DETERMINATION OF THE HETEROTROPHIC AND AUTOTROPHIC ACTIVE BIOMASS DURING ACTIVATED SLUDGE RESPIROMETRIC BATCH ASSAYS USING MOLECULAR TECHNIQUES

ARSHAD ISMAIL

April 2008

DETERMINATION OF THE HETEROTROPHIC AND AUTOTROPHIC ACTIVE BIOMASS DURING ACTIVATED SLUDGE RESPIROMETRIC BATCH ASSAYS USING MOLECULAR TECHNIQUES

ARSHAD ISMAIL

Thesis submitted in compliance with the requirements for Doctoral Degree in Technology in the Department of Biotechnology, Durban University of Technology

DETERMINATION OF THE HETEROTROPHIC AND AUTOTROPHIC ACTIVE BIOMASS DURING ACTIVATED SLUDGE RESPIROMETRIC BATCH ASSAYS USING MOLECULAR TECHNIQUES

ARSHAD ISMAIL

I hereby declare that this thesis represents my own work, unless stated to the contrary in the text, and that it has not been submitted in part, or in whole to any other Technikon/University

_____

A. ISMAIL

I hereby approve the final submission of the following thesis

_____ _____

Supervisor
Prof. F. Bux
(D.Tech: Biotechnology, DUT)

Date

_____ _____

Co-supervisor
Prof. M.C. Wentzel
(PhD: Civil Engineering, UCT)

Date

DEDICATION

To my parents….for their constant support and encouragement

ABSTRACT

Activated sludge models now in use worldwide for the design and operation of treatment systems use hypothetical concentrations of active organisms. In order to validate and calibrate model outputs, concentrations and activities of organisms responsible for nitrification and denitrification need to be reflected by actual measurements. This research has been initiated by the observation of an increasing gap of suitable techniques that exist in the direct measurement and separation of active biomass components, responsible for COD removal and denitrification.

The separation and accurate quantification of active biomass components in activated sludge is of paramount importance in models, used for the management and design of wastewater treatment plants. Accurate estimates of microbial population concentrations and the direct, *in situ* determination of kinetic parameters could improve the calibration and validation of existing models of biological nutrient removal activated sludge systems. The aim of this study was to obtain correlations between heterotrophic active biomass (Z_{BH}) and autotrophic active biomass (Z_{BA}) concentrations predicted by mathematical models and quantitative information obtained by fluorescent *in situ* hybridizations (FISH). Separate respirometric batch tests were applied to mixed liquors drawn from a well defined parent anoxic/aerobic activated sludge system in order to quantify the Z_{BH} and Z_{BA} concentrations. Similarly, fluorescent labeled, 16S rRNA-targeted oligonucleotide probes specific for ammonia and nitrite oxidizers were used in combination with DAPI staining to validate the Z_{BH} and Z_{BA} active biomass component in activated sludge respirometric batch tests. For the direct enumeration and simultaneous *in situ* analysis of the distribution of nitrifying bacteria, *in situ* hybridization with oligonucleotide probes were used. Probes (NSO 1225, NSR 1156 and NIT3) were used to target the nitrifiers and the universal probe (EUB MIX) was used to target all Eubacteria. Deducting the lithoautotrophic population from the total bacterial population revealed the Z_{BH} population in the modified batch test, whereas only quantifying the nitrifiers revealed the Z_{BA} population in autotrophic batch test. A conversion factor of 8.49×10^{-11}

mgVSS/cell (Holder-Snymann *et al*., 2004) was applied to express the Z_{BH} and Z_{BA} in terms of COD concentration. Z_{BH} values obtained by molecular probing correlated closely with values obtained from the modified batch test. However, the trend of consistently poor correspondence of measured and theoretical concentrations was evident. A similar result was observed for the Z_{BA} determination, with a close to moderate correspondence between measured and theoretical values and poor correspondence between measured values obtained by molecular probing and batch test.

Reasons for the large discrepancies between measured (batch test) and theoretical (parent system) values in the modified batch test were investigated using DNA fingerprinting techniques such as polymerase chain reaction (PCR) and denaturing gradient gel electrophoresis (DGGE). Microbial community profiles obtained from the parent system was compared to the profiles obtained from the modified batch test. PCR-DGGE profiles revealed shifts in population dominance between the batch test and the parent system, as well as population variability during the course of the batch test at defined So/Xo ratios. Therefore rendering the modified batch test an unsuitable technique to directly quantify the $Z_{BH(0)}$ with sufficient accuracy. The integration of molecular techniques (eg. FISH), are now required to expand model calibration and validation efforts, suggesting information gained by FISH can be incorporated into current design and operating guidelines and in particular, can be used for model development and validation. However, applicability of this knowledge still warrants further development to ensure direct practical benefits.

PREFACE

Aspects of the work covered in this thesis can be found in the following publications

Refereed Articles

P. Padayachee, A. Ismail, and F. Bux. (2006) Elucidation of the microbial community structure within a laboratory scale activated sludge process using a combination of molecular techniques. *Water SA vol 32 (5)*

A. Ismail, M.C. Wentzel and F. Bux. (2007) Using respirometric techniques and fluorescent in situ hybridization to evaluate the heterotrophic active biomass in activated sludge. *Biotechnology and Bioengineering vol 98 (3)*

A.P. Degenaar, A. Ismail and F. Bux (2008) Comparative evaluation of the microbial community in biological processes treating industrial and domestic wastwaters. *J. Applied Microbiology vol 104 (2)*

A. Ismail, P. Padayachee and F. Bux. (2008) Using molecular techniques to assess steady-state behaviour in a laboratory scale activated sludge system *Bioscience and Bioengineering* (Submitted)

A. Ismail, M.C. Wentzel and F. Bux (2008) Elucidation of the batch test procedure to quantify the ordinary heterotrophic organism in activated sludge mixed liquor. *Bioscience and Bioengineering* (In preparation)

Conference Proceedings

Ismail A.A.H, Holder F. and Bux F. (2004) Determining of the heterotrophic active biomass using novel molecular techniques. *WISA BIENNIAL CONFERENCE & EXHIBITION* 2-5 May. ICC, Cape Town.

P. Padayachee, A.A.H Ismail, and F. Bux (2006) Elucidation of the microbial community structure within a laboratory scale activated sludge process using a combination of molecular techniques. *WISA BIENNIAL CONFERENCE & EXHIBITION* 21-25 May. ICC, Durban.

A. Ismail, M.C. Wentzel and **F. Bux**. (2006) Integrating modeling and fluorescent *in situ* hybridization to determine the heterotrophic active biomass in activated sludge. *IWA world congress and exhibition,* 10-14 September 2006, Beijing China

Poster Presentation

A. Ismail, M.C. Wentzel and F. Bux (2006) Using modeling and molecular techniques to quantify the heterotrophic active biomass in activated sludge. 14th Biennial Congress of South African Society for Microbiology, 9-12 April. CSIR International Convention Centre, Pretoria

Research Report

F. HOLDER-SNYMAN, A.A.H. ISMAIL, D.D. MUDALY, and F. BUX (2005) Determination of heterotrophic active bacteria in activated sludge using novel molecular techniques, *WRC report K5/1178/05*

ACKNOWLEDGEMENTS

I wish to express my sincere gratitude and appreciation to the following people for their assistance in the completion of this thesis.

- Prof. F. Bux for his constant participation and interest during the course of this study.
- Prof M.C. Wentzel (UCT) for his assistance and guidance through the engineering technology aspects of this study.
- Prof. N. Lee (TUM, Germany) for her invaluable comments and critical appraisal.
- My colleagues: A. Degenaar, P. Padayachee, S. Maharaj, N.N. Goba and L.N. Zondi for their technical assistance during the course of this study
- To my Family, for their love, support and encouragement.
- The National Research Foundation for their financial assistance.

TABLE OF CONTENTS

LIST OF TABLES

LIST OF FIGURES

LIST OF ABBREVIATIONS

ALF1b	Oligonucleotide probe specific for the alpha-subclass of *Proteobacteria*
AO	Autotrophic organisms
BET42a	Oligonucleotide probe specific for the beta-subclass of *Proteobacteria*
BNR	Biological nutrient removal
COD	Chemical oxygen demand
COD_{FE}	Total filtered effluent COD concentration (mgCOD/L)
COD_{ML}	Total unfiltered mixed liquor COD concentration (mgCOD/L)
$COD_{t=0}$	Total unfiltered COD concentration at the start of the test (mgCOD/L)
$COD_{t=T}$	Total unfiltered COD concentration at the end of the test (mgCOD/L)
COD_{FIL}	Filtered COD
DAPI	4',6-diamidino-2-phenylindole
DGGE	Denaturing gradient gel electrophoresis
DNA	Deoxyribonucleic acid
rDNA	Ribosomal DNA
DO	Dissolved oxygen
EBPR	Excess biological phosphorous removal
EPS	Exopolymeric substance
EUB338	Oligonucleotide probe specific for most members of the kingdom Bacteria
f_{CV}	COD to VSS ratio of mixed liquor (mgCOD/mgVSS)
f_{VB}	VSS to biomass ratio of mixed liquor (mgVSS/cell)
$f_{S,up}$	Unbiodegradable particulate fraction of the influent (mgCOD/mgCOD)
$f_{S,us}$	Unbiodegradable soluble fraction of the influent (mgCOD/mgCOD)
FISH	Fluorescent *in situ* hybridization
GAM42a	Oligonucleotide probe specific for the gamma-subclass of *Proteobacteria*
GPBHGC	Gram-positive bacteria with high G+C DNA content
HGC69a	Oligonucleotide probe specific for *Actinobacter*
INF	Influent
MLSS	Mixed liquor suspended solids
MLVSS	Mixed liquor volatile suspended solids (volatile suspended solids)

NDEBPR	Nitrification denitrification excess biological phosphorus removal
NOB	Nitrite-oxidizing bacteria
OHO	Ordinary heterotrophic organism
OUR	Oxygen utilization rate
$OUR_{H(t)}$	OHO active biomass oxygen utilization rate at time t (mgO/L/h)
$OUR_{M(t)}$	OUR measured at time t (mgO/L/h)
$OUR_{N(t)}$	AO oxygen utilization rate at time t (mgO/L/h)
OUR_{NO2}	OUR for NO_2^- nitrification (mgO/L/h)
OUR_{NO3}	OUR for NO_3^- nitrification (mgO/L/h)
PAO	Polyphosphate accumulating organism
PCR	Polymerase chain reaction
PSS	Protein synthesizing system
RBCOD; S_{bsi}	Readily biodegradable COD (mgCOD/L)
RFLP	Restriction fragment length polymorphism
RNA	Ribonucleic acid
SBCOD;S_{bpi}	Slowly biodegradable COD (mgCOD/L)
SBR	Sequenced batch reactor
SCFA	Short chain fatty acid
S_0/X_0	Initial substrate (S_0) to initial biomass (X_0) ratio
TKN	Total Kjedahl nitrogen (mgN/L)
V	Volume (L)
VFA	Volatile fatty acid
WRC	Water Research Commission
Z_{BA}	AO active biomass concentration (mgCOD/L)
$Z_{BA(0)}$	AO active biomass concentration at the start of the test (mgCOD/L)
Z_{BH}	OHO active biomass concentration (mgCOD/L)
$Z_{BH(0)}$	OHO active biomass concentration at the start of the test (mgCOD/L)

CHAPTER 1

General Introduction

1.1 The Active Biomass Concept

In order to optimize the design and operation of the single sludge activated sludge system over the past two decades a number of steady state design models (Marais and Ekama, 1976; WRC, 1984; Wentzel *et al*., 1990; Maurer and Gujer, 1994) and kinetic simulation models (Dold *et al.,* 1980, 1991; Van Haandel *et al.,* 1981; Henze *et al.,* 1987, 1995; Wentzel *et al*., 1992; Gujer *et al.,* 1995) have been developed, to progressively include aerobic COD removal and nitrification, anoxic denitrification and anaerobic /anoxic/aerobic biological excess phosphorus removal. These models enable system design and operational parameters to be readily identified, provide guidance in selecting values for these parameters and quantify the expected behaviour of the system.

These groups of models are based, to a large degree, on a common conceptual framework which has been developed from an understanding of the interactions between the components making up the mixed liquor in the bioreactor and the influent wastewater. This conceptual framework will be outlined briefly in this chapter, to provide an overview of the current understanding of the processes that give rise to the various mixed liquor components and how these processes relate to the influent wastewater. From this overview, the importance of the mixed liquor component ordinary heterotrophic organism (OHO) and autotrophic organism (AO) active biomass will be evident with particular emphasis placed on the quantification and identification of these groups.

1.2 Biological Transformation of the Organic Carbonaceous Material in the Bioreactor

The biodegradable components of the influent wastewater are biologically transformed in the bioreactor to other components or products, gaseous, soluble or particulate (Cronje *et al.*, 2005). In the steady state design and dynamic kinetic simulation models, the biological transformations of the organic carbonaceous materials are explicitly included, and directly influence the organic solids in the bioreactor. It is important, therefore, to gain a basic understanding of the approach adopted in the models to describe these transformations.

1.2.1 Organism groups

In the bioreactor of the activated sludge system a wide diversity of microorganisms have been identified. Therefore, including a complete description of every species in both the steady state design and dynamic kinetic simulation models would be impractical. Instead microorganisms that fulfill a particular function in the activated sludge system are grouped together as a single entity which has been called a "surrogate" organism. This surrogate organism is assigned a set of unique characteristics that reflect the behaviour of the group. Thus for modelling of activated sludge systems the "organizational level" (Odum, 1971) that is followed is the mass behaviour of a population or a group of selected organisms; these populations or groups are identified and selected based on their functions. The principal organism groups, their functions and the zones in which these functions are performed are summarized in Table 1.1. This research considers only the anoxic/aerobic activated sludge system. Thus, two groups need to be taken into account;

- Heterotrophic organisms unable to accumulate polyphosphate (polyP), termed ordinary heterotrophic organisms (OHO)
- Autotrophic organisms (AO) mediating nitrification, termed autotrophs or nitrifiers

The biological transformations mediated by these two groups are described in Table 1.1.

Table 1.1: Principle organism groups included in models for activated sludge systems (Cronje *et al*., 2005).

Organism	**Biological Process**	**Zone**
Ordinary heterotrophs - OHO (unable to accumulate polyP)	• COD removal (organic degradation; DO uptake) • Ammonification (organic N→NH_4^+)	Aerobic Aerobic
	• Denitrification (organic degradation; NO_3^-→NO_2^- →N_2)	Anoxic
	• Fermentation (F-RBCOD→SCFA)	Anaerobic
PolyP heterotrophs –PAO accumulate polyP)	• P release (SCFA uptake ; PHA storage	Anaerobic
	• P release (SCFA uptake; PHA storage) • P uptake (PHA degradation; denitrification)	Anoxic Anoxic
	• P uptake; P removal (PHA degradation; DO uptake)	Aerobic
Autotrophs-AO (nitrifiers)	• Nitrification (NH_4^+→NO_2^- →NO_3^-; DO uptake)	Aerobic

1.2.2 Ordinary heterotrophic organisms (OHO)

The heterotrophic organisms obtain both energy and carbon from complex organic compounds. Conceptually, in the models this "surrogate" heterotroph is subjected to two main biological processes; (i) synthesis or growth and (ii) endogenous mass loss/death

(i) Synthesis/ growth

For the heterotrophic organisms, the organic material in the influent serves two functions: (a) it is the supply of materials which are transformed into new cell materials, and (b) it is the supply of energy to achieve these transformations. In terms of models, on entry into the bioreactor some of the influent organic materials are transformed (via a number of biochemical pathways, collectively called anabolism) to new heterotroph cell material. Accepting the general formulation for protoplasm as $C_5H_7O_2N$ (McCarthy 1964), with glucose as an example substrate the synthesis reaction can be summarized as:

$$5C_6H_{12}O_6 + 6NH_3 \rightarrow 6C_5H_7O_2N + 18H_2O \quad (1.1)$$

The energy required for the synthesis/growth process is generated from the hydrolysis of organic molecules. This is achieved by the heterotrophs to give hydrogen ions, electrons and carbon dioxide. For example, consider the organic molecule glucose:

$$C_6H_{12}O_6 + H_2O \rightarrow 6CO_2 + 24H^+ + 24e^- \quad (1.2)$$

Because it releases electrons the molecule is termed an electron donor and on yielding the electrons, the molecule is said to be oxidized. The electrons (and protons) are captured by the heterotrophs, and are transferred via an internal sequential set of oxidation reduction (redox) reactions eventually to a molecule which can accept them; this molecule is called the terminal electron acceptor. In this series of redox reactions, free energy is released which is captured by an organism (collectively this process is called catabolism). The energy captured by the organism principally is used by the organism for the

transformation reactions that synthesize new cell mass, Eq. (1.1). From biogenetics it is possible to determine the amount of glucose that must be oxidized to synthesize one mole of new cell mass (WRC, 1984).

In the oxidation of substrate, if oxygen is present (aerobic conditions) the terminal electron acceptor is oxygen (O_2) which is reduced to water (H_2O), i.e.

$$O_2 + 4H^+ + 4e^- \rightarrow 2H_2O \tag{1.3}$$

If oxygen is absent, but nitrate (or nitrite) is present (anoxic conditions), the nitrate (NO_3^-) (or nitrite, NO_2^-) serves as terminal electron acceptor and is reduced to nitrogen gas (N_2), giving rise to denitrification process:

$$NO_3^- + 12H^+ + 10e^- \rightarrow N_2 + 6H_2O \tag{1.4}$$

Thus, of the original biodegradable organic material present, a part is oxidized to yield free energy. This free energy is utilized by the heterotrophs to "reorganize" the remaining organic material into new cell mass, the free energy being lost as heat in the re-organization. Noting that the heterotrophic organisms use electron transfer (redox) reactions to generate the free energy, the transformation of the biodegradable organic material can best be traced by monitoring the transformations in electrons. This has the advantage, *inter alia*, that, due to the indestructibility and hence conservation of electrons, electron mass balances can be conducted. Accordingly, of the electrons present in the biodegradable organic material (measured via COD test) (WRC, 1984), a fraction is transformed into new heterotrophic cell mass, and the remainder pass to the terminal electron acceptor, oxygen if aerobic and nitrate if anoxic.

Now, the ratio of electrons captured in new cell mass to the electrons present in the biodegradable substrate is termed the yield (Y_{ZH}), i.e.

$$Y_{ZH} = \frac{e^{-} \text{ in synthesized material}}{e^{-} \text{ in biodegradable material}} \qquad (1.5a)$$

Accepting the COD test as a measure of the electrons, then

$$Y_{ZH} = \frac{COD \text{ in synthesized material}}{COD \text{ in biodegradable material}} \qquad (1.5b)$$

And, from a mass balance on electrons (COD)
COD of biodegradable material = COD of synthesized material + e^- to electron acceptor.

For activated sludge systems with the wide diversity of biodegradable organics in the influent and heterotrophs in the bioreactor, it has been found that the yield can be accepted to be approximately constant, at Y_{ZH} = 0.666 mgCOD/mgCOD (Dold *et al*., 1980; 1991). In other words, for every biodegradable organic COD utilized, a constant fraction will be transformed to heterotrophic active biomass, and the balance of the electrons will pass to the electron acceptor.

A question that needs to be addressed is how much of the influent biodegradable material will be transformed in the bioreactor, within the residence time in the system? This is a problem of kinetics or rates. In considering the kinetics of biodegradable organic material transformation, it is subdivided into two components, readily biodegradable (soluble) COD (S_{bsi}) and slowly biodegradable (particulate) COD (S_{bpi}) (Fig. 1.1). This division is based on observed biological responses of activated sludge mixed liquor to domestic wastewater (Dold *et al.,* 1980; Van Haandel *et al*., 1981), that is, the division is a biokinetic one. Under dynamic loading of activated sludge (short sludge age cyclic loading, plugflow reactors, batch tests) two distinct rates of utilization of domestic wastewater biodegradable COD substrate were apparent with either oxygen (Dold *et al*., 1980; Ekama *et al*., 1986) or nitrate (Van Haandel *et al*., 1981; Ekama *et al*., 1986) as electron acceptor (aerobic or anoxic conditions respectively). Readily biodegradable COD (RBCOD) was taken up rapidly by the sludge and metabolized, giving rise to a high

oxygen or nitrate utilization rate, respectively. Slowly biodegradable COD (SBCOD) was taken up much more slowly and metabolized, giving rise to oxygen or nitrate utilization rates about 1/10 of the rate with RBCOD.

To explain these observations, the RBCOD was hypothesized to consist of simple *soluble* molecules that can be adsorbed readily by the organism and metabolized for energy and cell synthesis, whereas the SBCOD was assumed to be made up particulate/colloidal/ complex organic molecules that require extra cellular adsorption and enzymatic breakdown (hydrolysis) prior to adsorption and utilization.

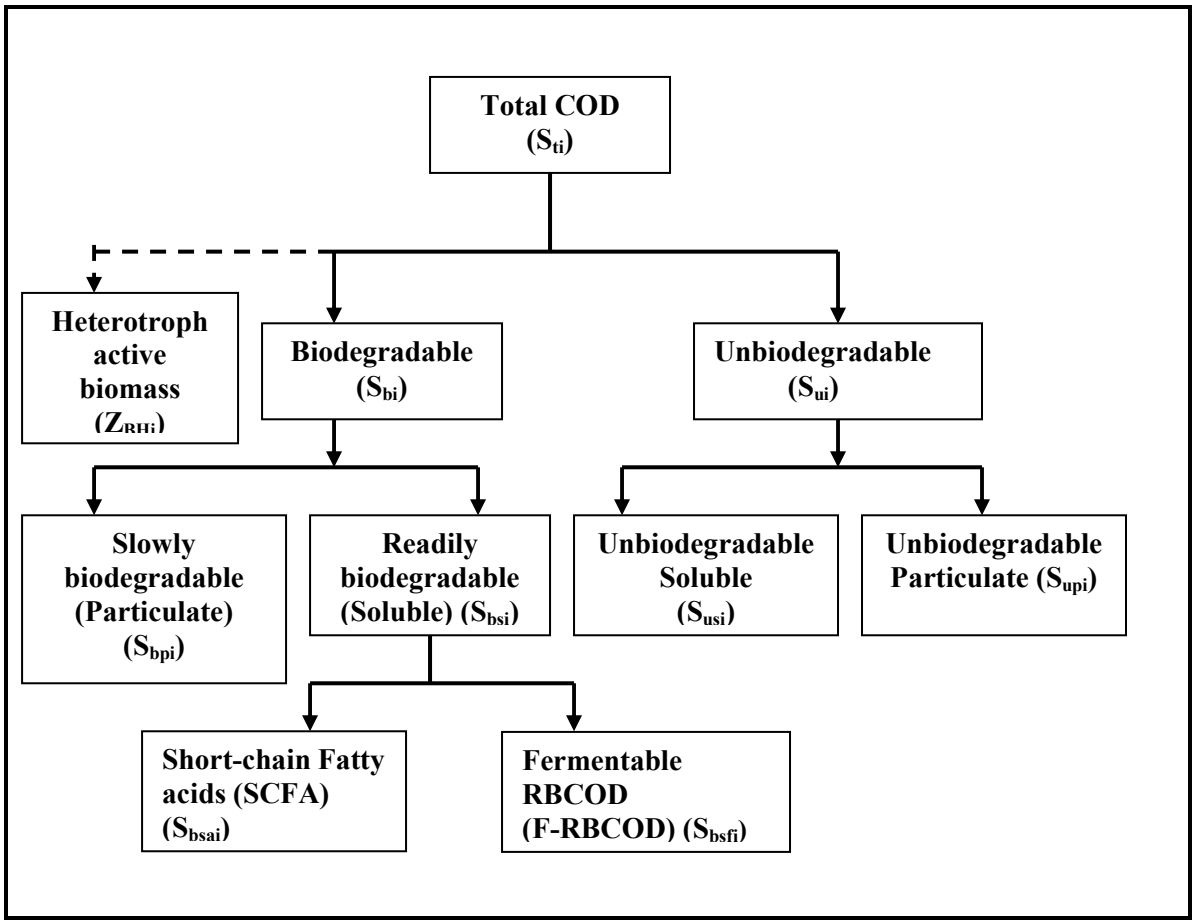

Fig 1.1: The division of influent COD into its different constituents (Cronje *et al.,* 2005)

The hypothesized difference in molecule size between RBCOD and SBCOD has been used to classify the RBCOD as a biodegradable soluble COD and the SBCOD as a biodegradable particulate COD. Since the RBCOD is soluble, it is exposed to biological treatment only as long as the liquid remains in the reactor, i.e. for the hydraulic retention time which is relatively short (~ 6-24h). However, the rate of RBCOD utilization is high and for sludge ages greater than about 3 days the concentration of RBCOD in the effluent is negligible even though the hydraulic retention time is short. Accordingly, for completely aerobic systems it can be safely assumed that all the RBCOD will be utilized in the system (Cronje *et al.,* 2005). For the SBCOD, the extracellular breakdown (hydrolysis) is slow and forms the limiting rate in the utilization of SBCOD. Although the rate of SBCOD utilization is relatively slow, the SBCOD does not appear in the effluent. This is because on entry of the influent into the bioreactor, the SBCOD becomes enmeshed in the mixed liquor, settles out in the secondary settling and is retained in the system. Therefore, the particulate biodegradable organics (SBCOD) are exposed to biological treatment for as long as the solid (settleable) material is retained in the system, i.e. for the sludge age. Thus even though the utilization of the SBCOD is around 10 times slower than that for the RBCOD, because the sludge age in most activated sludge systems is usually more than 10 times longer than the hydraulic retention time, the SBCOD is completely utilized also. From simulation studies using dynamic kinetic models (Dold *et al*., 1991) all the SBCOD is completely utilized for sludge ages greater than about 2 to 3 days and temperatures greater than 20ºC (5 to 6 days at 14ºC). Accordingly, for most activated sludge systems it is sufficient to assume all the SBCOD will be utilized in the system.

Thus, for activated sludge systems at 20ºC for sludge ages greater than 3 days all the biodegradable organic material in the influent, whether soluble or particulate, will be transformed in the bioreactor by biological action mediated by the heterotrophic active biomass. The products of transformation are:

- Gaseous- carbon dioxide (only considered if the fate of the carbon is traced) and nitrogen, produced if nitrate acts as terminal electron acceptor, Eq. (1.4), i.e. anoxic conditions;

- Soluble –water, produced when oxygen acts as a terminal electron acceptor, Eq. (1.3), i.e. aerobic conditions;
- Particulate – new heterotrophic active biomass.

The particulate heterotrophic active biomass will settle out in the secondary settling to be retained in the system and thus will be another component of the mixed liquor solids. Since the influent SBCOD is totally utilized for systems with sludge ages > 3d at 20ºC, the SBCOD will not be significant component of the mixed liquor solids, and hence can be neglected (Cronje *et al.,* 2005).

(ii) Endogenous mass loss/death

The endogenous mass loss phenomenon is the loss of active organism mass with time. The phenomenon can be observed as a reduction in organism active biomass when the organism population is aerated with no substrate added. The phenomenon also manifests itself as a decrease in specific organism yield with increase in sludge age. In models, two conceptual approaches have been followed to describe this phenomenon; endogenous respiration and death regeneration (Cronje *et al*., 2005).

Endogenous respiration

In this approach active organism mass is lost at a constant specific rate. Of the active organism mass that is lost, a part (the biodegradable fraction, about 80%) is oxidized to provide energy for maintenance of the active mass remaining and the balance (the unbiodegradable fraction, about 20%) remains as particulate unbiodegradable organic fraction accumulating in the system, and is called endogenous residue. The oxidation of the biodegradable part of the active mass lost gives rise directly to endogenous oxygen consumption under aerobic conditions, and indirectly to a nitrate demand (denitrification) under anoxic conditions. The simplicity of this approach allows analytical solutions to be readily determined (Cronje *et al*., 2005).

Death-regeneration

This approach is used in the dynamic kinetic simulation models. In the death-regeneration approach an attempt is made to separate out the process which takes place during the organisms "death phase". Disappearance of live active mass is hypothesized to be due to the net effect of death (natural or predation) and regeneration of organisms: on death the cell material is released through lysis; a part is particulate unbiodegradable endogenous residue (about 8%); the remaining part (about 92%) is biodegradable and adds to the slowly biodegradable COD (SBCOD) which passes through the path of adsorption, hydrolysis and synthesis of new cell mass (i.e. regeneration), discussed above. The synthesis of new cell mass gives rise to an associated aerobic oxygen or anoxic nitrate demand. Thus, in death-regeneration the oxygen or nitrate demand arises in fact from the energy requirements for resynthesis of organism active mass (regeneration) from the SBCOD liberated from the organism death. The main implication of this approach is that "maintenance energy" *per se* (the oxygen/nitrate requirement for maintenance) is considered to be so small that it can be combined with, and completely masked by, the oxygen/nitrate demand for resynthesis of new cell mass from the lysed biodegradable substrate.

Comparing the two approaches, for the mixed cultures present in the activated sludge system predation is likely to be a significant cause for death of organisms, "liberating" substrate for synthesis of new cell mass (predator and others). Thus, conceptually the death regeneration would appear superior. However, provided all the biodegradable COD has been depleted and a terminal electron acceptor (oxygen or nitrate) is continually available, with the appropriate selection of constants the two approaches give the same nett result, i.e. same loss of heterotrophic active biomass, utlilization of oxygen/nitrate and generation of endogenous residue (Dold *et al.,* 1980; 1991). If a terminal electron acceptor is not available, then the endogenous-respiration approach is deficient and the death-regeneration approach preferable. Also the two approaches do deviate slightly when significant biodegradable COD is present, e.g. Batch tests (Cronje *et al.,* 2005).

1.2.3 Autotrophic organisms (AO)

In the activated sludge system, the autotrophic organisms of importance are the nitrifiers. These organisms mediate the process of nitrification, whereby free and saline ammonia is oxidized to nitrate via nitrite (detailed description in Chapter 2).

Part of the energy released in the single nitrification process is used for synthesis of new nitrifier organism active mass (growth), i.e. accepting $C_5H_7O_2N$ as a generalized formulation for nitrifier protoplasm (MacCarty, 1964), then:

$$5CO_2 + NH_4^+ + 2H_2O \rightarrow C_5H_7O_2N + 5O_2 + H^+ \qquad (1.6)$$

Recognizing that ammonia serves as the "substrate" for the nitrifiers, the specific yield is expressed in terms of the ammonia utilized, i.e.

$$Y_{ZA} = \frac{COD \text{ of nitrifiers formed}}{NH_4^+ - N \text{ utilized}} \qquad (1.7)$$

The nitrifier active biomass that is formed in the activated sludge system is important in considering the mixed liquor solids, because it is particulate and so will settle in the secondary settling tank to be retained in the system. The nitrifier active biomass, therefore, will be one component making up the mixed liquor solids.

As with the heterotroph active biomass, the nitrifier active biomass also is subjected to endogenous mass loss/death. Although conceptually for consistency, this endogenous mass loss/death should result in the generation of an endogenous residue, compared to the other mixed liquor fractions the relative amount of endogenous residue generated by the autotrophs is so small it is of little practical importance and can be neglected (Cronje *et al.,* 2005).

1.2.4 Phosphate accumulating organisms (PAO)

The phosphate accumulating organisms (PAO) are a specified group of heterotrophic organisms able to accumulate P intracellularly in long chains polyphosphate (PolyP). In terms of the models, only those heterotrophic organisms exhibiting this behavior in the activated sludge system are included in the PAO group. To stimulate P behavioural patterns typical of the surrogate PAO group (P release, uptake and excess removal) requires the presence of an anaerobic reactor, with the influent wastewater fed to this reactor (Wong *et al*., 2005). This research does not focus on activated sludge systems that include anaerobic reactors, and hence quantifying the PAOs does not fall within the ambit of the current research project.

1.3 Modern Methods of Identifying and Quantifying Active Biomass Components

In recent years, a great variety of analytical and molecular tools have been developed to analyze and quantify active biomass components in activated sludge systems. In this section, existing methods within the molecular biology and engineering domains will be reviewed, providing combined insights for the quantification of mixed liquor components.

1.3.1 Fluorescent *in situ* hybridization (FISH)

FISH using rRNA-targeted oligonucleotide probes is frequently applied to quantify the composition of microbial communities in different environments (Wagner *et al.,* 1994c; Alfreider *et al*., 1996; Kämpfer *et al.,* 1996; Snaidr *et al*., 1997; Llobet-Brossa *et al.*, 1998). In such studies cell numbers are generally obtained by manual counting in an epifluorescence microscope. Usually the relative abundance of a probe target population is determined by comparison of the obtained numbers:

- with counts of all bacterial cells detectable by FISH (via simultaneous hybridization with a bacterial probe (Wagner *et al*., 1993; Glöckner *et al*., 1996; DeLong *et al*., 1999; Ravenschlag *et al.*, 2001) or probe set (Daims *et al*., 1999), or
- with counts of all organisms containing DNA (by simultaneous application of nucleic acid staining dyes (Hicks *et al.*, 1992; Wallner *et al*., 1995; Ramsing *et al*., 1996).

Although quantitative FISH has provided novel insights into the structure and dynamics of microbial communities, it suffers from its tediousness and its limited accuracy for samples containing densely aggregated cells like activated sludge flocs or biofilms. The latter problem can in part be ameliorated by the use of confocal laser scanning microscopy (CLSM) for the detection of probe-labeled cells (Wagner *et al*., 1998). However, even if optical CLSM sections are recorded, it is not feasible to count manually a sufficient number of cells in each hybridization experiment in a reasonable time period to obtain statistically reliable results. This limitation has two reasons. Firstly, manual counting itself is very time consuming and thus generally not more than a few thousand cells per hybridization experiment were counted in previous publications. Secondly, manual counting requires high magnification CLSM-sections which allow single cell resolution within clusters. However, such images only contain relatively few cells and therefore many images need to be recorded, rendering the procedure even more time consuming (Daims *et al.*, 2001c).

Therefore, more precise methods are required to quantify the composition of the microflora in samples containing clustered cells. In principal, flow cytometry is a more efficient and accurate alternative for quantification of fluorescently labeled bacterial cells (Wallner *et al.,* 1997). However, for the analysis of microbial flocs and biofilms flow cytometry is of limited use since it necessitates efficient dispersion of clustered bacteria prior to the measurement, a requirement which frequently cannot be fulfilled (Wallner *et al.*, 1995; Wallner *et al.,* 1997). To overcome the limitations of manual cell counting procedures, semi-automated digital image analysis tools were developed which quantify fluorescently labeled bacteria in environmental samples (Bloem *et al*., 1995; Ramsing *et al*., 1996). But such solutions are not able to efficiently count cells in dense clusters or

biofilms since single cell recognition within these structures cannot be automated. This problem can be circumvented by measuring the areas of specifically stained bacteria in randomly acquired optical CLSM sections. This approach only requires the software to differentiate between labeled biomass (including cell clusters) and unlabeled background but does not rely on single cell recognition within clusters. The abundance of a particular population is then expressed as fraction of the area occupied by all bacteria (Bouchez *et al.,* 2000; Schmid *et al.,* 2000).

For this purpose, an environmental sample is hybridized simultaneously with different rRNA-targeted oligonucleotide probes: one specific probe that targets the population which is to be quantified, and one domain-specific probe set that detects most bacteria. The population specific and the domain-specific probes are labeled with different fluorochromes. Following FISH, the fluorescence conferred by the different probes is recorded in separate CLSM images. The areas of the labeled cells in these images are measured by digital image analysis. Since this approach analyses low magnification images and can partly be automated it allows rapid quantification of high numbers of bacteria thereby significantly improving the statistical accuracy of the measurement (Bouchez *et al.,* 2000; Schmid *et al.,* 2000).

CLSM based methods to semi-automatically measure the biovolume of fluorescently labeled bacteria (Heydorn *et al.,* 2000) could theoretically be applied to determine absolute cell numbers of probe-defined bacterial populations on membrane filters. However, biovolume-based quantification is only accurate if serial optical sections are recorded using small vertical step intervals and subsequently are combined to image stacks. This procedure is extremely time consuming and leads to significant bleaching of FISH labeled bacterial cells.

Daims *et al*., (2001c) developed a semi-automated procedure for determining cell concentrations of bacterial populations in complex samples by FISH and CLSM using the area-based quantification method (Schmid *et al.,* 2000). Spiking of the samples with known amounts of *E.coli* cells, which were used as internal standards for the subsequent

FISH analysis, allowed to infer the absolute cell numbers of probe-target bacteria from their measured areas by digital analysis of CLSM images. However the accuracy of the developed method depends on relatively homogeneous distribution of reference cells (used for spiking) within the environmental sample. Since composition and density of aggregates or flocs might vary between different environments, special pretreatment (e.g. homogenization) of other samples may be necessary to ensure optimal dispersal of the cells used for spiking.

1.3.2 Isotope labeling and microautoradiography

Several isotope-based methods have been introduced in recent years for cultivation independent characterization of active microorganisms in environmental samples. The novel methodologies include direct isotope analysis of extracted biomarkers, including amino acids, fatty acids, and nucleic acids (Pelz *et al*., 1998; Roslev and Iversen, 1999; Bodelier *et al*., 2000; Boschker and Middelburg, 2002; MacGregor *et al.*, 2002), stable isotope probing (SIP) of DNA or RNA (Radajewski *et al*., 2000; Manefield *et al*., 2002), and a new isotope microarray (Adamczyk *et al.*, 2003).

Microautoradiography (MAR) in combination with fluorescence *in situ* hybridization (FISH) has also been developed for cultivation independent identification of active bacteria in environmental matrices (Andreasen and Nielsen, 1997; Lee *et al.,* 1999; Ouverney and Fuhrman, 1999). When targeting heterotrophic bacteria, the traditional MAR approach has been based on the addition of typically ^{14}C- or ^{3}H-labeled organic substrates to environmental samples under defined incubation conditions. Labeled substrate and/or labeled degradation products are then taken up by active heterotrophs and often assimilated into various biomass components. MAR based on inorganic $^{14}CO_2$ as the labeled precursor has been used successfully to target autotrophic organisms, e.g., chemolithotrophic nitrifiers from activated sludge (Lee *et al.,* 1999) and autotrophic *Achromatium* cells from freshwater sediments (Gray *et al*., 1999). Combined with FISH, the current MAR approach often provides excellent information about activity and identity at the single-cell level in complex environments.

Advances in isotope labeling strategies may further expand the potential applications of the MAR approach. For example, isotope labeling of metabolic active heterotrophic bacteria may be improved by using $^{14}CO_2$ as isotope source. This suggestion is based on the old observation that most, if not all, heterotrophic organisms assimilate CO_2 during biosynthesis in various carboxylation reactions induced by enzymes such as pyruvate carboxylase, phosphoenolpyruvate carboxylase, coenzyme A carboxylase, etc. (Dijkuizen and Harder, 1985). This phenomenon, often described as "heterotrophic CO_2 assimilation," has been used recently for quantification of microbial activity in environmental samples (Roslev *et al.,* 2004; Hesseloe *et al.,* 2005).

FISH combined with MAR ($HetCO_2$-MAR) made it possible for the first time on a single-cell level to distinguish better between uptake and storage of organic compounds and metabolism that initiates true growth. This was clearly illustrated by the unique information on electron acceptors preferences by "*Ca.* Microthrix parvicella" that was obtained with the $HetCO_2$-MAR approach (Hesseloe *et al.,* 2005).

1.3.3 Respirometric Batch Assays

(i) Determination of ordinary heterotrophic organism (OHO) active biomass

Kappelar and Gujer (1992) describe a simple batch test procedure to quantify heterotrophic active biomass in activated sludge mixed liquor. Where a small quantity of mixed liquor is added to centrifugated wastewater and the oxygen utilization rate (OUR) response is monitored with time. From the observed exponential increase in OUR, the initial OUR in the batch test can be determined and the heterotrophic active biomass concentration can be derived. This procedure was modified and extended by Wentzel *et al.* (1995) and Mbewe *et al.* (1995), for the characterization of municipal wastewaters. The batch test was conducted on unsettled municipal wastewater without the addition of activated sludge mixed liquor. From the OUR-time response and a flocculated-filtered COD measurement at the end of the test, the wastewater heterotrophic active biomass,

readily biodegradable COD (RBCOD) and unbiodegradable soluble COD (USCOD) could be determined. Mbewe *et al.* (1995) found that the RBCOD and USCOD measured in the batch test correlate closely to that measured via conventional methods. However they were not able to evaluate the results for wastewater heterotrophic active biomass, since no conventional methods were available. They did note that measurements appeared to reflect operational changes at the wastewater treatment plant where the wastewater was collected – at the treatment plant, due to operational problems with sludge handling unit processes, on occasion waste activated sludge mixed liquor was discharged into the sewer at a point upstream of where the wastewater was collected; the batch test method could correctly detect the increase in OHO active biomass during these periods.

Ubisi *et al.* (1997a, b) extended this simple batch test method to quantify the OHO active biomass concentration in an activated sludge system. In this test a small sample of mixed liquor is drawn from the activated sludge system and mixed with raw wastewater in a batch reactor where the OUR and nitrite and nitrate concentrations are monitored with time. In parallel, a similar batch test is conducted on the raw wastewater without the addition of mixed liquor. From analysis of the OUR and nitrate and nitrite responses of the two parallel tests, the mixed liquor OHO active biomass concentration can be quantified.

Wentzel *et al*. (1998) evaluated this batch test method by drawing mixed liquor samples from a well defined laboratory-scale anoxic/aerobic activated sludge system operated at 12 and 20d sludge age. They compared the results from the batch tests with theoretical values for OHO active biomass concentrations from steady state design (WRC, 1984) and kinetic simulation models (Dold *et al.,* 1991). From the comparison they concluded that the results obtained were both encouraging and perplexing. With the parent system at 12d sludge age, the agreement between measured and theoretical values was remarkably good. However, the parent system at 20d sludge age, the agreement was poor, with the theoretical values being about 2 times those measured. Wentzel *et al*. (1998) could provide no explanation for this inconsistency, but concluded that the results do indicate

that the batch test method may prove to be a valuable tool that can be used to provide greater insight into the behaviour of aerobic and anoxic /aerobic activated sludge systems.

In evaluating the modified batch test Cronje *et al.* (2000) proposed to eliminate potential errors by:

- physically removing the OHO active biomass from the wastewater. This was achieved through flocculation of the wastewater with aluminum sulphate followed by filtration.
- using exponential fits for the nitrate-time profiles to determine nitrification OURs.

Considering the above, Cronje *et al*. (2000) obtained results that showed a reasonable agreement between the modified batch test values and theoretical values obtained from steady state design model (WRC, 1984).

Lee *et al*. (2003) investigated the variability for the inconsistencies between measured and theoretical values by:

- re-evaluating the modified batch test procedure
- application of batch aerobic digestion to quantify OHO active biomass
- development of kinetic models and application of these to the parent and batch tests responses.

In examining possible causes for the lack of 1:1 correspondence between theoretical and measured OHO active biomass concentrations, Lee *et al.* (2003) noted that the modified batch test method to quantify OHO active biomass relies on a single OHO population with constant kinetics. Observations made by Lee *et al.* (2003) suggest that this may not be true, and that the batch test conditions may cause the overall OHO behaviour to deviate significantly from that in the steady state system.

(ii) Determination of Autotrophic active (AO) biomass

Following the extensive evaluation of the batch test procedure for measuring the OHO active biomass concentration, a preliminary investigation was initiated to determine whether a similar batch test could be developed to quantify AO active biomass concentration (Cronje *et al.* 2002). In the batch test a small quantity of mixed liquor

drawn from the parent system is mixed with activated sludge system effluent supplemented with ammonium chloride (50 mg NH_4^+ L^{-1} batch volume), the AO substrate. The nitrate and nitrite concentrations with time are then monitored. From the increase in the nitrate and nitrite concentrations with time, the AO active biomass concentration at the start of the test can be determined (Beeharry, 1999). In examining the correspondences between the measured versus theoretical AO active biomass concentrations from a set of nine such batch tests, although the values are of similar magnitude, the theoretical values were approximately 2½ times the measured values (Beeharry, 1999).

1.4 Research Aim and Objectives

Previous studies have integrated molecular techniques to validate modeling results. Rittmann *et al.,* (1999) compared model-translated measures to the direct probing measures of community structure. This was accomplished by RNA extraction and subsequent slot-blot hybridization with probes NSO1225 (ammonia oxidizers) and EUB338 (for all active bacteria), which confirmed that the ratio of active nitrifiers to active heterotrophs was mainly explained by the ratio of TKN:BOD_L removed. The specific rRNA contents of all bacteria and ammonium oxidizers were estimated as 11,000 and 14,000 ng rRNA/mgVSS_{active}, respectively. Extracted rRNA measures a lumped parameter incorporating both rRNA levels (which are often correlated to growth activity) and cell abundance. However, the relationship between these two types of fractions was not determined experimentally and thus hybridization results did not necessarily provide information on the contribution of various populations to biomass concentration as needed in the model (Oerther *et al*., 1999). Furthermore, the populations targeted by the rRNA probes does not encompass all members of the model populations eg. Nitrite-oxidizing bacteria.

Vogelsang *et al.,* (2002) used FISH with 16S rRNA-targeted oligonucleotide probes to monitor selective enrichement and to determine the spatial distribution of nitrifiers in gel

beads. Experimental results were compared to computer modelled population distributions and estimated overall activity of the same system. Fluorescently labelled, 16S rRNA-targeted oligonucleotide probes specific for ammonia and nitrite oxidizers were used in combination with DAPI staining to monitor the selectivity of the enrichment process. However the limited FISH data available was insufficient for full and proper model verification. Due to the semi-quantitative approach applied they did not have exact and reliable data suitable for a direct recalibration between community structure expressed as cell numbers and expressed as model biomass (Vogelsang *et al*., 2002).

The quantification of active biomass components (heterotrophic and autotrophic) is a significant parameter within activated sludge steady state design and kinetic simulation models. It is of paramount importance that these parameters are independently quantified and validated to provide accurate estimates of microbial population concentrations and the direct, *in situ* determination of kinetic parameters. Specific bacterial groups in complex open communities such as activated sludge may be detected directly by fluorescence *in situ* hybridization (FISH), using 16S rRNA-targeted oligonucleotide probes. By merging engineering and technology of wastewater treatment systems with molecular biological techniques, it will allow suitable quantitative data to replace VSS as the "active biomass" measurement and to define specific COD, oxygen, and nutrient utilization rates among other kinetic information. Therefore improving the calibration and validation of existing models of biological nutrient removal activated sludge systems. With the consideration of the above, this research was initiated by acknowledging the increasing gap between engineering technology and molecular biology in addressing the active biomass concept.

The principal aim of this research was to merge the engineering and technology aspects of wastewater treatment systems (Batch tests) with molecular biological techniques (FISH) in order to accurately quantify the heterotrophic and autotrophic active biomass components.

To achieve this aim, the following objectives were carried out:

- To monitor and operate a parent aerobic/anoxic activated sludge system which was representative of a full scale activated sludge system.
- Determination of the OHO and AO active biomass concentration using the modified batch test and FISH analysis.
- Comparison of the OHO and AO active biomass concentrations obtained from the batch test with that obtained from FISH analysis.
- Comparison of the measured OHO and AO active biomass concentrations with theoretical values predicted by the steady state model.
- Comparison of microbial profiles obtained from the batch test and parent system using PCR-DGGE.

CHAPTER 2

Literature Review

2.1 Nutrient Overload: Unbalancing the Global Nitrogen Cycle

As a basic building block of plant and animal proteins, nitrogen is a nutrient essential to all forms of life (Fig 2.1). Recent studies have shown that excess nitrogen from human activities such as agriculture, energy production, and transport has begun to overwhelm the natural nitrogen cycle with a range of ill effects from diminished soil fertility to toxic algal blooms (Vitousek, 1997). Until recently, the supply of nitrogen available to plants and animal has become limiting. Although it is the most abundant element in the atmosphere, plants cannot use nitrogen from the air until it is chemically transformed, or fixed, into ammonium or nitrate compounds that plants can metabolize. In nature, only certain bacteria and algae (and, to a lesser extent, lightning) have this ability to fix atmospheric nitrogen, and the amount that they make available to plants is comparatively small. Other bacteria break down nitrogen compounds in dead matter and release it to the atmosphere again. As a consequence, nitrogen is a precious commodity, a limiting nutrient, in most undisturbed natural systems (Bitton, 1995).

Driven by a massive increase in the use of fertilizer, the burning of fossil fuels, and an upsurge in land clearing and deforestation, the amount of nitrogen available for uptake at any given time has more than doubled since the 1940s. In other words, human activities now contribute more to the global supply of fixed nitrogen each year than natural processes do, with human-generated nitrogen totalling about 210 million metric tons per year, while natural processes contribute about 140 million metric ton (Table 2.1) (Vitousek, 1997).

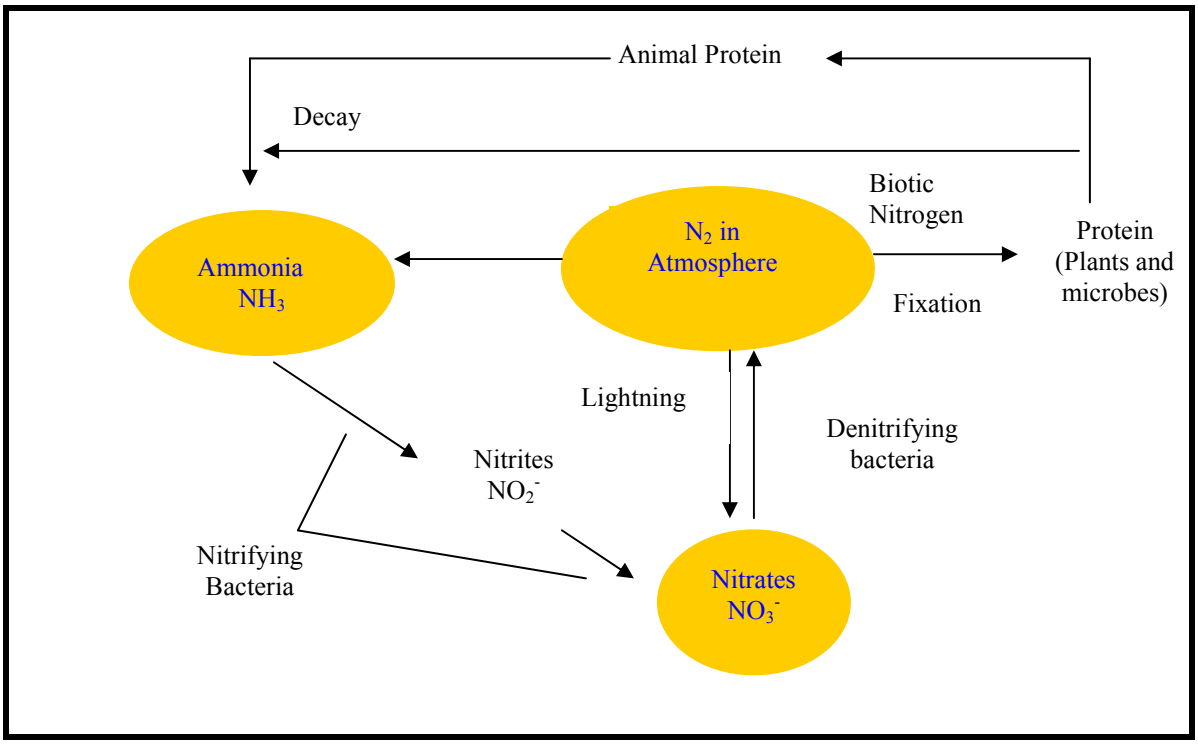

Fig. 2.1: Schematic representation of the nitrogen cycle (Stryer, 1981)

Although terrestrial ecosystems are vulnerable to the global nitrogen glut, aquatic ecosystems in lakes, rivers, and coastal estuaries have probably suffered the most so far. They are the ultimate receptacle of much of the nutrient overload, which tends to accumulate in runoff or to be delivered directly in the form of raw or treated sewage. (Sewage is very high in nitrogen from protein in the human diet). In these aquatic systems, excess nitrogen often greatly stimulates the growth of algae and other aquatic plants. When this extra plant matter dies and decays, it can deprive the water of its dissolved oxygen, suffocating many aquatic organisms (Vitousek, 1997).

This overfertilization process, called eutrophication (Steyn *et al.,* 1975), is one of the most serious threats to aquatic environments today, particularly in coastal estuaries and inshore waters where most commercial fish and shellfish species breed. One of the more troubling aspects of this nutrient assault on aquatic systems has been a steady rise in toxic algal blooms, which can take a heavy toll on fish, seabirds, and marine mammals (Vitousek, 1997).

Table 2.1: Global sources of biologically available (fixed) nitrogen (Vitousek, 1997).

A Global Glut of Nitrogen	
ANTHROPOGENIC SOURCES	**ANNUAL RELEASE OF FIXED NITROGEN (teragrams)**
Fertilizer	80
Legumes and other plants	40
Fossil fuels	20
Biomass burning	40
Wetland draining	10
Land clearing	20
Total from human sources	**210**
NATURAL SOURCES	
Soil bacteria, algae, lightning, etc.	140

Limitation of nutrient discharges into waters from point sources (sewers) is frequently achieved by intercepting and treating biological means, either by way of biological trickling filters or activated sludge systems. Both these systems utilize naturally occurring bacteria to reduce the nutrient concentrations entering waters. Artificial conditions favourable for the controlled growth of these bacteria are created within these systems and results in concentrations of at least a million times that found in the natural environment. The bacteria in these systems utilize the nutrients for growth and in this way the nutrients pass from the liquid phase into a solid phase and are concentrated in the biological culture (Lilley *et al*., 1997)

2.2 Activated Sludge Process

Since its development by Ardern and Lockett in 1914, the activated sludge system has gained increasing importance in the treatment of municipal wastewaters. This is a consequence of its adaptability to variation in wastewater composition, high rates of removal of organic material and ability to remove nutrients nitrogen (N) and phosphorus (P) to low levels without chemical addition (Casey *et al*., 1995).

Its initial development as an aerobic process was a consequence of its greater economy and surety of effluent quality than the trickling filter, especially with regard to nitrification. Barnard introduced significant developments in the activated sludge system in 1973 and 1975. By incorporating anoxic and anaerobic zones he demonstrated that a high percentage of the influent N and P could be removed by biological mechanisms in the system without the aid of chemical addition (Wentzel *et al*., 1992). It was later demonstrated that through the imposition of specific environmental conditions and substrate supply, the growth of certain species could be promoted so as to fulfill some desired function. Examples are:

- with a sufficiently long aerobic sludge age, nitrifying organisms develop and produce an effluent low in ammonia
- with the appropriate sludge age, and a sequence of in-series reactors operating in anaerobic, anoxic and aerobic states, with inter-reactor recycles, different species of microorganisms develop that
    - Nitrifiy;
    - Denitrify; and
    - Store phosphorus in excess of their metabolic requirements (WRC, 1984; Casey *et al*., 1995)

By these means the eutrophic elements, N and P, are removed from the wastewater biologically.

2.2.1 Biological nutrient removal system configurations

A number of mainstream nutrient removal systems have evolved in South Africa over the years. For the purpose of this investigation three common wastewater treatment processes for nitrogen removal will be discussed. These include Wuhrmann process (Fig. 2.2), Modified Ludzack-Ettinger process (detailed in Chapter 3) and Bardenpho process (Fig. 2.3). However other systems such as the Phoredox process, 3-stage Phoredox process, UCT process, modified UCT process and Johannesburg process were designed to incorporate both P and N removal (Lilley *et al*., 1997). These systems, however, are beyond the scope of this study and will not be discussed further.

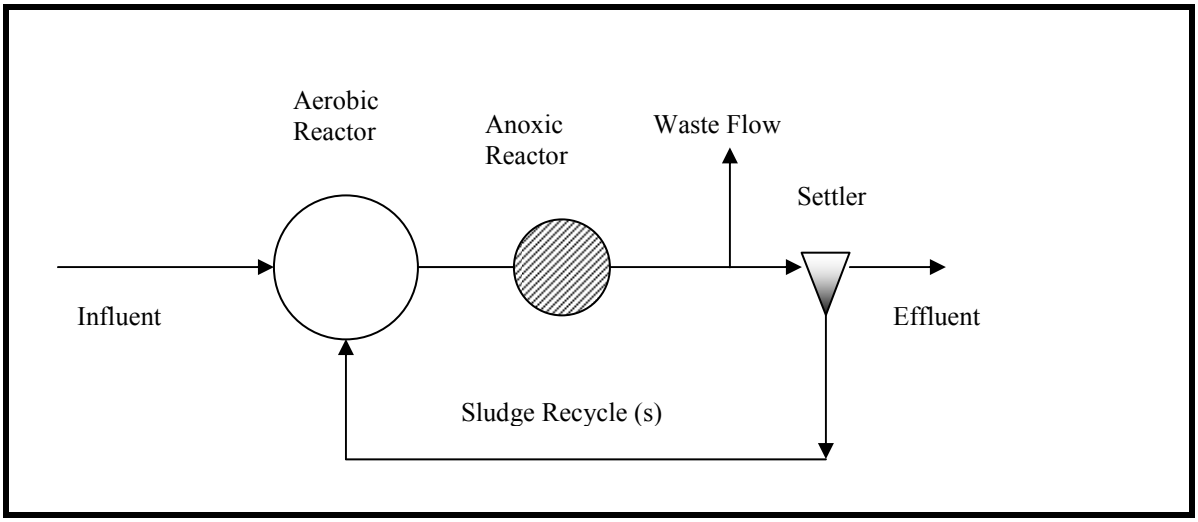

Fig. 2.2: The Wuhrmann process for nitrogen removal (Lilley *et al*., 1997).

The Wuhrmann process comprises an aerobic zone followed by an anoxic zone. The influent is discharged directly into the aerobic zone in which nitrification takes place. The flow is then discharged to the anoxic zone. The underflow from the clarifier (s-recycle) is returned to the aerobic zone. The substrate source for denitrification in the anoxic zone is obtained from death of organisms. However, the release rate of substrate is very low. This unfortunately leads to large anoxic zones and small aerobic zones. Theoretically, complete denitrification could be achieved. However, this is not practically possible

because the anoxic zone would have to be very large due to the slow denitrification rate which may lead to a loss of nitrification (WRC, 1984; Lilley *et al*., 1997).

The Bardenpho system (Fig. 2.3) was developed to overcome incomplete denitrification of the modified Ludzack-Ettinger (MLE) system. Barnard (1973) considered that low nitrate concentration discharged from the aeration zone could be denitrified in a secondary anoxic zone placed after the aerobic zone, to give a relatively nitrate-free effluent. Prior to discharge to the clarifier a flash aeration basin was introduced after the second anoxic zone to strip the nitrogen bubbles from the sludge. This assisted with sedimentation of the sludge. The flash aeration also served to nitrify any ammonia released within the anoxic zone.

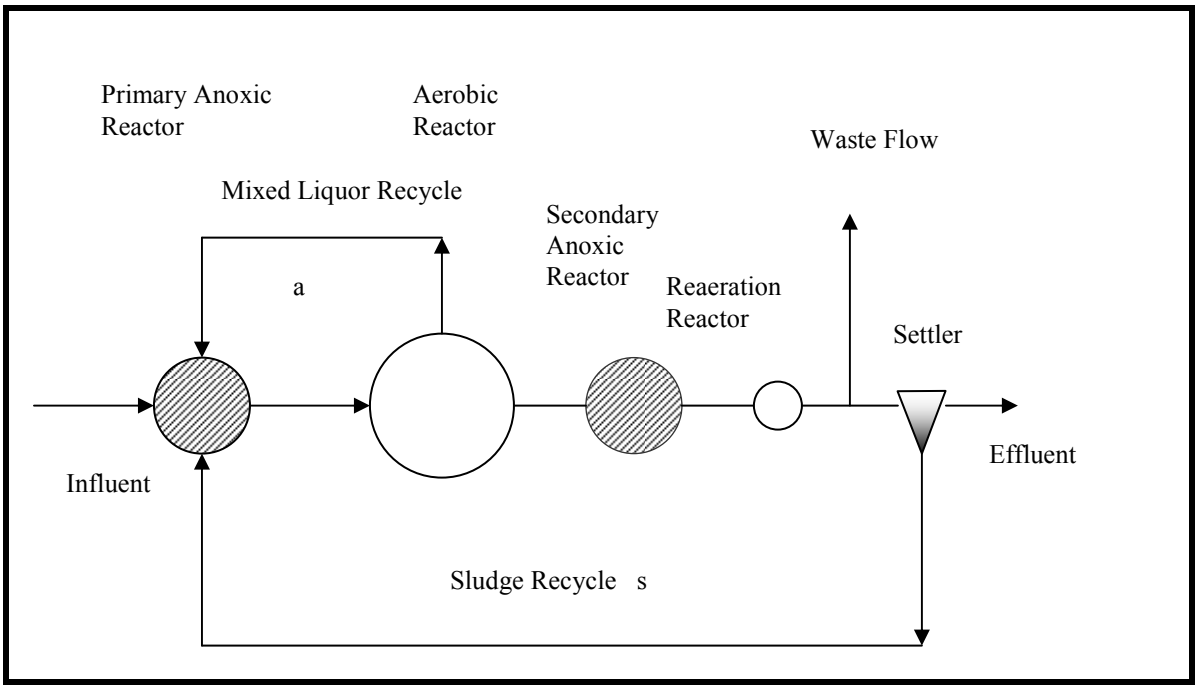

Fig. 2.3: The Bardenpho process for nitrogen removal (Lilley *et al*., 1997).

For a fixed underflow s-recycle ratio, the mixed liquor a-recycle governs the distribution of nitrate between the primary and secondary anoxic zones. The best denitrification performance will be obtained when a- and s-recycle values are chosen such that the primary anoxic zone is just loaded to its denitrification potential (maximum amount of

nitrate the reactor could remove) and the nitrate concentration in the flow leaving this zone will thus be zero (WRC, 1984; Lilley *et al*., 1997).

Table 2.2: Advantages and disadvantages of nitrogen removal processes (Lilley *et al*., 1997).

Process	**Advantages**	**Disadvantages**
Wuhrmann	Theoretically possible to remove all nitrate	Large anoxic mass fraction required which may inhibit nitrification Due to organisms die-off, ammonia and organic nitrogen are discharged with the effluent Low denitrification rate
Modified Ludzack-Ettinger	High rate of denitrification Simple configuration Higher N-removal than the Bardenpho system for $^{TKN}/_{COD}$ ratios > 0.1	Complete denitrification cannot be achieved Effluent nitrate concentration will be greater than 5mgN/L a-recycle limiting
Bardenpho	Theoretically possible to remove all the nitrate, but not possible in practice Higher N-removal than the MLE system for $^{TKN}/_{COD}$ ratios < 0.1	Complex configuration a-recycle limiting Mainly used for treating raw wastewaters where $^{TKN}/_{COD}$ ratios < 0.1.

The balance of nitrate generated in the aerobic zone (and not recycled to the primary anoxic zone) flows to the secondary anoxic zone. If this load of nitrate to the secondary anoxic zone is less than the denitrification potential of this zone then complete denitrification will be achieved. In practice the Bardenpho system for nitrogen removal is

appropriate if the calculated effluent nitrate concentration is greater than 7 mgN/L (which is usually the case for $^{TKN}/_{COD}$ ratios > 0.1 mgN/mg COD) then the MLE process is better suited for higher nitrogen removal efficiency (Table 2.2) (Lilley *et al*., 1997).

2.3 Microbial Community Analysis

The activated sludge treatment process uses undefined populations of bacteria to treat a variety of wastes. The conditions in a reactor are manipulated to promote the presence and activity of desirable organisms, such as ammonia oxidizers, and to discourage the growth of undesirable organisms such as the bacteria associated with foaming. The design and maintenance of such systems is, in effect, the engineering and the bacterial population and its activities (Curtis and Craine, 1998)

Unfortunately, it is difficult to engineer something that cannot be measured. Consequently, the explicit engineering of bacterial populations has been impeded by the crude, labour intensive and inadequate nature of the tools available to quantify and identify bacteria: suspended solids measurements (MLOSS), morphological examination and culture (Bitton, 1995).

However, progress has been made recently with the advent of 16S rRNA based technology, in particular: fluorescent *in situ* hybridization (FISH) (Amman *et al*., 1995), the polymerase chain reaction (PCR) and denaturing gradient gel electrophoresis (DGGE) (Muyzer *et al*., 1993). These techniques exploit differences between the ribosomal gene sequences of different organisms. In FISH, individual bacteria can be identified and enumerated using fluorescent probes targeted at specific signature sequences in ribosomal RNA. DGGE allows the comparison of rDNA sequences by separating them into discrete bands based on their sequence. The above molecular techniques are detailed in the following sections.

2.3.1 FISH…..early years

The earliest histochemistry techniques consisted of the use of different sorts of natural and synthetic dyes to stain cellular structures and sub-cellular accumulations. These compounds were generally non-specific because they had affinities for certain general categories of molecules, be they basic proteins, nucleic acids, lipids or carbohydrates. Even the more specific stains for cellular accumulations and macromolecular complexes such as hemosiderin, amyloid, elastin and reticular fibers were not generally applicable to investigation of all the biomolecules of interest. The ability to detect specific molecular identities was first demonstrated using antigen-antibody interactions. Early in the 1940s, antibodies were conjugated to fluorochromes without loss of their epitope-binding specificity (Jeffery *et al*., 2003). Decades later, the first antibody dependent fluorescent detection of nucleic acid hybrids was achieved (Rudkin and Stollar, 1977); however, this technology was soon replaced by the advent of fluorescent nucleic acid probes. The earliest *in situ* hybridizations, performed in the late 1960s, were not fluorescent at all, such as enzyme-based chromogenic reporters (Hougaard *et al.,* 1997) and gold-based probe systems used in electron microscopy (Puvion-Dutilleul and Puvion, 1996). FISH for visualization of nucleic acids developed as an alternative to older methods that used radiolabeled probes (Gall and Pardue, 1969). Early methods of isotopic detection employed non-specific labeling strategies, such as the random incorporation of radioactive modified bases into growing cells, followed by autoradiography. Several drawbacks of isotopic hybridization (Levsky and Singer, 2003) inspired the development of new techniques.

FISH with rRNA-targeted oligonucleotide probes is a cultivation-independent technique that allows phylogenetic identification of bacteria in mixed assemblages without prior cultivation (DeLong *et al.*, 1989; Amann *et al.*, 1990a; Amann *et al.*, 1990b; Amann *et al.*, 1996). The first application of fluorescent *in situ* detection was reported in 1980, when RNA that was directly labeled on the 3′ end with fluorophore was used as a probe for specific DNA sequences (Bauman *et al*., 1980). Enzymatic incorporation of fluorophore-modified bases throughout the length of the probe has been widely used for the preparation of fluorescent probes; one color is synthesized at a time (Wiegant *et al*.,

1991). The use of amino-allyl modified bases (Langer *et al*., 1981), which could later be conjugated to any sort of hapten or fluorophore, was critical for the development of *in situ* technologies because it allowed production of an array of low-noise probes by simple chemistry. Low probe specific activity prevented the assessment of nucleic acids with low copy number by FISH. Methods of indirect detection allowed signal output to be increased artificially by the use of secondary reporters that bind to the hybridization probes. In the early 1980s, assays featuring nick-translated, biotinylated probes, and secondary detection by fluorescent streptavidin conjugates were used for detection of DNA (Manuelidis *et al*., 1982) and mRNA (Singer and Ward, 1982) targets. Approximately a decade later, improved labeling of synthetic, single-stranded DNA probes allowed the chemical preparation of hybridization probes carrying enough fluorescent molecules to allow direct detection (Kislauskis *et al*., 1993).

Many variations with regards to the specifications, sensitivity and resolution have since been introduced such as polynucleotide DNA probes and oligonucleotide probes targeting mRNA (Trebesius *et al.*,1994; Wagner *et al.*, 1998; DeLong *et al.*, 1999).

2.3.2 Fluorescence *in situ* hybridization with rRNA-targeted oligonucleotide probes

Fluorescence *in situ* hybridization (FISH) with rRNA-targeted oligonucleotide probes is a cultivation-independent technique that allows the directly visualization of specific bacteria (or other microorganisms) in their habitats (DeLong *et al.*, 1989; Amann, 1995; Amann *et al.*,1995). The oligonucleotide probes are specific for single species, whole genera, or even phyla and domains according to the sequence conservation at their target sites on the rRNA (Amann *et al.*, 1995). FISH with rRNA-targeted probes can be combined effectively with comparative rRNA sequence analysis: A first overview of the bacterial community composition in an environmental sample is obtained by hybridization of the sample with existing probes that target different phylogenetic groups of bacteria. In parallel, rRNA gene libraries of the sample are established and screened

for sequences of new or otherwise interesting bacteria. Based on these rRNA sequences, new probes are developed which detect the corresponding organisms *in situ*. This "rRNA approach" (Amann *et al.*, 1995) proved to be highly useful for investigating microbial communities in numerous different, natural and artificial habitats. Up to seven different populations can be detected in the same experiment if several oligonucleotide probes, which have been labeled with different fluorochromes, are applied simultaneously (Amann *et al.*, 1996). Probes of nested specificity can be used to distinguish bacterial populations with a successively increasing resolution (Amann *et al.*, 1995).

The existing set of rRNA-targeted oligonucleotide probes has been extended continuously. Different probes of broad specificity cover for example the different subclasses of the *Proteobacteria* (Manz *et al.*, 1992), the *Cytophaga-Flavobacterium-Bacteroides* phylum (Manz *et al.*, 1996), gram-positive bacteria with high and low DNA G+C content (Roller *et al.*, 1994; Meier *et al.*, 1999), the planctomycetes (Neef *et al.*, 1998), most *Bacteria* (Amann *et al.*, 1990a), and the *Archaea* (Burggraf *et al.*, 1994). In addition, many probes have been designed that detect smaller groups, for example the ammonia-oxidizing bacteria in the beta subclass of *Proteobacteria* (Wagner *et al.*, 1995; Mobarry *et al.*, 1996; Pommering-Röser *et al.*, 1996; Juretschko *et al.*, 1998), diverse filamentous bacteria (Wagner *et al.*, 1994a), or different *Yersinia* species (Trebesius *et al.*, 1998).

The practical value of FISH is perhaps best demonstrated by the numerous studies on microbial consortia in wastewater treatment plants. FISH was applied to examine the high bacterial diversity in activated sludge without the constraints of cultivation-dependent methods (Wagner *et al.*, 1993; Manz *et al.*, 1994; Amann *et al*., 1996; Kämpfer *et al.*, 1996; Snaidr *et al.*, 1997). Specific probes were used to monitor defined groups of bacteria living in wastewater treatment plants, like nitrifiers (Wagner *et al.*, 1995; Mobarry *et al.*, 1996; Juretschko *et al.*, 1998) or floc-forming bacteria (Wagner *et al.*, 1994a; Rosselló-Mora *et al.*, 1995; Erhart *et al.*, 1997). The application spectrum of FISH can be amalgamated with, other techniques such as dot-blot hybridizations and

DGGE to elucidate microbial community structure and diversity. These extensions will be discussed in the following sections.

2.3.3 Methodological aspects of FISH

rRNAs are the main target molecules for FISH for several reasons: they can be found in all living organisms; they are relatively stable and occur in high copy numbers (usually several thousand per cell); and they include both variable and highly conserved sequence domains (Amann *et al*., 1995; 1990b). Signature sequences unique to a chosen group of microorganisms, ranging from whole phyla to individual species, can therefore be identified by comparative sequence analysis. Bacteria and archaea contain 5S, 16S, and 23S rRNAs with lengths of approximately 120, 1500 and 3000 nucleotides, respectively. In the vast majority of applications FISH probes target 16S rRNA. The public databases now include 16S rRNA sequences for most cultured microbial species, as well as numerous sequences directly retrieved from the environment (Maidak *et al*., 2000; Van de Peer *et al*., 2000). Probes are designed using sequence information from these databases and program packages such as ARB (Amann *et al*., 2000; 2001).

A typical FISH protocol includes four steps: the fixation and permeabilisation of the sample; hybridization; washing steps to remove unbound probe; and the detection of labelled cells by microscopy or flow cytometry (Amann, 1995). FISH is fully compatible with direct count methods (Glöckner *et al*., 1996; Maruyama and Sunamura, 2000).

The oligonucleotide probes used in FISH are generally between 15 and 30 nucleotides long and covalently linked at the 5′-end to a single fluorescent dye molecule. Common fluorophors include fluorescein, tetramethylrhodamine, Texas red and, increasingly, carbocyanine dyes like Cy3 or Cy5 (Southwick *et al.*, 1990). The carbocyanine dyes have greatly increased the sensitivity of FISH (Glöckner *et al*., 1996), but further improvements are still needed. The microorganisms living in oligotrophic environments, such as the open ocean, are typically small with low cellular rRNA content. The profound influence of cellular growth rate and nutritional status on cell detection by FISH has been

described (Amann *et al*., 1995). A recent study on this topic focused on *Rhodopseudomonas palustris* (Oda *et al*., 2000).

Polynucleotide probes consisting of nearly full-length 16S and/or 23S rRNA genes and each labelled with several fluorochrome molecules were shown to detect almost all cells present in marine bacterioplankton. However, probes of this size contain many conserved regions and are only able to discriminate between distantly related groups, such as the bacteria, crenarchaeota and euryarchaeota (DeLong *et al*., 1999). Shorter polynucleotide probes that target a defined variable region of approximately 250 nucleotides of the 23S rRNA have been shown to allow differentiation among genera (Trebesius *et al*., 1994). Oligonucleotide probes can be labelled at both the 5′- and 3′-end, and/or several probes applied simultaneously, thereby targeting each rRNA molecule with several fluorophores (Lee *et al*., 1993; Ouverney and Fuhrman, 2000).

There have also been attempts to improve FISH detection by boosting cellular ribosome content before fixation. Samples are preincubated in a cocktail of substrate and antibiotics, which should in theory result in cell activation and rRNA synthesis without cell division. In drinking water (Kalmbach *et al*., 2000), over 50% of all bacteria detected could be affiliated to the β-subclass of proteobacteria. Improved fluorescence signals were also reported for an oligotrophic cooling water system after pretreatment with glucose and chloramphenicol (MacDonald and Brozel, 2000). The problem with this approach is the inevitable selectivity of substrates and antibiotics.

2.3.4 Probe sensitivity and specificity

The current coverage of the *Bacteria* by group-specific probes is summarized in Table 2.3. In addition to the probes of broad specificity, which target whole phyla, numerous subphylum-, genus-, and species-specific probes are currently available for detailed analyses of microbial communities. This can be illustrated by the coverage of the nitrifying bacteria by oligonucleotide probes on different taxonomic levels. The nitrite-oxidizers of the genus *Nitrospira* can be distinguished from all other known bacteria by

the *Nitrospira*-phylum- and genus-specific probes (Fig. 2.4) (Daims *et al*., 2001a). All other known, aerobic, lithotrophic nitrifiers belong to different subclasses of the *Proteobacteria*. The α, β and γ-subclasses of this phylum are covered by subphylum specific probes (Fig. 2.4). Additional probes target particular groups within these subclasses, like the genus *Nitrobacter* in the alpha-subclass (Wagner *et al.*, 1996) or the ammonia oxidizers in the beta-subclass. Most members of the latter group are detected by the probes Nso190 and Nso1225 (Fig. 2.5). They can be further differentiated by means of subgroup- and species-specific probes. For example *Nitrosococcus mobilis* (which groups phylogenetically with the genus *Nitrosomonas*; (Teske *et al.*, 1994; Purkhold *et al.*, 2000) is targeted by the species-specific probe NmV and is detected also by probe NEU (specific for a sublineage of the genus *Nitrosomonas*) and probe Nsm156, which is specific for the genus *Nitrosomonas* (Fig. 2.5). Such probe binding patterns are used in microbial ecology like fingerprints to detect and quantify single bacterial species or higher taxa by *in situ* or membrane hybridization. This approach was also applied in different parts of this thesis, for example to quantify ammonia- and nitrite- oxidizing bacteria in batch tests (Chapter 4 and 5).

The abundance of bacteria stained by FISH with specific probes is usually expressed as a fraction of the total bacterial population in an environmental sample ("relative abundance"). For this purpose, the total bacterial population is quantified by counting the cells which have been labeled by a *Bacteria*-specific probe, mostly by probe EUB338 (Amann *et al.*, 1990a). Therefore, the quantification accuracy is strongly influenced by the coverage of the *Bacteria* by this probe. Previous studies demonstrated repeatedly that in environmental samples a significant fraction of the cells stained by the DNA-binding dye DAPI was not detected by EUB338 (Daims *et al*., 1999). The new probes EUB338-II and EUB338-III (Daims *et al*., 1999) cover two additional bacterial phyla (the *Planctomycetes* and the *Verrucomicrobia*) and a few members of other bacterial lineages, which are not targeted by the original probe EUB338.

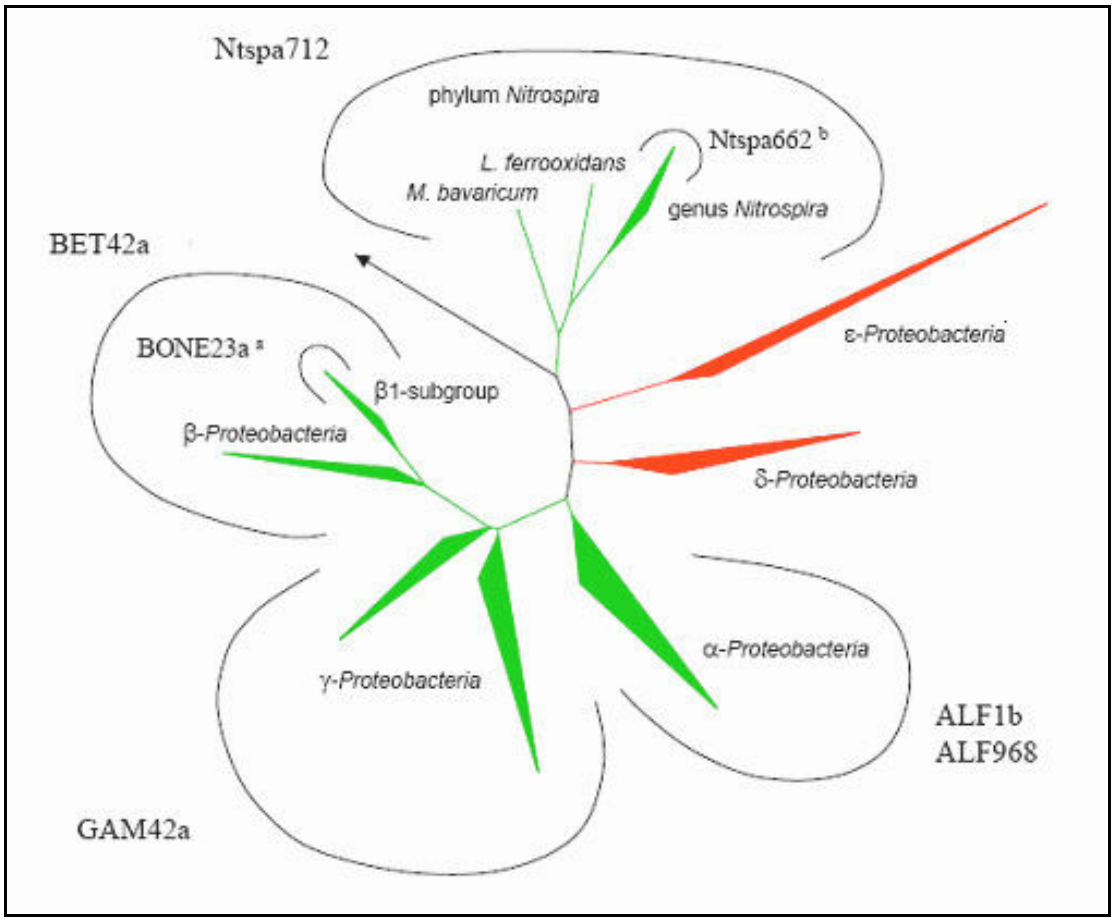

Fig 2.4: Diagrammatic representation of proteobacteria and the phylum *Nitrospira* showing the coverage of these phyla by group-specific, rRNA-targeted oligonucleotide probes. Additional probes were designed by Amann *et al.* (1996) [a] and Daims *et al.* (2001a) [b].

Table 2.3: Coverage of the main prokaryotic lines of descent by group-specific, rRNA- targeted oligonucleotide probes (Loy *et al*., 2003).

Probe	**Target site (rRNA position)**	**Target group and total coverage (%)**	**Reference**
ALF 1b	16S	α-*Proteobacteria*	Manz *et al*., 1992
ALF968	16S	84.7	Neef *et al*., 1998
BET42a	23S	β-*Proteobacteria* 92.6	Manz *et al*., 1992
GAM42a	23S	γ-*Proteobacteria* 90.8	Manz *et al*., 1992
CFB286	16S	*Cytophagales*	Wellar *et al*., 2000
CFB563	16S	90.5	Wellar *et al*., 2000
CFB719	16S		Wellar *et al*., 2000
CFB927	16S		Wellar *et al*., 2000
CFB1082	16S		Wellar *et al*., 2000
CF319	16S		Manz *et al*., 1996
Pla46	16S	*Planctomycetales*	Neef *et al*., 1998
Pla886	16S	95.1	Neef *et al*., 1998
EUB388-II	16S		Daims *et al*., 1999
EUB388-III	16S	*Verrucomicrobiales* 70	Daims *et al*., 1999
Ntspa712	16S	*Nitrospira* 85	Daims *et al*., 2001a
HGC	23S	High G+C gram positive bacteria 82.5	Roller *et al*., 1994
EUB388	16S	Domain *Bacteria*	Amann *et al*., 1990b
EUB388-II	16S	91.8	Daims *et al*., 1999
EUB388-III	16S		Daims *et al*., 1999

In total less than 2% of all 16S rRNA sequences in the current ARB database are complementary to EUB338-II and III at the probe target site (Daims *et al*., 1999) (Table 2.3).

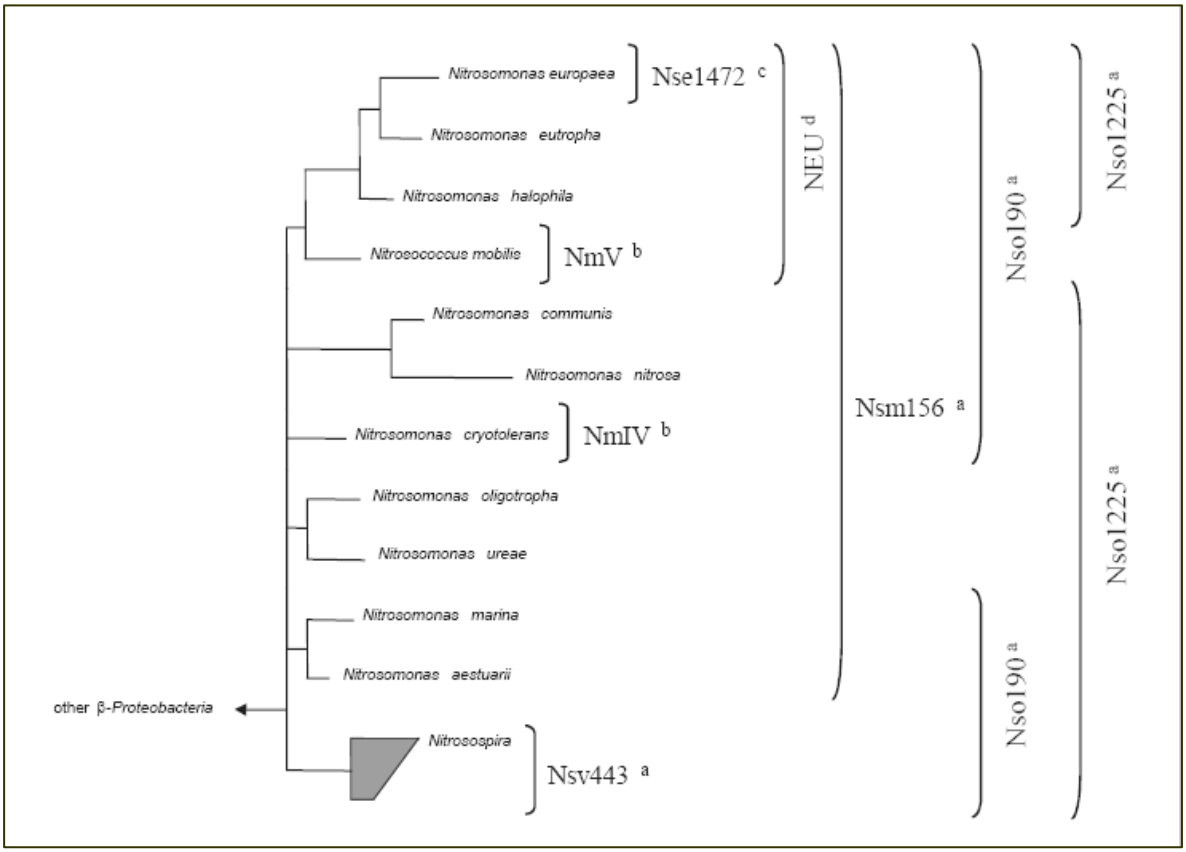

Fig 2.5: Coverage of the ammonia-oxidizers in the beta-subclass of *Proteobacteria* by rRNA-targeted oligonucleotides probes. The dendrogram contains only representative members of the phylogenetic clades proposed by Purkhold *et al*. (2000). The brackets indicate the coverage of the probes. Probe names are located on the right of the corresponding brackets. Probes were designed by Mobarry *et al*. (1996) [a], Pommering – Rőser *et al*. (1996) [b], Juretschko *et al*. (1998) [c] and Wagner *et al*. (1995) [d].

However, some of the organisms in the target groups of these probes were found to be abundant in various natural and engineered habitats and could thus be of major ecological importance. *Planctomycetes* were isolated from freshwater and marine samples (Hirsch and Müller, 1985; Schlesner, 1986) and were detected in activated sludge, biofilm and

terrestrial habitats by molecular methods (Liesack and Stackebrandt, 1992; Bond *et al.*, 1995; Snaidr *et al.*, 1997; Zarda *et al.*, 1997; Neef *et al.*, 1998; Schmid *et al.*, 2000). Verrucomicrobia were found not only in aquatic environments (Staley *et al.*, 1976; Schlesner, 1987; Hiorns *et al.*, 1997; Zwart *et al.*, 1998) but also in sediments and soils (Liesack and Stackebrandt, 1992; Janssen *et al.*, 1997; Wise *et al.*, 1997).

An uncultured bacterium belonging to the *Verrucomicrobia* was identified as a main metabolizer in a grassland soil (Felske and Akkermans, 1998). The importance of EUB338-II and III is also emphasized by the high abundance of different bacterial populations, which were detected by these probes but not by EUB338, in a biofilm sample (Daims *et al*., 1999). Moreover, almost all DAPI-stained cells in this biofilm could be assigned to the *Bacteria* by using a mixture of all three probes EUB338, EUB338-II and EUB338-III. Consequently, the new EUB338 variants should be used together with probe EUB338 in all quantification experiments to obtain more accurate results.

Nogueira *et al*. (2002) followed a top to bottom approach to characterize microbial population in biofilm reactors (Fig 2.6). Samples were first hybridized with EUB probe set (EUB388, EUB388-II and EUB388-III), then followed by subphylum specific probes (α-, β- and γ- *Proteobacteria*) and lastly characterization of ammonia and nitrite oxidizing bacteria using genus and species specific probes. This approach provided a high resolution analysis of microbial community structure in biofilm reactors. A similar approach was adopted in this thesis to characterize the microbial community in a lab-scale anoxic/aerobic activated sludge system (low resolution analysis) and modified batch test (high resolution analysis).

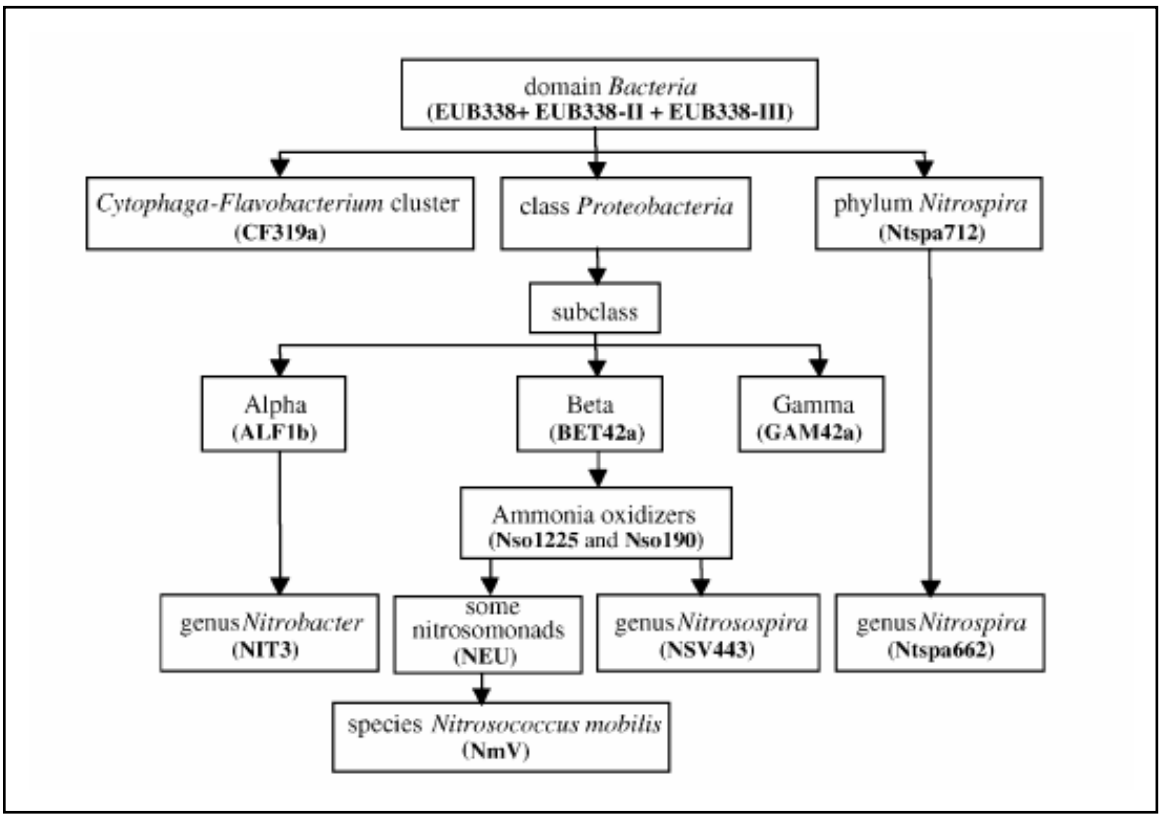

Fig 2.6: Specificity of rRNA-target oligonucleotide probes used for the *in situ* identification of nitrifiers and heterotrophic bacteria (Nogueira *et al*., 2002).

2.4 Genetic Fingerprinting Techniques

Genetic fingerprinting techniques provide a pattern or profile of the genetic diversity in a microbial community. One of the fingerprinting techniques that has been used in microbial ecology for more than a decade is the electrophoretic separation in high resolution polyacrylamide gels of low molecular weight rRNA molecules (5S rRNA and tRNA) extracted from natural samples (Hőfle, 1988). Another genetic fingerprinting technique, DGGE of PCR amplified ribosomal DNA fragments has been introduced into microbial ecology and has gained increased popularity amongst environmental microbiologist (Muyzer *et al*., 1993; Muyzer *et al*., 1995; Kowalchuk *et al*., 1997; Nicolaison and Ramsing, 2002; Dar *et al*., 2005).

2.4.1 Polymerase Chain Reaction (PCR)

The polymerase chain reaction (PCR) for gene amplification was first introduced by Saiki and colleagues in 1985. PCR quickly and efficiently produces many copies of specific DNA regions. Standard DNA cloning methods achieve similar results with viral or plasmid vectors, but with much greater effort. Thus, it is evident that PCR replaced or modified many applications of cloning technology. The main limitations of PCR are the size of the region that can be amplified, and the requirement for some knowledge of the sequences flanking the 'target' DNA (Giovannoni, 1991).

The PCR reaction mixture consists of template DNA, deoxynucleotide triphosphates (dNTPs), primers and DNA polymerase (*Taq polymerase*). PCR reactions can be broken down into three steps (Fig. 2.7), which are repeated in cycles:

- The melting of duplex sample DNA (94°C)
- The annealing of two primers to opposite DNA strands (eg. 53°C)
- The extension of primers by enzymatic nucleotide additions to produce a copy of the target gene (72°C)

The specificity of the PCR reaction is governed by the oligonucleotide primers which hybridize to opposite DNA strands at opposite ends of the DNA target, and direct the replication of the intervening region. Thus, the mechanism of PCR is simple primer-directed DNA synthesis, with the added dimensions that the process is repetitive, and the number of copies produced increases exponentially (Giovannoni, 1991).

In theory, with each replication cycle, the number of copies of the DNA target doubles. Copies of the target DNA are produced according to the equation:

$$N = N_o I^x$$

Where x is the number of cycles, N_o is the starting number of copies, and I is the efficiency of the reaction expressed as the number of complete target molecules produced per cycle from each template molecule. In theory, the maximum value for I is 2. An example will serve to illustrate the remarkable outcome of this process. Starting with a

single copy of 1-kilobase piece of DNA, after 36 complete cycles of synthesis, 10^{11} copies, or 100ng, of DNA would be produced (Giovannoni, 1991).

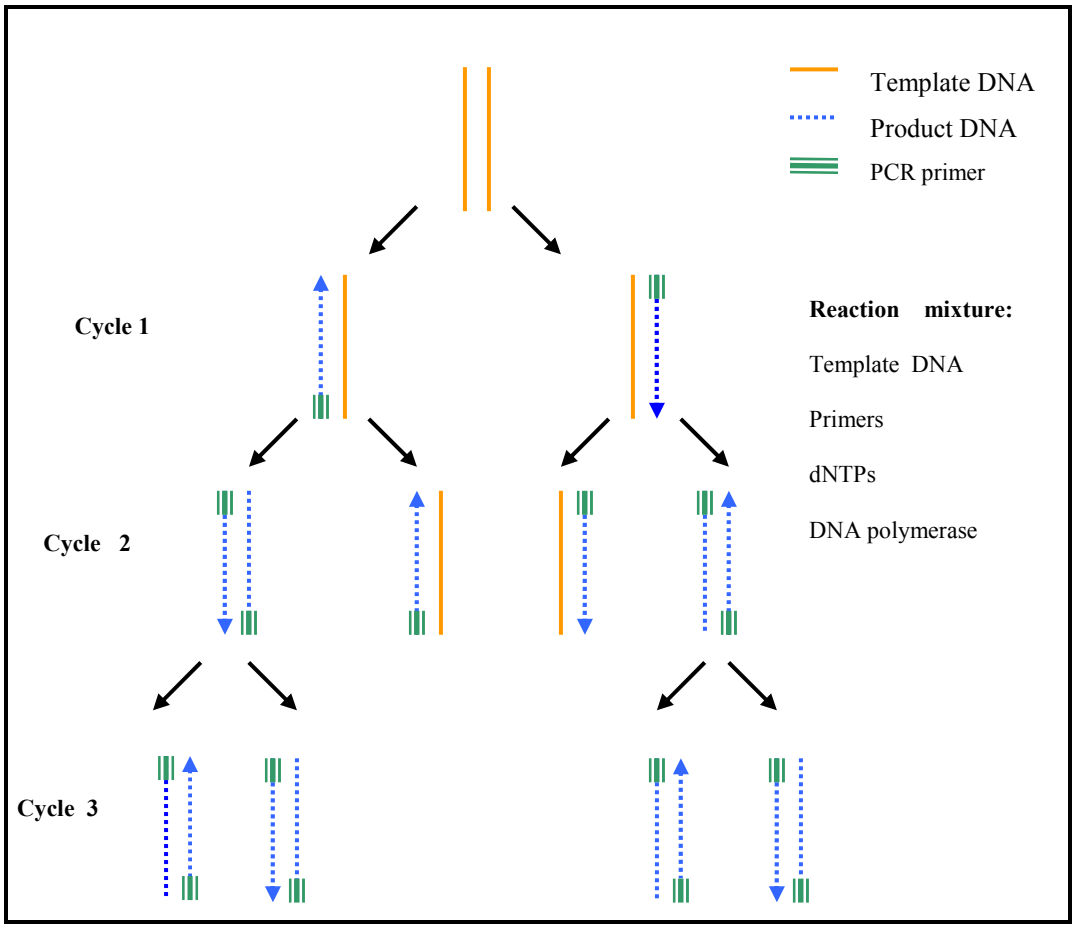

Fig. 2.7: A schematic outline of the polymerase chain reaction (Giovannoni, 1991)

2.4.2 *Thermus aquaticus* DNA Polymerase

The first PCR experiments used the Klenow fragment of *Escherichia coli* DNA polymerase 1 to catalyze the extension of the annealed primers (Saiki *et al*., 1985). The Klenow fragment is irreversibly denatured at 94°C. After each denaturing step fresh enzyme is added to the reaction. The process is tedious and prone to errors. The substitution of the thermostable DNA polymerase isolated from *Thermus aquaticus* (*Taq*

polymerase) (Chen *et al*., 1976) circumvented these problems (Saiki *et al*., 1988). In addition, the primer elongation step of the reaction could be run at higher temperatures, improving specificity. The result was a greatly simplified procedure that increased the yield, sensitivity, and the length of products that could be amplified.

Thermus aquaticus is a thermophilic eubacterium that can routinely be isolated from hotsprings and household water heaters (Giovannoni, 1991). Innis and colleagues (1988) studied the enzymology of the *T. aquaticus* DNA polymerase. *Taq* DNA polymerase exhibits an unusually high optimal processing activity, 8000 bases per minute at 75°C, and significant extension rates at much lower temperatures: 90 bases per a minute at 37°C and 15 bases per a minute at 22°C. Taq polymerase does not possess a 3' exonuclease activity, which may in part explain the high processing rate of the enzyme (Giovannoni, 1991).

2.4.3 Reduction of PCR bias caused by reannealing of templates

Multitemplate PCR has been frequently used in microbial ecology to determine the microbial community structure in environmental samples. However, it has been reported that the analysis of microbial communities based on multitemplate PCR can contain wrong information on the abundance and diversity of genes (Head *et al*., 1998; Kanagawa, 2003; Von Wintzingerode *et al.,* 1997). This problem is classified into two categories: bias and artifact (Kanagawa, 2003).

Artifact problems can be caused by the formation of a heteroduplex and a chimera. A heteroduplex is formed in PCR by cross-hybridization of heterologous sequences (Jensen and Straus, 1993; Qiu *et al*., 2001; Thompson *et al*., 2002) and can give data for nonexistent genes by further analysis using cloning and sequencing (Wu *et al*., 2001), denaturing gradient gel electrophoresis (Liu *et al*., 2002; Speksnijder *et al*., 2001; Yoshie *et al*., 2001) and terminal restriction fragment length polymorphism (T-RFLP) (Osborn *et al*., 2000). Intrastrand reannealing of the PCR product can also cause additional gene

diversity in T-RFLP analysis (Egert and Friedrich, 2003). A chimera is formed from an incompletely extended primer (Pääbo *et al*., 1990; Shuldiner *et al*., 1989) and template switching (Odelberg *et al*., 1995; Patel *et al*., 1996) during multitemplate PCR and gives artificial gene diversity.

Artifactual bands hamper interpretation and analysis of DGGE gels since they lead to an overestimation of sequence diversity. Moreover, the increased overlap of bands will make identification and retrieval of bands for sequencing more troublesome. Janse *et al*., (2004) isolated DNA from microorganisms from Lake Loosdrecht (Netherlands). PCR cycling was slightly adapted from Van Hannen *et al*. (1998) with an elongation temperature of 72ºC and a final extension step of 3 min at 72ºC. DGGE analysis, essentially performed as described in Muyzer *et al*. (1993), yielded profiles with artifactual double bands for all major sequences in the community profile. However, the intensity of artifactual bands was significantly decreased when the final elongation step at 72ºC was extended. An elongation step of 30 min appeared to be sufficient to effectively eliminate artifactual bands. The same result was obtained with DNA from Lake Hinge Sø (Denmark), which had a eukaryotic community profile strongly divergent from that of lake Loosdrecht (Janse *et al*., 2004). Modification of the PCR protocol by a simple extension of the final elongation step therefore seems a generally applicable remedy to prevent the formation of artifactual double bands.

Bias can be caused in multitemplate PCR by differences in primer binding energy (Polz and Cavanaugh, 1998; Ishii and Fuku, 2001; Lueders and Friedrich, 2003) and reannealing of templates (Mathieu-Daude *et al*., 1996; Suzuki and Giovannoni, 1996). Reannealing of templates has been reported to cause a strong bias toward 1:1 mixtures of genes in final PCR products, regardless of the initial ratio of the templates. The mechanism of this bias has been explained as the amplification rate of more abundant PCR products declining faster with the reannealing of PCR products than that of less abundant products in the same tube; hence, the final product concentrations are biased toward a 1:1 ratio independent of the initial template concentrations (Mathieu-Daude *et al*., 1996; Suzuki and Giovannoni, 1996). It has been reported that the PCR with low

amplification efficiencies and low PCR product yields did not show bias (Suzuki and Giovannoni, 1996). Kurata *et al*., (2004) produced the same result even with high PCR product yields they did not observe the bias in some cases.

Kurata *et al*. (2004) reevaluated the 1:1 bias by using a real-time quantitative PCR method to monitor amplification efficiencies and the amount of PCR product. They found that the reannealing of products at the annealing step does not cause the bias, but the preferential homoduplex formation by reannealing of the products during the decrease in temperature from the denaturation to the annealing step does cause the bias.

2.4.3.1 Real-time monitoring of PCR products

PCR bias and artifacts which occur randomly can be avoided by mixing the replicate PCR amplifications. Reproducible events are considered to occur in the late stages of PCR, and can be avoided by stopping the PCR earlier (Kanagwa, 2003). However a stoppage too early will result in not enough PCR product for subsequent analyses. One needs to know when to stop the PCR to obtain enough product while avoiding PCR bias and artifacts. For this purpose, real-time monitoring of the PCR products would be useful. There are three methods for monitoring the PCR product in real time (Mackay *et al*., 2002); (i) double stranded DNA-specific dyes (Higuchi *et al*., 1993), (ii) sequence-specific fluorescent probes (Hollard *et al*., 1991; Cardullo *et al*., 1988), and (iii) sequence-specific fluorescent primers (Kurata *et al*., 2001).

Double-stranded DNA-specific dyes

The DNA-binding fluorogenic molecules, SYBR® Green I and YO-PRO-1, are often used for monitoring the amount of PCR product. These molecules emit fluorescence when associated with double-stranded DNA, and so the fluorescence intensity indicates the amount of PCR product. When used in PCR, the fluorescent intensity increases as the amount of PCR product increases, and reaches a maximum value (Higuchi *et al*., 1993). The maximum fluorescent intensity is obtained when all the fluorogenic molecules in the

reaction mixture are associated with the PCR product, or when there is no further increase in PCR product. Therefore, careful consideration of the data is needed to decide when to stop the PCR (Kanagwa, 2003).

Sequence-specific fluorescent probes

TaqMan® probes (Hollard *et al*., 1991) and HybProbes (Cardullo *et al*., 1988) are very commonly used for real time monitoring of PCR products (Kanagwa, 2003). TaqMan® probes (Hollard *et al*., 1991) hybridize to the targeted PCR products, and are degraded by *Taq* polymerase with its exonuclease activity at the extension step. By this degradation, the fluorophores on the probes are let free and emit fluorescence. HybProbes (Cardullo *et al*., 1988) consist of two probes, and emit fluorescence when both hybridize to the targeted PCR products. To monitor multitemplate PCR products, a common sequence needs to be identified in the products in order to design the probes. However in many cases, the design is difficult because of differences in the sequence among targets even in conserved regions. When there are suitable sequences in the products, probes can be designed for real-time monitoring. With these methods, no increase in fluorescence intensity may indicate the total consumption of the probes, and careful consideration is needed to decide when the PCR should be stopped.

Sequence-specific fluorescent primers

Real-time monitoring with a fluorescent primer has recently been developed (Kurata *et al.,* 2001). When a primer containing a BODIPY® FL-modified cytosine at its 5′ end is used for PCR, its fluorescence is quenched by the quinine in the target, complementary to the modified cytosine. The quenched rate is proportional to the amount of PCR product. With this method, the quench rate shows the rate of consumption of the modified primer, therefore this method is suitable for monitoring the late stages of PCR. In PCR with this primer, a slight but significant decrease in the fluorescent intensity means that the PCR is approaching the end. The fluorescence of some other dyes, 5-FAM and TAMRA, is also quenched by their interaction with quinine (Torimura *et al.,* 2001) and these dyes also can

be used for this method.

2.4.4 Theoretical and practical aspects of DGGE

In DGGE (Fischer and Lerman, 1979, 1983; Myers *et al*., 1987) DNA fragments of the same length but with different sequences can be separated. Separation is based on the decreased electrophoretic mobility of a partially melted double-stranded DNA molecule in polyacrylamide gels containing a linear gradient of DNA denaturants (a mixture of urea and formamide). The melting of DNA fragments proceeds in discrete so-called *melting domains:* stretches of base pairs with an identical melting temperature. Once a domain with the lowest melting temperature reaches its melting temperature (*Tm*) at a particular position in the denaturing or temperature gradient gel, a transition of a helical to a partially melted molecule occurs, and migration of the molecule will practically halt. Sequence variation within such domains causes the melting temperatures to differ, and molecules with different sequences will stop migrating at different positions in the gel. By using DGGE, 50% of the sequence variants can be detected in DNA fragments up to 500 bp (Myers *et al*., 1985). This percentage can be increased to nearly 100% by the attachment of a GC-rich sequence, a so-called GC-clamp, to one side of the DNA fragment (Myers *et al*., 1985; Sheffield *et al*., 1989). A sequence of guanines (G) and cytosines (C) is added to the 5'-end of one of the PCR primers, co-amplified and thus introduced into the amplified DNA fragments (Sheffield *et al*., 1989; Sheffield *et al*., 1992). The GC-rich sequence acts as a high melting domain preventing the two DNA strands from complete dissociation into single strands. The length of the GC-clamp can vary between 30 and 50 nucleotides (Muyzer *et al*., 1997). As an alternative to GC-clamps, chemical clamps have been used (Muyzer and Smalla, 1998). One of the PCR primers is labelled at its 5'-end with a photoactivatable compound, such as psoralene, which intercalates between the base plates of both DNA strands and will covalently link them together after UV irradiation. The use of a so-called *ChemiClamp* has the advantage that both primers have a similar length, but also has disadvantages. Firstly, DGGE bands with this clamp cannot be reamplified directly, because of the covalent bond, and

secondly, irradiation of the PCR products with UV might damage the amplified DNA causing multiple bands or even a smear in the DGGE analysis (Cariello *et al*., 1988).

DNA bands in DGGE profiles can be visualised using ethidium bromide. Recently, SYBR Green I was introduced as an alternative to ethidium bromide (Muyzer *et al*., 1997). The advantage of SYBR Green I is the lack of background staining, Which makes it possible to observe less dominant DNA fragments. A more sensitive detection method is silver staining (Felske *et al*., 1996). However, silver staining also stains single stranded DNA, and silver stained gels cannot be used for subsequent hybridization analysis (Heuer and Smalla, 1997).

Prior to DGGE analysis of DNA fragments it is necessary to determine the melting behaviour of the DNA fragments. Furthermore, to obtain the best separation of different DNA fragments, it is necessary to optimize the gradient and the duration of electrophoresis (Muyzer and Smaller, 1998).

2.4.5 Application of DGGE in microbial ecology

DGGE of PCR amplified 16S rDNA fragments were first used to profile community complexity of a microbial mat and bacterial biofilms (Muyzer *et al*., 1993). For this purpose bacterial genomic DNA was extracted from natural samples, and segments of the 16S rRNA genes were amplified in the polymerase chain reaction (Saiki *et al*., 1988). This resulted in a mixture of PCR products obtained from the different bacteria present in the sample. The individual PCR products were subsequently separated by DGGE. The result was a pattern of bands, for which the number of bands corresponded to the number of predominant members in the microbial communities. To obtain more detailed information about some of the community members, DGGE profiles were blotted onto nylon membranes and hybridised with a radioactively-labelled oligonucleotide probe specific for sulfate-reducing bacteria (Amann *et al*., 1992). In a subsequent study, Muyzer and de Waal (1994) were able to identify community members by sequencing of DNA eluted from excised DGGE bands (Fig. 2.8). Additional information about

particular bacterial populations within the community can be obtained by hybridization analysis with taxon specific probes. Furthermore, individual bands can be excised from the gels and sequenced to identify the community members (Fig 2.8). These techniques are also used to monitor the success of isolation of bacteria in pure cultures, and to screen clone libraries for redundancy.

Ferris *et al.* (1997) used PCR-DGGE to study the re-establishment of a microbial mat after removal of the entire cyanobacterial layer. The results showed that previously undetected cyanobacteria colonized the remaining part of the mat, and that other cyanobacteria which were present before the disturbance remained undetected for up to 40 days. In a subsequent study, DGGE was used to evaluate seasonal distributions of bacterial populations along a thermal gradient in a hot spring microbial mat (Ferris and Ward, 1997). Similar DGGE patterns were found for samples collected at the same site and for sites with the same temperature, regardless of the season. However, different profiles were seen for samples from sites with different temperatures.

Nicolaison and Ramsing (2002) developed and employed DGGE of PCR amplicons of ammonia monooxgenase gene (*amoA*) to investigate the diversity of ammonia-oxidizing bacteria in four habitats. The results were compared to DGGE of PCR-amplified partial 16S rDNA sequences made with primers specific for ammonia-oxidizing bacteria. The *Nitrosomonas*-like sequences were found within a denaturant range from 30% to 46%, whereas the *Nitrosospira*-like sequences migrated to 50% to 60% denaturant. The majority of retrieved sequences from all four habitats with high ammonia loads were *Nitrosomonas*-like and only few *Nitrosospira*-like sequences were detected.

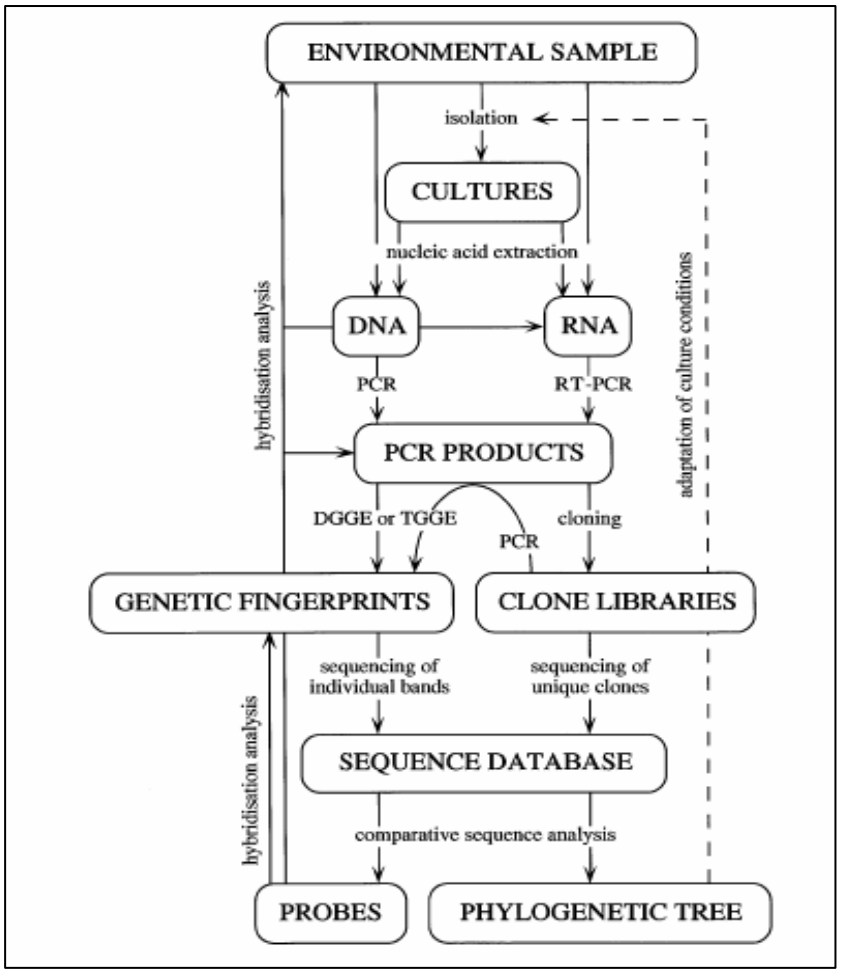

Fig. 2.8: Flow diagram of the different steps in the study of the structure and function of microbial communities (Muyzer and de Waal, 1994).

Dar *et al.* (2005) describes a three-step nested–PCR–DGGE strategy to detect sulfate-reducing bacteria (SRB) in complex microbial communities from industrial bioreactors. The largest number of bands was observed in DGGE patterns of products obtained with primers specific for the *Desulfovibrio-Desulfomicrobium* group, indicating a large diversity of these SRBs. In addition, members of other phylogenetic SRB groups, i.e., *Desulfotomaculum*, *Desulfobulbus*, and *Desulfococcus-Desulfonema-Desulfosarcina*, were detected. Bands corresponding to *Desulfobacterium* and *Desulfobacter* were not detected in the bioreactor samples.

2.4.6 Limitations of DGGE

One of the limitations of DGGE is the separation of only relatively small fragments, up to 500 base-pairs (Myers *et al*., 1985). This limits the amount of sequence information for phylogenetic inferences as well as for probe design. It has been demonstrated that it is not always possible to separate DNA fragments which have a certain amount of sequence variation. Vallaeys *et al*. (1997) found that 16S rDNA fragments obtained from different methane-oxidizing bacteria could not be resolved by DGGE although they had substantial sequence variation. A similar result was described by Buchholz-Cleven *et al*. (1997) who demonstrated that it was not possible to separate rDNA fragments differing in two to three nucleotides under the electrophoretic conditions they used. In contrast to these failures of separation, Nübel *et al*. (1996) could separate DNA fragments from different *rrN* operons, some of which were only differing in one base-pair. Furthermore, Kowalchuk *et al*. (1997) nicely demonstrated that double bands in the DGGE patterns were a result of the presence of a so-called *wobble base* (either a C or a T) in the reverse primer. When a mixture of the reverse primers was used, two bands were visible in the DGGE pattern, while when the two primers were used in separate PCR reactions only one band per reaction was found.

The use of different regions of the 16S rRNA and different DGGE conditions might result in different resolutions of separation. As the melting behaviour and the mobility in denaturing gradient gels of rDNA fragments for which sequences are known can be predicted by using computer algorithms (Lerman and Silverstein, 1987), it might be helpful to perform a comparative analysis of the different 16S rRNA sequences present in the databases to find those regions for which an optimal separation in DGGE can be expected. Similar computer simulations have been performed to identify the optimal combination of different tetrameric restriction enzymes for RFLP screening of SSU rDNA clone libraries (Moyer *et al*., 1996), or to analyse the hybridization potential between primers and probes and SSU rRNA sequences (Brunk *et al*., 1996).

Related to the problem of resolution might be the maximum number of different DNA fragments which can be separated by DGGE. For instance, by using DNA-DNA reannealing experiments Torsvik *et al*. (1990a, b) found that there might be as many as 104 different genomes present in soil samples. It is obvious that DGGE cannot separate all of the 16S rDNA fragments obtained from such a variety of microorganisms. In general, these electrophoretic techniques will only display the rDNA fragments obtained from the predominant species present in the community. Several different studies revealed that bacterial populations that make up 1% or more of the total community can be detected by PCR-DGGE (Muyzer *et al*., 1993; Murray *et al*., 1996). A similar value has been found by Lee *et al*. (1996) using PCR-SSCP to characterize bacterial community structures.

Furthermore, comigration of DNA fragments can be a problem for retrieving clean sequences from individual bands. Another problem in the study of community diversity on the basis of 16S rRNA genes, using DGGE or cloning strategies is the presence in some bacteria of multiple *rrN* operons with sequence microheterogeneity. DGGE can visualize this sequence heterogeneity (Nübel *et al*., 1996) which might lead to an overestimation of the number of bacteria within natural communities. The same is true for the double bands in the DGGE patterns which were produced by the use of degenerate primers in the PCR reactions (Kowalchuk *et al*., 1997).

2.5 The Importance of Nitrogen Elimination for Wastewater Treatment

The transformations of nitrogen compounds carried out by microorganisms are key steps of the biogeochemical nitrogen cycle. Reduced nitrogen is released as ammonia primarily during the decomposition of organic substance (ammonification). A part of this released ammonia is directly assimilated and incorporated into biomass, while the remaining ammonia is oxidized to nitrate by aerobic, ammonia-oxidizing and nitrite-oxidizing bacteria. Thereupon, the nitrate is either assimilated or it is used by facultatively anaerobic bacteria as alternative electron acceptor in the absence of oxygen

(denitrification). The end products of denitrification are gaseous dinitrogen and smaller amounts of nitric (NO) and nitrous (N_2O) oxide. Nitrogen-fixing bacteria close the cycle by reducing dinitrogen to ammonia (Bock *et al.*, 1992).

These natural processes are influenced strongly by human activities. Nitrogen compounds like ammonia and nitrate are main components of fertilizers and wastewater. Their release in the environment has to be minimized, because ammonia and nitrite are highly toxic to aquatic life (ammonia already at a concentration of 0.01 mg/l) (Arthur *et al.*, 1987). Nitrite and nitrate can also be harmful to humans (Schneider and Selenka, 1974). Nitrogen compounds in sewage water contribute to the eutrophication of natural waters, a process which causes incalculable ecological damage. The efficient elimination of nitrogen is therefore one of the most important processes in modern wastewater treatment. It takes place during a two-phase process in biological wastewater treatment plants (Henze *et al.*, 1997).

In the first stage (nitrification), ammonia is transformed to nitrate by ammonia- and nitrite oxidizing bacteria under aerobic conditions. The nitrate is reduced to gaseous N_2, nitric and nitrous oxide in the following, anaerobic denitrification stage. The next sections deal with the first of these two phases, nitrification, and with the microorganisms involved in this process.

2.5.1 Chemolitho – Autotrophic Oxidation of Ammonia and Nitrite

Chemolithotrophic nitrification is a two-step process, consisting of the conversion of ammonia to nitrite, which is in turn converted to nitrate. These steps are carried out by two different groups of organisms, the ammonia-oxidizing bacteria and the nitrite-oxidizing bacteria (AOB and NOB), respectively. There are no known autotrophic bacteria that can catalyze the production of nitrate from ammonia in one step. This study focuses on the application of molecular tools and engineering technology to quantify these organisms, which all have in common the ability to utilize ammonia as a sole source of energy and carbon dioxide as the chief source of carbon (Hooper *et al.,* 1997). AOB are chemolitho-autotrophs and are obligate aerobes, although some species may be

highly tolerant of low oxygen or anoxic environments (Bodelier *et al*., 1996). Further to their physiological uniformity, Head *et al.* (1993) used 16S rRNA gene sequence data to indicate that all known aerobic AOB isolates were restricted to two evolutionarily distinct lineages of the class *Proteobacteria*. Furthermore, it was demonstrated that all strains isolated from terrestrial and freshwater environments belonged to a single (monophyletic) evolutionary group within the β-subclass of the class *Proteobacteria*, providing evidence of their descent from a single chemolithoautotrophic ammonia-oxidizing ancestor.

Four genera belonging to this lineage have been described so far: *Nitrosomonas* (with *Nitrosococcus mobilis*), *Nitrosospira*, *Nitrosolobus*, and *Nitrosovibrio* (Woese *et al.*, 1984; Head *et al.*, 1993; Teske *et al.*, 1994; Utåker *et al.*, 1995; Pommering-Röser *et al.*, 1996). Reclassification of the latter three genera in the single genus *Nitrosospira* has been suggested (Head *et al.*, 1993), but has been discussed controversially due to ultrastructural features (Teske *et al.*, 1994). The only known aerobic ammonia oxidizing bacteria, which are not members of the beta-subclass of *Proteobacteria*, are *Nitrosococcus oceani* (Watson, 1965; Trüper and de Clari, 1997) and *N. halophilus* (Koops *et al.*, 1990). These two species group with the gamma-subclass of *Proteobacteria* (Woese *et al.*,1985; Head *et al.*, 1993; Teske *et al.*, 1994).

The chemolithotrophic oxidation of ammonia to nitrite is catalyzed by two enzymes: the membrane-bound ammonia monooxygenase (McTavish *et al.*, 1993; Hooper *et al.*, 1997), which oxidizes ammonia to hydroxylamine (Eq. 2.1), and the periplasmatic hydroxylamine oxidoreductase (Bergmann *et al.*, 1994; Sayavedra-Soto *et al.*, 1994), which oxidizes hydroxylamine to nitrite (Eq. 2.2). Only the oxidation of hydroxylamine is exergonic and is therefore regarded as the actual energy source in lithotrophic ammonia oxidation (Bock *et al.*, 1992).

Ammonia monooxygenase: $NH_3 + O_2 + 2H^+ + 2e^- \rightarrow NH_2OH + H_2O$ (2.1)

Hydroxylamine oxidoreductase: $NH_2OH + H_2O \rightarrow HNO_2 + 4H^+ + 4e^-$ (2.2)

The conversion of ammonia to nitrite yields little energy due to the high standard redox potentials of the two redox couples NH_2OH/NH_3 (+899 mV) and NO_2^-/NH_2OH (+66 mV). Consequently, ammonia-oxidizers are slow-growing bacteria. They depend also on reverse electron flow to regenerate reduction equivalents (reduced pyridine nucleotides; Bock *et al.*, 1992). It has to be mentioned, however, that the metabolism of ammonia-oxidizing bacteria is surprisingly versatile. Anoxic reduction of nitrite (denitrification) by *Nitrosomonas europaea* with pyruvate as electron donor has been observed (Abeliovich and Vonhak, 1992), and *N. eutropha* can reduce nitrite with hydrogen as electron donor at low oxygen pressure (Bock *et al.*, 1995). While ammonia-oxidizers are widely distributed in soils, freshwater, brackish and marine environments, the requirements of individual species for ammonia concentration, oxygen pressure, pH and temperature differ (Koops and Möller, 1992).

Nitrite-oxidizing bacteria perform the second step of nitrification, the oxidation of nitrite to nitrate. This physiological group is phylogenetically more heterogenous than the ammonia-oxidizers as all four described genera of nitrite-oxidizers belong to different lines of descent. The genera *Nitrobacter*, *Nitrococcus* and *Nitrospina* are group within different subclasses of the phylum *Proteobacteria*. The genus *Nitrobacter* (Winogradsky, 1892) with the four described species *N. winogradskyi* (Watson and Waterbury, 1971), *N. hamburgensis* (Bock *et al.*, 1983), *N. vulgaris* (Bock *et al.*, 1990), and *N. alkalicus* (Sorokin *et al.*, 1998) belongs to the alpha-subclass of *Proteobacteria* (Stackebrandt *et al.*, 1988). The genera *Nitrococcus* and *Nitrospina* (Watson and Waterbury, 1971) contain to date only one species, respectively: *Nitrococcus mobilis* which is a member of the gamma-subclass of *Proteobacteria*, while *Nitrospina gracilis* groups with the delta-subclass of *Proteobacteria* (Teske *et al.*, 1994). The nitrite-oxidizers of the genus *Nitrospira* form a distinct phylum in the domain *Bacteria* together with the genera *Leptospirillum*, *Thermodesulfovibrio* and "*Magnetobacterium bavaricum*" (Ehrich *et al.*, 1995). Two species, which were found in completely different habitats, have been assigned to this genus so far: *N. marina* was isolated from ocean water (Watson *et al.*, 1986), whereas *N. moscoviensis* was obtained from a heating system in Moscow (Ehrich *et al.*, 1995). Except for *Nitrospira*, only *Nitrobacter* species occur in various habitats

like soils, building stones, freshwater, brackish water, and even in acid sulfidic ores (Bock and Koops, 1992). In contrast, *Nitrospina* and *Nitrococcus* appear to be obligately halophilic and hence exclusively marine (Watson and Waterbury, 1971).

The integral membrane enzyme nitrite oxidoreductase catalyzes the chemolithotrophic oxidation of nitrite to nitrate in *Nitrobacter* cells (Tanaka *et al.*, 1983; Sundermeyer-Klinger *et al.*, 1984). This reaction is reversible and the oxygen, which is incorporated into nitrate, stems from water (Eq. 2.3):

Nitrite oxidoreductase: $NO_2^- + H_2O \leftrightarrow NO_3^- + 2H^+ + 2e^-$ (2.3)

The nitrite oxidoreductase of *Nitrobacter* has been studied extensively. The holoenzyme consists of three subunits in *N. hamburgensis* (Sundermeyer-Klinger *et al.*, 1984), but only of two subunits in *N. winogradskyi* and *N. vulgaris* (Bock *et al.*, 1990). Nitrite oxidoreductase contains molybdenum, iron-sulfur clusters, and manganese (Ingledew and Halling, 1976; Sundermeyer-Klinger *et al.*, 1984; Bock *et al.*, 1992). Much less is known about the composition of the nitrite-oxidizing systems of the other nitrite-oxidizers. Biochemical data indicate substantial differences between the nitrite oxidoreductase of *Nitrobacter* and the nitrite-oxidizing systems of *Nitrospira marina* and *N. moscoviensis* (Watson *et al.*, 1986; Ehrich *et al.*, 1995). While *Nitrococcus* and *Nitrospina* seem to be obligate chemolithotrophs (Watson and Waterbury, 1971), *Nitrobacter* and *Nitrospira* possess alternative metabolic pathways. Organotrophic growth in absence of nitrite, for example with acetate or pyruvate, was reported for *Nitrobacter* (Bock, 1976). *Nitrospira marina* cultures reached higher cell densities in media containing nitrite and pyruvate than in pure nitrite medium, indicating that this species can grow mixotrophically (Watson *et al.*, 1986). *N. moscoviensis* is able to reduce nitrate with hydrogen as electron donor under anoxic conditions (Ehrich *et al.*, 1995). *Nitrobacter* can also grow by denitrification in anoxic environments (Freitag *et al.*, 1987; Bock *et al.*, 1988) and possesses a dissimilatoric nitrite reductase, which reduces nitrite to nitric oxide (NO) (Ahlers *et al.*, 1990). This reaction might be a link between dissimilatory and assimilatory pathways, because nitric oxide can serve as electron donor for the reduction of NAD+

(Freitag and Bock, 1990). With respect to energy metabolism, the nitrite-oxidizers are confronted with similar problems as the ammonia-oxidizers. The standard redox potential of the NO_3^-/NO_2^- couple is extremely high (+420 mV). Consequently, the growth rates of nitrite-oxidizing bacteria are very low.

Chemolithotrophic, anaerobic oxidation of ammonia to N_2 is carried out by physiologically specialized planctomycetes (ANAMMOX organisms) (Strous *et al.*, 1999; Schmid *et al.*, 2000). Although this process may in future be exploited in wastewater treatment, at present no large-scale reactors exist that were designed specifically for anaerobic ammonia oxidation.

2.5.2 The key nitrite-oxidizers in wastewater treatment plants

According to a traditional concept, *Nitrosomonas* and *Nitrobacter* are responsible for nitrification in wastewater treatment plants (Henze *et al.*, 1997). This opinion is based on the experience that *Nitrosomonas* and *Nitrobacter* species can be isolated from practically any activated sludge. In contrast, *Nitrobacter* was not detected in aquarium biofilters by quantitative dot blot (Pillay *et al*., 1989a; 1989b; Hovanec and DeLong, 1996) or in activated sludge by FISH (Wagner *et al.*, 1996) with rRNA-targeted probes. These findings indicated that other nitrite-oxidizers could be more important for the nitrification process in wastewater treatment. This hypothesis was corroborated when *Nitrospira*-related bacteria were detected in a nitrite-oxidizing, laboratory-scale reactor by rRNA sequence analysis (Burrell *et al.*, 1998). Ribosomal RNA sequences affiliated to *Nitrospira* were also retrieved from freshwater aquaria (Hovanec *et al.*, 1998). Quantitative dot blot hybridization of total rRNA with *Nitrospira*-specific probes was performed in the same study. These experiments confirmed the high abundance of *Nitrospira*-like bacteria in the aquarium samples. Finally, FISH of activated sludge with *Nitrospira*-specific probes demonstrated for the first time that *Nitrospira*-like bacteria were a dominant population in a full-scale wastewater treatment plant (Juretschko *et al.*, 1998). Although *Nitrobacter* was not detectable in this sludge by FISH, a *Nitrobacter*

strain could be isolated from the same sample. Attempts to isolate the *Nitrospira* like bacteria were not successful (Juretschko *et al.*, 1998).

These results unmasked the dogma claiming that *Nitrobacter* species were the important nitrite-oxidizers in wastewater treatment as a mere artifact of cultivation. Later studies confirmed this conclusion repeatedly by using FISH and microsensors to correlate the spatial localization of *Nitrospira*-like bacteria with zones of active nitrite oxidation in biofilms (Schramm *et al.*, 1998; Okabe *et al.*, 1999; Schramm *et al.*, 1999; Schramm *et al.*, 2000).

2.6 Current Research Approach

In view of the above sections this research has been initiated to help bridge the gap that exists between the scientific and engineering paradigms of biological wastewater treatment processes. Application of novel analytical and investigative methods such as FISH has led to new insights in micro- and macroscopic processes in bioreactors. However, the question is still open as to whether or not the application of novel molecular techniques and the subsequent increase in knowledge are of significant practical relevance and of substantial applied value. Therefore, there is a need for further research focusing on integrating molecular based methods such as FISH with engineering technology (respirometric batch assays) in order to accurately quantify heterotrophic and autotrophic active biomass components. For validation, independent quantification of active biomass components and close correspondence to theoretical values is required. In order to realize the applied value of molecular techniques to accurately determine active biomass composition in activated sludge processes and validate current models, research should focus on:

- To establish whether molecular techniques in combination with engineering paradigms (mass balances) can be used to assess steady-state behaviour of a laboratory scale anoxic/aerobic activated sludge system. To determine microbial

community structure in both the aerobic and anoxic zones and to establish any difference in community structure. The application of FISH in combination with mass balance equations to monitor system performance could provide useful information about populations shifts as early indicators of upcoming malfunctions in wastewater treatment systems, so that corrective measures could be implemented in time.

- Mathematical modeling is powerful tool for process analysis and design. However one major limitation with activated sludge models is that many kinetic and stoichiometric paramaters are not easily identifiable. To provide a means of improving design and operation, the transformation of results from a microscale to macroscale level is needed which requires the thorough correlation with data describing the reactor systems from which samples are taken. Here, the modified batch test method will be re-evaluated, by comparing the measured OHO and AO active biomass concentrations with the theoretical values predicted by the steady-state model. In addition to the modified batch test, FISH analysis will be performed and quantitative data obtained by FISH expressed as COD based units will allow the active comparison of results obtained by molecular probing and steady-state model. This will establish whether the integration of FISH can be used to expand model calibration and validation efforts.

- In addressing the above concerns, it needs to be established whether discrepancies between measured and theoretical OHO active biomass concentrations arise from the activated sludge theory (i.e the theoretical) or from the batch test procedure itself (i.e the measured). Should any inconsistencies occur between the measured and theoretical OHO and AO active biomass concentrations, identify possible causes for the inconsistencies. Application of molecular techniques (PCR-DGGE) will be useful in examing possible reasons for the inconsistencies by monitoring microbial community structure with time. This will establish whether molecular techniques can be used to address key concerns in the engineering technology paradigm.

CHAPTER 3

The Modified Ludzack-Ettinger Process for Nitrogen Removal

3.1 Introduction

Ludzack and Ettinger in 1962 were the first to propose a single sludge nitrification-denitrification process utilizing the biodegradable material in the influent as an energy source for denitrification. In 1973, Barnard proposed an improvement of the Ludzack-Ettinger process, by completely separating the anoxic and aerobic reactors, recycling the underflow from the settler to the anoxic reactor, and providing an additional recycle from the aerobic to the anoxic reactor (Fig. 3.1) (WRC, 1984).

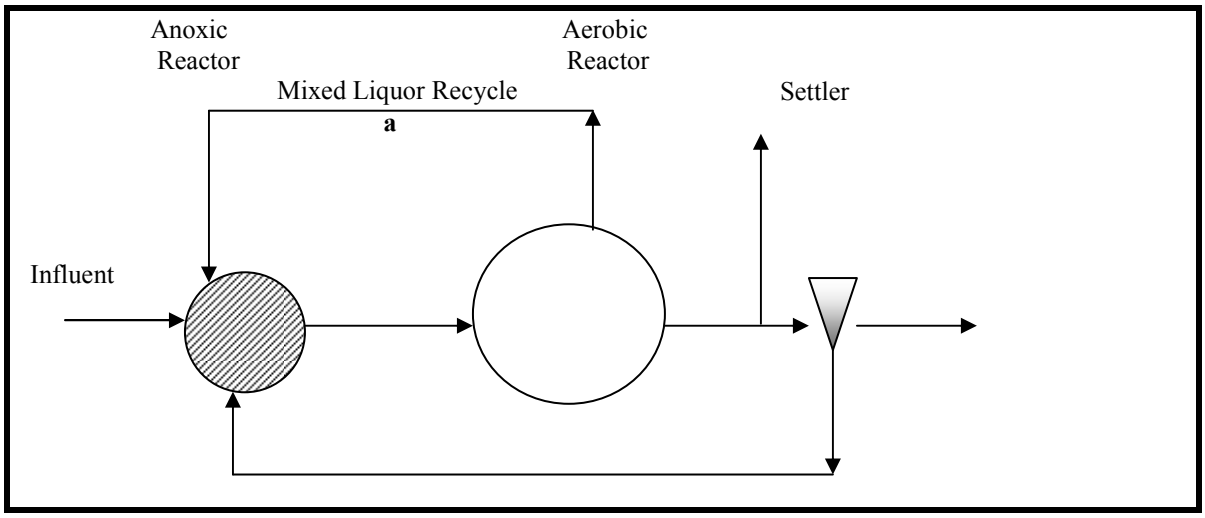

Fig. 3.1: The modified Ludzack-Ettinger process for nitrogen removal (WRC, 1984)

In this process, the influent is discharged directly into the anoxic zone. The anoxic zone is virtually free of oxygen but contains nitrite and nitrate or has a substantial input of nitrate. This zone is fundamental to the biological removal of nitrogen because the absence of oxygen allows non-polyP organisms to utilize nitrate as an electron acceptor,

reducing it to nitrogen gas, thus carrying out denitrification of mixed liquor and allowing the elemental nitrogen formed to escape to the atmosphere as a gas. The aerobic zone is aerated by introducing either air or oxygen. In this environment the utilization of biodegradable organic matter is virtually completed while ammonium nitrogen is converted to nitrate by the nitrifiers present in the population of microorganisms. A recycle (A-recycle) from the aerobic zone recycles nitrite and nitrate back to the anoxic zone. The underflow recycle (S-recycle) from the clarifiers also recycles nitrite, nitrate and mixed liquor to the anoxic basin. As the influent contains substrates or COD that can be used rapidly, a high rate of denitrification in the anoxic zone is observed. Complete denitrification cannot be achieved because part of the total flow from the aerobic reactor (containing nitrite and nitrate) is discharged directly with the effluent and is not recycled back to the anoxic zone (Lilley *et al.,* 1997).

To aid in the design and operation of the single sludge activated sludge system, over the past three decades a suite of steady state design models (WRC, 1984; Wentzel *et al.,* 1990; Maurer and Gujer, 1994) and kinetic simulation models (Dold *et al.,* 1980, 1991; Van Haandel *et al*., 1981; Henze *et al*., 1987; Wentzel *et al.*, 1992; Henze *et al*., 1995) have been developed. These models are based on the behavioral kinetics of an assemblage of microorganisms performing a particular function in the activated sludge system. This assemblage is grouped together as a single entity and is referred to as the 'surrogate' organism. This surrogate organism is assigned a set of unique characteristics that reflect the behaviour of the group, but may not reflect the characteristic of an individual species. A similar approach has been adopted for the 'non-organism' components of the activated sludge mixed liquor, e.g. inert organics. Together, the surrogate organism and non-organism groups make up the activated sludge mixed liquor organic (volatile) suspended solids (MLOSS) (Cronje *et al*., 2000).

In terms of models, in the non-nitrifying aerobic COD removal activated sludge system, the MLOSS is made up of three components;

- Ordinary heterotrophic organisms (OHO) active biomass,
- Endogenous residue and

- Inert material

With the inclusion of nitrification in the system, a fourth component is included;

- Autotrophic organism (AO) active biomass.

With the inclusion of denitrification through the incorporation of anoxic reactors, no additional surrogate organism is included, and the OHO above are considered to be facultative mediating the denitrification process.

Parallel to the developments in modeling, microbial community analysis has been identified as the key component in the design and monitoring of biological wastewater treatment systems (Cloete and Muyima, 1997). In the last years, a battery of molecular techniques has been developed to study microbial ecology in general and community structures in particular (Stahl, 1997; Wagner and Amann, 1997; Burlage *et al*., 1998; Atlas and Bartha, 1998). Specific bacterial groups in complex open communities such as activated sludge may be detected directly by fluorescence *in situ* hybridization (FISH), using 16S rRNA-targeted oligonucleotide probes (Stahl and Amann, 1991; Amann *et al*., 1995; Wagner and Amann, 1997). FISH has played a major role in the identification of abundant microorganisms in wastewater treatment plants (Wagner *et al*., 1994b). Recent research has focused on assigning key processes to groups of microorganisms identified *in situ* by FISH (Crocetti *et al*., 2000).

This chapter describes the configuration and operation of a 10 d laboratory-scale anoxic/aerobic activated sludge system and details the response of this system. Group-specific oligonucleotide probes were applied for *in situ* analysis of microbial community structure in the system. Special attention was given to the demonstration of cultivation independent monitoring of community composition.

3.2 Materials and Methods

3.2.1 Parent system

The parent laboratory-scale system layout and operational details are shown in Fig. 3.2. The system was fed 24 L/d raw (unsettled) municipal wastewater obtained from Southern Works (Durban, South Africa) in 2003 and Isipingo (Durban, South Africa) in 2004. The wastewater obtained from Southern works was primarily domestic with < 15% industrial contribution, whereas Isipingo is totally domestic. The wastewater was collected in batches, stored in 25 L containers at 4°C and served as feed for both the parent system and batch tests. For the parent system, daily wastewater was drawn from the storage containers after thorough mixing and diluted with tap water to approximately 500 mgCOD/L (COD of undiluted sewage ranged from 800 to 1200 mgCOD/L). To maintain pH in the aerobic reactor at ±7.5, the alkalinity of the influent was increased by 200 mg/L (as $CaCO_3$). A buffer solution was made up in a separate container by dissolving 67.2 g sodium bicarbonate ($NaHCO_3$) in to 1 L of distilled water. By adding 100 ml of the buffer solution to the 20 L diluted wastewater an increase in alkalinity of 200 mg/L (as $CaCO_3$) was achieved. After thorough mixing, samples were drawn for influent analysis.

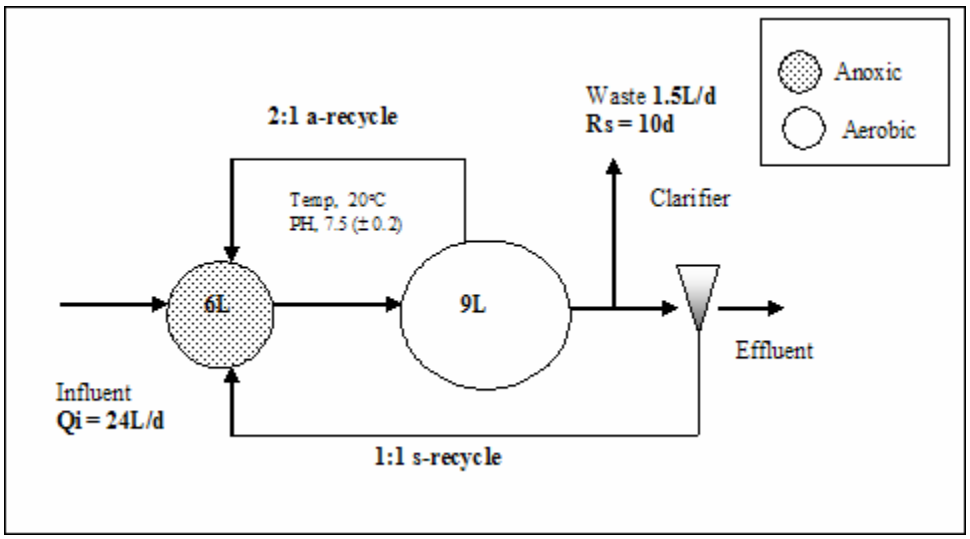

Fig. 3.2: Schematic layout and operational data for parent laboratory-scale Modified-Ludzack Ettinger (MLE) anoxic/aerobic activated sludge system

3.2.2 Sampling and measurements

The oxygen utilization rate (OUR) in the aerobic reactor was measured continually by using an automated technique (Randall *et al*., 1991). A dissolved oxygen (DO) probe (YSI) from an automated DO meter/OUR logger (Hi Tech Microsystems, South Africa) was immersed in the mixed liquor. The low and high DO set points of the meter were 2.0 and 5.0 mgO/L respectively. When the DO reached ±5.0 mgO/L the air switched off automatically and the decrease in DO with time was monitored; when the DO reached ±2.0 mgO/L, the air was switched on automatically and the cycle repeated. Automatically, for each cycle the slope of the DO-time data during the air off period was determined by linear regression; this gives the OUR, which was stored by the meter (together with the regression analysis and time data). The OUR results were downloaded from the DO meter to a PC the following day whilst the system was still feeding on the previous day's feed. OUR results with the regression correlation coefficient less than 0.99 (R^2 = 0.99) were rejected, the mean OUR determined from the remaining data and recorded as the OUR for the day. The number of OUR readings ranged from 120 to 150 per day.

Daily monitoring included influent COD (Appendix 1), TKN (Appendix 2); all reactors nitrate and nitrite (Technicon Auto Analyser II, Ireland); aerobic reactor VSS (Appendix 3), COD and TKN, OUR; effluent COD, TKN (Standard Methods, 1985), nitrate and nitrite (Table 3.1). To ensure steady state, the parent system was run for more than five sludge ages before mixed liquor was harvested for the batch test.

Table 3.1: Daily tests conducted on parent MLE activated sludge system

Test	Influent	Anoxic Reactor	Aerobic Reactor	Effluent
COD	☒		☒	☒
TKN	☒		☒	☒
NO_3^-		❄	❄	❄
NO_2^-		❄	❄	❄
OUR			❖	
MLVSS		⌘	⌘	
VSS		⌘	⌘	
pH		❖	❖	
DSVI			❖	

☒ Unfiltered sample
❄ Sample filtered through 0.45 μm filter paper
❖ Direct measurement
⌘ Centrifuge pellet

3.2.3 Sampling, cell fixation and sonication

Samples for FISH analyses were taken from the anoxic and aerobic zones of the laboratory-scale activated sludge system conducted in 2004 for the duration of 18 WW

batches. Samples of mixed liquor were collected at three intervals during each WW batch and fixed for 1.5 h at 4ºC with 4% paraformaldehyde (Appendix 4). Cells were fixed by the addition of three volumes of fixative to one volume of sample. Cells are then washed in 1x PBS (130 mM NaCl, 10 mM sodium phosphate buffer, pH 7.2) and then resuspended in PBS/cold absolute ethanol (1:1 v/v). For the detection of gram-positive prokaryotes samples were fixed with a 1:1 mixture of PBS and absolute ethanol (v/v) (Amann, 1995). Fixed samples were then sonicated with Virsonic 100 sonicator (Virtis, USA), to break up the flocs. Sonication was carried out at 8 watts for 6 minutes (Appendix 4).

3.2.4 Membrane filtration and staining with DAPI

Membrane filtration was carried out as described by Porter and Feig (1980) with the following modification. Cellulose acetate (Millipore, 0.22 µm pore size, 25 mm diameter) filters were stained for 24 h in Sudan Black (0.3% w/v in 60% ethanol) (Appendix 5). Dual staining of cells with DAPI and fluorescent oligonucleotides was modified from the method of Hicks *et al*. (1992) so that cells were stained after *in situ* hybridization with DAPI (0.25 µg/ml) for 5 minutes (Appendix 7).

3.2.5 Oligonucleotide probes and hybridization

Oligonucleotides probes used during the present study are given in Table 3.2. A volume of 10 µl of sonicated sample was spotted onto pretreated slides (Appendix 6) and allowed to dry. Spotted cells were then dehydrated by serial immersions through 60%, 80% and 96% (v/v) ethanol (3 minutes each). Samples of 10 µl hybridizations solution (0.9 M NaCl, 20 mM Tris/HCl, pH 7.2, 0.01% SDS, 50 ng probe, X% (v/v) formamide) were applied to each spot and incubated for 2 h at 46ºC in an isotonically equilibrated humidity chamber (Appendix 7). Probe was removed from the slide by rinsing in 2 ml pre-warmed washing solution (20 mM Tris/HCl, 0.01% SDS, 5 mM EDTA, YM NaCl). The salt concentration and formamide concentration was adjusted according to the formula of Lathe (1985). Slides were rapidly transferred into washing solution and incubated at 48ºC

for 20 minutes. Slides were then rinsed briefly with distilled water, air-dried and mounted in Mounting media antifading solution (Bio-Rad, USA) for viewing by microscopy.

3.2.6 Microscopy and image analysis

Cells were visualized with a Zeiss Axiolab microscope (Carl Zeiss, Germany) fitted for epifluorescence with a 50 W mercury high-pressure bulb and Zeiss filter sets 02, 09 and 15. Images were captured using a Hamamatsu (Japan) CCD camera. 30 microscopic fields under the 100X objective were randomly selected for enumeration

Table 3.2: Probe sequences and formamide percentages for *in situ* hybridization

Probe	Specificity	Sequence (5' - 3')	rRNA Target Site	F[1]	Reference
EUB388 I,II,III	Eubacteria	I: GCTGCCTCCCGTAGGAGT II: GCAGCCACCCGTAGGTGT III: GCTGCCACCCGTAGGTGT	16S, 338 - 355	20	Daims *et al*., 1999
ALF1b	Proteobacteria (Alpha)	CGTTCGYTCTGAGCCAG	16S, 19-35	20	Wagner *et al*., 1993
BET42a	Proteobacteria (Beta)	GCCTTCCCACTTCGTTT	23S, 1027 - 1043	35	Wagner *et al*., 1993
GAM42a	Proteobacteria (Gamma)	GCCTTCCCACATCGTTT	23S, 1027 - 1043	35	Wagner *et al*., 1993
HGC69a	Gram +ve Bacteria with high G+C content	TATAGTTACCACCGCCGT	16S, 1901 - 1918	25	Onuki *et al*., 2000

EUB 388, EUB 388-II and EUB 388-III were collectively used in equimolar concentrations and referred to as EUB MIX

[1] percentage formamide (v/v) in the hybridization buffer

3.3 Data Interpretation

3.3.1 Nitrogen and COD mass balances

The reliability of the experimental measurements was checked by means of COD and nitrogen (N) mass balances on steady state periods (Ekama *et al*., 1986). A brief description of the method for calculating the N and COD mass balances for the parent MLE system is given below. The average data from sewage Batch No. 1 in 2004 is used as an example.

Nitrogen mass balance

In the N mass balance, the influent TKN mass must be accounted for by the sum of the mass of TKN and nitrate in the effluent, mass of nitrate denitrified to nitrogen gas in the anoxic reactor and the mass of N abstracted through the waste sludge (WRC, 1984):

Mass of Influent TKN = mass of effluent TKN + mass of effluent NO_3 + mass of N denitrified + mass of TKN wasted

$$MN_{ti} = MN_{te} + MN_{ne} + MN_d + MN_w \quad (mgN/d) \qquad (3.1)$$

The mass of Nitrate denitrified (MN_d)

MN_d = anoxic NO_3 denitrification (Where Secondary Settling Tank (SST)) denitrification did not occur)

= anoxic reactor • (NO_3^- mass in – NO_3^- mass out)

$$= [NO_{3(AE)} \bullet Qi \bullet a + NO_{3(FE)} \bullet Qi \bullet s] - [NO_{3(AN)} \bullet Qi \bullet (1 + a + s)]$$

OR

= (anoxic + SST) • NO_3^- denitrification (Where SST denitrification did occur)

= anoxic reactor • (NO_3^- mass in – NO_3^- mass out) + SST• (NO_3^- mass in – NO_3^- mass out)

$$= [NO_{3(AE)} \bullet Qi \bullet a + NO_{3(AE)} \bullet Qi \bullet s] - [NO_{3(AN)} \bullet Qi \bullet (1 + a + s)] + Qi \bullet [NO_{3(AE)} - NO_{3(FE)}]$$

Where

Qi = influent flow rate (24 L/d)

a = a-recycle ratio = 2

s = s-recycle ratio = 1

$NO_{3(AE)}$ = NO_3 concentration in the aerobic reactor (3.9 mgN/L)

$NO_{3(FE)}$ = NO_3 concentration in the filtered effluent (7.9 mgN/L)

$NO_{3(AN)}$ = NO_3 concentration in the anoxic reactor (0.6 mgN/L)

$Qi \bullet [NO_{3(AE)} - NO_{3(FE)}]$ = Only calculated when $NO_{3(AE)} > NO_{3(FE)}$

i.e. only calculated when denitrification occurs in SST

For Batch no.1:

$MNO_{3,d}$ = $[(3.9 \bullet 24 \bullet 2) + (7.9 \bullet 24 \bullet 1)] - [(0.6 \bullet 24 \bullet (1+2+1)]$

= 319.2 mgN/d

The mass of effluent TKN (MN_{te}) was taken as the unfiltered TKN concentration of the effluent (N_{te}) multiplied by the effluent flow rate (Qi – Qw):

For Batch no.1: $MN_{te} = N_{te} \bullet (Qi - Qw)$

= $5.3 \bullet (24 - 1.5)$

= 119.25 mgN/d

The mass of effluent NO_3 (MN_{ne}) was calculated as the concentration of nitrate and nitrite in the effluent ($NO_{3(FE)} + NO_{2(FE)}$) multiplied by the effluent flow rate (Qi – Qw):

For Batch no.1: $MN_{ne} = (NO_{3(FE)} + NO_{2(FE)}) \bullet (Qi - Qw)$

= $(7.9 + 0) \bullet (24 - 1.5)$

= 177.75 mgN/d

The mass of N in the waste sludge (MN_w) was found by adding the NO_3 concentration in the aerobic reactor ($NO_{3(AE)}$) and the NO_2 concentration in the aerobic reactor ($NO_{2(AE)}$) to the measured mixed liquor TKN concentration (N_{ML}) and multiplying this value by the waste flow (Qw):

For Batch no. 1: $MN_w = (N_{ML} + NO_{3(AE)} + NO_{2(AE)}) \bullet Qw$

$= (234.6 + 3.9 + 0) \bullet 1.5$

$= 357.7$ mgN/d

The influent N mass (MN_{ti}) was taken as the influent TKN concentration (N_{ti}) multiplied by the influent flow rate (Qi):

For Batch no.1: $MN_{ti} = N_{ti} \bullet Qi$

$= 38.8 \bullet 24 = 931.2$ mgN/d

By substituting the masses calculated above in Eq. (3.1), the N mass balance is given by

$$\text{Nbal (\%)} = 100 \bullet (MN_{te} + MN_{ne} + MN_d + MN_w)/ MN_{ti} \quad (3.2)$$

For Batch no.1:

NBal (%) = 100 • (119.25 + 177.75 + 319.2 + 357.7) / 931.2

= 104.5 %

COD mass Balance

In the COD mass balance, the influent COD mass must be accounted for by the sum of the masses of effluent COD, carbonaceous oxygen demand for denitrification and the COD mass of the waste sludge:

Mass of Influent COD	=	mass of effluent COD	+	mass of carbonaceous oxygen demand	+	equivalent mass of oxygen demand for denitrification	+	mass of COD wasted

$$MS_{ti} = MS_{te} + MO_c + MO_d + MX_{svw} \text{ (mgCOD/L)} \quad (3.3)$$

The mass of effluent COD (MS_{te}) was taken as the unfiltered COD concentration of the effluent (S_{te}) multiplied by the effluent flow rate (Qi – Qw):

$$MS_{te} = S_{te} \bullet (Qi - Qw)$$

For Batch no. 1:

$= 46 \bullet (24 – 1.5) = 1035$ mgCOD/d

From the direct measurement of OUR in the aerobic reactor, the total oxygen demand (MO_t) can be calculated. However, the total oxygen demand is the sum of carbonaceous oxygen demand (MO_c) and the oxygen demand for nitrification (MO_n):

$$MO_t = 24 \bullet OUR \bullet V_{(AE)} = MO_c + MO_n \quad \text{(mgO/d)} \quad (3.4)$$

Where

$V_{(AE)}$ = volume of the aerobic reactor (L)

OUR = mean oxygen utilization rate measured in the aerobic reactor (mgO/L/h)

Therefore, to be able to calculate MO_c, an estimation for MO_n is essential. The oxygen demand for nitrification is related to the mass of nitrate generated from ammonia ($MNO_{3,g}$) and the mass of nitrite nitrified to nitrate ($MNO_{2,g}$):

$$MO_n = 4.57 \bullet MNO_{3,g} - 3.43 \bullet MNO_{2,g} \quad \text{(mgO/d)} \quad (3.5)$$

$$= 4.57 \bullet Qi \bullet (1 + a + s) \bullet [NO_{3(AE)} - NO_{3(AN)}] - 3.43 \bullet Qi \bullet (1 + a + s) \bullet [NO_{2(AE)} - NO_{2(AN)}]$$

Where

4.57 = mg of oxygen utilized per mg NH_4-N nitrified to NO_3-N

3.43 = mg of oxygen utilized per mg NO_2-N nitrified to NO_3-N

$MNO_{3,g} = Qi \bullet (1 + a + s) \bullet [NO_{3(AE)} - NO_{3(AN)}]$

$MNO_{2,g} = Qi \bullet (1 + a + s) \bullet [NO_{2(AE)} - NO_{2(AN)}]$

For Batch no.1: $MNO_{3,g} = 24 \bullet (1+ 2 +1) \bullet [3.9 – 0.6] = 316.8$ mgN/d

$MNO_{2,g} = 24 \bullet (1+ 2 +1) \bullet [0 – 0] = 0$ mgN/d

$MO_n = 4.57 \bullet 316.8 - 3.43 \bullet 0 = 1447.8$ mgN/d

The carbonaceous oxygen demand (MO_c) was calculated by substituting Eq. (3.5) into Eq. (3.4) and solving for MO_c:

$$MO_c = (24 \bullet OUR \bullet V_{AE}) - MO_n \quad \text{(mgO/d)} \quad (3.6)$$

For Batch no.1: $MO_c = (24 \bullet 30.6 \bullet 9) - 1447.8$

$MO_c = 5161.8$ mgO/d

The equivalent mass of oxygen demand for denitrification (MO_d) was calculated from:

$$MO_d = 2.86 \bullet MNO_{3,d} + 1.71 \bullet MNO_{2,d} \qquad \text{(mgO/d)} \qquad (3.7)$$

Where

2.86 = oxygen equivalent of nitrite as electron acceptor (mgO/mgNO_3-N) ($NO_3 \rightarrow N_2$)

1.71 = oxygen equivalent of nitrite as electron acceptor (mgO/mgNO_3-N) ($NO_2 \rightarrow N_2$)

$MNO_{3,d}$ = mass of nitrate denitrified into nitrogen gas (mgN/d)

$MNO_{2,d}$ = mass of nitrate denitrified into nitrogen gas (mgN/d)

For Batch no.1: $MO_d = 2.86 \bullet 319.2 + 1.71 \bullet 0$

$MO_d = 912.91$ mgO/d

The mass of COD in the waste sludge (MX_{SVW}) was calculated by multiplying the measured mixed liquor COD concentration (COD_{ML}) by the waste flow rate (Qw):

$$MX_{SVW} = (COD_{ML}) \bullet Qw \qquad \text{(mgCOD/d)} \qquad (3.9)$$

For Batch no.1: $MX_{SVW} = (3720) \bullet 1.5$

$MX_{SVW} = 5580$ mgCOD/d

The mass of influent COD (MS_{ti}) was taken as the influent COD concentration (Sti) multiplied by the influent flow rate (Qi):

$$MS_{ti} = S_{ti} \bullet Qi$$

For Batch no.1: $MS_{ti} = 502.6 \bullet 24$

$MS_{ti} = 12062.4$ mgCOD/d

By substituting the masses calculated above into Eq. (3.3), the COD mass balance is given by:

$$\text{COD bal (\%)} = 100 \bullet (MS_{te} + MO_c + MO_d + MX_{svw}) / MS_{ti} \quad (3.10)$$

For Batch no.1: COD bal (%) = 100 • (1035 + 5161.8 + 912.91 + 5580)/ 12062.4

COD bal (%) = 105.2 %

3.3.2 Determination of unbiodegradable soluble and particulate fractions

The unbiodegradable soluble ($f_{S,us}$) and particulate ($f_{S,up}$) fractions of the influent COD were determined using methods detailed by Ekama *et al*. (1986).

Unbiodegradable soluble COD fractions ($f_{S,us}$)

According to Ekama *et al.* (1986), the unbiodegradable soluble COD is given by the COD of the filtered effluent of the activated sludge system.

$$f_{S,us} = S_{te} / S_{ti} \quad (3.11)$$

Where

S_{te} = filtered effluent COD concentration (mgCOD/L)

S_{ti} = unfiltered influent COD concentration (mgCOD/L)

Unbiodegradable particulate COD fractions ($f_{S,up}$)

Following the method of Ekama *et al*. (1986), the measured mixed liquor suspended solids (MLVSS) was used to determine the influent unbiodegradable particulate COD fraction, $f_{S,up}$.

$$MX_V = \frac{MS_{ti}(1 - f_{S,us} - f_{S,up})Y_H \bullet R_S}{(1 + b_H \bullet R_S)}(1 + f \bullet b_H \bullet R_S) + f_{S,up} \bullet MS_{ti} \bullet R_S / f_{CV} \quad (3.12)$$

MX_V = total volatile solids mass (mgVSS)

= $X_v \bullet V_p$

X_v = MLVSS concentration (mgVSS/L)

V_p = System volume

Y_H = OHO active biomass yield (VSS units)

= 0.45 mgVSS/mgCOD

R_s = sludge age (d)

b_H = net specific endogenous mass loss rate (endogenous mass loss theory, WRC, 1984)

= 0.24/d at 20ºC

f = endogenous residue fraction

= 0.20

f_{CV} = COD/VSS ratio of mixed liquor (mgCOD/mgVSS)

MS_{ti} = total influent COD mass fed per day (mgCOD/d)

= $Qi \bullet S_{ti}$

Qi = influent flow rate

S_{ti} = influent COD concentration (mgCOD/L)

3.4 Results

3.4.1 Parent System

The parent system was operated for two years. In 2003 and 2004 the parent system comprised of 18 and 22 WW batches, respectively. Daily results for the parent activated system at 10d sludge age conducted during 2003 and 2004 are listed in Appendix 8 (Tables 8.1-8.3) and Appendix 9 (Tables 9.1-9.3) respectively. Each sewage batch was accepted as a steady state period. For each sewage batch the daily data were averaged and the sample standard deviations calculated. The averages and standard deviations are listed in Tables 3.3 (a, b) and 3.5 (a, b) for 2003 and 2004, respectively.

The results of the N and COD mass balances calculated for each sewage batch during 2003 and 2004 are listed in Table 3.4 and 3.6 and are shown graphically in Fig. 3.3 (a, b) and Fig 3.4 (a, b). In 2003 the 18 WW batches produced COD and N mass balances in the range 90-110%. However of the 22 WW batches in 2004 the N mass balances for

WW batches 2 and 7 fell outside the range of 90-110%, while the COD mass balance were in the acceptable range. Batch tests conducted with WW batches that resulted in having poor N mass balances were rejected.

For the average data on each wastewater batch (Tables 3.3 and 3.5), the $f_{S,us}$ values were calculated using Eq. (3.11), and the values are listed in Tables 3.4 and 3.6 for parent systems conducted during 2003 and 2004, respectively.

Table 3.3 (a): Parent system steady state data for 2003; for each sewage batch the data have been averaged and the sample standard deviations (Stdev) listed

WW Batch No.	TKN (mgN/L)						NITRATE (mgN/L)					
	Influent		***Effluent***		***Mixed Liquor***		***Anoxic***		***Aerobic***		***Effluent***	
	Mean	Stdev	Mean	Stdev	Mean	Stdev	Mean	Stdev	Mean	Stdev	Mean	Stdev
1	41.0	9.7	8.8	5.1	158.8	57.3	1.2	0.3	6.2	1.0	8.2	2.3
2	32.4	3.0	4.4	1.2	129.9	40.6	1.2	0.3	4.2	2.4	9.3	3.1
3	46.4	4.9	3.6	1.3	204.0	23.0	2.0	1.2	8.1	1.9	12.0	2.4
4	28.7	3.2	3.1	1.9	158.3	48.3	3.0	2.1	6.4	0.9	8.3	1.6
5	31.7	2.0	2.2	0.9	243.0	24.4	1.1	1.4	1.8	2.1	7.8	2.0
6	31.9	1.1	1.7	0.8	204.1	16.8	0.2	0.4	2.7	1.2	7.3	1.5
7	33.8	1.0	3.5	1.4	205.4	15.4	1.0	0.5	3.8	1.9	7.9	0.8
8	32.4	1.0	3.0	1.9	198.9	16.5	1.2	0.3	3.4	1.5	9.1	1.8
9	34.4	2.5	3.4	1.3	204.5	14.9	1.2	0.9	4.3	1.4	7.8	1.7
10	33.5	1.5	2.5	1.1	209.2	10.4	1.2	1.0	3.7	2.1	9.5	1.7
11	33.9	2.5	4.3	1.0	173.0	54.8	3.6	3.4	6.3	4.7	10.4	4.7
12	32.3	1.8	3.6	1.6	112.5	7.2	0.9	1.0	2.4	1.6	12.1	3.2
13	33.3	4.3	2.2	1.1	205.1	14.6	1.3	1.6	5.0	0.9	7.8	0.8
14	34.3	1.1	1.9	0.9	217.3	20.9	0.5	0.4	4.7	0.8	6.9	1.2
15	32.3	2.5	1.7	0.8	204.1	16.8	0.2	0.4	3.1	1.2	7.4	2.0
16	36.1	2.5	1.9	0.8	201.8	40.0	0.2	0.4	4.8	0.9	7.5	1.2
17	34.1	2.1	3.0	1.9	198.9	16.5	1.2	0.3	4.8	2.0	7.7	0.9
18	37.7	0.6	4.6	1.0	218.3	8.0	0.6	0.6	3.6	1.3	9.2	0.5

Table 3.3 (b): Parent system steady state data for 2003; for each sewage batch the data have been averaged and the sample standard deviations (Stdev) listed

WW Batch No.	COD (mgCOD/L)						OUR (mgO/L/h)		VSS (mgVSS/L)	
	Influent		*Effluent*		*Mixed Liquor*					
	Mean	Stdev	Mean	Stdev	Mean	Stdev	Mean	Stdev	Mean	Stdev
1	479.8	13.7	47.8	1.5	3656.3	527.6	31.8	3.1	2383.8	129.3
2	462.6	49.7	38.3	10.2	2812.9	690.7	30.6	0.4	1921.1	370.5
3	488.8	24.7	33.8	7.3	3446.6	169.6	31.1	0.5	2274.8	130.6
4	489.8	25.3	38.6	16.9	2813.7	323.5	30.8	0.1	1908.7	215.1
5	518.8	23.7	29.6	4.2	3320.6	278.3	30.5	0.2	2239.8	163.5
6	521.8	24.4	47.8	8.1	2871.0	560.9	32.2	0.3	1957.6	285.5
7	517.4	30.1	29.0	12.6	3203.0	266.2	31.4	0.2	2171.0	136.9
8	508.1	20.3	45.9	12.8	3157.5	424.4	31.0	0.2	2189.3	210.8
9	500.0	9.9	52.2	10.3	2829.8	464.0	30.6	0.1	1913.5	252.4
10	498.0	14.3	32.4	9.3	3190.9	434.5	30.4	0.1	2129.5	264.5
11	503.7	15.8	34.5	2.1	3608.7	152.9	30.2	0.1	2410.2	155.3
12	502.3	15.5	33.6	7.2	3304.9	255.4	30.7	0.2	2204.0	96.1
13	494.0	15.7	38.9	11.4	3325.4	165.4	30.6	0.1	2189.0	112.3
14	490.6	15.7	29.4	9.3	2988.8	156.3	30.4	0.1	1984.4	130.7
15	496.7	12.8	32.3	12.2	3212.8	109.7	30.9	1.2	2139.8	90.8
16	477.2	38.4	35.8	13.2	3052.2	468.8	29.9	0.1	2089.2	311.6
17	485.3	32.8	30.8	10.3	3145.3	277.5	30.2	0.9	2051.3	247.7
18	492.7	21.9	30.0	2.0	3325.3	123.7	30.5	0.6	2200.0	90.0

Table 3.4: Steady state N and COD mass balances, wastewater fractions and mixed liquor parameters for parent system in 2003 Data calculated from Table 3.3.

WW Batch No.	MASS BALANCE (%)		WASTEWATER FRACTIONS		MIXED LIQUOR		
	N	*COD*	*Unbio. Soluble* ($f_{S,us}$) *(mgCOD/mgCOD)*	*Unbio. Partic.* ($f_{S,up}$) *(mgCOD/mgCOD)*	*COD/VSS* (f_{cv}) *(mgCOD/mgVSS)*	*TKN/VSS* (f_N) *(mgN/mgVSS)*	*Active Fraction* (f_{av})
1	102.8	109.4	0.0938	0.2838 *	1.53	0.0671	0.2694*
2	105.0	102.4	0.0819	0.1616	1.46	0.0662	0.3976
3	103.9	96.8	0.0692	0.2347	1.52	0.0899	0.3188
4	103.6	92.4	0.0800	0.1303	1.48	0.0772	0.4318
5	107.4	99.0	0.0571	0.177	1.48	0.1085	0.3772
6	103.8	96.4	0.0921	0.1165	1.47	0.1067	0.4634
7	104.2	95.4	0.0566	0.1623	1.48	0.0950	0.3964
8	107.6	100.6	0.0906	0.1845	1.44	0.0915	0.3603
9	102.0	95.6	0.1045 *	0.1343	1.48	0.1087	0.4318
10	109.0	98.9	0.0652	0.1791	1.50	0.0996	0.3830
11	99.2	100.4	0.0687	0.2466	1.50	0.0715	0.3045
12	108.5	104.6	0.0672	0.1967	1.50	0.0512 *	0.3581
13	106.4	98.9	0.0789	0.2099	1.51	0.0935	0.3393
14	106.2	92.3	0.0595	0.1453	1.51	0.1097	0.4181
15	105.4	99.4	0.0651	0.1826	1.50	0.0957	0.3709
16	104.9	95.9	0.0751	0.1852	1.47	0.0998	0.3720
17	103.1	96.8	0.0638	0.1758	1.55 *	0.0982	0.3951
18	107.8	100.8	0.0609	0.2048	1.51	0.0993	0.3501
MEAN			**0.0721**	**0.1781**	**1.49**	**0.0928**	0.3743
Std deviation			**0.012**	**0.034**	**0.022**	**0.014**	0.0480

*Shaded blocks indicate data rejected as outliers at 95% confidence interval.

Table 3.5 (a): Parent system steady state data for 2004; for each sewage batch the data have been averaged and the sample standard deviations (Stdev) listed

WW Batch No.	TKN (mgN/l)						NITRATE (mgN/L)					
	Influent		*Effluent*		*Mixed Liquor*		*Anoxic*		*Aerobic*		*Effluent*	
	Mean	Stdev	Mean	Stdev	Mean	Stdev	Mean	Stdev	Mean	Stdev	Mean	Stdev
1	38.8	6.3	5.3	2.1	234.6	20.7	0.6	1.0	3.9	1.9	7.9	1.5
2	48.3	2.9	4.3	0.9	229.8	12.4	1.8	0.4	7.9	1.8	15.4	0.3
3	42.8	4.3	4.4	0.4	233.8	5.7	1.2	0.7	5.7	0.5	9.4	1.1
4	31.2	2.2	1.7	0.8	204.1	16.8	0.2	0.4	2.8	1.5	6.6	1.3
5	32.2	2.8	4.4	1.2	129.9	38.5	0.3	0.7	2.7	1.2	8.1	1.6
6	33.7	1.6	4.4	1.2	129.9	38.5	0.9	0.7	4.3	2.5	9.8	1.2
7	33.2	3.5	2.6	1.1	209.2	10.4	1.2	1.0	8.4	3.6	12.5	4.7
8	46.4	9.9	6.1	4.0	231.4	55.5	0.8	1.2	6.6	3.0	10.1	2.7
9	41.9	3.4	3.5	0.9	223.7	21.9	1.2	1.0	6.4	1.3	9.4	1.2
10	41.8	6.1	5.0	1.9	213.3	24.5	2.0	2.2	7.0	3.0	9.4	3.7
11	50.3	9.1	5.1	1.9	227.8	31.0	2.0	0.9	7.9	1.3	12.2	1.5
12	49.3	5.1	4.5	0.5	220.8	13.3	2.7	1.1	9.5	1.7	12.0	1.9
13	62.0	4.2	4.6	0.7	217.1	10.5	2.9	1.3	10.3	3.5	18.6	5.2
14	45.4	6.7	5.7	1.9	200.2	32.7	2.3	1.7	7.5	2.9	12.3	2.3
15	45.0	8.9	6.1	3.8	231.4	52.6	1.3	1.9	5.8	2.6	8.6	2.4
16	39.3	3.7	4.4	0.7	226.5	24.9	1.5	0.8	5.7	1.4	9.1	2.1
17	32.5	1.8	2.5	1.1	209.2	10.4	1.8	1.0	5.9	1.4	7.8	1.5
18	35.4	1.2	6.4	1.8	135.5	35.4	1.8	1.1	6.6	1.8	8.2	1.5
19	42.1	5.4	4.4	0.8	201.3	49.3	0.9	0.5	7.2	2.3	8.9	2.5
20	40.1	2.0	4.3	1.3	229.5	7.6	0.8	0.7	6.5	0.4	8.0	0.6
21	40.9	3.1	4.5	0.6	197.3	13.9	1.3	0.8	7.2	1.4	8.7	0.9
22	41.4	3.2	4.4	0.7	226.5	24.9	1.2	0.9	6.1	1.2	9.1	1.8

Table 3.5 (b): Parent system steady state data for 2004; for each sewage batch the data have been averaged and the sample standard deviations (Stdev) listed

WW no.	COD (mgCOD/L)						OUR (mgO/L/h)		VSS (mgVSS/L)	
	Influent		*Effluent*		*Mixed Liquor*					
	Mean	Stdev	Mean	Stdev	Mean	Stdev	Mean	Stdev	Mean	Stdev
1	502.6	48.8	46.0	10.1	3720.0	553.2	30.6	0.3	2352.4	153.1
2	492.0	52.6	57.0	11.9	2727.5	208.2	27.3	0.5	1860.0	205.0
3	504.0	10.2	47.2	9.5	3188.0	254.6	30.3	0.1	1979.6	273.6
4	500.2	43.0	47.2	5.7	2796.5	159.4	31.7	1.4	1897.8	163.2
5	490.7	21.8	39.5	4.4	2648.2	367.4	30.8	0.3	1816.8	186.0
6	512.1	22.5	48.3	7.3	3029.0	344.5	31.7	1.5	1860.3	213.5
7	513.4	29.5	53.7	9.2	2906.8	218.2	32.0	0.3	1948.3	141.3
8	516.4	25.0	48.2	9.6	2962.9	193.5	34.0	1.2	2028.7	189.2
9	506.0	16.1	46.8	7.8	3652.8	426.3	26.7	1.9	2341.6	252.0
10	491.1	29.6	41.5	7.6	3043.6	357.7	35.3	1.1	2076.0	232.6
11	511.7	23.7	40.5	7.4	3112.8	432.7	34.0	1.2	2023.7	256.2
12	474.4	22.3	43.9	5.8	3207.0	366.5	30.4	0.6	2151.6	315.5
13	446.8	45.9	40.0	6.0	3578.0	314.9	29.6	1.4	2434.5	338.7
14	492.3	32.7	43.1	5.3	3145.0	227.1	31.3	1.6	2088.2	137.8
15	489.2	30.4	37.0	6.1	2852.9	453.2	33.5	0.3	1933.6	277.7
16	479.4	25.2	40.2	4.5	2949.4	307.5	30.3	0.8	1985.0	239.0
17	432.0	44.5	40.3	6.1	2442.9	202.4	30.0	0.3	1708.4	139.7
18	420.0	39.9	44.0	9.5	2254.5	215.1	30.1	0.4	1659.4	446.7
19	449.2	40.0	39.1	8.2	2903.7	372.1	30.7	0.7	1914.5	239.2
20	478.2	29.8	44.0	5.8	3237.4	181.7	32.5	0.3	1996.3	201.6
21	478.4	15.2	45.7	6.5	3378.0	268.6	31.5	0.9	2319.3	182.1
22	487.5	28.3	37.0	6.1	3282.9	260.3	31.0	0.2	2133.0	154.1

Table 3.6: Steady state N and COD mass balances, wastewater fractions and mixed liquor parameters for parent system in 2004

WW No	MASS BALANCE (%)		WASTEWATER FRACTIONS		MIXED LIQUOR		
	N	*COD*	*Unbio. Soluble* ($f_{S,us}$) (mgCOD/mgCOD)	*Unbio. Partic.* ($f_{S,up}$) (mgCOD/mgCOD)	*COD/VSS* (f_{cv}) (mgCOD/mgVSS)	*TKN/VSS* (f_N) (mgN/mgVSS)	*Active Fraction* (f_{av})
1	105.6	105.9	0.0916	0.2669	1.59	0.1002	0.2946
2	119.2*	87.3	0.1175 *	0.1302	1.47	0.1250	0.4284
3	102.6	95.1	0.0935	0.1512	1.64	0.1201	0.4172
4	102.6	98.6	0.0948	0.1266	1.48	0.1081	0.4418
5	100.7	96.0	0.0808	0.1042	1.49	0.0716	0.4716
6	108.4	97.7	0.0946	0.1162	1.64	0.0704 *	0.4687
7	160.0*	89.5	0.1047	0.1302	1.50	0.1080	0.4309
8	109.0	94.6	0.0933	0.1364	1.47	0.1135	0.4216
9	104.6	92.4	0.0928	0.2493	1.57	0.0965	0.3100
10	102.8	102.1	0.0845	0.1736	1.48	0.1048	0.3791
11	102.7	95.3	0.0793	0.1379	1.57	0.1137	0.4294
12	101.7	94.8	0.0928	0.2115	1.53	0.1053	0.3399
13	102.7	105.9	0.0901	0.3394 *	1.49	0.0907	0.2299*
14	105.3	97.0	0.0880	0.1873	1.51	0.0961	0.3673
15	98.4	97.3	0.0757	0.1282	1.50	0.1228	0.4381
16	106.4	95.9	0.0839	0.1638	1.49	0.1154	0.3942
17	109.1	98.7	0.0937	0.1452	1.43	0.1231	0.4142
18	103.5	96.9	0.1055	0.1204	1.42	0.0854	0.4395
19	108.2	97.6	0.0881	0.1933	1.52	0.1072	0.3671
20	110.2	101.3	0.0923	0.1951	1.64	0.1161	0.3657
21	105.1	100.6	0.0957	0.2566	1.46	0.0994	0.2861
22	104.9	98.1	0.0775	0.1768	1.47	0.0851	0.3733
MEAN			**0.0902**	**0.1667**	1.52	0.1019	0.3879
Std deviation			**0.008**	**0.047**	0.0651	0.0155	0.0638

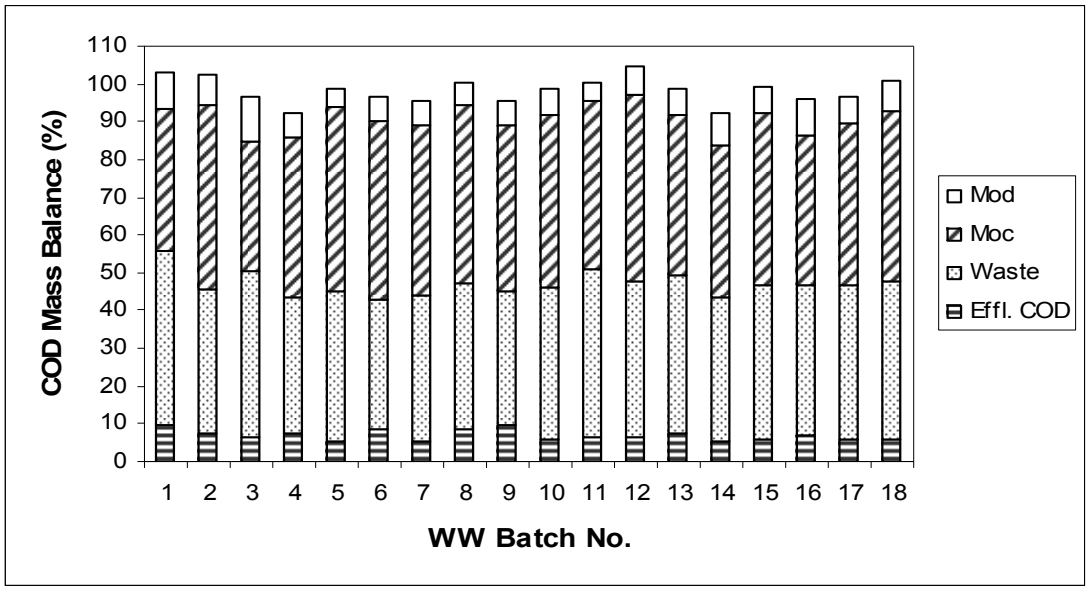

Fig. 3.3 (a): Graphical representation of the percentage COD mass balance for various WW batches for the parent system in 2003.

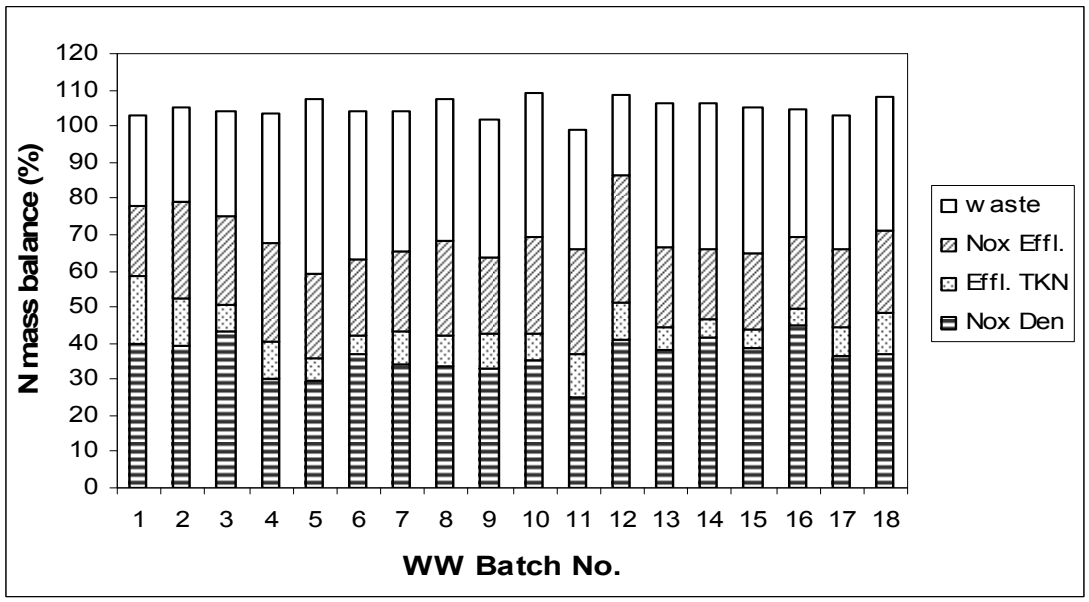

Fig. 3.3 (b): Graphical representation of the percentage N mass balance for various WW batches for the parent system in 2003.

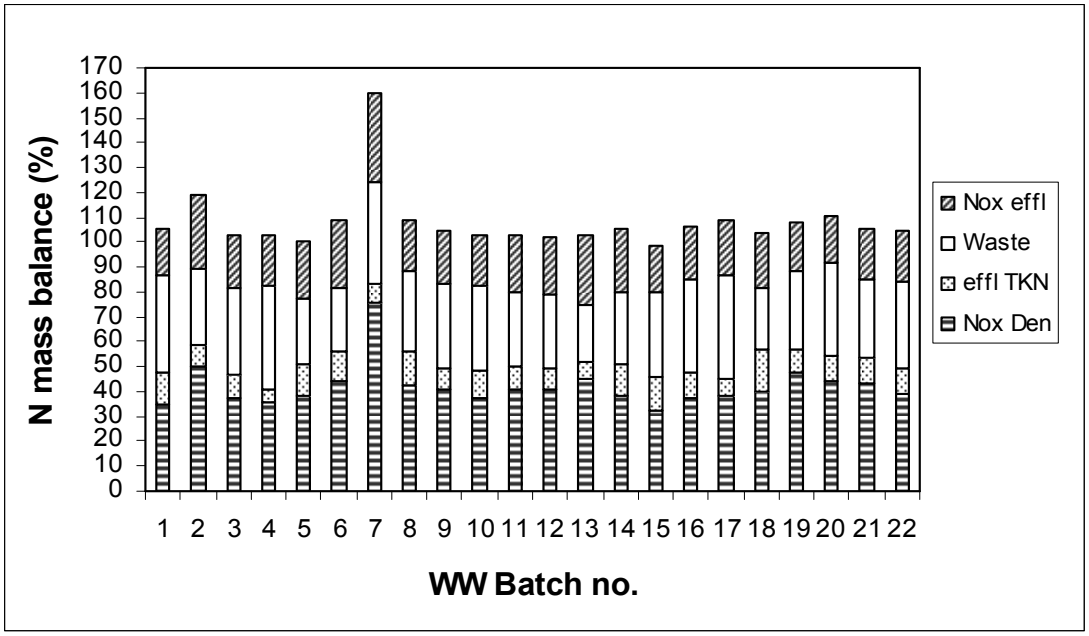

Fig. 3.4 (a): Graphical representation of the percentage N mass balance for various WW batches for the parent system in 2004.

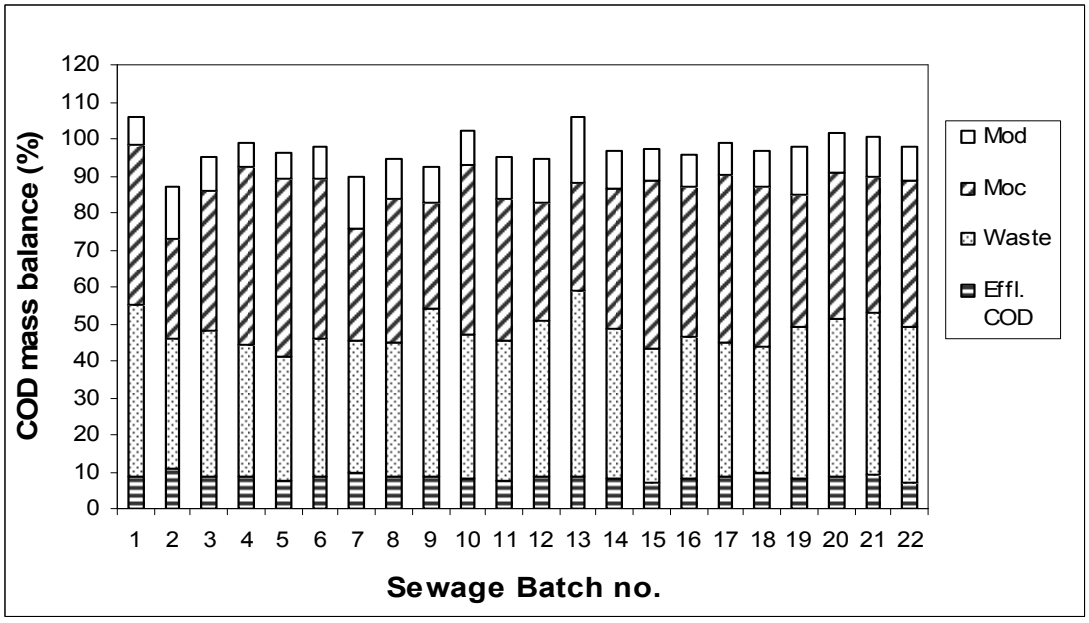

Fig. 3.4 (b): Graphical representation of the percentage COD mass balance for various WW batches for the parent system in 2004.

Influent WW mean $f_{S,us}$ were 0.0721 ± 0.012 and 0.0902 ± 0.008 for 2003 and 2004 systems respectively. The $f_{S,us}$ data from all the WW batches conducted in 2003 and 2004 were analysed using a statistical plot (Fig. 3.5 a, b respectively). Rejecting the outliers at 95% confidence limit, $f_{S,us}$ = 0.1045 (Table 3.4) and $f_{S,us}$ = 0.1175 (Table 3.6), the data was statistically plotted to determine its distribution in 2003 (Fig. 3.5a) and 2004 (Fig. 3.5b).

Influent WW mean $f_{S,up}$ were 0.0781 ± 0.034 and 0.1667 ± 0.047 for 2003 and 2004 systems respectively. The $f_{S,up}$ data from all the WW batches conducted in 2003 and 2004 were analysed using a statistical plot (Fig. 3.6 a, b respectively). Rejecting the outliers at 95% confidence limit, $f_{S,up}$ = 0.2838 (Table 3.4) and $f_{S,up}$ = 0.3394 (Table 3.6), the data was statistically plotted to determine its distribution in 2003 (Fig. 3.6a) and 2004 (Fig. 3.6b).

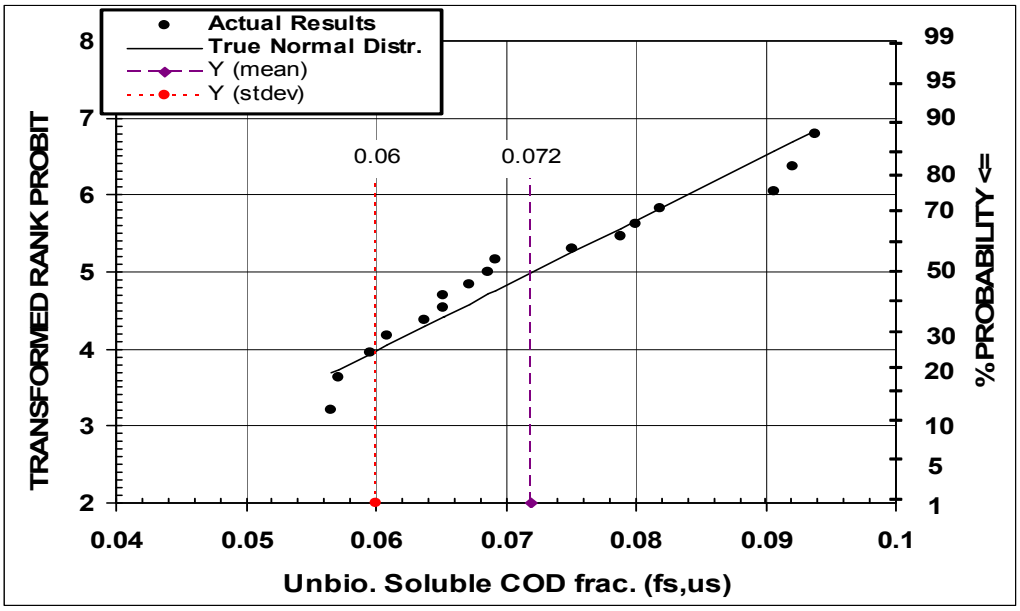

Fig. 3.5 (a): Statistical plot of influent unbiodegradable soluble COD fractions ($f_{S,us}$) for parent system in 2003 fed with wastewater from Southern Works.

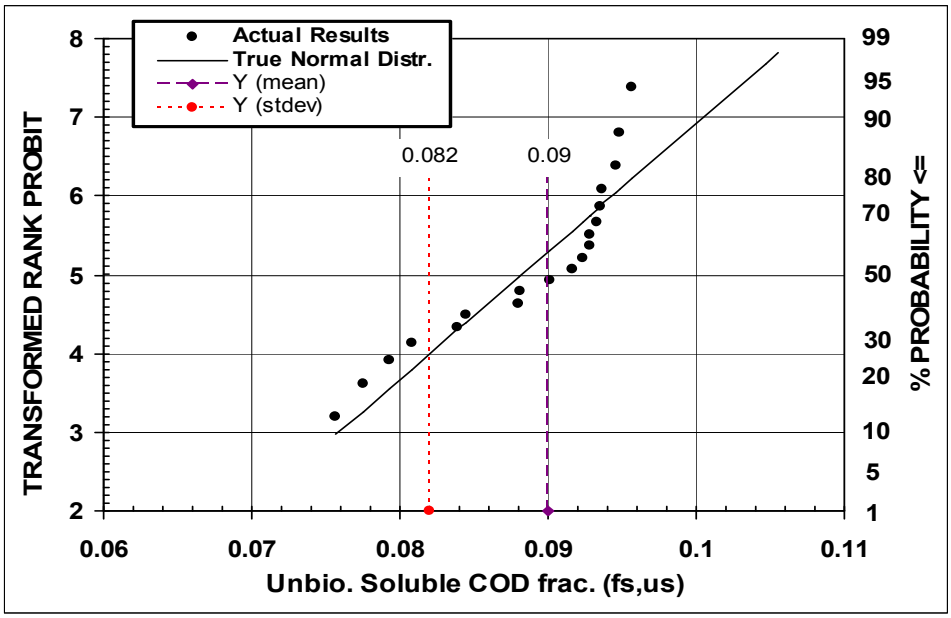

Fig. 3.5 (b): Statistical plot of influent unbiodegradable soluble COD fractions ($f_{S,us}$) for parent system in 2004 fed with wastewater from Isipingo.

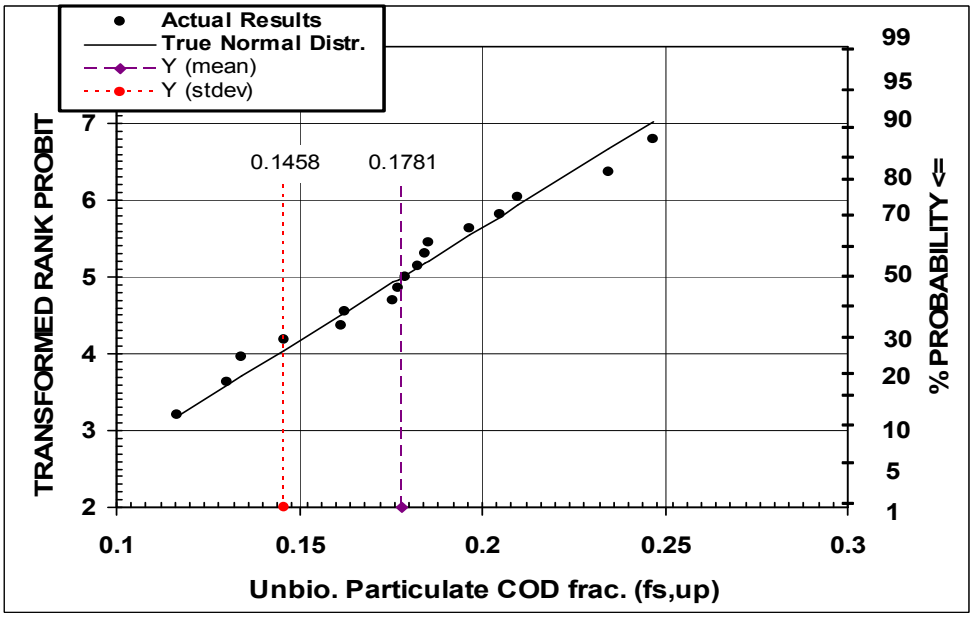

Fig. 3.6 (a): Statistical plot of influent unbiodegradable soluble COD fractions ($f_{S,up}$) for parent system in 2003 fed with wastewater from Southern Works.

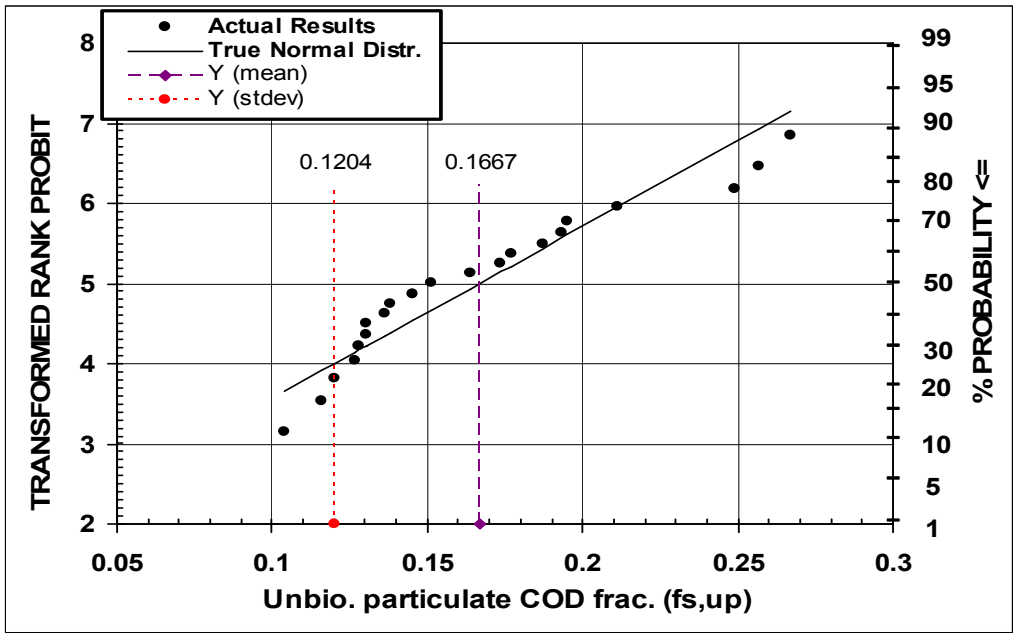

Fig. 3.6 (b): Statistical plot of influent unbiodegradable soluble COD fractions ($f_{S,up}$) for parent system in 2004 fed with wastewater from Isipingo.

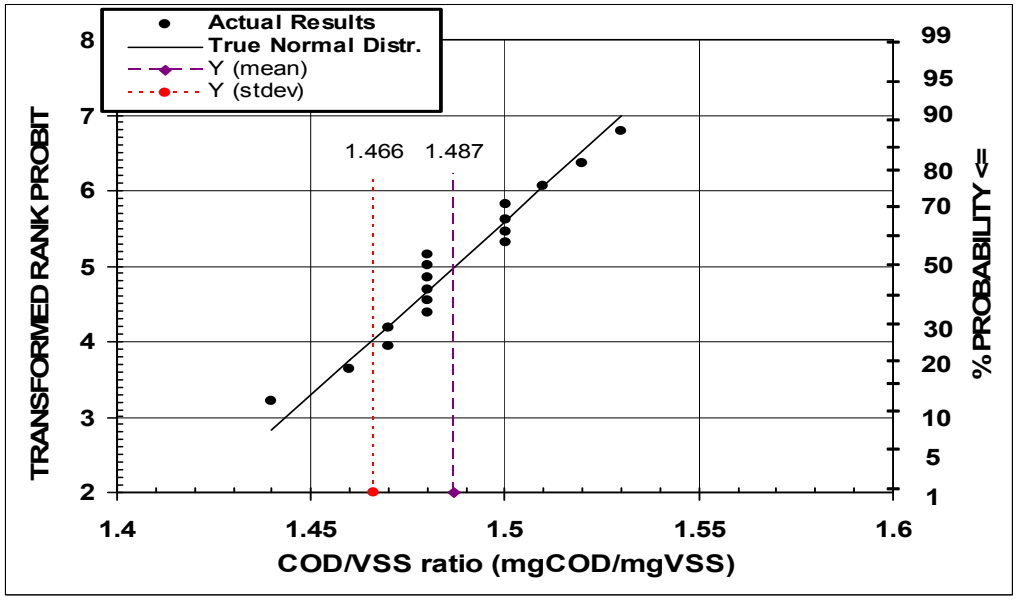

Fig. 3.7 (a): Statistical plot of COD/VSS ratio for parent system in 2003 fed with wastewater from Southern Works.

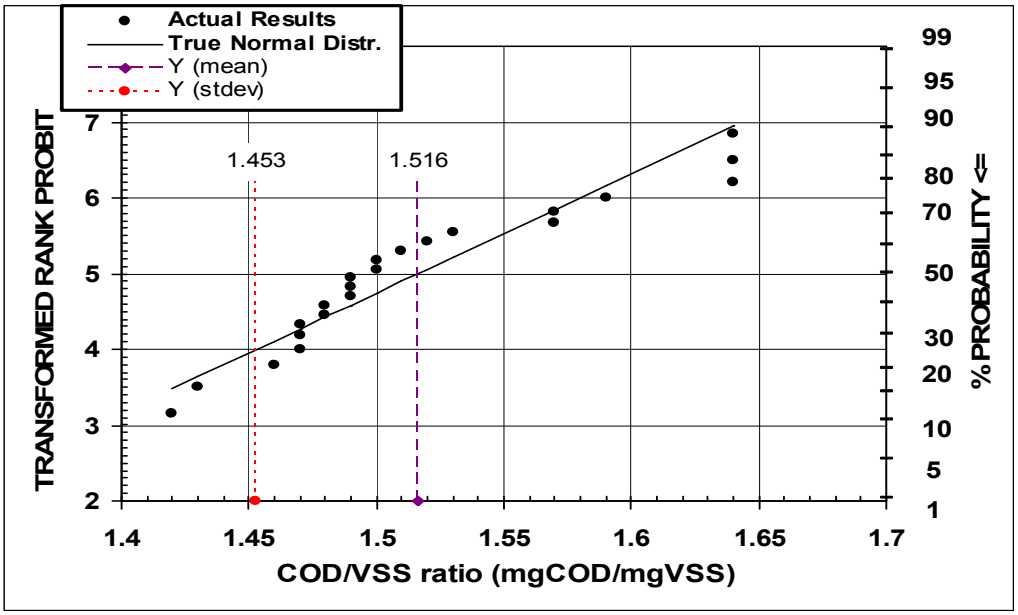

Fig. 3.7 (b): Statistical plot of COD/VSS ratio for parent system in 2004 fed with wastewater from Isipingo.

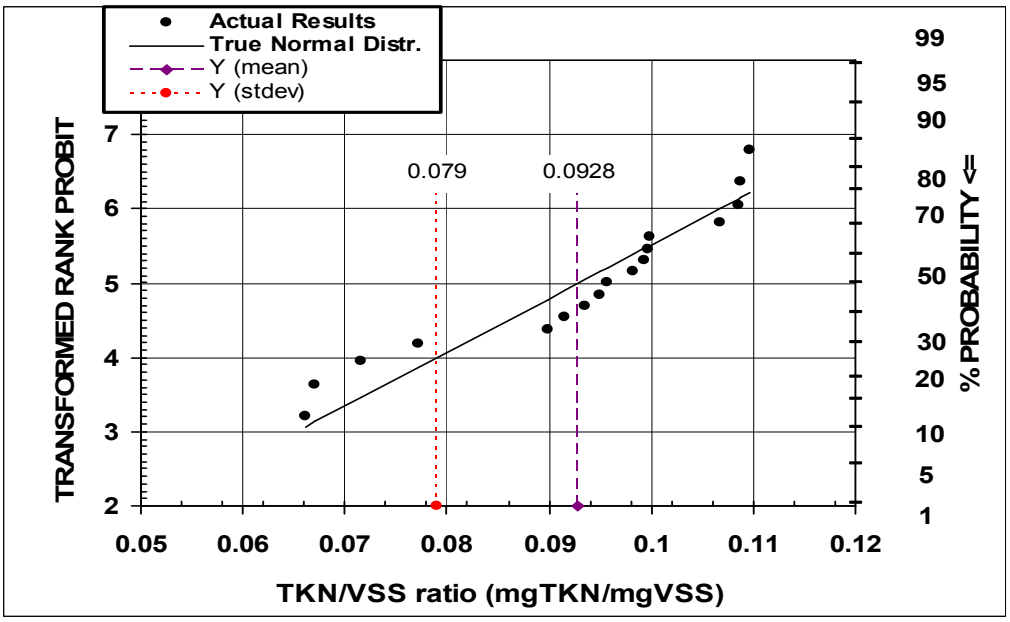

Fig. 3.8 (a): Statistical plot of TKN/VSS ratio for parent system in 2003 fed with wastewater from Southern Works.

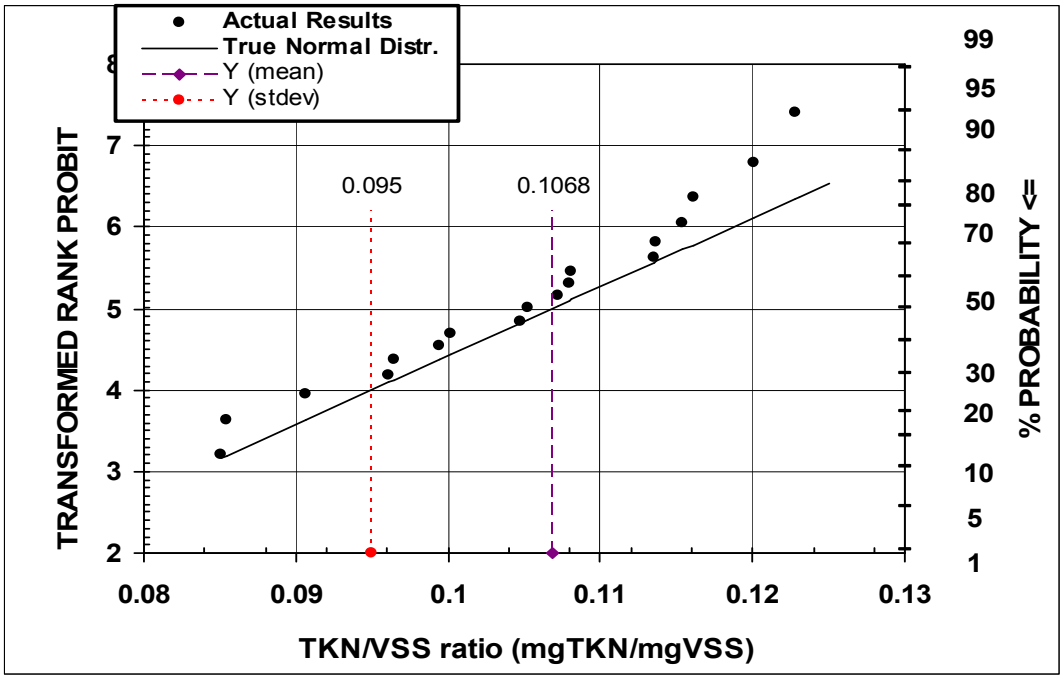

Fig. 3.8 (b): Statistical plot of TKN/VSS ratio for parent system in 2004 fed with wastewater from Isipingo.

Three independent measurements were made on the mixed liquor organic solids, volatile suspended solids (VSS), COD and TKN. To verify reliability of these measurements, the ratios of COD/VSS (f_{cv}) and TKN/VSS (f_N) for the parent system mixed liquor were calculated for each WW batch in 2003 and 2004 (Table 3.4 and 3.6, respectively). Statistical plots for these ratios were constructed (Fig. 3.7 and Fig. 3.8). The means for COD/VSS ratio were 1.49 ± 0.022 and 1.52 ± 0.065 for 2003 and 2004 systems respectively. The means for TKN/VSS ratio were 0.0928 ± 0.014 and 0.1019 ± 0.0155 for 2003 and 2004 systems respectively.

3.4.2 Microbial community analysis

The detectability of bacteria by FISH is dependent on their ribosomal content and consequently on their physiological state (Amann *et al.,* 1995). The microbial composition and diversity in the parent anoxic/aerobic activated sludge system conducted

during 2004 was analysed using FISH. The EUB probe mix (Table 3.2) was used to assess the overall physiological state of bacterial sludge communities with respect to viability and activity. In the sludge samples taken at different intervals within each WW batch for the aerobic zone, the percentages of bacterial cells giving a clear fluorescence signal after hybridization varied between 69.40% (±4.21%) and 89.13% (±4.25%) of all DAPI-stained cells (Fig. 3.9). *In situ* probing of activated sludge samples from the anoxic zone yielded 68.97% (±5.15%) to 98.56% (±2.87%) of detectable cells (Fig 3.9).

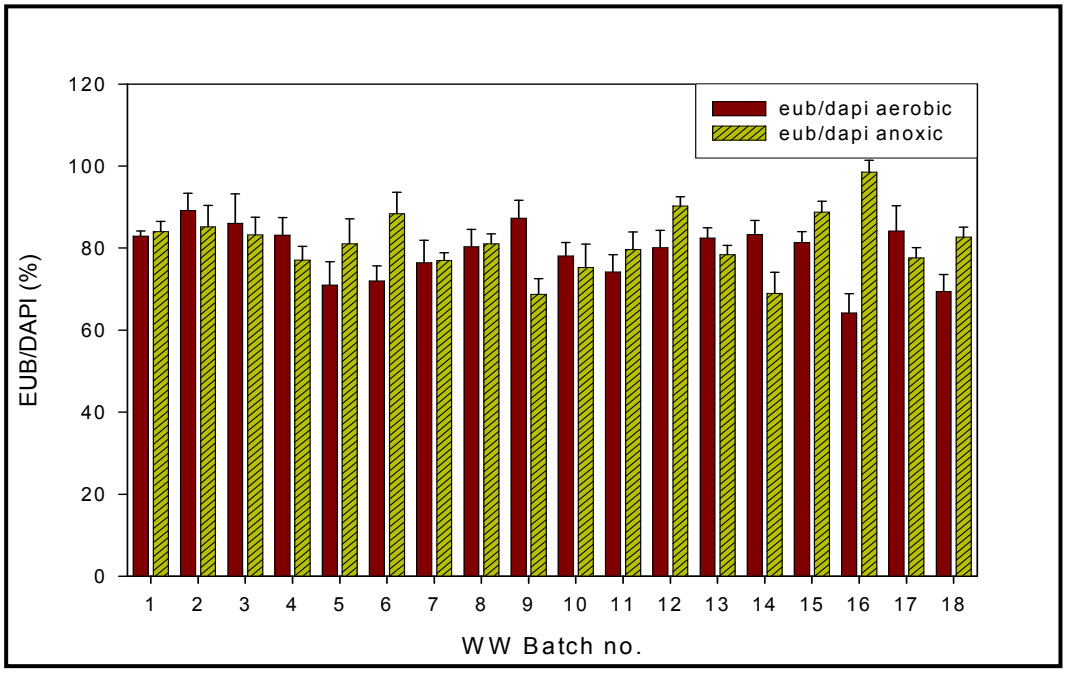

Fig. 3.9: Percentages of EUB-detectable cells relative to DAPI counts in WW batch samples taken from the parent system conducted in 2004.

FISH analysis was also performed to characterize the overall phylogenetic composition and diversity of the microbial population in the parent system. The probes applied covered only the group-specific probes (α-, β-, and γ- subclass of *Proteobacteria*) in order to assess the overall performance of the parent system. Cells hybridizing with probe BET42a in the aerobic and anoxic zones accounted for 26.09% (±3.15%) to 40.25% (±2.21%) and 10.75% (±0.37%) to 20.18% (±0.54%) of the cells detectable with EUB, respectively (Fig 3.10 and Fig 3.11).

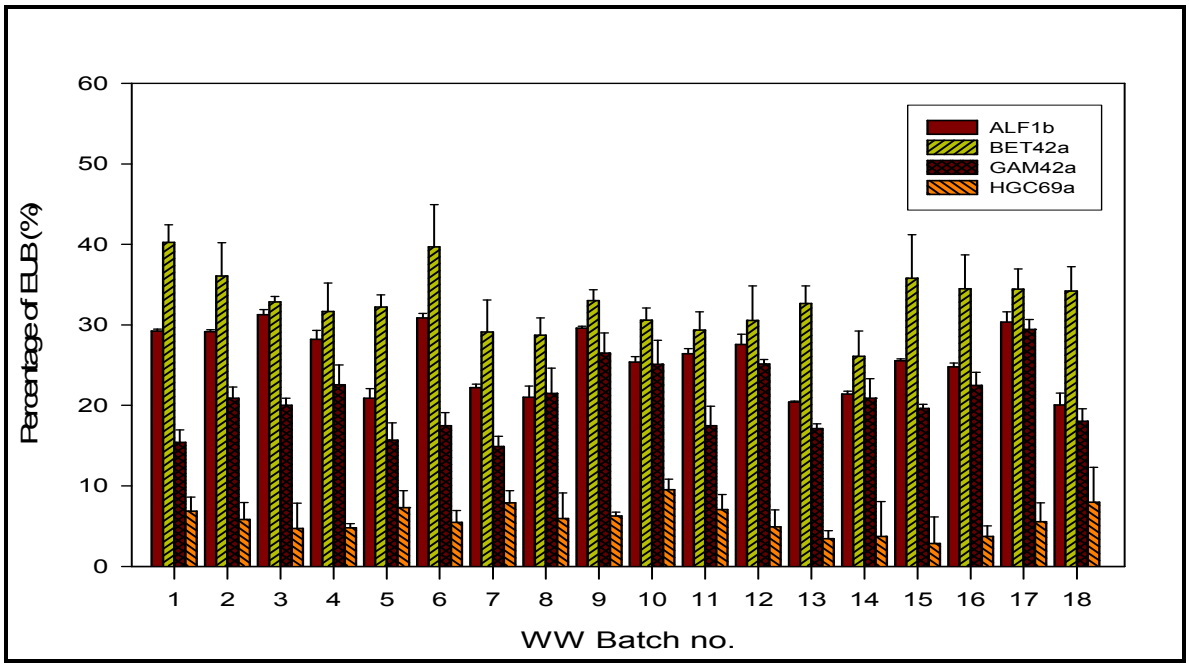

Fig. 3.10: Percentages of Group-specific probes relative to EUB counts in WW batch samples taken from the aerobic zone of the parent system conducted in 2004.

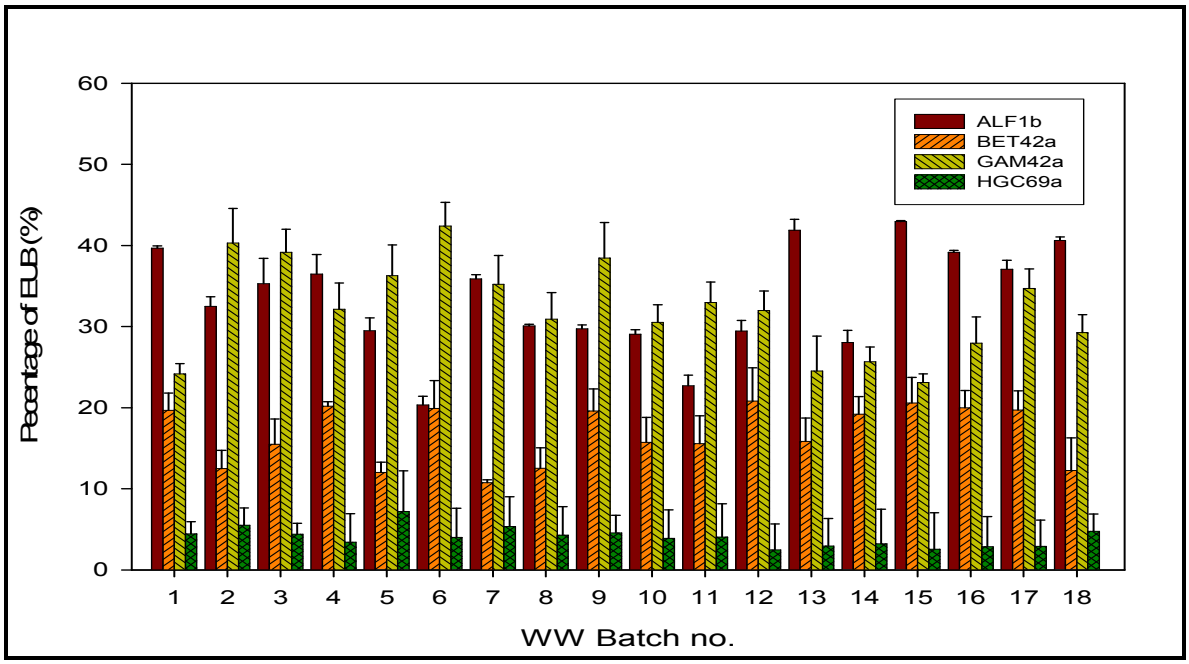

Fig. 3.11: Percentages of Group-specific probes relative to EUB counts in WW batch samples taken from the anoxic zone of the parent system conducted in 2004.

Bacteria affiliated to the α- subclass of *Proteobacteria* represented 20.05% (±1.47%) to 31.27% (±0.65%) and 20.33% (±1.1%) to 42.97% (±0.12%) of cells detectable by EUB in the aerobic and anoxic zones respectively. With probe GAM42a, specific members of the γ- subclass of *Proteobacteria*, 14.89% (±1.28%) to 29.43% (±1.24%) and 23.12% (±1.06) to 42.41% (±2.89) of hybridized EUB cells could be detected in the aerobic and anoxic zones respectively. Probe HGC69a, which is complementary to a 23S rRNA signature of bacteria with a high DNA G+C content, accounted for 2.84% (±3.29) to 9.49% (±1.34) and 2.46% (±3.2%) to 7.21% (±5.02) of the total number of cells hybridized with EUB in the aerobic and anoxic zones respectively (Fig 3.10 and Fig 3.11).

3.5 Discussion

3.5.1 COD and nitrogen mass balances

For the parent system operated in 2003, COD and N mass balances were in the acceptable range of 90% to 110% (Fig. 3.3a and b respectively). However of the 22 WW batches in 2004 the N mass balances for WW batches 2 and 7 exceeded 110% (Fig. 3.4a), while the COD mass balance were below 90% for the same WW batches. For these sewage batches, the nitrate concentrations in the aerobic reactor and effluent were high as compared to preceding and subsequent sewage batches (Table 3.5a). Large sample dilutions were used in the analytical procedure for nitrate, thus making it more susceptible to dilution errors. For this reason, the nitrate concentrations of the aerobic reactor and effluent seemed to have been overestimated, resulting in high N mass balances.

Three independent measurements were made on the mixed liquor organics solids, volatile suspended solids (VSS), COD and TKN. To verify the reliability of these measurements, the ratios of COD/VSS and TKN/VSS for the parent system mixed liquor were calculated for each WW batch (Table 3.6). Statistical plots for these ratios were constructed (Figs.

3.7b and 3.8b) to determine the distribution of the data. From the statistical plots it is evident that the data are normally distributed; this indicates that (i) an infinite number of parameters had an influence on the measurements (ii) each influence was small and (iii) no single factor has had a dominating influence on the measurements. Accordingly, it can be accepted that the errors in the COD mass balances do not lie in the measurement of the mixed liquor organic solids. Taking account of the above, it would appear that the main source of error in the COD mass balances lies in the measurement of OUR. Thus the measurement of OUR is critical for good COD mass balances. Batch tests conducted with WW batches that resulted in having poor COD and N mass balances were rejected.

3.5.2 Unbiodegradable soluble ($fs_{,us}$) and particulate ($fs_{,up}$) COD fractions

From the statistical plots for both Southern works (Fig. 3.5a) and Isipingo (Fig. 3.5b) raw wastewater the data were normally distributed giving mean $fs_{,us}$ values of 0.0721 (±0.012) and 0.0902 (±0.008) respectively. The mean $fs_{,us}$ values obtained for both the parent systems are similar and this could be attribute to the same COD feed concentration entering these systems (±500 mgCOD/L) (Lee *et al*., 2003). The mean $fs_{,us}$ values obtained for both Southern works and Isipingo raw wastewater were in the range of acceptable values of 0.04- 0.10 mgCOD/mgCOD for municipal raw wastewaters in South Africa (WRC, 1984).

The $fs_{,up}$ data for wastewater batches obtained from Southern Works and Isipingo were analysed using a statistical plot (Figs. 3.6a and 3.6b respectively). From the statistical plots for both Southern works and Isipingo raw wastewater the data were normally distributed giving mean $fs_{,up}$ values of 0.1781 (±0.034) and 0.1667 (±0.047) respectively. The mean $fs_{,up}$ values obtained for both parent systems are similar, this could also be attributed to the same feed COD concentration entering these systems (±500 mgCOD/L) (Lee *et al*., 2003). The mean $fs_{,up}$ values obtained for both Southern works and Isipingo raw wastewater were in the range of acceptable values of 0.07- 0.20 mgCOD/mgCOD for municipal raw wastewaters in South Africa (WRC, 1984).

3.5.3 Microbial community analysis

Microbial community composition of parent anoxic/aerobic activated sludge system conducted in 2004 was analysed using FISH. On a division level, the microbial composition of the aerobic (Fig. 3.10) and anoxic (Fig. 3.11) zones showed the dominance of *Proteobacteria* (α-, β-, and γ- subclass) which accounted for 82.3% (±1.3%) and 79.2% (±2.1%) respectively. Proteobacteria has been recognized as the key division in municipal wastewater treatment systems (Wagner *et al*., 1993; Wagner *et al*., 1994; Snaidr *et al*., 1997). Fluorescently labeled oligonucleotide probes were used for the *in situ* enumeration of important phylogenetic groups (α-, β-, and γ- subclass of *Proteobacteria*) in the aerobic and anoxic zones. On this level, the community structure in the samples from the aerobic zone differed to a samples taken from the anoxic zone. FISH analyses revealed β-subclass *Proteobacteria* to constitute the predominant group of bacteria with the sludge community of the aerobic reactor (Fig. 3.10). A numerical domination of β- *Proteobacteria* has been observed in many natural and made habitats, such as drinking water (Kalmbach *et al*., 1997) and activated sludge (Wagner *et al.*, 1993; Manz *et al.,* 1994). In the anoxic reactor rRNA molecules hybridizing with probes ALF1b and GAM42a were more frequent than molecules hybridizing with probes BET42a and HGC69a (Fig. 3.11). Application of group-specific probes showed different intensities of bacterial community composition in the aerobic and anoxic zones. Interestingly, the relationship between bacterial production, activity, and microbial community structure in samples from the aerobic zones differs from the observations in the anoxic reactor. The distinctive difference in the dominant bacterial groups present in the aerobic and anoxic zone reflects the diversity of organisms in the parent system. Importantly, it has to be considered that in each of the different compartments in a modern BNR plant, only a particular fraction of the biomass will be active, but all of the biomass is exposed to all conditions repeatedly (Wilderer *et al*., 2002). Operation assessment via microscopic sludge investigation affords sophisticated, methods of observation and interpretation.

Besides providing phylogenetic information, FISH can be used to assess the physiological state of single bacterial cells (Kalmbach *et al*., 1997). In conventional activated sludge, substrate degradation is coupled to biomass growth, i.e. the cells gain excess energy for anabolic reactions. As a consequence of high cellular rRNA contents, generally 70-90% of cells stained by DAPI were also detectable by FISH (Wagner *et al.*, 1993; Manz *et al.,* 1994). In the aerobic and anoxic reactor sludge, 81.4% (±3.6%) and 79.2% (±4.2%) respectively, of cells contained enough rRNA molecules for visualization by FISH (Fig. 3.9). The results obtained for the parent system aerobic and anoxic zones were in agreement with those previously found in conventional activated sludges. Cells with low rRNA contents are often associated with dormant, starved, or very slowly growing cells, all representing stages of low metabolic activity but are known to actively participate in metabolic transformations (Witzig *et al*., 2002).

Recently, it was shown that several members of the two environmentally important bacterial phyla *Planctomycetales* and *Verrucomicrobia* could not be detected by probe EUB338 (Daims *et al*., 1999). These bacteria may account for an unknown fraction of DAPI stained cells which are not visualized by *in situ* hybridization. In this study, however, additional hybridization experiments with the probe set recommended by Daims *et al.* (1999) did result in increasing probe specific cell counts, indicating that *Planctomycetales* and *Verrucomicrobia* were present in significant numbers.

3.5.4 Reactor performance versus microbial monitoring

The microbial community structure was continuously monitored throughout the duration of the parent aerobic/anoxic activated sludge system using FISH. The aerobic and anoxic reactors were individually monitored to establish the diversity in microbial consortia present and reflected steady state behaviour in the parent system. FISH analyses with group-specific probes revealed consistencies in the microbial composition in all wastewater batches, which were evident in the aerobic and anoxic zones. In order to define steady state behavior in the parent system COD and nitrogen mass balances were applied. Mass balance equations include kinetic and stoichiometric parameters that allow

descriptions of biomass growth, biomass decay, substrate utilization, hydroloysis etc. Mass balance results for the parent system were in the acceptable range of 90-110%, except for batches 2 and 7 which exceeded the N mass balance range. This was mainly due to the high aerobic nitrate levels. Similarly, microbial population dynamics was monitored in the aerobic and anoxic zones; consistencies in group-specific probe frequencies were suggestive of steady state behaviour. However, group-specific probes provided low resolution monitoring of microbial community structure in the parent system.

In order to assess the microbial community composition, structure and stability in relation to steady state behaviour, a more comprehensive set of specific oligonucleotide probes on a population (species) level must be applied. This would enable high resolution analyses and rapid monitoring of population shifts as early indicators of upcoming malfunctions in wastewater treatment systems, so that corrective measures could be implemented in time.

3.6 Conclusion

A thorough knowledge of the bacterial populations responsible for a functioning activated sludge process can only originate from the combination of different approaches. In this chapter the principal applicability of *in situ* hybridization with fluorescent labeled rRNA-targeted oligonucleotides was demonstrated. Group-specific nucleic acid probes facilitated monitoring of the microbial composition in a steady state parent activated sludge system. The characteristic difference in the bacterial communities present in the aerobic and anoxic zone confirms the diversity of organisms present in the parent system. This information is useful for the monitoring of the activated sludge processes because it was found that the zones have unique bacteria proliferating in them even though there is a continuous established flow rate of the influent that enters the system to the effluent that leaves the system. The consistency in the parent system data lends support to application of the steady state design procedure in determining theoretical and measured OHO active biomass concentrations in the parent system and batch test, respectively (Chapter 4).

CHAPTER 4

Integrating Molecular Biology and Modeling to Determine the Heterotrophic Active Biomass

4.1 Introduction

Current mathematical models describing the behavior of the activated sludge process are not based on the direct measurement of the different components comprising the biomass. Current techniques incorporating aspects of molecular biology and microbiology are making it possible to quantify the key microbial group's active in the process, with a view to improving the process description and design.

Historically the mixed liquor organic suspended solids (MLOSS) have been measured as a lumped parameter, via the VSS or COD test (Standard Methods, 1985). Specific rates for these biological processes (denitrification; oxygen utilization) are often expressed in terms of this lumped parameter, but only part of the MLOSS, the heterotrophic active biomass (Z_{BH}) is responsible for mediating the biological processes for COD removal and denitrification (Wentzel *et al*., 1998).

The batch test procedure developed by Kappeler and Gujer (1992) presented a means of quantifying the Z_{BH} concentration through monitoring the organisms OUR response with time in a batch reactor. This procedure was extended by Wentzel *et al*. (1995), Ubisi *et al*. (1997a, b) Cronje *et al*. (2002) and Lee *et al*., (2003) to quantify the heterotrophic active biomass concentration drawn from aerobic and anoxic/aerobic activated sludge systems. In the research of Ubisi *et al*. (1997 a,b) and Wentzel *et al*. (1998), the measured and theoretical Z_{BH} concentrations of mixed liquor from the 12d sludge age parent system showed a close 1:1 correlation while those for mixed liquor from the 20d sludge age parent system showed poor correlation. Ubisi *et al*. (1997a, b) and Wentzel *et al.* (1998) did not provide any explanation for this inconsistency. In the investigation of

Cronje *et al*. (2002) on mixed liquor drawn from a 10 day sludge age parent system, a reasonably close 1:1 correlation was found. In contrast, in the investigation of Beeharry *et al*. (2001) on mixed liquor from 10 day sludge age parent system, the correspondence line between measured and theoretical Z_{BH} fell parallel to the 1:1 correspondence. Lee *et al*. (2003) investigation on mixed liquors from 10 and 20 day sludge age parent systems found similar correspondence to that of Beeharry *et al.* (2001). To explain these observations, Novak *et al.* (1994) proposed that the batch conditions may favour growth of sections of Z_{BH} population (e.g fast growing Z_{BH}), causing the community structure to change with time in the batch test. This change in community structure will effect a change in the observed response, which is not taken into account in the batch test analysis.

Parallel to the developments in the engineering and technology of the activated sludge system, significant advances have been made in the microbiological and biochemical areas. Fluorescent *in situ* hybridization (FISH) with rRNA-targeted nucleic acid probes is a new molecular tool for rapid, reliable and cultivation-independent monitoring and quantification of phylogenetically defined bacterial populations in activated sludge samples (Amann *et al*. 1995). The detectability of bacteria by such oligonucleotide probes is not only dependant on the penetration of the labeled probes into cells but also on the ribosome contents and consequently on the growth rates of cells (DeLong *et al*., 1989). Because substantial portions of the 16S rRNA sequences are similar among all known organisms, low stringency hybridization permits the identification of rRNA genes from unknown organisms and thus can be used as targets for hybridization probes with various specificities. The ubiquity of the rRNA ensures that the probes can be designed to identify virtually any organism or group related organisms (Amann *et al*. 1995). The application of this technique allows for the detection and quantification of actively growing microorganisms with relatively high cellular rRNA content.

The engineering and technology paradigm (modeling) has largely worked independently of the molecular biology paradigm. To facilitate links and overlap between the two paradigm sets, the new developments in the molecular biology analytical techniques

(FISH) can be implemented to address the deficiency in the engineering and technology paradigm of the active biomass concept. This should prove possible because, in contrast to the more traditional analytical techniques, the new techniques provide quantitative information, a prerequisite for modeling. Some initial integration between modeling and these techniques has been initiated (Urbain *et al*., 1998; Wagner *et al*., 1998; Vogelsang *et al*., 2002; Gao *et al*., 2004), but this is still in its infancy.

In this chapter respirometric batch test were applied to mixed liquors drawn from a well defined parent anoxic/aerobic activated sludge system (Chapter 3) in order to quantify the Z_{BH} concentrations. Similarly fluorescent labeled, 16S rRNA-targeted oligonucleotide probes specific for ammonia and nitrite oxidizers were used in combination with DAPI staining to validate the Z_{BH} active biomass component in activate sludge respirometric batch tests. For the direct enumeration and simultaneous *in situ* analysis of the distribution of nitrifying bacteria, *in situ* hybridization with oligonucleotide probes were used. Probes (NSO 1225, NSR 1156 and NIT3) were used to target the nitrifiers and the universal probe (EUB MIX) was used to target all Eubacteria. Deducting the lithoautotrophic population from the total bacteria population revealed the Z_{BH} population in the modified batch test. The modified batch test method is used to correlate heterotrophic active biomass concentrations to results comparable to molecular probing. This provides a platform to employ suitable alternative technology to evaluate the heterotrophic active biomass component of activated sludge.

4.2 Materials and Methods

4.2.1 Wastewater preparation

The preparation of the wastewater for the modified batch test incorporates flocculating and filtering the raw wastewater. The raw wastewater was drawn from the storage tanks and diluted to the same concentration as the feed for the parent system (500 mgCOD/L).

4.2.2 Flocculation/settling

A volume of 10 ml of stock AL $(SO_4).15H_2O$ (50g/L) was added per L wastewater, the mixture was stirred rapidly (~200rpm) for 2 minutes (rapid mix phase) and then slowly (~1rpm) for 30 minutes. The mixture was allowed to settle for a further 30 minutes.

4.2.3 Filtration

The clear supernatant that developed in the settling cylinders was drawn off and filtered through a 0.45 μm glass fibre filter (Whatman's GF/C). The flocculated-filtered wastewater was stored overnight in a cold room at 4ºC.

4.2.4 Filtered wastewater and mixed liquor batch test

As described above, the modified batch tests were conducted using a mixture of flocculated-filtered wastewater and the mixed liquor drawn from the parent system. The single batch reactor configuration is illustrated in Fig. 4.1.

The required volume of flocculated-filtered wastewater was measured, preheated to 20ºC in a warm water bath and placed in a continually stirred batch reactor maintained at a constant temperature of 20ºC. The pH of the flocculated-filtered wastewater was raised to 7.5 by adding sodium bicarbonate ($NaHCO_3$) prior to the commencement of the batch test. The required volume of mixed liquor was harvested from the aerobic reactor of the parent system and added to flocculated-filtered wastewater, giving a combined volume of 5 L for the mixture in the batch reactor. Immediately after the mixed liquor was added to the flocculated-filtered wastewater, a sample was drawn to obtain the initial total COD concentration (Standard Methods, 1985). The oxygen supply and OUR response in the batch test were measured using an automated technique (Randall *et al*., 1991). At regular intervals, samples were drawn from the batch reactor, immediately filtered through 0.45μm filter paper, 2-3 drops of $HgCl_2$ (sample preservation) were added to the filtrate which was stored for subsequent nitrate and nitrite analysis. At the end of the batch tests,

the contents of the batch reactor were homogenized in a liquidizer, a sample drawn and the final COD concentration measured. The OUR results were downloaded from the DO meter to a computer.

4.2.5 Sampling, cell fixation and sonication

A grab sample of mixed liquor was collected at the start of each batch test and fixed for 1.5 hr at 4ºC with 4% paraformaldehyde (Appendix 4). Cells were fixed by the addition of three volumes of fixative to one volume of sample. Cells were then washed in 1x PBS (130 mM NaCl, 10 mM sodium phosphate buffer, pH 7.2) and then resuspended in PBS/cold absolute ethanol (1:1 v/v). For the detection of gram-positive prokaryotes samples were fixed with a 1:1 mixture of PBS and absolute ethanol (v/v) (Amann, 1995). Fixed samples were then sonicated with Virsonic 100 sonicator (Virtis, USA), to break up the flocs. Sonication was carried out at 8 watts for 6 minutes (Appendix 4).

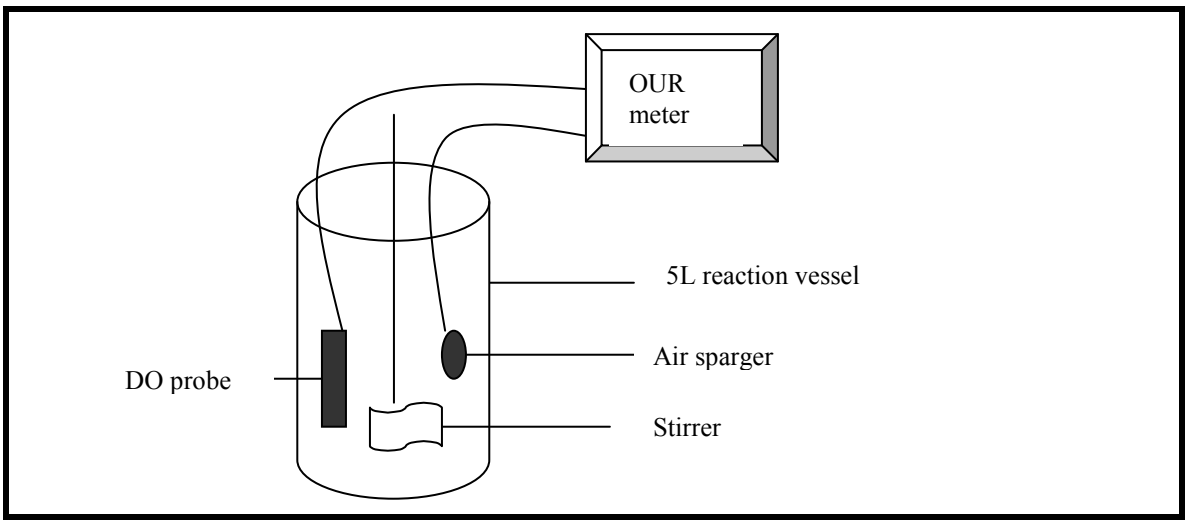

Fig. 4.1: A schematic representation of a single batch reactor used to conduct batch tests with mixed liquor added to flocculated-filtered wastewater.

4.2.6 Membrane filtration and staining with DAPI

Membrane filtration was carried out as described by Porter and Feig (1980) with the following modification. Cellulose acetate (Millipore, 0.22 µm pore size, 25 mm diameter) filters were stained for 24 h in Sudan Black (0.3% w/v in 60% ethanol) (Appendix 5). Dual staining of cells with DAPI and fluorescent oligonucleotides was modified from the method of Hicks *et al*. (1992) so that cells were stained after *in situ* hybridization with DAPI (0.25 µg/ml) for 5 minutes (Appendix 7).

4.2.7 Oligonucleotide probes and hybridization

Oligonucleotides probes used during the present study are shown in Table 4.1. A volume of 10 µl of sonicated sample was spotted onto pretreated slides (Appendix 6) and allowed to dry. Spotted cells were then dehydrated by serial immersions through 60%, 80% and 96% (v/v) ethanol (3 minutes each). Samples of 10 µl hybridizations solution (0.9M NaCl, 20 mM Tris/HCl, pH 7.2, 0.01% SDS, 50 ng probe, X% (v/v) formamide) were applied to each spot and incubated for 2 h at 46ºC in an isotonically equilibrated humidity chamber (Appendix 7). Probe was removed from the slide by rinsing in 2ml pre-warmed washing solution (20 mM Tris/HCl, 0.01% SDS, 5 mM EDTA, YM NaCl). The salt concentration and formamide concentration was adjusted according to the formula of Lathe (1985). Unlabeled competitor oligonucleotides probes were used in equimolar amounts. Results with all probes used for the quantification were corrected for non-specific binding according to results with NON338 as a negative control. Slides were rapidly transferred into washing solution and incubated at 48ºC for 20 minutes. Slides were then rinsed briefly with distilled water, air-dried and mounted in Mounting media antifading solution (Bio-Rad, USA) for viewing by microscopy.

4.2.8 Microscopy and image analysis

Cells were visualized with a Zeiss Axiolab microscope (Carl Zeiss, Germany) fitted for epifluorescence with a 50W mercury high-pressure bulb and Zeiss filter sets 02, 09 and

15. Images were captured using a Hamamatsu (Japan) CCD camera. Microscopic fields (n = 30) under the 100X objective were randomly selected for enumeration

Table 4.1: Probe sequences and formamide percentages for *in situ* hybridization

Probe	Sequence	% F[1]	fluor	Reference
EUB 388	5'- GCT GCC TCC CGT AGG AGT -3'	20	Fluorescein	Amann *et al*., 1990b
EUB 388 -II	5'- GCA GCC ACC CGT AGG TGT -3'	20	Fluorescein	Daims *et al*, 1999
EUB 388-III	5'- GCT GCC ACC CGT AGG TGT -3'	20	Fluorescein	Daims *et al*, 1999
NON388	5'- ACTCCTACGGGAGGCAGC-3'	20	Fluorescein	Manz *et al.,*1992
NIT 3	5'- CCT GTG CTC CAT GCT CCG - 3'	40	Fluorescein	Wagner *et al*., 1996
CNIT 3	5'- CCT GTG CTC CAG GCT CCG -3'	40	unlabeled	Wagner *et al*., 1996
NSR 1156	5'- CCC GTT CTC CTG GGC AGT -3'	30	Fluorescein	Schramm *et al*., 1999
NSO 1225	5'- CGC CAT TGT ATT ACG TGT GA -3'	35	Fluorescein	Mobarry *et al*., 1996

EUB 388, EUB 388-II and EUB 388-III were collectively used in equimolar concentrations and referred to as EUB MIX

[1] percentage formamide (v/v) in the hybridization buffer

4.3 Data Interpretation

Calculation procedures for the modified batch test developed by Wentzel *et al*. (1995) and Mbewe *et al*. (1995) are detailed in this section. The batch test was analyzed to determine the following:

- COD recovery (%)
- OHO active biomass concentration at the start of the batch test, $Z_{BH\ (0)}$ (mgCOD/L)
- RBCOD, μ_H (/d) and
- SBCOD, K_{mp} (/d)

To evaluate the measured OHO active biomass concentration determined in the batch test, the theoretical values for the parent system from which the mixed liquor was drawn were calculated. The steady state theory (WRC, 1984) for anoxic/aerobic activated sludge system was used to calculate the theoretical OHO active biomass concentration in the parent system, which was compared to the batch test measured concentrations. To illustrate the calculation procedures for the modified batch tests, data from one batch test (Batch test no. B1/03, Sewage batch no. 13) was extracted and used in the following sections.

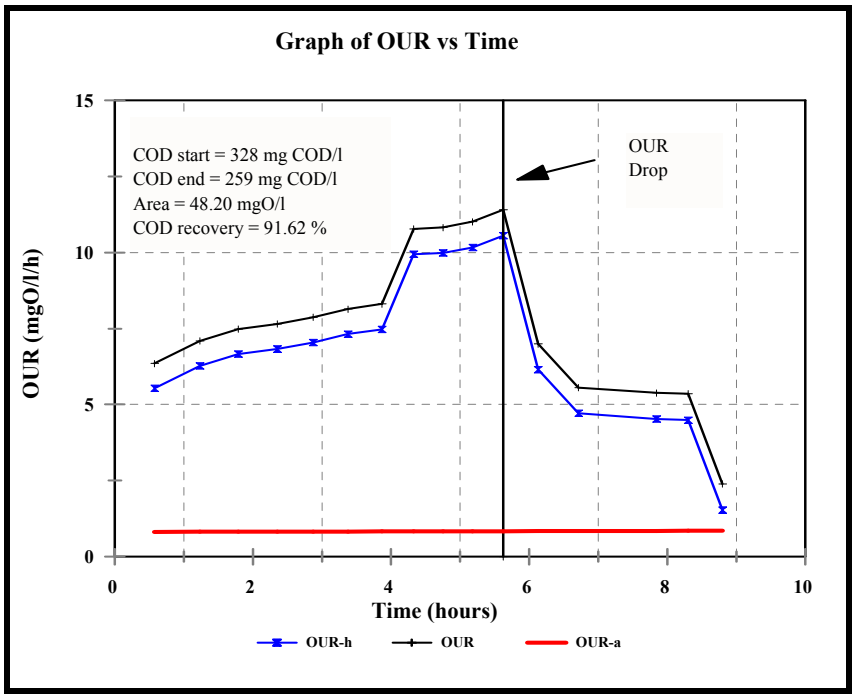

Fig 4.2: Oxygen Utilization Rate (OUR) response with time for a modified batch test on mixture of flocculated- filtered wastewater (4.5 L) and mixed liquor (0.5 L) drawn from the aerobic reactor. Batch Test No. B1/03, Sewage Batch No. 13.

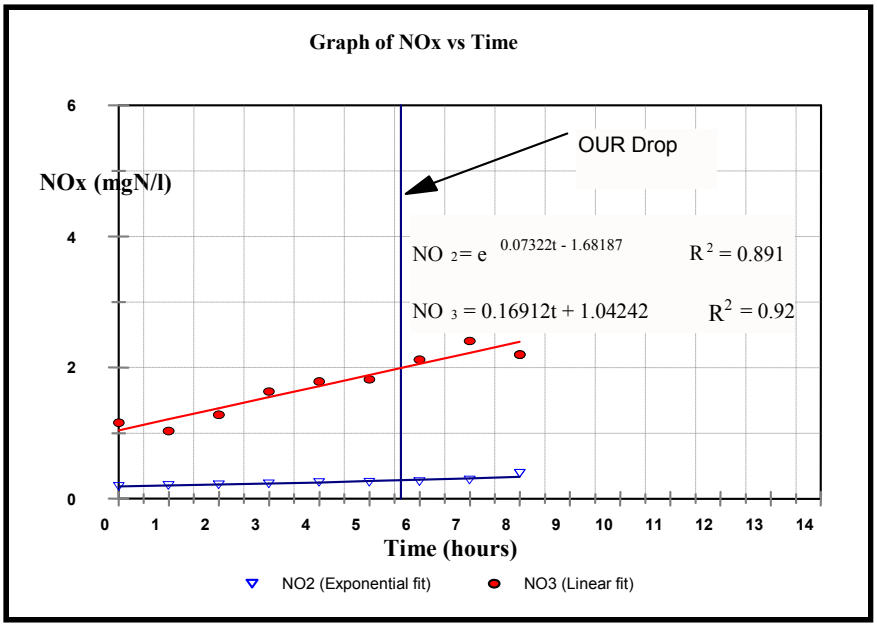

Fig 4.3: Nitrate and nitrite concentrations with time for modified batch test B1/03.

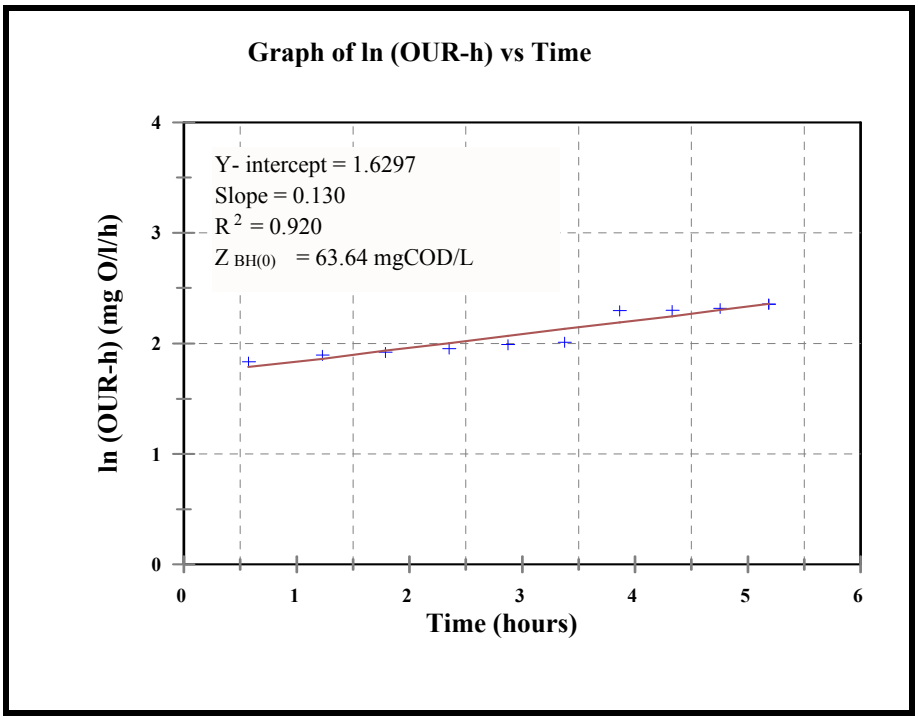

Fig 4.4: Ln OUR due to OHO active biomass versus time for OUR data up to the precipitous drop in OUR, in batch test B1/03.

4.3.1 Batch test data

4.3.1.1 Separating the OUR into it's OHO and nitrification components

In a batch test, mixed liquor is drawn from a nitrifying activated sludge system and thus nitrification can be expected and observed. The OUR due to nitrification must be taken into account in deriving estimates for %COD recovery and $Z_{BH(0)}$ since both parameters are determined from the OUR for OHOs only ($OUR_{H(t)}$). This can be done by noting that the measured OUR at any time t ($OUR_{M(t)}$) is made up of the OUR due to OHO growth ($OUR_{H(t)}$) and due to nitrification by autotrophic organisms (AO) ($OUR_{N(t0)}$, i.e.

$$OUR_{M(t)} = OUR_{H(t)} + OUR_{N(t)} \quad \text{(mgO/L/h)} \quad (4.1)$$

Rearranging Eq. (4.1):

$$OUR_{H(t)} = OUR_{M(t)} - OUR_{N(t)} \quad \text{(mgO/L/h)} \quad (4.2)$$

Accordingly, to determine $OUR_{H(t)}$, an estimate for $OUR_{N(t)}$ is essential. The $OUR_{N(t)}$ can be determined from the nitrite/nitrate concentration – time profile. In determining $OUR_{N(t)}$ from the nitrate concentration – profile, Ubisi *et al*. (1997a,b) noted that for the batch tests, ammonia-N is available in excess and nitrification proceeds at the maximum rate. Furthermore, they noted that since the yield and maximum specific growth rate of AOs are relatively low, the nitrification rate can be assumed to be constant within the time scale of the batch test. Accepting a constant nitrification rate slope of a "best fit" linear line to the nitrate (mgN/l) time profile (h) is the constant nitrification rate ($\Delta NO_3^-/\Delta t$, mgN/l/h), and the $OUR_{N(t)}$ is given by:

$$OUR_{N(t)} = 4.57 \bullet (\Delta NO_3^-/\Delta t) \quad \text{(mgO/L/h)} \quad (4.3)$$

However, Cronje (2000) proposed that the nitrification rate is not constant, but is approximated by an exponential fit to the measured NO_3^- concentration time – data. From such an exponential fit, the nitrification rate can be found at each time interval from the slope of the exponential equation, i.e. from the differential of the exponential equation and the corresponding $OUR_{N(t)}$ determined via eq. (4.3).

Beeharry *et al*. (2001) suggested that the nitrite concentrations should also be considered, since a detectable amount of nitrite was also generated in all batch tests. He also recommended that the nitrite/nitrate concentrations could be best represented by either linear or an exponential increase.

In this investigation, similarly to Beeharry *et al*. (2001) and Lee *et al*. (2003) significant nitrite concentrations were observed in the batch tests (Fig. 4.3). Therefore separate

nitrite and nitrate nitrification had to be taken into account. To accommodate both nitrite and nitrate nitrification, the following stiochiometry was accepted:

$$NH_4^+ + {}^3/_2\, O_2 \rightarrow NO_2^- + H_2O + 2H^+ \quad (4.4)$$

$$NO_2^- + {}^1/_2\, O_2 \rightarrow NO_3^- \quad (4.5)$$

From the stoichiometric equations above, for every 1mg NH_4^- - N nitrified to 1 mg NO_2^- - N, 3.43 mg O are required and for 1 mg NO_2^- - N nitrified to 1 mg NO_3^- - N, 1.14 mg O are required. Thus, for nitrification of NH_4^+ - N to NO_3^- - N, 4.57 mgO/mgN are required.

In Fig. 4.3, nitrite and nitrate concentrations were separated and "best fit" lines fitted to the individual profiles, linear or exponential were evaluated. From the regression analysis of the data in Fig. 4.3, the following were obtained:

$$NO_{2(t)} = e^{0.07322t - 1.68187} \quad [R^2 = 0.891] \quad (mgN/l) \quad (4.6)$$

$$NO_{3(t)} = 0.16912t + 1.04242 \quad [R^2 = 0.92] \quad (mgN/l) \quad (4.7)$$

Hence, differentiating the equations to determine an expression for the appropriate nitrification rate yields for batch test no. B1/03:

$$d(NO_2^-)/dt = 0.07322 \bullet e^{0.07322t - 1.68187} \quad (mgN/l/h) \quad (4.8)$$

$$d(NO_3^-)/dt = 0.16912 \quad (mgN/l/h) \quad (4.9)$$

From the individual profile fits, the OUR for NO_2^- nitrification (OUR_{NO2}) and NO_3^- nitrification (OUR_{NO3}) could be determined:

$$OUR_{NO2} = 3.43 \bullet (d(NO_2^-)/dt) \quad (mgO/l/h) \quad (4.10)$$

$$OUR_{NO3} = 4.57 \bullet (d(NO_3^-)/dt) \quad (mgO/l/h) \quad (4.11)$$

$$OUR_N = OUR_{NO2} + OUR_{NO3} \quad (mgO/l/h) \quad (4.12)$$

OUR_N was subtracted from the measured OUR_M (Fig. 4.2) at each time interval, to give the OUR_H for OHOs only (Fig. 4.3).

4.3.1.2 Derivation of equations for COD recovery

The acceptability of data from the batch test can be evaluated by doing a COD mass balance, as follows (Wentzel *et al.*, 1995)

$$\% \text{ COD Recovery} : = \frac{COD_{t=T} + \int_{t=0}^{t=T} OUR_{H(t)} \bullet dt}{COD_{t=0}} \bullet 100 \quad (4.13)$$

Where

t = time (h)

$COD_{t=T}$ = total unfiltered COD concentration at end of test (t=T) (mgCOD/l)

$COD_{t=0}$ = total unfiltered COD concentration at start of test (t=0) (mgCOD/l)

$OUR_{H(t)}$ = OHO active biomass oxygen utilization rate at time t (mgCOD/l)

$\int_{t=0}^{t=T} OUR_{H(t)} \bullet dt$ = integral area under the OHO OUR versus time plot between start and end of batch test (mgO/l)

= oxygen concentration consumed over the batch test by OHO active biomass

The integration of the $OUR_{M(t)}$ in the batch test can be calculated directly using an automated technique (Randall *et al.*, 1991). In Eq. (4.2), the OUR due to OHO growth

only ($OUR_{H(t)}$) equals the measured total OUR ($OUR_{M(t)}$) minus the OUR due to nitrification ($OUR_{N(t)}$). The $OUR_{N(t)}$ is made up of the nitrate and nitrite nitrification OURs (Eq. 4.12). Thus, the integration of the $OUR_{H(t)}$ can be calculated as follows;

$$\int_{t=0}^{t=T} OUR_{H(t)} \bullet dt = \int_{t=0}^{t=T} OUR_{M(t)} \bullet dt - \int_{t=0}^{t=T} OUR_{NO3(t)} \bullet dt - \int_{t=0}^{t=T} OUR_{NO2(t)} \bullet dt \qquad (4.14)$$

Using data in Fig. 4.2 and 4.3 as an example, $COD_{t=0}$ = 328 mgCOD/L; $COD_{t=T}$ = 259 mgCOD/L; T (time when the last sample is taken) = 8 h; and the expression developed above for OUR_{NO2} and OUR_{NO3}:

$$\int_{t=0}^{t=T} OUR_{M(t)} \bullet dt = 48.20 \text{ mgO/l}$$

$$\int_{t=0}^{t=T} OUR_{NO3(t)} \bullet dt = \int_{t=0}^{t=T} 0.7729 \bullet dt = 0.7729 \bullet T = 6.18 \text{ mgO/l}$$

$$\int_{t=0}^{t=T} OUR_{NO2(t)} \bullet dt = \int_{t=0}^{t=T} 0.2511 \bullet \exp(0.0732 \bullet t - 1.6819) \bullet dt$$

$$= 3.43 \bullet (e^{0.0732 \bullet T - 1.6819} - e^{-1.6819}) = 0.51 \text{ mgO/l}$$

$$\int_{t=0}^{t=T} OUR_{H(t)} \bullet dt = 48.20 - 6.18 - 0.51 = 41.51 \text{ mgO/l}$$

$$\% \text{ COD recovery} = \frac{259 + 41.51}{328} \bullet 100 = 91.62 \%$$

COD recoveries between 90 – 110 % indicate that the test results are acceptable.

4.3.1.3 Derivation of equations for OHO active biomass concentration, $Z_{BH(0)}$

From the simplified UCT model (Wentzel *et al*., 1995) to describe the process in the batch tests, the rate of growth of OHO active biomass (dZ_{BH}/dt) is given by:

dZ_{BH}/dt = growth on RBCOD + growth on SBCOD - death

$$\frac{dZ_{BH}}{dt} = \mu_{HT} \frac{S_{bs}}{K_{SH} + S_{bs}} \bullet Z_{BH} + K_{MPT} \frac{S_{ads}/Z_{BH}}{K_{SP} + S_{ads}/Z_{BH}} \bullet Z_{BH} - b_{HT} \bullet Z_{BH} \qquad (4.15)$$

where

Z_{BH} = OHO active Biomass concentration (mgCOD/l)

μ_{HT} * = maximum specific growth rate of OHO on RBCOD at temperature T (/d)

S_{bs} = RBCOD concentration (mgCOD/l)

K_{SH} = half saturation constant for RBCOD

= 5 mgCOD/l

K_{MPT}* = maximum specific growth rate of OHO on SBCOD at temperature T (/d)

S_{ads} = adsorbed SBCOD concentration (mgCOD/l)

K_{SP} = half saturation constant for SBCOD

= 0.027 mgCOD/mgCOD

b_{HT} = OHO specific death rate at temperature T (/d)

μ_{HT}, K_{MPT} and b_{HT} are temperature dependent.

It can be accepted that during the initial stages of the batch test (before RBCOD is depleted and the OUR drops precipitously) $S_{bs} >> K_{SH}$ and $S_{ads} / Z_{BH} >> K_{SP}$, and therefore,

$$\frac{dZ_{BH}}{dt} = (\mu_{HT} + K_{MPT} - b_{HT}) \bullet Z_{BH} \qquad (4.16)$$

Integrating Eq (4.16) and solving yields the OHO active biomass concentration at time t [$Z_{BH(t)}$, mgCOD/l] in terms of initial OHO active biomass concentration [$Z_{BH(0)}$, mgCOD/l], time (t, in h) and the net specific growth rate ($\mu_{HT} + K_{MPT} - b_{HT}$) viz;

$$Z_{BH(t)} = Z_{BH(0)}\, e^{(\mu_{HT} + K_{MPT} - b_{HT})\, t/24} \qquad (4.17)$$

The OUR at time t ($OUR_{(t)}$, mgO/l) is a function of $Z_{BH(t)}$, the net specific growth rate and OHO yield coefficient, Y_{ZH} = 0.666 mgCOD/mgCOD:

$$OUR_{(t)} = \frac{1 - Y_{ZH}}{Y_{ZH}} (\mu_{HT} + K_{MPT})\, Z_{BH(t)} / 24 \qquad (4.18)$$

Substituting Eq. (4.17) for $Z_{BH(t)}$ in Eq. (4.18) and taking natural log yields

$$\text{Ln } OUR_{(t)} = \text{Ln}\left[\frac{1 - Y_{ZH}}{Y_{ZH}} (\mu_{HT} + K_{MPT})\, Z_{BH(0)} / 24 \right] + (\mu_{HT} + K_{MPT} - b_{HT})t/24 \qquad (4.19)$$

Which is a straight line with,

$$\text{Slope} = (\mu_{HT} + K_{MPT} - b_{HT})/24 \qquad (4.20)$$

$$\text{y-intercept} = \text{Ln } OUR_{(t=0)} = \text{Ln}\left[\frac{1 - Y_{ZH}}{Y_{ZH}} (\mu_{HT} + K_{MPT})\, Z_{BH(0)} / 24 \right] \qquad (4.21)$$

To determine the OHO active biomass at the start of the batch test ($Z_{BH(0)}$), the OHO active biomass OUR values for the data up to precipitous drop in OUR were plotted as Ln (OUR_H) versus time (for example, the Ln (OUR_H) from the data in Fig. 4.3 are plotted in Fig. 4.5), and linear regression applied to determine the y-intercept, slope and correlation coefficient. From the slopes and y-intercept, Eqs. (4.20) and (4.21) respectively, $Z_{BH(0)}$ can be determined (Wentzel *et al*., 1995):

$$Z_{BH(0)} = \frac{(e^{\text{y-intercept}}) \bullet 24}{\frac{1 - Y_{ZH}}{Y_{ZH}} \bullet (\text{slope} \bullet 24 + b_{HT})} \quad (4.22)$$

Where

$Z_{BH(0)}$ = OHO active biomass concentration at the start of the batch test (mgCOD/l *batch reactor*)

Y_{ZH} = OHO active biomass yield, COD units (mgCOD/mgCOD)
0.666 mgCOD/mgCOD (Dold *et al*., 1980, 1991; Wentzel *et al*., 1995)

b_{HT} = OHO specific death rate at temperature T (/d)
b_{H20} $1.029^{(T-20)}$

b_{H20} = OHO specific death rate at 20°C
= 0.62/d (death/regeneration theory, Dold *et al*., 1980; Wentzel *et al*., 1995)

Note that Eq. (4.15) for the batch tests, the death regeneration theory (Dold *et al*., 1980) is used (b_{H20} = 0.62/d), whereas in Eq. (4.27) below for the steady state system, the endogenous respiration theory (Dold *et al*., 1980; WRC, 1984; Lee *et al*., 2003) is used (b_{H20} = 0.24/d).

4.3.1.4 Derivation of Equations for maximum specific growth rates

From the analysis of an $OUR_{H(t)}$ (mgO/l/h) versus time (h) response in the batch test, valuable information regarding the OHO active biomass growth rates can also be determined. Wentzel *et al*. (1995) and Mbewe *et al*. (1995) concluded that the $OUR_{H(t)}$ before the precipitous drop could be separated into the OUR contribution due to RBCOD degradation and the OUR contribution due to SBCOD degradation (see Fig. 4.2). This is equivalent to separating the overall growth rate (μ_{HT} + K_{MPT}) into its μ_{HT} and K_{MPT} components. The derived equation for K_{MPT} (OHO maximum specific growth rate on SBCOD) and μ_{HT} (OHO maximum specific growth rate on RBCOD) will be repeated here to illustrate the calculation procedures.

In terms of the UCT model, growth of OHO active biomass on RBCOD and SBCOD is independent and concomitant (Wentzel *et al*., 1995). The OUR's (mgO/l/h) associated with these two growth processes are given by Eq. (4.15), which can be separated to give:

$$(1)\quad OUR_{RBCOD(t)} \bullet 24 = \frac{1 - Y_{ZH}}{Y_{ZH}} \bullet \mu_{HT} \bullet Z_{BH(0)}\ e^{(\mu_{HT} + K_{MPT} - b_{HT})\, t/24} \qquad (4.23)$$

$$(2)\quad OUR_{SBCOD(t)} \bullet 24 = \frac{1 - Y_{ZH}}{Y_{ZH}} \bullet K_{MPT} \bullet Z_{BH(0)}\ e^{(\mu_{HT} + K_{MPT} - b_{HT})\, t/24} \qquad (4.24)$$

Heterotrophic maximum specific growth rate on SBCOD, K_{MPT}

Up to the precipitous decrease, the OUR is the sum of the OURs associated with the RBCOD and SBCOD utilization [Eq. (4.23) + Eq. (4.24)]. The precipitous drop in OUR signifies the depletion of RBCOD, the remaining OUR is that of SBCOD [Eq. (4.24)]. If the precipitous decrease occurs at t=s hours at which time the OUR is $OUR_{SBCOD(t)}$, then from Eq. (4.24) K_{MPT} is given by:

$$K_{MPT} = \frac{OUR_{SBCOD(t=s)} \bullet 24}{\frac{1 - Y_{ZH}}{Y_{ZH}} \bullet Z_{BH(0)}\ e^{(\mu_{HT} + K_{MPT} - b_{HT}) \bullet (t=s)/24}} \qquad (4.25)$$

Where

$OUR_{SBCOD(t=s)}$ = OUR due to SBCOD only, *i.e.* observed OUR immediately following the precipitous drop in OUR (mgO/l/h)

(t = s) = time immediately following the precipitous drop in OUR (h)

$(\mu_{HT} + K_{MPT} - b_{HT})/24$ = slope of Ln $OUR_{(t)}$ versus time (h) plot.

T = Temperature (ºC)

Using data from Figs. 4.2 and 4.4 as an example, time s = 5.63h; $OUR_{SBCOD(t\ =\ 5.63h)}$ = 4.720 mgO/l/h; slope Ln $OUR_{(t)}$ vs time plot = 0.130 (Fig. 4.4); $Z_{BH(0)}$ = 63.64 mg COD/l; T = 20ºC:

$$K_{MPT20} = \frac{4.720 \bullet 24}{\frac{1-0.666}{0.666} \bullet 63.64 \bullet e^{0.130 \bullet 5.63}} = 1.71/d$$

Heterotrophic maximum specific growth rate on RBCOD, μ_{HT}

For the UCT model (Wentzel *et al*., 1995) the value for μ_{HT} can be calculated from the value for K_{MPT} derived above and the slope of the Ln OUR versus time plot, as follows

$$\mu_{HT} = \text{Slope} \bullet 24 - K_{MPT} + b_{HT} \qquad (4.26)$$

For the example above,

$$\mu_{HT} = 0.130 \bullet 24 - 1.71 + 0.62 = 2.03/d$$

4.3.2 Theoretical OHO active biomass concentration in the parent system

In order to evaluate the modified batch test procedure, the measured OHO active biomass concentrations determined in the batch tests was compared with the theoretical values for the parent system from which the mixed liquor is drawn. The steady state theory (WRC,1984) and the kinetic simulation models (Dold *et al*., 1991) for anoxic/aerobic activated sludge systems gave theoretical OHO active biomass concentrations that were in close agreement (Ubisi *et al*., 1997a,b; Cronje *et al*., 2000; Lee *et al*., 2003). Since the steady state theory is simpler and provides a direct analytical solution, this will be used to calculate the theoretical OHO active biomass concentration in the parent system, and added to the batch test. This calculation procedure is summarized below.

From WRC (1984), the OHO active biomass fraction of the mixed liquor volatile suspended solids (VSS) (f_{av}) can be determined from:

$$f_{av} = MX_{BH} / MX_V$$
$$= MX_{BH} / (MX_{BH} + MX_E + MX_I + MX_{BA}) \quad (4.27)$$

Where

MX_V = mass of volatile suspended solids = $V \bullet X_V$, VSS units (mg VSS)

MX_{BH} = mass of OHO active biomass = $V \bullet X_{BH}$, VSS units (mg VSS)

MX_E = mass of endogenous material = $V \bullet X_E$, VSS units (mg VSS)

MX_I = mass of inert material = $V \bullet X_I$, VSS units (mg VSS)

MX_{BA} = mass of AO active biomass = $V \bullet X_{BA}$, VSS units (mg VSS)

V = system volume (l)

X_{BH} = OHO active biomass concentration, VSS units (mg VSS/l)

X_E = endogenous material concentration, VSS units (mg VSS/l)

X_I = inert material concentration, VSS units (mg VSS/l)

X_V = volatile suspended solids concentration, VSS units (mg VSS/l)

In Eq. (4.27), for activated systems receiving "normal" municipal wastewaters (influent TKN/COD ratio < 0.12 mgN/mgCOD) the AO active biomass (MX_{BA}) component of the mixed liquor organic suspended solids is very small compared to the other three components (< 2% of the total for the parent system here). Thus, with very little error, the AO active biomass can be neglected when calculating the mixed liquor VSS (Wentzel *et al*., 1995). Accordingly, from WRC (1984), substituting in Eq. (4.27) for $MX_{BA} = 0$ and $MX_V = (MX_{BH} + MX_E + MX_I)$:

$$\frac{1}{f_{av}} = 1 + f_E\, b_{HT}\, R_s + \frac{f_{s,up}(1 + b_{HT} R_s)}{f_{cv} Y_H (1 - f_{s,us} - f_{s,up})} \quad (4.28)$$

f_E = fraction of OHO active biomass that is endogenous residue 0.2 (endogenous residue theory, Dold *et. al*., 1980)

b_{HT} = specific endogenous mass loss rate at temperature T (/d) b_{HT} $1.029^{(T-20)}$

b_{H20} = specific endogenous mass loss rate at 20°C 0.24/d at 20°C (endogenous respiration theory, (Dold *et al*., 1980)

Rs = sludge age (d)

$f_{s, up}$ = fraction of influent substrate that is unbiodegradable particulate

$f_{s, us}$ = fraction of influent substrate that is unbiodegradable soluble

f_{CV} = COD to VSS ratio of mixed liquor organic suspended solids (mgCOD/mgVSS)

Y_H = OHO active biomass yield, VSS units (mgVSS/mgCOD) 0.45mgVSS/mgCOD (WRC, 1984)

Knowing f_{av} and the concentration of mixed liquor VSS that was drawn from the parent system [Xv (PS)] to be added to the batch tests, the theoretical OHO active biomass concentration in the batch reactor due to the added mixed liquor [$X_{BH}(Theo.)_{BT}$, COD units] is given by:

$$Z_{BH}(Theo.)_{BT} = \frac{[Xv\,(PS) \bullet f_{av} \bullet f_{cv} \bullet V_{ML}]}{(V_{ML} + V_{WW})} \qquad (4.29)$$

Where

$Z_{BH}(theor)_{BT}$ = theoretical OHO active biomass concentration in batch test reactor due to added mixed liquor, COD units (mgCOD/l batch reactor)

Xv (PS) = mixed liquor VSS concentration measured in parent system

V_{ML} = volume of mixed liquor from parent system added to batch test (l)

V_{WW} = volume of wastewater added to batch test

As an illustration, for batch test no. B1 conducted with Sewage batch no. 13/03 (2 Sept 2003) the theoretical OHO active biomass concentration in the batch reactor due to the

addition of the mixed liquor sample drawn from the parent system was calculated as follows:

Using data from the parent system during sewage batch no. 13/03 as an example, Xv (PS) = 2250 mgVSS/l; fav = 0.3668; f_{cv} = 1.45 mgCOD/mgVSS (Appendix 8, Table 8.3); V_{ML} = 0.5 L and V_{WW} = 4.5 L. Substituting these values into Eq. (4.8).

$$Z_{BH}\,(\text{Theor})_{BT} = \frac{2250 \cdot 0.3668 \cdot 1.45 \cdot 0.5}{(0.5 + 4.5)} = 119.67 \text{ mgCOD/l}$$

Note that in Eq. (4.28) the parent system mixed liquor organic suspended solids are expressed in VSS units [X_V (PS)], whereas the OHO active biomass is expressed in COD units. This is done because conventionally the mixed liquor organic suspended solids in activated sludge systems are measured via the VSS test, whereas the kinetic model used to develop the batch test are in terms of the COD parameter. However, the two units of measure are directly related through the COD/VSS ratio of the mixed liquor organic suspended solids (f_{cv}), which was available from direct measurements.

4.4 Results

This section documents the results obtained for the parent system, batch tests and FISH analysis. Also, illustrated is a comparison between the theoretical OHO active biomass concentration in the parent system [$Z_{BH(0)}$ (Theo.)], the OHO active biomass concentrations measured at the start of the batch tests [$Z_{BH(0)}$ (Meas.)] and the OHO active biomass at the start of the test determined by molecular probing [($Z_{BH(0)}$ Probe)]. The calculation procedures for the parent system and batch test are fully detailed in sections 4.3.1 and 4.3.2 above.

4.4.1 Parent system data

Each sewage batch constituted a steady state period during which the characteristics of the sewage batch governed the parent system behavior. Therefore each sewage batch was analyzed separately to determine the various parent systems parameters, as set out in Chapter 3. During 8 out of a total of 40 sewage batches (18 sewage batches in 2003 and 22 sewage batches in 2004), modified batch tests were conducted. For these sewage batches the various parent system parameters and the average data (From Tables 3.3 (a, b), 3.4, 3.5 (a, b), and 3.6 - Chapter 3) are listed in Table 4.2 and 4.3.

Table 4.2: Steady state results for 10d sludge age parent laboratory-scale anoxic/aerobic activated sludge system for those sewage batches during which batch tests were performed. Averages are listed with sample standard deviations in parenthesis.

Sew. Batch No.	COD (mg/l)		TKN (mgN/l)		Nitrate (mgN/l)			OUR mgO/l/h	Mixed liquor (mg/l)		
	Inf	Eff	Inf	Eff	AX	AE	Eff		VSS	COD	TKN
13/03	494.0 (15.7)	38.9 (11.4)	33.3 (4.3)	2.2 (1.1)	1.3 (1.6)	5.0 (0.9)	7.8 (0.8)	30.6 (0.1)	2189.0 (112.3)	3325.4 (165.4)	205.1 (14.6)
14/03	490.6 (15.7)	29.4 (9.3)	34.3 (1.1)	1.9 (0.9)	0.5 (0.4)	4.7 (0.8)	6.9 (1.2)	30.4 (0.1)	1984.4 (130.7)	2988.8 (156.3)	217.3 (20.9)
15/03	496.7 (12.8)	32.3 (12.2)	32.3 (2.5)	1.7 (0.8)	0.2 (0.4)	3.1 (1.2)	7.4 (2.0)	30.9 (1.2)	2139.8 (90.8)	3212.8 (109.7)	204.1 (16.8)
16/03	477.2 (38.4)	35.8 (13.2)	36.1 (2.5)	1.9 (0.8)	0.2 (0.4)	4.8 (0.9)	7.5 (1.2)	29.9 (0.1)	2089.2 (311.6)	3052.2 (468.8)	201.8 (40.0)
17/03	485.3 (32.8)	30.8 (10.3)	34.1 (2.1)	3.0 (1.9)	1.2 (0.3)	4.8 (2.0)	7.7 (0.9)	30.2 (0.9)	2051.3 (247.7)	3145.3 (277.5)	198.9 (16.5)
18/03	492.7 (21.9)	30.0 (2.0)	37.7 (0.6)	4.6 (1.0)	0.6 (0.6)	3.6 (1.3)	9.2 (0.5)	30.5 (0.6)	2200.0 (90.0)	3325.3 (123.7)	218.3 (8.0)
21/04	478.4 (15.2)	45.7 (6.5)	40.9 (3.1)	4.5 (0.6)	1.3 (0.8)	7.2 (1.4)	8.7 (0.9)	31.5 (0.9)	2319.3 (182.1)	3378.0 (268.6)	197.3 (13.9)
22/04	487.5 (28.3)	37.0 (6.1)	41.4 (3.2)	4.4 (0.7)	1.2 (0.9)	6.1 (1.2)	9.1 (1.8)	31.0 (0.2)	2133.0 (154.2)	3282.9 (260.3)	226.5 (24.9)

To formulate a theoretical estimate for OHO active biomass concentration present in the parent system during each sewage batch period, the following were determined from the data in Table 4.2:

- Influent wastewater unbiodegradable soluble and particulate fractions ($f_{s,us}$ and $f_{s,up}$ respectively); system COD and N mass balances (Ekama *et al*., 1986) and the COD and TKN to VSS ratios for the mixed liquor (f_{CV} and f_N respectively). The calculation procedures are set out in detail in Chapter 3 and the results for each

sewage batch during which the modified batch tests were conducted are listed in Table 4.3.

- The OHO active biomass fractions of the mixed liquor organic suspended solids (f_{av}) were determined for each sewage batch using the steady state design model [Eq. (4.27)]. The steady state design model proved to be more direct and simpler when determining the OHO active biomass fractions (f_{av}) (Ubisi *et al*., 1997a, b; Cronje *et al*., 2000).

Table 4.3: Steady state COD and N mass balances, wastewater fractions and mixed liquor parameters for the 10 days sludge age parent laboratory-scale anoxic/aerobic activated sludge system.

ww Batch No.	Mass balance (%)		Wastewater COD fractions		Mixed liquor		
	COD	N	Unbiod. Soluble (fs,us)	Unbio. Particulate (fs,up)	COD/VSS ratio (mgCOD/mgVSS) ❖ (fCV)	TKN/VSS ratio (mgN/mgVSS) (fN)	Active Fraction (fav)
13/03	98.9	106.4	0.0789	0.2099	1.51	0.0935	0.3393
14/03	92.3	106.2	0.0595	0.1453	1.51	0.1097	0.4181
15/03	99.4	105.4	0.0651	0.1826	1.50	0.0957	0.3709
16/03	95.9	104.9	0.0751	0.1852	1.47	0.0998	0.3720
17/03	96.8	103.1	0.0638	0.1758	1.55 *	0.0982	0.3951
18/03	100.8	107.8	0.0609	0.2048	1.51	0.0993	0.3501
21/04	100.6	105.1	0.0957	0.2566	1.46	0.0994	0.2861
22/04	98.1	104.9	0.0775	0.1768	1.47	0.0851	0.3733

* Shaded blocks rejected as outliers

4.4.2 Batch test data

Table 4.4: COD recovery, regression data from Ln (OUR_H) versus time plot and heterotrophic active biomass at the start of the batch test ($Z_{BH(0)}$)

Sew Batch No.	Batch Test No.	Volume (L)		COD Recov (%)	Regression			Growth Rate (/d)		$Z_{BH(0)}$ (mgCOD/l)			
					Y-int	slope	R^2	K_{mp}	μ_H	Measured		Theoretical	
		WW	ML							Batch	ML	Batch	ML
13/03	B1	4.5	0.5	91.6	1.6297	0.130	0.919	1.71	2.03	63.6	636.4	119.7	1196.7
14/03	B2	4.5	0.5	103.4	1.4849	0.065	0.923	0.92	1.25	94.8	947.7	123.5	1234.7
15/03	B3	4.6	0.4	95.0	0.1098	0.310	0.930	1.38	6.67	6.5	80.7	93.9	1174.3
16/03	B4	4.5	0.5	97.2	1.4247	0.076	0.940	0.84	1.60	79.4	793.6	100.5	1004.8
17/03	B5	4.5	0.5	94.8	1.4252	0.143	0.916	2.17	1.89	47.7	477.4	108.9	1088.6
17/03	B6	4.5	0.5	92.3	0.6194	0.176	0.987	1.00	3.84	17.9	179.0	127.2	1272.3
17/03	B7	4.5	0.5	93.4	0.6954	0.182	0.997	1.64	3.35	18.7	187.2	124.3	1243.4
18/03	B8	4.5	0.5	89.4	1.3005	0.191	0.991	2.07	3.12	32.9	329.4	129.3	1292.6
21/04	B9	4.5	0.5	98.2	1.3572	0.105	0.566	1.67	1.46	57.7	577.1	97.8	978.2
21/04	B10	4.5	0.5	93.8	0.9814	0.101	0.983	1.71	1.34	40.7	407.1	97.8	978.2
21/04	B11	4.6	0.4	90.5	0.8483	0.131	0.973	0.75	3.02	28.9	360.8	77.8	972..0
21/04	B12	4.6	0.4	103.2	1.4150	0.094	0.930	1.59	1.28	66.8	834.6	77.8	972.0
21/04	B13	4.4	0.6	94.8	0.8347	0.179	0.987	2.31	2.6	21.9	182.3	132.6	1105.2
21/04	B14	4.5	0.5	105.5*	1.2230	0.087	0.930	1.65	1.06	58.2	582.3	110.5	1105.2
22/04	B15	4.4	0.6	89.5	0.9556	0.231	0.891	2.41	3.76	19.7	163.8	147.7	1231.0
22/04	B16	4.4	0.6	91.6	1.1559	0.153	0.961	1.13	3.15	34.6	288.1	147.7	1231.0

For the batch tests, measured OUR, NO_3 and NO_2 - time data are shown graphically in Appendix 10. Following the procedures set out in Section 4.3.1 above, the OHO active biomass concentrations measured at the start of the test were calculated and are listed in Appendix 10; the results are summarized in Table 4.4.

The %COD recoveries for all the batch tests were calculated using Eq. (4.13) and the results are listed in Appendix 10. The %COD recovery for each batch test is summarized in Table 4.4. In general, %COD recoveries were good, with only 2 out of 16 batch tests yielding %COD recoveries < 90%. Batch 14 yielded %COD recovery > 105%.To determine wether these low and high %COD recoveries arose from random effects, or whether they were a discernable trend, a statistical plot of the %COD recovery for all the modified batch tests was constructed (Fig 4.5). The mean %COD recovery was 95.23% with sample standard deviation of 5.0%.

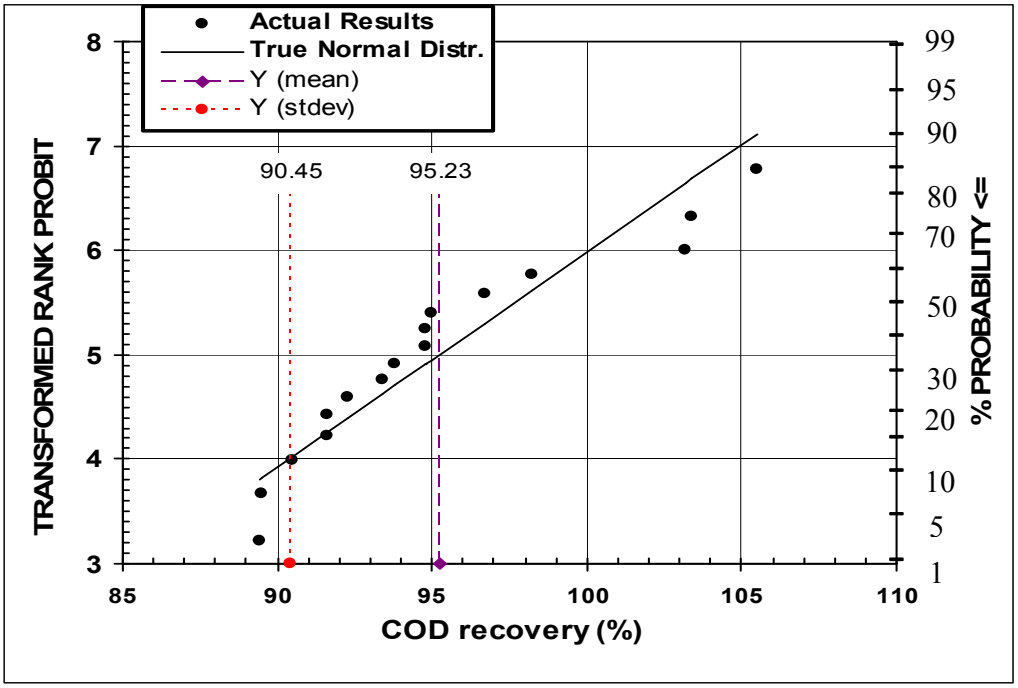

Fig 4.5: Statistical plot of %COD for all the modified batch tests conducted with flocculated – filtered wastewater and mixed liquor drawn from the 10 days sludge age MLE activated sludge system.

For K_{MP}, a statistical plot for K_{MP} values for all the modified batch tests was constructed (Fig. 4.6). From Fig. 4.6, the mean K_{MP} was 1.56/d with sample standard deviation of 0.523/d.

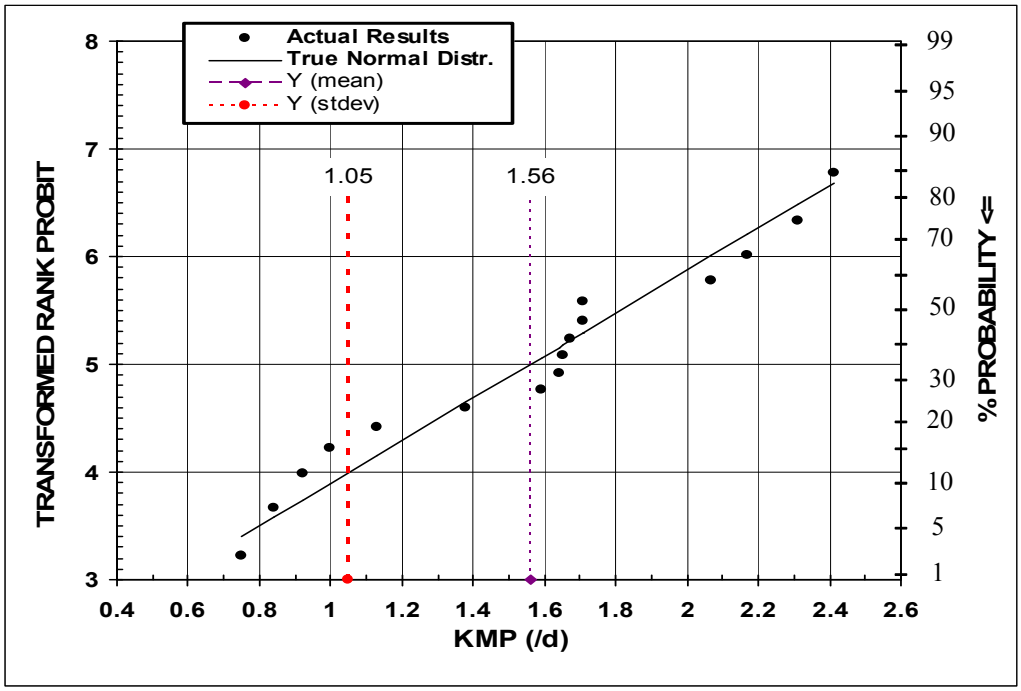

Fig 4.6: Statistical plot of K_{MP} recovery for all the modified batch tests conducted with flocculated – filtered wastewater and mixed liquor drawn from the 10d sludge age MLE activated sludge system.

In Table 4.4, the measured OHO active biomass concentration at the start of each batch test [$Z_{BH(0)}$(Meas.)] is compared to the theoretical OHO active biomass concentration at the start of the batch test due to the mixed liquor sample which was drawn from the parent system and added to the batch test [$Z_{BH(0)}$(Theo.)]. The theoretical values were predicted via the steady state model (see section 4.3.2). To illustrate the comparison, the measured versus theoretical mixed liquor OHO active biomass data for all the batch test are shown in Fig. 4.8.

For μ_H, a statistical plot for μ_H values for all the modified batch tests was constructed (Fig. 4.7). From Fig. 4.7, the mean μ_H was 2.59 /d with sample standard deviation of 1.40 /d.

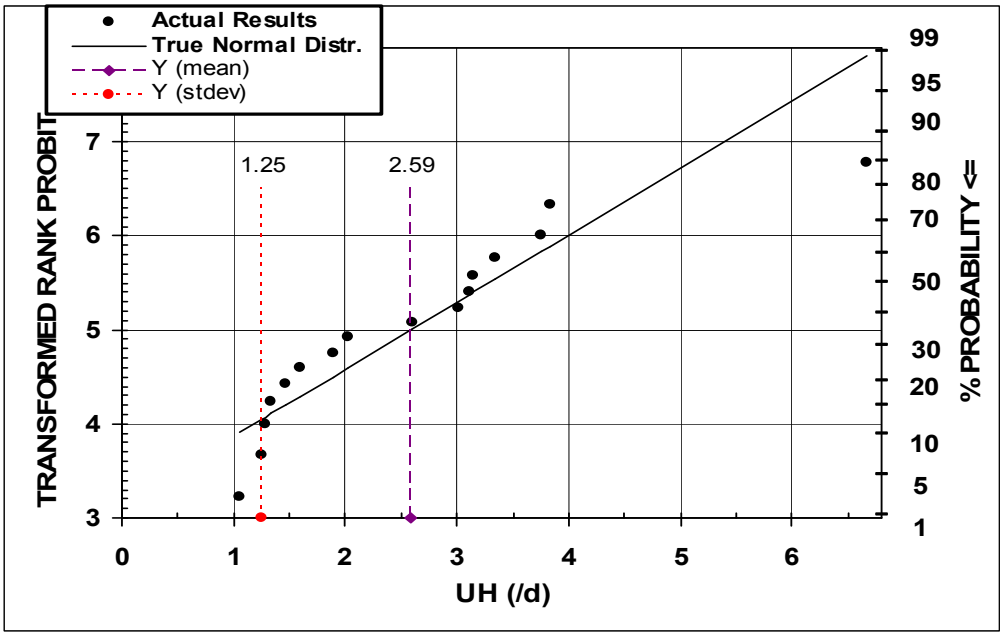

Fig. 4.7 Statistical plot of μ_H recovery for all the modified batch tests conducted with flocculated – filtered wastewater and mixed liquor drawn from the 10 days sludge age MLE activated sludge system.

4.4.3 FISH analysis data

The oligonucleotide probes used were targeted to the cells 16S rRNA, which provides a phylogenetic identification based directly on cell genetic code (Stahl, 1997). The following nitrifying probes were used, NSO 1225 complemenary to a signature region of all known ammonia oxidizers in the beta-subclass of *Proteobacteria* (Mobarry *et al.,* 1996), NIT3 complementary to a region of all previously sequenced *Nitrobacter species* (Wagner *et al*., 1996) and NSR 1156 specific for freshwater *Nitrospira spp*. EUB388 probe mix (consisting of probes EUB338, EUB338-II, and EUB338-III) was used to target the domain bacteria (Daims *et. al.,* 1999), which includes the nitrifiers. The probes used and their sequences are listed in Table 4.1. Cell counts for the determination of the heterotrophic active biomass concentration for each batch test was converted to mass

units (mgCOD/l) in order to determine what fraction of the measured VSS is metabolically active.

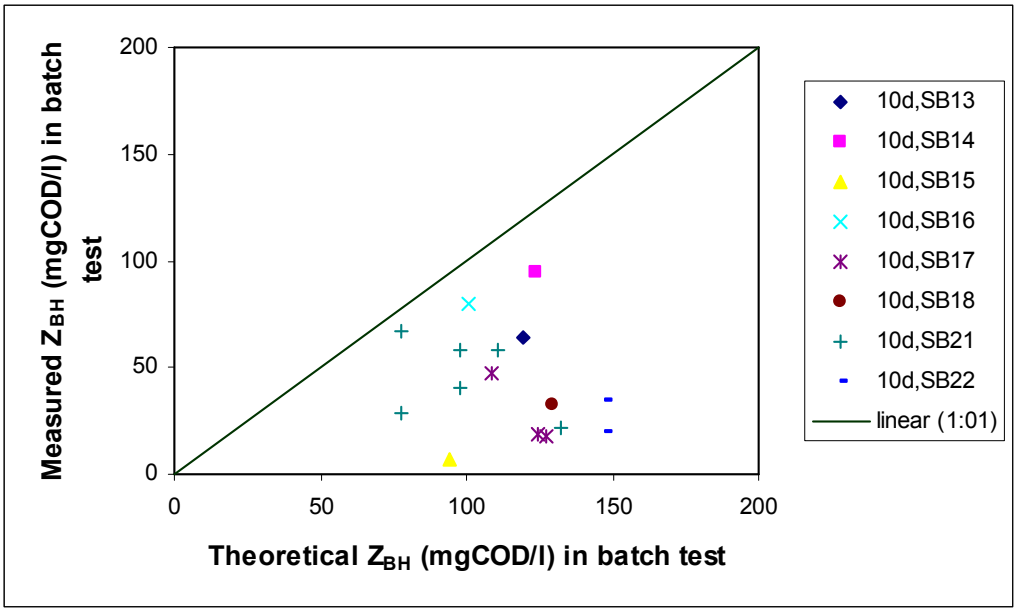

Fig. 4.8: Modified batch test results; graph of measured versus theoretical heterotrophic active biomass concentration at the start of the test [$Z_{BH(0)}$] for various sewage batches (SB) for the 10 d (sludge age) MLE activated sludge system

To determine the heterotrophic active biomass concentration at the beginning of each batch test, the total nitrifying population (sum of NSO 1225, NIT3 and NSR 1156 cell counts) was subtracted from cell counts obtained from EUB388 probe mix (Table 4.5). The following equation was applied to convert cell counts (cells/ml) to mass units (mgCOD/l). In order to make a conversion from cell numbers to mass units a conversion factor (F_{VB}) of 8.49 x 10-11 mgVSS/cell (Mudaly *et al.*, 2001; Holder-Snymann *et al.,* 2005) was applied in the following equation:

$$Z_{BH} = \frac{CC \bullet F_{(CV)} \bullet F_{(VB)} \bullet V_{(0)}}{V_{(M)} \bullet 1000 \bullet DF} \quad (4.30)$$

Where

Z_{BH} = Heterotrophic active biomass (mgCOD/l)

CC = Cell counts (cells/ml)

Fcv = COD to VSS ratio of the mixed liquor (mgCOD/mgVSS)

$V_{(0)}$ = Original volume of fixed sample (ml)

$V_{(M)}$ = Volume of fixed sample remaining (ml)

DF = Dilution factor

In Table 4.5, the measured OHO active biomass concentration at the start of each batch test [$Z_{BH(0)}$ (meas.)] is compared to the probe OHO active biomass concentration at the start of the test [$Z_{BH(0)}$ (probe)]. In sludge samples taken at the start of each batch test, bacterial cells stained with DAPI varied between 1.88 (± 0.09) and 3.15 (±0.07) x 10^9 cells/ml. Cells hybridizing with EUB probe mix ranged from 1.39 (±0.08) to 2.61 (±0.06) x 10^9 cells/ml. The percentages of cells giving a clear fluorescence signal after hybridization varied between 64% (±7.58%) and 94% (±4.16%) of all DAPI-stained cells. The MLVSS concentrations in parent system ranged between 1.6590 and 2.4340 g L^{-1} (Fig. 4.11). As shown in Fig. 4.11, the percentages of FISH detectable cells had minor fluctuations with changing operating conditions. The nitrifiers (combination of probes NSO 1225, NSR1156 and NIT3) ranged from 0.33 (±0.01) to 0.66 (±0.02) x 10^9 cells/ml (Table 4.5). Comprehensive FISH data including DAPI and probe cell counts for each batch test are listed in Appendix 11. The modified batch test translated OUR response into parameters that reflect the $Z_{BH(0)}$ and are directly comparable to the $Z_{BH(0)}$ measures from the molecular probes. The probe values ranged from 242.14 to 628.49 mgCOD/L, while the measured values ranged from 80.7 to 834.6 mgCOD/L (Table 4.5). Theoretical values predicted via steady-state model ranged from 972 to 1292 mgCOD/L (Table 4.4). To illustrate the comparison, the measured versus probe mixed liquor OHO active

biomass data for all the batch tests are shown in Fig. 4.9. The comparison between theoretical and probe mixed liquor OHO active biomass data are shown in Fig. 4.10.

Table 4.5: Probe cell counts and heterotrophic active biomass concentration at the start of each batch test ($Z_{BH(0)}$)

Batch test no.	No. (± SD) of cells ($10^9 \cdot ml^{-1}$)			Probe measured $Z_{BH(0)}$ (mgCOD/l)	Measured $Z_{BH(0)}$ (mgCOD/l) ML
	DAPI	EUB Mix	Nitrifiers (NSO, NIT, NSR)		
B1/03	3.03 ± 0.23	2.03 ± 0.15	0.33 ± 0.01	501.32	636.4
B2/03	3.15 ± 0.07	2.61 ± 0.06	0.47± 0.05	628.49	947.7
B3/03	2.40 ± 0.02	1.94 ± 0.13	0.41 ± 0.02	469.46	80.7
B4/03	2.13 ± 0.12	1.94 ± 0.23	0.59 ± 0.04	396.47	793.6
B5/03	1.84 ± 0.60	1.95 ± 0.06	0.44 ± 0.04	367.12	477.4
B6/03	1.93 ± 0.16	1.78 ± 0.22	0.35± 0.03	436.52	179
B7/03	2.16 ± 0.06	1.56 ± 0.11	0.56 ± 0.02	299.63	187.2
B8/03	2.28 ± 0.07	1.60 ± 0.18	0.55 ± 0.05	326.97	329.4
B9/04	2.99 ± 0.13	2.39 ± 0.22	0.66 ± 0.02	522.97	577.1
B10/04	2.82 ± 0.09	2.28 ± 0.25	0.59 ± 0.001	496.46	407.1
B11/04	1.81± 0.87	1.41 ± 0.27	0.58 ± 0.02	244.30	360.8
B12/04	2.01 ± 0.13	1.89 ± 0.08	0.58 ± 0.02	380.68	834.6
B13/04	1.88 ± 0.09	1.39 ± 0.08	0.58 ± 0.01	242.14	182.3
B14/04	1.99 ± 0.05	1.67 ± 0.09	0.60 ± 0.02	321.87	582.3
B15/04	2.10 ± 0.06	1.47 ± 0.06	0.38 ± 0.01	331.53	163.8
B16/04	2.49 ± 0.05	2.24 ± 0.07	0.39 ± 0.01	563.20	288.1

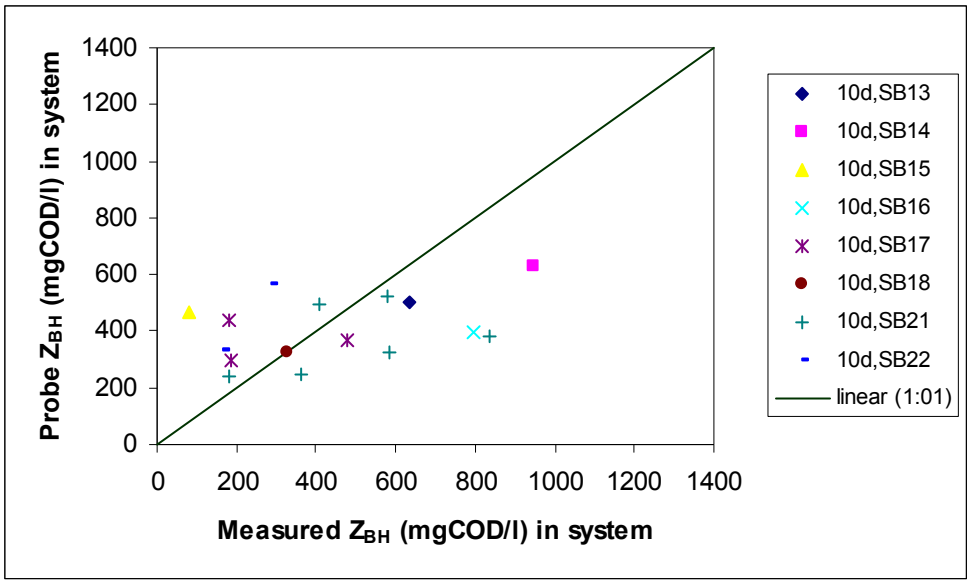

Fig. 4.9: Modified batch test results; graph of measured versus probe heterotrophic active biomass concentration at the start of the test [$Z_{BH(0)}$] for various sewage batches (SB) for the 10 d (sludge age) MLE activated sludge system.

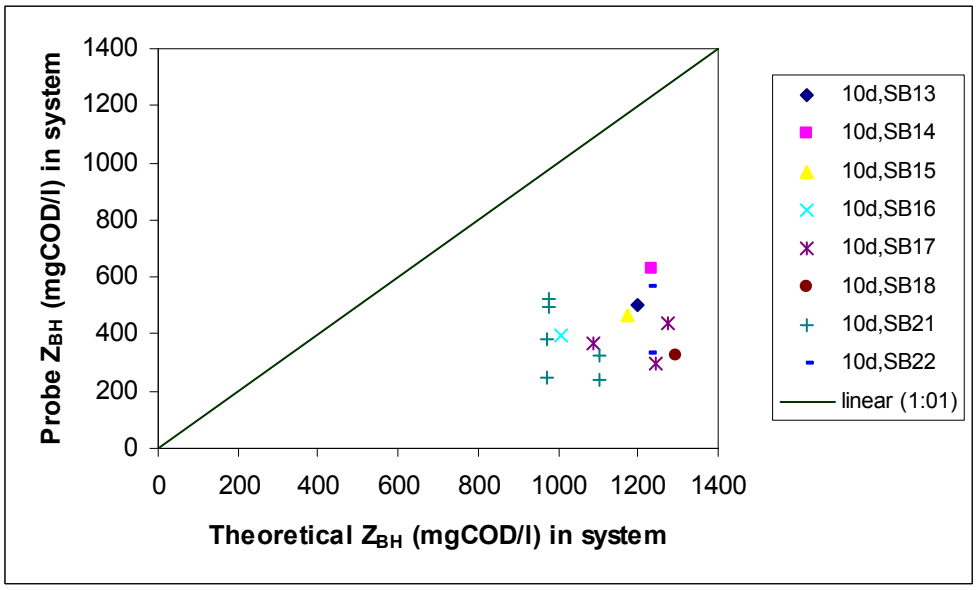

Fig. 4.10: Theoretical versus probe heterotrophic active biomass concentration at the start of the test [$Z_{BH(0)}$] for various sewage batches (SB) for the 10 d (sludge age) MLE activated sludge system.

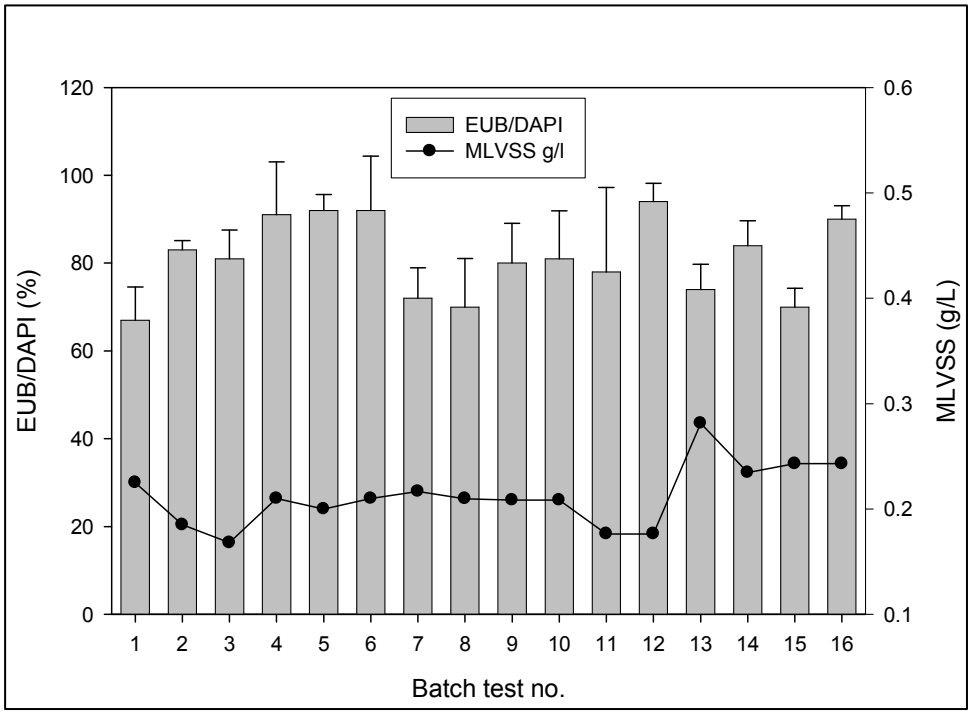

Fig. 4.11: Percentage of EUB-detectable cells relative to DAPI counts in activated sludge samples taken at the start of each modified batch test.

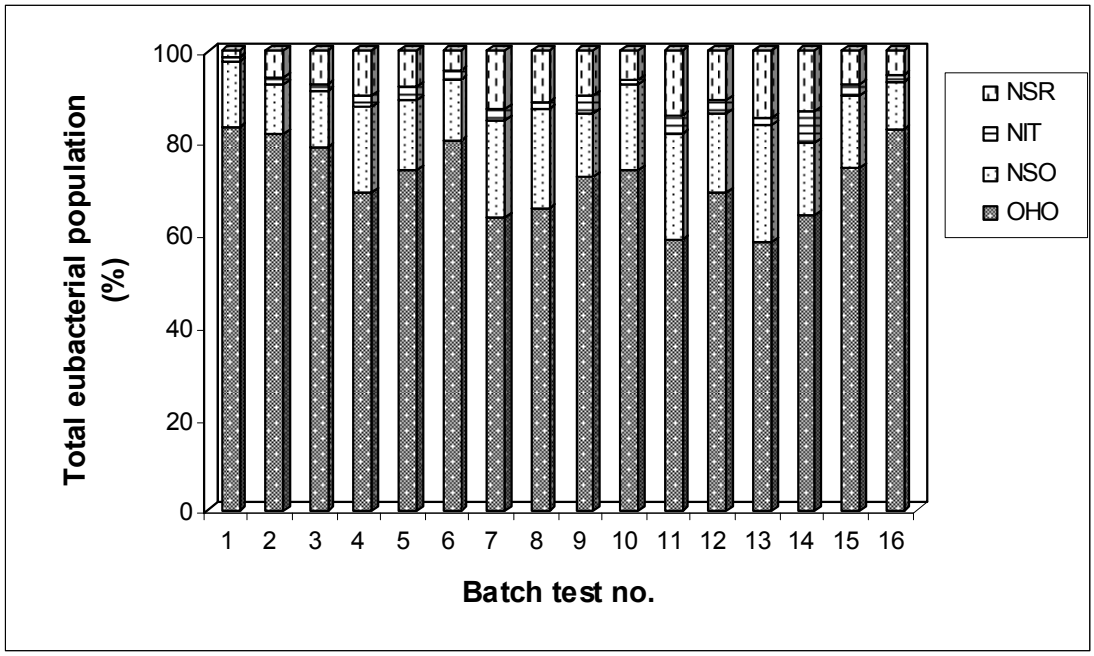

Fig. 4.12: Composition of nitrifying and OHO population for 16 batch tests.

Quantification of the nitrifying population was carried out using probes specific for ammonia (NSO 1225) and nitrite (NIT3 and NSR1156) oxidizing bacteria at the beginning of each batch test (Fig. 4.12). Ammonia oxidizing bacterial (AOB) population ranged from 10.56 to 25.68%, while the nitrite oxidizing bacterial (NOB) population ranged from 0.75 to 7.14% with probe NIT3 and 1.49 to 14.86% with probe NSR1156. The ordinary heterotrophic population (OHO) ranged from 58.11 to 83.58% of the total eubacterial population.

4.5 Discussion

4.5.1 COD recovery and maximum specific growth rates (K_{MP} and μ_H)

In general, good %COD recoveries were achieved with only one batch test (No.14) yielding %COD recovery > 105% (Table, 4.4). To determine whether this high %COD recovery arose from random effects, or whether they were a discernable trend, a statistical plot of the %COD recovery for all modified batch tests were constructed (Fig. 4.5). From the statistical plot this point deviates significantly from the "true" normal distribution line. This would indicate that the %COD recovery for this data did not arise from random effects. Most likely, the dominating cause was the difficulty in accurately measuring OUR values. Since this deviation was relatively small (<1%) this data point was retain. The good %COD recoveries lend credibility to the reliability of the measurements and the batch test procedure.

For each of the batch tests, the values for K_{MP} and μ_H were calculated using Eq. (4.25) and Eq. (4.26) respectively (Table 4.4). For K_{MP}, a statistical plot of the K_{MP} values for all the modified batch tests were constructed (Fig. 4.6). From Fig. 4.6 the mean K_{MP} was 1.56/d ± 0.523/d. This is significantly larger than the K_{MP} value measured by Cronje *et al*. (2000) (0.84/d), but close to the values measured by Beeharry *et al.* (2001) (1.49 and 1.38/d) and Lee *et al*. (2003) (1.37/d).

In Lee *et al*. (2003) a clearly discernable trend in μ_H values was observed, as the volume in mixed liquor added to the batch test increased, the value for μ_H decreased. This indicated that the mixed liquor had a dominating influence. However in this investigation, a trend could not be observed due to the limited range of mixed liquor quantities used in the batch test. For μ_H, a statistical plot of the μ_H values for all the modified batch tests was constructed (Fig. 4.7). From Fig. 4.7 the mean μ_H was 2.59/d ± 1.40/d. This is significantly larger than the μ_H value measured by Cronje *et al*. (2000) (0.84/d), but close to the values measured by Cronje *et al.* (2005) (2.8/d).

4.5.2 Comparison between measured and theoretical OHO active biomass for 10 days sludge age MLE activated sludge system

In Table 4.4, the measured OHO active biomass concentration at the start of each batch test [$Z_{BH(0)}$(meas.)] is compared to the theoretical OHO active biomass concentration at the start of the test due to mixed liquor sample which was drawn from the parent system and added to the batch test [$Z_{BH(0)}$(theor.)]; theoretical values were predicted via the steady state design model. To illustrate the comparison, the measured versus theoretical mixed liquor OHO active biomass data for all the batch tests are shown in Fig. 4.8. From Fig. 4.8 there is a correspondence between measured and theoretical $Z_{BH(0)}$, but the values plot parallel to and below the 1:1 correspondence line. Lee *et al*. (2003) identified three trend regions when examining the correspondence between measured and theoretical $Z_{BH(0)}$. The first, in the region of theoretical $Z_{BH(0)}$ from 0 to about 30 mgCOD/l as the theoretical $Z_{BH(0)}$ increases, the measured values decrease, to approach near zero. The second, in the region from 30 to 150 mgCOD/l theoretical $Z_{BH(0)}$, as theoretical increases, the measured values increase parallel to 1:1 correspondence line between the measured values and the theoretical values. In this investigation data was primarily collected in this region and exhibited similar trend to that observed by Beeharry *et al*. (2001) and Lee *et al*. (2003). This was evident for batch tests conducted on SB's 13, 15, 17 and 22 (Fig. 4.8). The third, above 150 mgCOD/l theoretical $Z_{BH(0)}$, as the theoretical $Z_{BH(0)}$ increases

further the measured $Z_{BH(0)}$ values increase sharply. Thus, it is evident that the trends observed in this investigation are consistent with those of Lee *et al*. (2003).

4.5.3 Comparison between measured and probe OHO active biomass for 10 days sludge age MLE activated sludge system

In Table 4.5, the measured OHO active biomass concentration at the start of each batch test [$Z_{BH(0)}$ (meas.)] is compared to the probe OHO active biomass concentration at the start of the test [$Z_{BH(0)}$ (probe)]. The modified batch test translated OUR response into parameters that reflect the $Z_{BH(0)}$ and are directly comparable to the $Z_{BH(0)}$ measures from the molecular probes. The $Z_{BH(0)}$ values obtained by molecular probing correlated closely with measured $Z_{BH(0)}$ (ML) values obtained from the modified batch tests (Fig. 4.9). However molecular probing provides a more accurate quantification of the Z_{BH} than the modified batch tests since rRNA-targeted oligonucleotide probes are used for the direct enumeration of individual cells. The discrepancies in measured Z_{BH} values could be attributed to sensitivity in regression analysis of Ln OUR data (Cronje *et al*., 2002) or the presence of unknown nitrifiers.

4.5.4 Comparison between theoretical and probe OHO active biomass for 10 days sludge age MLE activated sludge system

In Fig. 4.10, the theoretical OHO active biomass concentration [$Z_{BH(0)}$ (theor.)] predicted by steady-state model is compared to the probe OHO active biomass concentration at the start of the test [$Z_{BH(0)}$ (probe)]. The $Z_{BH(0)}$ values obtained by molecular probing correlated poorly with theoretical $Z_{BH(0)}$ (ML) values obtained from the steady-state model (Fig. 4.10). This could be attributed to the failure of properly defining the active biomass fraction represented in the steady-state model. The steady-state model suggests that the active biomass fraction is related to the biodegradable fraction of the MLVSS and neglects the autotrophic active biomass component. Hence, the entire biodegradable biological VSS belong to living cells only (WRC, 1984; Ekama *et al*., 1986). The

MLVSS contains both dead and living cells, the active biomass is only part of the biodegradable solids. Papkov *et al*., (2000) developed a mathematical expression to calculate the active fraction in activated sludge of both heterotrophic and autotrophic biomass. As a result of this approach, the calculated active biomass fraction was less than the values calculated according to the conventional approach. Furthermore, Holder-Snyman *et al*., (2005) investigated the relationship between measured VSS and metabolically active cells using FISH. They concluded that VSS is not a true reflection of metabolically active cells and only 20% of the measured VSS was found to represent metabolically active biomass.

4.5.5 Composition and dynamics of NOB populations

Microbial nitrification (oxidation of NH_4^+ to NO_3^- via NO_2^-) is carried out by two phylogenetically unrelated groups of lithoautotrophic bacteria, the AOB and the NOB. The *Nitrospira*-specific probe was used together with a previously published probe for the *in situ* detection of *Nitrobacter* (Wagner *et al.*, 1996) to investigate the community structure of nitrite-oxidizing bacteria in activated sludge respirometric batch test (Fig 4.12). Nitrite oxidation was catalyzed in all batch tests mainly by *Nitrospira*-like bacteria (1.49 to 14.86% of EUB) confirming the recently recognized importance of these bacteria for nitrite oxidation in several environments (Juretschko *et al*., 1998; Wagner *et al*., 1998; Daims *et al*., 2000). *Nitrobacter* could only be detected in small amounts (0.75 to 7.14% of EUB) (Fig. 4.12).

The factors that cause the dominance of nitrite-oxidizing *Nitrospira*-like bacteria over *Nitrobacter* in most bioreactors have not yet been elucidated. Schraam and coworkers (1999) postulated that *Nitrobacter spp.* could be r-strategists with low substrate affinity for nitrite and relatively high growth rates at increased nitrite concentrations. On the contrary, *Nitrospira spp*. could be K-strategist with a high substrate affinity for nitrite and lower growth rates. Thus it seems that *Nitrobacter* was out competed by *Nitrospira* in all batch tests and is consistent with the "K/r hypothesis" mentioned above.

Nitrite is an intermediary product of nitrification. Therefore, the nitrite concentration will increase only if the ammonia-oxidizers produce more nitrite than the nitrite-oxidizers can consume. The large population of ammonia-oxidizing bacteria in batch test 14 amounted to 15.48% of the total eubacterial population (Fig 4.12). Although *Nitrospira*-like bacteria were the dominant nitrite-oxidizing population in batch test 14, *Nitrobacter* also occurred in significant amounts (7.14% of EUB). One might expect that *Nitrobacter spp.* should have overgrown *Nitrospira* in batch test 14 due to their presumably high growth rates at increased nitrite concentrations. Thus the dominance of *Nitrospira* in batch test 14 may rather be completely independent from the nitrite concentration. The ability of *Nitrospira*-like bacteria to take up pyruvate was demonstrated by Daims *et al*. (2001a). Therefore it is possible that these organisms possess the capability to grow mixotrophically with other organic carbon sources, which are present in wastewater but cannot be used by *Nitrobacter*.

4.5.6 Quantification accuracy of $Z_{BH(0)}$ using model outputs and FISH

Previous studies have integrated molecular techniques to validate modelling results. Urbain *et al*. (1998) compared microbial population levels predicted by the mathematical model and rRNA levels using dot blot hybridizations. However their conclusion relied upon the assumption that the fraction of rRNA for the specific nitrifier population is equivalent to the fraction of biomass (expressed as COD) for the 'theoretical' population (Oerther *et al.*, 1999). Andreoletta *et al.* (2001) combined respirometric tests with flow cytometry techniques (FCM) to determine the active fraction. In order to assess the viable fraction of the biomass, biovolume was converted into biomass on the basis of carbon content per cell volume. Results obtained in this study, indicated that the maximum growth rate should be in the order 11/d for a good correlation. Discrepancies between model and experimental data could also be attributed to the failure to separate and quantify the nitrifier population.

The conversion factor to transform VSS based concentrations to COD based concentrations is either determined experimentally or by assuming that 85% of the total

biomass is organic, resulting in conversion factor of 1.42 gCOD/gVSS (Grady and Daigger, 1998). Thus to maintain the convenience of expressing microbial population concentrations in COD based units as is done in current models it was necessary for the conversion of hybridization outputs into COD based values. A conversion factor of 8.49^{-11} mgVSS/cell (Holder-Snymann *et al*., 2005) was applied in this study to determine the correlation between measured values obtained from the modified batch test and probe values obtained by FISH. Good correspondences between measured and probe $Z_{BH(0)}$ values were observed (Fig. 4.9). This could be attributed to the quantitative accuracy carried out with whole cell hybridization rather than extracted rRNA. Extracted rRNA measures a 'lumped' parameter, which reflects both the rRNA content and abundance of the target population. In contrast, whole cell hybridizations can determine abundance and rRNA content independently when the intensities of probe conferred hybridization signals are quantified (Oerther *et al*., 1999). Starving or chemical inhibition do not cause a measurable decrease of the cellular ribosome content in ammonia-oxidizing bacteria (Wagner *et al*., 1995). Therefore, active and inactive ammonia-oxidizer cells cannot be distinguished by FISH with rRNA-targeted probes, and the assumption that all quantified, probe-stained cells were metabolically active leads to over or underestimation of activity. This problem can be circumvented only by methods to detect active cells specifically. The combined application of FISH and microautoradiography (Lee *et al.,* 1999; Daims *et al*., 2001b) establishes an alternative approach to determine the active nitrifier populations by using existing, rRNA-targeted probes.

The batch test measured $Z_{BH(0)}$ were consistently lower than the corresponding theoretical values (Fig. 4.8). Lee *et al.* (2003) explained that the OHO maximum specific growth rates increased with time, and this behaviour is not reflective of a single OHO population with fixed kinetics that defines the modified batch test procedure. This results in the underestimation of $Z_{BH(0).}$ Grady *et al*. (1996) proposed substrate competition between different OHO groups as a possible cause. These possibilities were investigated using DNA fingerprinting techniques such as polymerase chain reaction (PCR) and denaturing gradient gel electrophoresis (DGGE) (Chapter six). This will enable the close monitoring

of microbial community profiles along the duration of the batch test, as well as to compare the microbial profile between the parent system and the modified batch test.

4.6 Conclusion

In terms of merging engineering and technology of wastewater systems with knowledge gained from microbiological and molecular biological analytical methods, it is necessary to provide as much quantitative information as possible. This data is crucial for the validation of models. It is timely for the new microbiological and moleculr techniques to provide suitable quantitative data to replace VSS as the "active biomass" measurement.

In this study FISH analysis in combination with mathematical modelling constituted a suitable approach in quantifying the OHO active biomass concentrations by analysing the lithoautotrophic populations. In order to assess the quantification accuracy of OHO active biomass concentrations, a comparison between mathematical modelling, FISH and theoretical concentrations were obtained. The batch test measured and probe $Z_{BH(0)}$ values were consistently lower than the corresponding theoretical values. This was attributed to the high dependency of the theoretical concentration on VSS measurement and the inability of the VSS measurement to distinguish between live and dead cells. However there was an improved correlation between molecular probing values and the modified batch test (measured $Z_{BH(0)}$) values. The ability of FISH to provide a direct measurement of OHO active biomass concentration would take precedent over indirect methods (modified batch test). The integration of molecular techniques (FISH), are now required to expand model calibration and validation efforts.

CHAPTER 5

Integrating Molecular Biology and Modeling to Determine the Autotrophic Active Biomass

5.1 Introduction

The optimization of biological nitrogen removal from sewage water is among the most challenging tasks in modern wastewater treatment. Despite their importance, knowledge about the identity and ecology of the microorganisms catalyzing N-removal in WWTPs is still scarce. The lack of fundamental microbiological understanding, which is more or less directly reflected in the frequent failure of N-removal in plants worldwide, hampers knowledge-driven process improvements. Exploitation of new microbial pathways, growth and maintenance of stable and highly active microbial consortia as well as efficient bioaugmentation strategies are achievable goals if we shift our research focus from empirical studies to investigations embracing key fundamental issues of microbial ecology of wastewater treatment.

Microbial community analysis has been identified as the key to the design of biological wastewater treatment systems (Cloete and Muyima, 1997). A battery of molecular techniques has been developed to study microbial ecology in general and community structures in particular (Stahl, 1997; Wagner and Amann, 1997; Burlage *et al.*, 1998; Atlas and Bartha, 1998). Specific bacterial groups in complex open communities such as activated sludge may be detected directly by fluorescence *in situ* hybridization (FISH), using 16S rRNA-targeted oligonucleotide probes (Stahl and Amann, 1991; Amann *et al*., 1995; Wagner and Amann, 1997).

For instance, by using fluorescent labelled probes specific for ammonia and nitrite oxidisers, the spatial distribution of nitrifiers in a biofilm may be evaluated by *in situ* hybridization (Wagner *et al*., 1996; Mobarry *et al.,* 1996; Schramm *et al*., 1998).

According to Atlas and Bartha (1998), understanding the structure and functioning of an ecosystem requires and necessitates quantitative information. When microbial ecosystems are applied as catalysts in biological wastewater treatment, a proper quantitative description can only be obtained by complex mathematical models, such as the standard models applied for activated sludge systems (Henze *et al*., 1995; Gujer *et al.,* 1999). A fundamental parameter in those biokinetic models is the biomass concentration of the particular microbial population involved in each particular process. The validity of such models cannot be verified as long as those fundamental factors remain unknown. Specific populations identified by FISH may possibly be quantified by counting, and compared to total bacterial numbers simply obtained by staining with the DNA-intercalating dye 4,6-diamidino-2-phenylindole (DAPI) to estimate their relative abundance.

This aspect of the study focuses on the enumeration of the nitrifying bacterial community present in a lab-scale parent system using batch tests and molecular techniques. Since a vast majority of the bacteria, including important nitrifiers, can still not be isolated and grown as pure cultures, the introduction of molecular approaches proves vital for the characterization and quantification of ammonia and nitrite oxidizing bacterial population present in the reactor.

5.2 Material and Methods

5.2.1 Autotrophic batch test

The Autotrophic batch tests were conducted using a mixture of effluent wastewater and the mixed liquor drawn from the parent system. The single batch reactor configuration is illustrated in Fig. 5.1. Each batch test was conducted for a period of 48 h. The required volume of effluent wastewater was measured and placed in a continually stirred batch reactor maintained at a constant temperature of 20ºC. A volume of 83.3 ml of stock NH_4Cl (11.46 g/L) solution was added to 5 liters of wastewater. This produced a final

concentration of 50 mgN/L in the batch reactor. The required volume of mixed liquor was harvested from the aerobic reactor of the parent system (Chapter 3) and added to wastewater, giving a combined volume of 5 L for the mixture in the batch reactor. Immediately after the mixed liquor was added to the wastewater, a sample was drawn to obtain the initial total COD concentration (Standard Methods, 1985). The oxygen supply and OUR response in the batch test were measured using an automated technique (Randall *et al*., 1991). The sampling regime for nitrate and nitrite analyses was as follows; samples where taken at half hour intervals for the first 7 h, thereafter every hour for the next 5 hours, this was followed by 2 h intervals for 12 h, then 6 h intervals for the next 12 h and finally at the end of the 48 h period. Samples drawn from the batch reactor, were immediately filtered through 0.45 μm filter paper, 2-3 drops of $HgCl_2$ were added to the filtrate which was stored for subsequent nitrate and nitrite analysis. At the end of the batch tests, the contents of the batch reactor were homogenized in a liquidizer, a sample drawn and the final COD concentration measured. The OUR results were downloaded from the DO meter to a computer.

The pH was monitored throughout the duration of the batch test. For adequate nitrification, the pH should be kept in a range of 7.2-7.6. At the start of the batch test the pH was high due to the addition of ammonium chloride. However, as the batch test proceeded, the pH decreased due to the oxidation of ammonia and the release of hydrogen ions (H^+). This resulted in the gradual decrease in pH in the reactor to below 7.2. In order to maintain the desired pH (7.2-7.6) a few drops of sodium hydrogen carbonate solution ($NaHCO_3$) were added to the reactor. If the pH is not maintained in the specified range, the nitrification rate will decrease.

5.2.2 Sampling, cell fixation and sonication

A grab sample of mixed liquor was collected at the start of each batch test and fixed for 1.5 h at 4ºC with 4% paraformaldehyde (Appendix 4). Cells were fixed by the addition of three volumes of fixative to one volume of sample. Cells are then washed in 1x PBS (130 mM NaCl, 10 mM sodium phosphate buffer, pH 7.2) and then resuspended in PBS/cold

absolute ethanol (1:1 v/v). For the detection of gram-positive prokaryotes samples were fixed with a 1:1 mixture of PBS and absolute ethanol (v/v) (Amann, 1995). Fixed samples were then sonicated with Virsonic 100 sonicator (Virtis, USA), to break up the flocs and facilitate quantification of the nitrifiers. Sonication was carried out at 8 watts for 6 minutes (Appendix 4).

5.2.3 Membrane filtration and staining with DAPI

Membrane filtration was carried out as described by Porter and Feig (1980) with the following modification. Cellulose acetate (Millipore, 0.22 μm pore size, 25 mm diameter) filters were stained for 24 h in Sudan Black (0.3% w/v in 60% ethanol) (Appendix 5). Dual staining of cells with DAPI and fluorescent oligonucleotides was modified from the method of Hicks *et al*. (1992) so that cells were stained after *in situ* hybridization with DAPI (0.25 μg/ml) for 5 minutes (Appendix 7).

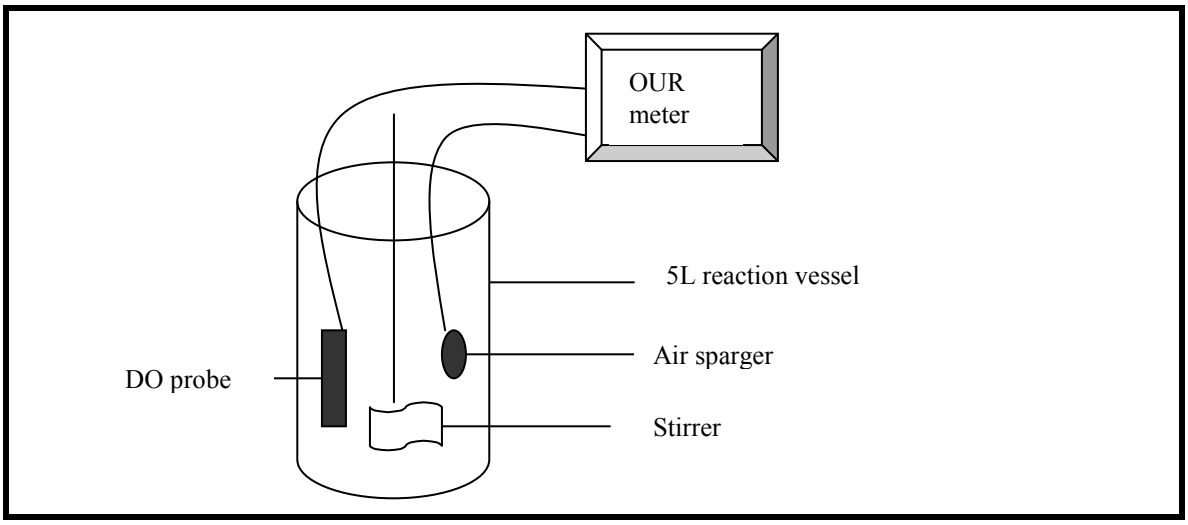

Fig. 5.1: A schematic representation of a single batch reactor used to conduct batch tests with mixed liquor added to wastewater.

5.2.4 Oligonucleotide probes and hybridization

Oligonucleotides probes used during the present study are given in Table 5.1. A volume of 10 µl of sonicated sample was spotted onto pretreated slides (Appendix 6) and allowed to dry. Spotted cells were then dehydrated by serial immersions through 60%, 80% and 96% (v/v) ethanol (3 min each). Samples of 10 µl hybridizations solution (0.9 M NaCl, 20 mM Tris/HCl, pH 7.2, 0.01% SDS, 50 ng probe, X% (v/v) formamide) were applied to each spot and incubated for 2 h at 46ºC in an isotonically equilibrated humidity chamber (Appendix 7). Probe was removed from the slide by rinsing in 2 ml pre-warmed washing solution (20 mM Tris/HCl, 0.01% SDS, 5 mM EDTA, YM NaCl). The salt concentration and formamide concentration was adjusted according to the formula of Lathe (1985). Unlabeled competitor oligonucleotides probes were used in equimolar amounts. Results with all probes used for the quantification were corrected for non-specific binding according to results with NON338 as a negative control. Slides were rapidly transferred into washing solution and incubated at 48ºC for 20 minutes. Slides were then rinsed briefly with distilled water, air- dried and mounted in Mounting media antifading solution (Bio-Rad, USA) for viewing by microscopy.

5.2.5 Microscopy and image analysis

Cells were visualized with a Zeiss Axiolab microscope (Carl Zeiss, Germany) fitted for epifluorescence with a 50W mercury high-pressure bulb and Zeiss filter sets 02, 09 and 15. Images were captured using a Hamamatsu (Japan) CCD camera. Microscopic fields (n = 30) under the 100X objective were randomly selected for enumeration.

Table 5.1: Probe sequences and formamide percentages for *in situ* hybridization

Probe	Sequence	% F[1]	fluor	Reference
EUB 388	5'- GCT GCC TCC CGT AGG AGT -3'	20	Fluorescein	Amann *et al*., 1990b
EUB 388 -II	5'- GCA GCC ACC CGT AGG TGT -3'	20	Fluorescein	Daims *et al*, 1999
EUB 388-III	5'- GCT GCC ACC CGT AGG TGT -3'	20	Fluorescein	Daims *et al*, 1999
NON388	5'- ACT CCT ACG GGA GGC AGC -3'	20	Fluorescein	Manz *et al.,*1992
NIT 3	5'- CCT GTG CTC CAT GCT CCG - 3'	40	Fluorescein	Wagner *et al*., 1996
CNIT 3	5'- CCT GTG CTC CAG GCT CCG -3'	40	unlabeled	Wagner *et al*., 1996
NSR 1156	5'- CCC GTT CTC CTG GGC AGT -3'	30	Fluorescein	Schramm *et al*., 1999
NSO 1225	5'- CGC CAT TGT ATT ACG TGT GA -3'	35	Fluorescein	Mobarry *et al*., 1996

[1] percentage formamide (v/v) in the hybridization buffer

5.3 Development of Equations for Batch test procedure

5.3.1 Growth and Death rate equations

For nitrifier growth, Monod Kinetics can be applied. The following were established.

- The mass of organisms generated is a fixed fraction of the mass of the substrate utilized (WRC, 1984).

$$M(\Delta Z_{BA}) = Y_n * M(N_a) \qquad (5.1)$$

Where

$M(\Delta Z_{BA})$ = mass of nitrifiers generated, (mgCOD)

$M(\Delta N_a)$ = mass of ammonia as N utilized, [mg(NH_3-N)]

Y_n = mass of nitrifiers generated per unit mass of ammonia utilized, [mgX_n/mg(NH_3-N)]

Differentiating equation (5.1)

$$\frac{dZ_{BA}}{dt} = Y_n \frac{dN_a}{dt}$$

- The specific rate of growth, that is, the rate of growth per unit mass of organisms per unit time, is related to the concentration of the substrate surrounding the organism

$$\mu_{nT} = \frac{\mu_{nmT} * N_a}{k_{nT} + N_a} \qquad (5.2)$$

Where

μ_n = specific growth rate (/d)

μ_{nm} = maximum specific growth rate (/d)

k_n = half saturation constant, i.e. the concentration at which $\mu_{nm} = ½ \mu_{nm}$ [mg(NH_3-N)/L]

N_a = concentration of ammonia surrounding the organisms, [mg(NH_3-N)/L)

T subscript refers to temperature, ºC

The growth rate is given by the product of the specific growth rate and organism mass:

$$\frac{dZ_{BA}}{dt} = \mu_{nT} * Z_{BA} \qquad (5.3)$$

Substituting Eq. (5.2) for μ_{nT} in Eq. (5.3)

$$\frac{dZ_{BA}}{dt} = \frac{\mu_{nmT} * N_a}{k_{nT} + N_a} * Z_{BA}$$

Herbert (1958) showed that generally an organisms mass undergoes a continuous mass loss, called endogenous mass loss. Furthermore, Ekama and Marais (1984) found that this loss occurs independently of the growth. Thus, the formulation of endogenous mass loss is:

$$\frac{dZ_{BA}}{dt} = -b_{nT} * Z_{BA}$$

Where

b_{nT} = specific endogenous mass loss rate for ammonium oxidizing bacteria, such as AO per day, at temperature T

Combining the growth and death rate equations:

$$\frac{dZ_{BA}}{dt} = \text{growth on ammonia} - \text{death}$$

$$\Rightarrow \quad \frac{dZ_{BA}}{dt} = \mu_A * \frac{N_a}{K_{SA} + N_a} * Z_{BA} - b_A * Z_{BA} \qquad (5.4)$$

Conditions should be created in the Batch test such that:

$$N_a >> K_{SA(}(K_{SA} \sim 1 mgN/L)$$

i.e. substrate concentration (N_a) ensures rate operates at the maximum

$$\frac{N_a}{K_{SA} + N_a} \approx \frac{N_a}{N_a} = 1$$

From equation (5.4):

$$\frac{dZ_{BA}}{dt} = \mu_{nm} * Z_{BA} - b_A * Z_{BA} \qquad (5.5)$$
$$= (\mu_{nm} - b_A) * Z_{BA}$$

Rearranging equation (5.5):

$$\frac{dZ_{BA}}{Z_{BA}} = (\mu_{nm} - b_A)dt \tag{5.6}$$

Integrating both sides of the equation (5.6):

$$\int \frac{dZ_{BA}}{Z_{BA}} = \int (\mu_{nm} - b_A)dt$$

$$\Rightarrow \ln Z_{BA(t)} = (\mu_{nm} - b_A)t + c \tag{5.7}$$

Taking exponentials on both sides of equation (5.7):

$$Z_{BA(t)} = e^{(\mu_{nm} - b_A)t} * e^{c} \tag{5.8}$$

At time t = 0

$$Z_{BA(t)} = Z_{BA(0)}$$

$$\Rightarrow Z_{BA(0)} = e^{0} * e^{c} \qquad (e^0 = 1)$$

$$\Rightarrow e^{c} = Z_{BA(0)}$$

Equation (5.8) then becomes:

$$Z_{BA(t)} = Z_{BA(0)} * e^{(\mu_{nm} - b_A)t} \tag{5.9}$$

Thus, by knowing the initial concentration of nitrifiers, $Z_{BA(0)}$ and the μ_{nm} value, the concentration of nitrifiers at any time, t, can be calculated (accepting the b_A value to be 0.04/d) (Ekama and Marais, (1984).

5.3.2 Nitrification Rate

Nitrate concentrations were determined and "best fit" lines fitted to the individual profiles, only exponential fit was evaluated. For the example in Fig 5.2 exponential fit to nitrate concentration – time profiles gave good correlation to the experimental data: From the regression analysis of the data in Fig 5.2 the following were obtained:

$$NO_{3(t)} = e^{0.02892(t) + 2.29654} \qquad [R^2 = 0.83] \qquad (mgN/l) \qquad (5.10)$$

Hence, differentiating the above equation to determine an expression for the appropriate nitrification rate yield for batch test no. AB4:

$$d(NO_3^-)/dt = 0.02892 \bullet e^{0.02892(t) + 2.29659} \qquad (mgN/l/h) \qquad (5.11)$$

Taking *ln* of both sides of equation (5.11)

$$\ln\left(\frac{dNO_3}{dt}\right) = \ln\left(0.02892\right) + (0.0289\ (t) + 2.29659)$$

This is the form of a straight line graph $\boldsymbol{y = b + mx}$

Slope = {0.0289 (t) + 2.29659} and y-intercept = ln [0.02892]

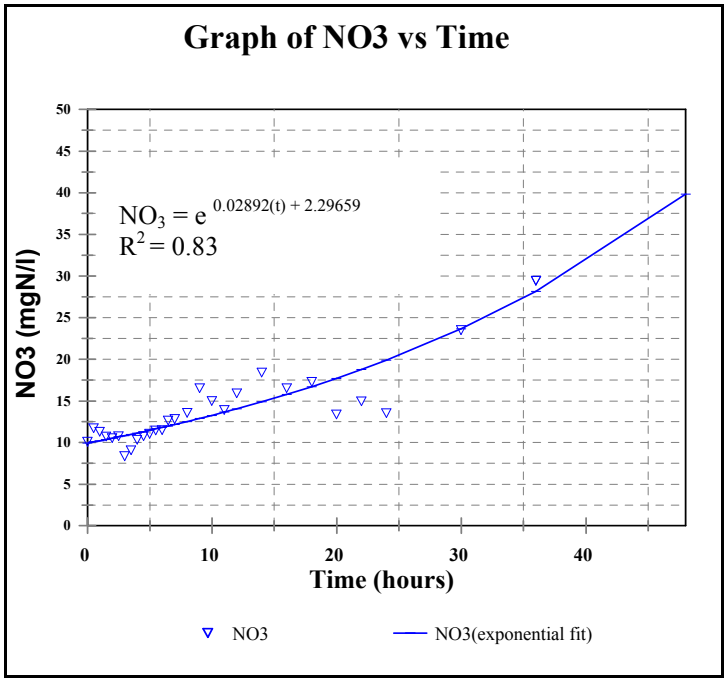

Fig 5.2: Nitrate concentrations with time for autotrophic batch test no. AB4.

The rate of nitrate production, $\frac{dNO_3}{dt}$ can be formulated as follows:

$$\frac{dZ_{BA}}{dt} = -Y_{ZA} * \frac{dN_a}{dt}$$

$$\frac{dN_a}{dt} = -\frac{dNO_3}{dt}$$

The stoichiometric ratio of ammonia utilization to nitrate production being 1:1

$$\therefore \frac{dZ_{BA}}{dt} = +Y_{ZA}\frac{dNO_3}{dt}$$

Substituting equation (5.4) into the above and rearranging

$$\frac{dNO_3}{dt} = \frac{1}{Y_{ZA}} * \mu_{nm} * \frac{N_a}{K_{SA} + N_a} * Z_{BA} \tag{5.12}$$

As before, conditions in the Batch Test should be created such that:

$$N_a >> K_{SA(}(K_{SA} \sim 1mgN/L)$$

$$\frac{N_a}{K_{SA} + N_a} \approx \frac{N_a}{N_a} = 1$$

From equation (5.12):

$$\frac{dNO_3}{dt} = \frac{1}{Y_{ZA}} * \mu_{nm} * Z_{BA}$$

And

$$\left(\frac{dNO_3}{dt}\right)_t = \frac{1}{Y_{ZA}} * \mu_{nm} * Z_{BA(t)} = \frac{\mu_{nm}}{Y_{ZA}} * Z_{BA(t)} \tag{5.13}$$

Substituting equation (5.9) into equation (5.13)

$$\left(\frac{dNO_3}{dt}\right)_t = \frac{\mu_{nm}}{Y_{ZA}} * Z_{BA(0)} * e^{(\mu_{nm} - b_A)t} \qquad (5.14)$$

Taking *ln* of both sides of equation (5.14)

$$\ln\left(\frac{dNO_3}{dt}\right)_t = \ln\left(\frac{\mu_{nm}}{Y_{ZA}} * Z_{BA(0)}\right) + (\mu_{nm} - b_A)t$$

This is in the form of a straight line graph $\boldsymbol{y = b + mx}$

A plot of $\ln\left(\frac{dNO_3}{dt}\right)_t$ versus time is shown below for batch test no. AB4.

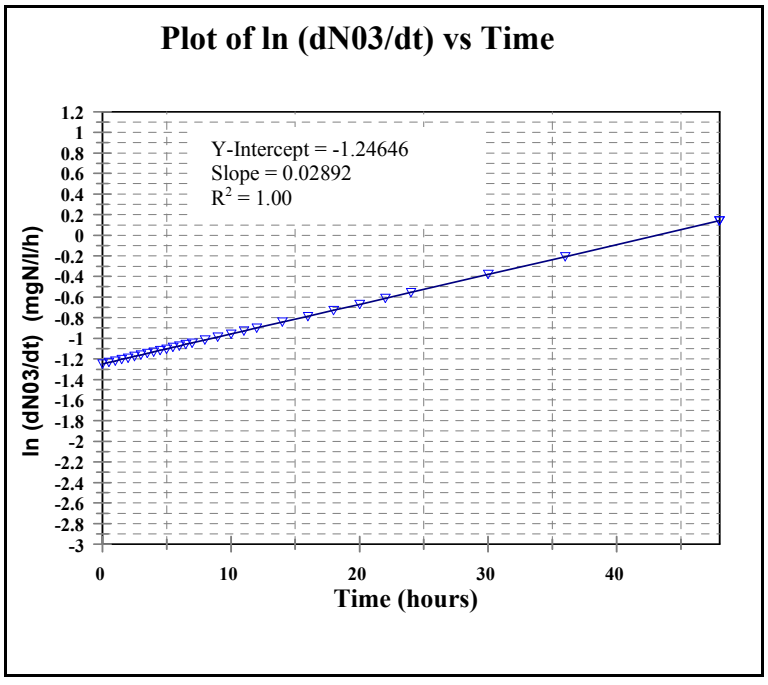

Fig. 5.3: Expected plot of *ln* (rate of change in nitrate concentration) versus time for batch test no. AB4

The slope of the above straight line graph is:

$$\left(\mu_{nm} - b_A\right) \tag{5.15}$$

Rearranging equation (5.15)

$$\mu_{nm} = slope + b_A \tag{5.16}$$

Using the data in Fig. 5.3, μ_{nm} can be determined.

μ_{nm} = 0.02892 + (0.04/24)

= 0.030586 /h

= 0.73 /d

And its y-intercept is:

$$\ln\left(\frac{dNO_3}{dt}\right)_{t=0} = \ln\left(\frac{\mu_{nm}}{Y_{ZA}} * Z_{BA(0)}\right)$$

$$\text{y - intercept} = \ln\left(\frac{\mu_{nm}}{Y_{ZA}} * Z_{BA(0)}\right) \tag{5.17}$$

Taking exponentials on both sides of equation (5.17)

$$e^{y-\text{int}\,ercept} = \frac{\mu_{nm}}{Y_{ZA}} * Z_{BA(0)} \tag{5.18}$$

Rearranging equation (5.18):

$$Z_{BA(0)} = \frac{e^{y-\text{int}\,ercept}}{\frac{1}{Y_{ZA}} * (slope + b_A)} \tag{5.19}$$

Where

Y_{ZA} = 0.15 g cell COD/g N utilized

Using data in Fig. 5.2, the initial concentration of nitrifiers at t = 0 can be calculated for batch test no. AB4.

$$Z_{BA(0)} = \frac{e^{0.02892} * 24}{\frac{1}{0.15} * [(0.02892 * 24) + 2.29659 + 0.04]}$$

$$= 1.22 \text{ mgCOD/L}$$

5.3.3 Theoretical autotrophic active biomass concentration in the parent system

In order to evaluate the autotrophic batch test procedure, the measured autotrophic active biomass concentrations determined in the batch tests will be compared with the theoretical values for the parent system from which the mixed liquor is drawn. Since the steady state theory is simpler and provides a direct analytical solution, this was used to calculate the theoretical autotrophic active biomass concentration in the parent system, and then compared to the batch test. This calculation procedure is summarized below.

From WRC (1984), the nitrifier mass fraction of the mixed liquor volatile suspended solids M(Xn) can be determined as follows:

$$M(Xn) = \frac{(QiNne + MNd)Yn * Rs}{(1 + bnT * Rs)} \qquad (5.20)$$

Where,

$QiNne$ = Obtained from N mass balance (Chapter 3)

MNd = Obtained from N mass balance (Chapter 3)

Yn = mass of nitrifiers generated per unit mass of ammonia utilized [$mgX_n/mg(NH_3\text{-}N)$]

bnT = endogenous respiration rate of nitrifying bacteria at TºC = 0.04/d

Rs = sludge age

As an illustration, for batch test no. AB4 conducted with sewage batch no. 12/04 (26 July 2004) the theoretical autotrophic active biomass concentration in the batch reactor due to the addition of the mixed liquor sample drawn from the parent system was calculated as follows:

Using data from the parent system during sewage batch no. 12/04 as an example, QiNne = 269.7 mgN/d; Yn = 0.10; Mnd = 482.5 mgN/d (Appendix 9, Table 9.1); fcv = 1.53 mgCOD/mgVSS, V_{ML} = 0.5L and V_{WW} = 4.5L Substituting these values into Eq. (5.20).

$$MXn = \frac{(269.7 + 482.5) * 0.10 * 10}{(1 + 0.04) * 10}$$

$$= 72.33 \text{ mgVSS}$$

Total volume of anoxic and aerobic Vp = 15 L

$$Xn = \frac{M(Xn)}{Vp} = \frac{72.33}{15}$$

$$= 4.822 \text{ mgVSS/L}$$

In 500 ml, $Xn = \frac{500 * 4.822}{1000} = 2.411 \text{ mgVSS}$

500 ml in 4.5L reactor,

$$Xn = \frac{2.411}{4.5}$$

$$= 0.5358 * 1.48$$

$$= 0.793 \text{ mgCOD/L}$$

5.4 Results

This section will document the results obtained for the parent system, batch tests and FISH analysis. Also, illustrated is a comparison between the theoretical autotrophic active biomass concentration in the parent system [$Z_{BA(0)}$ (Theo.)], the autotrophic active biomass concentrations measured at the start of the batch tests [$Z_{BA(0)}$ (Meas.)] and the autotrophic active biomass at the start of the test determined by molecular probing [($Z_{BA(0)}$ Probe)]. The calculation procedures for the parent system and batch test are fully detailed in sections 5.3.2 and 5.3.3 above.

5.4.1 Parent system data

Each sewage batch constituted a steady state period during which the characteristics of the sewage batch governed the parent system behavior. Therefore, each sewage batch was analyzed separately to determine the various parent system parameters, as set out in Chapter 3. During 6 out of a total of 22 sewage batches (22 sewage batches in 2004), autotrophic batch tests were conducted. For these sewage batches the various parent system parameters and the average data [From Tables 3.5 (a, b) and 3.6 in Chapter 3] are listed in Table 5.2 and 5.3.

Table 5.2: Steady state results for the parent laboratory-scale anoxic/aerobic activated sludge system for those WW batches used during autotrophic batch tests. Averages are listed with sample standard deviations in parenthesis.

Sew batch no.	COD (mg/l)		TKN (mgN/l)		Nitrate (mgN/l)			OUR mgO/l/h	Mixed liquor (mg/l)		
	Inf	Eff	Inf	Eff	Anoxic	Aerobic	Eff		VSS	COD	TKN
8/04	516.4 (2.5)	48.2 (9.6)	46.4 (9.9)	6.1 (4.0)	0.8 (1.2)	6.6 (3.0)	10.1 (2.7)	34.0 (1.2)	2028.7 (189.2)	2962.9 (193.5)	231.4 (55.5)
9/04	506 (16.1)	46.8 (7.8)	41.9 (3.4)	3.5 (0.9)	1.2 (1.0)	6.4 (1.3)	9.4 (1.2)	26.7 (1.9)	2341.6 (251.9)	3652.8 (426.3)	223.7 (21.9)
12/04	474.4 (22.3)	43.9 (5.8)	49.3 (5.1)	4.5 (0.5)	2.7 (1.1)	9.5 (1.7)	12.0 (1.9)	30.4 (0.6)	2151.6 (315.5)	3207 (366.5)	220.8 (13.3)
14/04	492.3 (32.7)	43.1 (5.3)	45.4 (6.7)	5.7 (1.9)	2.3 (1.7)	7.5 (2.9)	12.3 (2.3)	31.3 (1.6)	2088.2 (137.8)	3145 (227.1)	200.2 32.7
16/04	479.4 (25.2)	40.2 (4.5)	39.3 (3.7)	4.4 (0.7)	1.5 (0.8)	5.7 (1.4)	9.1 (2.1)	30.3 (0.8)	1985 (239.0)	2949.4 (307.5)	226.5 (24.9)
18/04	420.0 (39.9)	44.0 (9.5)	35.4 (1.2)	6.4 (1.8)	1.8 (1.1)	6.6 (1.8)	8.2 (1.5)	30.1 (0.4)	1659.4 (446.7)	2254.5 (215.1)	135.5 (35.4)

To formulate a theoretical estimate for autotrophic active biomass concentration present in the parent system during each sewage batch period, the following were determined from the data in Table 5.2 and 5.3:

- System COD and N mass balances fell within the acceptable range of 90-110% (Table 5.3) (Ekama *et al*., 1986); mass of nitrate in the effluent and mass of nitrate denitrified (MN_{ne} and MN_d respectively) and the COD and TKN to VSS ratios for the mixed liquor (f_{CV} and f_N respectively). The calculation procedures are set out in detail in Chapter 3 and the results for each sewage batch during which the modified batch tests were conducted are listed in Table 5.3.

- The theoretical autotrophic active biomass was determined for each sewage batch using the steady state design model [Eq. (5.20)] (WRC, 1984).

Table 5.3: Steady state COD and N mass balances, nitrate utilization and mixed liquor parameters for the 10 days sludge age parent laboratory-scale anoxic/aerobic activated sludge system.

ww Batch No.	Mass balance (%)		Mass of effluent NO_3 (MN_{ne}) (mgN/d)	Mass of NO_3 denitrified (MN_d) (mgN/d)	Mixed liquor	
	COD	N			COD/VSS ratio (mgCOD/mgVSS) (fCV)	TKN/VSS ratio (mgN/mgVSS) (fN)
8/04	94.6	109.0	226.9	478.4	1.47	0.1135
9/04	92.4	104.6	212.5	415.0	1.57	0.0965
12/04	94.8	101.7	269.7	482.5	1.53	0.1053
14/04	97.0	105.3	277.1	431.2	1.51	0.0961
16/04	95.9	106.4	205.3	352.1	1.49	0.1154
18/04	96.9	103.5	184.3	340.0	1.42	0.0854

5.4.2 Batch test data

For the batch tests, NO_3 and NO_2 - time data and Ln (rate of change of nitrates) are shown graphically in Appendix 12. Following the procedures set out in Section 5.3.2 above, the autotrophic active biomass concentrations measured at the start of the test were calculated and are listed in Appendix 12 and the results are summarized in Table 5.4.

The μ_{nm} values for all the batch tests were calculated using Eq. (5.16) and are listed in Table 5.4. For μ_{nm}, a statistical plot for μ_{nm} values for all the modified batch tests was constructed (Fig. 5.4). From Fig. 5.4, the mean μ_{nm} was 0.788/d with sample standard deviation of 0.199/d.

Table 5.4: Regression data from Ln (rate of change of nitrates) versus time plot and autotrophic active biomass at the start of the batch test ($Z_{BA(0)}$)

Sew batch no.	Batch test no.	Volume (L)		Regression			Growth Rate (/d)	$Z_{BA(0)}$ (mgCOD/l)			
								Measured		Theoretical	
		WW	ML	Y-int	Slope	R^2	μ_{nm}	Batch	ML	Batch	ML
8/04	AB1	4.6	0.4	-0.65	0.041	1.00	1.03	1.05	13.15	0.582	7.27
9/04	AB2	4.5	0.5	-4.67	0.041	1.00	1.02	1.36	13.63	0.662	6.61
12/04	AB3	4.5	0.5	-0.97	0.026	1.00	0.66	1.10	11.02	0.793	7.93
12/04	AB4	4.5	0.5	-1.25	0.029	1.00	0.73	1.22	12.22	0.793	7.93
14/04	AB5	4.5	0.5	-2.30	0.033	1.00	0.82	1.91	19.01	0.747	7.47
14/04	AB6	4.65	0.35	-2.36	0.041	1.00	1.01	2.02	28.84	0.506	7.22
16/04	AB7	4.5	0.5	-1.31	0.031	1.00	0.78	1.26	12.59	0.588	5.88
16/04	AB8	4.5	0.5	-1.35	0.035	1.00	0.89	1.30	12.98	0.588	5.88
18/04	AB9	4.5	0.5	-1.44	0.018	1.00	0.47	1.20	11.99	0.553	5.53
18/04	AB10	4.5	0.5	-1.44	0.018	1.00	0.47	1.20	11.99	0.553	5.53

In Table 5.4, the measured autotrophic active biomass concentration at the start of each batch test [$Z_{BH(0)}$(Meas.)] is compared to the theoretical autotrophic active biomass concentration at the start of the batch test due to the mixed liquor sample which was drawn from the parent system and added to the batch test [$Z_{BH(0)}$(Theo.)]. The theoretical values were predicted via the steady state model (see section 5.3.3). To illustrate the comparison, the measured versus theoretical mixed liquor autotrophic active biomass data for all the batch tests are shown in Fig. 5.5.

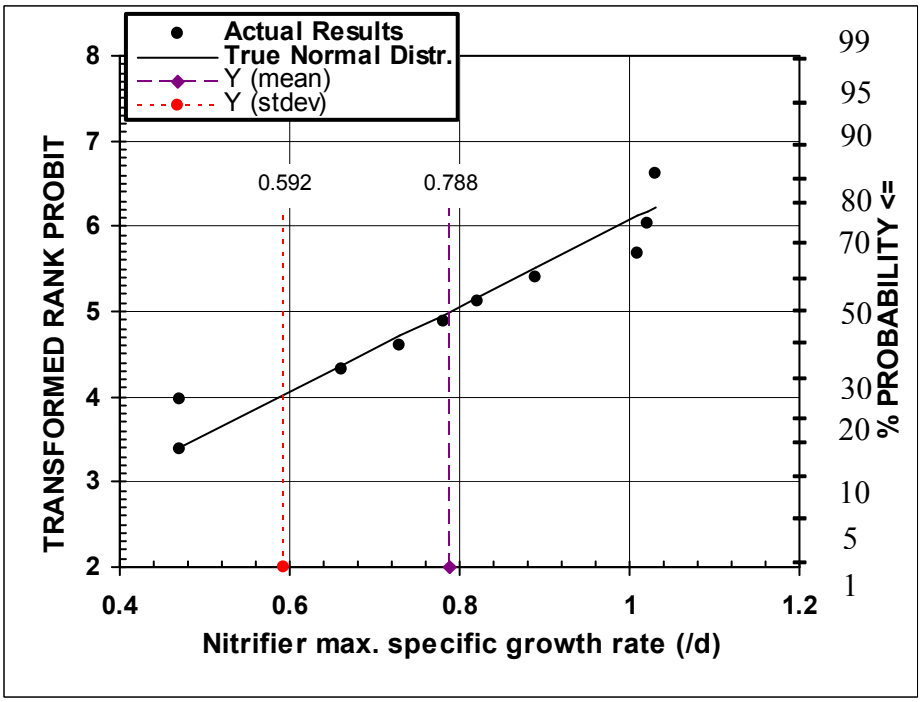

Fig 5.4: Statistical plot of μ_{nm} data for all autotrophic batch tests

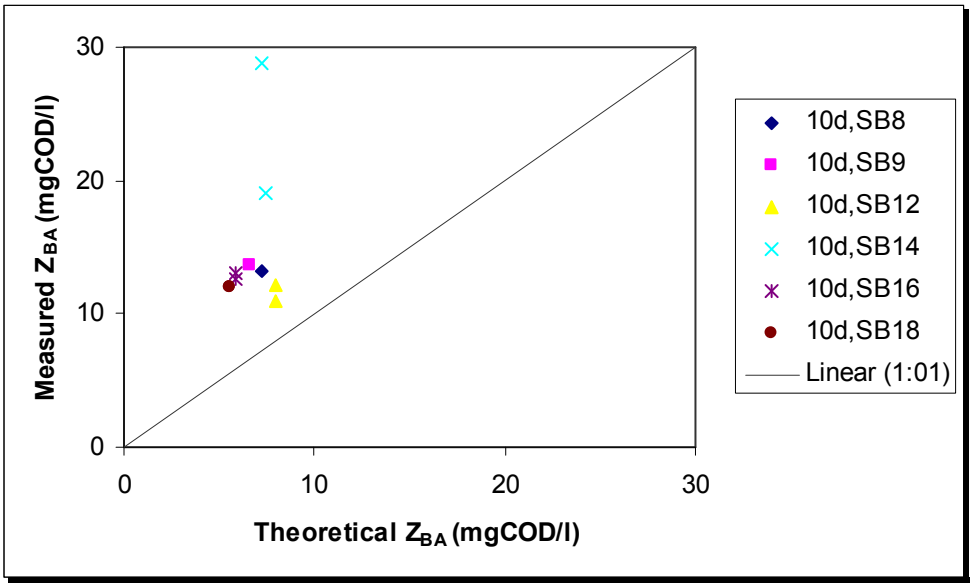

Fig. 5.5: Autotrophic batch test results; graph of measured versus theoretical autotrophic active biomass concentration at the start of the test [$Z_{BA(0)}$] for various sewage batches (SB) for the 10 d (sludge age) MLE activated sludge system

5.4.3 Quantification of ammonia and nitrite oxidizing bacteria

The existence of ammonia and nitrite oxidizers were identified and quantified with a set of 16S rRNA-targeted oligonucleotide probes (Table 5.1). The following nitrifying probes were used, NSO 1225 complementary to a signature region of all known ammonia oxidizers in the beta-subclass of *Proteobacteria* (Mobarry *et al.,* 1996), NIT3 complementary to a region of all previously sequenced *Nitrobacter* species was used along with an unlabeled competitor CNIT3 (Wagner *et al*., 1996) and NSR 1156 specific for freshwater *Nitrospira spp*. EUB388 probe mix (consisting of probes EUB338, EUB338-II, and EUB338-III) was used to target the domain bacteria (Daims *et. al*., 1999). To determine the autotrophic active biomass concentration at the start of each batch test, the sum of the ammonia and nitrite oxidizing cell counts (sum of NSO 1225, NIT3 and NSR 1156 cell counts) consolidated the nitrifying population (Table 4.5). Cell counts for the determination of the autotrophic active biomass concentration for each batch test was converted to mass units (mgCOD/l) in order to determine what fraction of the measured VSS is metabolically active. In order to make a conversion from cell numbers to mass units a conversion factor (FVB) of 8.49 x 10-11 mgVSS/cell (Holder-Snymann *et al.,* 2005; Mudaly *et al.,* 2001) was applied in the following equation:

$$Z_{BA} = \frac{CC \bullet F_{(CV)} \bullet F_{(VB)} \bullet V_{(0)}}{V_{(M)} \bullet 1000 \bullet DF} \qquad (5.21)$$

Where

Z_{BA} = Autotrophic active biomass (mgCOD/l)

CC = Cell counts (cells/ml)

Fcv = COD to VSS ratio of the mixed liquor (mgCOD/mgVSS)

$V_{(0)}$ = Original volume of fixed sample (ml)

$V_{(M)}$ = Remaining volume of fixed sample (ml)

DF = Dilution factor

In Table 5.5, the measured autotrophic active biomass concentration at the start of each batch test [$Z_{BA(0)}$ (meas.)] is compared to the probe autotrophic active biomass concentration at the start of the test [$Z_{BA(0)}$ (probe)]. In sludge samples taken at the start of each batch test, cells hybridizing with EUB probe mix ranged from 6.21 (±1.29) to 14.3 (±1.11) x 10^9 cells/ml. Cells hybridizing with probe Nso1225 varied between 0.81 (±0.009) and 4.20 (±0.26) x 10^9 cells/ml. Cells hybridized to probes NIT3 and NSR1156 acounted for 0.04 (±0.002) to 0.58 (±0.02) x 10^9 cells/ml and 0.35 (±0.04) to 0.84 (±0.04) x 10^9 cells/ml of detectable cells, respectively. Comprehensive FISH data including DAPI and probe cell counts for each batch test are listed in Appendix 13. The batch test translated NO_3 and NO_2 - time profiles into parameters that reflect the $Z_{BA(0)}$ and are directly comparable to the $Z_{BA(0)}$ measures from the molecular probes.The probe values ranged from 39.17 (±0.50) to 163.22 (± 8.68) mgCOD/L, while the measured values ranged from 80.7 to 834.6 mgCOD/L (Table 5.5). To illustrate the comparison, the measured versus probe mixed liquor autotrophic active biomass data for all the batch test are shown in Fig. 5.6.

Table 5.5: Ammonia oxidisers (Nso1225), nitrite oxidizers (NIT3 + NSR1156) and measured autotrophic active biomass concentrations at the start of each batch test ($Z_{BA(0)}$)

Batch test no.	No. (± SD) of cells ($10^8 \cdot ml^{-1}$)				Probe measured $Z_{BA(0)}$ (mgCOD/l)	Measured $Z_{BA(0)}$ (mgCOD/l) ML
	EUB mix	Nitrifiers				
		NSO1225	NIT3	NSR1156		
B1/03	8.02 ± 0.08	1.04 ± 0.13	0.05 ± 0.001	0.47 ± 0.01	46.65 ± 3.81	13.15
B2/03	8.79 ± 0.34	1.48 ± 0.16	0.04 ± 0.002	0.69 ± 0.03	70.80 ± 5.83	13.63
B3/03	7.51 ± 0.24	1.68 ± 0.12	0.18 ± 0.02	0.35 ± 0.009	68.82 ± 3.88	11.02
B4/03	6.21 ± 1.29	0.81± 0.009	0.07 ± 0.002	0.37 ± 0.01	39.17± 0.50	12.22
B5/03	6.31 ± 0.09	1.26 ± 0.15	0.14 ± 0.007	0.35 ± 0.04	53.92 ± 5.21	19.01
B6/03	7.93 ± 0.21	1.16 ± 0.13	0.58 ± 0.02	0.77± 0.02	77.36 ± 3.57	28.84
B7/03	14.3 ± 1.11	4.20 ± 0.26	0.34 ± 0.03	0.84 ± 0.04	163.22 ± 8.68	12.59
B8/03	13.1 ± 0.92	2.77± 0.14	0.17 ± 0.005	0.51 ± 0.007	105.05 ± 4.19	12.98
B9/04	10.2 ± 1.10	0.85± 0.02	0.12 ± 0.009	0.49 ± 0.02	42.36 ± 0.97	11.99
B10/04	8.67 ± 0.14	1.18 ± 0.01	0.10 ± 0.01	0.43 ± 0.006	49.53 ± 1.76	11.99

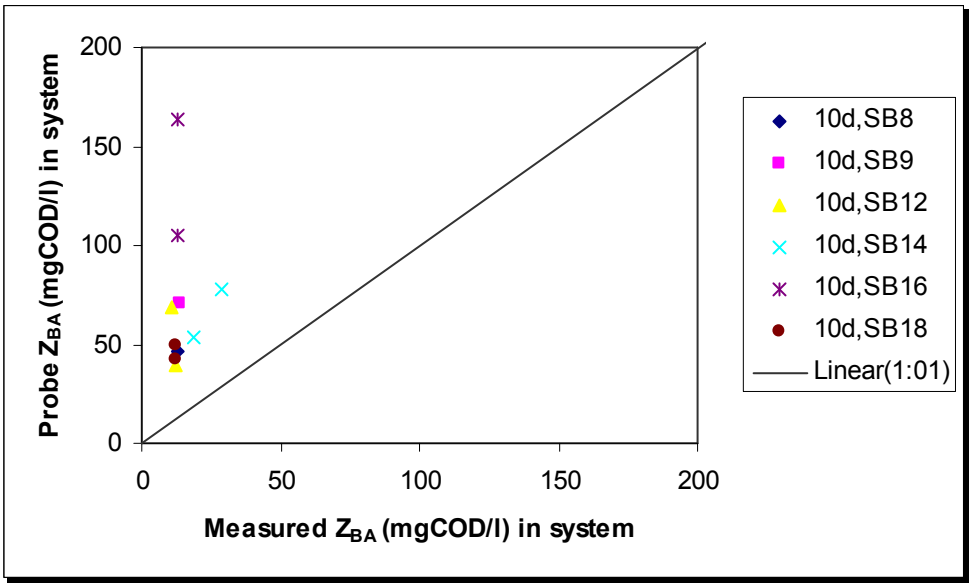

Fig. 5.6: Measured versus probe autotrophic active biomass concentration at the start of the test [$Z_{BA(0)}$] for various sewage batches (SB) for the 10d sludge age MLE activated sludge system.

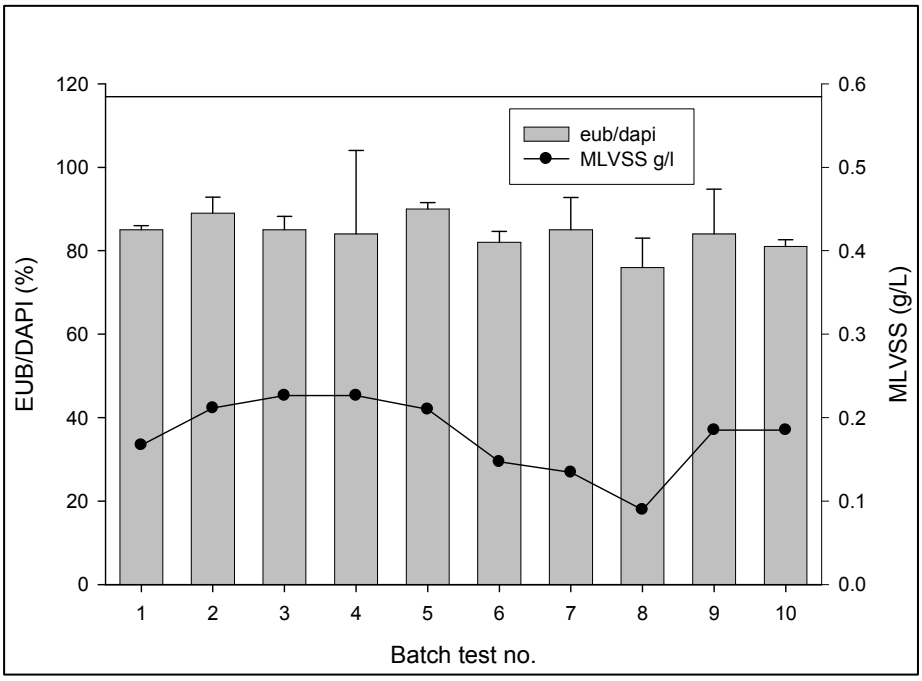

Fig. 5.7: Percentage of EUB-detectable cells relative to DAPI counts in activated sludge samples taken at the start of each autotrophic batch test.

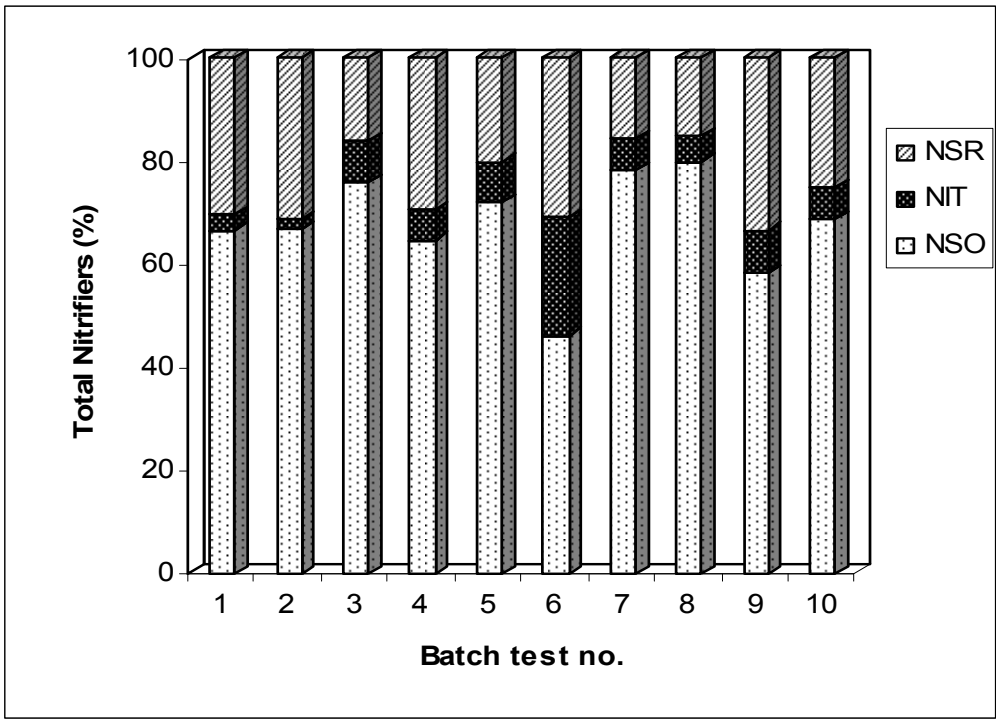

Fig. 5.8: Composition of ammonia oxidizers (Nso1225) and nitrite oxidizers (NIT3+NSR1156)

The EUB/DAPI ratio was used to assess the abundance of metabolically active cells present in each batch test. In sludge samples taken at the start of each batch test, the percentages of cells giving a clear fluorescence signal after hybridization varied between 76% (±7.03%) and 90% (±1.54%) of all DAPI-stained cells (Fig. 5.7). In order to assess if the MLVSS fraction is a true reflection of the metabolically active cells present in the biomass, MLVSS concentrations were compared with results from hybridization experiments in each batch test. The MLVSS concentrations in all the batch tests ranged between 0.0895 and 0.2264 g/L. As shown in Fig. 5.7, the percentages of FISH-detectable cells were almost identical and were not affected by changing operating conditions.

The AOB group specific probe Nso1225 and the genus specific probes for NOB (NIT3+NSR1156) were applied to analyze the composition of nitrifiers in ten autotrophic batch tests. Ammonia oxidizers ranged from 46.15% to 80% of the total nitrifier

population. *Nitrospira sp* was found to be the dominant nitrite oxidizer ranging from 15% to 33.33%., whilst *Nitrobacter sp* ranged from 1.79% to 23.08% of the total nitrifier population (Fig 5.8).

5.5 Discussion

5.5.1 Maximum specific growth rates (μ_{nm})

Models that are dependant on the Monod relationship are frequently used to describe microbial growth kinetics in both pure (Senn *et al*., 1994; Owens and Legan, 1987) and mixed cultures (Gujer *et al*., 1995). Monod's model relates the growth rate to the concentration of a single growth-controlling substrate via the maximum specific growth rate (μ_{nm}) and the substrate affinity constant (K_s). Since the growth is a result of catabolic and anabolic enzymatic activities, these processes, i.e., substrate utilization or growth-association product formation can be quantitatively described based on growth models (Kovarova-Kovar and Egli, 1998).

Here we provide a new batch test method to measure μ_{nm} and determine the initial concentration of nitrifiers $Z_{BA(0)}$. μ_{nm} values ranged from 0.47 – 1.03/d. For $\mu_{nm,}$ a statistical plot of the μ_{nm} values for all autotrophic batch tests was constructed (Fig 5.4); the mean μ_{nm} was 0.788/d with sample standard deviation of 0.199/d. The mean value falls within in the acceptable range for raw municipal WW in South Africa (0.3 – 0.8/d, WRC, 1984). From the statistical plot (Fig. 5.4) it is evident that the data are normally distributed; this indicates that (i) the μ_{nm} value is influenced by an infinite number of parameters, that is, no single parameter had a single major influence (ii) each parameter has a small influence on the μ_{nm} value and (iii) each parameter influencing the μ_{nm} value is independent and random.

Microbial growth kinetics of suspended cells is usually determined through conducting batch, continuous-culture, or fed-batch experiments in the laboratory. Although, in

theory (Wanner, 1994), the latter technique should overcome some of the disadvantages which hamper the conventional methods of batch and chemostat cultivation, it has never been routinely used to experimentally estimate kinetic parameters (e.g., μ_{max} and K_s). In batch-culture experiments, either the consumption of the growth-controlling substrate or the increase in biomass concentration is monitored as a function of time. Inherent in this system is that the cell's environment and hence the cell's composition and physiological state change during the experiment (Grady *et al*., 1996). Therefore, it is the growth in carbon-limited continuous culture, mostly under (slow) transient conditions or sometimes close to steady-state conditions, that probably resembles the growth conditions experienced by microorganisms in nature most of the time (Kovarova-Kovar and Egli, 1998).

5.5.2 Comparison between measured and theoretical AO active biomass for 10 days sludge age MLE activated sludge system

In Table 5.4, the measured AO active biomass concentration at the start of each batch test [$Z_{BA(0)}$(meas.)] is compared to the theoretical AO active biomass concentration at the start of the test due to mixed liquor sample which was drawn from the parent system and added to the batch test [$Z_{BA(0)}$(theor.)]; theoretical values were predicted via the steady state design model. To illustrate the comparison, the measured versus theoretical mixed liquor AO active biomass data for all the batch tests are shown in Fig. 5.5.

From Fig. 5.5, poor correspondence between measured and theoretical $Z_{BA(0)}$ values were evident. In examining possible causes for the lack of correspondence between theoretical and measured AO active biomass concentrations, it was noted that the batch test method to quantify AO active biomass relies on a single AO population with constant kinetics. Observations made in this research, and previously (e.g. Daigger and Grady, 1982; Novak *et al.*, 1994; Grady *et al*., 1996) suggest that this may not be true, and that the batch test conditions may cause the overall AO behaviour to deviate significantly from that of the steady state system. The batch test method, and its interpretation in terms

of the procedures described in sections 5.2 and 5.3, is particularly sensitive to any changes in AO kinetics as time proceeds in the batch test, since these kinetics are applied to the start of the test to determine the AO active biomass concentration. This sensitivity, can explain the variability in correlations between batch test measured AO active biomass concentrations and the theoretical values. Further reasons for the inconsistencies between measured and theoretical values were evaluated using molecular techniques (Chapter 6).

5.5.3 Comparison between measured and probe AO active biomass for 10 days sludge age MLE activated sludge system

In Table 5.5, the measured AO active biomass concentration at the start of each batch test [$Z_{BA(0)}$ (meas.)] is compared to the probe AO active biomass concentration at the start of the test [$Z_{BA(0)}$ (probe)]. The batch test translated nitrate- time profiles into parameters that reflect the $Z_{BA(0)}$ and are directly comparable to the $Z_{BA(0)}$ measures from the molecular probes. The $Z_{BA(0)}$ values obtained by molecular probing correlated poorly with measured $Z_{BA(0)}$ (ML) values obtained from the modified batch tests (Fig. 5.6).

As mentioned above, model data used to record nitrifying autotrophic biomass were compared to microscopic activity of the batch test. However, adequate FISH data available in this particular case was clearly sufficient for full and proper model verification. The quantitative approach applied here, did not have reliable and exact correspondence between nitrifying community structure expressed as cell numbers and expressed as model biomass. The large degree of variability could be ascribed to the fact that active and inactive ammonia-oxidizers cells cannot be distinguished by FISH with rRNA-targeted probes, and the assumption that all quantified, probe-stained cells were metabolically active leads to unprecise activity estimations. Schraam *et al*. (1999) combined microsensor measurements and FISH to investigate the *in situ* structure and function of the nitrifying bioreactor. In examining the aggregates from the top of the reactor and in the central parts of all aggregates, ammonium was virtually absent and no ammonium oxidation activity was detected. Nevertheless, ammonia-oxidizing bacteria were detectable by FISH, although in significantly lower numbers than in the active

zones. This again demonstrates the capacity of ammonia-oxidizing bacteria to maintain their ribosomes, even under conditions not conducive to activity and growth (Wagner *et al*., 1995; Schramm *et al*., 1996).

The microscopic detection of microbial cells and the ability to estimate their abundance in reactors provide valuable information about population structure, but lack proof that the organisms in question are actually performing a certain function. Recently, FISH has been combined with microautoradiography (MAR) to determine specific uptake of organic and inorganic radiolabeled substrates by activated sludge microbial communities (Lee *et al*., 1999). FISH and MAR have been used to demonstrate that members of the nitrite-oxidizing genus *Nitrospira* in activated sludge, which could not be cultivated in the laboratory, are able to fix atmospheric CO_2. They were far more abundant *in situ* than were *Nitrobacter* cells (Daims *et al*., 2000). This technique is essential for improving mathematical models and understanding why certain physiological conditions must be optimized in order for nitrification to persist in a particular reactor setting (Wilderer *et al*., 2002).

5.5.4 Nitrifying population dynamics

The FISH analysis of nitrifying bacteria in ten autotrophic batch test revealed notably high concentration of ammonia oxidizers (Fig. 5.8). The occurrence of both *Nitrobacter* and *Nitrospira*-like bacteria were detected in all batch tests, the quantification of their populations yielded much higher cell numbers for *Nitrospira* than for *Nitrobacter* (Fig. 5.8). The quantitative dominance of *Nitrospira*-like bacteria over *Nitrobacter*, which corresponds to the results of other studies (Burrell *et al*., 1998; Juretschko *et al*., 1998; Schramm *et al*., 1998; Schramm *et al*., 1999) indicates that the former are more successful under the growth conditions in most WWTPs. Therefore, they should be regarded as the actual key organisms of nitrite oxidation in wastewater treatment. Increased concentration of *Nitrobacter* (23.08%) in batch test 6 (Fig. 5.7) could be due to its capability to grow mixotrophically (Daims *et al*., 2001a). The factors, however, which select for *Nitrospira* or *Nitrobacter* are still unknown and deserve further investigation

since detailed knowledge about this topic would help to improve the growth conditions for the most efficient nitrite-oxidizers and hence to increase both stability and performance of nitrifying bioreactors (Daims *et al*., 2001a).

5.6 Conclusion

Engineering design, efficient operation, and assessment of alternative process control strategies for nitrification require information about the quantities and activities of AOB and NOB in activated sludge treatment systems. In this study, batch test procedure designed to quantify the autotrophic component of activated sludge revealed large discrepancies between measured and theoretical AO active biomass concentration, therefore rendering it an unsuitable practice to directly quantify the AO active biomass with sufficient accuracy. However, FISH analysis shows promise in accurately quantifying the AO active biomass and therefore replacing indirect methods (batch test). FISH analysis confirms its reliability over conventional techniques in identifying and quantifying key microbial communities (nitrifiers) in activated sludge. This proves vital in understanding and monitoring key microbial process, which could be beneficial in the detection of earlier malfunctions in WWTP's.

CHAPTER 6

Using PCR-Denaturing Gradient Gel Electrophoresis to compare Microbial Community Structure between the Modified Batch Test and the Parent System under Defined So/Xo conditions

6.1 Introduction

It is now well established among microbiologist that only a small fraction of all bacteria have being isolated and characterized (Wayne *et al*., 1987; Ward *et al*., 1992). Comparison of the percentage of culturable bacteria with total cell counts form different habitats showed enormous discrepancies (Amann *et al*., 1995). In order to obtain a better understanding of the role of microbial diversity in the maintenance of various ecosystems, alternative approaches which complement the traditional microbiological procedures are required.

Denaturing gradient gel electrophoresis of 16S rDNA fragments, generated by the polymerase chain reaction (PCR-DGGE), has become a popular method among microbial ecologists to study the diversity of natural microbial populations. This method constitutes direct extraction of the community DNA and amplification of typically 200–600 bp long 16S rDNA fragments. These fragments are separated according to their melting point on a denaturing gradient gel (Muyzer and Smalla, 1998). PCR-DGGE is considered a rapid and reliable method for the relative comparison of different bacterial communities. The method also provides a comparison of the true sequences if DGGE bands are excised and sequenced (Muyzer and Smalla, 1998). The PCR-DGGE was originally developed to analyze fragments from single organisms where comprehensive knowledge of the nucleotide sequence was available (Muyzer *et al*., 1993). Muyzer *et al*. (1995) used DGGE analysis of PCR amplified rDNA fragments to provide information on the genetic diversity of microbial communities found around hydrothermal vents. DGGE analysis of

16S rDNA fragments has been used to study the presence and activity of sulphate reducing bacteria in a stratified water column of Mariager Fjord in Denmark (Teske *et al*., 1996). DGGE of PCR amplified 16S rRNA gene fragments has been applied to profile the distribution of microbial populations inhabiting regions with different temperatures in a hot spring cyanobacterial community (Ferris *et al*., 1996). The results of these studies have shown the enormous wealth of microbial diversity and at the same time the limitations of traditional cultivation techniques to retrieve this diversity.

The batch test procedure (see chapter four) developed by Kappeler and Gujer (1992) presented a means of quantifying the heterotrophic active biomass (Z_{BH}) concentration through monitoring the organisms OUR response with time in the batch reactor. The modifications of the batch test (Wentzel *et al*., 1995; Ubisi *et al*., 1997a, b; Cronje *et al*., 2002) have been extensively evaluated and correspondences between the measured (Batch test) and theoretical (Parent system, see chapter three) Z_{BH} has been observed with a large degree of variability (Lee *et al*., 2003). The batch test measured Z_{BH} were consistently lower than the corresponding theoretical values (chapter four). Lee *et al*. (2003) explained that the ordinary heterotrophic organisms (OHO) maximum specific growth rates increased with time, and this behaviour is not reflective of a single OHO population with fixed kinetics that defines the modified batch test procedure. This results in the underestimation of Z_{BH}. Grady *et al*. (1996) proposed substrate competition between different OHO groups as a possible cause.

During a batch experiment, an initial substrate concentration (So) is in contact with an initial quantity of microbial culture (Xo). The parameter So represents the carbon and energy source for biosynthesis, while Xo represents a source of carbon and energy consumption. After being put into contact with the substrate, microorganisms of mixed culture start to remove the substrate, which is demonstrated by changes in substrate removal and biomass growth curves or lines. Therefore the most important parameter in batch cultivation of mixed cultures is the ratio of initial substrate concentration to initial biomass concentration (So/Xo as COD/Biomass) (Chudoba *et al*. 1992)

At high substrate to biomass ratios the batch assay will measure the maximum rate of substrate oxidation, but it does not represent the growth rate and physiological state of bacteria in the original treatment environment. The greater the batch reactor So/Xo ratio, the greater the change in the bacterial community away from that of the original wastewater environment, and the more likely it is that the measured kinetics will reflect the characteristics of the fastest growing bacteria, or changes in the physiological state of the bacterial community. Hence, lower So/Xo ratios (<2) are preferred in batch assays. Under these conditions, bacterial cell multiplication rate is assumed not to be altered from that of the original treatment environment (Chudoba *et al.,* 1991, 1992).

This chapter will aim to address reasons for the inconsistencies between the measured and theoretical Z_{BH} values, by providing a comparison of bacterial communities between the batch test and parent system using PCR-DGGE analysis. This study also explores the significance of defined So/Xo ratios in a mixed batch culture.

6.2 Materials and Methods

6.2.1 DNA extractions

Samples of 25 mL were taken in one-hour intervals from each of the three-batch test (Batch test 10, 11 and 15) previously discussed in chapter four. The phenol-chloroform extraction technique (Appendix 14) produced a high yield of DNA from the 0.2 g activated sludge pellet samples (Mayer and Palmer, 1996; Kuhn *et al*., 2002). The samples were incubated with lysis buffer and then exposed to a cycle of freezing and thawing the cells which was carried out five times. The removal of proteins and RNA contaminants was done by treating the samples with phenol-chloroform (25:24) and 98% chloroform. The extracted DNA was precipitated with absolute isopropyl alcohol and quantification of the DNA was done using a spectrophotometer according to Maniatis *et al*. (1982).

6.2.2 PCR

The variable V3 region of 16S rDNA was enzymatically amplified in the PCR with primers to conserved regions of the 16S rRNA genes. The nucleotide sequences of the primers are as follows: primer 1, 5'-CGCCCGCCGCGCCGGCGGGCGGGGCGGG GGCACGGGGGGCCTACGGGAGGCAGCAG-3' primer 2, 5'-ATTACCGCGGCTG CTGG-3' corresponding respectively to positions (in *E. coli*) 341-358 and 534-517. Primer 1 has at its 5' end a 40-nucleotide GC-rich sequence (GC clamp). A combination of primers 1 and 2 was used to amplify the 16S rDNA regions (Muyzer *et al.,* 1993). PCR amplification was carried out on a Hybaid Thermal Cycler (Hybaid limited, Ashford, UK) in 0.2 ml reaction volumes. The reaction mixture and PCR procedure is detailed in Appendix 15.

6.2.3 DGGE

All DGGE gels were prepared using a D-gene denaturing gel electrophoresis system (Bio-Rad, Hercules, Ca, USA). PCR products were loaded onto a 7.5% (wt/vol) acrylamide gel (37.5:1, acrylamide: N,N'-methylene-bis-acrylamide) in 1 x TAE buffer with gradients which were formed with 7.5% (wt/vol) acrylamide stock solutions. An optimum denaturant range of 20% to 50% was determined. Parallel DGGE gels (Appendix 16) containing a linear gradient of 20% to 50% parallel to the direction of electrophoresis were run with PCR products obtained from batch test samples. Gels were run for 3 hours at a constant 200V at 60°C by which time the bands had stabilized. Gels were stained with ethidium bromide (1 mg/ml) and photographed with UV transillumination (302 nm) (Hoefer Pharmacia Biotech Inc, USA). DGGE profiles of batch tests at defined So/Xo ratios were determined.

6.3 Data Interpretation

The ratio So/Xo can have a number of interpretations, e.g. So = total, biodegradable or biodegradable soluble COD; Xo = TSS, VSS or OHO active biomass. In this investigation, the initial substrate concentrations, So, were determined by measuring the COD concentrations of the flocculated and filtered sewage before addition to the batch reactor and taking due account of the dilution by addition of mixed liquor (chapter four). This interpretation of So is not equal to the biodegradable substrate concentration on which OHO active biomass would grow since some portion of this So would be unbiodegradable. However, since the sewage is flocculated and filtered which would remove virtually all unbiodegradable particulates; it can be regarded as reasonably representative of the biodegradable substrate concentration. The initial biomass concentration (Xo) was calculated from the parent system analysis with the steady state model (WRC, 1984). Thus in this research, Xo is not represented by VSS or TSS concentration, but is represented by the OHO active biomass concentration calculated by the steady state model. In order to further evaluate the meaning of Xo, EUB cell counts from FISH analysis was also used to express Xo in all modified batch test.

From the above, formulations for So and Xo, using steady state model were as follows (Lee *et al*., 2003):

$$So = COD_{filt.} \frac{V_{reactor} - V_{ML}}{V_{reactor}} \qquad \text{(mgCOD/L)} \qquad (6.1)$$

$$Xo = f_{av} \bullet X_V \bullet \frac{V_{ML}}{V_{reactor}} \qquad \text{(mgMLAVSS/L)} \qquad (6.2)$$

Where:

$COD_{filt.}$ = COD concentration of flocculated and filtered sewage (mgCOD/L)

$V_{reactor}$ = Volume of batch reactor (5 L)

V_{ML} = Volume of mixed liquor added to batch reactor (L)

f_{av} = OHO active fraction of VSS, calculated with Eqn. (4.27)

X_V = VSS concentration of the parent system (mgVSS/L)

Formulations of Xo, using FISH model were as follows:

$$Xo = \frac{EUB \bullet F_{(CV)} \bullet F_{(VB)} \bullet V_{(0)}}{V_{(M)} \bullet 1000 \bullet DF} \quad \text{(mgCOD/L)} \qquad (6.3)$$

Where

Xo = Active biomass (mgCOD/L)

EUB = EUB mix Cell counts (cells/ml)

F_{VB} = Conversion factor 8.49 x 10^{-11} mgVSS/cell

Fcv = COD to VSS ratio of the mixed liquor (mgCOD/mgVSS)

$V_{(0)}$ = Original volume of fixed sample (ml)

$V_{(M)}$ = Measured volume of sample remaining (ml)

DF = Dilution factor

6.4 Results

This section presents the results obtained for the parent system, batch tests and FISH analysis. Also illustrated is a comparison between So/Xo ratios obtained via steady state model and FISH. This chapter addresses reasons for inconsistencies between measured and theoretical OHO active biomass (Chapter four) by comparing microbial profiles observed during the parent system and batch tests at defined So/Xo ratios. The calculation procedures for the batch test are fully detailed in section 6.3 above.

6.4.1 So/Xo ratios

The initial substrate to biomass (So/Xo) ratio used in batch test experiments is particularly important because it influences both parameter identifiability and the expression of culture history. In order to investigate the biological meaning of Xo, biomass was determined using steady state model (Eq. 6.2) and FISH analysis (Eq. 6.3) (Parent system and batch test data used in the above equations are listed in Table 6.2). The biomass determined by the steady state model (Xo-steady state) for all 16 batch tests ranged from 54.38 – 99.14 mgMLAVSS/L. Whereas the biomass determined by FISH (Xo-EUB, Table 6.2) ranged from 411.37- 767.13 mgCOD/L (Table 6.1).

So/Xo ratios obtained from steady state model and FISH analysis (Table 6.1) reveal ratios ranging from 0.71 – 1.77 and 0.1 – 0.24 respectively. As shown in Fig. 6.1, So/Xo –FISH ratios were consistently lower than ratios obtained by steady state model. FISH ratios were ≤ 0.24 whereas steady state ratios were ≤ 1.77 in all batch tests. Maximum specific growth rates (μ_H), as calculated from the batch test data with analytical procedure by Wentzel *et al.* (1995) (Chapter four), do not remain constant. As the So/Xo ratio increases the μ_H values increase, this was evident for batch tests 1-4. For batch test 5-8, So/Xo ratios were more or less constant but revealed fluctuating μ_H values. A similar pattern could be observed for the remaining of the batch tests. For batch tests 1, 2, 4, 9, 10, 12, and 14; So/Xo ratios were more or less equal to their concomitant μ_H values.

Table 6.1: Substrate to biomass ratios for 16 modified batch tests determined by steady state model and FISH analysis

Batch Test No.	So (mgCOD/L)	Xo-Steady State (mgMLAVSS/L)	Xo-FISH (mgCOD/L)	So/Xo Steady state	So/Xo-FISH
B1/03	142.2	82.53	599.80	1.72	0.24
B2/03	115.2	85.74	767.13	1.34	0.15
B3/03	106.72	62.63	594.16	1.70	0.18
B4/03	91.8	69.29	572.67	1.32	0.16
B5/03	68.4	75.60	496.69	0.90	0.14
B6/03	65.52	84.82	542.69	0.77	0.12
B7/03	77.4	84.01	468.99	0.92	0.17
B8/03	91.8	84.49	497.56	1.09	0.18
B9/04	118.8	67.00	711.60	1.77	0.17
B10/04	118.8	67.00	679.53	1.77	0.17
B11/04	77.28	54.38	411.37	1.42	0.19
B12/04	75.44	54.38	550.53	1.39	0.14
B13/04	72.16	90.22	416.70	0.80	0.17
B14/04	68.4	75.18	500.69	0.91	0.14
B15/04	72.16	99.14	446.30	0.73	0.16
B16/04	70.4	99.14	680.37	0.71	0.10

Table 6.2: Parent system data and batch test (Chapter 4) parameters with EUB cell counts for 16 batch tests.

Batch Test No.	Batch test Data				Parent System Data		
	WW (L)	ML (L)	COD Filtrate (mgCOD/L)	EUB Count (cells/ml)	Fav	Fcv (mgCOD /mgVSS)	Xv (mgVSS/L)
B1/03	4.5	0.5	158	2.03E+09	0.3668	1.45	2250
B2/03	4.5	0.5	128	2.61E+09	0.4083	1.44	2100
B3/03	4.6	0.4	116	1.94E+09	0.3728	1.50	2100
B4/03	4.5	0.5	102	1.94E+09	0.3229	1.45	2146
B5/03	4.5	0.5	76	1.69E+09	0.3780	1.44	2000
B6/03	4.5	0.5	72.8	1.78E+09	0.4039	1.50	2100
B7/03	4.5	0.5	86	1.56E+09	0.3877	1.48	2167
B8/03	4.5	0.5	102	1.60E+09	0.4027	1.53	2098
B9/04	4.5	0.5	132	2.39E+09	0.3215	1.46	2084
B10/04	4.5	0.5	132	2.28E+09	0.3215	1.46	2084
B11/04	4.6	0.4	84	1.41E+09	0.3084	1.43	2204
B12/04	4.6	0.4	82	1.89E+09	0.3084	1.43	2204
B13/04	4.4	0.6	82	1.39E+09	0.3206	1.47	2345
B14/04	4.5	0.5	76	1.67E+09	0.3206	1.47	2345
B15/04	4.4	0.6	82	1.47E+09	0.4082	1.49	2024
B16/04	4.4	0.6	80	2.24E+09	0.4082	1.49	2024

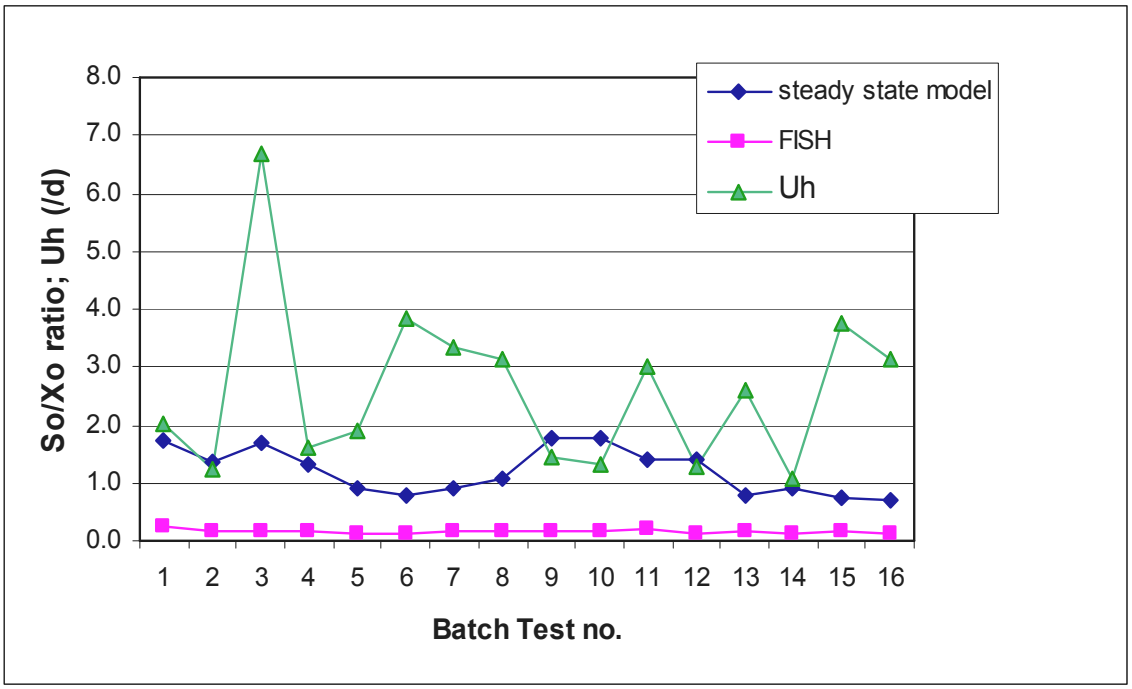

Fig 6.1: Comparison of So/Xo ratios obtained by steady state model and FISH analysis.

6.4.2 PCR-DGGE analysis

Three batch tests (B10/04, B11/04 and B15/04) were selected with defined So/Xo ratios for PCR- DGGE analysis (Table 6.1). The So/Xo ratio in these batch tests reflects the ratio range in all 16 batch tests as determined by steady state model. So/Xo ratios in B10, B11 and B15 were 1.77, 1.42 and 0.73 respectively (Table 6.1).

The 16S rDNA gene fragments amplified from mixed liquor batch test samples were resolved using DGGE analysis. DGGE analysis of the microbial communities present in the parent system (Fig. 6.2, lane P) demonstrated the presence of twelve distinguishable bands in the separation pattern. Based on the band intensities four prominent bands were observed in lane P (positions B2, B3, B4 and B5) (Fig. 6.2). The occurrences of these bands were consistent through out the batch test except in lanes 3 and 8. Lanes 1 and 3 showed dominant bands in the B1 position, which were either not visible or showed weak

intensities through out the duration of the batch test. After 8 hours, only one high intensity band was observed at the B2 position of the parent system.

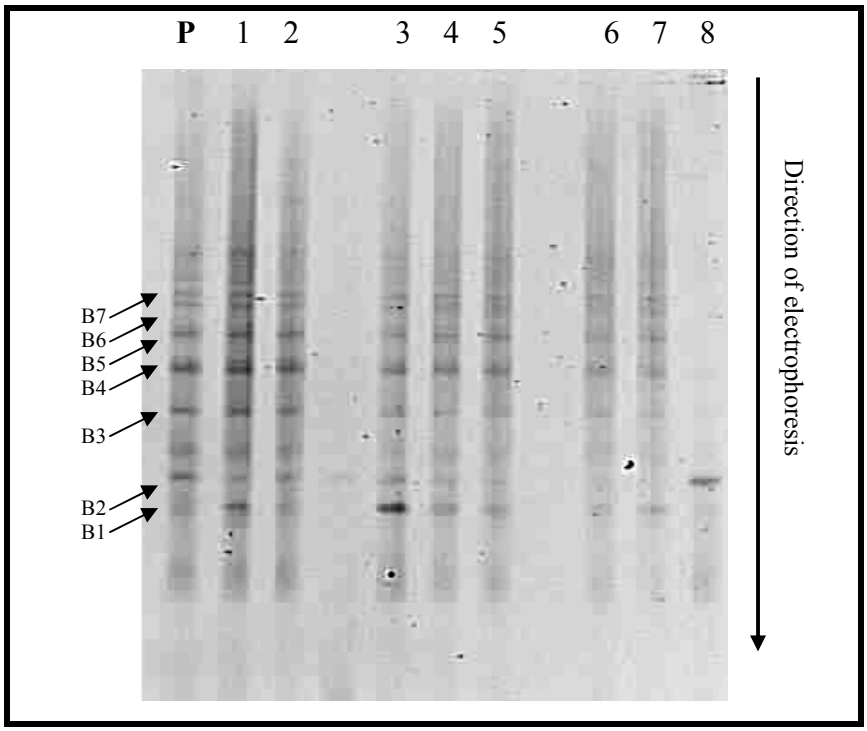

Fig. 6.2: Negative image of an ethidium bromide-stained DGGE pattern of PCR products obtain from a B15/04 with So/Xo ratio of 0.73. The batch test was sampled every hour for a period of 8 hours (Lanes 1-8). The PCR products were eletrophoresed on a 40-60% denaturing, 7.5% polyacrylamide gel. Lane P = parent system.

Figure 6.3 represents DGGE analysis of amplified 16S rDNA fragments of mixed liquor sampled at regular intervals from B11/04 with So/Xo ratio of 1.42. Based on the band intensities two prominent bands were observed throughout the batch test (Positions C1 and C2), except in lanes 3, 5, and 8 (absence of bands at the C1 position). Weak bands were observed in lanes 1, 2, 3, 4, and 6 at the C3 position and lanes 1, 3, and 6 at the C5 position. The bacterial band pattern obtained for the parent system (Lane P) showed the presence of nine species with only a few dominant species (positions C4, C5 and C6). Low intensities were observed in positions C1 and C2 (Lane P).

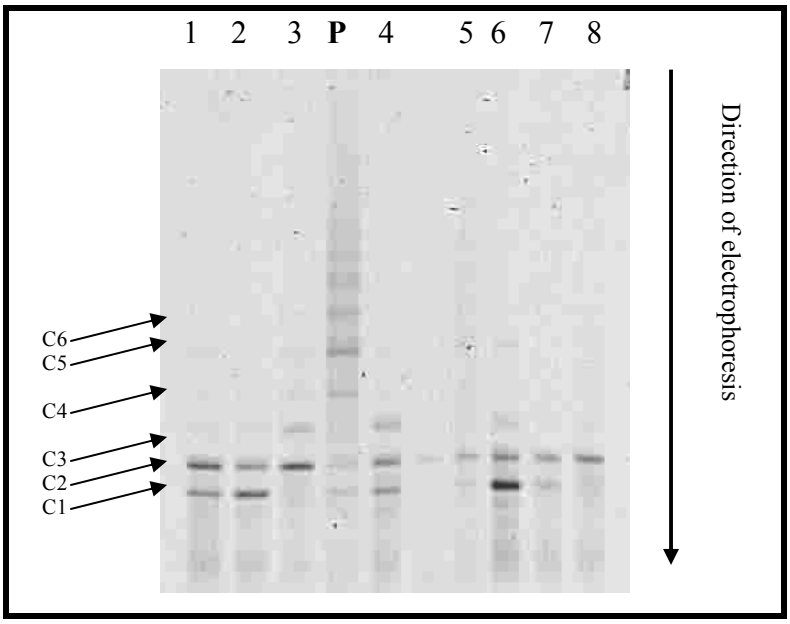

Fig. 6.3: Negative image of an ethidium bromide-stained DGGE pattern of PCR products obtain from B11/04 with So/Xo ratio of 1.42. The batch test was sampled every hour for a period of 8 hours (Lanes 1- 8). The PCR products were eletrophoresed on a 40-60% denaturing, 7.5% polyacrylamide gel. Lane P = parent system.

Figure 6.4 represents the DGGE pattern of 16S rDNA fragments of mixed liquor sampled at regular intervals from B10/04 with So/Xo ratio of 1.72. The DGGE analysis of batch test 10/04 showed 2 prominent bands in lanes 1, 2, 3 and 6 at positions D1, D2 and D3. Weak intensity bands were visible at position D3 (Lanes 1, 2, and 3) and D5 (Lanes 1 and 3). Similarly, these bands were visible in the parent system (Lane P), with dominant bands located in positions D1 and D2. After 3 hours there was a shift in dominance, in Lanes 4 and 8 a single dominant band was evident in position D2; lane 5 dominant bands were evident at positions D1 and D5 and lane 7 positions D2 and D3.

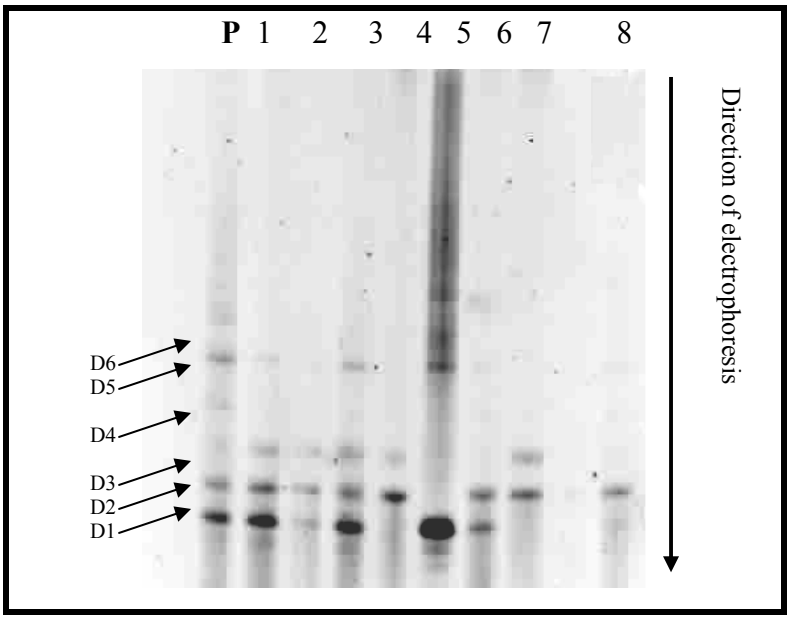

Fig 6.4: Negative image of an ethidium bromide-stained DGGE pattern of PCR products obtain from B10/04 with So/Xo ratio of 1.77. The batch test was sampled every hour for a period of 8 hours (Lanes 1-8). The PCR products were eletrophoresed on a 40-60% denaturing, 7.5% polyacrylamide gel. Lane P = parent system.

6.5 Discussion

6.5.1 So/Xo ratio

Knowledge of microbial growth and substrate utilization kinetics is important for monitoring the fate of organic compounds in natural and engineered environments. During biodegradation studies, the ratio of initial substrate concentration, So, to the initial biomass concentration, Xo, is one of the major factors affecting the identifiability of the different kinetic parameters (Grady *et al.,* 1996). At low So/Xo ratio a relatively high amount of biomass is supplied with a low quantity of substrate. The initial energy level is then low as well, and the increase in cell mass reflects only the increase in molecular polymer content in the biomass. Consequently, weight changes do not necessarily reflect

similar changes in cell number. Due to the fact that the cell replication is a process energetically enough demanding, no, or only negligible cell multiplication takes place at low So/Xo ratios during exogenous substrate removal (Grady *et al.*, 1996; Pitter and Chudoba, 1990; Chudoba, 1991). Low So/Xo ratios (<2) were observed for all batch test (Fig. 6.1), using steady state model. To maintain the convenience of expressing biomass concentrations in VSS based units as is done in steady state model, it was necessary to convert hybridization outputs into VSS (or COD) based values. This result was achieved by using FISH with a universal probe (EUBmix, Table 6.2) and DAPI (a compound that forms highly fluorescent complexes with DNA). FISH analysis revealed extremely low ratios (<0.24), as a result of increased biomass values (411.37- 767.13 mgCOD/L) (Table 6.1). Biomass data obtained with FISH analysis provides the fraction of a population's biomass that contains rRNA and is therefore potentially active. The biomass concentration was determined by assuming the ratio of active cells to total cells is a good approximation to determine the fraction of active biomass in a system (Oerther *et al*., 1999).

Conversely, under high So/Xo ratios a relatively low amount of biomass is supplied with a higher quantity of substrate. The initial energy level is higher, thus sufficient for different synthetic reactions which take place during cell replication cycle, like enzyme, protein and nucleic acids syntheses. Consequently, the number of microorganisms increases during the exogenous substrate removal, which is indicated by increasing rates of substrate removal and biomass growth. It is obvious that the portion of substrate consumed for energy production by catabolic processes will be higher as well, because of higher energetic demand of cell multiplication and maintenance processes (Chudoba *et al*., 1992). All batch tests conducted in this study did not display high So/Xo ratios due to the relatively low initial substrate concentrations (Table 6.1).

6.5.2 OUR vs. So/Xo ratio

Lee *et al*. (2003) suggest that low So/Xo conditions are unlikely to be represented in batch tests because none of the batch tests conducted are substrate limiting during the

first few hours as indicated by the precipitous drop in OUR. Batch tests conducted in this study were similar to the conditions to that of Lee *et al*. (2003).

By only monitoring OUR it is not possible to tell how the cell has allocated its resources. Small variations in cell maintenance have been shown to have a great influence on cell growth (Stouthamer and van Versevld, 1987). Characteristically, adding nutrients to batch cultures stimulates bacterial growth and alters the physiology of the bacteria (Dawes and Sutherland, 1992). Pollard *et al*. (1998) have suggested that when excess substrate was added to the batch reactor, bacteria progressively channeled more energy into new cell synthesis and less into cell maintenance. The rapid increase in bacterial growth was a normal response of bacteria that have been exposed to a sudden increase in the nutrients. These changes were due to either bacteria adapting to the new nutrient environment (Dawes and Sutherland, 1992), or the selection of sub-populations of bacteria that were more able to efficiently use the higher concentration of nutrients (Grady *et al*., 1996).

Energy generated from the oxidation of substrate by the bacterial cell in the batch reactor environment is allocated into a complex array of cellular functions. Oxygen utilization rates (OUR) are related only to the initial energy generated from substrate oxidation. On its own, the OUR does not indicate how the cell used the energy from substrate oxidation. The energy resource may be allocated to cell maintenance, new cell synthesis, endogenous polymers (that can again be oxidized) and secreted exopolymers (Jorand *et al*., 1995)

Other researchers (Grady *et al*., 1996; Ellis *et al*., 1996) similarly explained that So/Xo ratios must be low for kinetic growth parameters to represent those of the original treatment environment. The purpose of low ratios is to ensure minimal changes of the bacterial physiological state and community structure away from those of the original treatment process.

6.5.3 Maximum specific growth rate of RBCOD (μ_H) under various So/Xo conditions

From Fig. 6.1, there is a high degree of variability between So/Xo ratios and their corresponding μ_H values. The highest values for μ_H exceed the μ_H values usually used in the design of activated sludge systems (1.5 – 3.5/d) (Dold *et al*., 1991). Batch test conditions with respect to So/Xo ratio could have a significant impact on the maximum specific growth rates (Lee *et al.*, 2003). Significantly, the conditions may favour the growth of a part of the OHO community over another, causing a change in microbial OHO community structure with time in the batch test. Since interpretation of the batch test data is based on a single consistent OHO population representing the entire OHO community, change in the community structure with time will reflect as changes in the behavioural characteristics of the single surrogate OHO population group (Lee *et al*., 2003). Lee *et al*. (2003) further explains, if the fast growing group of the OHO community is favoured and their proportion of the OHO population increases with time in the batch test; this would result in an increase of the maximum specific growth rate with time of the entire OHO population. This could be evident for Batch test no. 3 (Fig. 6.1) with the possibility of the fast growing group been favoured resulting in an increased μ_H value. These changes with time in the batch test are not taken in to account in the current analytical and calculation procedures, because a single OHO population with fixed constant kinetics is accepted.

According to Grady *et al*. (1996), the larger the So/Xo, the greater the change in the community structure and the more the batch test measured kinetics will reflect the characteristics of the fastest growing population group, rather than the characteristics of the original culture. Similarly, the greater the number of sequential enrichments performed, the more the measured parameters will reflect the kinetics of the fastest growing population group.

6.5.4 Competition models to evaluate OHO behaviour

To explain observations similar to those above, Novak *et al.* (1994) and Grady *et al*. (1996) proposed substrate competition between different OHO groups as a possible cause. Lee *et al*. (2003) investigated this possibility by developing a kinetic model for competition between two OHO populations, one a fast grower the other a slow grower based on the concepts of Novak *et al*. (1994). The second OHO group was incorporated into the simplified kinetic model used to analyze the batch test data (Wentzel *et al*., 1995) as follows (Lee *et al*., 2003): (1) the single OHO active biomass was subdivided into two, a fast grower (Z_{BH1}) and a slow grower (Z_{BH2}); (2) All OHO mediated processes were duplicated, with the new processes allocated to the second OHO group; (3) the absorbed SBCOD was split into two, S_{ads1} and S_{ads2}, utilized by Z_{BH1} and Z_{BH2} respectively.

In comparing the various estimates for OHO active biomass concentrations, Lee *et al*. (2003) found that the two OHO population kinetic models gave concentrations that were significantly closer to the theoretical values than single OHO population model. Lee *et al*. (2003) further explains that the competition hypothesis, in agreement with previous researchers, is the only feasible explanation for the observations in the batch tests. However the kinetic models are largely hypothetical and insufficient information is available to separate the two OHO populations and quantify the individual kinetic processes. In order to elucidate the above premise, further investigations were facilitated by molecular based techniques such as PCR-DGGE.

6.5.5 Analysis of bacterial community in the parent system and batch test by PCR-DGGE technique.

In DGGE (Fischer and Lerman, 1979, 1983; Myers *et al*., 1987) DNA fragments of the same length but with different sequences can be separated. Separation is based on the decreased electrophoretic mobility of a partially melted double stranded DNA molecule in polyacrylamide gel containing a linear gradient of DNA denaturants (a mixture of urea and formamide). DNA molecules with different sequences stop migrating at different

positions. In order to compare the bacterial community in parent system with that of batch test, DGGE analysis was performed.

The sensitivity of the detection of 16S rDNA sequence variants by this approach was demonstrated by different band intensities and profiles observed at various So/Xo ratios in a batch test. Each band on a gel represents a species of distinctive duplex stability (Curtis and Craine, 1998). A DGGE analysis of the microbial community in each of the batch test clearly identified a number of species. The bacterial pattern obtained from sludge samples in the parent system (Fig 6.2, Lane P) showed the presence of four dominant species (indicated by the intensities of the bands), which were consistence with batch test samples except at 1 and 3 h (Fig 6.2). Lanes 1, 3 (position B1) showed a shift in a single dominant species away from the bacterial pattern of the parent system. The relative intensities of the bands infer the general changes in relative abundance of the dominant members of the community (Lyautey *et al*., 2005).

DGGE analysis of PCR products from batch test B11/04 samples (So/Xo = 1.42) revealed two dominant bands at position C1 and C2, which were consistent throughout the batch test except at hours 3 and 8 (position C1). In contrast, the DGGE profile of the parent system (Fig. 6.3, Lane P) revealed weak band intensities at position C1 and C2. The above observation is suggestive of a qualitative shift in microbial community away from the original treatment environment. Similarly, the DGGE profile obtained for batch test B10/04 (So/Xo = 1.77) did not show a perceptible trend during the course of the experiment. Lanes 4 (position D1), 5 (position D2), 7 (position D1) and 8 (position D1) showed the absence of prominent DGGE bands in the separation pattern, which is indicative of a shift away from the original bacterial community structure (Fig. 6.4, Lane P).

By comparing the DGGE profiles of the parent system and batch tests at defined So/Xo ratios, it is clear that the bacterial community in both systems differed. At So/Xo of 0.73, there were changes in the relative abundance of the dominant members of the community, suggesting low population variability. At So/Xo of 1.42 and 1.77, microbial

communities demonstrated the absence of distinguishable bands in the separation pattern of the parent system, suggesting high population variability.

6.6 Conclusion

In evaluating the modified batch test to quantify OHO active biomass, the measured values were in poor agreement with the theoretical values predicted by the activated sludge models. In examining reasons for the inconsistencies, it was noted that the modified batch test method relies on a single OHO population with constant kinetics representing the entire OHO community, change in the community structure with time will reflect as changes in the behavioural characteristics of the single surrogate OHO population group. Application of molecular techniques (PCR-DGGE) revealed shifts in population dominance between batch test and parent system, as well as population variability during the course of the batch test at defined So/Xo ratios. Therefore, suggesting a community shift away from the original treatment environment, rendering the batch test inadequate to accurately quantify mixed liquor components in activated sludge. Yet again, novel molecular technique shows its powerful advantage over conventional techniques in addressing key concerns in the engineering technology paradigm.

CHAPTER 7

General Conclusion and Recommendations

Biological wastewater treatment has been applied for more than a century to ameliorate anthropogenic damage to the environment. But only during the last decade the use of molecular tools has provided new insights into the composition and dynamics of activated sludge microbial communities. This study focuses on the use of molecular techniques in concurrence with mathematical modeling to assess system performance, quantification of mixed liquor components and providing a suitable means to monitor population variability.

FISH analysis in combination with mass balances (N and COD) was used to assess steady-state behaviour in a parent laboratory scale anoxic/aerobic activated sludge systems. FISH analysis was independently conducted on the aerobic and anoxic zones to determine the community structure in these zones. Both zones exhibited different community structures, with *β- Proteobacteria* predominating in the aerobic zone and *α-* and *γ-Proteobacteria* predominating in the anoxic zone. FISH analyses with group-specific probes revealed consistencies in the microbial composition in all wastewater batches, which were evident in the aerobic and anoxic zones. COD and Nitrogen mass balances were in the acceptable range of 90-110%, except for WW batches 2 and 7 in 2004 which fell outside the acceptable range. This was mainly due to high aerobic nitrate levels. FISH analysis in combination with mass balance equations provides a useful tool to monitor steady state behaviour. Although in this study only group-specific probes were evaluated, to obtain high resolution analysis a more comprehensive set of probes targeting population (species) should be applied.

Mixed liquor harvested from the parent anoxic/aerobic activated sludge system was used to conduct batch tests for the quantification of the OHO and AO active biomass components of mixed liquor. In addition to the batch test procedure FISH analysis with

fluorescent labeled, 16S rRNA-targeted oligonucleotide probes specific for ammonia and nitrite oxidizers were used in combination with DAPI staining to validate the Z_{BH} and Z_{BA} active biomass component in activate sludge respirometric batch tests. Results obtained were both perplexing and encouraging. For the heterotrophic batch tests correlations between the measured values obtained from the batch test and by molecular probing revealed close to moderate correspondences. However, the comparison of theoretical (parent system) values to the measured (batch test) and probe values were consistently poor. The batch test measured and probe $Z_{BH(0)}$ values were consistently lower than the corresponding theoretical values. This was attributed to the high dependency of the theoretical concentration on VSS measurement and the inability of the VSS measurement to distinguish between live and dead cells. However there was an improved correlation between molecular probing values and the modified batch test (measured $Z_{BH(0)}$) values. The ability of FISH to provide a direct measurement of OHO active biomass concentration would take precedent over indirect methods (modified batch test). The integration of molecular techniques (FISH), are now required to expand model calibration and validation efforts.

In evaluating the batch test procedure to quantify the AO active biomass, poor correspondences were observed between the measured, probe and theoretical $Z_{BA(0)}$ values. The large degree of variability could be attributed to the populations targeted by rRNA probes may not correspond to the theoretical populations in the model. Currently available rRNA probes may not encompass all members of the model populations or may target members that are not part of the model populations. Furthermore, batch test conditions may cause the overall AO behaviour to deviate significantly from that of the steady state system. The batch test method is particularly sensitive to any changes in AO kinetics as time proceeds in the batch test, since these kinetics are applied to the start of the test to determine the AO active biomass concentration. This sensitivity, can explain the variability in correlations between batch tests measured AO active biomass concentrations and the theoretical values.

In addressing reasons for the large discrepancies between measured and theoretical values, PCR-DGGE analysis revealed a change in population dominance between the batch test and parent system, as well as during the course of the batch test at defined So/Xo ratios. The batch test method and its interpretation in terms of procedures described in Chapter 4 and 5, is particularly sensitive to any changes in OHO or AO kinetics as time proceeds in the batch test, since these kinetics are applied at the start of the test to determine the OHO or AO active biomass concentrations. Unfortunately, the sensitivity renders the batch test as an unsuitable method to quantify the OHO or AO active biomass concentration with sufficient accuracy.

The causes for the lack of a 1:1 correspondence between OHO and AO active biomass measured in the batch test and that predicted theoretically with the activated sludge models was shown to lie in the modified batch test itself. This was supported by results obtained from PCR-DGGE analyses, which clearly showed a change in community structure away form the original treatment environment (parent system). Furthermore, it must be remembered that in the parent activated sludge systems, the OHO population is dominated by the slow growing OHO population group, to the extent of near exclusion of the fast growers. Thus, for the activated sludge system the current models incorporating a single OHO population are adequate, provided extremes in dynamic loading are not encountered (e.g. selector reactors).

However integration of novel molecular techniques (FISH) aimed at providing quantitative information, are now required to expand model calibration and validation efforts. However, it is necessary to clearly indicate how the biomass is defined and what the limitations of the probes may be. Effectively incorporating quantitative information from microscopic fields into kinetic parameters will be beneficial to the practical process of designing and operating advanced reactor systems for biological wastewater treatment.

In view of this research, the following recommendations can be made:

- CLSM (confocal laser scanning microscopy) in combination with FISH is a powerful approach to investigate microbial community structure and aggregate architecture (3D- analysis). The principle involves excitation of a fluorophore by a focussed laser beam. Once an image has been digitized it can be analysed by image processing to derive quantitative information. This technique can be used to assess AOB and NOB in the batch test and parent system and improve the accuracy in quantifying the above populations as well as provide important spatial information.

- FISH in combination with microautoradiography (MAR) can be used to determine specific uptake of organic and inorganic radiolabeled substrates by activated sludge microbial communities. This technique will prove useful in identifying and quantifying the key AOB's and NOB's responsible for the increased nitrification rates during respirometric batch assays.

- Real-time PCR (RT-PCR) can be used as a quantitative tool to analyse microbial communities based on their genetic information. Real-time monitoring of PCR products reduces PCR artifacts and biases. This technique can be used to quantify AOB's and NOB's and validate results obtained by FISH.

- Using three-step nested PCR-DGGE (primers specific for AOB's and NOB's) will provide a profile of only AOB and NOB in complex microbial communities. This will allow a comparison of only AOB and NOB between batch test and parent system unlike one-step PCR-DGGE which profiles the entire microbial community.

REFERENCES

Abeliovich A and Vonhak A (1992) Anaerobic metabolism of *Nitrosomonas europaea*. *Arch. Microbiol*. **158**: 267-270

Adamczyk J, Hesselsoe M, Iversen N, Lehner A, Nielsen PH, Schloter M, Roslev P and Wagner M (2003) The isotope array, a new tool that employs substrate-mediated labeling of rRNA for determination of microbial community structure and function. *Appl. Environ. Microbiol*. **69:** 6875–6887

Ahlers B, König W and Bock E (1990) Nitrite reductase activity in *Nitrobacter vulgaris*. *FEMS Microbiol. Lett.* **67**: 121-126

Alfreider A, Pernthaler J, Amann R, Sattler B, Glöckner FO, Wille A and Psenner R **(**1996) Community analysis of the bacterial assemblages in the winter cover and pelagic layers of a high mountain lake by *in situ* hybridization. *Appl. Environ. Microbiol.* **62:** 2138-2144

Amann RI (1995) In situ identification of micro-organisms by whole cell hybridization with rRNA-targeted nucleic acid probes. In: *Molecular Microbial Ecology Manual*. Akkeman ADC, van Elsas, JD and de Bruigin FJ (Eds.) Kluwer Academic Publishers, Dortrecht.

Amann R, Fuchs BM and Behrens S (2001) The identification of microorganisms by fluorescence *in situ* Hybridisation. *Curr. Opinion in Biotechnology* **12**: 231-236

Amann R and Ludwig W (2000) Ribosomal RNA-targeted nucleic acid probes for studies in microbial ecology. *FEMS Microbiol. Rev*. **24**: 555-565

Amann R, Snaidr J, Wagner M, Ludwig W and Schleifer KH (1996) *In situ* visualization of high genetic diversity in a natural microbial community. *J. Bacteriol*. **178**: 3496–3500

Amann RI, Binder BJ, Olson RJ, Chisholm SW, Devereux R and Stahl DA (1990a) Combination of 16S rRNA-targeted oligonucleotide probes with £ow cytometry for analyzing mixed microbial populations. *Appl. Environ. Microbiol*. **56**: 1919-1925

Amann RI, Krumholz L, Stahl DA (1990b) Fluorescent oligonucleotide probing of whole cells for determinative, phylogenetic and environmental studies in microbiology. *J. Bacteriol*. **172**: 762-770

Amann RI, Ludwig W and Schleifer K.-H (1995) Phylogenetic identification and in situ detection of individual microbial cells without cultivation. *Microbiol. Rev*. **59**: 143-169

Amann RI, Stromley J, Devereux R, Key R and Stahl DA (1992) Molecular and microscopic identification of sulfate-reducing bacteria in multispecies biofilms. *Appl. Environ. Microbiol*. **58**: 614–623

Andreasen K and Nielsen PH (1997) Application of Microautoradiography to the study of substrate uptake by filamentous microorganisms in activated sludge. *Appl. Environ. Microbiol.* **63:** 3662–3668

Andreottola G, Foladori P, Gelmini A and Ziglio G (2001) Biomass active fraction evaluated by direct method and respirometric techniques. *IWA conference on activated sludge population dynamics*, Rome, 11 -13 July, 273-279

Ardern E and Lockett WT (1914) Experiments on the oxidation of sewage without the aid of filters. *J. Soc. Chem. Ind*. **33**: 523

Arthur JW, West CW, Allen KN and Hedke SF (1987). Seasonal toxicity of ammonia to five fish and nine invertebrate species. *Bull. Environ. Contam. Toxicol*. **38**: 324-331.

Atlas RM and Bartha R (1998) Quantitative ecology: numbers, biomass, and activities. In Atlas RM and R Bartha, *Microbial Ecology: Fundamentals and Applications*, Benjamin/Cummings Science Publishing, Menlo Park CA: 218–263

Bauman JG, Wiegant J, Borst P and van Duijn P (1980) A new method for fluorescence microscopical localization of specific DNA sequences by in situ hybridization of fluorochrome labelled RNA. *Exp. Cell Res*. **128**: 485-490

Beeharry AO (1999) Measurement of the nitrifier maximum specific growth rate. BSc undergraduate thesis, Dept. Civil Eng., Univ. of Cape Town, Rondebosch 7701, South Africa.

Beeharry AO, Wentzel MC and Ekama GA (2001) Evaluation of batch test for measurement of active biomass in activated sludge mixed liquor. *Res. Rept. W112*, Dept. Civil Eng., Univ. of Cape Town, Rondebosch 7701, South Africa.

Bergmann DJ, Arciero DM and Hooper AB (1994) Organization of the *hao* gene cluster of *Nitrosomonas europaea*: Genes for two tetraheme c cytochromes. *J. Bacteriol*. **176**: 3148-3153.

Bitton G (1995) *Wastewater Microbiology*. John Wiley and sons, New York

Bloem J, Veninga M and Shepherd J (1995) Fully automatic determination of soil bacterium numbers, cell volumes, and frequencies of dividing cells by confocal laser scanning microscopy and image analysis. *Appl. Environ. Microbiol.* **61**(3): 926-936

Bock E (1976) Growth of *Nitrobacter* in the presence of organic matter. II. Chemoorganotrophic growth of *Nitrobacter agilis*. *Arch. Microbiol*. **108**: 305-312

Bock E and Koops H-P (1992) The genus *Nitrobacter* and related genera. In: *The prokaryotes*. Balows A, Trüper HG, Dworkin M, Harder W and Schleifer K-H (Eds.), 2302-2309, Springer-Verlag, New York.

Bock E, Koops H-P, Ahlers B and Harms H (1992) Oxidation of inorganic nitrogen compounds as energy source. In: *The prokaryotes*. Balows H, Trüper HG, Dworkin M, Harder W and Schleifer K-H (Eds.), 414-430, Springer-Verlag, New York.

Bock E, Koops H-P, Möller UC and Rudert M (1990) A new facultatively nitrite oxidizing bacterium, *Nitrobacter vulgaris* sp. nov. *Arch. Microbiol*. **153**: 105-110.

Bock E, Schmidt I, Stüven R and Zart D (1995) Nitrogen loss caused by denitrifying *Nitrosomonas* cells using ammonia or hydrogen as electron donors and nitrite as electron acceptor. *Arch. Microbiol*. **163**: 16-20.

Bock E, Sundermeyer-Klinger H and Stackebrandt, E (1983) New facultative lithoautotrophic nitrite-oxidizing bacteria. *Arch. Microbiol*. **136**: 281-284.

Bock E, Wilderer PA and Freitag A (1988) Growth of *Nitrobacter* in absence of dissolved oxygen. *Wat. Res*. **22**: 245-250.

Bodelier PLE, Libochant JA, Blom CWPM, Laanbroek HJ (1996) Dynamics of nitrification and denitrification in root-oxygenated sediments and adaptation of ammonia-oxidizing bacteria to low-oxygen or anoxic habitats. *Appl. Environ. Microbiol.* 62: 4100–7

Bodelier PL, Roslev P, Henckel T, and Frenzel P (2000) Stimulation by ammonium-based fertilizers of methane oxidation in soil around rice roots. *Nature* **403:** 421–424.

Bond PL, Hugenholtz P, Keller J and Blackall LL (1995) Bacterial community structures of phosphate-removing and non-phosphate-removing activated sludges from sequencing batch reactors. *Appl. Environ. Microbiol*. **61**: 1910-1916

Boschker HTS and Middelburg JJ (2002) Stable isotopes and biomarkers in microbial ecology. *FEMS Microbiol. Ecol*. **40:** 85–95

Bouchez T, Patureau D, Dabert P, Juretschko S, Doré J, Delgenès P, Moletta R and Wagner M (2000) Ecological study of a bioaugmentation failure. *Environ. Microbiol*. **2**(2)**:** 179-190

Brunk CF, Avaniss-Aghajani E and Brunk CA (1996) A computer analysis of primer and probe hybridization potential with small-subunit rRNA sequences. *Appl. Environ. Microbiol.* **62**: 872–879

Buchholz-Cleven BEE, Rattunde B and Straub KL (1997) Screening for genetic diversity of isolates of anaerobic Fe(II)oxidizing bacteria using DGGE and whole-cell hybridization. *System. Appl. Microbiol*. **20**: 301–309

Burggraf S, Mayer T, Amann R, Schadhauser S, Woese CR and Stetter KO (1994) Identifying members of the domain Archaea with rRNA-targeted oligonucleotide probes. *Appl. Environ. Microbiol*. **60**: 3112-3119

Burlage RS, Atlas RM, Stahl D, Geesey G and Sayler G (eds), (1998) *Techniques in Microbial Ecology.* Oxford University Press, New York.

Burrell PC, Keller J and Blackall LL (1998) Microbiology of a nitrite-oxidizing bioreactor. *Appl. Environ. Microbiol*. **64**: 1878-1883

Cardullo RA, Agrawal S, Flores C, Zamecnik PC, and Wolf DE (1988) Detection of nucleic acid hybridization by nonradioactive fluorescence resonance energy transfer. *Proc. Natl. Acad. Sci. USA* **85**: 8790-8794

Cariello NF, Keohavong P, Sanderson BJS and ThillyWG (1988) DNA damage produced by ethidium bromide staining and exposure to ultraviolet light. *Nucleic Acids Res*. **16**: 4157

Casey TG, Ekama GA, Wentzel MC and Marais GvR (1995) Filamentous organism bulking in nutrient removal activated sludge systems Paper 1: a historical overview of causes and control. *Wat. SA* **21** (3): 231-237

Chen A, Edgar DB and Trela JM (1976) Deoxyribonucleic acid polymerase from the extreme thermophile *Thermus aquaticus*. *J. Bacteriol.* **127**: 1550-1557

Chudoba P, Capdeville B and Chudoba J (1992) Explanation of the biological meaning of the So/Xo ratio in batch cultivation. *Wat. Sci. Tech*. **26** (3-4): 743-751

Chudoba P, Chang J and Capdeville B (1991) Synchronised division of activated sludge microoganisms. *Wat. Res*. **25** (7): 817-822

Cloete, TE and Muyima NYO (1997) Microbial Community Analysis: the Key to Design of Biological Wastewater Treatment Systems. *IAWQ Scientific and Technical Report No. 5.* University Press, Cambridge.

Crocetti GR, Hugenholtz P, Bond PL, Schuler A, Keller J, Jenkins D and Blackall LL (2000) Identification of polyphosphate-accumulating organisms and design of 16S rRNA-directed probes for their detection and quantification. *Appl. Environ. Microbiol*. **66**: 1175-1182

Cronje GL, Beeharry AO, Lakay MT, Wentzel MC and Ekama GA (2005) Activity of heterotrophic and autotrophic biomass in BNR activated sludge. *Res. Report 1179/1/05,* Water Research Commision, P/Bag X03, Gezina 0031, South Africa.

Cronje GL, Beeharry AO, Wentzel MC, Ekama GA (2002) Active biomass in activated sludge mixed liquor. *Wat. Res*. **36**: 439-444

Cronje GL, Wentzel MC and Ekama GA (2000) Measurement of active heterotrophic organism concentration in nitrification –denitrification activated sludge systems. *Res. Rep. W102*, Dept. Civil Eng., Univ. of Cape Town, Rondebosch 7701, South Africa

Curtis TP and Craine NG (1998) The comparison of the diversity of activated sludge plants. *Wat. Sci. Tech*. **37** (4-5): 71-78

Daigger GT and Grady CPL (Jr) (1982) The dynamics of microbial growth on soluble substrate. *Wat. Res*. **16**: 365-382

Daims H, Brühl A, Amann R, Schleifer K-H and Wagner M (1999) The domain-specific probe EUB338 is insufficient for the detection of all bacteria: development and evaluation of a more comprehensive probe set. *System. Appl. Microbiol*. **22**: 434–44

Daims H, Nielsen JL, Nielsen PH, Schleifer KH and Wagner M (2001a) *In situ* characterization of *Nitrospira*-like nitrite-oxidizing bacteria active in wastewater treatment plants. *Appl. Environ. Microbiol*. **67**: 5273–5284

Daims H, Purkhold U, Bjerrum L, Arnold E, Wilderer PA and Wagner M (2001b) Nitrification in sequencing biofilm batch reactors: lessons from molecular approaches. *Wat. Sci. Tech*. **43**: 9–18.

Daims H, Ramsing NB, Schliefer K-H and Wagner M (2001c) Cultivation-independent, semiautomatic determination of absolute bacterial cell numbers in environmental samples by fluorescence *in situ* hybridization. *Appl. Environ. Microbiol*. **67** (12): 5810-5818

Daims H, Nielsen PH, Nielsen JL, Juretschko S and Wagner M (2000) Novel *Nitrospira*-like bacteria as dominant nitrite-oxidizers in biofilms from wastewater treatment plants: diversity and *in situ* physiology. *Wat. Sci. Tech*. **41**: 85–90

Dar SA, Kuenen JG and Muyzer G (2005) Nested PCR-Denaturing Gradient Gel Electrophoresis approach to determine the diversity of sulphate-reducing bacteria in complex microbial communities. *Appl. Environ. Microbiol*. **71**(5): 2325-2330

Dawes IW and Sutherland IW (1992) *Microbial Physiology*. Blackwell Scientific Publications, Oxford.

DeLong EF, Taylor LT, Marsh TL and Preston CM (1999) Visualization and enumeration of marine planktonic archaea and bacteria by using polyribonucleotide probes and fluorescent *in situ* hybridization. *Appl. Environ. Microbiol*. **65**: 5554-5563

DeLong EF, Wickham GS and Pace NR (1989) Phylogenetic stains: ribosomal RNA-based probes for the identification of single microbial cells. *Science* **243**: 1360-1363

Dijkhuizen L and Harder W (1985) Microbial metabolism of carbon dioxide *In* H. Dalton (ed.), *Comprehensive biotechnology*, *vol 1*: *the principles of biotechnology*. Pergamon Press, Ltd., Oxford, England.

Dold PL, Ekama GA and Marais GVR (1980) A general model for the activated sludge process. *Prog. Water Technology* **12** (60): 47-77

Dold P, Wentzel, MC, Billing AE, Ekama GA and Marais GVR (1991) Activated sludge simulation programs. *Water Research Commision*, PO Box 824, Pretoria 0001, South Africa.

Egert M and Friedrich MW (2003) Formation of pseudo-terminal restriction fragments, a PCR-related bias affecting terminal restriction fragment length polymorphism analysis of microbial community structure. *Appl. Environ. Microbiol*. **69**: 2555–2562

Ehrich S, Behrens D, Lebedeva E, Ludwig W and Bock E (1995) A new obligately chemolithoautotrophic, nitrite-oxidizing bacterium, *Nitrospira moscoviensis* sp. nov. and its phylogenetic relationship. *Arch. Microbiol*. **164**: 16-23

Ekama GA, Dold PL and Marais GVR (1986) Procedure for determining influent COD fractions and the maximum specific growth rate of heterotrophs in activated sludge. *Wat. Sci. Tech.* **18**: 91-114

Ekama GA and Marais GVR (1984) Two improve sludge settleability parameters. IMIESA, **9**(6): 20

Ellis TG, Barbeau DS, Smets BF and Grady CPLJ (1996) Respirometric technique for determination of extant kinetic parameters describing biodegradation. *Wat. Environ. Res*. **68** (5): 917-926.

Erhart R, Bradford D, Seviour RJ, Amann R and Blackall LL (1997) Development and use of fluorescent in situ hybridization probes for the detection and identification of "*Microthrix parvicella*" in activated sludge. *System. Appl. Microbiol*. **20**: 310-318

Felske A and Akkermans AD (1998) Prominent occurrence of ribosomes from an uncultered bacterium of the *Verrucomicrobiales* cluster in grassland soils. *Lett. Appl. Microbiol*. **26**: 219-223

Felske A, Engelen B, Nübel U and Backhaus H (1996) Direct ribosomal isolation from soil to extract bacterial rRNA for community analysis. *Appl. Environ. Microbiol*. **62**: 4162–4167

Ferris MJ, Muyzer G and Ward DM (1996) Denaturing gradient gel electrophoresis profiles of 16s RNA-defined populations inhabiting a hot spring microbial mat community. *Appl. Env. Microbiol*. **62**: 340-346

Ferris MJ, Nold SC, Revsbech NP and Ward NM (1997) Population structure and physiological changes within a hot spring microbial mat community following disturbance. *Appl. Environ. Microbiol*. **63**: 1367–1374

Ferris MJ and Ward DM (1997) Seasonal distributions of dominant 16S rRNA defined populations in a hot spring microbial mat examined by denaturing gradient gel electrophoresis. *Appl. Environ. Microbiol*. **63**: 1375–1381

Fisher SG and Lerman LS (1979) Length-independent separation of DNA restriction fragments in two dimensional gel electrophoresis. *Cell* **16**: 191-200

Fisher SG and Lerman LS (1983) DNA fragments differing by single-base pair substitutions are separated in denaturing gradient gels: Correspondence with melting theory. *Proc. Natl. Acad. Sci. USA* **80**: 1579-1583

Freitag A and Bock E (1990) Energy conservation in *Nitrobacter*. *FEMS Microbiol. Lett.* **66**: 157-162

Freitag A, Rudert M and Bock E (1987) Growth of *Nitrobacter* by dissimilatoric nitrate reduction. *FEMS Microbiol. Lett*. **48**: 105-109.

Gall JG and Pardue ML (1969) Formation and detection of RNA-DNA hybrid molecules in cytological preparations. *Proc. Natl. Acad. Sci. USA* **63**: 378-383.

Gao M, Yang M, Li H, Wang Y and Pan F (2004) Nitrification and sludge characteristics in a submerged membrane bioreactor on synthetic inorganic wastewater. *Desalination* **170**: 171-185

Giovannoni SJ (1991). The polymerase chain reaction, *In* E. Stackerbrandt and M. Goodfellow (ed.), *Nucleic acid techniques in bacterial systematics*. John Wiley & Sons, Chichester, England.

Glöckner FO, Amann R, Alfreider A, Pernthaler J, Psenner R, Trebesius K, Schleifer K-H (1996) An *in situ* hybridization protocol for detection and identification of planktonic bacteria**.** *System. Appl. Microbiol*, **19**: 403-406

Grady L and Diagger G (1998) *Biological Wastewater Treatment: principles and practice*. Marcel Dekker, Inc., New York.

Grady CPL, Smits BF, Barbeau DS (1996) Variability in kinetic parameter estimates: a review of possible causes and proposed terminology. *Wat. Res*. **30**(3): 742-748

Gray ND, Howarth R, Pickup RW, Jones JG and Head IM (1999) Substrate uptake by uncultured bacteria from the genus *Achromatium* determined by microautoradiography. *Appl. Environ. Microbiol*. **65:** 5100–5106.

Gujer W, Henze M, Mino T, Matsuo T, Wentzel MC and Marais GvR (1995). The activated sludge model No. 2: Biological Phosphorus removal. *Wat. Sci. Tech*. **31**(2): 1-11.

Gujer W, Henze M, Mino T and van Loosdrecht MCM (1999) Activated Sludge Model No. 3. *Wat. Sci. Tech.* **39**(1): 183–193

Head IM, Hiorns WD, Embley TM, McCarthy AJ, Saunders JR (1993) The phylogeny of autotrophic ammonium oxidizing bacteria as determined by analysis of 16S ribosomal RNA gene sequences. *J. Gen. Microbiol.* **139**: 1147–53

Head IM, Saunders JR and Pickup RW (1998) Microbial evolution, diversity, and ecology: a decade of ribosomal RNA analysis of uncultivated microorganisms. *Microb. Ecol*. **35**: 1–21

Henze M, Grady CPL (Jr), Gujer W, Marais GvR and Matsuo T (1987) Activated sludge model No. 1. *IAWQ Scientific and Technical Report No. 1*, IAWQ, London

Henze M, Gujer W, Mino T, Wentzel MC and Marais GVR (1995) Activated Sludge Model No. 2. *IAWQ Scientific and Technical Report No. 3,* IAWQ, London.

Henze M, Harremoës P, la Cour Jansen J and Arvin E (1997) *Wastewater treatment*. Springer-Verlag, Berlin.

Herbert D (1958) Recent progress in microbiology. *VII. International congress on microbiology.* Tunevall Alinquist and Wiksell (eds), Stockholm.

Hesselsoe M, Nielsen JL, Roslev P and Nielsen PH (2005) Isotope labeling and microautoradiography of active heterotrophic bacteria on the basis of assimilation of $^{14}CO_2$. *Appl. Environ. Microbiol*. **71** (2): 646-655

Heuer H, Krsek M, Baker P, Smalla K and Wellington EMH (1997) Analysis of actinomycete communities by specific amplification of genes encoding 16S rRNA and gel electrophoretic separation in denaturing gradients. *Appl. Environ. Microbiol*. **63**: 3233–3241

Heydorn A, Nielsen AT, Hentzer M, Sternberg C, Givskov M, Ersboll BK and Molin S (2000). Quantification of biofilm structures by the novel computer program COMSTAT. *Microbiol.* **146**: 2395-407

Hicks RE, Amann RI and Stahl DA (1992) Dual staining of natural bacterioplankton with 4', 6-diamidino-2-phenylindole and fluorescent oligonucleotide probes targeting kingdom level 16S rRNA sequences. *Appl. Environ. Microbiol.* **58**: 2153-2163

Higuchi R, Fockler C, Dollinger G and Watson R (1993) Kinetic PCR analysis: real-time monitoring of DNA amplitication reactions. *Bio/Technology*. **11**: 1026-1030

Hiorns WD, Methé BA, Nierzwicki-Bauer SA and Zehr JP (1997) Bacterial diversity in Adirondack mountain lakes as revealed by 16S rRNA gene sequences. *Appl. Environ. Microbiol*. **63**: 2957-2960

Hirsch P and Müller M (1985) *Planctomyces limnophilus* sp. nov., a stalked and budding bacterium from freshwater. *System. Appl. Microbiol*. **6**: 276-280

Höfle MG (1988) Identifcation of bacteria by low molecular weight RNA profiles: a new chemotaxonomic approach. *J. Microbiol. Meth*. **8**: 235–248

Holder-Snyman F, Ismail AAH, Mudaly DD, and Bux F (2005) Determination of heterotrophic active bacteria in activated sludge using novel molecular techniques, *WRC report K5/1178/05*

Hollard PM, Abramson RD, Watson R and Gelfand DH (1991) Detection of specific polymerase chain reaction product by utilizing the 5'→3' exonuclease activity of *Thermus aquaticus* DNA polymerase. *Proc. Natl. Acad. Sci. USA*. **88**: 7276-7280

Hooper AB, Vannelli T, Bergmann DJ and Arciero D (1997) Enzymology of the oxidation of ammonia to nitrite by bacteria. *Antonie van Leeuwenhoek J. Gen. Mol. Microbiol.* **71**: 59–67

Hougaard DM, Hansen H and Larsson LI (1997) Non-radioactive *in situ* hybridization for mRNA with emphasis on the use of oligodeoxynucleotide probes. *Histochem. Cell Biol.* **108**: 335-344

Hovanec TA and DeLong EF (1996) Comparative analysis of nitrifying bacteria associated with freshwater and marine aquaria. *Appl. Environ. Microbiol*. **62**: 2888-2896

Hovanec TA, Taylor LT, Blakis A and Delong EF (1998) *Nitrospira*-like bacteria associated with nitrite oxidation in freshwater aquaria. *Appl. Environ. Microbiol*. **64**: 258-264.

Ingledew WJ and Halling PJ (1976) Paramagnetic centers of the nitrite oxidizing bacterium *Nitrobacter*. *FEBS Lett*. : 90-93

Innis MA, Myambo KB, Gelfand DH and Brow MAD (1988) DNA sequencing with *Thermus aquaticus* DNA polymerase, and direct sequencing of PCR amplified DNA. *Proc. Natl. Acad. Sci. USA* **85**: 9436-9440

Ishii K and Fukui M (2001) Optimization of annealing temperature to reduce bias caused by a primer mismatch in multitemplate PCR. *Appl. Environ. Microbiol*. **67**: 3753–3755

Janse I, Bok J and Zwart G (2004) A simple remedy against artifactual double bands in denaturing gradient gel electrophoresis *J. Microbiol. Meth.* **57**: 279-281

Janssen PH, Schuhmann A, Mörschel E and Rainey FA (1997) Novel anaerobic ultramicrobacteria belonging to the *Verrucomicrobiales* lineage of bacterial descent isolated by dilution culture from anoxic rice paddy soil. *Appl. Environ. Microbiol*. **63**: 1382-1388

Jeffery M, Singer L and Singer RH (2003) Fluorescent *in situ* hybridization: past, present and future. *J. cell Sci.* **116**: 2833-2838

Jensen MA and Straus N (1993) Effect of PCR conditions on the formation of heteroduplex and single-stranded DNA products in the amplification of bacterial ribosomal DNA spacer regions. *PCR Methods Appl*. **3**: 186–194

Jorand F, Zartarian F, Thomas F, Block JC, Bottero JY, Villemin G, Urbain V and Manem J (1995) Chemical and structural (2D) linkage between bacteria within activated sludge flocs. *Wat. Res*. **29**(7): 1639-1647

Juretschko S, Timmermann G, Schmid M, Schleifer K-H, Pommering-Röser A, Koops H-P and Wagner M (1998) Combined molecular and conventional analyses of nitrifying bacterium diversity in activated sludge: *Nitrosococcus mobilis* and *Nitrospira*-like bacteria as dominant populations. *Appl. Environ. Microbiol*. **64**: 3042-3051

Kalmbach S, Manz W, Bendinger B, Szewzyk U (2000) *In situ* probing reveals aquabacterium commune as a widespread and highly abundant bacterial species in drinking water biofilms. *Wat Res*, **34**: 575-581

Kalmbach S, Manz W and Szewzyk U (1997) Dynamics of biofilm formation in drinking water: phylogenetic affiliation and metabolic potential of single cells assessed by formazan reduction and in situ. *FEMS Microbiol. Ecol.* **22**: 265-279

Kämpfer P, Erhart R, Beimfohr C, Böhringer J, Wagner M and Amann R (1996) Characterization of bacterial communities from activated sludge: culture-dependent numerical identification versus in situ identification using group- and genus-specific rRNA-targeted oligonucleotide probes. *Microb. Ecol*. **32**: 101-121

Kanagawa T (2003) Bias and artifacts in multitemplate polymerase chain reactions (PCR). *J. Biosci. Bioeng*. **96:** 317–323

Kappeler J and Gujer W (1992) Estimation of kinetic parameters of heterotrophic biomass under aerobic conditions and characterization wastewater for activated sludge modeling. *Wat. Sci. Tech.* **25** (6): 125-140

Kislauskis EH, Li Z, Singer RH and Taneja KL (1993) Isoformspecific 3′-untranslated sequences sort alpha-cardiac and beta-cytoplasmic actin messenger RNAs to different cytoplasmic compartments. *J. Cell Biol.* **123**: 165-172

Koops H-P, Böttcher B, Möller UC, Pommering-Röser A and Stehr G (1990) Description of a new species of *Nitrosococcus*. *Arch. Microbiol*. **154**: 244-248.

Koops H-P and Möller UC (1992) The lithotrophic ammonia-oxidizing bacteria. In: *The prokaryotes*. Balows A, Trüper HG, Dworkin M, Harder W and Schleifer K-H (Eds.), Springer-Verlag, New York.

Kovarova-kovar K and Egli T (1998) Growth kinetics of suspended microbial cells: from single-substrate-controlled growth to mixed substrate kinetics. *Microbiol. Molec. Biol. Rev*. **62** (3): 646-666

Kowalchuk GA, Stephen JR, de Boer W, Prosser JI, Embley TM and Woldendorp JW (1997) Analysis of ammonia-oxidizing bacteria of the β-subdivision of the class *Proteobacteria* in coastal sand dunes by denaturing gradient gel electrophoresis and sequencing of PCR-amplified 16S ribosomal DNA fragments. *Appl. Environ. Microbiol*. **63**: 1489–1497

Kuhn RC, Rock CM and Oshima KH (2002) Occurrence of *Cryptosporidium* and *Giardia* in Wild Ducks along the Rio Grande River Valley in Southern New Mexico. *Appl. Environ. Microbiol*. **68** (1): 161-165

Kurata S, Kanagawa T, Magariyama Y, Takatsu K, Yamada K, Yokomaku T and Kamagata Y (2004) Reevaluation and reduction of a PCR bias caused by reannealing of templates. *Appl. Environ. Microbiol*. **70** (12): 7545-7549

Kurata S, Kanagawa T, Yamada K, Torimura M, Yokomaku T, Kamagata Y and Kurane, R (2001) Fluorescent quenching-based quantitative detection of specific DNA/RNA using a BODIPY@ FL-labeled probe or primer. *Nucleic Acid Res*. **29**: e34

Langer PR, Waldrop AA and Ward DC (1981) Enzymatic synthesis of biotin-labeled polynucleotides: novel nucleic acid affinity probes. *Proc. Natl. Acad. Sci. USA* **78**: 6633-6637

Lathe R (1985) Synthetic oligonucleotide probes deduced from amino acid sequence data. Theoretical and practical considerations. *J. Mol. Biol*. **183**: 1-2

Lee BJ, Wentzel MC, Ekama GA (2003) Batch test for the measurement of ordinary heterotrophic organism active mass in activated sludge mixed liquor. *Res. Rept. W84,* Dept. of Civil Eng., University of Cape Town, Rondebosch 7700, South Africa

Lee D-H, Zo Y-G and Kim S-J (1996) Nonradioactive method to study genetic profiles of natural bacterial communities by PCR-Single-Strand-Conformation Polymorphism. *Appl. Environ. Microbiol*. **62**: 3112–3120

Lee N, Nielsen PH, Andreasen K, Juretschko S, Nielsen JL, Schleifer KH, and Wagner M (1999) Combination of fluorescent in situ hybridization and microautoradiography: a new tool for structure-function analysis in microbial ecology. *Appl. Environ. Microbiol*. **65:** 1289–1297

Lee SH, Malone C, Kemp PF (1993) Use of multiple 16S rRNA-targeted fluorescent probes to increase signal strength and measure cellular RNA from natural planktonic bacteria. *Mar. Ecol. Prog. Ser.* **101**: 193-201

Lerman LS and Silverstein K (1987) Computational simulation of DNA melting and its application to denaturing gradient gel electrophoresis. *Methods Enzymol.* **155**: 482–501

Levsky JM and Singer RH (2003) Fluorescence in situ hybridization: past, present and future. *J. Cell Sci.* **116**: 2833-2838

Liesack W and Stackebrandt E (1992) Occurrence of novel groups of the domain *Bacteria* as revealed by analysis of genetic material isolated from an Australian terrestrial environment. *J. Bacteriol*. **174**: 5072-5078

Lilley ID, Pybus PJ and Power SPB (1997) Operating manual for biological nutrient removal wastewater treatment works. *Res Report No. TT 83/97* Water Research Commision, P/Bag X03, Gezina 0031, South Africa.

Liu W-T, Huang C-L, Hu JY, Song L, Ong SL and Ng WJ **(**2002). Denaturing gradient gel electrophoresis polymorphism for rapid 16s rDNA clone screening and microbial diversity study. *J. Biosci. Bioeng*. **93**: 101–103

Llobet-Brossa E, Rosselló-Mora R and Amann R (1998) Microbial community composition of wadden sea sediments as revealed by fluorescence *in situ* hybridization. *Appl. Environ. Microbiol*. **64** (7): 2691-2696

Loy A, Horn M and Wagner M (2003) probeBase: an online resource for rRNA-targeted oligonucleotide probes. *Nucleic Acid Res*. **31** (1): 514-516

Lueders T and Friedrich MW (2003) Evaluation of PCR amplification bias by terminal restriction fragment length polymorphism analysis of small subunit rRNA and *mcrA* genes by using defined template mixtures of methanogenic pure cultures and soil DNA extracts. *Appl. Environ. Microbiol*. **69:** 320–326

Lyautey E, Lacoste B, Ten-Hage L, Rols J-L, and Garabetian F (2005) Analysis of bacterial diversity in river biofilms using 16S rDNA PCR-DGGE: Methodology settings and fingerprints interpretation. *Wat. Res*. **39**: 380-388

MacCarthy PL (1964) Thermodynamics of the biological synthesis and growth. *Proc. 11th Int. Conf. on Water Pollution Res.*, Tokyo, Japan, 169-199

MacDonald R and Brozel VS (2000) Community analysis of bacterial biofilms in a simulated recirculating cooling-water system by fluorescent *in situ* hybridization with rRNA-targeted oligonucleotide probes. *Wat. Res*. **34**: 2439-2446

MacGregor BJ, Bruchert V, Fleischer S and Amann R (2002) Isolation of small-subunit rRNA for stable isotopic characterization. *Environ. Microbiol*. **4:** 451–464

Mackay IM, Arden KE and Nitsche A (2002) Real-time PCR in virology. *Nucleic Acids Res.* **30:** 1292-1305

Maidak BL, Cole JR, Lilburn TG, Parker CT, Saxman PR, Stredwick JM, Garrity GM, Li B, Olsen GJ, Pramanik S (2000) The RDP (Ribosomal Database Project) continues**.** *Nucleic Acids Res*. **28**: 173-174

Manefield M, Whiteley AS, Griffiths RI and Bailey MJ (2002) RNA stable isotope probing, a novel means of linking microbial community function to phylogeny. *Appl. Environ. Microbiol.* **68:** 5367–5373

Maniatis T, Fritsch EF and Sambrook J (1982) *Molecular Cloning: A Laboratory Manual*. USA: Cold Spring Harbor Laboratory.

Manuelidis L, Langer-Safer PR and Ward DC (1982) High-resolution mapping of satellite DNA using biotin-labeled DNA probes. *J. Cell Biol.* **95**: 619-625

Manz W, Amann R, Ludwig W, Vancanneyt M and Schleifer KH (1996) Application of a suite of 16S rRNA-specific oligonucleotide probes designed to investigate bacteria of the phylum cytophaga-flavobacter-bacteroides in the natural environment. *Microbiology* **142**: 1097-1106

Manz W, Amann R, Ludwig W, Wagner M and Schleifer K-H (1992) Phylogenetic oligodeoxynucleotide probes for the major subclasses of proteobacteria: problems and solutions. *System. Appl. Microbiol.* **15**: 593-600

Manz W, Wagner M, Amann R and Schleifer K-H (1994) *In situ* characterization of the microbial consortia active in two wastewater treatment plants. *Wat. Res*. **28**: 1715-1723

Marais GVR and Ekama GA (1976) The activated sludge process: Part 1 – Steady state behavior. *Wat. SA* **2** (4): 163-200

Maruyama A and Sunamura M (2000) Simultaneous direct counting of total and specific microbial cells in seawater, using a deep-sea microbe as target**.** *Appl. Environ. Microbiol*. **66**: 2211-2215

Mathieu-Daude F, Welsh J, Vogt T and McClelland M (1996) DNA rehybridization during PCR: the 'Cot effect' and its consequences. *Nucleic Acids Res.* **24**: 2080–2086

Maurer M and Gujer W (1994) Prediction of the performance of enhance biological phosphorus removal plants. *Wat. Sci. Tech*. **30** (6): 333-334

Mayer CL and Palmer CJ (1996) Evaluation of PCR, Nested PCR, and Fluorescent Antibodies for Detection of *Giardia* and *Cryptosporidium* Species in Wastewater. *Amer. Soc. Microbiol*. **62**(6): 2081-2085

Mbewe A, Wentzel MC and Ekama, GA (1995) Characterisation of Municipal Wastewaters, *UCT Report No. W 84.* Dept. Civil Eng., Univ. of Cape Town, Rondebosch 7701, South Africa.

McTavish H, Fuchs JA and Hooper AB (1993) Sequence of the gene coding for ammonia monooxygenase in *Nitrosomonas europaea*. *J. Bacteriol*. **175**: 2436-2444

Meier H, Amann R, Ludwig W and Schleifer K-H (1999) Specific oligonucleotide probes for in situ detection of a major group of gram-positive bacteria with low DNA G+C content. *System. Appl. Microbiol*. **22**: 186-196

Mobarry BK, Wagner M, Urbain V, Rittmann BE and Stahl DA (1996) Phylogenetic probes for analyzing abundance and spatial organization of nitrifying bacteria. *Appl. Environ. Microbiol*. **62**: 2156-2162

Moyer CL, Tiedje JM, Dobbs FC and Karl DM (1996) A computer-simulated restriction fragment length polymorphism analysis of bacterial small-subunit rRNA genes: Efficacy of selected tetrameric restriction enzymes for studies of microbial diversity in nature. *Appl. Environ. Microbiol*. **62**: 2501–2507

Mudaly DD, Atkinson BW and Bux F (2001) FISHing for biomass in activated sludge mixed liquor: the slippery VSS fraction. In: *Advances in Water and Wastewater Treatment Technology in - Molecular Technology, nutrient removal, sludge reduction and environmental health*, Matsuo T, Hanaki K, Takizawa S and Satoh H (eds), Elsevier Science, Amsterdam: Netherlands

Murray AE, Hollibaugh JT and Orrego C (1996) Phylogenetic compositions of bacterioplankton from two California estuaries compared by denaturing gradient electrophoresis of 16S rDNA fragments. *Appl. Environ. Microbiol*. **62**: 2676–2680

Muyzer G, Brinkhoff T, Nübel U, Santegoeds C, Schäfer H and Wawer C (1997) Denaturing gradient gel electrophoresis (DGGE) in microbial ecology. In: Akkermans

ADL, van Elsas JD and de Bruijn FJ (Eds) *Molecular Microbial Ecology Manual*. Kluwer Academic Publishers, Dordrecht, Netherlands

Muyzer G and deWaal EC (1994) Determination of the genetic diversity of microbial communities using DGGE analysis of PCR amplified 16S rRNA. *NATO ASI Series* **G35**: 207–214

Muyzer G, de Waal EC and Uitterlinden AG (1993) Profiling of complex microbial populations by denaturing gradient gel electrophoresis analysis of polymerase chain reactionamplified genes encoding for 16S rRNA. *Appl. Environ. Microbiol*. **59**: 695–700

Muyzer G and Smalla K (1998) Application of denaturing gradient gel electrophoresis (DGGE) and temperature gradient gel electrophoresis (TGGE) in microbial ecology. *Antonie van Leewenhoek* **73**: 127-141

Muyzer G, Teske A, Wirson CO and Jannasch HW (1995) Phylogenetic relationship of *Thiomicrospira* species and their identification in deep-sea hydrothermal vent samples by denaturing gradient gel electrophoresis of 16s rDNA. *Appl. Env. Microbiol*. **59**: 695-700

Myers RM, Fischer SG, Lerman LS and Maniatis T (1985) Nearly all single base substitutions in DNA fragments joined to a GC clamp can be detected by denaturing gradient gel electrophoresis. *Nucleic Acids Res*. **13**: 3131–3145

Myers RM, Maniatus T and Lerman LS (1987) Detection and localization of single base changes by denaturing gradient gel electrophoresis. *Methods Enzymol*. **155**: 501-527

Neef A, Amann R, Schlesner H and Schleifer K-H (1998) Monitoring a widespread bacterial group: in situ detection of Planctomycetes with 16S rRNA-targeted probes. *Microbiology* **144**: 3257-3266

Nicolaison MH and Ramsing NB (2002) denaturing gradient gel electrophoresis (DGGE) approaches to study diversity of ammonia-oxidizing bacteria. *J. Microbial. Methods* **50**: 189-203

Nogueira R, Melo LF, Purkhold U, Wuertz S and Wagner M (2002) Nitrifying and heterotrophic population dynamics in biofilm reactors: effects of hydraulic retention time and the presence of organic carbon. *Water Res,* **36**: 469-481

Novak L, Larrea L and Wanner J (1994) Estimation of maximum specific growth rate of heterotrophic and autotrophic biomass: a combined technique of mathematical modeling and batch cultivations. *Wat. Sci. Tech*. **30** (11): 171-180

Nübel U, Engelen B, Felske A, Snaidr J, Wieshuber A, Amann RI, Ludwig W and Backhaus H (1996) Sequence heterogeneities of genes encoding 16S rRNAs in *Paenibacillus polymyxa* detected by temperature gradient gel electrophoresis. *J. Bacteriol*. **178:** 5636–5643

Oda Y, Slagman SJ, Meijer WG, Forney LJ and Gottschal JC (2000) Influence of growth rate and starvation on fluorescent *in situ* hybridization of *Rhodopseudomonas palustris*. *FEMS Microbiol. Ecol*. **32**: 205-213

Odelberg SJ, Weiss RB, Hata A and White R (1995) Template-switching during DNA synthesis by *Thermus aquaticus* DNA polymerase I. *Nucleic Acids Res*. **23:** 2049–2057
Odum (1971) *Fundamentals of Ecology*. WB Saunders Co., London.

Oerther DB, de los Reyes FL and Raskin L (1999) Interfacing phylogenetic oligonucleotide probe hybridization with representations of microbial populations and specific growth rates in mathematical models of activated sludge processes. *Wat. Sci. Tech*. **39** (1): 11-20

Okabe S, Satoh H and Watanabe Y (1999) *In situ* analysis of nitrifying biofilms as determined by in situ hybridization and the use of microelectrodes. *Appl Environ Microbiol* **65**: 3182– 3191

Onuki M, Satoh H, Mino T and Matsuo T (2000) Application of Molecular Methods to Microbial Community Analysis of Activated Sludge. *Wat. Sci. Technol.* **42**(3-4): 17-22

Osborn AM, Moore ERB and Timmis KN **(**2000) An evaluation of terminal-restriction fragment length polymorphism (T-RFLP) analysis for the study of microbial community structure and dynamics. *Environ. Microbiol*. **2**: 39–50

Ouverney CC and Fuhrman JA (1999) Combined microautoradiography-16S rRNA probe technique for determination of radioisotope uptake by specific microbial cell types in situ. *Appl. Environ. Microbiol*. **65:** 3264

Ouverney CC and Fuhrman JA (2000) Marine planktonic archaea take up amino acids. *Appl. Environ. Microbiol*. **66**: 4829-4833

Owens JD and Legan JD (1987) Determination of the Monod substrate saturation constant for microbial growth. *FEMS Microbiol. Rev.* **46:** 419–432

Pääbo S, Irwin DM and Wilson AC **(**1990) DNA damage promotes jumping between templates during enzymatic amplification. *J. Biol. Chem*. **265:** 4718–4721

Patel R, Lin C, Laney M, Kurn N, Rose S and Ullman EF (1996) Formation of chimeric DNA primer extension products by template switching onto an annealed downstream oligonucleotide. *Proc. Natl. Acad. Sci*. *USA* **93**: 2969–2974

Pelz O, Cifuentes LA, Hammer BT, Kelley CA and Coffin RB (1998) Tracing the assimilation of organic compounds using δ13C analysis of unique amino acids in the bacterial peptidoglycan cell wall. *FEMS Microbiol. Ecol*. **25:** 229–240

Pillay B, Roth G and Oellermann RA (1989) Nitrification and the enumeration of marine nitrifying bacteria in a closed prawn-culture system. *S. Afr. Mar. Sci. J.* **8**: 325-332

Pillay B, Roth G and Oellermann RA (1989) Cultural characteristics and identification of marine nitrifying bacteria from a closed prawn-culture system. *S. Afr. Mar. Sci. J.* **8**: 333-343

Pitter P and Chudoba J (1990) *Biodegradablity of organic substances in the aquatic environment.* CRC Press, Boca Raton, USA

Pollard PC, Steffens MA, Biggs CA and Lant PA (1998) Bacterial growth dynamics in activated sludge batch assays. *Wat. Res*. **32** (3): 587-596

Polz MF and Cavanaugh CM (1998) Bias in template-to-product ratios in multitemplate PCR. *Appl. Environ. Microbiol*. **64**: 3724–3730

Pommering-Röser A, Rath G and Koops H-P (1996) Phylogenetic diversity within the genus *Nitrosomonas*. *System. Appl. Microbiol*. **19**: 344-351

Porter KG and Feig Y (1980) The use of DAPI for identifying and counting aquatic microflora. *Limnol. Oceanogr*. **25**: 943-948

Purkhold U, Pommering-Röser A, Juretschko S, Schmid MC, Koops H-P and Wagner M (2000) Phylogeny of all recognized species of ammonia oxidizers based on comparative 16S rRNA and *amoA* sequence analysis: implications for molecular diversity surveys. *Appl. Environ. Microbiol.* **66**: 5368-5382

Puvion-Dutilleul F and Puvion E (1996) Non-isotopic electron microscope in situ hybridization for studying the functional subcompartmentalization of the cell nucleus. *Histochem. Cell Biol.* **106**: 59-78

Qiu X, Wu L, Huang H, McDonel PE, Palumbo AV, Tiedje JM and Zhou J (2001) Evaluation of PCR-generated chimeras, mutations, and heteroduplexes with 16S rRNA gene-based cloning. *Appl. Environ. Microbiol*. **67:** 880–887

Radajewski S, Ineson P, Parekh NR and Murrell JC (2000) Stable-isotope probing as a tool in microbial ecology. *Nature* **403:** 646–649

Ramsing NB, Fossing H, Ferdelman TG, Andersen F and Thamdrup B (1996) Distribution of bacterial populations in a stratified fjord (Mariager Fjord, Denmark) quantified by *in situ* hybridization and related to chemical gradients in the water column. *Appl. Environ. Microbiol*. **62**(4)**:** 1391-1404

Randall EW, Wilkinson A and Ekama GA (1991) An instrumentation for the direct determination of oxygen utilization rate. *Wat. SA* **17**(1): 11-18

Ravenschlag K, Sahm K and Amann R (2001) Quantitative molecular analysis of the microbial community in marine arctic sediments (Svalbard). *Appl. Environ. Microbiol*. **67**(1)**:** 387-95

Roller C, Wagner M, Amann R, Ludwig W and Schleifer K-H (1994) In situ probing of gram-positive bacteria with high DNA G + C content using 23S rRNA-targeted oligonucleotides. *Microbiology* **140**: 2849-2858

Roslev P and Iversen N (1999) Radioactive fingerprinting of microorganisms that oxidize atmospheric methane in different soils. *Appl. Environ. Microbiol*. **65:** 4064–4070

Roslev P, Larsen MB, Jørgensen D and Hesselsoe M (2004) Use of heterotrophic CO_2 assimilation as a measurer of metabolic activity in planktonic and sessile bacteria. *J. Microbiol. Methods* **59:** 381–393

Rosselló-Mora RA, Wagner M, Amann R and Schleifer K-H (1995) The abundance of *Zoogloea ramigera* in sewage treatment plants. *Appl. Environ. Microbiol*. **61**: 702-707

Rudkin GT and Stollar BD (1977) High resolution detection of DNA-RNA hybrids in situ by indirect immunofluorescence. *Nature* **265**: 472-473

Saiki RK, Gelfand DH, Stoffel S, Scharf SJ, Higuchi R, Horn GT, Mullis KB, and Ehrlich HA (1988) Primer-directed enzymatic amplification of DNA with a thermostable DNA polymerase. *Science* **239**: 487-491.

Saiki RK, Scharf SJ, Faloona F, Mullis KB, Horn GT, Erlich HA, and Arnheim N (1985) Enzymatic amplification of beta-globin genomic sequences and restriction site analysis for diagnosis of sickle cell anemia. *Science* **230**: 1350-1354

Sayavedra-Soto LA, Hommes NG and Arp DJ (1994) Characterization of the gene encoding hydroxylamine oxidoreductase in *Nitrosomonas europaea*. *J. Bacteriol*. **176**: 504-510

Schlesner H (1986) *Pirella marina* sp. nov., a budding, peptidoglycan-less bacterium from brackish water. *System. Appl. Microbiol*. **8**: 177-180

Schlesner H (1987) *Verrucomicrobium spinosum* gen. nov., sp. nov.: a fimbriated prosthecate bacterium. *System. Appl. Microbiol*. **10**: 54-56

Schmid M, Twachtmann U, Klein M, Strous M, Juretschko S, Jetten M, Metzger JW, Schleifer K-H and Wagner M (2000) Molecular evidence for a genus-level diversity of bacteria capable of catalyzing anaerobic ammonium oxidation. *System. Appl. Microbiol*. **23**: 93-106

Schneider B and Selenka F (1974) Behaviour and effects of nitrate and nitrite in the organism. I. Changes of methemoglobine concentration in the organism depending on the way of administration of nitrite. *Zentralbl.-Bakteriol*. **159**: 113-129

Schramm A, De Beer D, Gieseke A, Amann R (2000) Microenvironments and distribution of nitrifying bacteria in a membrane-bound biofilm. *Environ. Microbiol.* **2**: 680–686

Schraam A, De Beer D, van den Heuvel JC, Ottengraf S and Amann R (1999) Microscale distribution of populations and activities of *Nitrosospira* and *Nitrospira* spp. along a macroscale gradient in a nitrifying bioreactor: quantification by in situ hybridization and the use of microsensors. *Appl. Environ. Microbiol*. **65**: 3690-3696

Schramm A, De Beer D, Wagner M and Amann R (1998) Identification and activities *in situ* of *Nitrosospira* and *Nitrospira* spp. as dominant populations in a nitrifying fluidized bed reactor. *Appl. Environ. Microbiol.* **64**: 3480–3485

Schramm A, Larsen LH, Revsbech NP, Ramsing NB, Amann R and Schleifer K-H (1996) Structure and function of a nitrifying biofilm as determined by *in situ* hybridization and the use of microelectrodes. *Appl. Environ. Microbiol*. **62**: 4641–4647

Senn H, Lendenmann U, Snozzi M, Hamer G and Egli T (1994) The growth of *Escherichia coli* in glucose-limited chemostat cultures: a reexamination of the kinetics. *Biochim. Biophys. Acta* **1201**: 424–436

Sheffield VC, Beck JS, Stone EM and Myers RM (1992) A simple and efficient method for attachment of a 40-base pair, GC-rich sequence to PCR-amplified DNA. *BioTechniques* **12**: 386–387

Sheffield VC, Cox DR and Myers RM (1989) Attachment of a 40bp G+C rich sequence (GC-clamp) to genomic DNA fragments by polymerase chain reaction results in improved detection of single-base changes. *Proc. Natl. Acad. Sci. USA* **86:** 232–236

Shuldiner AR, Nirula A and Roth J **(**1989) Hybrid DNA artifact from PCR of closely related target sequences. *Nucleic Acids Res*. **17:** 4409

Singer RH and Ward DC (1982) Actin gene expression visualized in chicken muscle tissue culture by using in situ hybridization with a biotinated nucleotide analog. *Proc. Natl. Acad. Sci. USA* **79**: 7331-7335

Snaidr J, Amann R, Huber I, Ludwig W and Schleifer K-H (1997) Phylogenetic analysis and *in situ* identification of bacteria in activated sludge. *Appl. Environ. Microbiol.* **63**: 2884-2896

Sorokin DY, Muyzer G, Brinkhoff T, Kuenen JG and Jetten MSM (1998) Isolation and characterization of a novel facultatively alkaliphilic *Nitrobacter* species, *N. alkalicus* sp. nov. *Arch. Microbiol*. **170**: 345-352.

Southwick PL, Ernst LA, Tauriello EW, Parker SR, Mujumdar RB, Mujumdar SR, Clever HA, Waggoner AS (1990) Cyanine dye labeling reagents - carboxymethylindocyanine succinimidyl esters. *Cytometry*. **11**: 418-430

Speksnijder AG, Kowalchuk GA, De Jong S, Kline E, Stephen JR and Laanbroek HJ (2001) Microvariation artifacts introduced by PCR and cloning of closely related 16S rRNA gene sequences. *Appl. Environ. Microbiol*. **67:** 469–472

Stackebrandt E, Murray RGE and Trüper HG (1988). *Proteobacteria* classis nov., a name for the phylogenetic taxon that includes the "purple bacteria and their relatives". *Int. J. Syst. Bacteriol.* **38**: 321-325

Stahl DA (1997) Molecular approaches for the measurement of density, diversity, and phylogeny. In Hurst CJ, Knudsen GR, McInerney MJ, Stetzenbach LD and Walter MV (eds), *Manual of Environmental Microbiology*. American Society for Microbiology Press, Washington DC.

Stahl DA and Amann R (1991) Development and application of nucleic acid probes. In Stackebrandt E. and M. Goodfellow (eds), *Sequencing and Hybridization Techniques in Bacterial Systematics.* John Wiley & Sons, Chichester.

Staley JT, de Bont JAM and de Jonge K (1976) *Prosthecobacter fusiformis* nov. gen. et sp., the fusiform caulobacter. *Antonie van Leeuwenhoek* **42**: 333-342

Standard Methods for the Examination of Water and Wastewater (1985). 16th edn, American Public Health Assoc., 1015 15th Str. NW, Washington DC 20005, USA

Steyn DJ, Toerien DF and Visser JH (1975) Eutrophication levels of some SA impoundments II Hartbeesport Dam. *Water SA* **1** (3): 93-101

Stouthamer AH and van Verseveld HW (1987) Microbial energetics should be considered in manipulation metabolism for biotechnological purposes. *Trends Biotechnol*. **5**: 149-155

Strous M, Fuerst JA, Kramer EHM, Logemann S, Muyzer G, van de Pas-Schoonen KT, Webb RI, Kuenen JG and Jetten MSM (1999) Missing lithotroph identified as new planctomycete. *Nature* **400**: 446-449

Stryer L (1981) *Biochemistry* (2nd edn.). WH Freeman & Co, San Francisco.

Sundermeyer-Klinger H, Meyer W, Warninghoff B and Bock E (1984) Membrane-bound nitrite oxidoreductase of *Nitrobacter*: evidence for a nitrate reductase system. *Arch. Microbiol*. **140**: 153-158

Suzuki MT and Giovannoni SJ (1996) Bias caused by template annealing in the amplification of mixtures of 16S rRNA genes by PCR. *Appl. Environ. Microbiol.* **62:** 625–630

Tanaka Y, Fukumori Y and Yakamaka T (1983) Purification of cytochrome a_1c_1 from *Nitrobacter agilis* and characterization of nitrite oxidation system of the bacterium. *Arch. Microbiol*. **135**: 265-271

Teske A, Alm E, Regan JMST, Rittmann BE and Stahl DA (1994) Evolutionary relationships among ammonia- and nitrite-oxidizing bacteria. *J. Bacteriol*. **176**: 6623-6630

Teske A, Wawer C, Muyzer G and Ramsing NB (1996) Distribution of sulfate-reducing bacteria in a stratified Fjord (Mariager Fjord, Denmark) as evaluated by most-probable-number counts and denaturing gradient gel electrophoresis of PCR-amplified ribosomal DNA fragments. *Appl. Environ. Microbiol*. **62**: 1405–1415

Thompson JR, Marcelino LA, and Polz MF (2002) Heteroduplexes in mixed-template amplifications: formation, consequence and elimination by 'reconditioning PCR'. *Nucleic Acids Res*. **30:** 2083–2088

Torimura M, Kurata S, Yamada K, Yokomaku T, Kamagata Y, Kanagawa T and Kurane R (2001) Fluorescence-quenching phenomenon by photo-induced electron transfer between a fluorescent dye and a nucleotide base. *Anal. Sci*., **17**: 155-160

Torsvik V, Goksoyr J and Daale FL (1990a) High diversity in DNA of soil bacteria. *Appl. Envrion. Microbiol*. **56**: 782–787

Torsvik V, Salte K, Sorkeim R & Goksoyr J (1990b) Comparison of phenotypic diversity and DNA heterogeneity in a population of soil bacteria. *Appl. Environ. Microbiol*. **56:** 776–781

Trebesius K, Amann R, Ludwig W, Mühlegger K, Schleifer K-H (1994) Identification of whole fixed bacterial cells with nonradioactive 23S rRNA-targeted polynucleotide probes. *Appl. Environ. Microbiol*. **60**: 3228-3235

Trebesius K, Harmsen D, Rakin A, Schmelz J and Heesemann J (1998) Development of rRNA-targeted PCR and in situ hybridization with fluorescently labelled oligonucleotides for detection of *Yersinia* species. *J. Clin. Microbiol*. **36**: 2557-2564

Trüper HG and de Clari L (1997) Taxonomic note: necessary correction of specific epithets formed as substantives (nouns) "in apposition". *Int. J. Syst. Bacteriol*. **47**: 908-909

Ubisi MF, Jood TW, Wentzel MC and Ekama GA (1997a) Activated sludge mixed liquor heterotrophic active biomass. *Wat. SA* **23**(3): 239-248

Ubisi MF., Wentzel MC. and Ekama GA (1997b) Organic and inorganic components of activated sludge mixed liquor. *Res. Rept. W94*, Dept. Civil Eng., Univer. of Cape, Ronderbosch 7700, South Africa.

Urbain V, Mobarry B, de Silva V, Stahl DA, Rittmann BE and Manem J (1998) Integration of performance, molecular biology and modeling to describe the activated sludge process. *Wat. Sci. Tech*. **37**(4-5): 223-229

Utåker JB, Bakken L, Jiang QQ and Nes IF (1995) Phylogenetic analysis of seven new isolates of ammonia-oxidizing bacteria based on 16S rRNA gene sequences. *System. Appl. Microbiol*. **18**: 549-559

Vallaeys T, Topp E, Muyzer G, Macheret V, Laguerre G and Soulas G (1997) Evaluation of denaturing gradient gel electrophoresis in the detection of 16S rDNA sequence variation in rhizobia and methanotrophs. *FEMS Microbiol. Ecol.* **24**: 279–285

Van de Peer Y, De Rijk P, Wuyts L, Winkelmans T and De Wachter R (2000) The European small subunit ribosomal RNA database**.** *Nucleic Acids Res*. **28**: 175-176.

Van Haandel APC, Ekama GA and Marias GVR (1981) The activated sludge process 3 – Single sludge denitrification. *Wat. Res*. **15**: 1135-1152

Van Hannen EJ, van Agterveld MP, Gons HJ and Laanbroek HJ (1998) Revealing genetic diversity of eukaryotic microorganisms in aquatic environments by denaturing gradient gel electrophoresis. *J. Phycol*. **34**: 206–213

Vitousek PM (1997) Human Alteration of the Global Nitrogen Cycle: Causes and Consequences. *Issues in Ecology* **1**: 4-6

Vogelsang C, Schramm A, Picioreanu C, Van Loosdrecht MCM and ∅stgaard K (2002) Microbial community analysis by FISH for mathematical modeling of selective enrichment of gel-entrapped nitrifiers obtained from domestic wastewater. *Hydrobiologia.* **419**: 165-178

Von Wintzingerode F, Gobel UB and Stackebrandt E **(**1997) Determination of microbial diversity in environmental samples: pitfalls of PCR-based rRNA analysis. *FEMS Microbiol. Rev*. **21:** 213–229

Wagner M and Amann R (1997) Molecular techniques for determining microbial community structures in activated sludge. In Cloete TE and Muyima NYO (eds), Microbial Community Analysis: The Key to Design of Biological Waste-water Treatment Systems. *IAWQ Scientific and Technical Report No. 5*, University Press, Cambridge: 61–72

Wagner M, Amann R, Kämpfer P, Assmus B, Hartmann A, Hutzler P, Springer N and Schleifer K-H (1994a) Identification and *in situ* detection of gram-negative filamentous bacteria in activated sludge. *System. Appl. Microbiol*. **17**: 405-417

Wagner M, Aßmuss B, Hartmann A, Hutzler P and Amann R (1994b) In situ analysis of microbial consortia in activated sludge using fluorescently labelled, rRNA-targeted

oligonucleotide probes and confocal laser scanning microscopy. *J. Microscopy* **176**: 181-187.

Wagner M, Erhart R, Manz W, Amann R, Lemmer H, Wedl D and Schleifer K-H (1994c). Development of an rRNA-targeted oligonucleotide probe specific for the genus *Acinetobacter* and its application for *in situ* monitoring in activated sludge. *Appl. Environ. Microbiol*. **60**: 792-800

Wagner M, Amann R, Lemmer H and Schleifer K-H (1993) Probing activated sludge with oligonucleotides specific for *Proteobacteria*: inadequacy of culture-dependent methods for describing microbial community structure. *Appl. Environ. Microbiol*. **59**: 1520-1525

Wagner M, Hutzler P and Amann R (1998) 3-D analysis of complex microbial communities by combining confocal laser scanning microscopy and fluorescence *in situ* hybridization (FISH) *In* Wilkinson MHF and Schut F (ed.), *Digital image analysis of microbes*. John Wiley & Sons, Chichester.

Wagner M, Rath G, Amann R, Koops H-P and Schleifer K-H (1995) *In situ* identification of ammonia-oxidizing bacteria. *System. Appl. Microbiol*. **18**: 251-264

Wagner M, Rath G, Koops H-P, Flood J and Amann R (1996) *In situ* analysis of nitrifying bacteria in sewage treatment plants. *Wat. Sci. Tech*. **34**: 237-244

Wallner G, Erhart R and Amann R (1995) Flow cytometric analysis of activated sludge with rRNA-targeted probes. *Appl. Environ. Microbiol*. **61**(5)**:** 1859-1866

Wallner G, Fuchs B, Spring S, Beisker W and Amann R (1997) Flow sorting of microorganisms for molecular analysis. *Appl Environ Microbiol*. **63**(11)**:** 4223-31

Wanner J (1994) Activated sludge bulking and foaming control. Technomic Publishing Co., Inc., Lancaster, Pa.

Ward DM, Bateson MM, Weller R and Ruff-Roberts (1992) Ribosomal RNA analysis of microorganisms as they occur in nature. *Adv. Microb. Ecol*. **12**: 219–286

Watson SW (1965) Characteristics of a marine nitrifying bacterium, *Nitrosocystis oceanus* sp. n. *Limnol. Oceanogr*. **10(Suppl.)**: R274-R289

Watson SW, Bock E, Valois FW, Waterbury JB and Schlosser U (1986) *Nitrospira marina* gen. nov. sp. nov.: a chemolithotrophic nitrite-oxidizing bacterium. *Arch. Microbiol*. **144**: 1-7

Watson SW and Waterbury JB (1971) Characteristics of two marine nitrite oxidizing bacteria, *Nitrospina gracilis* nov. gen. nov. sp. and *Nitrococcus mobilis* nov. gen. nov. sp. *Arch. Mikrobiol*. **77**: 203-230

Wayne LG, Brenner DJ, Colwell RR, Grimont PAD, Kandler O, Krichevsky MI, Moore LH, Moore WEC, Murray RGE, Stackebrandt E, Starr MP and Truper HG (1987) Report of the ad hoc committee on reconciliation of approaches to bacterial systematics. *Int. J. Syst. Bacteriol.* **37:** 463–464

Weller R, Glöckner FO and Amann R (2000) 16S rRNA-targeted oligonucleotide probes for the in situ detection of members of the phylum Cytophaga-Flavobacterium-Bacteroides. *System. Appl. Microbiol*. **23**: 107-114

Wentzel MC, Dold PL, Ekama GA and Marais GvR (1990). Biological excess phosphorus removal – steady state process design. *Wat. SA* **16**(1): 29-48

Wentzel MC, Ekama GA and Marais GvR (1992) Processes and modeling of nitrification denitrification biological excess phosphorus removal systems- a review. *Wat. Sci. Tech.* **25**(6): 59-82

Wentzel MC, Mbewe A and Ekama GA (1995) Batch test for the measurements of readily biodegradable COD and active organisms concentrations in municipal wastewaters. *Wat. SA* **21**(2): 117-124

Wentzel MC, Ubisi MF and Ekama GA (1998) Heterotrophic active biomass component of activated sludge mixed liquor. *Wat. Sci. Tech*. **37**(4-5): 79-87

Wiegant J, Ried T, Nederlof PM, van der Ploeg M, Tanke HJ and Raap AK (1991). *In situ* hybridization with fluoresceinated DNA. *Nucleic Acids. Res.* **19**: 3237-3241

Wilderer PA, Bungartz H-J, Lemmer H, Wagner M, Keller J and Wuertz S (2002) Modern scientific methods and their potential in wastewater science and technology. *Wat Res.* **36**: 370-393

Winogradsky S (1892) Contributions a la morphologie des organismes de la nitrification. *Arch. Sci. Biol*. (St. Petersb.) **1**: 88-137

Wise MG, McArthur JV and Shimkets LJ (1997) Bacterial diversity of a carolina bay as determined by 16S rRNA gene analysis: confirmation of novel taxa. *Appl. Environ. Microbiol.* **63**: 1505-1514

Witzig R, Manz W, Rosenberger S, Kruger U, Kraume M and Szewzyk U (2002) Microbial aspects of a bioreactor with submerged membranes for aerobic treatment of municipal wastewater. *Wat. Res*. **36:** 394-402

Woese CR, Weisburg WG, Hahn CM, Paster BJ, Zablen LB, Lewis BJ, Macke TJ, Ludwig W and Stackebrandt E (1985) The phylogeny of the purple bacteria: the gamma subdivision. *System. Appl. Microbiol*. **6**: 25-33

Woese CR, Weisburg WG, Paster BJ, Hahn CM, Tanner RS, Krieg NR, Koops H-P, Harms H and Stackebrandt E (1984) The phylogeny of the purple bacteria: the beta subdivision. *System. Appl. Microbiol*. **5**: 327-336.

Wong M-T, Mino T, Seviour RJ, Onuki M and Liu W-T (2005) *In situ* identification and characterization of the microbial community structure of full-scale enhanced biological phosphorous removal plants in Japan. *Wat Res*. **39**: 2901-2914

WRC (1984) Theory, Design and operation of nutrient removal Activated Sludge processes. *Water research Commission*, PO Box 824, Pretoria 0001, South Africa

Yoshie S, Noda N, Miyano T, Tsuneda S, Hirata A and Inamori Y (2001) Microbial community analysis in the denitrification process of saline-wastewater by denaturing gradient gel electrophoresis of PCR-amplified 16s rDNA and the cultivation method. *J. Biosci. Bioeng*. **92**: 346–353

Wu J-H, Liu W-T, Tseng I-C and Cheng S-S (2001) Characterization of a 4-methylbenzoate-degrading methanogenic consortium as determined by small-subunit rDNA sequence analysis. *J. Biosci. Bioeng*. **91:** 449–455

Zarda B, Hahn D, Chatzinotas A, Schönhuber W, Neef A, Amann RI and Zeyer J (1997) Analysis of bacterial community structure in bulk soil by in situ hybridization. *Arch. Microbiol*. **168**: 185-192

Zwart G, Huismans R, van Agterveld MP, Van de Peer Y, de Rijk P, Eenhoorn H, Muyzer G, van Hannen EJ, Gons HJ and Laanbroek HJ (1998) Divergent members of the bacterial division *Verrucomicrobiales* in a temperate freshwater lake. *FEMS Microbiol. Ecol.* **25**: 159-169

APPENDIX 1

Chemical oxygen demand (COD) test
(Standard methods, 1985)

Reagents

1.1 Standard potassium dichromate ($K_2Cr_2O_7$) solution, 0.250N

Dissolve 12,259 g, $K_2Cr_2O_7$ (primary standard grade) previously dried at 103ºC for 3 hours and then cooled in a desiccator, in distilled water and make up to 1000 mL

1.2 Sulphuric acid (H_2SO_4) reagent

Dissolve 15 g of silver sulphate (Ag_2SO_4) in 2500 mL of concentrated (<98%) H_2SO_4 using a magnetic stirrer. Dissolution takes place between 1 and 2 days.

1.3 Standard ferrous ammonia sulphate [Fe $(NH_4)_2(SO_4)_2$] 0.05N

Dissolve 100 g analytical grade Fe $(NH_4)_2(SO_4)_2 . 6H_2O$ in distilled water using a 5 L volumetric flask. Add 100 mL of concentrated H_2SO_4 and make up to 5000mL.

Standardization: Pipette 5 mL of standard $K_2Cr_2O_7$ (1.1) solution into a Erlenmeyer flask, and dilute to 50 mL with distilled water. Add 15 mL of the H_2SO_4 (1.2) and allow to cool before titrating with Fe $(NH_4)_2(SO_4)_2$ titrant, using 2 drops of ferroin indicator (1.4)

$$\text{Normality Fe } (NH_4)_2(SO_4)_2 = \frac{\text{mL } K_2Cr_2O_7 * 0.25}{\text{mL Fe } (NH_4)_2(SO_4)_2}$$

1.4 Ferrion indicator

Dissolve 1.485 g 1,10-phenanthroline monohydrate, together with 0.695 g $FeSO_4.7H_2O$ in distilled water and dilute to 100 mL.

1.5 Mercuric sulphate ($HgSO_4$) powder

Procedure

1. Collect the correct number of clean, dry 250 mL Erlenmeyer flasks with the ground-glass 24/40 necks. Two flasks are used for each test. Include 2 extra flasks if influent COD is being tested and 2 extra flasks if reactor or effluent COD is being tested.
2. Place approximately 0.04 g $HgSO_2$ powder in each flask. This is the equivalent to the volume of 2 match heads.
3. Place 8-10 glass beads (± 3mm diameter) in each flask.
4. For each influent sample pipette 10 mL of unfiltered influent into each of the two flasks. Pipette 10mL of distilled water into each of the two flasks (these are the blanks)
5. Add 5 mL of $K_2Cr_2O_7$ solution to each of the flasks.
6. In turn, carefully add 15 mL of the H_2SO_4 COD acid (1.2) to each flask, ensuring that no vapour escapes from the flask. This is most easily done by pouring the acid down the wall of the flask while the flask is tilted. Immediately attach the flask to the jacket condenser.
7. Once acid has been added to each flask ensure that the flasks are level on the heating pad. Allow the contents of the flask to boil for 2 hours. Ensure that the water flow rate in the condensers is swift enough to condense all vapour rising up the condensers.
8. Allow the flasks to cool to room temperature with the condensers still in position
9. Pour approximately 80 mL of distilled water through the top opening of each of the condensers into the sample mixture, ensuring that the side walls of the condensers are well washed.
10. Remove the flasks from the condensers and the heating pad and add 2 drops of ferroin indicator to each flask.
11. Titrate with Fe $(SO_4)_2$ (NH_4) solution until one drop of titrant changes the solution colour to reddish brown.

Calculation:

$$\text{mg/L COD} = \frac{(a-b) * N * 8000}{\text{mL sample}}$$

where

a = average mL $Fe(SO_4)_2(NH_4)$ used to titrate blank of same volume as sample

b = average mL $Fe(SO_4)_2(NH_4)$ used to titrate sample

N = normality of $Fe(SO_4)_2(NH_4)$

APPENDIX 2

Total kjeldahl nitrogen (TKN) test (Standard methods, 1985)

Reagents

2.1 Mercuric sulphate ($HgSO_4$) solution

Dissolve 40 g red mercuric oxide (HgO) in 250 mL of 1 H_2SO_4: 5 water (50 mL : 250 mL) and dilute to 800 mL with distilled water.

2.2 Sulphuric acid (H_2SO_4)- mercuric sulphate ($HgSO_4$)-potassium sulphate (K_2SO_4) solution

Dissolve 333.75 g K_2SO_4 in 1800 mL distilled water and add 500 mL concentrated H_2SO_4. Add 62.5 mL $HgSO_4$ solution and dilute to 2500 mL. This reagent crystallizes at temperature lower than 14ºC.

2.3 7N Sulphuric acid (H_2SO_4)

Dilute 485 mL concentrated H_2SO_4 (>98%) in distilled water and make up to 2500 mL with distilled water.

2.4 Digestion mixture

Mix the two solutions made up in 2.2 and 2.3 above to give 5000 mL of digestion mixture

2.5 Mixed indicator

Mix two volumes of 0.2% methyl red in 95% alcohol with 1 volume of 0.2% methylene blue in 95% alcohol. This solution must be made fresh every 30 days.

2.6 Boric acid (H_3BO_3)

Dissolve 100 g H_3BO_3 in distilled water. Add 100 mL of mixed indicator (or 40 mL blue and 80 mL red), and dilute to 5000 mL.

2.7 Sulphuric acid H_2SO_4 solution 0.02N

Prepare a stock solution of 0.1 N H_2SO_4 by diluting 2.8 mL concentrated H_2SO_4 to 1000 mL. Dilute 200 mL of the 0.1 N H_2SO_4 stock solution to 1000 mL with distilled water to give a 0.02 N stock solution. Standardize this solution as outlined in section 102.3 (c) – Alkalinity of "Standard Methods", p.54

2.8 Standard Sulphuric acid (H_2SO_4) solution 0.001 N

Dilute 100 mL of the 0.02 N H_2SO_4 stock solution to 2000 mL to give an approximately 0.001 N H_2SO_4 solution.

2.9 Sodium Hydroxide (NaOH)- sodium thiosulphate solution ($Na_2S_2O_3.5H_2O$)

Dissolve 500 g NaOH and 25 g $Na_2S_2O_3.5H_2O$ in distilled water and make up to 1000 mL. This procedure is done in a plastic container as the reaction is highly exothermic.

Procedure

1. Pipette 25 mL influent sample or a 50mL reactor or effluent sample into a 250 mL Kjeldahl flask. Add 10 mL digestion mixture (2.4) and 3 glass beads (approximately 3 mm diameter). Prepare a blank by placing a volume of distilled water equal in volume to that of the sample with digestion mixture and beads, in a second kjeldahl flask. Follow the same procedure for the sample and the blank.
2. Digest the sample mixture on a heating pad until the sample is clear, and heat for another 20 minutes.
3. Transfer the Kjeldahl flask to the micro steam distillation apparatus and allow cooling for approximately 30 min.

4. Pipette 50 mL of H_3BO_3 solution (2.6) into a 100 mL Erlenmeyer flask and place in position on the steam distillation apparatus with nozzle of the condenser immersed in the solution.
5. Add about 100 mL of distilled water to the contents of the Kjeldahl flask to dissolve the sediment.
6. Add 10 mL of the NaOH solution (2.9) to the contents of the Kjeldahl flask via the top opening of the steam distillation apparatus, and immediately seal the apparatus by placing the steam line in position.
7. Steam distil until the volume of the H_3BO_3 solution in the Erlenmeyer flask is approximately 100 mL.
8. Titrate the contents of the Erlenmeyer flask for the sample and the blank with standardized 0.02 N H_2SO_4 (2.7).

Calculation

$$\text{TKN mgN/L} = \frac{(a-b)* N *14000}{A}$$

Where

a = mL 0.001N H_2SO_4 for sample

b = mL 0.001N H_2SO_4 for blank

N = actual normality of 0.001N H_2SO_4

A = mL sample

APPENDIX 3

Determination of MLSS and MLVSS
(Standard methods, 1985)

Determination of MLSS

1. Place 100 mL of activated sludge mixed liquor in a centrifuge tube. Centrifuge at 4000 xg for 8 min
2. Discard the supernatant and quantitatively scoop the sludge into a pre-weighed crucible.
3. place the crucible into a drying oven at 105ºC and leave overnight. Remove from oven and allow to cool in a dessicator.
4. Re-weigh crucible.
5. determine the MLSS according to the following calculation:

$$\text{MLSS (g/L)} = \frac{\text{mass of (crucible + sludge) – mass of (crucible) in grams x 10}}{\text{100 mL}}$$

Determination of MLVSS

1. Place the pre-weighed crucible (from the MLSS determination) into a muffle furnace
2. Ash at 550ºC for 1 hour. Remove the crucible and allow to cool in dessicator.
3. Re-weigh the crucible.
4. Determine the MLVSS according to the following equation:

$$\text{MLVSS (g/L)} = \frac{\text{mass of (crucible + sludge) – mass of (crucible + ash) x 10}}{\text{100 mL}}$$

APPENDIX 4

Cell fixation and sonication

1. Cell fixation with 4% paraformaldehyde (Amann, 1995)

Introduction:

The hybridization process exposes the cells to increased temperature, detergents and variable osmotic gradients. Fixation is an essential procedure for maintaining the morphological integrity of the cells. In order to minimize auto-fluorescence, fresh (not older than 24 h) 4% paraformaldehyde in phosphate buffered saline (PBS) solutions are routinely prepared.

Solutions:

1 x PBS / 3 x PBS

130 mM sodium chloride (NaCl) / 390 mM

10 mM sodium phosphate buffer / 30 mM

pH 7.2

4% paraformaldehyde in PBS

- In a fume cupboard, heat 65 mL of ddH_2O to 60 ^oC.
- Add 4 g of paraformaldehyde.
- Add 2 – 3 drops 2 M sodium hydroxide solution and stir rapidly until the solution has clarified (usually takes 1 - 2 min).
- Remove from heat source and add 33 mL of 3 x PBS. Adjust pH to 7.2 with conc. HCl.
- Filter solution through a 0.45 μm membrane filter.
- Quickly cool down to 4^oC and store in a refrigerator or on ice.

Procedure:

In a 15 mL polypropylene centrifuge tube, add three volumes of paraformaldehyde fixative to one volume of sample and hold for 1½ h at 4^{o}C. Pellet fixed cells by centrifugation (5000 x g) for 10 min and decant fixative. Wash fixed cells twice, in 1 x PBS and resuspend to half the original volume of sample. Fill to the original volume with ice-cold, 98 % ethanol and vortex.

Note: Fixed cells may now be stored in the freezer (-20^{o}C) for several months.

2. Cell dispersion using sonication

Introduction:

The activated sludge floc has been found to be highly compact. In order to obtain accurate cell counts, it is often necessary to disperse the cells by sonication using a Virsonic 100 sonicator (Virtis U.S.A.) at low frequency, after paraformaldehyde fixation.

Procedure:

- Fill a 2 mL micro-test tube with 1 mL fixed sample.
- In order to prevent spillage of the sample, cover the opening of the micro-test tube with parafilm.
- Pierce a small hole in the centre of the parafilm covering using the tip of the sonication probe
- Insert the probe so that the tip of the probe is approximately 1 cm above the base of the micro- test tube and sonicate at 5 watts for 5 min for an MLSS = 2500 - 3000 mg/L.

APPENDIX 5

Membrane filtration and staining with DAPI

Sample preparation:

A volume of 5ul sonicated sample, 100 µl of 1% nonidet (Sigma) and 895 µl of 1xPBS was added together to prepare a dilution of 1000 µl, in an eppendorf tube. 1% nonidet was added to disperse the cells after they have been sonicated.

Preparation of 60% Sudan Black:

Weigh 0.3 g of Sudan Black.
Prepare 60% Ethanol = 60 ml of 99.99% ethanol (Saarchem) + 40 ml distilled water.
Add 100 ml of 60% ethanol.

Membrane Filtration:

Nucleopore filters (Millipore), with pore size of 0.22 µm were used. These are pre-treated by staining with 60% sudan black overnight. These stained filters are then washed with distilled water, to wash-off the excess sudan black solution that was not absorbed by the filter. A backing filter (Osmotics Laboratory) with a pore size of 0.45µm was placed on a rubber filter, which was placed at the mouth of a filtering conical flask; this was wet with distilled water. The Nucleopore filter is then placed on top of the backing filter; a 15 ml glass tower was clamped onto the conical flask. The sample, which was diluted to 1000 µl, was filtered through using a vacuum filter. A volume of 1 ml (0.5 µg/ml) DAPI stain (Sigma) was added to the filter (to give a final concentration of 0.25 µg/ml). The tower was covered with foil, to prevent the DAPI from absorbing light and becoming less effective in staining the cells. The DAPI stain was left for, 5 minutes thereafter filtered through with a vacuum. Excess stain that was not absorbed by

the cells, were washed 7 times with distilled water. The 0.22 μm filter was then mounted onto a microscope slide, which contained 1 drop of glycerol/PBS mixture (95:5 v/v) (Sigma). A drop of anti-fading mounting medium, vectashield (Vector laboratories, USA) was added to the surface of the mounted filter paper. A coverslip was placed making sure minimum airspaces were formed. The coverslip edges are then laminated onto the slide using clear nail polish. The slide is then ready to view using the Zeiss Axiolab microscope (50 Watts high pressure mercury bulb and Zeiss filter set 01) fitted for epifluorescence microscopy.

Microscopy and image analysis:

View the mounted filter under an epifluorescence (100 x objective) microscope (Zeiss Axioplan) using an appropriate filter set for DAPI fluorescence (Zeiss filter set 02). Select thirty random fields for cells counts using the image analysis software Macro. Determine the mean total cell count using the following equation:

TCC = MTCC x DF x MF

Where:

TCC	=	Total cell count.
MTCC	=	Mean total cell count.
DF	=	Dilution factor.
MF	=	Total number of microscopic fields on filter (17594 fields under 1000 x magnification).

APPENDIX 6

Pretreatment of microscope slides, immobilization of fixed cells and probe dilutions

1. Pretreatment of microscopic slides

Introduction:

8-Well teflon coated diagnostic microscope slides are routinely used. The teflon coating which is hydrophobic prevents mixing of adjacent wells. Thereby samples can be hybridised simultaneously on the same slide. Poly-L-lysine is used as an adhesive, the polycationic nature of this molecule allows interaction with the anionic sites of cells surfaces, resulting in strong adhesive properties.

Solutions:

(1:10) Poly - L-Lysine (Sigma diagnostics, U.S.A. Procedure no. P8920)
Allow solution to reach room temperature (18 - 26^{o}C) before use.
Dilute 1:10 with dH_2O.

Procedure:

- Clean slide surface by soaking in a warm soap solution for 1 h, rinse thoroughly with dH_2O and air dry.
- Immerse clean slides in diluted (1:10) Poly-L-Lysine solution for 10 min.
- Drain Poly-L-Lysine solution from slides and dry in an oven for one hour at 60^{o}C or at room temperature overnight.
- Store treated slides in a sealed container.

2. Immobilization of fixed microbial cells on treated microscope slides

Procedure:

- Dilute sonicated sample in ddH_2O and add 0.1 volume of 1% Igepal Ca-30.
- Spot 10 μL of sonicated sample onto each well of a pre-treated microscope slide.
- Allow the spots to air dry.
- Dehydrate the spots through successive passages through 50%, 80% and 98% v/v ethanol washes (lasting 3 min each).
- Subsequently slides can be stored dry at room temperature in a desiccator indefinitely.

3. Probe dilutions

Introduction:

Fluorescently labelled oligonucleotide probes are known to be extremely light sensitive and begin to fade and degrade rapidly once exposed to light. In order to prevent this, all centrifuge tubes and eppendorfs used during the hybridisation should be covered with foil and should be stored in the freezer at -4^{o}C. Unnecessary thawing and freezing of probes solutions can also lead to degradation, therefore in order to prevent this, the stock probe solution is sub-divided into 1 μL aliquots and then freezing at -4^{o}C until required for hybridization.

Procedure:

Dilute probe according to manufacturer's instructions with sterile ddH_2O, so that the precise concentration is obtained.

Calculation of stock probe concentration:

E.g. concentration of probe EUB338 = yield (μg)

Dilution volume from data sheet (200 μL)

= 168 μg / 200 μL

= 0.84 μg/μL X 1000 (μg→ μg)

= 840 ng/μL

Calculation of working probe dilution:

Since 50 ng of probe is required per hybridisation and10 μL of hybridisation solution is required per spot, a working concentration of 5 ng/μL is used.

$M_1V_1 = M_2V_2$

(840 ng/μL)(1 μL) = (5ng/μL)(V_2)

V_2 = (840 ng/μL X 1 μL) / 5ng/μL

167 μL hyb.buffer + 1 μL probe

Therefore 16 hybridizations can be performed using 10 μL of probe/hybridization solution (containing 50 ng of probe) per hybridization

APPENDIX 7

Whole cell hybridization (Amann, 1995)

Introduction:

In order to minimize non-specific binding through evaporative concentration, hybridization is carried out in a sealed 50 mL polypropylene screw top centrifuge tube. This serves as a useful and portable hybridization chamber. Thereafter hybridization was carried out according to Amann (1995) as follows:

Materials

50 mL polypropylene screw top centrifuge tube
Whatman 3MM filter paper
Coverslips
Anti-fading mounting medium

Solutions:

Hybridisation buffers

Preparation of EUB hybridization buffer

1. Mass out the following:
   - 0.24 g Tris HCl
   - 0.186 g EDTA
   - 0.01 g sodium dodecyl sulphate
   - 5.26 g NaCl
   - **20 ml formamide**
2. Dissolve in 80 ml distilled water.
3. Adjust to pH 7.2.
4. Make up to 100 ml.

Wash buffers

Preparation of EUB wash buffer

1. Mass out the following:
   - 2.42 g Tris HCl
   - 1.86 g EDTA
   - 0.10 g sodium dodecyl sulphate
   - **11.1 g NaCl**
2. Dissolve in 800 ml distilled water.
3. Adjust to pH 8.0.
4. Make up to 1 L.

Preparation of NSO 1225 hybridization buffer

1. Mass out the following:
   - 0.24 g Tris HCl
   - 0.186 g EDTA
   - 0.01 g sodium dodecyl sulphate
   - 5.26 g NaCl
   - **35 ml formamide**

2. Dissolve in 80 ml distilled water.
3. Adjust to pH 7.2.
4. Make up to 100 ml.

Preparation of NSO 1225 wash buffer

1. Mass out the following:
   - 2.42 g Tris HCl
   - 1.86 g EDTA
   - 0.10 g sodium dodecyl sulphate
   - **4.67 g NaCl**

2. Dissolve in 800 ml distilled water.
3. Adjust to pH 8.0.
4. Make up to 1 L.

Preparation of NSR 116 hybridization buffer

1. Mass out the following:
   - 0.24 g Tris HCl
   - 0.186 g EDTA
   - 0.01 g sodium dodecyl sulphate
   - 5.26 g NaCl
   - **30 ml formamide**

2. Dissolve in 80 ml distilled water.
3. Adjust to pH 7.2.
4. Make up to 100 ml.

Preparation of NSR 116 wash buffer

1. Mass out the following:
   - 2.42 g Tris HCl
   - 1.86 g EDTA
   - 0.10 g sodium dodecyl sulphate
   - **7 g NaCl**

2. Dissolve in 800 ml distilled water.
3. Adjust to pH 8.0.
4. Make up to 1 L.

Preparation of NIT3 hybridization buffer

1. Mass out the following:
   - 0.24 g Tris HCl
   - 0.186 g EDTA
   - 0.01 g sodium dodecyl sulphate
   - 5.26 g NaCl
   - **40 ml formamide**

2. Dissolve in 80 ml distilled water.
3. Adjust to pH 7.2.
4. Make up to 100 ml.

Preparation of NIT 3 wash buffer

1. Mass out the following:
   - 2.42 g Tris HCl
   - 1.86 g EDTA
   - 0.10 g sodium dodecyl sulphate
   - **3.27 g NaCl**

2. Dissolve in 800 ml distilled water.
3. Adjust to pH 8.0.
4. Make up to 1 L.

Preparation of ALF1b hybridization buffer

1. Mass out the following:
   - 0.24 g Tris HCL
   - 0.186 g EDTA
   - 0.01 g sodium dodecyl sulphate
   - 5.26 g NaCl
   - **20 ml formamide**

2. Dissolve in 80 ml distilled water.
3. Adjust to pH 7.2.
4. Make up to 100 ml.

Preparation of ALF1b wash buffer

1. Mass out the following:
   - 2.42 g Tris HCL
   - 1.86 g EDTA
   - 0.10 g sodium dodecyl sulphate
   - **11.1 g NaCl**

2. Dissolve in 800 ml distilled water.
3. Adjust to pH 8.0.
4. Make up to 1 L.

Preparation of BET42a / GAM42a hybridisation buffer

1. Mass out the following:
   - 0.24 g Tris HCL
   - 0.186 g EDTA
   - 0.01 g sodium dodecyl sulphate
   - 5.26 g NaCl
   - **35 ml formamide**

2. Dissolve in 80 ml distilled water.
3. Adjust to pH 7.2.
4. Make up to 100 ml.

Preparation of BET42a / GAM42a wash buffer

1. Mass out the following:
   - 2.42 g Tris HCL
   - 1.86 g EDTA
   - 0.10 g sodium dodecyl sulphate
   - **4.67 g NaCl**

2. Dissolve in 800 ml distilled water.
3. Adjust to pH 8.0.
4. Make up to 1 L.

Preparation of HGC69a hybridization buffer

1. Mass out the following:
   - 0.24 g Tris HCL
   - 0.186 g EDTA
   - 0.01 g sodium dodecyl sulphate
   - 5.26 g NaCl
   - **25 ml formamide**

2. Dissolve in 80 ml distilled water.
3. Adjust to pH 7.2.
4. Make up to 100 ml.

Preparation of HGC69a wash buffer

1. Mass out the following:
   - 2.42 g Tris HCL
   - 1.86 g EDTA
   - 0.10 g sodium dodecyl sulphate
   - **8.77 g NaCl**

2. Dissolve in 800 ml distilled water.
3. Adjust to pH 8.0.
4. Make up to 1 L.

0.25 µg/mL DAPI solution

0.25 µg/mL DAPI in sterile ddH_2O.

Procedure:

- Soak a slip of Whatman 3MM paper in hybridization buffer and place in tube.
- Allow the chamber to equilibrate for 5 min at the hybridization temperature.
- Dilute and mix probe in pre-warmed hybridization buffer to a concentration of 50 ng/µL

  (According to Appendix 6. PROBE DILUTION).
- Spot 10 µL of hybridization buffer/probe mix onto each spot of fixed cells.
- Quickly transfer slide to the pre-warmed moisture chamber and hybridize for 1.5 h at 46 ^{o}C.
- Remove slide from moisture chamber and immediately stop hybridization by rinsing the probe from the slides with wash buffer pre-warmed to 48 ^{o}C.
- Transfer the slide to a 50 mL polypropylene tube filled with pre-warmed wash buffer.
- Incubate for 20 min at 48 ^{o}C.
- Remove wash buffer by rinsing slide in ddH_2O, shake away excess water and air dry.
- Spot 10 uL of 0.25 g/mL DAPI solution onto each spot of fixed cells and stain in the dark for 10 min at room temperature.
- Remove stain by rinsing slide in ddH_2O, shake away excess water and air dry.
- In order to prevent fading of the bound probe, apply 1 drop of anti-fading mounting medium to each spot.
- Cover slide with a coverslip, laminate with clear nail varnish and allow to air dry.

Microscopy and Image analysis:

View slide with an epifluorescence microscope (Zeiss Axioplan) using appropriate filter sets for DAPI (02), rhodamine (15) and fluorescein (09).

Select twenty random fields for enumeration by image analysis.

The cell count for each probe is determined using the following equation:

$$\frac{n(\mathrm{Pr}obe)}{n(DAPI)} * \frac{100}{1}$$

Where:

n(Probe)	=	Average number of cells bearing probe conferred fluorescence.
n(DAPI)	=	Average number of cells bearing DAPI conferred fluorescence.

APPENDIX 8

Comprehensive data for 10 days anoxic/aerobic activated sludge system

TABLE 8.1 Daily analysis for various sewage batches conducted during 2003. Daily analysis includes: TKN (influent, effluent and mixed liquor); Nitrate (influent, effluent and aerobic); nitrogen mass balance. Mean and standard deviation are calculated for each batch

TABLE 8.2 Daily analysis for various sewage batches conducted during 2003. Daily analysis includes: COD (influent, effluent and mixed liquor); OUR; COD mass balance. Mean and standard deviation are calculated for each batch.

TABLE 8.3 Wastewater fractions and mixed liquor parameters for parent system in 2003. Wastewater fractions include: *fs,us* and *fs,up*; mixed liquor parameters include: *Xv, Fcv, Fn* and *Fav*. Mean and standard deviations are calculated for each batch.

TABLE 8.1: Daily experimental data and nitrogen mass balance for parent system in 2003

Nitrogen mass balance **2003**

System condition and parameters

	Rs	V	Q	a	s	Yh		Fcv				Qw		
Unit	day	L	(L/d)	Recycle ratio		mgVss/mgCOD		mgCOD/mgVSS				L		
Value	10.0	15.0	24.0	2.0	1.0	0.5		1.48				1.5		

Batch no	Date	TKN (IN)	TKN (AE)	TKN (FE)	NO3 (AN)	NO3 (AE)	NO3 (FE)	MNd	%	MNte	%	MNne	%	MNw	%	MNti	Nbal (%)
1	5-May	29.9	106.4	3.9	1.2	5.9	6.9	333.6	46.5	88.2	12.3	155.3	21.6	168.5	23.5	718.1	103.8
	6-May	44.8	150.0	8.4	1.5	7.3	10.8	465.6	43.3	189.0	17.6	243.0	22.6	236.0	21.9	1075.2	105.4
	7-May	48.2	220.0	14.0	0.9	5.4	6.9	338.4	29.3	315.0	27.3	155.3	13.4	338.1	29.3	1155.8	99.2
	Mean	41.0	158.8	8.8	1.2	6.2	8.2	379.2	39.7	197.4	19.0	184.5	19.2	247.5	24.9	983.0	102.8
	Std	9.7	57.3	5.1	0.3	1.0	2.3	74.9		113.6		50.7		85.4		233.0	3.2
	8-May	34.0	220.0	4.7	1.4	4.0	8.4	261.1	32.0	106.2	13.0	189.0	23.2	336.1	41.2	816.0	109.4
	9-May	34.7	112.0	5.6	1.3	6.7	7.8	384.0	46.1	126.0	15.1	175.5	21.1	178.1	21.4	833.3	103.6
	10-May	31.4	109.2	3.4	1.2	5.0	6.8	289.9	38.5	75.6	10.0	153.0	20.3	171.4	22.8	752.6	91.7
	11-May	33.0	120.4	6.7	0.6	4.8	6.8	333.6	42.1	151.2	19.1	153.0	19.3	187.8	23.7	792.0	104.2
	12-May	36.0	189.0	5.0	1.2	6.9	8.4	412.3	47.7	113.4	13.1	189.0	21.9	293.8	34.0	864.0	116.7
	13-May	32.5	109.2	3.4	1.4	7.5	8.5	428.9	55.0	75.6	9.7	191.0	24.5	175.0	22.5	779.5	111.7
	14-May	28.0	117.6	4.5	1.6	1.5	7.6	105.6	15.7	100.8	15.0	170.1	25.3	178.7	26.6	672.0	82.6
	15-May	28.0	120.4	5.0	0.7	2.5	8.5	256.3	38.1	113.4	16.9	190.8	28.4	184.4	27.4	672.0	110.8
	16-May	36.0	100.8	2.8	1.2	1.4	14.9	309.1	35.8	63.0	7.3	335.7	38.9	153.3	17.7	864.0	99.7

	17-May	30.2	100.8	3.4	1.4	1.4	15.2	295.9	40.8	75.6	10.4	341.3	47.0	153.3	21.1	725.8	**119.3**
2	**Mean**	32.4	129.9	4.4	1.2	4.2	9.3	307.7	39.2	100.1	13.0	208.8	27.0	201.2	25.8	777.1	105.0
	Std	3.0	40.6	1.2	0.3	2.4	3.1	93.2		27.6		69.9		61.9		71.0	11.3
	19-May	49.8	180.0	4.0	3.4	8.5	14.8	433.7	36.3	90.2	7.5	331.9	27.8	282.7	23.7	1195.2	**95.3**
	20-May	45.4	180.0	3.4	1.2	5.6	13.6	477.1	43.8	75.6	6.9	305.1	28.0	278.3	25.6	1088.6	**104.4**
	21-May	52.9	220.0	2.8	1.2	10.8	12.5	701.0	55.2	63.0	5.0	280.1	22.1	346.2	27.3	1269.4	**109.5**
	22-May	41.3	230.0	5.6	3.2	7.7	10.6	314.6	31.7	126.0	12.7	237.8	24.0	356.5	35.9	992.2	**104.3**
	23-May	42.5	210.0	2.2	0.9	7.9	8.8	505.0	49.5	50.4	4.9	198.0	19.4	326.9	32.0	1020.0	**105.9**
3	**Mean**	46.4	204.0	3.6	2.0	8.1	12.0	486.3	43.3	81.0	7.4	270.6	24.2	318.1	28.9	1113.1	103.9
	Std	4.9	23.0	1.3	1.2	1.9	2.4	140.3		29.2		53.3		36.0		117.3	5.3
Batch no	**Date**	**TKN (IN)**	**TKN (AE)**	**TKN (FE)**	**NO3 (AN)**	**NO3 (AE)**	**NO3 (FE)**	**MNd**		**MNte**		**MNne**		**MNw**		**MNti**	**Nbal (%)**
	28-May	30.8	210.0	5.6	4.4	7.6	10.4	193.0	26.1	126.0	17.1	234.0	31.7	326.4	44.2	738.7	**119.0**
	29-May	28.4	188.0	1.7	1.3	5.7	6.8	310.1	45.4	37.8	5.5	153.0	22.4	290.6	42.6	682.6	**116.0**
	30-May	24.3	126.0	3.4	5.2	6.8	7.3	5.3	0.9	75.6	12.9	164.3	28.1	199.2	34.1	584.2	**76.1**
	3-Jun	35.8	134.4	1.7	1.2	5.4	9.4	369.6	43.0	37.8	4.4	211.5	24.6	209.7	24.4	860.2	**96.3**
	4-Jun	33.6	109.2	1.7	1.3	6.7	9.4	421.0	52.2	37.8	4.7	211.5	26.2	173.8	21.6	806.4	**104.7**
	5-Jun	31.4	109.2	1.7	1.2	5.7	8.8	369.6	49.1	37.8	5.0	198.0	26.3	172.4	22.9	752.6	**103.3**
4	**Mean**	28.7	158.3	3.1	3.0	6.4	8.3	219.5	30.4	69.3	10.1	187.3	27.1	247.1	35.9	689.5	103.6
	Std	3.2	48.3	1.9	2.1	0.9	1.6	160.6		41.8		36.5		73.2		76.5	19.6
Batch no	**Date**	**TKN (IN)**	**TKN (AE)**	**TKN (FE)**	**NO3 (AN)**	**NO3 (AE)**	**NO3 (FE)**	**MNd**		**MNte**		**MNne**		**MNw**		**MNti**	**Nbal (%)**
	9-Jun	33.6	220.0	2.2	0.6	5.4	7.6	383.0	47.5	50.4	6.3	170.1	21.1	338.1	41.9	806.4	**116.8**

	10-Jun	29.1	230.0	1.7	0.7	0.4	6.9	121.1	17.3	37.8	5.4	154.1	22.1	345.6	49.5	698.9	**94.2**
	11-Jun	33.6	255.0	1.1	0.2	0.2	8.5	195.8	24.3	25.2	3.1	191.3	23.7	382.9	47.5	806.4	**98.6**
	12-Jun	30.3	280.0	2.8	0.4	1.5	5.3	158.8	21.8	63.0	8.7	119.3	16.4	422.2	58.1	727.2	**105.0**
	13-Jun	32.0	230.0	3.4	0.5	1.3	10.8	276.6	36.0	75.6	9.8	241.9	31.5	347.0	45.2	768.0	**122.5**
5	**Mean**	31.7	243.0	2.2	1.1	1.8	7.8	227.0	29.4	50.4	6.7	175.3	23.0	367.2	48.4	761.4	107.4
	Std	2.0	24.4	0.9	1.4	2.1	2.0	104.5		19.9		45.6		35.3		47.9	12.0
	17-Jun	33.0	223.0	2.2	0.2	4.6	5.5	330.8	41.8	50.4	6.4	124.2	15.7	341.4	43.1	792.0	**106.9**
	18-Jun	32.0	215.0	2.1	1.3	3.6	5.5	181.9	23.7	47.9	6.2	122.9	16.0	327.8	42.7	768.0	**88.6**
	19-Jun	31.0	205.0	1.1	0.2	3.4	8.6	346.1	46.5	25.2	3.4	192.6	25.9	312.5	42.0	744.0	**117.8**
	20-Jun	30.0	225.0	1.7	0.0	1.3	6.8	222.0	30.8	37.8	5.3	153.0	21.3	339.4	47.1	720.0	**104.5**
	21-Jun	33.0	218.0	2.8	0.3	2.1	5.7	213.4	26.9	63.0	8.0	127.1	16.1	330.2	41.7	792.0	**92.6**
	22-Jun	30.3	185.0	2.8	0.1	3.5	7.5	342.4	47.1	63.0	8.7	168.8	23.2	282.8	38.9	727.2	**117.8**
	23-Jun	32.0	190.0	1.7	0.0	3.7	7.3	349.0	45.4	37.8	4.9	164.3	21.4	290.5	37.8	768.0	**109.6**
	24-Jun	33.0	210.0	1.1	0.1	1.1	9.7	275.3	34.8	25.2	3.2	218.0	27.5	316.7	40.0	792.0	**105.5**
	25-Jun	32.0	178.0	1.1	0.2	1.3	8.7	253.0	32.9	25.2	3.3	194.6	25.3	268.9	35.0	768.0	**96.6**
	26-Jun	33.0	192.0	0.6	0.2	2.6	7.9	297.5	37.6	12.6	1.6	177.8	22.4	291.8	36.8	792.0	**98.4**
6	**Mean**	31.9	204.1	1.7	0.2	2.7	7.3	281.1	36.8	38.8	5.1	164.3	21.5	310.2	40.5	766.3	103.8
	Std	1.1	16.8	0.8	0.4	1.2	1.5	61.5		17.1		32.7		25.3		27.5	9.9
	27-Jun	33.0	210.0	2.7	1.3	5.0	7.0	282.2	35.6	60.8	7.7	158.4	20.0	322.6	40.7	792.0	**104.0**
	28-Jun	34.0	220.0	2.1	0.3	5.7	6.8	408.0	50.0	47.7	5.8	153.0	18.8	338.6	41.5	816.0	**116.1**
	29-Jun	33.0	198.0	3.1	0.2	4.0	7.8	361.9	45.7	70.2	8.9	175.5	22.2	303.1	38.3	792.0	**115.0**
	30-Jun	33.0	167.0	1.1	0.6	5.8	7.8	405.6	51.2	25.2	3.2	175.5	22.2	259.2	32.7	792.0	**109.3**
	1-Jul	35.0	210.0	3.5	1.2	4.9	9.4	340.3	40.5	78.8	9.4	211.5	25.2	322.3	38.4	840.0	**113.4**
	2-Jul	36.0	210.0	3.9	1.4	5.5	7.3	304.3	35.2	87.8	10.2	164.3	19.0	323.2	37.4	864.0	**101.8**
	3-Jul	33.0	211.0	2.8	1.6	1.5	8.6	129.6	16.4	63.0	8.0	192.6	24.3	318.8	40.3	792.0	**88.9**
	4-Jul	34.0	210.0	5.6	0.7	2.5	8.5	256.3	31.4	126.0	15.4	190.8	23.4	318.8	39.1	816.0	**109.3**
	5-Jul	34.0	220.0	5.7	1.2	1.4	8.5	155.0	19.0	127.1	15.6	191.3	23.4	332.1	40.7	816.0	**98.7**
	6-Jul	33.0	198.0	4.2	1.4	1.4	7.6	114.2	14.4	95.2	12.0	171.0	21.6	299.1	37.8	792.0	**85.8**
7	**Mean**	33.8	205.4	3.5	1.0	3.8	7.9	275.8	33.9	78.2	9.6	178.4	22.0	313.8	38.7	811.2	104.2

	Std	1.0	15.4	1.4	0.5	1.9	0.8	110.2		32.3		18.1		22.5		24.8	10.6
	7-Jul	32.0	195.0	3.7	1.4	4.0	8.4	246.7	32.1	83.3	10.8	189.0	24.6	298.6	38.9	768.0	**106.4**
	8-Jul	31.0	184.0	1.1	1.3	4.7	7.8	264.0	35.5	25.2	3.4	175.5	23.6	283.1	38.0	744.0	**100.5**
	9-Jul	31.4	184.0	1.1	1.2	4.0	6.8	265.9	35.3	25.2	3.3	153.0	20.3	282.1	37.4	753.6	**96.4**
	10-Jul	31.3	167.0	1.1	0.6	4.8	7.8	372.0	49.6	25.2	3.4	175.5	23.4	257.7	34.4	750.0	**110.7**
	11-Jul	32.0	210.0	0.6	1.2	4.9	8.4	318.5	41.5	12.6	1.6	189.0	24.6	322.3	42.0	768.0	**109.7**
	12-Jul	33.3	210.0	3.9	1.4	4.5	8.5	358.6	44.9	87.8	11.0	191.0	23.9	321.7	40.3	798.0	**120.2**
	13-Jul	33.0	211.0	2.8	1.6	1.5	11.6	127.7	16.1	63.0	8.0	260.1	32.8	318.8	40.3	792.0	**97.2**
	14-Jul	34.0	210.0	5.6	0.7	2.5	8.5	351.6	43.1	126.0	15.4	190.8	23.4	318.8	39.1	816.0	**121.0**
	15-Jul	32.6	220.0	5.7	1.2	1.4	12.5	204.5	26.2	127.1	16.3	280.1	35.8	332.1	42.5	781.4	**120.8**
	16-Jul	33.2	198.0	4.2	1.4	1.4	10.6	113.3	14.2	95.2	11.9	237.6	29.8	299.1	37.5	797.0	**93.5**
8	**Mean**	32.4	198.9	3.0	1.2	3.4	9.1	262.3	33.8	67.1	8.5	204.2	26.2	303.4	39.0	776.8	107.6
	Std	1.0	16.5	1.9	0.3	1.5	1.8	92.1		43.2		40.9		23.5		23.9	10.6
Batch no	**Date**	**TKN (IN)**	**TKN (AE)**	**TKN (FE)**	**NO3 (AN)**	**NO3 (AE)**	**NO3 (FE)**	**MNd**		**MNte**		**MNne**		**MNw**		**MNti**	**Nbal (%)**
	17-Jul	33.0	205.0	2.7	2.4	5.1	7.6	193.4	24.4	60.8	7.7	170.1	21.5	315.1	39.8	792.0	**93.4**
	18-Jul	35.0	194.0	2.1	0.3	4.1	6.1	312.5	37.2	47.7	5.7	136.8	16.3	297.1	35.4	840.0	**94.5**
	19-Jul	36.0	210.0	3.1	0.2	4.4	5.6	325.9	37.7	70.2	8.1	125.6	14.5	321.6	37.2	864.0	**97.6**
	20-Jul	36.0	197.0	4.1	0.5	4.8	6.7	342.2	39.6	92.7	10.7	150.3	17.4	302.7	35.0	864.0	**102.8**
	21-Jul	35.0	180.0	0.6	0.2	4.5	6.6	351.4	41.8	12.6	1.5	147.6	17.6	276.8	32.9	840.0	**93.8**
	22-Jul	33.0	210.0	4.5	0.5	4.0	7.0	312.3	39.4	101.3	12.8	158.0	19.9	321.0	40.5	792.0	**112.7**
	23-Jul	38.0	220.0	4.6	1.2	6.5	8.6	402.2	44.1	104.0	11.4	192.6	21.1	339.8	37.3	912.0	**113.9**
	24-Jul	33.0	210.0	4.6	1.7	2.5	10.5	208.3	26.3	103.5	13.1	235.8	29.8	318.8	40.2	792.0	**109.4**
	25-Jul	29.0	189.0	3.6	2.2	1.4	9.9	91.7	13.2	80.1	11.5	221.9	31.9	285.6	41.0	696.0	**97.6**
	26-Jul	36.0	230.0	4.5	2.5	5.4	9.2	238.8	27.6	101.3	11.7	207.7	24.0	353.0	40.9	864.0	**104.3**
9	**Mean**	34.4	204.5	3.4	1.2	4.3	7.8	277.9	33.1	77.4	9.4	174.6	21.4	313.1	38.0	825.6	102.0
	Std	2.5	14.9	1.3	0.9	1.4	1.7	93.0		30.1		37.8		23.4		60.1	7.8
	27-Jul	33.1	214.0	1.7	3.5	5.8	10.3	174.0	21.9	37.8	4.8	230.6	29.0	329.7	41.5	794.9	**97.1**
	28-Jul	35.1	220.0	1.9	0.5	4.6	9.7	329.8	39.1	41.8	5.0	217.1	25.8	336.9	40.0	842.9	**109.8**
	29-Jul	33.6	218.0	2.8	0.3	3.2	6.6	366.7	45.5	63.0	7.8	147.6	18.3	331.8	41.1	806.4	**112.7**
	30-Jul	30.3	185.0	2.8	0.1	2.3	9.9	305.2	42.0	63.0	8.7	221.9	30.5	280.9	38.6	727.2	**119.8**
	31-Jul	33.3	210.0	3.9	1.4	7.5	8.5	502.6	63.0	87.8	11.0	191.0	23.9	326.2	40.9	798.0	**138.8**

	1-Aug	33.0	211.0	2.8	1.6	1.5	11.6	201.6	25.5	63.0	8.0	260.1	32.8	318.8	40.3	792.0	**106.5**
	2-Aug	33.0	211.0	2.8	1.6	1.5	11.6	98.2	12.4	63.0	8.0	260.1	32.8	318.8	40.3	792.0	**93.4**
	3-Aug	36.0	215.0	0.6	0.2	5.3	7.3	455.9	52.8	12.6	1.5	163.1	18.9	330.4	38.2	864.0	**111.3**
	4-Aug	34.0	210.0	1.7	1.3	3.6	9.5	304.3	37.3	37.8	4.6	212.6	26.1	320.3	39.3	816.0	**107.2**
	5-Aug	33.2	198.0	4.2	1.4	1.4	10.6	111.8	14.0	95.2	11.9	237.6	29.8	299.1	37.5	797.0	**93.3**
10	**Mean**	33.5	209.2	2.5	1.2	3.7	9.5	285.0	35.3	56.5	7.1	214.2	26.8	319.3	39.8	803.0	109.0
	Std	1.5	10.4	1.1	1.0	2.1	1.7	137.5		24.7		37.5		17.1		35.9	13.6
Batch no	**Date**	**TKN (IN)**	**TKN (AE)**	**TKN (FE)**	**NO3 (AN)**	**NO3 (AE)**	**NO3 (FE)**	**MNd**		**MNte**		**MNne**		**MNw**		**MNti**	**Nbal (%)**
	6-Aug	30.6	220.0	5.5	1.5	2.1	7.5	136.8	18.6	122.6	16.7	168.8	23.0	333.2	45.4	734.4	**103.7**
	7-Aug	35.4	180.0	2.8	0.5	3.6	6.8	284.6	33.5	63.0	7.4	153.0	18.0	275.3	32.4	849.6	**91.3**
	8-Aug	36.7	240.0	4.6	1.2	4.0	7.5	256.9	29.2	102.6	11.6	168.8	19.2	365.9	41.5	880.8	**101.5**
	9-Aug	35.7	180.0	4.5	2.5	3.5	7.5	105.6	12.3	100.8	11.8	168.8	19.7	275.2	32.1	857.8	**75.8**
	13-Aug	31.4	106.0	3.4	7.9	12.2	16.1	212.4	28.2	75.6	10.0	362.2	48.1	177.3	23.6	752.6	**109.9**
	14-Aug	33.6	112.0	5.0	8.0	12.3	16.9	231.6	28.7	113.4	14.1	380.0	47.1	186.5	23.1	806.4	**113.0**
11	**Mean**	33.9	173.0	4.3	3.6	6.3	10.4	204.7	25.1	96.3	11.9	233.6	29.2	268.9	33.0	813.6	99.2
	Std	2.5	54.8	1.0	3.4	4.7	4.7	69.8		22.7		106.9		75.9		59.7	13.7
	16-Aug	32.4	106.0	3.9	0.4	0.8	11.8	283.2	36.4	88.2	11.3	265.5	34.1	160.2	20.6	777.6	**102.5**
	17-Aug	31.4	112.0	2.8	0.5	3.4	9.8	350.4	46.5	63.0	8.4	220.5	29.3	173.1	23.0	753.1	**107.2**
	18-Aug	34.7	117.0	5.0	1.0	3.5	13.5	396.0	47.5	113.4	13.6	302.6	36.3	180.8	21.7	833.3	**119.1**
	19-Aug	33.6	112.0	5.6	0.5	3.6	10.6	379.2	47.0	126.0	15.6	238.5	29.6	173.4	21.5	806.4	**113.7**
	20-Aug	32.1	120.0	4.5	0.4	4.2	8.8	372.6	48.4	101.3	13.1	197.6	25.6	186.3	24.2	770.4	**111.3**
	23-Aug	29.1	100.8	1.1	0.5	0.9	11.8	280.8	40.2	25.2	3.6	265.0	37.9	152.5	21.8	698.9	**103.5**
	25-Aug	32.5	120.0	2.2	3.2	0.4	18.4	151.5	19.4	50.4	6.5	414.6	53.2	180.6	23.2	779.5	**102.3**
12	**Mean**	32.3	112.5	3.6	0.9	2.4	12.1	316.3	40.8	81.1	10.3	272.0	35.2	172.4	22.3	774.2	108.5
	Std	1.8	7.2	1.6	1.0	1.6	3.2	85.8		36.3		71.5		12.1		42.2	6.5

26-Aug	36.8	210.0	3.4	2.7	6.2	7.8	225.6	25.6	75.6	8.6	175.5	19.9	324.3	36.7	882.7	**90.7**
27-Aug	36.6	220.0	2.1	3.5	6.2	8.9	171.6	19.6	47.3	5.4	200.3	22.8	339.3	38.7	877.9	**86.4**
28-Aug	29.1	214.0	1.7	3.5	5.8	7.3	116.4	16.7	37.8	5.4	163.1	23.3	329.7	47.2	698.9	**92.6**
29-Aug	35.1	220.0	1.9	0.5	4.6	8.7	379.9	45.1	41.8	5.0	194.6	23.1	336.9	40.0	842.9	**113.1**
30-Aug	26.9	189.0	1.7	0.2	4.5	6.6	359.1	55.7	37.8	5.9	148.1	22.9	290.3	45.0	645.1	**129.5**
31-Aug	30.2	190.0	1.1	0.0	4.2	7.4	374.7	51.6	25.2	3.5	166.5	22.9	291.3	40.1	725.8	**118.2**
1-Sep	32.5	185.0	1.7	0.1	4.0	8.3	382.7	49.1	37.8	4.8	186.8	24.0	283.5	36.4	779.5	**114.3**
2-Sep	39.0	213.0	4.5	0.1	4.5	7.8	394.4	42.1	101.3	10.8	175.5	18.8	326.3	34.9	936.0	**106.6**
13 **Mean**	33.3	205.1	2.2	1.3	5.0	7.8	300.6	38.2	50.6	6.2	176.3	22.2	315.2	39.9	798.6	106.4
Std	4.3	14.6	1.1	1.6	0.9	0.8	111.4		25.1		17.3		22.9		102.4	15.2
5-Sep	36.0	225.0	2.2	0.1	6.5	8.2	495.6	57.4	50.4	5.8	184.8	21.4	347.3	40.2	864.0	**124.8**
6-Sep	33.2	185.0	1.1	0.2	4.5	6.3	350.4	44.0	25.2	3.2	142.2	17.8	284.3	35.7	796.8	**100.7**
7-Sep	34.1	195.2	2.2	0.6	4.6	7.6	342.4	41.8	50.4	6.2	169.9	20.8	299.7	36.6	818.4	**105.4**
8-Sep	36.0	240.0	1.1	0.7	4.0	8.6	332.5	38.5	25.2	2.9	192.6	22.3	366.0	42.4	864.0	**106.1**
9-Sep	33.0	235.0	2.0	0.2	4.3	5.3	313.0	39.5	45.0	5.7	119.7	15.1	359.0	45.3	792.0	**105.6**
10-Sep	34.0	201.0	0.6	0.2	4.6	5.2	324.9	39.8	12.6	1.5	116.3	14.3	308.4	37.8	816.0	**93.4**
11-Sep	34.0	221.0	3.0	0.8	4.2	7.2	297.6	36.5	67.5	8.3	162.0	19.9	337.8	41.4	816.0	**106.0**
12-Sep	34.0	236.0	3.0	1.2	4.8	7.2	288.0	35.3	67.5	8.3	162.0	19.9	361.2	44.3	816.0	**107.7**
14 **Mean**	**34.3**	**217.3**	**1.9**	**0.5**	**4.7**	**6.9**	**343.0**	**41.6**	**43.0**	**5.2**	**156.2**	**18.9**	**332.9**	**40.5**	**822.9**	**106.2**
Std	**1.1**	**20.9**	**0.9**	**0.4**	**0.8**	**1.2**	**65.2**		**20.3**		**28.1**		**31.3**		**27.2**	**8.8**
15-Sep	35.0	223.0	2.2	0.2	5.3	6.3	379.1	45.1	50.4	6.0	140.6	16.7	342.4	40.8	840.0	**108.6**
16-Sep	31.0	215.0	2.1	1.3	3.6	5.5	183.8	24.7	47.9	6.4	124.7	16.8	327.8	44.1	744.0	**92.0**
17-Sep	33.6	205.0	1.1	0.2	4.5	6.5	353.3	43.8	25.2	3.1	146.3	18.1	314.3	39.0	806.4	**104.0**
18-Sep	29.1	225.0	1.7	0.0	2.5	5.3	247.5	35.4	37.8	5.4	119.7	17.1	341.3	48.8	698.9	**106.8**
19-Sep	33.6	218.0	2.8	0.3	3.2	6.6	287.5	35.7	63.0	7.8	147.6	18.3	331.8	41.1	806.4	**102.9**
20-Sep	35.0	185.0	2.8	0.1	2.3	9.9	338.1	40.3	63.0	7.5	221.9	26.4	280.9	33.4	840.0	**107.6**
21-Sep	32.0	190.0	1.7	0.0	2.6	8.0	314.2	40.9	37.8	4.9	180.7	23.5	288.8	37.6	768.0	**107.0**

	22-Sep	35.0	210.0	1.1	0.1	2.1	10.7	346.3	41.2	25.2	3.0	240.5	28.6	318.2	37.9	840.0	110.7
	23-Sep	31.0	178.0	1.1	0.2	1.5	9.6	287.8	38.7	25.2	3.4	215.1	28.9	269.3	36.2	744.0	107.2
	24-Sep	28.0	192.0	0.6	0.2	3.6	5.6	290.3	43.2	12.6	1.9	126.0	18.8	293.3	43.7	672.0	107.5
15	**Mean**	32.3	204.1	1.7	0.2	3.1	7.4	302.8	38.9	38.8	4.9	166.3	21.3	310.8	40.3	776.0	105.4
	Std	2.5	16.8	0.8	0.4	1.2	2.0	57.2		17.1		44.9		26.1		60.6	5.2
	25-Sep	33.0	215.0	0.6	0.2	5.3	6.3	379.1	47.9	12.6	1.6	140.6	17.8	330.4	41.7	792.0	108.9
	26-Sep	39.0	210.0	1.7	1.3	3.6	9.5	277.7	29.7	37.8	4.0	212.6	22.7	320.3	34.2	936.0	90.6
	27-Sep	39.0	220.0	2.2	0.2	5.4	7.5	415.4	44.4	50.4	5.4	167.6	17.9	338.0	36.1	936.0	103.8
	28-Sep	39.0	215.0	1.7	0.0	6.3	7.1	468.8	50.1	37.8	4.0	159.3	17.0	331.9	35.5	936.0	106.6
	29-Sep	36.0	198.0	1.1	0.3	5.2	7.6	408.5	47.3	25.2	2.9	170.1	19.7	304.8	35.3	864.0	105.2
	30-Sep	38.0	220.0	2.8	0.1	5.5	6.9	423.8	46.5	63.0	6.9	155.0	17.0	338.3	37.1	912.0	107.5
	1-Oct	34.0	220.0	3.4	0.0	4.7	6.5	378.7	46.4	75.6	9.3	147.2	18.0	337.0	41.3	816.0	115.0
	2-Oct	35.0	220.0	2.2	0.1	4.1	6.0	329.8	39.3	50.4	6.0	134.1	16.0	336.2	40.0	840.0	101.2
	3-Oct	33.6	210.0	1.2	0.2	4.5	8.6	407.8	50.6	27.9	3.5	192.6	23.9	321.8	40.0	805.4	118.0
	4-Oct	34.0	89.6	1.7	0.2	3.6	9.0	371.4	45.5	37.8	4.6	202.1	24.8	139.7	17.1	816.0	92.0
16	**Mean**	36.1	201.8	1.9	0.2	4.8	7.5	386.1	44.8	41.9	4.8	168.1	19.5	309.8	35.8	865.3	104.9
	Std	2.5	40.0	0.8	0.4	0.9	1.2	53.1		18.6		26.5		60.7		59.3	8.7

Batch no	Date	TKN (IN)	TKN (AE)	TKN (FE)	NO3 (AN)	NO3 (AE)	NO3 (FE)	MNd		MNte		MNne		MNw		MNti	Nbal (%)
	5-Oct	32.0	195.0	3.7	1.4	4.0	8.4	261.1	34.0	83.3	10.8	189.0	24.6	298.6	38.9	768.0	108.3
	6-Oct	36.0	184.0	1.1	1.3	6.7	7.8	384.0	44.4	25.2	2.9	175.5	20.3	286.1	33.1	864.0	100.8
	7-Oct	31.4	184.0	1.1	1.2	5.0	6.8	289.9	38.5	25.2	3.3	153.0	20.3	283.6	37.6	753.6	99.7
	8-Oct	31.3	167.0	1.1	0.6	5.8	6.2	367.2	49.0	25.2	3.4	139.5	18.6	259.2	34.6	750.0	105.5
	9-Oct	35.0	210.0	0.6	1.2	6.9	7.4	388.3	46.2	12.6	1.5	166.5	19.8	325.3	38.7	840.0	106.3
	10-Oct	38.0	210.0	3.9	1.4	7.5	8.5	428.9	47.0	87.8	9.6	191.0	20.9	326.2	35.8	912.0	113.4
	11-Oct	34.0	211.0	2.8	1.6	1.5	8.3	123.4	15.1	63.0	7.7	186.8	22.9	318.8	39.1	816.0	84.8
	12-Oct	34.0	210.0	5.6	0.7	2.5	8.5	256.3	31.4	126.0	15.4	190.8	23.4	318.8	39.1	816.0	109.3
	13-Oct	34.0	220.0	5.7	1.2	3.4	6.5	202.8	24.9	127.1	15.6	146.9	18.0	335.0	41.1	816.0	99.5
	14-Oct	35.0	198.0	4.2	1.4	4.6	8.3	283.7	33.8	95.2	11.3	186.8	22.2	303.8	36.2	840.0	103.5
17	**Mean**	34.1	198.9	3.0	1.2	4.8	7.7	298.6	36.4	67.1	8.2	172.6	21.1	305.5	37.4	817.6	103.1
	Std	2.1	16.5	1.9	0.3	2.0	0.9	94.5		43.2		19.8		23.8		50.8	7.8
	15-Oct	37.0	219.0	4.6	1.4	4.9	8.6	309.4	34.8	103.5	11.7	193.3	21.8	335.8	37.8	888.0	106.1

	16-Oct	38.0	226.0	5.6	0.3	3.6	9.5	376.8	41.3	126.0	13.8	213.8	23.4	344.4	37.8	912.0	**116.3**
	17-Oct	38.0	210.0	3.7	0.3	2.3	9.4	309.6	33.9	82.1	9.0	211.5	23.2	318.4	34.9	912.0	**101.1**
18	**Mean**	37.7	218.3	4.6	0.6	3.6	9.2	331.9	36.7	103.9	11.5	206.2	22.8	332.9	36.8	904.0	107.8
	Std	0.6	8.0	1.0	0.6	1.3	0.5	38.9		21.9		11.2		13.3		13.9	7.8

TABLE 8.2: Daily experimental data and COD mass balance for parent system in 2003

COD mass balance **2003**

	Rs	V	Q	a	s	Yh		Fcv				Qw		V (Aerobic)
Unit	day	L	(L/d)	Recycle ratio		mgVss/mgCOD		mgCOD/mgVSS				L		
Value	**10**	**15**	**24**	**2**	**1**	**0.45**		**1.48**				**1.5**		**9**

Batch no	Date	COD(IN)	COD (ml)	COD (FE)	OUR	Mste		Msti	MXsvw		Moc		Mod		COD bal (%)
1	5-May	470.0	3077.0	47.0	29.4	1057.5	9.4	11280.0	4615.5	40.9	4286.3	38.0	954.1	8.5	96.7
	6-May	475.0	3500.0	50.0	31.4	1125.0	9.9	11400.0	5250.0	46.1	4227.0	37.1	1331.6	11.7	104.7
	7-May	500.0	3704.0	47.0	30.1	1057.5	8.8	12000.0	5556.0	46.3	4523.0	37.7	967.8	8.1	100.9
	Mean	479.8	3656.3	47.8	31.8	1092.0	9.4	11514.0	5466.8	44.4	5215.0	37.6	813.4	9.4	109.4
	Stdev	13.7	527.6	1.5	3.1	39.9		328.1	761.0		1743.7		569.7		17.6
	8-May	486.0	3537.0	54.0	29.8	1215.0	10.4	11664.0	5305.5	45.5	5267.8	45.2	746.8	6.4	107.5
	9-May	438.0	2904.0	37.0	30.3	832.5	7.9	10512.0	4356.0	41.4	4167.1	39.6	1098.2	10.4	99.4
	10-May	390.0	1927.0	24.6	30.6	554.4	5.9	9360.0	2890.5	30.9	4929.2	52.7	829.2	8.9	98.3
	13-May	390.0	1927.0	24.6	30.7	554.4	5.9	9360.0	2890.5	30.9	3965.9	42.4	1226.6	13.	92.3

													11	
	14-May	489.0	3358.0	35.2	30.7	792.0	6.7	11736.0	5037.0	42.9	6633.5	56.5	302.0	2.6	108.8
	15-May	510.0	3183.0	42.2	30.7	950.4	7.8	12240.0	4774.5	39.0	5841.5	47.7	733.1	6.0	100.5
	16-May	500.0	3467.0	45.0	30.8	1012.5	8.4	12000.0	5200.5	43.3	6573.8	54.8	884.1	7.4	113.9
	17-May	498.0	2200.0	44.0	30.9	990.0	8.3	11952.0	3300.0	27.6	6681.0	55.9	846.3	7.1	98.9
2	**Mean**	462.6	2812.9	38.3	30.6	862.7	7.7	11103.0	4219.3	37.7	5507.5	49.3	833.3	7.7	102.4
	Std	49.7	690.7	10.2	0.4	228.8		1192.8	1036.1		1099.3		274.5		7.0
	19-May	478.0	3508.0	37.0	31.9	832.5	7.3	11472.0	5262.0	45.9	4666.2	40.7	1240.3	10.8	104.6
	20-May	513.0	3398.0	33.4	30.9	752.4	6.1	12312.0	5097.0	41.4	4763.7	38.7	1364.6	11.1	97.3
	21-May	485.0	3704.0	44.0	30.9	990.0	8.5	11640.0	5556.0	47.7	2465.0	21.2	2005.0	17.2	94.6
	22-May	513.0	3367.0	29.9	30.7	673.2	5.5	12312.0	5050.5	41.0	4672.3	37.9	899.9	7.3	91.7
	23-May	455.0	3256.0	24.6	30.9	554.4	5.1	10920.0	4884.0	44.7	3596.8	32.9	1444.2	13.2	96.0
3	**Mean**	488.8	3446.6	33.8	31.1	760.5	6.5	11731.2	5169.9	44.1	4032.8	34.3	1390.8	11.9	96.8
	Std	24.7	169.6	7.3	0.5	164.3		593.3	254.4		999.1		401.4		4.8
Batch no	**Date**	**COD(IN)**	**COD (ml)**	**COD (FE)**	**OUR**	**Mste**		**Msti**	**MXsvw**		**Moc**		**Mod**		**COD bal (%)**
	28-May	528.0	3071.0	24.5	30.9	551.3	4.4	12672.0	4606.5	36.4	5263.9	41.5	551.9	4.4	86.6
	29-May	462.0	2534.0	58.1	30.9	1306.8	11.8	11088.0	3801.0	34.3	4742.0	42.8	886.8	8.0	96.8
	30-May	462.0	2314.0	51.0	31.0	1148.4	10.4	11088.0	3471.0	31.3	5991.8	54.0	15.1	0.1	95.8
	3-Jun	489.0	2828.0	26.4	30.8	594.0	5.1	11736.0	4242.0	36.1	4810.2	41.0	1057.1	9.0	91.2
	4-Jun	503.0	3076.0	19.4	30.6	435.6	3.6	12072.0	4614.0	38.2	4258.0	35.3	1203.9	10.0	87.1
	5-Jun	495.0	3059.0	52.0	30.7	1170.0	9.8	11880.0	4588.5	38.6	4663.4	39.3	1057.1	8.9	96.6
4	**Mean**	489.8	2813.7	38.6	30.8	867.7	7.5	11756.0	4220.5	35.8	4954.9	42.3	795.3	6.7	92.4
	Std	25.3	323.5	16.9	0.1	380.7		607.8	485.3		601.2		442.8		4.7
Batch no	**Date**	**COD(IN)**	**COD (ml)**	**COD (FE)**	**OUR**	**Mste**		**Msti**	**MXsvw**		**Moc**		**Mod**		**COD bal (%)**

	9-Jun	529.0	3472.0	35.2	30.6	792.0	6.2	12696.0	5208.0	41.0	4492.9	35.4	1095.5	8.6	91.3
	10-Jun	499.8	3335.0	24.6	30.5	554.4	4.6	11995.2	5002.5	41.7	6704.6	55.9	346.2	2.9	105.1
	11-Jun	515.0	3261.0	29.9	30.7	673.2	5.4	12360.0	4891.5	39.6	6620.2	53.6	560.0	4.5	103.1
	12-Jun	554.0	3640.0	26.4	30.4	594.0	4.5	13296.0	5460.0	41.1	6102.6	45.9	454.1	3.4	94.8
	13-Jun	496.0	2895.0	31.6	30.3	711.0	6.0	11904.0	4342.5	36.5	6160.5	51.8	791.0	6.6	100.8
5	**Mean**	518.8	3320.6	29.6	30.5	664.9	5.3	12450.2	4980.9	40.0	6016.2	48.5	649.4	5.2	99.0
	Std	23.7	278.3	4.2	0.2	94.3		567.7	417.5		892.6		298.8		5.8
Batch no	**Date**	**COD(IN)**	**COD (ml)**	**COD (FE)**	**OUR**	**Mste**		**Msti**	**MXsvw**		**Moc**		**Mod**		**COD bal (%)**
	17-Jun	544.0	2600.0	56.0	32.5	1260.0	9.7	13056.0	3900.0	29.9	5095.8	39.0	946.1	7.2	85.8
	18-Jun	508.0	2780.0	44.0	32.7	990.0	8.1	12192.0	4170.0	34.2	6043.3	49.6	520.3	4.3	96.2
	19-Jun	492.0	2900.0	48.0	32.5	1080.0	9.1	11808.0	4350.0	36.8	5638.1	47.7	989.8	8.4	102.1
	20-Jun	516.0	2740.0	50.0	32.2	1125.0	9.1	12384.0	4110.0	33.2	6416.4	51.8	635.1	5.1	99.2
	21-Jun	524.0	2240.0	52.0	32.3	1170.0	9.3	12576.0	3360.0	26.7	6147.8	48.9	610.2	4.9	89.8
	22-Jun	520.0	2020.0	40.0	32.1	900.0	7.2	12480.0	3030.0	24.3	5425.6	43.5	979.4	7.8	82.8
	23-Jun	516.0	3760.0	44.0	32.0	990.0	8.0	12384.0	5640.0	45.5	5321.6	43.0	998.0	8.1	104.6
	24-Jun	580.0	3760.0	32.0	32.0	720.0	5.2	13920.0	5640.0	40.5	6471.1	46.5	787.3	5.7	97.8
	25-Jun	506.0	2870.0	60.0	31.8	1350.0	11.1	12144.0	4305.0	35.4	6393.6	52.6	723.6	6.0	105.2
	26-Jun	512.0	3040.0	52.0	31.9	1170.0	9.5	12288.0	4560.0	37.1	5835.7	47.5	850.9	6.9	101.0
6	**Mean**	521.8	2871.0	47.8	32.2	1075.5	8.6	12523.2	4306.5	34.4	5878.9	47.0	804.1	6.4	96.4
	Std	24.4	560.9	8.1	0.3	183.0		586.8	841.3		493.6		176.0		7.8
	27-Jun	450.0	3060.0	40.0	31.7	900.0	8.3	10800.0	4590.0	42.5	5215.3	48.3	807.2	7.5	106.6
	28-Jun	510.0	3230.0	14.0	31.8	315.0	2.6	12240.0	4845.0	39.6	4493.2	36.7	1166.9	9.5	88.4
	29-Jun	498.0	3010.0	26.0	31.6	585.0	4.9	11952.0	4515.0	37.8	5149.6	43.1	1035.1	8.7	94.4
	30-Jun	560.0	3640.0	16.0	31.5	360.0	2.7	13440.0	5460.0	40.6	4531.5	33.7	1160.0	8.6	85.7
	1-Jul	552.0	3000.0	40.0	31.3	900.0	6.8	13248.0	4500.0	34.0	5179.1	39.1	973.3	7.3	87.2
	2-Jul	518.0	3670.0	42.0	31.5	945.0	7.6	12432.0	5505.0	44.3	5016.1	40.3	870.4	7.0	99.2
	3-Jul	524.0	3070.0	14.0	31.3	315.0	2.5	12576.0	4605.0	36.6	6778.2	53.9	370.7	2.9	96.0
	4-Jul	518.0	2990.0	18.0	31.2	405.0	3.3	12432.0	4485.0	36.1	5947.3	47.8	733.1	5.9	93.1
	5-Jul	516.0	3360.0	44.0	31.2	990.0	8.0	12384.0	5040.0	40.7	6653.8	53.7	443.4	3.6	106.0

	6-Jul	528.0	3000.0	36.0	31.2	810.0	6.4	12672.0	4500.0	35.5	6743.7	53.2	326.7	2.6	97.7
7	**Mean**	517.4	3203.0	29.0	31.4	652.5	5.3	12417.6	4804.5	38.8	5570.8	45.0	788.7	6.4	95.4
	Std	30.1	266.2	12.6	0.2	284.0		722.0	399.3		891.6		315.0		7.3
Batch no	**Date**	**COD(IN)**	**COD (ml)**	**COD (FE)**	**OUR**	**Mste**		**Msti**	**MXsvw**		**Moc**		**Mod**		**COD bal (%)**
	7-Jul	526.0	3720.0	36.0	31.2	810.0	6.4	12624.0	5580.0	44.2	5572.3	44.1	705.6	5.6	100.3
	8-Jul	520.0	2960.0	50.0	31.1	1125.0	9.0	12480.0	4440.0	35.6	5234.6	41.9	755.0	6.1	92.6
	9-Jul	544.0	3440.0	48.0	31.0	1080.0	8.3	13056.0	5160.0	39.5	5458.7	41.8	760.5	5.8	95.4
	10-Jul	496.0	2700.0	68.0	31.2	1530.0	12.9	11904.0	4050.0	34.0	4901.1	41.2	1063.9	8.9	97.0
	11-Jul	480.0	3240.0	52.0	30.9	1170.0	10.2	11520.0	4860.0	42.2	5094.9	44.2	910.9	7.9	104.5
	12-Jul	489.0	3500.0	40.0	31.0	900.0	7.7	11736.0	5250.0	44.7	5344.7	45.5	1025.5	8.7	106.7
	13-Jul	528.0	3400.0	52.0	30.7	1170.0	9.2	12672.0	5100.0	40.2	6644.3	52.4	365.2	2.9	104.8
	14-Jul	503.0	3276.0	19.4	30.9	435.6	3.6	12072.0	4914.0	40.7	5882.5	48.7	1005.6	8.3	101.4
	15-Jul	495.0	3059.0	52.0	30.7	1170.0	9.8	11880.0	4588.5	38.6	6558.7	55.2	584.8	4.9	108.6
	16-Jul	500.0	2280.0	42.0	30.8	945.0	7.9	12000.0	3420.0	28.5	6659.4	55.5	324.0	2.7	94.6
8	**Mean**	508.1	3157.5	45.9	31.0	1033.6	8.5	12194.4	4736.3	38.8	5735.1	47.1	750.1	6.2	100.6
	Std	20.3	424.4	12.8	0.2	287.9		487.3	636.6		666.0		263.4		5.5
	17-Jul	500.0	2220.0	56.0	30.8	1260.0	10.5	12000.0	3330.0	27.8	5481.6	45.7	553.2	4.6	88.5
	18-Jul	508.0	2360.0	60.0	30.6	1350.0	11.1	12192.0	3540.0	29.0	4951.3	40.6	893.7	7.3	88.0
	19-Jul	489.0	3500.0	40.0	30.6	900.0	7.7	11736.0	5250.0	44.7	4758.3	40.5	932.1	7.9	100.9
	20-Jul	495.0	3059.0	52.0	30.7	1170.0	9.8	11880.0	4588.5	38.6	4753.4	40.0	978.8	8.2	96.7
	21-Jul	498.0	2730.0	60.0	30.6	1350.0	11.3	11952.0	4095.0	34.3	4742.7	39.7	1004.9	8.4	93.6
	22-Jul	490.0	2730.0	48.0	30.5	1080.0	9.2	11760.0	4095.0	34.8	5051.1	43.0	893.1	7.6	94.6
	23-Jul	508.0	2740.0	52.0	30.5	1170.0	9.6	12192.0	4110.0	33.7	4252.0	34.9	1150.4	9.4	87.6
	24-Jul	520.0	2660.0	50.0	30.4	1125.0	9.0	12480.0	3990.0	32.0	6219.7	49.8	595.8	4.8	95.6
	25-Jul	502.0	3689.0	34.0	30.5	765.2	6.4	12048.0	5533.5	45.9	6956.4	57.7	262.2	2.2	112.2
	26-Jul	490.0	2610.0	70.0	30.4	1575.0	13.4	11760.0	3915.0	33.3	5320.3	45.2	683.0	5.8	97.7
9	**Mean**	500.0	2829.8	52.2	30.6	1174.5	9.8	12000.0	4244.7	35.4	5248.7	43.7	794.7	6.6	95.6
	Std	9.9	464.0	10.3	0.1	231.8		237.6	696.0		801.5		266.0		7.3
	27-Jul	504.0	2642.0	27.0	30.5	607.5	5.0	12096.0	3963.0	32.8	5583.3	46.2	497.6	4.1	88.1
	28-Jul	504.0	2839.0	39.0	30.3	877.5	7.3	12096.0	4258.5	35.2	4756.9	39.3	943.1	7.8	89.6
	29-Jul	474.0	3120.0	45.0	30.3	1012.5	8.9	11376.0	4680.0	41.1	5250.5	46.2	1048.8	9.2	105.4

	30-Jul	490.0	2720.0	30.0	30.4	675.0	5.7	11760.0	4080.0	34.7	5607.0	47.7	873.0	7.4	95.5
	31-Jul	485.0	3558.0	30.0	30.4	675.0	5.8	11640.0	5337.0	45.9	3886.0	33.4	1437.3	12.3	97.4
	1-Aug	484.0	3307.0	20.8	30.4	468.0	4.0	11616.0	4960.5	42.7	6579.5	56.6	576.6	5.0	108.3
	2-Aug	508.0	2770.0	37.4	30.5	842.4	6.9	12192.0	4155.0	34.1	6592.5	54.1	280.7	2.3	97.4
	3-Aug	520.0	3704.0	20.8	30.5	468.0	3.8	12480.0	5556.0	44.5	4391.7	35.2	1303.7	10.4	93.9
	4-Aug	511.0	3828.0	27.0	30.3	607.5	5.0	12264.0	5742.0	46.8	5531.4	45.1	870.4	7.1	104.0
	5-Aug	500.0	3421.0	47.0	30.4	1057.5	8.8	12000.0	5131.5	42.8	6566.5	54.7	319.9	2.7	109.0
10	**Mean**	498.0	3190.9	32.4	30.4	729.1	6.1	11952.0	4786.4	40.1	5474.5	45.8	815.1	6.8	98.9
	Std	14.3	434.5	9.3	0.1	209.4		342.6	651.8		940.3		393.3		7.5
Batch no	**Date**	**COD(IN)**	**COD (ml)**	**COD (FE)**	**OUR**	**Mste**		**Msti**	**MXsvw**		**Moc**		**Mod**		**COD bal (%)**
	6-Aug	520.0	3702.0	37.0	30.3	833.4	6.7	12480.0	5553.0	44.5	6270.8	50.2	391.2	3.1	104.6
	7-Aug	480.0	3504.0	36.1	30.3	812.0	7.0	11520.0	5256.0	45.6	5208.9	45.2	814.1	7.1	105.0
	8-Aug	495.0	3657.0	35.7	30.3	802.6	6.8	11880.0	5485.5	46.2	5323.0	44.8	734.9	6.2	103.9
	9-Aug	502.0	3689.0	34.0	30.1	765.2	6.4	12048.0	5533.5	45.9	6093.5	50.6	302.0	2.5	105.4
	13-Aug	522.0	3752.0	33.3	30.1	748.8	6.0	12528.0	5628.0	44.9	4632.6	37.0	607.3	4.8	92.7
	14-Aug	503.0	3348.0	31.2	30.2	702.0	5.8	12072.0	5022.0	41.6	4614.7	38.2	662.4	5.5	91.1
11	**Mean**	503.7	3608.7	34.5	30.2	777.3	6.4	12088.0	5413.0	44.8	5357.2	44.3	585.3	4.9	100.4
	Std	15.8	152.9	2.1	0.1	48.2		378.2	229.4		703.7		199.5		6.6
Batch no	**Date**	**COD(IN)**	**COD (ml)**	**COD (FE)**	**OUR**	**Mste**		**Msti**	**MXsvw**		**Moc**		**Mod**		**COD bal (%)**
	16-Aug	507.0	3224.0	29.0	30.5	652.5	5.4	12168.0	4836.0	39.7	6410.4	52.7	810.0	6.7	104.4
	17-Aug	517.0	3216.0	31.2	30.5	702.0	5.7	12408.0	4824.0	38.9	5317.9	42.9	1002.1	8.1	95.5
	18-Aug	512.0	3255.0	27.0	30.8	608.4	5.0	12288.0	4882.5	39.7	5543.8	45.1	1132.7	9.2	99.0
	19-Aug	480.0	3589.0	34.5	30.7	776.3	6.7	11520.0	5383.5	46.7	5260.4	45.7	1084.5	9.4	108.5
	20-Aug	490.0	3569.0	33.3	30.5	748.1	6.4	11760.0	5353.5	45.5	4936.6	42.0	1065.7	9.1	102.9
	23-Aug	490.0	3432.0	49.0	30.8	1102.5	9.4	11760.0	5148.0	43.8	6472.8	55.0	803.1	6.8	115.0

	25-Aug	520.0	2849.0	31.2	30.8	702.0	5.6	12480.0	4273.5	34.2	7898.7	63.3	433.3	3.5	106.6
12	**Mean**	502.3	3304.9	33.6	30.7	756.0	6.3	12054.9	4957.3	41.2	5977.2	49.5	904.5	7.5	104.6
	std	15.5	255.4	7.2	0.2	162.7		372.5	383.1		1028.3		245.4		6.4
	26-Aug	500.0	3466.0	35.4	30.6	795.6	6.6	12000.0	5199.0	43.3	5076.2	42.3	645.2	5.4	97.6
	27-Aug	490.0	3562.0	37.4	30.6	842.4	7.2	11760.0	5343.0	45.4	5444.7	46.3	490.9	4.2	103.1
	28-Aug	512.0	3487.0	58.0	30.7	1305.0	10.6	12288.0	5230.5	42.6	5615.7	45.7	332.9	2.7	101.6
	29-Aug	478.0	3274.0	31.2	30.7	702.0	6.1	11472.0	4911.0	42.8	4826.0	42.1	1086.6	9.5	100.5
	30-Aug	470.0	3078.0	54.0	30.6	1215.0	10.8	11280.0	4617.0	40.9	4702.9	41.7	1027.1	9.1	102.5
	31-Aug	505.0	3290.0	39.5	30.5	889.2	7.3	12120.0	4935.0	40.7	4766.0	39.3	1071.6	8.8	96.2
	1-Sep	485.0	3181.0	27.0	30.5	608.4	5.2	11640.0	4771.5	41.0	4861.4	41.8	1094.4	9.4	97.4
	2-Sep	512.0	3265.0	29.0	30.6	652.5	5.3	12288.0	4897.5	39.9	4680.0	38.1	1127.9	9.2	92.4
13	**Mean**	494.0	3325.4	38.9	30.6	876.3	7.4	11856.0	4988.1	42.1	4996.6	42.2	859.6	7.3	98.9
	Std	15.7	165.4	11.4	0.1	255.9		377.7	248.1		354.0		318.7		3.6
	5-Sep	474.0	2953.0	20.8	30.5	468.0	4.1	11376.0	4429.5	38.9	3806.8	33.5	1417.3	12.5	89.0
	6-Sep	513.0	2953.0	37.4	30.5	842.4	6.8	12312.0	4429.5	36.0	4697.0	38.2	1002.1	8.1	89.1
	7-Sep	478.0	2979.0	20.8	30.5	468.0	4.1	11472.0	4468.5	39.0	4844.5	42.2	979.2	8.5	93.8
	8-Sep	482.0	2941.0	16.6	30.4	374.4	3.2	11568.0	4411.5	38.1	5110.3	44.2	951.1	8.2	93.8
	9-Sep	486.0	3256.0	37.3	30.4	838.8	7.2	11664.0	4884.0	41.9	4772.1	40.9	895.1	7.7	97.7
	10-Sep	480.0	2704.0	27.0	30.5	607.5	5.3	11520.0	4056.0	35.2	4650.3	40.4	929.2	8.1	88.9
	11-Sep	513.0	3024.0	33.3	30.4	748.8	6.1	12312.0	4536.0	36.8	5068.3	41.2	851.1	6.9	91.0
	12-Sep	499.0	3100.0	41.6	30.3	936.0	7.8	11976.0	4650.0	38.8	4965.4	41.5	823.7	6.9	95.0
14	**Mean**	490.6	2988.8	29.4	30.4	660.5	5.6	11775.0	4483.1	38.1	4739.3	40.2	981.1	8.4	92.3
	Std	15.7	156.3	9.3	0.1	209.5		375.8	234.5		412.0		186.5		3.3

Batch no	**Date**	**COD(IN)**	**COD (ml)**	**COD (FE)**	**OUR**	**Mste**		**Msti**	**MXsvw**		**Moc**		**Mod**		**COD bal (%)**
	15-Sep	502.0	3397.0	23.0	30.3	517.5	4.3	12048.0	5095.5	42.3	4337.7	36.0	1084.1	9.0	91.6
	16-Sep	490.0	3256.0	22.0	33.3	495.0	4.2	11760.0	4884.0	41.5	6179.4	52.5	525.8	4.5	102.8

	17-Sep	504.0	3350.0	27.0	30.1	607.5	5.0	12096.0	5025.0	41.5	4610.6	38.1	1010.4	8.4	93.0
	18-Sep	513.0	3039.0	39.0	30.3	877.5	7.1	12312.0	4558.5	37.0	5433.7	44.1	707.8	5.7	94.0
	19-Sep	474.0	3120.0	45.0	32.5	1012.5	8.9	11376.0	4680.0	41.1	5721.4	50.3	822.3	7.2	107.6
	20-Sep	486.0	3256.0	37.3	32.0	838.8	7.2	11664.0	4884.0	41.9	5943.9	51.0	967.0	8.3	108.3
	21-Sep	495.0	3125.0	24.0	31.0	540.0	4.5	11880.0	4687.5	39.5	5575.1	46.9	898.5	7.6	98.5
	22-Sep	506.0	3245.0	21.0	30.0	472.5	3.9	12144.0	4867.5	40.1	5600.5	46.1	990.5	8.2	98.2
	23-Sep	485.0	3153.0	27.0	30.0	607.5	5.2	11640.0	4729.5	40.6	5884.2	50.6	823.1	7.1	103.5
	24-Sep	512.0	3187.0	58.0	30.0	1305.0	10.6	12288.0	4780.5	38.9	4980.1	40.5	830.3	6.8	96.8
15	**Mean**	496.7	3212.8	32.3	30.9	727.4	6.1	11920.8	4819.2	40.4	5426.7	45.6	866.0	7.3	99.4
	Std	12.8	109.7	12.2	1.2	274.2		308.0	164.5		599.4		163.6		5.9
	25-Sep	486.0	3537.0	54.0	29.9	1215.0	10.4	11664.0	5305.5	45.5	4253.5	36.5	1084.1	9.3	101.7
	26-Sep	438.0	2904.0	37.0	30.0	832.5	7.9	10512.0	4356.0	41.4	5475.2	52.1	794.2	7.6	109.0
	27-Sep	390.0	1927.0	24.6	29.9	554.4	5.9	9360.0	2890.5	30.9	4194.7	44.8	1188.2	12.7	94.3
	28-Sep	520.0	2787.2	22.9	30.1	514.8	4.1	12480.0	4180.8	33.5	3760.5	30.1	1340.7	10.7	78.5
	29-Sep	503.0	3016.0	45.0	29.8	1012.5	8.4	12072.0	4524.0	37.5	4258.5	35.3	1168.3	9.7	90.8
	30-Sep	465.0	3536.0	20.6	30.0	463.5	4.2	11160.0	5304.0	47.5	4083.8	36.6	1212.0	10.9	99.1
	1-Oct	498.0	3360.0	38.0	30.0	855.0	7.2	11952.0	5040.0	42.2	4450.9	37.2	1083.1	9.1	95.6
	2-Oct	474.0	3120.0	45.0	30.0	1012.5	8.9	11376.0	4680.0	41.1	4716.4	41.5	943.1	8.3	99.8
	3-Oct	503.0	3276.0	19.4	29.9	435.6	3.6	12072.0	4914.0	40.7	4548.6	37.7	1166.3	9.7	91.7
	4-Oct	495.0	3059.0	52.0	29.8	1170.0	9.8	11880.0	4588.5	38.6	4934.8	41.5	1062.3	8.9	99.0
16	**Mean**	477.2	3052.2	35.8	29.9	806.6	7.0	11452.8	4578.3	39.9	4467.7	39.3	1104.2	9.7	95.9
	Std	38.4	468.8	13.2	0.1	296.4		922.2	703.2		484.6		151.7		8.1

Batch no	Date	COD(IN)	COD (ml)	COD (FE)	OUR	Mste		Msti	MXsvw		Moc		Mod		COD bal (%)
	5-Oct	486.0	3537.0	54.0	29.8	1215.0	10.4	11664.0	5305.5	45.5	5278.6	45.3	746.8	6.4	107.6
	6-Oct	498.0	3100.0	20.0	29.6	450.0	3.8	11952.0	4650.0	38.9	4031.0	33.7	1098.2	9.2	85.6
	7-Oct	400.0	3590.0	28.0	30.8	630.0	6.6	9600.0	5385.0	56.1	4959.5	51.7	829.2	8.6	123.0
	8-Oct	472.0	2870.0	36.0	29.5	810.0	7.2	11328.0	4305.0	38.0	4110.3	36.3	1050.2	9.3	90.7
	9-Oct	496.0	3160.0	16.0	29.7	360.0	3.0	11904.0	4740.0	39.8	3945.3	33.1	1110.6	9.3	85.3
	10-Oct	492.0	3016.0	36.0	32.6	810.0	6.9	11808.0	4524.0	38.3	4361.2	36.9	1226.6	10.4	92.5
	11-Oct	502.0	2710.0	28.0	29.6	630.0	5.2	12048.0	4065.0	33.7	6408.9	53.2	352.8	2.9	95.1

	12-Oct	517.0	3300.0	30.0	30.7	675.0	5.4	12408.0	4950.0	39.9	5832.9	47.0	733.1	5.9	98.3
	13-Oct	480.0	2970.0	32.0	29.9	720.0	6.3	11520.0	4455.0	38.7	5512.9	47.9	580.0	5.0	97.8
	14-Oct	510.0	3200.0	28.0	29.9	630.0	5.1	12240.0	4800.0	39.2	5069.9	41.4	811.3	6.6	92.4
17	**Mean**	485.3	3145.3	30.8	30.2	693.0	6.0	11647.2	4718.0	40.8	4951.0	42.6	853.9	7.4	96.8
	Std	32.8	277.5	10.3	0.9	231.6		787.8	416.3		833.5		270.3		11.2
	15-Oct	510.0	3210.0	30.0	29.8	675.0	5.5	12240.0	4815.0	39.3	4901.3	40.0	884.8	7.2	92.1
	16-Oct	468.0	3310.0	28.0	30.9	630.0	5.6	11232.0	4965.0	44.2	5196.0	46.3	1077.6	9.6	105.7
	17-Oct	500.0	3456.0	32.0	30.7	720.0	6.0	12000.0	5184.0	43.2	5753.8	47.9	885.5	7.4	104.5
	18-Oct														
18	**Mean**	492.7	3325.3	30.0	30.5	675.0	5.7	11824.0	4988.0	42.2	5283.7	44.8	949.3	8.1	100.8
	Std	21.9	123.7	2.0	0.6	45.0		526.5	185.6		432.9		111.2		7.5

TABLE 8.3: Wastewater fractions and mixed liquor parameters for parent system in 2003.

2003

	Rs	Vp	Qi	bH	f	Yh		Qw
Unit	day	L	(L/d)	d		mgVss/mgCOD		L
Value	**10.0**	**15.0**	**24.0**	**0.24**	**0.2**	**0.45**		**1.5**

	date	Xv	Sti	Ste	Fcv	Msti	Mxv	Fs,us	Fs,up	Fav	Fn
	28/4/03	2500.0	498.2	37.9	1.74	11956.8	37500	0.0761	0.3494	0.2424	0.0000
	5-May	2200.0	470.0	47.0	1.40	11280	33000	0.1000	0.2240	0.3058	0.0484
	6-May	2400.0	475.0	50.0	1.46	11400	36000	0.1053	0.2869	0.2548	0.0625
	7-May	2435.0	500.0	47.0	1.52	12000	36525	0.0940	0.2750	0.2744	0.0903
1	**Mean**	2383.8	485.8	45.5	1.53	11659.2	35756.25	0.0938	0.2838	0.2694	0.0671
	Std	129.3	15.5	5.2	0.15	372.2399	1939.757	0.0127	0.0516	0.0277	0.0214
	date	**Xv**	**Sti**	**Ste**	**Fcv**	**Msti**	**Mxv**	**Fs,us**	**Fs,up**	**Fav**	**Fn**
	8-May	2100.0	486.0	54.0	1.68	11664	31500	0.1111	0.2412	0.3174	0.1048
	9-May	1956.0	438.0	37.0	1.48	10512	29340	0.0845	0.2089	0.3351	0.0573
	10-May	1345.0	390.0	24.6	1.43	9360	20175	0.0632	0.0638	0.5361	0.0812
	13-May	1320.0	390.0	24.6	1.46	9360	19800	0.0632	0.0573	0.5503	0.0827
	14-May	2168.0	489.0	35.2	1.55	11736	32520	0.0720	0.2119	0.3420	0.0542
	15-May	2134.0	510.0	42.2	1.49	12240	32010	0.0828	0.1725	0.3769	0.0564
	16-May	2200.0	500.0	45.0	1.58	12000	33000	0.0900	0.2205	0.3318	0.0458
	17-May	2146.0	498.0	44.0	1.03	11952	32190	0.0884	0.1164	0.3908	0.0470
2	**Mean**	1921.1	462.6	38.3	1.46	11103	28816.88	0.0819	0.1616	0.3976	0.0662
	Std	370.5									
	19-May	2400.0	478.0	37.0	1.46	11472	36000	0.0774	0.2726	0.2742	0.0750
	20-May	2200.0	513.0	33.4	1.54	12312	33000	0.0652	0.1881	0.3687	0.0818
	21-May	2400.0	485.0	44.0	1.54	11640	36000	0.0907	0.2901	0.2650	0.0917
	22-May	2276.0	513.0	29.9	1.48	12312	34140	0.0583	0.1934	0.3572	0.1011
	23-May	2098.0	455.0	24.6	1.55	10920	31470	0.0542	0.2295	0.3290	0.1001
	26-May										
	27-May										
3	**Mean**	2274.8	488.8	33.8	1.52	11731.2	34122	0.0692	0.2347	0.3188	0.0899
	Std	130.6	24.7	7.3	0.04	593.339	1958.704	0.0149	0.0459	0.0473	0.0114
	date	**Xv**	**Sti**	**Ste**	**Fcv**	**Msti**	**Mxv**	**Fs,us**	**Fs,up**	**Fav**	**Fn**
	28-May	2100.0	528.0	24.5	1.46	12672	31500	0.0464	0.1266	0.4403	0.1000
	29-May	1754.0	462.0	58.1	1.44	11088	26310	0.1257	0.1330	0.4135	0.1072
	30-May	1590.0	462.0	51.0	1.46	11088	23850	0.1105	0.0832	0.4962	0.0792
	3-Jun	1950.0	489.0	26.4	1.45	11736	29250	0.0540	0.1295	0.4336	0.0689
	4-Jun	2168.0	503.0	19.4	1.42	12072	32520	0.0385	0.1592	0.3942	0.0504
	5-Jun	1890.0	495.0	52.0	1.62	11880	28350	0.1051	0.1501	0.4131	0.0578
4	**Mean**	1908.7	489.8	38.6	1.48	11756	28630	0.0800	0.1303	0.4318	0.0772
	Std	215.1	25.3	16.9	0.07	607.8052	3226.844	0.0379	0.0264	0.0356	0.0228

9-Jun	2100.0	529.0	35.2	1.65	12696	31500	0.0665	0.1596	0.4128	0.1048
10-Jun	2356.0	499.8	24.6	1.42	11995.2	35340	0.0493	0.2123	0.3317	0.0976
11-Jun	2225.0	515.0	29.9	1.47	12360	33375	0.0581	0.1758	0.3755	0.1146
12-Jun	2450.0	554.0	26.4	1.49	13296	36750	0.0477	0.1883	0.3659	0.1143
13-Jun	2068.0	496.0	31.6	1.40	11904	31020	0.0637	0.1489	0.3999	0.1112

5	**Mean**	2239.8	518.8	29.6	1.48	12450.24	33597	0.0571	0.1770	0.3772	0.1085
	Std	163.5	23.7	4.2	0.10	567.7347	2452.911	0.0084	0.0248	0.0316	0.0073
	date	**Xv**	**Sti**	**Ste**	**Fcv**	**Msti**	**Mxv**	**Fs,us**	**Fs,up**	**Fav**	**Fn**
	17-Jun	1800.0	544.0	56.0	1.44	13056	27000	0.1029	0.0626	0.5340	0.1239
	18-Jun	1956.0	508.0	44.0	1.42	12192	29340	0.0866	0.1216	0.4355	0.1099
	19-Jun	1985.0	492.0	48.0	1.46	11808	29775	0.0976	0.1543	0.3927	0.1033
	20-Jun	1900.0	516.0	50.0	1.44	12384	28500	0.0969	0.1070	0.4578	0.1184
	21-Jun	1685.0	524.0	52.0	1.33	12576	25275	0.0992	0.0441	0.5642	0.1294
	22-Jun	1389.0	520.0	40.0	1.45	12480	20835	0.0769	-0.0282	0.7542	0.1332
	23-Jun	2100.0	516.0	44.0	1.79	12384	31500	0.0853	0.2073	0.3681	0.0905
	24-Jun	2146.0	580.0	32.0	1.75	13920	32190	0.0552	0.1232	0.4703	0.0979
	25-Jun	2250.0	506.0	60.0	1.28	12144	33750	0.1186	0.1790	0.3345	0.0791
	26-Jun	2365.0	512.0	52.0	1.29	12288	35475	0.1016	0.1936	0.3231	0.0812
6	**Mean**	1957.6	521.8	47.8	1.47	12523.2	29364	0.0921	0.1165	0.4634	0.1067
	Std	285.5								0.1295	0.0195

27-Jun	2050.0	450.0	40.0	1.49	10800	30750	0.0889	0.2241	0.3193	0.1024
28-Jun	2200.0	510.0	14.0	1.47	12240	33000	0.0275	0.1630	0.3974	0.1000
29-Jun	2050.0	498.0	26.0	1.47	11952	30750	0.0522	0.1476	0.4116	0.0966
30-Jun	2400.0	560.0	16.0	1.52	13440	36000	0.0286	0.1674	0.3973	0.0696
1-Jul	2060.0	552.0	40.0	1.46	13248	30900	0.0725	0.1050	0.4667	0.1019
2-Jul	2300.0	518.0	42.0	1.60	12432	34500	0.0811	0.2263	0.3303	0.0913
3-Jul	2100.0	524.0	14.0	1.46	12576	31500	0.0267	0.1226	0.4495	0.1005
4-Jul	2300.0	518.0	18.0	1.30	12432	34500	0.0347	0.1542	0.3868	0.0913
5-Jul	2250.0	516.0	44.0	1.49	12384	33750	0.0853	0.1970	0.3485	0.0978
6-Jul	2000.0	528.0	36.0	1.50	12672	30000	0.0682	0.1152	0.4566	0.0990

7	**Mean**	2171.0	517.4	29.0	1.48	12417.6	32565	0.0566	0.1623	0.3964	0.0950
	Std	136.9			0.07					0.0520	0.0098
	date	**Xv**	**Sti**	**Ste**	**Fcv**	**Msti**	**Mxv**	**Fs,us**	**Fs,up**	**Fav**	**Fn**
	7-Jul	2530.0	526.0	36.0	1.47	12624	37950	0.0684	0.2440	0.3027	0.0771
	8-Jul	2200.0	520.0	50.0	1.35	12480	33000	0.0962	0.1596	0.3725	0.0836
	9-Jul	2375.0	544.0	48.0	1.45	13056	35625	0.0882	0.1906	0.3498	0.0775
	10-Jul	1978.0	496.0	68.0	1.37	11904	29670	0.1371	0.1495	0.3789	0.0844
	11-Jul	2060.0	480.0	52.0	1.57	11520	30900	0.1083	0.2127	0.3350	0.1019
	12-Jul	2300.0	489.0	40.0	1.52	11736	34500	0.0818	0.2474	0.3020	0.0913
	13-Jul	2100.0	528.0	52.0	1.62	12672	31500	0.0985	0.1707	0.3891	0.1005
	14-Jul	2300.0	503.0	19.4	1.42	12072	34500	0.0385	0.1925	0.3561	0.0913
	15-Jul	2250.0	495.0	52.0	1.36	11880	33750	0.1051	0.2016	0.3230	0.0978
	16-Jul	1800.0	500.0	42.0	1.27	12000	27000	0.0840	0.0768	0.4937	0.1100
8	**Mean**	2189.3	508.1	45.9	1.44	12194.4	32839.5	0.0906	0.1845	0.3603	0.0915
	Std	210.8			0.11	487.3373	3161.345	0.0261	0.0498	0.0558	0.0110
	date	**Xv**	**Sti**	**Ste**	**Fcv**	**Msti**	**Mxv**	**Fs,us**	**Fs,up**	**Fav**	**Fn**

	17-Jul	1600.0	500.0	56.0	1.39	12000	24000	0.1120	0.0496	0.5548	0.1281
	18-Jul	1800.0	508.0	60.0	1.31	12192	27000	0.1181	0.0859	0.4757	0.1078
	19-Jul	2345.0	489.0	40.0	1.49	11736	35175	0.0818	0.2528	0.2938	0.0896
	20-Jul	2100.0	495.0	52.0	1.46	11880	31500	0.1051	0.1831	0.3553	0.0938
	21-Jul	1900.0	498.0	60.0	1.44	11952	28500	0.1205	0.1323	0.4147	0.0947
	22-Jul	1845.0	490.0	48.0	1.48	11760	27675	0.0980	0.1222	0.4386	0.1138
	23-Jul	1745.0	508.0	52.0	1.57	12192	26175	0.1024	0.0881	0.4991	0.1261
	24-Jul	1700.0	520.0	50.0	1.56	12480	25500	0.0962	0.0615	0.5456	0.1235
	25-Jul	2300.0	502.0	34.0	1.60	12048	34500	0.0677	0.2426	0.3187	0.0822
	26-Jul	1800.0	490.0	70.0	1.45	11760	27000	0.1429	0.1249	0.4221	0.1278
9	**Mean**	1913.5	500.0	52.2	1.48	12000	28702.5	0.1045	0.1343	0.4318	0.1087
	Std	252.4									

	date	**Xv**	**Sti**	**Ste**	**Fcv**	**Msti**	**Mxv**	**Fs,us**	**Fs,up**	**Fav**	**Fn**
	27-Jul	1745.0	504.0	27.0	1.51	12096	26175	0.0536	0.0667	0.5380	0.1226
	28-Jul	1900.0	504.0	39.0	1.49	12096	28500	0.0774	0.1160	0.4531	0.1158
	29-Jul	2100.0	474.0	45.0	1.49	11376	31500	0.0949	0.2087	0.3328	0.1038
	30-Jul	1850.0	490.0	30.0	1.47	11760	27750	0.0612	0.1075	0.4662	0.1000
	31-Jul	2300.0	485.0	30.0	1.55	11640	34500	0.0619	0.2500	0.3073	0.0913
	1-Aug	2100.0	484.0	20.8	1.57	11616	31500	0.0430	0.1906	0.3741	0.1005
	2-Aug	2000.0	508.0	37.4	1.39	12192	30000	0.0737	0.1228	0.4322	0.1055
	3-Aug	2500.0	520.0	20.8	1.48	12480	37500	0.0400	0.2347	0.3195	0.0860
	4-Aug	2500.0	511.0	27.0	1.53	12264	37500	0.0528	0.2630	0.2961	0.0840
	5-Aug	2300.0	500.0	47.0	1.49	12000	34500	0.0940	0.2309	0.3108	0.0861
10	**Mean**	2129.5	498.0	32.4	1.50	11952	31942.5	0.0652	0.1791	0.3830	0.0996
	Std	264.5	14.3	9.3	0.05	342.6018	3968.068	0.0194	0.0697	0.0840	

	date	**Xv**	**Sti**	**Ste**	**Fcv**	**Msti**	**Mxv**	**Fs,us**	**Fs,up**	**Fav**	**Fn**
	6-Aug	2623.0	520.0	37.0	1.41	12480	39345	0.0712	0.2601	0.2807	0.0839
	7-Aug	2342.0	480.0	36.1	1.50	11520	35130	0.0752	0.2620	0.2877	0.0769
	8-Aug	2324.0	495.0	35.7	1.57	11880	34860	0.0721	0.2540	0.3040	0.1033
	9-Aug	2562.0	502.0	34.0	1.44	12048	38430	0.0677	0.2735	0.2733	0.0703
	13-Aug	2400.0	522.0	33.3	1.56	12528	36000	0.0638	0.2343	0.3233	0.0442
	14-Aug	2210.0	503.0	31.2	1.51	12072	33150	0.0620	0.1958	0.3577	0.0507
11	**Mean**	2410.2	503.7	34.5	1.50	12088	36152.5	0.0687	0.2466	0.3045	0.0715
	Std	155.3	15.8	2.1	0.07	378.1555	2329.523	0.0051	0.0281	0.0316	0.0218
	16-Aug	2092.0	507.0	29.0	1.54	12168	31380	0.0572	0.1616	0.4009	0.0507
	17-Aug	2198.0	517.0	31.2	1.46	12408	32970	0.0603	0.1675	0.3846	0.0510
	18-Aug	2150.0	512.0	27.0	1.51	12288	32250	0.0528	0.1655	0.3942	0.0544
	19-Aug	2278.0	480.0	34.5	1.58	11520	34170	0.0719	0.2616	0.2974	0.0492
	20-Aug	2265.0	490.0	33.3	1.58	11760	33975	0.0679	0.2423	0.3160	0.0530
	23-Aug	2345.0	490.0	49.0	1.46	11760	35175	0.1000	0.2520	0.2867	0.0430
	25-Aug	2100.0	520.0	31.2	1.36	12480	31500	0.0600	0.1261	0.4268	0.0571
12	**Mean**	2204.0	502.3	33.6	1.50	12054.86	33060	0.0672	0.1967	0.3581	0.0512

	Std	96.1									
	date	**Xv**	**Sti**	**Ste**	**Fcv**	**Msti**	**Mxv**	**Fs,us**	**Fs,up**	**Fav**	**Fn**
	26-Aug	2344.0	500.0	35.4	1.48	12000	35160	0.0707	0.2310	0.3154	0.0896
	27-Aug	2300.0	490.0	37.4	1.55	11760	34500	0.0764	0.2500	0.3039	0.0957
	28-Aug	2245.0	512.0	58.0	1.55	12288	33675	0.1133	0.2240	0.3200	0.0953
	29-Aug	2000.0	478.0	31.2	1.64	11472	30000	0.0653	0.1889	0.3775	0.1100
	30-Aug	2100.0	470.0	54.0	1.47	11280	31500	0.1149	0.2177	0.3163	0.0900
	31-Aug	2145.0	505.0	39.5	1.53	12120	32175	0.0783	0.1862	0.3667	0.0886
	1-Sep	2200.0	485.0	27.0	1.45	11640	33000	0.0558	0.1988	0.3480	0.0841
B1/03	2-Sep	2250.0	512.0	29.0	1.45	12288	33750	0.0566	0.1822	0.3668	0.0947
13	**Mean**	2198.0	494.0	38.9	1.51	11856	32970	0.0789	0.2099	0.3393	0.0935
	Std	112.3	15.7	11.4	0.07			0.0232	0.0245	0.0287	0.0078
	5-Sep	1913.0	474.0	20.8	1.54	11376	28695	0.0439	0.1437	0.4263	0.1176
	6-Sep	1913.0	513.0	37.4	1.54	12312	28695	0.0730	0.1139	0.4617	0.0967
	7-Sep	2054.0	478.0	20.8	1.45	11472	30810	0.0435	0.1645	0.3903	0.0950
	8-Sep	2100.0	482.0	16.6	1.40	11568	31500	0.0345	0.1605	0.3912	0.1143
	9-Sep	1850.0	486.0	37.3	1.50	11664	27750	0.0767	0.1212	0.4462	0.1270
	10-Sep	1800.0	480.0	27.0	1.76	11520	27000	0.0563	0.1330	0.4578	0.1117
	11-Sep	2100.0	513.0	33.3	1.44	12312	31500	0.0649	0.1458	0.4083	0.1052
	12-Sep	2145.0	499.0	41.6	1.45	11976	32175	0.0834	0.1796	0.3631	0.1100
14	**Mean**	1984.4	490.6	29.4	1.51	11775	29765.63	0.0595	0.1453	0.4181	0.1097
	Std	130.7	15.7	9.3	0.11			0.0178	0.0224	0.0358	0.0106
	date	**Xv**	**Sti**	**Ste**	**Fcv**	**Msti**	**Mxv**	**Fs,us**	**Fs,up**	**Fav**	**Fn**
	15-Sep	2128.0	502.0	23.0	1.60	12048	31920	0.0458	0.1812	0.3861	0.1048
	16-Sep	1984.0	490.0	22.0	1.64	11760	29760	0.0449	0.1596	0.4161	0.1084
	17-Sep	2250.0	504.0	27.0	1.49	12096	33750	0.0536	0.1968	0.3556	0.0911
	18-Sep	2082.0	513.0	39.0	1.46	12312	31230	0.0760	0.1485	0.4046	0.1081
	19-Sep	2100.0	474.0	45.0	1.49	11376	31500	0.0949	0.2087	0.3328	0.1038
	20-Sep	2200.0	486.0	37.3	1.48	11664	33000	0.0767	0.2127	0.3324	0.0841
	21-Sep	2154.0	495.0	24.0	1.45	11880	32310	0.0485	0.1735	0.3786	0.0882
	22-Sep	2100.0	506.0	21.0	1.55	12144	31500	0.0415	0.1587	0.4081	0.1000
	23-Sep	2100.0	485.0	27.0	1.50	11640	31500	0.0557	0.1822	0.3728	0.0848
	24-Sep	2300.0	512.0	58.0	1.39	12288	34500	0.1133	0.2036	0.3220	0.0835
15	**Mean**	2139.8	496.7	32.3	1.50	11920.8	32097	0.0651	0.1826	0.3709	0.0957
	Std	90.8	12.8	12.2	0.07	307.9844	1361.429	0.0243	0.0226	0.0340	0.0103
	25-Sep	2438.0	486.0	54.0	1.45	11664	36570	0.1111	0.2826	0.2560	0.0882
	26-Sep	2254.0	438.0	37.0	1.29	10512	33810	0.0845	0.2452	0.2758	0.0932
	27-Sep	1500.0	390.0	24.6	1.28	9360	22500	0.0632	0.0976	0.4620	0.1467
	28-Sep	1604.0	520.0	22.9	1.74	12480	24060	0.0440	0.0146	0.6463	0.1340
	29-Sep	2100.0	503.0	45.0	1.44	12072	31500	0.0895	0.1650	0.3781	0.0943
	30-Sep	2300.0	465.0	20.6	1.54	11160	34500	0.0443	0.2682	0.2943	0.0957
	1-Oct	2230.0	498.0	38.0	1.51	11952	33450	0.0763	0.2115	0.3368	0.0987
	2-Oct	2146.0	474.0	45.0	1.45	11376	32190	0.0949	0.2148	0.3229	0.1025
	3-Oct	1980.0	503.0	19.4	1.65	12072	29700	0.0385	0.1412	0.4413	0.1061

	4-Oct	2340.0	495.0	52.0	1.31	11880	35100	0.1051	0.2111	0.3063	0.0383
16		2089.2	477.2	35.8	1.47	11452.8	31338	0.0751	0.1852	0.3720	0.0998
		311.6	38.4	13.2	0.15	922.2442	4673.932	0.0264	0.0826	0.1178	0.0287
	date	**Xv**	**Sti**	**Ste**	**Fcv**	**Msti**	**Mxv**	**Fs,us**	**Fs,up**	**Fav**	**Fn**
	5-Oct	2400.0	486.0	54.0	1.47	11664	36000	0.1111	0.2787	0.2617	0.0813
	6-Oct	1618.0	498.0	20.0	1.92	11952	24270	0.0402	0.0461	0.5955	0.1137
	7-Oct	2156.0	400.0	28.0	1.67	9600	32340	0.0700	0.3823	0.2152	0.0853
	8-Oct	2000.0	472.0	36.0	1.44	11328	30000	0.0763	0.1674	0.3780	0.0835
	9-Oct	2100.0	496.0	16.0	1.50	11904	31500	0.0323	0.1601	0.4039	0.1000
	10-Oct	2114.0	492.0	36.0	1.43	11808	31710	0.0732	0.1723	0.3719	0.0993
	11-Oct	1854.0	502.0	28.0	1.46	12048	27810	0.0558	0.0939	0.4875	0.1138
	12-Oct	1760.0	517.0	30.0	1.88	12408	26400	0.0580	0.0837	0.5339	0.1193
	13-Oct	2344.0	480.0	32.0	1.27	11520	35160	0.0667	0.2063	0.3153	0.0939
	14-Oct	2167.0	510.0	28.0	1.48	12240	32505	0.0549	0.1671	0.3877	0.0914
17		2051.3	485.3	30.8	1.55	11647.2	30769.5	0.0638	0.1758	0.3951	0.0982
		247.7	32.8	10.3	0.21	787.7502	3715.105	0.0218	0.0981	0.1181	0.0136
	15-Oct	2098.0	510.0	30.0	1.53	12240	31470	0.0588	0.1589	0.4027	0.1044
	16-Oct	2268.0	468.0	28.0	1.46	11232	34020	0.0598	0.2426	0.3048	0.0996
	17-Oct	2234.0	500.0	32.0	1.55	12000	33510	0.0640	0.2129	0.3427	0.0940
	18-Oct										
18		2200.0	492.7	30.0	1.51	11824	33000	0.0609	0.2048	0.3501	0.0993
		90.0	21.9	2.0	0.05	526.5434	1349.333	0.0027	0.0424	0.0493	0.0052

APPENDIX 9

Comprehensive data for 10 days anoxic/aerobic activated sludge system

TABLE 9.1 Daily analysis for various sewage batches conducted during 2004. Daily analysis includes: TKN (influent, effluent and mixed liquor); Nitrate (influent, effluent and aerobic); nitrogen mass balance. Mean and standard deviation are calculated for each batch

TABLE 9.2 Daily analysis for various sewage batches conducted during 2004. Daily analysis includes: COD (influent, effluent and mixed liquor); OUR; COD mass balance. Mean and standard deviation are calculated for each batch.

TABLE 9.3 Wastewater fractions and mixed liquor parameters for parent system in 2004. Wastewater fractions include: *fs,us* and *fs,up*; mixed liquor parameters include: *Xv, Fcv, Fn* and *Fav*. Mean and standard deviations are calculated for each batch.

TABLE 9.1: Daily experimental data and nitrogen mass balance for parent system in 2004

Nitrogen mass balance **2004**

System condition and parameters

	Rs	V	Q	a	s	Yh	Fcv				Qw		
Unit	day	L	(L/d)	Recycle ratio		mgVss/mgCOD	mgCOD/mgVSS				L		
Value	10	15	24	2	1	0.45	1.48				1.5		

Batch no.	Date	TKN (IN)	TKN (AE)	TKN (FE)	NO3 (AN)	NO3 (AE)	NO3 (FE)	MNd	%	MNte	%	MNne	%	MNw	%	MNti	Nbal (%)
	3-Apr	35.0	230.0	4.5	0.0	1.2	7.5	237.6	28.3	101.3	12.1	168.8	20.1	346.8	41.3	840.0	**101.7**
	4-Apr	33.0	220.0	2.8	0.2	4.2	8.5	386.4	48.8	63.0	8.0	191.3	24.1	336.3	42.5	792.0	**123.4**
	5-Apr	40.0	238.0	6.2	0.5	4.2	10.8	412.8	43.0	139.5	14.5	243.0	25.3	363.3	37.8	960.0	**120.7**
	6-Apr	45.0	288.0	5.6	1.2	5.4	8.2	340.8	31.6	126.0	11.7	184.5	17.1	440.1	40.8	1080.0	**101.1**
	7-Apr	33.0	221.0	6.2	3.2	7.1	6.3	184.8	23.3	139.5	17.6	141.8	17.9	342.2	43.2	792.0	**102.0**
	8-Apr	39.0	230.0	3.4	0.4	5.6	6.5	386.4	41.3	76.5	8.2	146.3	15.6	353.4	37.8	936.0	**102.8**
	9-Apr	44.0	246.0	8.4	0.0	3.9	6.7	348.0	33.0	189.0	17.9	150.8	14.3	374.9	35.5	1056.0	**100.6**
	10-Apr	50.0	216.0	8.9	0.0	3.4	8.9	376.8	31.4	200.3	16.7	200.3	16.7	329.1	27.4	1200.0	**92.2**
	11-Apr	39.0	230.0	4.0	0.0	1.2	8.9	271.2	29.0	90.0	9.6	200.3	21.4	346.8	37.1	936.0	**97.0**
	12-Apr	30.0	227.0	3.4	0.0	2.3	6.3	261.6	36.3	76.5	10.6	141.8	19.7	344.0	47.8	720.0	**114.4**
1	**Mean**	38.8	234.6	5.3	0.6	3.9	7.9	320.6	34.6	120.2	12.7	176.9	19.2	357.7	39.1	931.2	**105.6**
	Std	6.3	20.7	2.1	1.0	1.9	1.5	76.5		47.5		33.1		31.8		150.0	10.3
	13-Apr																
	14-Apr																
	15-Apr																
	16-Apr																
	17-Apr																
	18-Apr																
	19-Apr	50.0	246.0	5.6	2.1	8.2	15.5	564.0	47.0	126.0	10.5	348.8	29.1	381.3	31.8	1200.0	**118.3**
	20-Apr	50.0	216.0	4.3	1.3	8.2	15.5	640.8	53.4	96.8	8.1	348.8	29.1	336.3	28.0	1200.0	**118.6**
	21-Apr	44.0	230.0	4.0	1.5	5.4	15.6	489.6	46.4	90.0	8.5	351.0	33.2	353.1	33.4	1056.0	**121.6**

	22-Apr	49.0	227.0	3.4	2.1	9.8	14.9	626.4	53.3	76.5	6.5	335.3	28.5	355.2	30.2	1176.0	**118.5**
2	**Mean**	48.3	229.8	4.3	1.8	7.9	15.4	580.2	50.0	97.3	8.4	345.9	30.0	356.5	30.9	1158.0	**119.2**
	Std	2.9	12.4	0.9	0.4	1.8	0.3	69.0		20.9		7.2		18.6		68.9	1.6
Batch no.	**Date**	**TKN (IN)**	**TKN (AE)**	**TKN (FE)**	**NO3 (AN)**	**NO3 (AE)**	**NO3 (FE)**	**MNd**	**%**	**MNte**	**%**	**MNne**	**%**	**MNw**	**%**	**MNti**	**Nbal (%)**
	23-Apr	45.0	240.0	4.0	1.2	5.2	8.5	338.4	31.3	90.0	8.3	191.3	17.7	367.8	34.1	1080.0	**91.4**
	24-Apr	49.0	230.0	5.0	0.2	6.0	10.1	511.2	43.5	112.5	9.6	227.3	19.3	354.0	30.1	1176.0	**102.5**
	25-Apr	38.0	240.0	4.5	1.5	6.5	7.9	357.6	39.2	101.3	11.1	177.8	19.5	369.8	40.5	912.0	**110.3**
	26-Apr	42.0	229.0	4.0	2.1	5.6	10.5	319.2	31.7	90.0	8.9	236.3	23.4	351.9	34.9	1008.0	**98.9**
	27-Apr	40.0	230.0	4.5	1.2	5.4	9.8	379.2	39.5	101.3	10.5	220.5	23.0	353.1	36.8	960.0	**109.8**
3	**Mean**	42.8	233.8	4.4	1.2	5.7	9.4	381.1	37.0	99.0	9.7	210.6	20.6	359.3	35.3	1027.2	**102.6**
	Std	4.3	5.7	0.4	0.7	0.5	1.1	76.1		9.4		24.9		8.7		103.8	7.9
	2-May	33.6	223.0	2.2	0.2	5.3	5.3	356.3	44.2	50.4	6.3	119.3	14.8	342.4	42.5	806.4	**107.7**
	3-May	31.0	215.0	2.1	1.3	3.6	5.5	182.9	24.6	47.9	6.4	123.8	16.6	327.8	44.1	744.0	**91.7**
	4-May	33.6	205.0	1.1	0.2	4.5	6.7	358.1	44.4	25.2	3.1	150.8	18.7	314.3	39.0	806.4	**105.2**
	5-May	29.1	225.0	1.7	0.0	2.5	5.0	239.8	34.3	37.8	5.4	112.5	16.1	341.3	48.8	698.9	**104.7**
	6-May	33.6	218.0	2.8	0.3	3.2	6.1	276.5	34.3	63.0	7.8	137.3	17.0	331.8	41.1	806.4	**100.3**
	7-May	30.3	185.0	2.8	0.1	2.3	6.2	252.7	34.7	63.0	8.7	139.5	19.2	281.0	38.6	727.2	**101.2**
	8-May	32.0	190.0	1.7	0.0	2.6	7.2	294.2	38.3	37.8	4.9	162.0	21.1	288.8	37.6	768.0	**101.9**
	9-May	31.0	210.0	1.1	0.1	0.1	7.5	174.7	23.5	25.2	3.4	168.8	22.7	315.2	42.4	744.0	**91.9**
	10-May	31.0	178.0	1.1	0.2	1.5	9.6	287.8	38.7	25.2	3.4	215.1	28.9	269.3	36.2	744.0	**107.2**
	11-May	26.9	192.0	0.6	0.2	2.6	6.9	275.4	42.7	12.6	2.0	155.3	24.1	291.9	45.2	645.1	**114.0**
4		31.2	204.1	1.7	0.2	2.8	6.6	269.8	36.0	38.8	5.1	148.4	19.9	310.4	41.6	749.0	102.6
		2.2	16.8	0.8	0.4	1.5	1.3	61.5		17.1		29.9		26.1		51.7	6.9
Batch no.	**Date**	**TKN (IN)**	**TKN (AE)**	**TKN (FE)**	**NO3 (AN)**	**NO3 (AE)**	**NO3 (FE)**	**MNd**		**MNte**		**MNne**		**MNw**		**MNti**	**Nbal (%)**
	12-May	34.0	220.0	4.7	2.4	4.6	5.5	123.8	15.2	106.2	13.0	124.2	15.2	336.9	41.3	816.0	**84.7**
	13-May	34.7	112.0	5.6	0.5	3.6	10.5	373.7	44.8	126.0	15.1	235.1	28.2	173.3	20.8	833.3	**109.0**
	14-May	31.4	109.2	3.4	0.4	3.4	8.6	327.8	43.6	75.6	10.0	192.6	25.6	168.8	22.4	752.6	**101.6**

	15-May	31.4	120.4	6.7	0.0	1.3	6.8	223.2	29.7	151.2	20.1	153.0	20.3	182.5	24.2	752.6	**94.3**
	16-May	36.0	189.0	5.0	0.0	2.1	5.7	237.4	27.5	113.4	13.1	127.1	14.7	286.7	33.2	864.0	**88.5**
	17-May	32.5	109.2	3.4	0.0	3.5	9.0	384.0	49.3	75.6	9.7	201.6	25.9	169.1	21.7	779.5	**106.5**
	18-May	28.0	117.6	4.5	0.0	3.7	7.3	350.4	52.1	100.8	15.0	164.3	24.4	181.9	27.1	672.0	**118.6**
	19-May	28.0	120.4	5.0	0.0	1.1	9.7	286.8	42.7	113.4	16.9	218.0	32.4	182.3	27.1	672.0	**119.1**
	20-May	36.0	100.8	2.8	0.0	1.3	8.7	267.6	31.0	63.0	7.3	194.6	22.5	153.1	17.7	864.0	**78.5**
	21-May	30.2	100.8	3.4	0.0	2.6	9.0	338.4	46.6	75.6	10.4	202.1	27.8	155.0	21.4	725.8	**106.2**
5		32.2	129.9	4.4	0.3	2.7	8.1	291.3	38.2	100.1	13.1	181.3	23.7	199.0	25.7	773.2	100.7
		2.8	38.5	1.2	0.7	1.2	1.6	76.5		26.2		35.6		58.4		67.5	13.2
	22-May	34.0	220.0	4.7	0.6	0.7	10.5	228.0	27.9	106.2	13.0	236.3	29.0	331.1	40.6	816.0	**110.5**
	23-May	34.7	112.0	5.6	0.2	0.6	9.0	225.6	27.1	126.0	15.1	202.5	24.3	168.9	20.3	833.3	**86.8**
	24-May	31.4	109.2	3.4	1.5	6.7	8.5	381.6	50.7	75.6	10.0	191.3	25.4	173.9	23.1	752.6	**109.3**
	25-May	33.6	120.4	6.7	1.3	5.4	9.3	357.6	44.3	151.2	18.8	209.3	25.9	188.7	23.4	806.4	**112.4**
	26-May	37.0	189.0	5.0	0.0	5.0	8.4	441.6	49.7	113.4	12.8	189.0	21.3	291.0	32.8	888.0	**116.6**
	27-May	32.5	109.2	3.4	2.3	7.5	12.8	446.4	57.3	75.6	9.7	288.0	36.9	175.1	22.5	779.5	**126.4**
	28-May	35.0	117.6	4.5	0.8	5.0	9.9	400.6	47.7	100.8	12.0	222.5	26.5	183.9	21.9	840.0	**108.1**
	29-May	34.0	120.4	5.0	0.3	2.3	9.2	302.4	37.1	113.4	13.9	207.0	25.4	184.1	22.6	816.0	**98.9**
	30-May	33.0	100.8	2.8	0.3	2.4	10.3	333.6	42.1	63.0	8.0	231.8	29.3	154.8	19.5	792.0	**98.9**
	31-May	32.0	100.8	3.4	1.5	7.2	9.8	436.8	56.9	75.6	9.8	220.5	28.7	162.0	21.1	768.0	**116.5**
6		33.7	129.9	4.4	0.9	4.3	9.8	355.4	44.1	100.1	12.3	219.8	27.3	201.3	24.8	809.2	108.4
		1.6	38.5	1.2	0.7	2.5	1.2	78.4		26.2		27.2		56.4		37.3	10.6
	1-Jun	34.0	214.0	1.7	3.5	8.8	7.6	268.8	32.9	37.8	4.6	171.0	21.0	334.2	41.0	816.0	**99.5**
	2-Jun	42.0	220.0	2.4	0.5	3.5	8.2	316.8	31.4	54.0	5.4	184.5	18.3	335.3	33.3	1008.0	**88.3**
	3-Jun	33.6	218.0	2.8	0.3	9.1	21.0	916.8	113.7	63.0	7.8	472.5	58.6	340.7	42.2	806.4	**222.3**
	4-Jun	30.3	185.0	2.8	0.1	6.5	7.6	487.9	67.1	63.0	8.7	171.0	23.5	287.3	39.5	727.2	**138.8**
	5-Jun	33.3	210.0	3.9	1.4	8.5	7.3	448.8	56.2	87.8	11.0	164.3	20.6	327.8	41.1	798.0	**128.9**
	6-Jun	33.0	211.0	2.8	1.6	6.5	15.7	539.0	68.1	63.0	8.0	353.3	44.6	326.3	41.2	792.0	**161.8**
	7-Jun	33.0	211.0	2.8	1.6	9.5	14.5	654.2	82.6	63.0	8.0	326.3	41.2	330.8	41.8	792.0	**173.5**
	8-Jun	31.0	215.0	0.6	0.2	17.0	16.1	1179.0	158.5	12.6	1.7	362.3	48.7	348.0	46.8	744.0	**255.6**
	9-Jun	29.0	210.0	1.7	1.3	8.7	13.9	631.2	90.7	37.8	5.4	312.8	44.9	328.1	47.1	696.0	**188.2**
	10-Jun	33.2	198.0	4.2	1.4	5.6	13.0	446.4	56.0	95.2	11.9	292.5	36.7	305.4	38.3	797.0	**143.0**

7		33.2	209.2	2.6	1.2	8.4	12.5	588.9	75.7	57.7	7.2	281.0	35.8	326.4	41.2	797.7	**160.0**
		3.5	10.4	1.1	1.0	3.6	4.7										
Batch no.	**Date**	**TKN (IN)**	**TKN (AE)**	**TKN (FE)**	**NO3 (AN)**	**NO3 (AE)**	**NO3 (FE)**	**MNd**		**MNte**		**MNne**		**MNw**		**MNti**	**Nbal (%)**
	11-Jun	35.8	205.0	3.5	0.0	3.4	8.6	369.6	43.0	78.8	9.2	193.5	22.5	312.6	36.4	859.2	**111.1**
	12-Jun	37.0	308.0	2.4	0.0	3.5	9.3	391.2	44.1	54.0	6.1	209.3	23.6	467.3	52.6	888.0	**126.3**
	13-Jun	47.0	210.0	5.4	0.0	4.4	10.8	470.4	41.7	121.5	10.8	243.0	21.5	321.6	28.5	1128.0	**102.5**
	14-Jun	37.0	143.0	16.0	0.0	3.2	6.5	309.6	34.9	360.0	40.5	146.3	16.5	219.3	24.7	888.0	**116.6**
ab1	15-Jun	44.0	241.0	2.5	2.3	7.2	8.5	328.8	31.1	56.3	5.3	191.3	18.1	372.3	35.3	1056.0	**89.8**
	16-Jun	35.0	210.0	7.4	0.2	5.8	6.3	410.4	48.9	166.5	19.8	141.8	16.9	323.7	38.5	840.0	**124.1**
	17-Jun	56.0	188.0	4.2	0.3	10.5	11.5	751.2	55.9	94.5	7.0	258.8	19.3	297.8	22.2	1344.0	**104.3**
	18-Jun	58.0	234.0	5.2	2.1	11.5	14.7	703.0	50.5	117.0	8.4	330.5	23.7	368.3	26.5	1392.0	**109.1**
	19-Jun	58.0	333.0	8.4	3.1	8.6	11.5	391.9	28.2	189.0	13.6	259.4	18.6	512.4	36.8	1392.0	**97.2**
	20-Jun	56.0	242.0	6.2	0.2	7.5	13.1	657.6	48.9	139.5	10.4	295.7	22.0	374.3	27.8	1344.0	**109.2**
8	**Mean**	46.4	231.4	6.1	0.8	6.6	10.1	478.4	42.7	137.7	13.1	226.9	20.3	356.9	32.9	1113.1	109.0
	std	9.9	55.5	4.0	1.2	3.0	2.7	163.1		89.8		61.7		84.2		237.1	11.4
	21-Jun	39.0	222.0	2.1	0.8	4.4	9.4	360.0	38.5	47.3	5.0	211.5	22.6	339.6	36.3	936.0	**102.4**
ab2	22-Jun	45.0	238.0	4.5	0.2	4.5	9.4	422.2	39.1	101.3	9.4	210.8	19.5	363.8	33.7	1080.0	**101.7**
	23-Jun	44.0	258.0	3.5	1.4	5.9	9.5	378.2	35.8	78.8	7.5	213.8	20.2	395.8	37.5	1056.0	**101.0**
	24-Jun	48.0	236.0	4.0	0.8	7.5	8.7	489.8	42.5	90.0	7.8	196.0	17.0	365.2	31.7	1152.0	**99.0**
	25-Jun	39.0	224.0	4.5	2.3	6.4	9.9	327.6	35.0	101.3	10.8	222.1	23.7	345.6	36.9	936.0	**106.5**
	26-Jun	38.0	238.0	3.2	2.4	6.8	7.9	285.6	31.3	72.0	7.9	177.8	19.5	367.2	40.3	912.0	**99.0**
	27-Jun	39.0	211.0	4.4	0.2	5.6	8.3	450.7	48.2	99.0	10.6	187.7	20.0	324.9	34.7	936.0	**113.5**
	28-Jun	40.0	213.0	3.2	1.7	8.1	8.8	440.4	45.9	72.0	7.5	198.7	20.7	331.7	34.5	960.0	**108.6**
	29-Jun	42.0	221.0	3.2	2.5	7.3	12.0	397.0	39.4	72.0	7.1	269.6	26.7	342.5	34.0	1008.0	**107.2**
	30-Jun	45.0	176.0	2.2	0.0	7.2	10.6	598.8	55.4	49.5	4.6	237.4	22.0	274.8	25.4	1080.0	**107.5**
9	**Mean**	41.9	223.7	3.5	1.2	6.4	9.4	415.0	41.1	78.3	7.8	212.5	21.2	345.1	34.5	1005.6	104.6
	Std	3.4	21.9	0.9	1.0	1.3	1.2	88.5		19.8		26.4		32.3		81.9	4.7
	1-Jul	35.0	220.0	10.0	0.8	4.5	6.8	302.6	36.0	225.0	26.8	152.3	18.1	336.8	40.1	840.0	**121.0**
	2-Jul	42.0	226.0	5.0	0.8	5.3	6.8	346.3	34.4	112.5	11.2	152.8	15.2	347.0	34.4	1008.0	**95.1**
	3-Jul	34.0	248.0	4.5	0.4	4.4	6.3	318.0	39.0	101.3	12.4	141.1	17.3	378.5	46.4	816.0	**115.1**
	4-Jul	38.0	229.0	3.5	0.0	4.5	7.3	389.8	42.7	78.8	8.6	164.3	18.0	350.2	38.4	912.0	**107.8**

	5-Jul	46.0	168.0	4.5	2.6	10.5	11.4	529.7	48.0	101.3	9.2	257.2	23.3	267.8	24.3	1104.0	**104.7**
	6-Jul	35.0	182.0	3.5	1.3	6.5	7.7	374.9	44.6	78.8	9.4	173.7	20.7	282.7	33.7	840.0	**108.3**
	7-Jul	43.0	210.0	4.0	2.3	7.3	9.3	352.8	34.2	90.0	8.7	209.7	20.3	325.9	31.6	1032.0	**94.8**
	8-Jul	50.0	224.0	4.0	2.8	7.6	14.6	441.1	36.8	90.0	7.5	328.1	27.3	347.4	28.9	1200.0	**100.5**
	9-Jul	50.0	196.0	5.0	7.6	13.6	16.9	330.5	27.5	112.5	9.4	379.6	31.6	314.3	26.2	1200.0	**94.7**
	10-Jul	45.0	230.0	5.6	1.4	5.7	6.7	301.9	28.0	126.0	11.7	150.3	13.9	353.5	32.7	1080.0	**86.3**
10	**Mean**	41.8	213.3	5.0	2.0	7.0	9.4	368.8	37.1	111.6	11.5	210.9	20.6	330.4	33.7	1003.2	102.8
	Std	6.1	24.5	1.9	2.2	3.0	3.7	70.9		42.7		83.8		33.9		145.7	10.6
Batch no.	**Date**	**TKN (IN)**	**TKN (AE)**	**TKN (FE)**	**NO3 (AN)**	**NO3 (AE)**	**NO3 (FE)**	**MNd**		**MNte**		**MNne**		**MNw**		**MNti**	**Nbal (%)**
	11-Jul	53.0	230.0	4.5	2.1	5.2	14.0	382.8	30.1	101.3	8.0	313.9	24.7	352.8	27.7	1272.0	**90.5**
	12-Jul	48.0	220.0	2.8	2.9	8.7	12.7	445.0	38.6	63.0	5.5	286.2	24.8	343.1	29.8	1152.0	**98.7**
	13-Jul	64.0	238.0	7.3	1.2	7.9	14.1	602.9	39.3	164.3	10.7	317.7	20.7	368.9	24.0	1536.0	**94.6**
	14-Jul	68.0	288.0	5.6	0.8	8.0	13.1	621.8	38.1	126.0	7.7	294.5	18.0	444.0	27.2	1632.0	**91.1**
	15-Jul	45.0	221.0	6.2	1.2	7.5	10.3	491.5	45.5	139.5	12.9	232.2	21.5	342.7	31.7	1080.0	**111.7**
	16-Jul	47.0	230.0	3.4	1.2	6.9	10.3	462.0	41.0	76.5	6.8	231.1	20.5	355.3	31.5	1128.0	**99.7**
	17-Jul	44.0	246.0	4.4	1.6	8.4	12.4	545.5	51.7	99.0	9.4	279.2	26.4	381.5	36.1	1056.0	**123.6**
	18-Jul	50.0	216.0	8.9	2.5	7.7	11.4	405.4	33.8	200.3	16.7	256.7	21.4	335.6	28.0	1200.0	**99.8**
	19-Jul	39.0	162.0	4.0	3.7	8.2	10.4	289.2	30.9	90.0	9.6	233.3	24.9	255.4	27.3	936.0	**92.7**
	20-Jul	45.0	227.0	3.4	2.3	10.5	13.5	606.7	56.2	76.5	7.1	303.3	28.1	356.3	33.0	1080.0	**124.3**
11	**Mean**	50.3	227.8	5.1	2.0	7.9	12.2	485.3	40.5	113.6	9.4	274.8	23.1	353.6	29.6	1207.2	102.7
	Std	9.1	31.0	1.9	0.9	1.3	1.5	109.7		43.6		34.1		46.4		218.8	12.8
	21-Jul	48.0	210.0	4.5	3.5	10.8	12.3	477.6	41.5	101.3	8.8	276.8	24.0	331.2	28.8	1152.0	**103.0**
	22-Jul	39.0	244.0	4.0	1.7	5.5	9.5	328.8	35.1	90.0	9.6	213.8	22.8	374.3	40.0	936.0	**107.6**
	23-Jul	52.0	238.0	4.5	4.5	9.5	14.2	364.8	29.2	101.3	8.1	319.5	25.6	371.3	29.7	1248.0	**92.7**
	24-Jul	52.0	221.0	5.6	2.8	9.5	11.7	470.6	37.7	126.0	10.1	263.9	21.1	345.8	27.7	1248.0	**96.7**
	25-Jul	42.0	217.0	4.2	1.2	8.3	8.4	482.4	47.9	94.5	9.4	189.0	18.8	337.9	33.5	1008.0	**109.5**
ab3/4	26-Jul	48.0	213.0	5.0	3.2	10.3	11.2	456.7	39.6	112.5	9.8	252.7	21.9	335.0	29.1	1152.0	**100.4**
	27-Jul	54.0	218.0	4.5	3.5	11.5	13.5	540.0	41.7	101.3	7.8	303.8	23.4	344.3	26.6	1296.0	**99.5**
	28-Jul	52.0	224.0	4.5	3.2	10.7	14.2	547.7	43.9	101.3	8.1	319.5	25.6	352.1	28.2	1248.0	**105.8**
	29-Jul	54.0	198.0	4.0	1.3	9.2	11.8	600.0	46.3	90.0	6.9	265.5	20.5	310.8	24.0	1296.0	**97.7**
	30-Jul	52.0	225.0	4.5	2.2	9.5	13.0	556.8	44.6	101.3	8.1	292.5	23.4	351.8	28.2	1248.0	**104.4**
12	**Mean**	49.3	220.8	4.5	2.7	9.5	12.0	482.5	40.7	101.9	8.7	269.7	22.7	345.4	29.6	1183.2	101.7

	Std	5.1	13.3	0.5	1.1	1.7	1.9	85.1		10.7		43.0		18.7		122.9	5.3
Batch no.	**Date**	**TKN (IN)**	**TKN (AE)**	**TKN (FE)**	**NO3 (AN)**	**NO3 (AE)**	**NO3 (FE)**	**MNd**		**MNte**		**MNne**		**MNw**		**MNti**	**Nbal (%)**
	31-Jul	58.0	228.0	3.2	1.2	10.5	14.2	729.6	52.4	72.0	5.2	319.5	23.0	357.8	25.7	1392.0	**106.2**
	1-Aug	57.0	210.0	4.2	2.1	11.5	15.9	732.0	53.5	94.5	6.9	357.8	26.2	332.3	24.3	1368.0	**110.9**
	2-Aug	58.0	232.0	4.5	1.2	12.3	17.5	895.2	64.3	101.3	7.3	393.8	28.3	366.5	26.3	1392.0	**126.2**
	3-Aug	62.0	230.0	4.4	3.2	14.6	16.4	787.2	52.9	99.0	6.7	369.0	24.8	366.9	24.7	1488.0	**109.0**
	4-Aug	64.0	210.0	5.6	2.2	13.3	16.5	820.8	53.4	126.0	8.2	371.3	24.2	334.9	21.8	1536.0	**107.6**
	5-Aug	62.0	199.0	5.0	3.2	11.8	14.6	608.6	40.9	112.5	7.6	328.5	22.1	316.2	21.2	1488.0	**91.8**
	6-Aug	66.0	215.0	4.2	4.2	10.3	15.5	461.3	29.1	94.5	6.0	348.8	22.0	337.9	21.3	1584.0	**78.4**
	7-Aug	66.0	218.0	5.6	2.7	2.3	28.0	519.6	32.8	126.0	8.0	630.2	39.8	330.5	20.9	1584.0	**101.4**
	8-Aug	69.0	210.0	4.5	4.1	9.2	28.2	726.0	43.8	101.3	6.1	634.7	38.3	328.8	19.9	1656.0	**108.1**
	9-Aug	58.0	219.0	4.5	5.1	7.5	19.3	336.2	24.2	101.3	7.3	434.0	31.2	339.8	24.4	1392.0	**87.0**
13	**Mean**	62.0	217.1	4.6	2.9	10.3	18.6	661.7	44.7	102.8	6.9	418.7	28.0	341.1	23.0	1488.0	102.7
	Std	4.2	10.5	0.7	1.3	3.5	5.2	175.9		15.9		117.2		17.0		100.6	13.7
Batch no.	**Date**	**TKN (IN)**	**TKN (AE)**	**TKN (FE)**	**NO3 (AN)**	**NO3 (AE)**	**NO3 (FE)**	**MNd**		**MNte**		**MNne**		**MNw**		**MNti**	**Nbal (%)**
	10-Aug	55.0	221.0	5.0	3.2	10.2	15.2	547.2	41.5	112.5	8.5	342.0	25.9	346.8	26.3	1320.0	**102.2**
	11-Aug	54.0	196.0	4.0	1.2	11.2	13.4	742.6	57.3	90.0	6.9	301.5	23.3	310.8	24.0	1296.0	**111.5**
	12-Aug	55.0	210.0	4.5	3.2	10.2	15.5	555.1	42.1	101.3	7.7	349.4	26.5	330.3	25.0	1320.0	**101.2**
	13-Aug	45.0	220.0	4.0	1.2	8.5	9.2	513.8	47.6	90.0	8.3	206.8	19.1	342.8	31.7	1080.0	**106.8**
	14-Aug	40.0	132.0	4.5	1.2	7.1	11.3	496.6	51.7	101.3	10.5	253.1	26.4	208.7	21.7	960.0	**110.4**
	15-Aug	45.0	232.0	5.2	2.2	8.2	11.6	459.8	42.6	117.0	10.8	260.1	24.1	360.3	33.4	1080.0	**110.9**
ab5/6	16-Aug	46.0	223.0	10.0	0.3	5.2	7.9	406.6	36.8	225.0	20.4	177.8	16.1	342.3	31.0	1104.0	**104.3**
	17-Aug	37.0	215.0	7.3	3.0	1.6	13.6	115.2	13.0	164.3	18.5	305.1	34.4	324.9	36.6	888.0	**102.4**
	18-Aug	38.0	143.0	8.0	1.2	3.9	12.1	362.4	39.7	180.0	19.7	271.8	29.8	220.4	24.2	912.0	**113.4**
	19-Aug	39.0	210.0	4.2	6.8	9.1	13.5	112.8	12.1	94.5	10.1	303.8	32.5	328.7	35.1	936.0	**89.7**
14	**Mean**	45.4	200.2	5.7	2.3	7.5	12.3	431.2	38.4	127.6	12.2	277.1	25.8	311.6	28.9	1089.6	105.3
	Std	6.7	32.7	1.9	1.7	2.9	2.3	185.5		43.8		52.2		50.3		161.8	6.6
	20-Aug	35.8	205.0	3.5	6.1	5.6	15.0	41.8	4.9	78.8	9.2	338.4	39.4	315.9	36.8	859.2	**90.2**
	21-Aug	37.0	308.0	2.4	2.2	5.2	8.5	244.3	27.5	54.0	6.1	191.3	21.5	469.7	52.9	888.0	**108.0**
	22-Aug	47.0	210.0	5.4	0.0	2.9	8.0	331.7	29.4	121.5	10.8	180.0	16.0	319.4	28.3	1128.0	**84.4**
	23-Aug	37.0	143.0	16.0	0.0	1.1	7.5	230.9	26.0	360.0	40.5	167.9	18.9	216.1	24.3	888.0	**109.8**

	24-Aug	44.0	241.0	2.5	0.0	6.7	5.6	456.7	43.3	56.3	5.3	126.7	12.0	371.6	35.2	1056.0	**95.8**
	25-Aug	35.0	210.0	7.4	0.4	5.3	6.3	364.8	43.4	166.5	19.8	142.7	17.0	322.9	38.4	840.0	**118.7**
	26-Aug	42.0	188.0	4.2	0.8	4.5	9.0	359.3	35.6	94.5	9.4	201.8	20.0	288.8	28.6	1008.0	**93.7**
	27-Aug	58.0	234.0	5.2	0.2	7.8	9.5	587.5	42.2	117.0	8.4	213.8	15.4	362.7	26.1	1392.0	**92.0**
	28-Aug	58.0	333.0	8.4	0.2	8.9	8.2	601.0	43.2	189.0	13.6	184.5	13.3	512.9	36.8	1392.0	**106.8**
	29-Aug	56.0	242.0	6.2	2.8	10.1	8.5	425.3	31.6	139.5	10.4	191.3	14.2	378.2	28.1	1344.0	**84.4**
15		45.0	231.4	6.1	1.3	5.8	8.6	364.3	32.7	137.7	13.3	193.8	18.8	355.8	33.6	1079.5	**98.4**
		8.9	52.6	3.8	1.9	2.6	2.4	159.8		85.2		54.3		81.5		212.7	**11.7**

Batch no. ab7/8	**Date**	**TKN (IN)**	**TKN (AE)**	**TKN (FE)**	**NO3 (AN)**	**NO3 (AE)**	**NO3 (FE)**	**MNd**		**MNte**		**MNne**		**MNw**		**MNti**	**Nbal (%)**
	30-Aug	40.0	220.0	4.0	2.3	6.5	10.2	334.1	34.8	90.0	9.4	230.4	24.0	339.8	35.4	960.0	**103.6**
	31-Aug	46.0	210.0	3.2	1.2	6.0	13.5	496.8	45.0	72.0	6.5	303.8	27.5	324.0	29.3	1104.0	**108.4**
	1-Sep	38.0	260.0	4.5	2.8	2.9	11.0	133.2	14.6	101.3	11.1	246.8	27.1	394.4	43.2	912.0	**96.0**
	2-Sep	36.0	229.0	4.0	2.7	7.2	8.4	289.9	33.6	90.0	10.4	189.0	21.9	354.2	41.0	864.0	**106.8**
	3-Sep	40.0	276.0	4.5	0.5	4.1	7.1	319.2	33.3	101.3	10.5	159.8	16.6	420.2	43.8	960.0	**104.2**
	4-Sep	45.0	220.0	5.3	1.2	7.3	10.3	481.2	44.6	119.3	11.0	230.6	21.4	341.0	31.6	1080.0	**108.5**
	5-Sep	38.0	237.0	5.0	1.2	4.8	8.5	319.2	35.0	112.5	12.3	191.3	21.0	362.7	39.8	912.0	**108.1**
	6-Sep	36.0	210.0	4.2	0.6	5.5	7.2	379.2	43.9	94.5	10.9	162.0	18.8	323.3	37.4	864.0	**111.0**
	7-Sep	35.0	198.0	5.3	1.2	5.3	6.9	304.8	36.3	119.3	14.2	155.3	18.5	305.0	36.3	840.0	**105.3**
	8-Sep	39.0	205.0	3.5	0.8	7.2	8.2	463.7	49.5	78.8	8.4	184.5	19.7	318.2	34.0	936.0	**111.7**
16	**Mean**	39.3	226.5	4.4	1.5	5.7	9.1	352.1	37.0	97.9	10.5	205.3	21.6	348.3	37.2	943.2	106.4
	Std	3.7	24.9	0.7	0.8	1.4	2.1	109.2		16.1		47.2		36.0		88.4	4.5
	9-Sep	33.1	214.0	1.7	0.5	5.2	6.4	355.2	44.7	37.8	4.8	144.0	18.1	328.8	41.4	794.4	**109.0**
	10-Sep	35.1	220.0	1.9	2.9	6.4	6.0	173.8	20.6	41.8	5.0	135.0	16.0	339.6	40.3	842.9	**81.9**
	11-Sep	33.6	218.0	2.8	1.2	2.9	7.2	197.3	24.5	63.0	7.8	162.0	20.1	331.4	41.1	806.4	**93.5**
	12-Sep	30.3	185.0	2.8	0.8	4.2	6.3	274.1	37.7	63.0	8.7	141.8	19.5	283.7	39.0	727.2	**104.9**
	13-Sep	33.3	210.0	3.9	1.2	6.1	6.5	334.1	41.9	87.8	11.0	146.3	18.3	324.2	40.6	798.0	**111.8**
	14-Sep	33.0	211.0	2.8	1.2	6.3	10.3	430.8	54.4	63.0	8.0	230.6	29.1	325.9	41.1	792.0	**132.6**
	15-Sep	33.0	211.0	2.8	1.6	7.2	9.2	412.8	52.1	63.0	8.0	207.0	26.1	327.3	41.3	792.0	**127.5**
	16-Sep	31.0	215.0	0.6	2.5	6.5	9.1	291.8	39.2	12.6	1.7	204.8	27.5	332.3	44.7	744.0	**113.1**
	17-Sep	29.0	210.0	1.7	3.7	6.6	7.5	140.6	20.2	37.8	5.4	168.8	24.2	324.9	46.7	696.0	**96.6**
	18-Sep	33.2	198.0	4.2	2.3	7.2	9.3	346.1	43.4	95.2	11.9	209.3	26.3	307.7	38.6	797.0	**120.2**
17		32.5	209.2	2.5	1.8	5.9	7.8	295.7	37.9	56.5	7.2	174.9	22.5	322.6	41.5	779.0	**109.1**

		1.8	10.4	1.1	1.0	1.4	1.5	99.2		24.7		34.8		15.9		43.3	15.6
Batch no.	**Date**	**TKN (IN)**	**TKN (AE)**	**TKN (FE)**	**NO3 (AN)**	**NO3 (AE)**	**NO3 (FE)**	**MNd**		**MNte**		**MNne**		**MNw**		**MNti**	**Nbal (%)**
	19-Sep	35.0	178.0	5.0	1.7	4.3	9.8	276.0	32.9	112.5	13.4	220.5	26.3	273.4	32.5	840.0	**105.0**
ab9/10	20-Sep	36.0	115.0	8.0	1.2	5.4	8.6	350.4	40.6	180.0	20.8	193.5	22.4	180.6	20.9	864.0	**104.7**
	21-Sep	34.0	115.0	8.0	4.1	5.1	10.5	104.6	12.8	180.0	22.1	236.3	29.0	180.1	22.1	816.0	**85.9**
	22-Sep	38.0	218.0	4.0	0.4	5.4	7.8	407.0	44.6	90.0	9.9	175.5	19.2	335.1	36.7	912.0	**110.5**
	23-Sep	36.0	118.0	8.0	2.3	8.8	7.4	378.2	43.8	180.0	20.8	166.5	19.3	190.2	22.0	864.0	**105.9**
	24-Sep	34.0	115.0	8.0	2.4	7.5	7.4	307.2	37.6	180.0	22.1	166.5	20.4	183.8	22.5	816.0	**102.6**
	25-Sep	35.0	118.0	5.0	2.5	9.9	5.2	360.0	42.9	112.5	13.4	116.1	13.8	191.9	22.8	840.0	**92.9**
	26-Sep	36.0	118.0	8.0	2.3	7.5	8.5	343.4	39.8	180.0	20.8	191.5	22.2	188.3	21.8	864.0	**104.5**
	27-Sep	35.0	145.0	4.5	0.3	7.2	9.5	543.6	64.7	101.3	12.1	212.6	25.3	228.3	27.2	840.0	**129.3**
	28-Sep	35.0	115.0	5.0	0.9	5.1	7.3	329.8	39.3	112.5	13.4	164.3	19.6	180.2	21.4	840.0	**93.7**
18		35.4	135.5	6.4	1.8	6.6	8.2	340.0	39.9	142.9	16.9	184.3	21.7	213.2	25.0	849.6	**103.5**
		1.2	35.4	1.8	1.1	1.8	1.5	109.8		39.7		34.5		52.1		28.2	11.7
	29-Sep	40.0	210.0	5.6	1.2	7.5	9.9	483.1	50.3	126.0	13.1	221.6	23.1	326.3	34.0	960.0	**120.5**
	30-Sep	38.0	224.0	4.0	0.0	4.2	6.5	360.0	39.5	90.0	9.9	147.2	16.1	342.3	37.5	912.0	**103.0**
	1-Oct	38.0	234.0	3.4	0.3	4.5	6.0	330.2	36.2	75.6	8.3	134.1	14.7	357.8	39.2	912.0	**98.4**
	2-Oct	38.0	106.0	3.4	0.2	7.3	9.7	562.8	61.7	76.5	8.4	217.1	23.8	170.0	18.6	912.0	**112.5**
	3-Oct	40.0	112.0	3.4	1.2	6.2	7.1	352.3	36.7	76.5	8.0	159.3	16.6	177.3	18.5	960.0	**79.7**
	4-Oct	45.0	217.0	5.0	1.3	6.4	6.6	339.8	31.5	112.5	10.4	147.6	13.7	335.1	31.0	1080.0	**86.6**
	5-Oct	38.0	218.0	4.5	1.2	7.8	11.8	542.4	59.5	101.3	11.1	265.5	29.1	338.7	37.1	912.0	**136.8**
	6-Oct	42.0	237.0	4.5	0.7	6.9	9.8	499.2	49.5	101.3	10.0	220.5	21.9	365.9	36.3	1008.0	**117.7**
	7-Oct	48.0	229.0	5.0	1.2	12.4	13.5	802.8	69.7	112.5	9.8	302.6	26.3	362.1	31.4	1152.0	**137.2**
	8-Oct	54.0	226.0	5.3	1.4	8.9	8.6	499.0	38.5	119.3	9.2	193.3	14.9	352.4	27.2	1296.0	**89.8**
19		42.1	201.3	4.4	0.9	7.2	8.9	477.2	47.3	99.1	9.8	200.9	20.0	312.8	31.1	1010.4	108.2
		5.4	49.3	0.8	0.5	2.3	2.5	144.7		18.7		55.4		74.4		129.2	20.2
Batch no.	**Date**	**TKN (IN)**	**TKN (AE)**	**TKN (FE)**	**NO3 (AN)**	**NO3 (AE)**	**NO3 (FE)**	**MNd**		**MNte**		**MNne**		**MNw**		**MNti**	**Nbal (%)**
	9-Oct	42.0	226.0	3.5	0.3	6.2	8.3	469.9	46.6	78.8	7.8	186.8	18.5	348.4	34.6	1008.0	**107.5**
	10-Oct	42.0	232.0	2.4	0.8	6.5	7.9	424.8	42.1	54.0	5.4	177.8	17.6	357.8	35.5	1008.0	**100.6**
	11-Oct	41.0	218.0	5.4	1.3	5.9	8.8	369.6	37.6	121.5	12.3	198.0	20.1	335.9	34.1	984.0	**104.2**

	12-Oct	38.0	237.0	5.0	2.4	7.2	8.4	314.9	34.5	112.5	12.3	189.0	20.7	366.2	40.2	912.0	**107.7**
	13-Oct	40.0	229.0	3.4	0.5	7.1	7.9	482.4	50.3	76.5	8.0	177.8	18.5	354.2	36.9	960.0	**113.6**
	14-Oct	41.0	226.0	5.0	0.2	6.3	8.4	482.4	49.0	112.5	11.4	189.0	19.2	348.4	35.4	984.0	**115.1**
	15-Oct	43.0	232.0	5.6	0.1	6.4	7.8	484.8	47.0	126.0	12.2	175.5	17.0	357.6	34.7	1032.0	**110.8**
	16-Oct	38.0	218.0	6.2	0.6	6.4	7.4	427.9	46.9	139.5	15.3	167.2	18.3	336.6	36.9	912.0	**117.5**
	17-Oct	38.0	237.0	3.4	1.2	6.7	8.6	413.0	45.3	76.5	8.4	193.7	21.2	365.6	40.1	912.0	**115.0**
	18-Oct	38.0	240.0	3.4	0.8	6.5	6.9	400.8	43.9	76.5	8.4	155.3	17.0	369.8	40.5	912.0	**109.9**
20		40.1	229.5	4.3	0.8	6.5	8.0	427.1	44.3	97.4	10.2	181.0	18.8	354.0	36.9	962.4	110.2
		2.0	7.6	1.3	0.7	0.4	0.6	55.9		28.2		13.0		11.8		47.3	5.3

Batch no.	**Date**	**TKN (IN)**	**TKN (AE)**	**TKN (FE)**	**NO3 (AN)**	**NO3 (AE)**	**NO3 (FE)**	**MNd**		**MNte**		**MNne**		**MNw**		**MNti**	**Nbal (%)**
	19-Oct	44.0	186.0	5.0	0.3	7.2	8.5	519.8	49.2	112.5	10.7	191.3	18.1	289.9	27.4	1056.0	**105.4**
	20-Oct	48.0	203.0	4.5	1.2	10.4	9.5	613.0	53.2	101.3	8.8	213.8	18.6	320.1	27.8	1152.0	**108.3**
hetero	21-Oct	40.0	190.0	4.5	2.3	8.9	9.5	434.9	45.3	101.3	10.5	213.8	22.3	298.4	31.1	960.0	**109.2**
	22-Oct	40.0	200.0	5.0	2.7	7.2	8.4	289.9	30.2	112.5	11.7	189.0	19.7	310.7	32.4	960.0	**94.0**
	23-Oct	40.0	210.0	3.4	0.5	6.1	8.1	439.7	45.8	76.5	8.0	182.3	19.0	324.2	33.8	960.0	**106.5**
	24-Oct	41.0	176.0	5.0	1.2	6.8	9.2	432.0	43.9	112.5	11.4	207.0	21.0	274.2	27.9	984.0	**104.2**
	25-Oct	36.0	180.0	4.5	2.1	5.9	10.1	324.0	37.5	101.3	11.7	227.3	26.3	278.9	32.3	864.0	**107.8**
	26-Oct	40.0	218.0	4.5	0.6	6.5	7.7	441.4	46.0	101.3	10.5	173.9	18.1	336.8	35.1	960.0	**109.7**
	27-Oct	40.0	210.0	5.0	1.2	6.6	8.6	407.3	42.4	112.5	11.7	193.7	20.2	324.9	33.8	960.0	**108.2**
	28-Oct	40.0	200.0	3.4	0.8	6.0	7.3	386.4	40.3	76.5	8.0	164.3	17.1	309.0	32.2	960.0	**97.5**
21	mean	40.9	197.3	4.5	1.3	7.2	8.7	428.8	43.4	100.8	10.3	195.6	20.0	306.7	31.4	981.6	105.1
	std	3.1	13.9	0.6	0.8	1.4	0.9	91.3		13.9		19.7		20.9		75.4	5.3
	29-Oct	40.0	220.0	4.0	0.3	6.0	7.5	436.3	45.5	90.0	9.4	168.8	17.6	339.0	35.3	960.0	**107.7**
	30-Oct	46.0	210.0	3.2	1.2	6.3	13.5	511.2	46.3	72.0	6.5	303.8	27.5	324.5	29.4	1104.0	**109.7**
	31-Oct	38.0	260.0	4.5	2.8	2.9	11.0	133.2	14.6	101.3	11.1	246.8	27.1	394.4	43.2	912.0	**96.0**
	1-Nov	38.0	229.0	4.0	2.7	7.2	8.4	289.9	31.8	90.0	9.9	189.0	20.7	354.2	38.8	912.0	**101.2**
	2-Nov	42.0	276.0	4.5	0.5	5.6	7.8	408.0	40.5	101.3	10.0	175.5	17.4	422.4	41.9	1008.0	**109.8**
	3-Nov	45.0	220.0	5.3	1.2	6.3	8.9	400.8	37.1	119.3	11.0	200.3	18.5	339.5	31.4	1080.0	**98.1**
	4-Nov	46.0	237.0	5.0	0.8	7.2	8.5	472.8	42.8	112.5	10.2	191.3	17.3	366.3	33.2	1104.0	**103.5**
	5-Nov	39.0	210.0	4.2	0.6	6.5	7.7	441.4	47.2	94.5	10.1	173.9	18.6	324.8	34.7	936.0	**110.5**
	6-Nov	41.0	198.0	5.3	1.2	6.6	8.6	407.3	41.4	119.3	12.1	193.7	19.7	306.9	31.2	984.0	**104.4**
	7-Nov	39.0	205.0	3.5	0.8	6.0	8.6	417.6	44.6	78.8	8.4	193.5	20.7	316.5	33.8	936.0	**107.5**

22	mean	41.4	226.5	4.4	1.2	6.1	9.1	391.8	39.2	97.9	9.9	203.6	20.5	348.8	35.3	993.6	104.9
	std	3.2	24.9	0.7	0.9	1.2	1.8	107.4		16.1		41.3		36.5		76.9	5.1

TABLE 9.2: Daily experimental data and COD mass balance for parent system in 2004

COD mass balance 2004

	Rs	V	Q	a	s	Yh		Fcv				Qw		V (Aer)
Unit	day	L	(L/d)	Recycle ratio		mgVss/mgCOD		mgCOD/mgVSS				L		L
Value	**10**	**15**	**24**	**2**	**1**	**0.45**		**1.48**				**1.5**		**9**

Batch no	Date	COD(IN)	COD (ml)	COD (FE)	OUR	Mste	%	Msti	MXsvw	%	Moc	%	Mod	%	COD(%)
	3-Apr	554.0	4820.0	42.0	30.1	945.0	7.1	13296.0	7230.0	54.4	5975.1	44.9	679.5	5.1	**111.5**
1	4-Apr	566.0	4400.0	66.0	30.3	1485.0	10.9	13584.0	6600.0	48.6	4781.3	35.2	1105.1	8.1	**102.9**
	5-Apr	505.0	3790.0	60.0	30.6	1350.0	11.1	12120.0	5685.0	46.9	4990.7	41.2	1180.6	9.7	**109.0**
	6-Apr	552.0	3520.0	48.0	30.7	1080.0	8.2	13248.0	5280.0	39.9	4795.1	36.2	974.7	7.4	**91.6**
	7-Apr	428.0	3680.0	34.0	30.7	765.0	7.4	10272.0	5520.0	53.7	4913.7	47.8	528.5	5.1	**114.2**
	8-Apr	480.0	3460.0	40.0	30.7	900.0	7.8	11520.0	5190.0	45.1	4349.9	37.8	1105.1	9.6	**100.2**
	9-Apr	426.0	3900.0	50.0	30.8	1125.0	11.0	10224.0	5850.0	57.2	4941.8	48.3	995.3	9.7	**126.3**
	10-Apr	510.0	3520.0	40.0	30.9	900.0	7.4	12240.0	5280.0	43.1	5180.6	42.3	1077.6	8.8	**101.6**
	11-Apr	490.0	3130.0	40.0	30.8	900.0	7.7	11760.0	4695.0	39.9	6126.3	52.1	775.6	6.6	**106.3**
	12-Apr	515.0	2980.0	40.0	30.9	900.0	7.3	12360.0	4470.0	36.2	5663.2	45.8	748.2	6.1	**95.3**
	Mean	502.6	3720.0	46.0	30.6	1035.0	8.6	12062.4	5580.0	46.5	5171.8	43.2	917.0	7.6	**105.9**
	Stdev	48.8	553.2	10.1	0.3	227.5		1170.8	829.8		569.6		218.9		**10.0**
	13-Apr														

	14-Apr														
	15-Apr														
	16-Apr														
	17-Apr														
	18-Apr														
	19-Apr	464.0	2430.0	44.0	28.0	990.0	8.9	11136.0	3645.0	32.7	3371.8	30.3	1613.0	14.5	**86.4**
	20-Apr	434.0	2740.0	72.0	27.0	1620.0	15.6	10416.0	4110.0	39.5	2804.8	26.9	1832.7	17.6	**99.5**
	21-Apr	520.0	2890.0	52.0	27.0	1170.0	9.4	12480.0	4335.0	34.7	4121.0	33.0	1400.3	11.2	**88.4**
	22-Apr	550.0	2850.0	60.0	27.0	1350.0	10.2	13200.0	4275.0	32.4	2453.9	18.6	1791.5	13.6	**74.8**
2	Mean	492.0	2727.5	57.0	27.3	1282.5	11.0	11808.0	4091.3	34.8	3187.9	27.2	1659.4	14.2	**87.3**
	Stdev	52.6	208.2	11.9	0.5										10.1
Batch no	**Date**	**COD(IN)**	**COD (ml)**	**COD (FE)**	**OUR**	**Mste**		**Msti**	**MXsvw**		**Moc**		**Mod**		**COD bal (%)**
	23-Apr	515.0	3450.0	46.0	30.1	1035.0	8.4	12360.0	5175.0	41.9	4755.4	38.5	967.8	7.8	**96.5**
	24-Apr	490.0	3220.0	38.0	30.3	855.0	7.3	11760.0	4830.0	41.1	3995.9	34.0	1462.0	12.4	**94.8**
	25-Apr	498.0	2770.0	40.0	30.3	900.0	7.5	11952.0	4155.0	34.8	4349.0	36.4	1022.7	8.6	**87.2**
	26-Apr	512.0	3190.0	50.0	30.5	1125.0	9.2	12288.0	4785.0	38.9	5048.2	41.1	912.9	7.4	**96.6**
	27-Apr	505.0	3310.0	62.0	30.5	1395.0	11.5	12120.0	4965.0	41.0	4743.2	39.1	1084.5	8.9	**100.6**
	28-Apr														
	29-Apr														
	30-Apr														
	1-May														
3	Mean	504.0	3188.0	47.2	30.3	1062.0	8.8	12096.0	4782.0	39.5	4578.3	37.8	1090.0	9.0	**95.1**
	Stdev	10.2	254.6	9.5	0.1										**4.9**
	2-May	476.0	2897.0	54.0	32.1	1215.0	10.6	11424.0	4345.5	38.0	4724.3	41.4	1018.9	8.9	**98.9**
	3-May	408.0	2897.0	42.0	30.8	945.0	9.7	9792.0	4345.5	44.4	5645.8	57.7	523.0	5.3	**117.0**
	4-May	514.0	2674.0	51.0	30.5	1147.5	9.3	12336.0	4011.0	32.5	4684.1	38.0	1024.1	8.3	**88.1**
	5-May	538.0	2855.0	45.0	31.9	1012.5	7.8	12912.0	4282.5	33.2	5783.6	44.8	685.9	5.3	**91.1**
	6-May	512.0	2846.0	45.0	30.9	1012.5	8.2	12288.0	4269.0	34.7	5367.1	43.7	790.7	6.4	**93.1**
	7-May	464.0	2666.0	46.0	33.1	1035.0	9.3	11136.0	3999.0	35.9	6168.2	55.4	722.6	6.5	**107.1**
	8-May	562.0	2436.0	55.0	29.9	1237.5	9.2	13488.0	3654.0	27.1	5331.1	39.5	841.5	6.2	**82.0**
	9-May	505.0	2858.0	50.0	30.9	1125.0	9.3	12120.0	4287.0	35.4	6672.2	55.1	499.7	4.1	**103.8**
	10-May	498.0	2858.0	48.0	33.5	1080.0	9.0	11952.0	4287.0	35.9	6640.2	55.6	823.1	6.9	**107.3**

	11-May	525.0	2978.0	36.0	33.9	810.0	6.4	12600.0	4467.0	35.5	6256.6	49.7	787.7	6.3	**97.8**
4	Mean	500.2	2796.5	47.2	31.7	1062.0	8.9	12004.8	4194.8	35.3	5727.3	48.1	771.7	6.4	**98.6**
	Stdev	43.0	159.4	5.7	1.4										10.5
Batch no	**Date**	**COD(IN)**	**COD (ml)**	**COD (FE)**	**OUR**	**Mste**		**Msti**	**MXsvw**		**Moc**		**Mod**		**COD bal (%)**
	12-May	482.0	2763.0	34.0	30.5	765.0	6.6	11568.0	4144.5	35.8	5611.9	48.5	354.2	3.1	**94.0**
	13-May	485.0	2433.0	36.0	31.5	810.0	7.0	11640.0	3649.5	31.4	5461.5	46.9	1068.7	9.2	**94.4**
	14-May	517.0	2804.0	40.0	30.8	900.0	7.3	12408.0	4206.0	33.9	5352.1	43.1	937.6	7.6	**91.8**
	15-May	511.0	2442.0	40.0	30.7	900.0	7.3	12264.0	3663.0	29.9	6072.0	49.5	638.4	5.2	**91.9**
	16-May	519.0	3242.0	43.0	30.5	967.5	7.8	12456.0	4863.0	39.0	5662.2	45.5	678.8	5.4	**97.7**
	17-May	490.0	2936.0	38.0	30.6	855.0	7.3	11760.0	4404.0	37.4	5061.0	43.0	1098.2	9.3	**97.1**
	18-May	500.0	2836.0	34.0	30.8	765.0	6.4	12000.0	4254.0	35.5	5040.7	42.0	1002.1	8.4	**92.2**
	19-May	480.0	2812.0	38.0	30.8	855.0	7.4	11520.0	4218.0	36.6	6165.7	53.5	820.2	7.1	**104.7**
	20-May	448.0	2159.0	46.0	30.7	1035.0	9.6	10752.0	3238.5	30.1	6072.0	56.5	765.3	7.1	**103.3**
	21-May	475.0	2055.0	46.0	30.8	1035.0	9.1	11400.0	3082.5	27.0	5536.2	48.6	967.8	8.5	**93.2**
5	Mean	490.7	2648.2	39.5	30.8	888.8	7.6	11776.8	3972.3	33.7	5603.5	47.7	833.2	7.1	**96.0**
	Stdev	21.8	367.4	4.4	0.3										4.7
	22-May	514.0	3666.0	46.0	30.7	1035.0	8.4	12336.0	5499.0	44.6	6576.5	53.3	652.1	5.3	**111.6**
	23-May	559.0	3010.0	48.0	35.4	1080.0	8.1	13416.0	4515.0	33.7	7466.6	55.7	645.2	4.8	**102.2**
	24-May	507.0	3142.0	36.0	32.6	810.0	6.7	12168.0	4713.0	38.7	4751.6	39.1	1091.4	9.0	**93.4**
	25-May	501.0	3107.0	41.0	31.3	922.5	7.7	12024.0	4660.5	38.8	4966.4	41.3	1022.7	8.5	**96.2**
	26-May	521.0	2875.0	46.0	31.0	1035.0	8.3	12504.0	4312.5	34.5	4506.7	36.0	1263.0	10.1	**88.9**
	27-May	485.0	3165.0	60.0	32.1	1350.0	11.6	11640.0	4747.5	40.8	4643.6	39.9	1276.7	11.0	**103.2**
	28-May	511.0	3130.0	51.0	30.8	1147.5	9.4	12264.0	4695.0	38.3	4816.7	39.3	1145.6	9.3	**96.3**
	29-May	478.0	2382.0	52.0	30.5	1170.0	10.2	11472.0	3573.0	31.1	5701.9	49.7	864.9	7.5	**98.6**
	30-May	522.0	3173.0	45.0	31.9	1012.5	8.1	12528.0	4759.5	38.0	5962.6	47.6	954.1	7.6	**101.3**
	31-May	523.0	2640.0	58.0	30.9	1305.0	10.4	12552.0	3960.0	31.5	4165.1	33.2	1249.2	10.0	**85.1**
6	Mean	512.1	3029.0	48.3	31.7	1086.8	8.9	12290.4	4543.5	37.0	5355.8	43.5	1016.5	8.3	**97.7**
	Stdev	22.5	344.5	7.3	1.5	164.0		539.4	516.7		1048.1		236.3		7.6
	1-Jun	516.0	2855.0	53.0	31.6	1192.5	9.6	12384.0	4282.5	34.6	4489.6	36.3	768.8	6.2	**86.7**
	2-Jun	488.0	2778.0	36.0	31.6	810.0	6.9	11712.0	4167.0	35.6	5511.6	47.1	906.0	7.7	**97.3**
	3-Jun	514.0	2958.0	43.0	31.8	967.5	7.8	12336.0	4437.0	36.0	2979.6	24.2	2622.0	21.3	**89.2**

	4-Jun	522.0	3122.0	65.0	31.8	1462.5	11.7	12528.0	4683.0	37.4	4044.8	32.3	1395.3	11.1	**92.5**
	5-Jun	565.0	3268.0	60.0	31.9	1350.0	10.0	13560.0	4902.0	36.2	3784.1	27.9	1283.6	9.5	**83.5**
	6-Jun	553.0	2477.0	55.0	32.2	1237.5	9.3	13272.0	3715.5	28.0	4777.1	36.0	1541.7	11.6	**84.9**
	7-Jun	526.0	2864.0	52.0	32.2	1170.0	9.3	12624.0	4296.0	34.0	3478.2	27.6	1871.1	14.8	**85.7**
	8-Jun	485.0	2898.0	58.0	32.3	1305.0	11.2	11640.0	4347.0	37.3	-380.9	-3.3	3371.9	29.0	**74.3**
	9-Jun	480.0	3070.0	50.0	32.3	1125.0	9.8	11520.0	4605.0	40.0	3710.5	32.2	1805.2	15.7	**97.6**
	10-Jun	485.0	2778.0	65.0	32.5	1462.5	12.6	11640.0	4167.0	35.8	5168.7	44.4	1276.7	11.0	**103.7**
7	Mean	513.4	2906.8	53.7	32.0	1208.3	9.8	12321.6	4360.2	35.5	3756.3	30.5	1684.2	13.8	**89.5**
	Stdev	29.5	218.2	9.2	0.3	206.8		708.5	327.3		1651.2		792.4		8.5
Batch no	**Date**	**COD(IN)**	**COD (ml)**	**COD (FE)**	**OUR**	**Mste**		**Msti**	**MXsvw**		**Moc**		**Mod**		**COD bal (%)**
	11-Jun	520.0	2898.0	58.0	35.6	1305.0	10.5	12480.0	4347.0	34.8	6202.3	49.7	1057.1	8.5	**103.5**
	12-Jun	567.0	3233.0	60.0	35.3	1350.0	9.9	13608.0	4849.5	35.6	6097.9	44.8	1118.8	8.2	**98.6**
	13-Jun	507.0	2989.0	56.0	35.0	1260.0	10.4	12168.0	4483.5	36.8	5621.0	46.2	1345.3	11.1	**104.5**
	14-Jun	517.0	2867.0	56.0	34.7	1260.0	10.2	12408.0	4300.5	34.7	6095.6	49.1	885.5	7.1	**101.1**
	15-Jun	500.0	2952.0	38.0	34.4	855.0	7.1	12000.0	4428.0	36.9	5269.9	43.9	940.4	7.8	**95.8**
	16-Jun	479.0	2707.0	41.0	33.9	922.5	8.0	11496.0	4060.5	35.3	4867.7	42.3	1173.7	10.2	**95.9**
	17-Jun	547.0	3046.0	36.0	33.4	810.0	6.2	13128.0	4569.0	34.8	2735.1	20.8	2148.4	16.4	**78.2**
	18-Jun	517.0	2764.0	36.0	32.9	810.0	6.5	12408.0	4146.0	33.4	2986.8	24.1	2010.5	16.2	**80.2**
	19-Jun	512.0	2855.0	49.0	32.5	1102.5	9.0	12288.0	4282.5	34.9	4615.7	37.6	1120.9	9.1	**90.5**
	20-Jun	498.0	3318.0	52.0	32.0	1170.0	9.8	11952.0	4977.0	41.6	3702.7	31.0	1880.7	15.7	**98.1**
8	Mean	516.4	2962.9	48.2	34.0	1084.5	8.7	12393.6	4444.4	35.9	4819.5	39.0	1368.1	11.0	**94.6**
	Stdev	25.0	193.5	9.6	1.2	215.5		600.0	290.2		1291.6		466.5		9.1
	21-Jun	532.0	2858.0	48.0	28.7	1080.0	8.5	12768.0	4287.0	33.6	4617.6	36.2	1029.6	8.1	**86.3**
	22-Jun	496.0	3854.0	58.0	27.5	1305.0	11.0	11904.0	5781.0	48.6	4038.3	33.9	1207.4	10.1	**103.6**
	23-Jun	512.0	3797.0	34.0	29.0	765.0	6.2	12288.0	5695.5	46.4	4294.1	34.9	1081.8	8.8	**96.3**
	24-Jun	485.0	3375.0	52.0	24.2	1170.0	10.1	11640.0	5062.5	43.5	2290.1	19.7	1400.9	12.0	**85.3**
	25-Jun	522.0	3835.0	43.0	29.0	967.5	7.7	12528.0	5752.5	45.9	4449.9	35.5	936.9	7.5	**96.6**
	26-Jun	518.0	3986.0	41.0	26.5	922.5	7.4	12432.0	5979.0	48.1	3798.0	30.5	816.8	6.6	**92.6**
	27-Jun	506.0	4004.0	39.0	24.6	877.5	7.2	12144.0	6006.0	49.5	2927.1	24.1	1289.1	10.6	**91.4**
	28-Jun	511.0	4211.0	45.0	24.6	1012.5	8.3	12264.0	6316.5	51.5	2484.0	20.3	1259.5	10.3	**90.3**
	29-Jun	495.0	3158.0	56.0	26.3	1260.0	10.6	11880.0	4737.0	39.9	3577.2	30.1	1135.3	9.6	**90.1**
	30-Jun	483.0	3450.0	52.0	26.4	1170.0	10.1	11592.0	5175.0	44.6	2532.8	21.8	1712.6	14.8	**91.4**

9	Mean	506.0	3652.8	46.8	26.7	1053.0	8.7	12144.0	5479.2	45.1	3500.9	28.7	1187.0	9.8	**92.4**
	Stdev	16.1	426.3	7.8	1.9			386.0	639.4		877.3		253.0		5.4
	1-Jul	468.0	3224.0	48.0	34.9	1080.0	9.6	11232.0	4836.0	43.1	5908.6	52.6	865.6	7.7	**113.0**
	2-Jul	481.0	2942.0	38.0	34.9	855.0	7.4	11544.0	4413.0	38.2	5531.2	47.9	990.5	8.6	**102.1**
	3-Jul	472.0	2942.0	38.0	34.9	855.0	7.5	11328.0	4413.0	39.0	5814.3	51.3	909.5	8.0	**105.9**
	4-Jul	522.0	2886.0	38.0	34.7	855.0	6.8	12528.0	4329.0	34.6	5542.8	44.2	1114.7	8.9	**94.5**
	5-Jul	455.0	3271.0	32.0	34.6	720.0	6.6	10920.0	4906.5	44.9	3999.0	36.6	1514.9	13.9	**102.0**
	6-Jul	447.0	3111.0	38.0	34.4	855.0	8.0	10728.0	4666.5	43.5	5144.6	48.0	1072.2	10.0	**109.4**
	7-Jul	523.0	3083.0	36.0	34.3	810.0	6.5	12552.0	4624.5	36.8	5221.8	41.6	1009.0	8.0	**92.9**
	8-Jul	512.0	2970.0	48.0	36.6	1080.0	8.8	12288.0	4455.0	36.3	5819.6	47.4	1261.6	10.3	**102.7**
	9-Jul	511.0	2294.0	58.0	37.0	1305.0	10.6	12264.0	3441.0	28.1	5353.2	43.6	945.2	7.7	**90.1**
	10-Jul	520.0	3713.0	41.0	37.2	922.5	7.4	12480.0	5569.5	44.6	6148.7	49.3	863.5	6.9	**108.2**
10	Mean	491.1	3043.6	41.5	35.3	933.8	7.9	11786.4	4565.4	38.9	5448.4	46.3	1054.7	9.0	**102.1**
	Stdev	29.6	357.7	7.6	1.1	172.1		710.6	536.5		600.3		202.8		7.5

Batch no	**Date**	**COD(IN)**	**COD (ml)**	**COD (FE)**	**OUR**	**Mste**		**Msti**	**MXsvw**		**Moc**		**Mod**		**COD bal (%)**
	11-Jul	518.0	3196.0	32.0	35.6	720.0	5.8	12432.0	4794.0	38.6	6333.9	50.9	1094.8	8.8	**104.1**
	12-Jul	526.0	2989.0	34.0	35.3	765.0	6.1	12624.0	4483.5	35.5	5084.5	40.3	1272.6	10.1	**91.9**
	13-Jul	489.0	3250.0	34.0	35.0	765.0	6.5	11736.0	4875.0	41.5	4611.9	39.3	1724.2	14.7	**102.0**
	14-Jul	475.0	2450.0	52.0	34.7	1170.0	10.3	11400.0	3675.0	32.2	4336.3	38.0	1778.5	15.6	**96.1**
	15-Jul	521.0	3450.0	39.0	34.4	877.5	7.0	12504.0	5175.0	41.4	4664.4	37.3	1405.7	11.2	**97.0**
	16-Jul	523.0	3835.0	52.0	33.9	1170.0	9.3	12552.0	5752.5	45.8	4828.2	38.5	1321.3	10.5	**104.1**
	17-Jul	547.0	3328.0	41.0	33.4	922.5	7.0	13128.0	4992.0	38.0	4244.3	32.3	1560.2	11.9	**89.3**
	18-Jul	533.0	3140.0	47.0	32.9	1057.5	8.3	12792.0	4710.0	36.8	4811.8	37.6	1159.3	9.1	**91.8**
	19-Jul	505.0	2390.0	38.0	32.5	855.0	7.1	12120.0	3585.0	29.6	5036.9	41.6	827.1	6.8	**85.0**
	20-Jul	480.0	3100.0	36.0	32.0	810.0	7.0	11520.0	4650.0	40.4	3321.0	28.8	1735.2	15.1	**91.3**
11	Mean	511.7	3112.8	40.5	34.0	911.3	7.4	12280.8	4669.2	38.0	4727.3	38.5	1387.9	11.4	**95.3**
	Stdev	23.7	432.7	7.4	1.2	166.4		569.6	649.1		760.3		313.9		6.6
	21-Jul	490.0	3280.0	36.0	30.4	810.0	6.9	11760.0	4920.0	41.8	3355.1	28.5	1365.9	11.6	**88.9**
	22-Jul	502.0	3130.0	42.0	30.3	945.0	7.8	12048.0	4695.0	39.0	4871.2	40.4	940.4	7.8	**95.0**
	23-Jul	490.0	2950.0	50.0	30.3	1125.0	9.6	11760.0	4425.0	37.6	4351.2	37.0	1043.3	8.9	**93.1**
	24-Jul	438.0	2420.0	40.0	30.1	900.0	8.6	10512.0	3630.0	34.5	3557.7	33.8	1346.0	12.8	**89.7**

	25-Jul	494.0	3750.0	38.0	30.3	855.0	7.2	11856.0	5625.0	47.4	3441.0	29.0	1379.7	11.6	**95.3**
	26-Jul	480.0	3260.0	48.0	30.0	1080.0	9.4	11520.0	4890.0	42.4	3360.8	29.2	1306.2	11.3	**92.3**
	27-Jul	475.0	3420.0	52.0	30.0	1170.0	10.3	11400.0	5130.0	45.0	2959.4	26.0	1544.4	13.5	**94.8**
	28-Jul	480.0	2970.0	40.0	30.0	900.0	7.8	11520.0	4455.0	38.7	3180.9	27.6	1566.4	13.6	**87.7**
	29-Jul	445.0	3450.0	42.0	32.0	945.0	8.8	10680.0	5175.0	48.5	3439.6	32.2	1716.0	16.1	**105.6**
	30-Jul	450.0	3440.0	51.0	31.0	1147.5	10.6	10800.0	5160.0	47.8	3497.7	32.4	1592.4	14.7	**105.5**
12	Mean	474.4	3207.0	43.9	30.4	987.8	8.7	11385.6	4810.5	42.3	3601.5	31.6	1380.1	12.2	**94.8**
	Stdev	22.3	366.5	5.8	0.6	131.0		535.5	549.8		572.2		243.4		6.3
	31-Jul	528.0	3490.0	44.0	29.6	990.0	7.8	12672.0	5235.0	41.3	2320.0	18.3	2086.7	16.5	**83.9**
	1-Aug	400.0	3250.0	44.0	29.8	990.0	10.3	9600.0	4875.0	50.8	2304.2	24.0	2093.5	21.8	**106.9**
	2-Aug	426.0	3590.0	38.0	29.5	855.0	8.4	10224.0	5385.0	52.7	1508.7	14.8	2560.3	25.0	**100.8**
	3-Aug	440.0	3100.0	50.0	29.7	1125.0	10.7	10560.0	4650.0	44.0	1409.5	13.3	2251.4	21.3	**89.4**
	4-Aug	446.0	3790.0	34.0	29.6	765.0	7.1	10704.0	5685.0	53.1	1537.1	14.4	2347.5	21.9	**96.5**
	5-Aug	364.0	3970.0	36.0	29.6	810.0	9.3	8736.0	5955.0	68.2	2635.9	30.2	1740.7	19.9	**127.5**
	6-Aug	440.0	3830.0	32.0	29.7	720.0	6.8	10560.0	5745.0	54.4	3747.9	35.5	1319.3	12.5	**109.2**
	7-Aug	480.0	3810.0	34.0	29.9	765.0	6.6	11520.0	5715.0	49.6	6653.6	57.8	1486.1	12.9	**126.9**
	8-Aug	486.0	3800.0	44.0	32.1	990.0	8.5	11664.0	5700.0	48.9	4696.1	40.3	2076.4	17.8	**115.4**
13	9-Aug	458.0	3150.0	44.0	26.2	990.0	9.0	10992.0	4725.0	43.0	4595.3	41.8	961.6	8.7	**102.5**
	Mean	446.8	3578.0	40.0	29.6	900.0	8.5	10723.2	5367.0	50.6	3140.8	29.0	1892.3	17.8	**105.9**
	Stdev	45.9	314.9	6.0	1.4	134.2		1100.7	472.3		1735.4		503.0		14.5
	10-Aug	406.0	3270.0	46.0	33.4	1035.0	10.6	9744.0	4905.0	50.3	4132.6	42.4	1565.0	16.1	**119.4**
	11-Aug	505.0	3300.0	38.0	32.2	855.0	7.1	12120.0	4950.0	40.8	2570.4	21.2	2123.7	17.5	**86.6**
	12-Aug	485.0	3240.0	38.0	29.8	855.0	7.3	11640.0	4860.0	41.8	3374.4	29.0	1587.6	13.6	**91.7**
	13-Aug	485.0	3315.0	36.0	29.2	810.0	7.0	11640.0	4972.5	42.7	3089.4	26.5	1469.6	12.6	**88.8**
	14-Aug	500.0	2780.0	38.0	30.3	855.0	7.1	12000.0	4170.0	34.8	3943.3	32.9	1420.2	11.8	**86.6**
	15-Aug	500.0	3230.0	52.0	30.3	1170.0	9.8	12000.0	4845.0	40.4	3901.7	32.5	1315.1	11.0	**93.6**
	16-Aug	495.0	2870.0	48.0	32.2	1080.0	9.1	11880.0	4305.0	36.2	4812.2	40.5	1162.8	9.8	**95.6**
	17-Aug	522.0	3090.0	44.0	30.2	990.0	7.9	12528.0	4635.0	37.0	7120.0	56.8	329.5	2.6	**104.4**
	18-Aug	518.0	2890.0	46.0	32.4	1035.0	8.3	12432.0	4335.0	34.9	5809.5	46.7	1036.5	8.3	**98.3**
	19-Aug	507.0	3465.0	45.0	33.5	1012.5	8.3	12168.0	5197.5	42.7	6205.0	51.0	322.6	2.7	**104.7**
14	Mean	492.3	3145.0	43.1	31.3	969.8	8.2	11815.2	4717.5	40.2	4495.8	38.0	1233.3	10.6	**97.0**

	Stdev	32.7	227.1	5.3	1.6	119.3		783.8	340.6		1466.9		559.4		10.2
Batch no	**Date**	**COD(IN)**	**COD (ml)**	**COD (FE)**	**OUR**	**Mste**		**Msti**	**MXsvw**		**Moc**		**Mod**		**COD bal (%)**
	20-Aug	529.0	3024.0	47.0	33.1	1057.5	8.3	12696.0	4536.0	35.7	7375.7	58.1	119.4	0.9	**103.1**
	21-Aug	491.0	2664.0	31.0	33.3	697.5	5.9	11784.0	3996.0	33.9	5865.8	49.8	698.8	5.9	**95.5**
	22-Aug	457.0	3042.0	36.0	33.3	810.0	7.4	10968.0	4563.0	41.6	5918.3	54.0	948.6	8.6	**111.6**
	23-Aug	443.0	2106.0	36.0	33.5	810.0	7.6	10632.0	3159.0	29.7	6757.9	63.6	660.3	6.2	**107.1**
	24-Aug	454.0	2268.0	36.0	33.5	810.0	7.4	10896.0	3402.0	31.2	4296.6	39.4	1306.2	12.0	**90.1**
	25-Aug	517.0	3186.0	29.0	33.7	652.5	5.3	12408.0	4779.0	38.5	5142.8	41.4	1043.3	8.4	**93.6**
	26-Aug	504.0	2448.0	32.0	33.7	720.0	6.0	12096.0	3672.0	30.4	5631.8	46.6	1027.5	8.5	**91.4**
	27-Aug	473.0	3132.0	38.0	33.8	855.0	7.5	11352.0	4698.0	41.4	3940.3	34.7	1680.3	14.8	**98.4**
	28-Aug	515.0	3472.0	38.0	33.8	855.0	6.9	12360.0	5208.0	42.1	3499.3	28.3	1718.7	13.9	**91.3**
	29-Aug	509.0	3187.0	47.0	34.0	1057.5	8.7	12216.0	4780.5	39.1	4104.2	33.6	1216.3	10.0	**91.3**
15	Mean	489.2	2852.9	37.0	33.5	832.5	7.1	11740.8	4279.4	36.4	5253.3	44.9	1042.0	8.9	**97.3**
	Std	30.4	453.2	6.1	0.3	136.2		729.3	679.8		1281.4		481.8		7.5
	30-Aug	482.0	3150.0	41.0	32.4	922.5	8.0	11568.0	4725.0	40.8	5162.5	44.6	955.5	8.3	**101.7**
	31-Aug	463.0	2898.0	43.0	30.4	967.5	8.7	11112.0	4347.0	39.1	4454.1	40.1	1420.8	12.8	**100.7**
	1-Sep	509.0	2925.0	41.0	29.8	922.5	7.6	12216.0	4387.5	35.9	6397.2	52.4	381.0	3.1	**99.0**
	2-Sep	463.0	3096.0	32.0	29.9	720.0	6.5	11112.0	4644.0	41.8	4488.5	40.4	829.2	7.5	**96.1**
	3-Sep	522.0	3258.0	45.0	30.6	1012.5	8.1	12528.0	4887.0	39.0	5030.2	40.2	912.9	7.3	**94.5**
	4-Sep	500.0	3250.0	45.0	30.6	1012.5	8.4	12000.0	4875.0	40.6	3933.4	32.8	1376.2	11.5	**93.3**
	5-Sep	486.0	3222.0	38.0	29.9	855.0	7.3	11664.0	4833.0	41.4	4883.3	41.9	912.9	7.8	**98.5**
	6-Sep	472.0	2340.0	36.0	29.9	810.0	7.2	11328.0	3510.0	31.0	4313.0	38.1	1084.5	9.6	**85.8**
	7-Sep	454.0	2619.0	36.0	29.9	810.0	7.4	10896.0	3928.5	36.1	4664.0	42.8	871.7	8.0	**94.3**
	8-Sep	443.0	2736.0	45.0	29.9	1012.5	9.5	10632.0	4104.0	38.6	3672.5	34.5	1326.1	12.5	**95.1**
16	Mean	479.4	2949.4	40.2	30.3	904.5	7.9	11505.6	4424.1	38.4	4699.9	40.8	1007.1	8.8	**95.9**
	Std	25.2	307.5	4.5	0.8	102.2		605.5	461.2		755.5		312.3		4.6
Batch no	**Date**	**COD(IN)**	**COD (ml)**	**COD (FE)**	**OUR**	**Mste**		**Msti**	**MXsvw**		**Moc**		**Mod**		**COD bal (%)**
	9-Sep	369.0	2241.0	41.0	29.9	922.5	10.4	8856.0	3361.5	38.0	4389.9	49.6	1015.9	11.5	**109.4**
	10-Sep	434.0	2574.0	40.0	29.9	900.0	8.6	10416.0	3861.0	37.1	4918.4	47.2	497.0	4.8	**97.7**
	11-Sep	423.0	2367.0	40.0	30.0	900.0	8.9	10152.0	3550.5	35.0	5729.8	56.4	564.2	5.6	**105.8**
	12-Sep	409.0	2268.0	41.0	30.0	922.5	9.4	9816.0	3402.0	34.7	5005.9	51.0	783.9	8.0	**103.0**
	13-Sep	409.0	2691.0	49.0	31.0	1102.5	11.2	9816.0	4036.5	41.1	4541.9	46.3	955.5	9.7	**108.4**

	14-Sep	457.0	2620.0	40.0	29.9	900.0	8.2	10968.0	3930.0	35.8	4247.2	38.7	1232.1	11.2	**94.0**
	15-Sep	360.0	2750.0	27.0	29.9	607.5	7.0	8640.0	4125.0	47.7	4005.9	46.4	1180.6	13.7	**114.8**
	16-Sep	482.0	2430.0	34.0	29.9	765.0	6.6	11568.0	3645.0	31.5	4694.7	40.6	834.7	7.2	**85.9**
	17-Sep	484.0	2088.0	49.0	29.9	1102.5	9.5	11616.0	3132.0	27.0	5199.2	44.8	402.2	3.5	**84.7**
	18-Sep	493.0	2400.0	42.0	29.9	945.0	8.0	11832.0	3600.0	30.4	4330.5	36.6	989.8	8.4	**83.4**
17	Mean	432.0	2442.9	40.3	30.0	906.8	8.8	10368.0	3664.4	35.8	4706.3	45.8	845.6	8.3	**98.7**
	Std	44.5	202.4	6.1	0.3	137.3		1069.2	303.5		489.4		269.2		10.7
	19-Sep	511.0	2300.0	39.0	29.9	877.5	7.2	12264.0	3450.0	28.1	5333.2	43.5	789.4	6.4	**85.2**
	20-Sep	450.0	2583.0	43.0	29.9	967.5	9.0	10800.0	3874.5	35.9	4620.1	42.8	1002.1	9.3	**96.9**
	21-Sep	427.0	1845.0	43.0	29.9	967.5	9.4	10248.0	2767.5	27.0	6019.6	58.7	299.3	2.9	**98.1**
	22-Sep	374.0	1987.0	30.0	29.9	675.0	7.5	8976.0	2980.5	33.2	4273.5	47.6	1164.1	13.0	**101.3**
	23-Sep	400.0	2200.0	52.0	29.9	1170.0	12.2	9600.0	3300.0	34.4	3619.8	37.7	1081.8	11.3	**95.5**
	24-Sep	382.0	2178.0	58.0	30.0	1305.0	14.2	9168.0	3267.0	35.6	4242.5	46.3	878.6	9.6	**105.7**
	25-Sep	409.0	2313.0	38.0	29.9	855.0	8.7	9816.0	3469.5	35.3	3207.4	32.7	1029.6	10.5	**87.2**
	26-Sep	436.0	2358.0	58.0	31.2	1305.0	12.5	10464.0	3537.0	33.8	4457.9	42.6	982.2	9.4	**98.3**
	27-Sep	392.0	2450.0	34.0	29.9	765.0	8.1	9408.0	3675.0	39.1	3435.6	36.5	1554.7	16.5	**100.2**
	28-Sep	419.0	2331.0	45.0	29.9	1012.5	10.1	10056.0	3496.5	34.8	4637.6	46.1	943.1	9.4	**100.3**
18	Mean	420.0	2254.5	44.0	30.1	990.0	9.9	10080.0	3381.8	33.7	4384.7	43.5	972.5	9.8	**96.9**
	Std	39.9	215.1	9.5	0.4	214.2		958.4	322.6		856.5		314.2		6.3
	29-Sep	454.0	2025.0	45.0	29.5	1012.5	9.3	10896.0	3037.5	27.9	3601.4	33.1	1381.7	12.7	**82.9**
	30-Sep	491.0	3033.0	25.0	29.7	562.5	4.8	11784.0	4549.5	38.6	4568.1	38.8	1029.6	8.7	**90.9**
	1-Oct	457.0	3150.0	49.0	30.2	1102.5	10.1	10968.0	4725.0	43.1	4682.7	42.7	944.5	8.6	**104.4**
	2-Oct	443.0	2898.0	40.0	30.5	900.0	8.5	10632.0	4347.0	40.9	3475.2	32.7	1609.6	15.1	**97.2**
	3-Oct	454.0	2925.0	27.0	30.7	607.5	5.6	10896.0	4387.5	40.3	4446.2	40.8	1007.6	9.2	**95.9**
	4-Oct	517.0	2870.0	43.0	31.0	967.5	7.8	12408.0	4305.0	34.7	4465.0	36.0	971.9	7.8	**86.3**
	5-Oct	426.0	3090.0	41.0	31.1	922.5	9.0	10224.0	4635.0	45.3	3822.0	37.4	1551.3	15.2	**106.9**
	6-Oct	440.0	2890.0	32.0	31.4	720.0	6.8	10560.0	4335.0	41.1	4062.3	38.5	1427.7	13.5	**99.9**
	7-Oct	446.0	3465.0	45.0	31.6	1012.5	9.5	10704.0	5197.5	48.6	1901.1	17.8	2296.0	21.5	**97.2**
	8-Oct	364.0	2691.0	44.0	31.6	990.0	11.3	8736.0	4036.5	46.2	3537.4	40.5	1427.0	16.3	**114.4**
19	Mean	449.2	2903.7	39.1	30.7	879.8	8.3	10780.8	4355.6	40.7	3856.2	35.8	1364.7	12.9	**97.6**
	Std	40.0	372.1	8.2	0.7	184.8		959.4	558.2		822.3		413.8		9.5

	9-Oct	500.0	3270.0	36.0	32.2	810.0	6.8	12000.0	4905.0	40.9	4338.4	36.2	1344.0	11.2	**95.0**
	10-Oct	500.0	3540.0	42.0	32.2	945.0	7.9	12000.0	5310.0	44.3	4461.0	37.2	1214.9	10.1	**99.4**
	11-Oct	495.0	3240.0	50.0	32.3	1125.0	9.5	11880.0	4860.0	40.9	4952.2	41.7	1057.1	8.9	**101.0**
	12-Oct	486.0	3186.0	54.0	32.3	1215.0	10.4	11664.0	4779.0	41.0	4890.7	41.9	900.6	7.7	**101.0**
	13-Oct	472.0	3448.0	42.0	32.5	945.0	8.3	11328.0	5172.0	45.7	4115.8	36.3	1379.7	12.2	**102.5**
	14-Oct	454.0	3258.0	51.0	32.5	1147.5	10.5	10896.0	4887.0	44.9	4359.3	40.0	1379.7	12.7	**108.1**
	15-Oct	517.0	3250.0	45.0	32.5	1012.5	8.2	12408.0	4875.0	39.3	4260.4	34.3	1386.5	11.2	**93.0**
	16-Oct	426.0	3222.0	40.0	32.8	900.0	8.8	10224.0	4833.0	47.3	4533.7	44.3	1223.9	12.0	**112.4**
	17-Oct	438.0	2870.0	40.0	32.8	900.0	8.6	10512.0	4305.0	41.0	4678.3	44.5	1181.3	11.2	**105.3**
	18-Oct	494.0	3090.0	40.0	33.0	900.0	7.6	11856.0	4635.0	39.1	4629.5	39.0	1146.3	9.7	**95.4**
20	Mean	478.2	3237.4	44.0	32.5	990.0	8.7	11476.8	4856.1	42.4	4521.9	39.6	1221.4	10.7	**101.3**
	Std	29.8	181.7	5.8	0.3	131.2		716.1	272.6		269.7		159.7		6.1

Batch no	**Date**	**COD(IN)**	**COD (ml)**	**COD (FE)**	**OUR**	**Mste**		**Msti**	**MXsvw**		**Moc**		**Mod**		**COD bal (%)**
	19-Oct	480.0	3600.0	45.0	31.8	1012.5	8.8	11520.0	5400.0	46.9	3828.6	33.2	1486.7	12.9	**101.8**
	20-Oct	480.0	3540.0	50.0	33.6	1125.0	9.8	11520.0	5310.0	46.1	3208.3	27.8	1753.1	15.2	**98.9**
	21-Oct	470.0	3040.0	54.0	31.6	1215.0	10.8	11280.0	4560.0	40.4	3917.0	34.7	1243.8	11.0	**96.9**
	22-Oct	472.0	3270.0	56.0	31.7	1260.0	11.1	11328.0	4905.0	43.3	4877.3	43.1	829.2	7.3	**104.8**
	23-Oct	452.0	3540.0	46.0	31.6	1035.0	9.5	10848.0	5310.0	48.9	4370.9	40.3	1257.5	11.6	**110.4**
	24-Oct	484.0	3240.0	46.0	31.5	1035.0	8.9	11616.0	4860.0	41.8	4351.5	37.5	1235.5	10.6	**98.8**
	25-Oct	484.0	3050.0	40.0	30.5	900.0	7.7	11616.0	4575.0	39.4	4910.1	42.3	926.6	8.0	**97.4**
	26-Oct	470.0	3180.0	42.0	31.5	945.0	8.4	11280.0	4770.0	42.3	4191.6	37.2	1262.3	11.2	**99.0**
	27-Oct	480.0	3880.0	34.0	30.5	765.0	6.6	11520.0	5820.0	50.5	4236.3	36.8	1164.8	10.1	**104.0**
	28-Oct	512.0	3440.0	44.0	30.4	990.0	8.1	12288.0	5160.0	42.0	4293.7	34.9	1105.1	9.0	**94.0**
21	**Mean**	478.4	3378.0	45.7	31.5	1028.3	9.0	11481.6	5067.0	44.2	4218.5	36.8	1226.5	10.7	**100.6**
	Std	15.2	268.6	6.5	0.9	146.2		364.7	402.9		497.0		261.2		4.7
	29-Oct	512.0	3024.0	47.0	31.2	1057.5	8.6	12288.0	4536.0	36.9	4243.0	34.5	1247.9	10.2	**90.2**
	30-Oct	491.0	3664.0	31.0	31.1	697.5	5.9	11784.0	5496.0	46.6	4488.8	38.1	1462.0	12.4	**103.1**
	31-Oct	457.0	3042.0	36.0	31.0	810.0	7.4	10968.0	4563.0	41.6	6660.8	60.7	381.0	3.5	**113.2**
	1-Nov	443.0	3106.0	36.0	31.2	810.0	7.6	10632.0	4659.0	43.8	4756.3	44.7	829.2	7.8	**104.0**
	2-Nov	454.0	3268.0	36.0	30.9	810.0	7.4	10896.0	4902.0	45.0	4445.6	40.8	1166.9	10.7	**103.9**
	3-Nov	517.0	3186.0	29.0	31.0	652.5	5.3	12408.0	4779.0	38.5	4462.8	36.0	1146.3	9.2	**89.0**

	4-Nov	504.0	3448.0	32.0	30.7	720.0	6.0	12096.0	5172.0	42.8	3827.7	31.6	1352.2	11.2	**91.5**
	5-Nov	473.0	3132.0	38.0	30.9	855.0	7.5	11352.0	4698.0	41.4	4070.6	35.9	1262.3	11.1	**95.9**
	6-Nov	515.0	3772.0	38.0	30.7	855.0	6.9	12360.0	5658.0	45.8	4277.4	34.6	1164.8	9.4	**96.7**
	7-Nov	509.0	3187.0	47.0	30.8	1057.5	8.7	12216.0	4780.5	39.1	4369.3	35.8	1194.3	9.8	**93.3**
22	**Mean**	487.5	3282.9	37.0	31.0	832.5	7.1	11700.0	4924.4	42.2	4560.2	39.3	1120.7	9.5	**98.1**
	Std	28.3	260.3	6.1	0.2	136.2		679.6	390.4		779.7		307.1		7.7

TABLE 9.3: Wastewater fractions and mixed liquor parameters for parent system in 2004

	Rs	Vp	Qi	bH	f	Yh	Fcv	Qw
Unit	day	L	(L/d)	d		mgVss/mgCOD	mgCOD/mgVSS	L
Value	**10**	**15**	**24**	**0.24**	**0.2**	**0.45**	**1.48**	**1.50**

Batch no.	date	Xv	Sti	Ste	Fcv	COD ML	Msti	Mxv	Fs,us	Fs,up	Fav	Fn
	3-Apr	2380	554	42	2.03	4820	13296	35700	0.0758	0.2936	0.3108	0.0966
	4-Apr	2380	566	66	1.85	4400	13584	35700	0.1166	0.2602	0.3139	0.0924
	5-Apr	2036	505	60	1.86	3790	12120	30540	0.1188	0.2325	0.3407	0.1169
	6-Apr	2360	552	48	1.49	3520	13248	35400	0.0870	0.1862	0.3600	0.1220
	7-Apr	2530	428	34	1.45	3680	10272	37950	0.0794	0.3847	0.1920	0.0874
	8-Apr	2544	480	40	1.36	3460	11520	38160	0.0833	0.2812	0.2539	0.0904
	9-Apr	2344	426	50	1.66	3900	10224	35160	0.1174	0.4221	0.1772	0.1049
	10-Apr	2464	510	40	1.43	3520	12240	36960	0.0784	0.2409	0.2983	0.0877
	11-Apr	2196	490	40	1.43	3130	11760	32940	0.0816	0.1982	0.3403	0.1047
	12-Apr	2290	515	40	1.30	2980	12360	34350	0.0777	0.1698	0.3584	0.0991
1	Mean	2352.4	502.6	46	1.59	3720	12062.4	35286	0.0916	0.2669	0.2946	0.1002
	Stdev	153.05			0.25				0.0182	0.0826	0.0660	0.0120
	13-Apr											
	14-Apr											
	15-Apr											
	16-Apr											
	17-Apr											
	18-Apr											
	19-Apr	1662	464	44	1.46	2430	11136	24930	0.0948	0.0954	0.4787	0.1480
	20-Apr	1922	434	72	1.43	2740	10416	28830	0.1659	0.2243	0.2916	0.1124
	21-Apr	1736	520	52	1.66	2890	12480	26040	0.1000	0.0799	0.5202	0.1325
	22-Apr	2120	550	60	1.34	2850	13200	31800	0.1091	0.1212	0.4229	0.1071
2	Mean	1860	492	57	1.47	2727.5	11808	27900	0.1175	0.1302	0.4284	0.1250
	Stdev	204.96			0.14				0.0328	0.0650	0.0995	0.0189
	date	**Xv**	**Sti**	**Ste**	**Fcv**	**COD ML**	**Msti**	**Mxv**	**Fs,us**	**Fs,up**	**Fav**	**Fn**
	23-Apr	1686	515	46	2.05	3450	12360	25290	0.0893	0.0896	0.5311	0.1423
	24-Apr	1814	490	38	1.78	3220	11760	27210	0.0776	0.1379	0.4488	0.1268
	25-Apr	1860	498	40	1.49	2770	11952	27900	0.0803	0.1120	0.4579	0.1290
	26-Apr	2224	512	50	1.43	3190	12288	33360	0.0977	0.1890	0.3478	0.1030
	27-Apr	2314	505	62	1.43	3310	12120	34710	0.1228	0.2276	0.3002	0.0994
	28-Apr											
	29-Apr											
	30-Apr											
	1-May											
3	Mean	1979.6	504	47.2	1.64	3188	12096	29694	0.0935	0.1512	0.4172	0.1201
	Stdev	273.6	10.22	9.55	0.27				0.0182	0.0565	0.0924	0.0183
	2-May	1876	476	54	1.54	2897	11424	28140	0.1134	0.1609	0.3899	0.1189

	3-May	1820	408	42	1.59	2897	9792	27300	0.1029	0.2384	0.3127	0.1181
	4-May	1698	514	51	1.57	2674	12336	25470	0.0992	0.0684	0.5336	0.1207
	5-May	1992	538	45	1.43	2855	12912	29880	0.0836	0.1034	0.4649	0.1130
	6-May	1962	512	45	1.45	2846	12288	29430	0.0879	0.1233	0.4359	0.1111
	7-May	2108	464	46	1.26	2666	11136	31620	0.0991	0.1807	0.3357	0.0878
	8-May	1688	562	55	1.44	2436	13488	25320	0.0979	0.0222	0.6204	0.1126
	9-May	2100	505	50	1.36	2858	12120	31500	0.0990	0.1548	0.3800	0.1000
	10-May	1710	498	48	1.67	2858	11952	25650	0.0964	0.0934	0.4996	0.1041
	11-May	2024	525	36	1.47	2978	12600	30360	0.0686	0.1209	0.4452	0.0949
4	Mean	1897.8	500.2	47.2	1.48	2796.5	12004.8	28467	0.0948	0.1266	0.4418	0.1081
	Stdev	163.2	42.97	5.71	0.12				0.0122	0.0609	0.0935	0.0111
	date	**Xv**	**Sti**	**Ste**	**Fcv**	**COD ML**	**Msti**	**Mxv**	**Fs,us**	**Fs,up**	**Fav**	**Fn**
	12-May	1858	482	34	1.49	2763	11568	27870	0.0705	0.1235	0.4428	0.1184
	13-May	1810	485	36	1.34	2433	11640	27150	0.0742	0.0947	0.4716	0.0619
	14-May	1990	517	40	1.41	2804	12408	29850	0.0774	0.1165	0.4435	0.0549
	15-May	1658	511	40	1.47	2442	12264	24870	0.0783	0.0460	0.5715	0.0726
	16-May	1984	519	43	1.63	3242	12456	29760	0.0829	0.1424	0.4292	0.0953
	17-May	1716	490	38	1.71	2936	11760	25740	0.0776	0.0983	0.4984	0.0636
	18-May	1689	500	34	1.68	2836	12000	25335	0.0680	0.0715	0.5395	0.0696
	19-May	1906	480	38	1.48	2812	11520	28590	0.0792	0.1407	0.4161	0.0632
	20-May	1471	448	46	1.47	2159	10752	22065	0.1027	0.0607	0.5396	0.0685
	21-May	2086	475	46	1.17	2442	11400	31290	0.0968	0.1482	0.3640	0.0483
5	Mean	1816.8	490.7	39.5	1.49	2686.9	11776.8	27252	0.0808	0.1042	0.4716	0.0716
	Stdev	186.0	21.82	4.4	0.16				0.0110	0.0361	0.0650	0.0206
	22-May	2249	514	46	1.63	3666	12336	33735	0.0895	0.2278	0.3304	0.0978
	23-May	1809	559	48	1.66	3010	13416	27135	0.0859	0.0573	0.5607	0.0619
	24-May	2027	507	36	1.55	3142	12168	30405	0.0710	0.1511	0.4120	0.0539
	25-May	1776	501	41	1.75	3107	12024	26640	0.0818	0.1110	0.4822	0.0678
	26-May	1589	521	46	1.81	2875	12504	23835	0.0883	0.0337	0.6096	0.1189
	27-May	1860	485	60	1.70	3165	11640	27900	0.1237	0.1737	0.3880	0.0587
	28-May	1900	511	51	1.65	3130	12264	28500	0.0998	0.1363	0.4350	0.0619
	29-May	1611	478	52	1.48	2382	11472	24165	0.1088	0.0751	0.5128	0.0747
	30-May	1688	522	45	1.88	3173	12528	25320	0.0862	0.0688	0.5534	0.0597
	31-May	2094	523	58	1.26	2640	12552	31410	0.1109	0.1274	0.4029	0.0481
6	Mean	1860.3	512.1	48.3	1.64	3029	12290.4	27904.5	0.0946	0.1162	0.4687	0.0704
	Stdev	213.5	22.48	7.29	0.18				0.0159	0.0594	0.0894	0.0219
	1-Jun	2031	516	53	1.41	2855	12384	30465	0.1027	0.1363	0.4094	0.1054
	2-Jun	1973	488	36	1.41	2778	11712	29595	0.0738	0.1385	0.4126	0.1115
	3-Jun	1992	514	43	1.48	2958	12336	29880	0.0837	0.1313	0.4289	0.1094
	4-Jun	1962	522	65	1.59	3122	12528	29430	0.1245	0.1466	0.4106	0.0943
	5-Jun	2056	565	60	1.59	3268	13560	30840	0.1062	0.1208	0.4498	0.1021
	6-Jun	1840	553	55	1.35	2477	13272	27600	0.0995	0.0577	0.5364	0.1147
	7-Jun	1747	526	52	1.64	2864	12624	26205	0.0989	0.0750	0.5267	0.1208
	8-Jun	1798	485	58	1.61	2898	11640	26970	0.1196	0.1395	0.4232	0.1196
	9-Jun	1860	480	50	1.65	3070	11520	27900	0.1042	0.1627	0.4006	0.1129
	10-Jun	2224	485	65	1.25	2778	11640	33360	0.1340	0.1934	0.3106	0.0890
7	Mean	1948.3	513.4	53.7	1.50	2906.8	12321.6	29224.5	0.1047	0.1302	0.4309	0.1080
	Stdev	141.34	29.52	9.19	0.14				0.0181	0.0393	0.0644	0.0104

	date	Xv	Sti	Ste	Fcv	COD ML	Msti	Mxv	Fs,us	Fs,up	Fav	Fn
	11-Jun	2045	520	58	1.42	2898	12480	30675	0.1115	0.1408	0.4026	0.1002
	12-Jun	2100	567	60	1.54	3233	13608	31500	0.1058	0.1242	0.4403	0.1467
	13-Jun	1900	507	56	1.57	2989	12168	28500	0.1105	0.1364	0.4256	0.1105
	14-Jun	1982	517	56	1.45	2867	12408	29730	0.1083	0.1311	0.4201	0.0721
	15-Jun	2089	500	38	1.41	2952	12000	31335	0.0760	0.1566	0.3890	0.1154
	16-Jun	1956	479	41	1.38	2707	11496	29340	0.0856	0.1445	0.3993	0.1074
	17-Jun	1773	547	36	1.72	3046	13128	26595	0.0658	0.0507	0.5772	0.1060
	18-Jun	1804	517	36	1.53	2764	12408	27060	0.0696	0.0785	0.5170	0.1297
	19-Jun	2367	512	49	1.21	2855	12288	35505	0.0957	0.1766	0.3333	0.1407
	20-Jun	2271	498	52	1.46	3318	11952	34065	0.1044	0.2243	0.3117	0.1066
8	Mean	2028.7	516.4	48.2	1.47	2962.9	12393.6	30430.5	0.0933	0.1364	0.4216	0.1135
	Stdev	189.16	25	9.58	0.14				0.0177	0.0480	0.0785	0.0215
	21-Jun	1727	532	48	1.65	2858	12768	25905	0.0902	0.0604	0.5541	0.1285
	22-Jun	2644	496	58	1.46	3854	11904	39660	0.1169	0.3268	0.2210	0.0900
	23-Jun	2370	512	34	1.60	3797	12288	35550	0.0664	0.2485	0.3134	0.1089
	24-Jun	2400	485	52	1.41	3375	11640	36000	0.1072	0.2609	0.2704	0.0983
	25-Jun	2314	522	43	1.66	3835	12528	34710	0.0824	0.2388	0.3243	0.0968
	26-Jun	2460	518	41	1.62	3986	12432	36900	0.0792	0.2764	0.2874	0.0967
	27-Jun	2534	506	39	1.58	4004	12144	38010	0.0771	0.3025	0.2623	0.0833
	28-Jun	2367	511	45	1.78	4211	12264	35505	0.0881	0.3028	0.2785	0.0900
	29-Jun	2444	495	56	1.29	3158	11880	36660	0.1131	0.2333	0.2803	0.0904
	30-Jun	2156	483	52	1.60	3450	11592	32340	0.1077	0.2428	0.3081	0.0816
9	Mean	2341.6	506	46.8	1.57	3652.8	12144	35124	0.0928	0.2493	0.3100	0.0965
	Stdev	251.83	16.08	7.76	0.14				0.0173	0.0735	0.0906	0.0137
	date	Xv	Sti	Ste	Fcv	COD ML	Msti	Mxv	Fs,us	Fs,up	Fav	Fn
	1-Jul	2234	468	48	1.44	3224	11232	33510	0.1026	0.2466	0.2887	0.0985
	2-Jul	1780	481	38	1.65	2942	11544	26700	0.0790	0.1244	0.4559	0.1270
	3-Jul	1638	472	38	1.80	2942	11328	24570	0.0805	0.1019	0.4989	0.1514
	4-Jul	2066	522	38	1.40	2886	12528	30990	0.0728	0.1264	0.4285	0.1108
	5-Jul	2312	455	32	1.41	3271	10920	34680	0.0703	0.2652	0.2769	0.0727
	6-Jul	2072	447	38	1.50	3111	10728	31080	0.0850	0.2350	0.3107	0.0878
	7-Jul	2200	523	36	1.40	3083	12552	33000	0.0688	0.1555	0.3905	0.0955
	8-Jul	1908	512	48	1.56	2970	12288	28620	0.0938	0.1240	0.4445	0.1174
	9-Jul	2230	511	58	1.03	2294	12264	33450	0.1135	0.1277	0.3682	0.0879
	10-Jul	2320	520	41	1.60	3713	12480	34800	0.0788	0.2294	0.3283	0.0991
10	Mean	2076	491.1	41.5	1.48	3043.6	11786.4	31140	0.0845	0.1736	0.3791	0.1048
	Stdev	232.64	29.61	7.65	0.20				0.0146	0.0626	0.0768	0.0227
	11-Jul	2245	518	32	1.42	3196	12432	33675	0.0618	0.1719	0.3744	0.1024
	12-Jul	1584	526	34	1.89	2989	12624	23760	0.0646	0.0149	0.6472	0.1389
	13-Jul	1892	489	34	1.72	3250	11736	28380	0.0695	0.1542	0.4249	0.1258
	14-Jul	2254	475	52	1.09	2450	11400	33810	0.1095	0.1687	0.3221	0.1278
	15-Jul	2102	521	39	1.64	3450	12504	31530	0.0749	0.1716	0.3955	0.1051
	16-Jul	1680	523	52	2.28	3835	12552	25200	0.0994	0.1006	0.5274	0.1369
	17-Jul	2412	547	41	1.38	3328	13128	36180	0.0750	0.1785	0.3585	0.1020
	18-Jul	2028	533	47	1.55	3140	12792	30420	0.0882	0.1316	0.4343	0.1065
	19-Jul	1980	505	38	1.21	2390	12120	29700	0.0752	0.1010	0.4449	0.0818
	20-Jul	2060	480	36	1.50	3100	11520	30900	0.0750	0.1857	0.3648	0.1102

11	Mean	2023.7	511.7	40.5	1.57	3112.8	12280.8	30355.5	0.0793	0.1379	0.4294	0.1137
	Stdev	256.25	23.73	7.4	0.34				0.0152	0.0531	0.0956	0.0181
	date	**Xv**	**Sti**	**Ste**	**Fcv**	**COD ML**	**Msti**	**Mxv**	**Fs,us**	**Fs,up**	**Fav**	**Fn**
	21-Jul	2250	490	36	1.46	3280	11760	33750	0.0735	0.2153	0.3280	0.0933
	22-Jul	2024	502	42	1.55	3130	12048	30360	0.0837	0.1608	0.3968	0.1206
	23-Jul	2312	490	50	1.28	2950	11760	34680	0.1020	0.2024	0.3122	0.1029
	24-Jul	1934	438	40	1.25	2420	10512	29010	0.0913	0.1624	0.3579	0.1143
	25-Jul	2246	494	38	1.67	3750	11856	33690	0.0769	0.2564	0.3105	0.0966
	26-Jul	2264	480	48	1.44	3260	11520	33960	0.1000	0.2377	0.2974	0.0941
	27-Jul	1386	475	52	2.47	3420	11400	20790	0.1095	0.0379	0.6188	0.1573
	28-Jul	2194	480	40	1.35	2970	11520	32910	0.0833	0.1955	0.3341	0.1021
	29-Jul	2400	445	42	1.44	3450	10680	36000	0.0944	0.3195	0.2301	0.0825
	30-Jul	2506	450	51	1.37	3440	10800	37590	0.1133	0.3274	0.2127	0.0898
12	Mean	2151.6	474.4	43.9	1.53	3207	11385.6	32274	0.0928	0.2115	0.3399	0.1053
	Stdev	315.49	22.31	5.82	0.35				0.0135	0.0838	0.1122	0.0214
	31-Jul	2274	528	44	1.53	3490	12672	34110	0.0833	0.1967	0.3540	0.1003
	1-Aug	3204	400	44	1.01	3250	9600	48060	0.1100	0.4130	0.1261	0.0655
	2-Aug	2362	426	38	1.52	3590	10224	35430	0.0892	0.3639	0.2089	0.0982
	3-Aug	2102	440	50	1.47	3100	10560	31530	0.1136	0.2591	0.2780	0.1094
	4-Aug	2850	446	34	1.33	3790	10704	42750	0.0762	0.3928	0.1760	0.0737
	5-Aug	2146	364	36	1.85	3970	8736	32190	0.0989	0.5570	0.1236	0.0927
	6-Aug	2267	440	32	1.69	3830	10560	34005	0.0727	0.3545	0.2354	0.0948
	7-Aug	2348	480	34	1.62	3810	11520	35220	0.0708	0.2943	0.2748	0.0928
	8-Aug	2348	486	44	1.62	3800	11664	35220	0.0905	0.2934	0.2700	0.0894
	9-Aug	2444	458	44	1.29	3150	10992	36660	0.0961	0.2697	0.2517	0.0896
13	Mean	2434.5	446.8	40	1.49	3578	10723.2	36517.5	0.0901	0.3394	0.2299	0.0907
	Stdev	338.74	45.86	5.96	0.24				0.0148	0.1012	0.0725	0.0127
	10-Aug	2134	406	46	1.53	3270	9744	32010	0.1133	0.3390	0.2207	0.1036
	11-Aug	2202	505	38	1.50	3300	12120	33030	0.0752	0.1939	0.3550	0.0890
	12-Aug	2276	485	38	1.42	3240	11640	34140	0.0784	0.2226	0.3155	0.0923
	13-Aug	2200	485	36	1.51	3315	11640	33000	0.0742	0.2184	0.3302	0.1000
	14-Aug	2118	500	38	1.31	2780	12000	31770	0.0760	0.1480	0.3879	0.0623
	15-Aug	1992	500	52	1.62	3230	12000	29880	0.1040	0.1746	0.3834	0.1165
	16-Aug	2100	495	48	1.37	2870	11880	31500	0.0970	0.1647	0.3685	0.1062
	17-Aug	1842	522	44	1.68	3090	12528	27630	0.0843	0.1029	0.4878	0.1167
	18-Aug	1898	518	46	1.52	2890	12432	28470	0.0888	0.1096	0.4633	0.0753
	19-Aug	2120	507	45	1.63	3465	12168	31800	0.0888	0.1992	0.3606	0.0991
14	Mean	2088.2	492.3	43.1	1.51	3145	11815.2	31323	0.0880	0.1873	0.3673	0.0961
	Stdev	137.8	32.66	5.3	0.12				0.0133	0.0673	0.0747	0.0172
	date	**Xv**	**Sti**	**Ste**	**Fcv**	**COD ML**	**Msti**	**Mxv**	**Fs,us**	**Fs,up**	**Fav**	**Fn**
	20-Aug	1930	529	47	1.57	3024	12696	28950	0.0888	0.1120	0.4639	0.1062
	21-Aug	2100	491	31	1.27	2664	11784	31500	0.0631	0.1415	0.3938	0.1467
	22-Aug	2268	457	36	1.34	3042	10968	34020	0.0788	0.2360	0.2924	0.0926
	23-Aug	1590	443	36	1.32	2106	10632	23850	0.0813	0.0793	0.4953	0.0899
	24-Aug	1684	454	36	1.35	2268	10896	25260	0.0793	0.0942	0.4719	0.1431
	25-Aug	2308	517	29	1.38	3186	12408	34620	0.0561	0.1781	0.3633	0.0910
	26-Aug	2148	504	32	1.14	2448	12096	32220	0.0635	0.1217	0.4049	0.0875
	27-Aug	1980	473	38	1.58	3132	11352	29700	0.0803	0.1868	0.3708	0.1182

	28-Aug	1522	515	38	2.28	3472	12360	22830	0.0738	0.0135	0.6540	0.2188
	29-Aug	1806	509	47	1.76	3187	12216	27090	0.0923	0.1186	0.4710	0.1340
15	Mean	1933.6	489.2	37	1.50	2852.9	11740.8	29004	0.0757	0.1282	0.4381	0.1228
	Stdev	277.66	30.39	6.06	0.33				0.0116	0.0622	0.0984	0.0406
	30-Aug	2238	482	41	1.41	3150	11568	33570	0.0851	0.2157	0.3189	0.0983
	31-Aug	2056	463	43	1.41	2898	11112	30840	0.0929	0.1944	0.3399	0.1021
	1-Sep	2022	509	41	1.45	2925	12216	30330	0.0806	0.1376	0.4168	0.1286
	2-Sep	1952	463	32	1.59	3096	11112	29280	0.0691	0.1867	0.3738	0.1173
	3-Sep	2052	522	45	1.59	3258	12528	30780	0.0862	0.1537	0.4095	0.1345
	4-Sep	2234	500	45	1.45	3250	12000	33510	0.0900	0.2055	0.3339	0.0985
	5-Sep	2114	486	38	1.52	3222	11664	31710	0.0782	0.1984	0.3522	0.1121
	6-Sep	1402	472	36	1.67	2340	11328	21030	0.0763	0.0117	0.6502	0.1498
	7-Sep	1862	454	36	1.41	2619	10896	27930	0.0793	0.1475	0.3992	0.1063
	8-Sep	1918	443	45	1.43	2736	10632	28770	0.1016	0.1873	0.3478	0.1069
16	Mean	1985	479.4	40.2	1.49	2949.4	11505.6	29775	0.0839	0.1638	0.3942	0.1154
	Stdev	239.01	25.23	4.54	0.09				0.0093	0.0595	0.0960	0.0171
	9-Sep	1538	369	41	1.46	2241	8856	23070	0.1111	0.1761	0.3621	0.1391
	10-Sep	1900	434	40	1.35	2574	10416	28500	0.0922	0.1766	0.3537	0.1158
	11-Sep	1552	423	40	1.53	2367	10152	23280	0.0946	0.1130	0.4574	0.1405
	12-Sep	1636	409	41	1.39	2268	9816	24540	0.1002	0.1404	0.4020	0.1131
	13-Sep	1814	409	49	1.48	2691	9816	27210	0.1198	0.2191	0.3156	0.1158
	14-Sep	1926	457	40	1.36	2620	10968	28890	0.0875	0.1570	0.3796	0.1096
	15-Sep	1744	360	27	1.58	2750	8640	26160	0.0750	0.2774	0.2831	0.1210
	16-Sep	1736	482	34	1.40	2430	11568	26040	0.0705	0.0830	0.4977	0.1238
	17-Sep	1662	484	49	1.26	2088	11616	24930	0.1012	0.0643	0.5146	0.1264
	18-Sep	1576	493	42	1.52	2400	11832	23640	0.0852	0.0447	0.5764	0.1256
17	Mean	1708.4	432	40.3	1.43	2442.9	10368	25626	0.0937	0.1452	0.4142	0.1231
	Stdev	139.71	46.96	6.43	0.10				0.0152	0.0720	0.0942	0.0104
	date	**Xv**	**Sti**	**Ste**	**Fcv**	**COD ML**	**Msti**	**Mxv**	**Fs,us**	**Fs,up**	**Fav**	**Fn**
	19-Sep	2742	511	39	0.84	2300	12264	41130	0.0763	0.1550	0.3034	0.0649
	20-Sep	1850	450	43	1.40	2583	10800	27750	0.0956	0.1533	0.3869	0.0622
	21-Sep	1164	427	43	1.59	1845	10248	17460	0.1007	-0.0133	0.7089	0.0988
	22-Sep	1350	374	30	1.47	1987	8976	20250	0.0802	0.0940	0.4845	0.1615
	23-Sep	1500	400	52	1.47	2200	9600	22500	0.1300	0.1316	0.4170	0.0787
	24-Sep	1660	382	58	1.31	2178	9168	24900	0.1518	0.1862	0.3226	0.0693
	25-Sep	1814	409	38	1.28	2313	9816	27210	0.0929	0.1691	0.3523	0.0650
	26-Sep	1634	436	58	1.44	2358	10464	24510	0.1330	0.1296	0.4167	0.0722
	27-Sep	1664	392	34	1.47	2450	9408	24960	0.0867	0.1788	0.3664	0.0871
	28-Sep	1216	419	45	1.92	2331	10056	18240	0.1074	0.0201	0.6367	0.0946
18	Mean	1659.4	420	44	1.42	2254.5	10080	24891	0.1055	0.1204	0.4395	0.0854
	Stdev	446.73	39.93	9.52	0.27				0.0250	0.0677	0.1343	0.0296
	29-Sep	1450	454	45	1.40	2025	10896	21750	0.0991	0.0445	0.5678	0.1448
	30-Sep	1870	491	25	1.62	3033	11784	28050	0.0509	0.1239	0.4588	0.1198
	1-Oct	1862	457	49	1.69	3150	10968	27930	0.1072	0.2018	0.3591	0.1257
	2-Oct	1984	443	40	1.46	2898	10632	29760	0.0903	0.2081	0.3317	0.0534
	3-Oct	2043	454	27	1.43	2925	10896	30645	0.0595	0.1930	0.3518	0.0548
	4-Oct	1938	517	43	1.48	2870	12408	29070	0.0832	0.1141	0.4535	0.1120

	5-Oct	1900	426	41	1.63	3090	10224	28500	0.0962	0.2428	0.3138	0.1147
	6-Oct	2052	440	32	1.41	2890	10560	30780	0.0727	0.2136	0.3240	0.1155
	7-Oct	2362	446	45	1.47	3465	10704	35430	0.1009	0.3188	0.2320	0.0970
	8-Oct	1684	364	44	1.60	2691	8736	25260	0.1209	0.2720	0.2779	0.1342
19	Mean	1914.5	449.2	39.1	1.52	2903.7	10780.8	28717.5	0.0881	0.1933	0.3671	0.1072
	Stdev	239.19	39.97	8.21	0.11				0.0218	0.0805	0.0992	0.0308
	9-Oct	2234	500	36	1.46	3270	12000	33510	0.0720	0.2000	0.3450	0.1012
	10-Oct	1780	500	42	1.99	3540	12000	26700	0.0840	0.1403	0.4614	0.1303
	11-Oct	2345	495	50	1.38	3240	11880	35175	0.1010	0.2273	0.3002	0.0930
	12-Oct	1985	486	54	1.61	3186	11664	29775	0.1111	0.1900	0.3624	0.1194
	13-Oct	2004	472	42	1.72	3448	11328	30060	0.0890	0.2255	0.3419	0.1143
	14-Oct	2106	454	51	1.55	3258	10896	31590	0.1123	0.2576	0.2876	0.1073
	15-Oct	1859	517	45	1.75	3250	12408	27885	0.0870	0.1220	0.4658	0.1248
	16-Oct	1750	426	40	1.84	3222	10224	26250	0.0939	0.2282	0.3494	0.1246
	17-Oct	1800	438	40	1.59	2870	10512	27000	0.0913	0.1828	0.3740	0.1317
	18-Oct	2100	494	40	1.47	3090	11856	31500	0.0810	0.1771	0.3696	0.1143
20	Mean	1996.3	478.2	44	1.64	3237.4	11476.8	29944.5	0.0923	0.1951	0.3657	0.1161
	Stdev	201.63	29.84	5.83	0.19				0.0128	0.0419	0.0586	0.0127
	date	**Xv**	**Sti**	**Ste**	**Fcv**	**COD ML**	**Msti**	**Mxv**	**Fs,us**	**Fs,up**	**Fav**	**Fn**
	19-Oct	2502	480	45	1.44	3600	11520	37530	0.0938	0.2970	0.2475	0.0903
	20-Oct	2294	480	50	1.54	3540	11520	34410	0.1042	0.2725	0.2762	0.1011
	21-Oct	2084	470	54	1.46	3040	11280	31260	0.1149	0.2119	0.3215	0.1046
	22-Oct	2292	472	56	1.43	3270	11328	34380	0.1186	0.2591	0.2714	0.1034
	23-Oct	2490	452	46	1.42	3540	10848	37350	0.1018	0.3317	0.2178	0.0920
	24-Oct	2224	484	46	1.46	3240	11616	33360	0.0950	0.2241	0.3138	0.1016
	25-Oct	2106	484	40	1.45	3050	11616	31590	0.0826	0.1865	0.3557	0.1102
	26-Oct	2204	470	42	1.43	3150	11280	33060	0.0894	0.2277	0.3084	0.0989
	27-Oct	2652	480	34	1.46	3880	11520	39780	0.0708	0.3349	0.2278	0.0894
	28-Oct	2345	512	44	1.47	3440	12288	35175	0.0859	0.2207	0.3206	0.1023
21	Mean	2319.3	478.4	45.7	1.46	3375	11481.6	34789.5	0.0957	0.2566	0.2861	0.0994
	Stdev	182.11	15.2	6.5	0.03				0.0147	0.0514	0.0452	0.0068
	29-Oct	2024	512	47	1.49	3024	12288	30360	0.0918	0.1461	0.4082	0.0766
	30-Oct	2242	491	31	1.46	3264	11784	33630	0.0631	0.2075	0.3383	0.0937
22	Mean	2133	501.5	39	1.47	3144	12036	31995	0.0775	0.1768	0.3733	0.0851
	Stdev	154.15	14.85	11.3	0.03				0.0203	0.0434	0.0495	0.0121

APPENDIX 10

OUR vs. time plots for modified batch tests

Results for batch tests with mixture of flocculated-filtered wastewater (WW) and mixed liquor (ML) drawn from the 10 days sludge age parent activated sludge system:

- Batch test numbers
- Dates of batch test
- Volumes added
- COD recoveries
- *Measured* OHO active biomass present at the start of the batch test ($Z_{BH(0)}$) and *projected* parent system mixed liquor (ML) active biomass
- The *theoretical* parent system mixed liquor (ML) OHO active biomass and the *projected* active biomass present at the start of the batch test
- OUR vs. time and Ln (OUR) vs. time profiles for modified batch tests no. B1 – B16
- The nitrate/nitrite concentration vs. time profiles recorded during each batch test are also given

BATCH TEST 1 DATA										
% COD Recovery		**End Time=**	8.00					**COD filt.**	158	
COD t=o	**CODt=T**	**MOt**	**$MONO_2$**	**MOno3**	**MOn**	**MOc**	**% Recovery**	So(mgCOD/l)	Xo(mgMLVSS/l)	**So/Xo**
328.00	259.00	48.20	0.51	6.18	6.69	41.51	91.62	142.2	225	0.632
								So(mgCOD/l)	Xo(mgMLAVSS/l)	**So/Xo**
Parent System		**fcv=**	**1.450**	**Batch Result**				142.2	82.53	1.72
fav	**Xv**	**V_{ML}**	**ZBH(Theo)**	**$Z_{BH(0)}$**	**OURSBCOD**	**KMP**	**UH**	**t=s**		
0.3668	**2250**	500	119.6685	63.64	4.72	1.71	2.03	5.63		

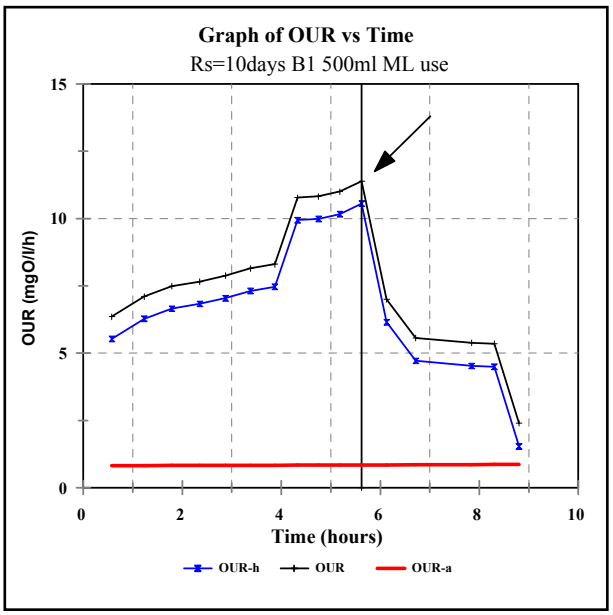

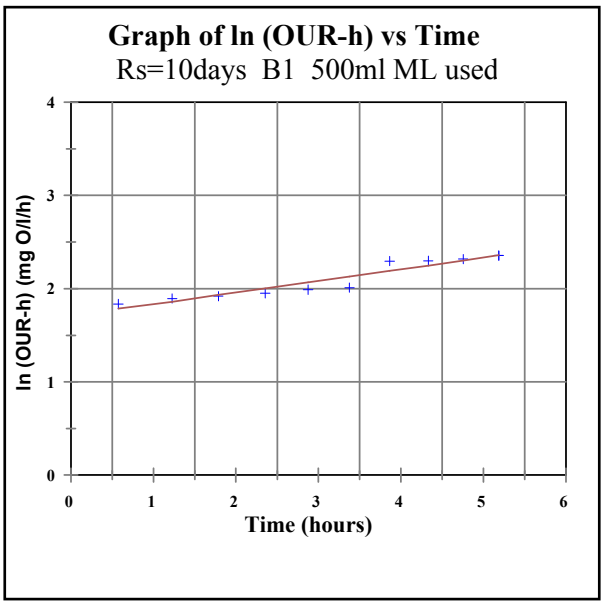

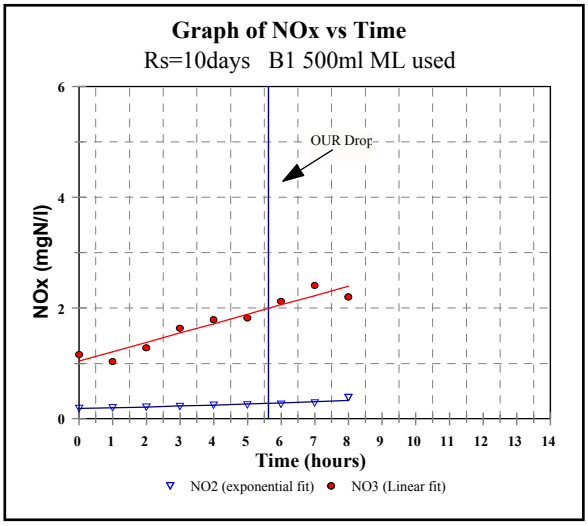

			Fitted Data			
Time	**NO_2**	**NO_3**	**NO_2**	**NO_3**	**Ln(NO_2)**	**Ln(NO_3)**
	conc.	**conc.**	**conc.**	**conc.**		
	[mg/l]	**[mg/l]**	**[mg/l]**	**[mg/l]**		
0.00	0.190	1.162	0.19	1.04	-1.66073	0.15014
1.00	0.207	1.037	0.20	1.21	-1.57504	0.03633
2.00	0.215	1.282	0.22	1.38	-1.53712	0.24842
3.00	0.230	1.640	0.23	1.55	-1.46968	0.49470
4.00	0.251	1.790	0.25	1.72	-1.38230	0.58222
5.00	0.255	1.822	0.27	1.89	-1.36649	0.59993
6.00	0.267	2.124	0.29	2.06	-1.32051	0.75330
7.00	0.288	2.412	0.31	2.23	-1.24479	0.88046
8.00	0.389	2.201	0.33	2.40	-0.94418	0.78891

Sew. Batch No./Year	Batch test No.	Batch test date	Volume (L)		COD Recov. (%)	Regression			$Z_{BH(0)}$ (mgCOD/l)			
			WW	ML		Y-int	Slope	R^2	Measured		Theoretical	
									Batch Test	ML	Batch Test	ML
SB13/03	1	2-sept	4.5	0.5	91.6	1.6297	0.130	0.919	63.6	636.4	119.7	1196.7

BATCH TEST 2 DATA										
% COD Recovery		**End Time=**	8.00					**CODfilt.**	128	
COD t=o	**CODt=T**	**MOt**	**MOno2**	**MOno3**	**MOn**	**MOc**	**% Recovery**	So(mgCOD/l)	Xo(mgMLVSS/l)	**So/Xo**
299.00	270.00	46.70	1.73	5.82	7.55	39.15	103.39	64	210	0.305
								So(mgCOD/l)	Xo(mgMLAVSS/l)	**So/Xo**
Parent System		**fcv=**	**1.440**	**Batch Result**				64	85.743	0.746
fav	**Xv**	**V_{ML}**	**ZBH(Theo)**	**ZBH(O)**	**OURSBCOD**	**KMP**	**UH**	**t=s**		
0.4083	**2100**	500	123.46992	94.77	2.76	0.92	1.25	6.482		

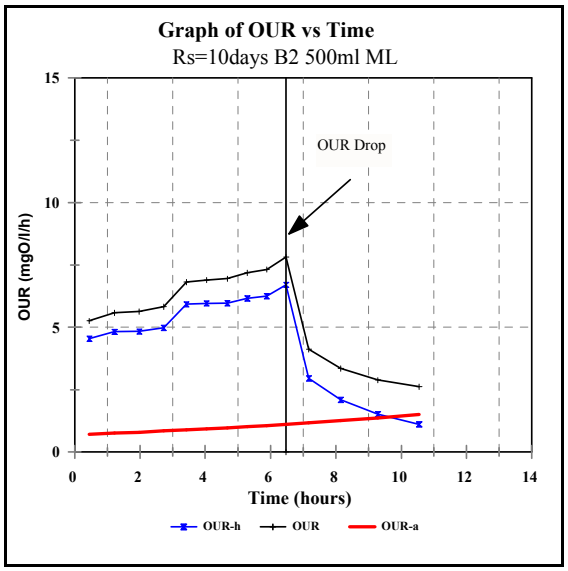

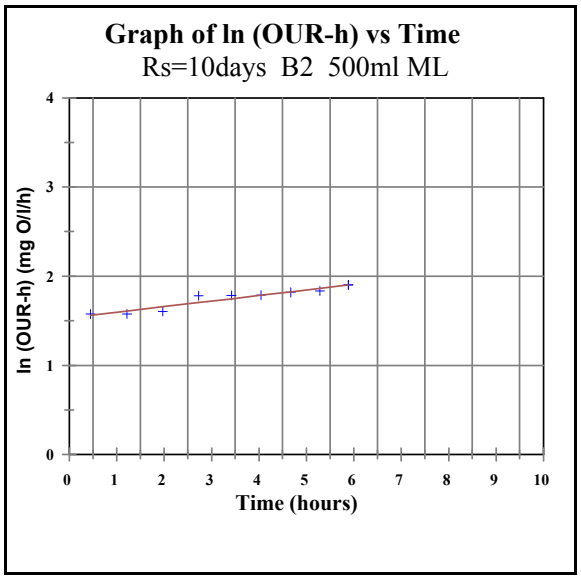

			Fitted Data			
Time	**NO_2**	**NO_3**	**NO_2**	**NO_3**	**Ln(NO_2)**	**Ln(NO_3)**
	conc.	**conc.**	**conc.**	**conc.**		
	[mg/l]	**[mg/l]**	**[mg/l]**	**[mg/l]**		
0.00	0.54	1.66	0.56	1.65	-0.61619	0.50682
1.00	0.64	1.76	0.60	1.78	-0.44629	0.56531
2.00	0.65	1.92	0.65	1.91	-0.43078	0.65233
3.00	0.68	2.03	0.71	2.05	-0.38566	0.70804
4.00	0.80	2.25	0.77	2.20	-0.22314	0.81093
5.00	0.83	2.25	0.83	2.36	-0.18633	0.81093
6.00	0.90	2.66	0.90	2.54	-0.10536	0.97833
7.00	0.95	2.80	0.98	2.73	-0.05129	1.02962
8.00	1.09	2.83	1.06	2.93	0.08434	1.04028

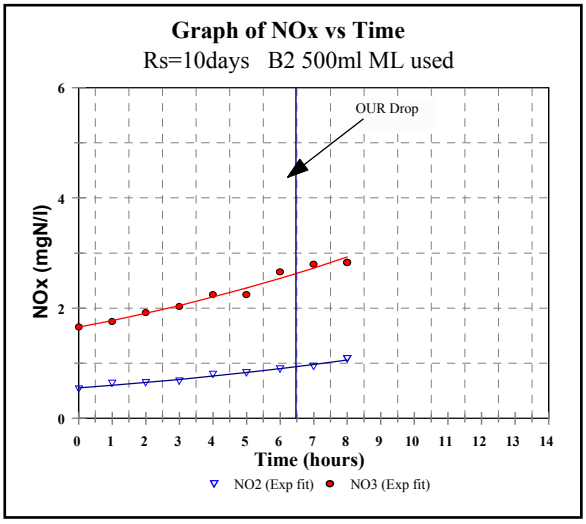

Sew. Batch No./Year	Batch test No.	Batch test date	Volume (l)		COD Recov. (%)	Regression			ZBH(0) (mgCOD/l)			
			WW	ML		Y-int	Slope	R^2	Measured		Theoretical	
									Batch Test	ML	Batch Test	ML
SB14/03	2	11-sept	4.5	0.5	103.4	1.4849	0.065	0.923	94.8	947.7	123.5	1234.7

BATCH TEST 3 DATA

% COD Recovery		End Time=	8.00					CODfilt.	116	
COD t=o	**CODt=T**	**MOt**	**MOno2**	**MOno3**	**MOn**	**MOc**	**% Recovery**	So(mgCOD/l)	Xo(mgMLVSS/l)	**So/Xo**
420.00	380.00	31.00	1.78	10.13	11.90	19.10	95.02	106.72	168	0.635
								So(mgCOD/l)	Xo(mgMLAVSS/l)	**So/Xo**

Parent System		fcv=	1.500	Batch Result				106.72	62.630	1.703
fav	**Xv**	**VML**	**ZBH(Theo)**	**ZBH(O)**	**OURSBCOD**	**KMP**	**UH**	**t=s**		
0.3728	**2100**	400	93.9456	6.46	1.12	1.38	6.67	5.789		

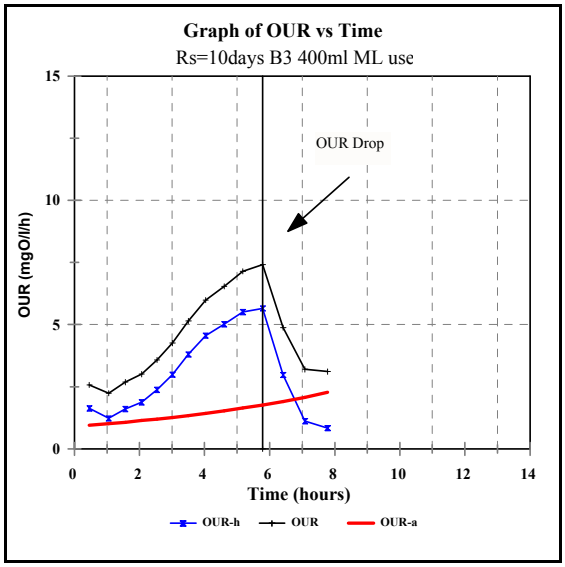

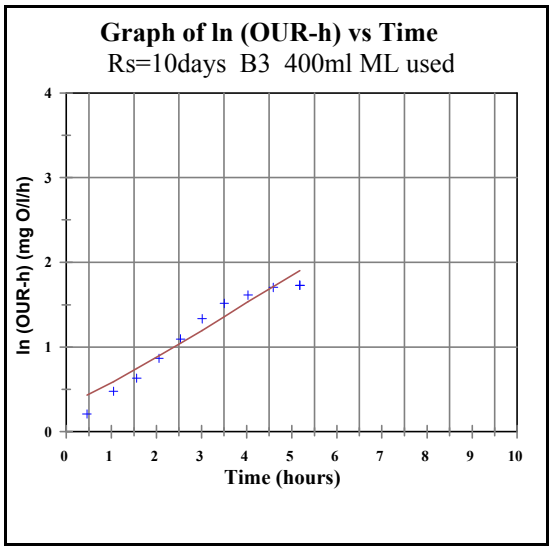

Time	NO_2	NO_3	Fitted Data NO_2	Fitted Data NO_3	$Ln(NO_2)$	$Ln(NO_3)$
	conc.	conc.	conc.	conc.		
	[mg/l]	[mg/l]	[mg/l]	[mg/l]		
0.00	0.09	1.89	0.08	1.85	-2.44185	0.63658
1.00	0.11	1.98	0.11	2.04	-2.25379	0.68310
2.00	0.15	2.19	0.14	2.25	-1.89712	0.78390
3.00	0.19	2.48	0.17	2.49	-1.66601	0.90826
4.00	0.20	2.94	0.22	2.74	-1.61445	1.07841
5.00	0.24	2.99	0.29	3.03	-1.43548	1.09527
6.00	0.29	3.36	0.37	3.34	-1.24827	1.21194
7.00	0.58	3.67	0.47	3.69	-0.54991	1.30019
8.00	0.68	4.01	0.60	4.07	-0.39008	1.38879

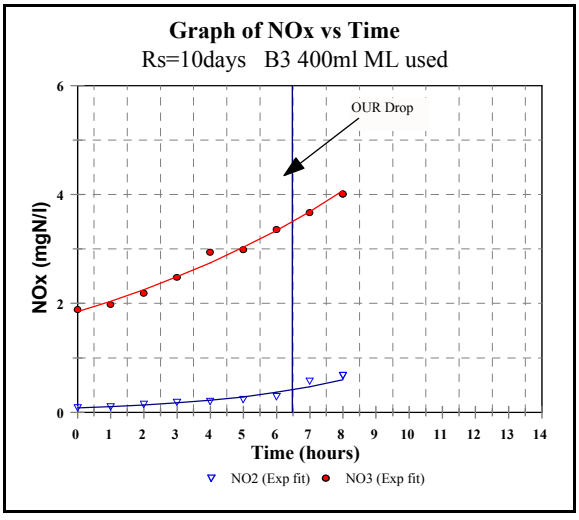

Sew. Batch No./year	Batch test No.	Batch test date	Volume (l)		COD Recov. (%)	Regression			ZBH(0) (mgCOD/l)			
			WW	ML		Y-int	Slope	R^2	Measured		Theoretical	
									Batch Test	ML	Batch Test	ML
SB15/03	3	23-sept	4.6	0.4	95.0	0.1098	0.310	0.930	6.5	80.7	93.9	1174.3

BATCH TEST 4 DATA										
% COD Recovery		**End Time=**	8.00					**CODfilt.**	102	
COD t=o	**CODt=T**	**MOt**	**MOno2**	**MOno3**	**MOn**	**MOc**	**% Recov.**	So(mgCOD/l)	Xo(mgMLVSS/l)	**So/Xo**
484.00	432.00	46.70	0.79	7.32	8.11	38.59	97.23	91.8	214.6	0.428
								So(mgCOD/l)	Xo(mgMLAVSS/l)	**So/Xo**
Parent System		**fcv=**	**1.450**	**Batch Result**				91.8	69.29434	1.325
fav	**Xv**	**V_{ML}**	**ZBH(Theo)**	**$Z_{BH(0)}$**	**OURSBCOD**	**KMP**	**UH**	**t=s**		
0.3229	**2146**	500	100.476793	79.36	2.27	0.84	1.60	6.482		

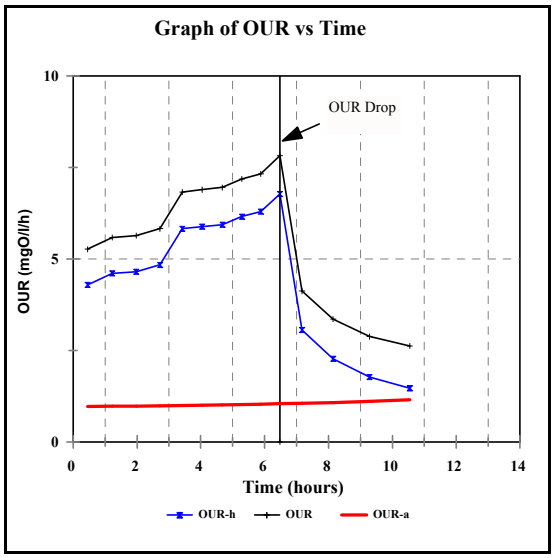

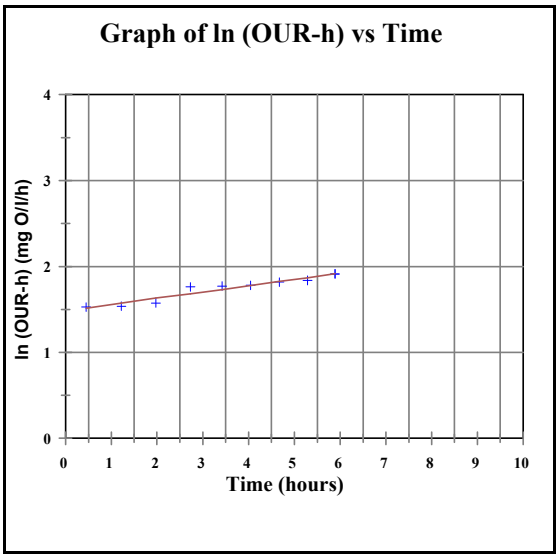

			Fitted Data			
Time	**NO_2**	**NO_3**	**NO_2**	**NO_3**	**Ln(NO_2)**	**Ln(NO_3)**
	conc.	**conc.**	**conc.**	**conc.**		
	[mg/l]	**[mg/l]**	**[mg/l]**	**[mg/l]**		
0.00	0.13	0.49	0.11	0.52	-2.01741	-0.71744
1.00	0.13	0.80	0.12	0.72	-2.01741	-0.22690
2.00	0.14	0.80	0.14	0.92	-2.00248	-0.22189
3.00	0.14	1.00	0.16	1.12	-1.96611	0.00399
4.00	0.14	1.51	0.19	1.32	-1.93794	0.40946
5.00	0.19	1.59	0.22	1.52	-1.63990	0.46058
6.00	0.25	1.78	0.25	1.72	-1.37437	0.57436
7.00	0.35	1.97	0.29	1.92	-1.03846	0.67905
8.00	0.37	1.98	0.34	2.12	-0.99696	0.68209

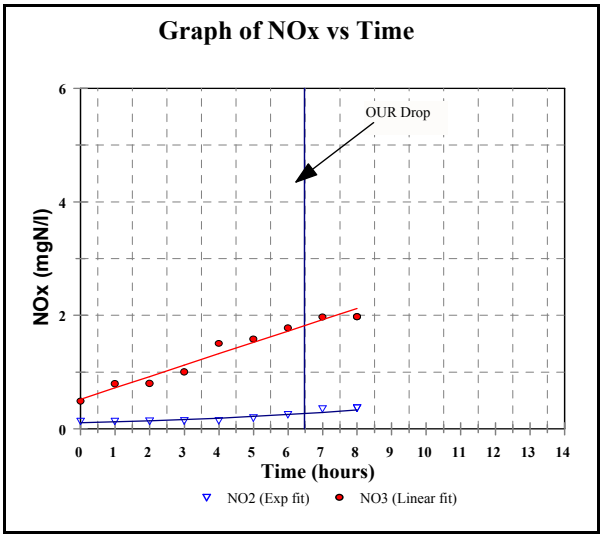

Sew. Batch No.	Batch test No.	Batch test date	Volume (l)		COD Recov. (%)	Regression			ZBH(0) (mgCOD/l)			
			WW	ML		Y-int	Slope	R^2	Measured		Theoretical	
									Batch Test	ML	Batch Test	ML
SB16/03	4	02-Oct	4.5	0.5	97.2	1.4247	0.076	0.940	79.4	793.6	100.5	1004.8

BATCH TEST 5 DATA										
% COD Recovery		End Time=	8.00					CODfilt.	76	
COD t=o	CODt=T	MOt	MOno2	MOno3	MOn	MOc	% Recovery	So(mgCOD/l)	Xo(mgMLVSS/l)	So/Xo
428.00	366.25	46.00	0.71	5.73	6.43	39.57	94.82	68.4	200	0.342
								So(mgCOD/l)	Xo(mgMLAVSS/l)	So/Xo
Parent System		fcv=	1.440	Batch Result				68.4	75.6	0.905
fav	Xv	VML	ZBH(Theo), BT	ZBH(O)	OURSBCOD	KMP	UH	t=s		
0.378	2000	500	108.864	47.74	4	2.17	1.89	4.282		

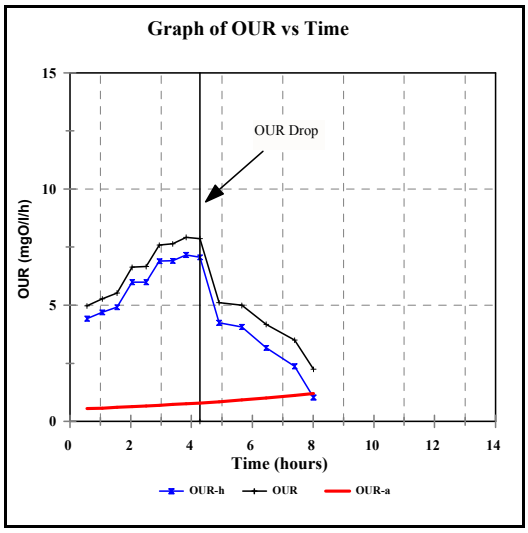

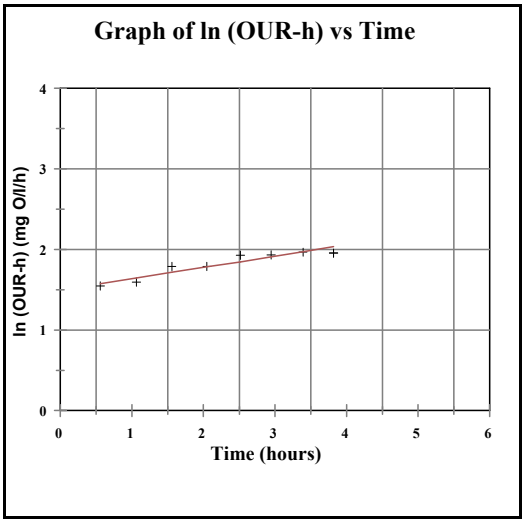

			Fitted Data			
Time	NO_2	NO_3	NO_2	NO_3	$Ln(NO_2)$	$Ln(NO_3)$
	conc.	conc.	conc.	conc.		
	[mg/l]	[mg/l]	[mg/l]	[mg/l]		
0.00	0.06	0.74	0.06	0.81	-2.76462	-0.29975
1.00	0.09	0.94	0.09	0.91	-2.44185	-0.06614
2.00	0.11	1.08	0.12	1.02	-2.21641	0.08066
3.00	0.15	1.17	0.14	1.14	-1.92415	0.15615
4.00	0.15	1.33	0.17	1.29	-1.87080	0.28141
5.00	0.23	1.34	0.19	1.45	-1.47841	0.29342
6.00	0.23	1.65	0.22	1.63	-1.46968	0.50259
7.00	0.24	1.90	0.25	1.83	-1.41882	0.64238
8.00	0.25	1.98	0.27	2.06	-1.37833	0.68310

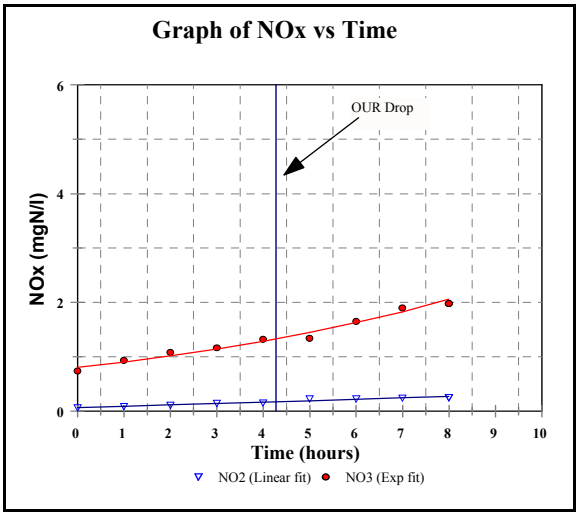

Sew. Batch No.	Batch test No.	Batch test date	Volume (L)		COD Recov. (%)	Regression			ZBH(0) (mgCOD/l)			
			WW	ML		Y-int	Slope	R2	Measured		Theoretical	
									Batch Test	ML	Batch Test	ML
SB17/03	5	08-Oct	4.5	0.5	94.8	1.4252	0.143	0.916	47.7	477.4	108.9	1088.6

BATCH TEST 6 DATA

% COD Recovery		End Time=	8.00					CODfilt.	72.8	
COD t=o	**CODt=T**	**MOt**	**MOno2**	**MOno3**	**MOn**	**MOc**	**% Recovery**	So(mgCOD/l)	Xo(mgMLVSS/l)	**So/Xo**
370.00	322.00	26.10	2.55	4.18	6.73	19.37	92.26	65.52	210	0.312
								So(mgCOD/l)	Xo(mgMLAVSS/l)	**So/Xo**
Parent System		**fcv=**	**1.500**	**Batch Result**				65.52	84.819	0.772
fav	**Xv**	**VML**	**ZBH(Theo)**	**ZBH(O)**	**OUR_{SBCOD}**	**K_{MP}**	**U_H**	**t=s**		
0.4039	**2100**	500	127.2285	17.90	1.11	1.00	3.84	6.211		

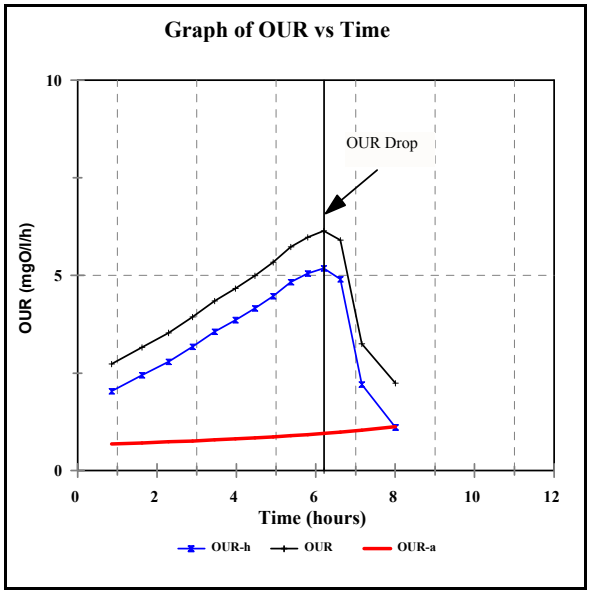

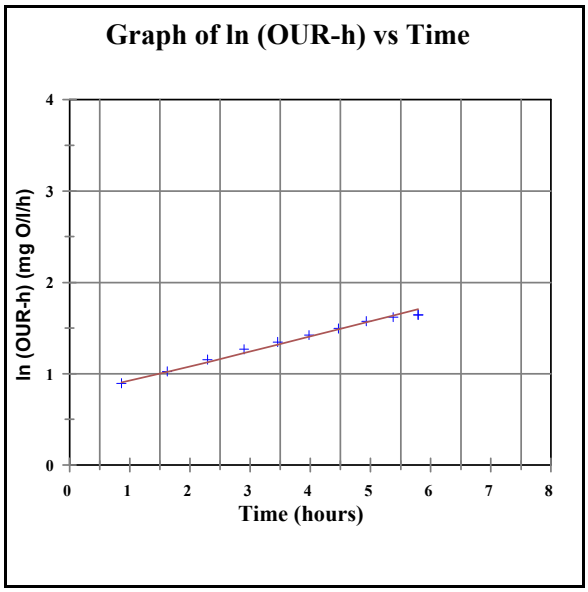

			Fitted Data			
Time	**NO_2**	**NO_3**	**NO_2**	**NO_3**	**Ln(NO_2)**	**Ln(NO_3)**
	conc.	**conc.**	**conc.**	**conc.**		
	[mg/l]	**[mg/l]**	**[mg/l]**	**[mg/l]**		
0.00	0.21	1.04	0.23	1.09	-1.57022	0.04210
1.00	0.28	1.21	0.27	1.21	-1.28735	0.19310
2.00	0.38	1.24	0.33	1.32	-0.98083	0.21350
3.00	0.44	1.53	0.39	1.44	-0.82554	0.42396
4.00	0.44	1.64	0.47	1.55	-0.82554	0.49470
5.00	0.48	1.67	0.57	1.66	-0.74024	0.51103
6.00	0.78	1.80	0.68	1.78	-0.25231	0.58667
7.00	0.78	1.88	0.81	1.89	-0.25103	0.63074
8.00	0.98	1.94	0.97	2.01	-0.02429	0.66475

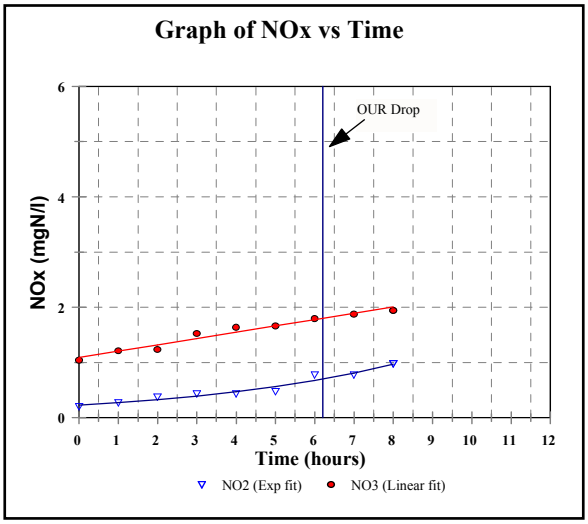

Sew. Batch No.	Batch test No.	Batch test date	Volume (l)		COD Recov. (%)	Regression			ZBH(0) (mgCOD/l)			
			WW	ML		Y-int	Slope	R^2	Measured		Theoretical	
									Batch Test	ML	Batch Test	ML
SB17/03	6	9-0ct	4.5	0.5	92.3	0.6194	0.176	0.987	17.9	179.0	127.2	1272.3

BATCH TEST 7 DATA										
% COD Recovery		**End Time=**	**8.00**					**CODfilt.**	**86**	
COD t=o	**CODt=T**	**MOt**	**MOno2**	**MOno3**	**MOn**	**MOc**	**% Recovery**	So(mgCOD/l)	Xo(mgMLVSS/l)	**So/Xo**
370.00	322.00	28.90	0.68	4.57	5.25	23.65	93.42	77.4	216.7	0.357
								So(mgCOD/l)	Xo(mgMLAVSS/l)	**So/Xo**
Parent System		**fcv=**	**1.480**	**Batch Result**				77.4	84.01459	0.921
fav	**Xv**	**VML**	**ZBH(Theo)**	**$Z_{BH(0)}$**	**OUR_{SBCOD}**	**K_{MP}**	**U_H**	**t=s**		
0.3877	2167	500	124.3415932	18.72	1.95	1.64	3.35	6.099		

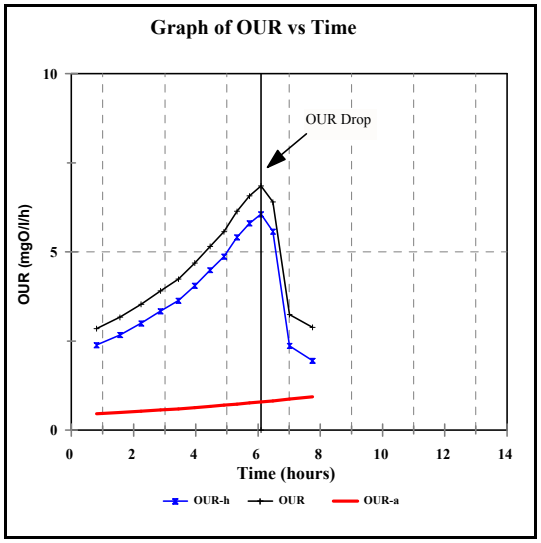

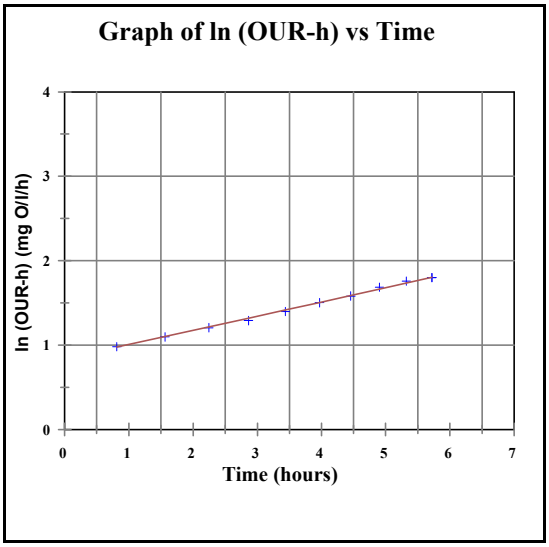

			Fitted Data			
Time	**NO2**	**NO3**	**NO2**	**NO3**	**Ln(NO2)**	**Ln(NO3)**
	conc.	**conc.**	**conc.**	**conc.**		
	[mg/l]	**[mg/l]**	**[mg/l]**	**[mg/l]**		
0.00	0.08	0.93	0.07	0.89	-2.47694	-0.07365
1.00	0.08	0.97	0.08	0.98	-2.47694	-0.02737
2.00	0.12	1.11	0.10	1.08	-2.16282	0.10256
3.00	0.12	1.16	0.12	1.18	-2.13707	0.14756
4.00	0.12	1.24	0.14	1.30	-2.12026	0.21188
5.00	0.12	1.39	0.16	1.43	-2.08747	0.32570
6.00	0.15	1.53	0.19	1.57	-1.87080	0.42723
7.00	0.21	1.63	0.23	1.72	-1.56542	0.48981
8.00	0.44	2.10	0.27	1.89	-0.83241	0.74241

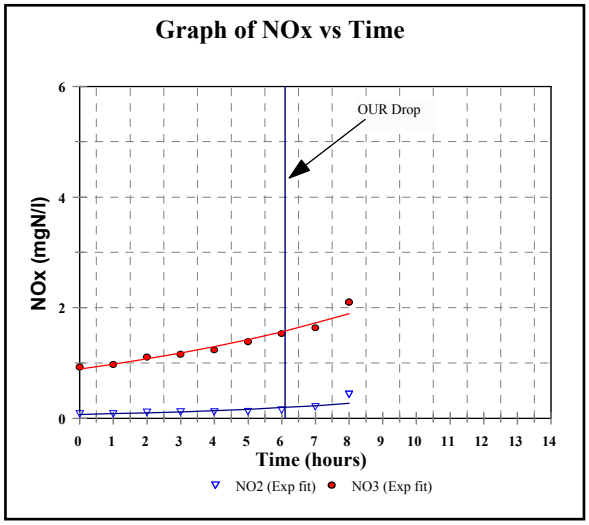

Sew. Batch No.	Batch test No.	Batch test date	Volume (L)		COD Recov. (%)	Regression			$Z_{BH(0)}$ (mgCOD/l)			
			WW	ML		Y-int	Slope	R^2	Measured		Theoretical	
									Batch Test	ML	Batch Test	ML
SB17/03	7	14-0ct	4.5	0.5	93.4	0.6954	0.182	0.997	18.7	187.2	124.3	1243.4

BATCH TEST 8 DATA										
% COD Recovery		**End Time=**	8.00					**CODfilt.**	102	
COD t=o	**CODt=T**	**MOt**	**MOno2**	**MOno3**	**MOn**	**MOc**	**% Recovery**	So(mgCOD/l)	Xo(mgMLVSS/l)	**So/Xo**
408.00	324.00	46.60	1.28	4.65	5.93	40.67	89.38	91.8	209.8	0.438
								So(mgCOD/l)	Xo(mgMLAVSS/l)	**So/Xo**

Parent System		**fcv=**	**1.530**	**Batch Result**				91.8	84.48646	1.087
fav	**Xv**	V_{ML}	**ZBH(Theo)**	**ZBH(O)**	OUR_{SBCOD}	K_{MP}	U_H	**t=s**		
0.4027	**2098**	500	129.3	32.94	3.82	2.07	3.12	5.18		

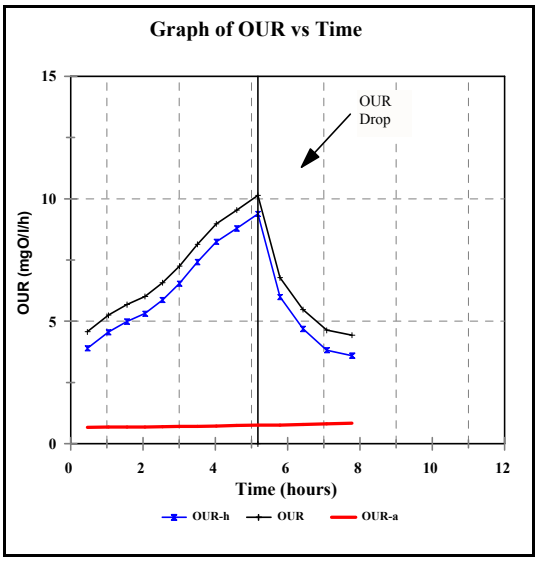

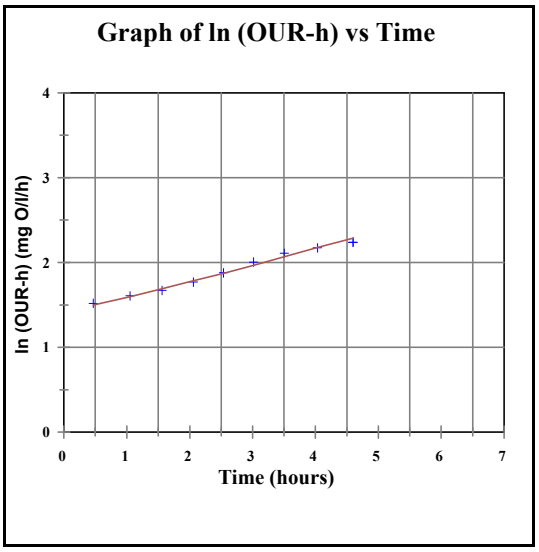

			Fitted Data			
Time	**NO_2**	**NO_3**	**NO_2**	**NO_3**	**Ln(NO_2)**	**Ln(NO_3)**
	conc.	**conc.**	**conc.**	**conc.**		
	[mg/l]	**[mg/l]**	**[mg/l]**	**[mg/l]**		
0.00	0.20	1.47	0.18	1.42	-1.59455	0.38730
1.00	0.21	1.48	0.21	1.55	-1.58475	0.39204
2.00	0.24	1.58	0.24	1.67	-1.42296	0.45806
3.00	0.30	1.74	0.28	1.80	-1.21402	0.55216
4.00	0.30	2.08	0.32	1.93	-1.20065	0.73285
5.00	0.31	2.09	0.37	2.06	-1.16796	0.73908
6.00	0.42	2.29	0.42	2.18	-0.87467	0.82899
7.00	0.46	2.30	0.48	2.31	-0.78746	0.83204
8.00	0.67	2.33	0.56	2.44	-0.40347	0.84372

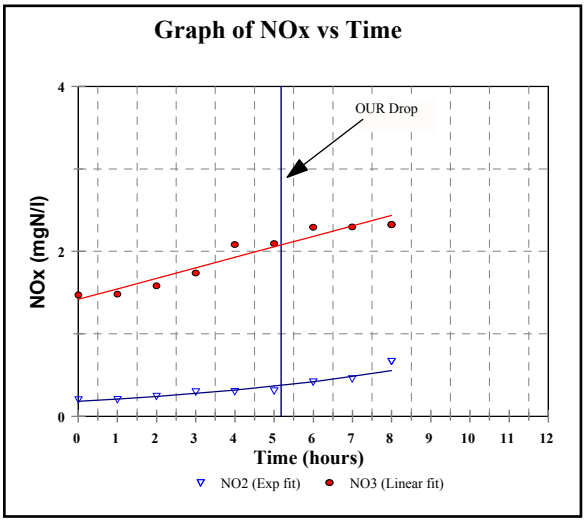

Sew. Batch No.	Batch test No.	Batch test date	Volume (L)		COD Recov. (%)	Regression			ZBH(0) (mgCOD/l)			
			WW	ML		Y-int	Slope	R^2	Measured		Theoretical	
									Batch Test	ML	Batch Test	ML
SB18/03	8	15-Oct	4.5	0.5	89.4	1.3005	0.191	0.991	32.9	329.4	129.3	1292.6

BATCH TEST 9 DATA										
% COD Recovery		**End Time=**	8.00					**CODfilt.**	132	
COD t=o	**CODt=T**	**MOt**	**MOno2**	**MOno3**	**MOn**	**MOc**	**% Recovery**	So(mgCOD/l)	Xo(mgMLVSS/l)	**So/Xo**
270.00	246.00	36.40	4.61	12.58	17.18	19.22	98.23	118.8	347.33	0.342
								So(mgCOD/l)	Xo(mgMLAVSS/l)	**So/Xo**
Parent System		**fcv=**	**1.460**	**Batch Result**				118.8	67.00	1.77
fav	**Xv**	**VML**	**ZBH(Theo)**	$Z_{BH(0)}$	OUR_{SBCOD}	K_{MP}	U_H	**t=s**		
0.3215	**2084**	500	97.820876	57.71	2.911686075	1.67	1.46	3.506		

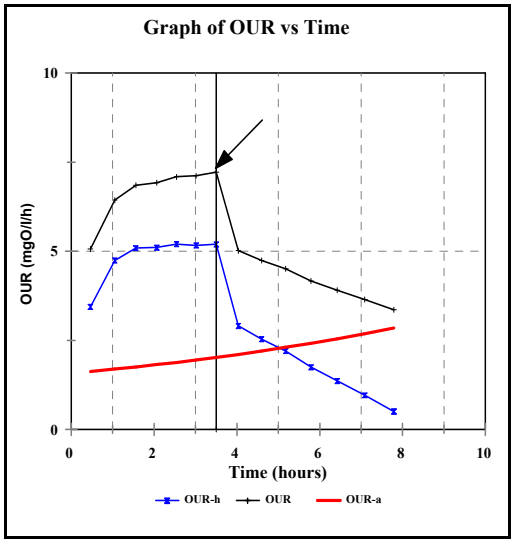

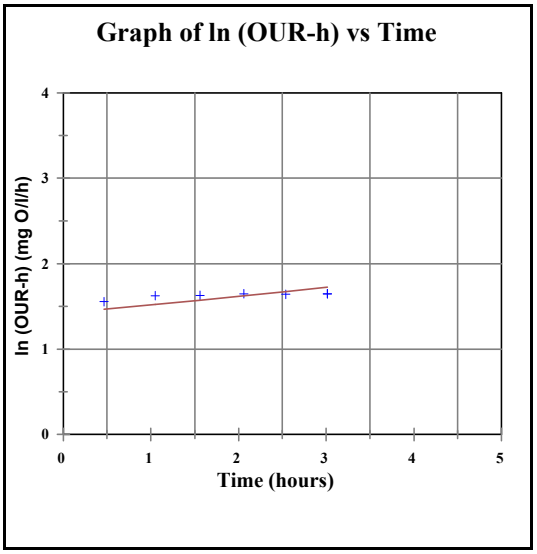

			Fitted Data			
Time	**NO2**	**NO3**	**NO2**	**NO3**	**Ln(NO2)**	**Ln(NO3)**
	conc.	**conc.**	**conc.**	**conc.**		
	[mg/l]	**[mg/l]**	**[mg/l]**	**[mg/l]**		
0.00	0.19	2.31	0.42	2.09	-1.66073	0.83725
1.00	0.71	2.51	0.59	2.32	-0.34249	0.92028
2.00	0.82	2.48	0.76	2.58	-0.19845	0.90826
3.00	0.99	2.64	0.93	2.87	-0.01005	0.97078
4.00	1.22	2.88	1.09	3.18	0.19885	1.05779
5.00	1.29	3.34	1.26	3.53	0.25464	1.20597
6.00	1.33	3.73	1.43	3.93	0.28518	1.31641
7.00	1.56	4.26	1.60	4.36	0.44469	1.44927
8.00	1.74	5.77	1.77	4.84	0.55389	1.75267

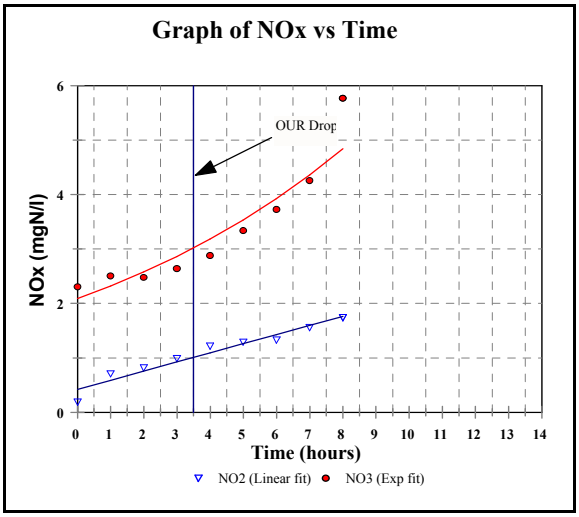

Sew. Batch No.	Batch test No.	Batch test date	Volume (l)		COD Recov. (%)	Regression			$Z_{BH(0)}$ (mgCOD/l)			
			WW	ML		Y-int	Slope	R^2	Measured		Theoretical	
									Batch Test	ML	Batch Test	ML
SB21/04	9	21-Oct	4.5	0.5	98.2	1.3572	0.105	0.566	57.7	577.1	97.8	978.2

BATCH TEST 10 DATA										
% COD Recovery		**End Time=**	8.00					**CODfilt.**	132	
COD t=o	**CODt=T**	**MOt**	**MOno2**	**MOno3**	**MOn**	**MOc**	**% Recovery**	So(mgCOD/l)	Xo(mgMLVSS/l)	**So/Xo**
276.00	244.00	25.80	2.56	8.41	10.98	14.82	93.78	118.8	208.4	0.570
								So(mgCOD/l)	Xo(mgMLAVSS/l)	**So/Xo**
Parent System		**fcv=**	**1.460**	**Batch Result**				118.8	67.0006	1.773
fav	**Xv**	**V_{ML}**	**ZBH(Theo)**	**$Z_{BH(0)}$**	**OUR_{SBCOD}**	**K_{MP}**	**U_H**	**t=s**		
0.3215	**2084**	500	97.820876	40.71	2.375226919	1.71	1.34	4.819		

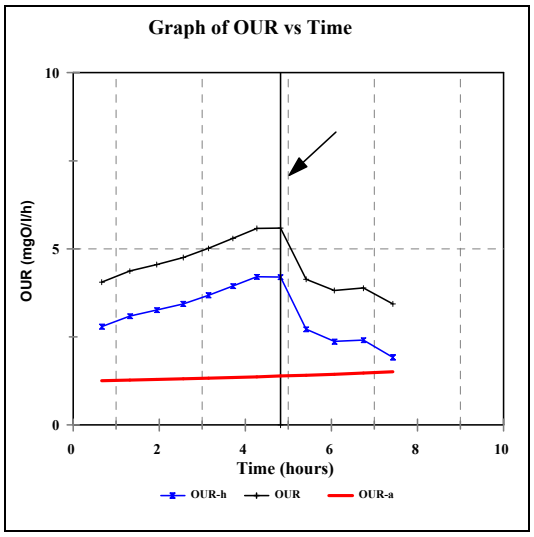

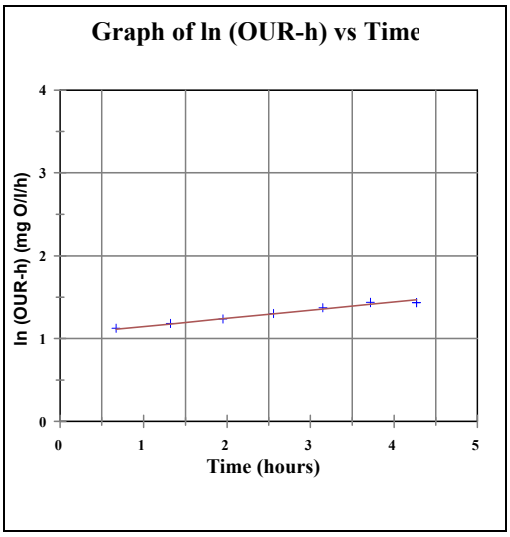

			Fitted Data			
Time	**NO_2**	**NO_3**	**NO_2**	**NO_3**	**Ln(NO_2)**	**Ln(NO_3)**
	conc.	**conc.**	**conc.**	**conc.**		
	[mg/l]	**[mg/l]**	**[mg/l]**	**[mg/l]**		
0.00	0.43	2.64	0.49	2.18	-0.84397	0.97078
1.00	0.48	2.12	0.55	2.41	-0.73397	0.75142
2.00	0.64	2.50	0.62	2.64	-0.44629	0.91629
3.00	0.80	2.86	0.69	2.87	-0.22314	1.05082
4.00	0.84	2.98	0.78	3.10	-0.17435	1.09192
5.00	1.00	3.28	0.87	3.33	0.00000	1.18784
6.00	1.02	3.47	0.98	3.56	0.01980	1.24415
7.00	1.40	3.99	1.10	3.79	0.33647	1.38379
8.00	0.82	4.10	1.24	4.03	-0.19845	1.41099

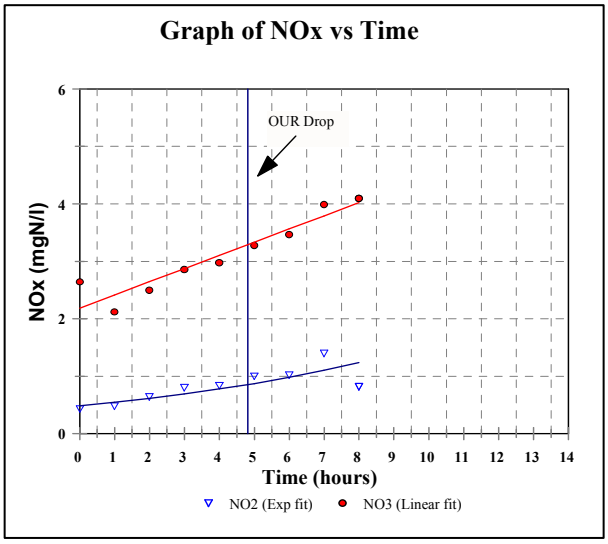

Sew. Batch No.	Batch test No.	Batch test date	Volume (L)		COD Recov. (%)	Regression			$Z_{BH(0)}$ (mgCOD/l)			
			WW	ML		Y-int	Slope	R^2	Measured		Theoretical	
									Batch Test	ML	Batch Test	ML
SB21/04	10	21OCT 04	4.5	0.5	93.8	0.9814	0.101	0.983	40.7	407.1	97.8	978.2

BATCH TEST 11 DATA										
% COD Recovery		**End Time=**	8.00					**CODfilt.**	84	
COD t=o	**CODt=T**	**MOt**	**MOno2**	**MOno3**	**MOn**	**MOc**	**% Recovery**	So(mgCOD/l)	Xo(mgMLVSS/l)	**So/Xo**
290.00	245.00	41.90	5.50	19.05	24.55	17.35	90.47	77.28	176.32	0.438
								So(mgCOD/l)	Xo(mgMLAVSS/l)	**So/Xo**
Parent System		**fcv=**	**1.430**	**Batch Result**				77.28	54.377088	1.421
fav	**Xv**	**VML**	**ZBH(Theo)**	**$Z_{BH(0)}$**	**OUR_{SBCOD}**	**K_{MP}**	**U_H**	**t=s**		
0.3084	**2204**	400	77. 8	28.86	0.95158904	0.75	3.02	5.66		

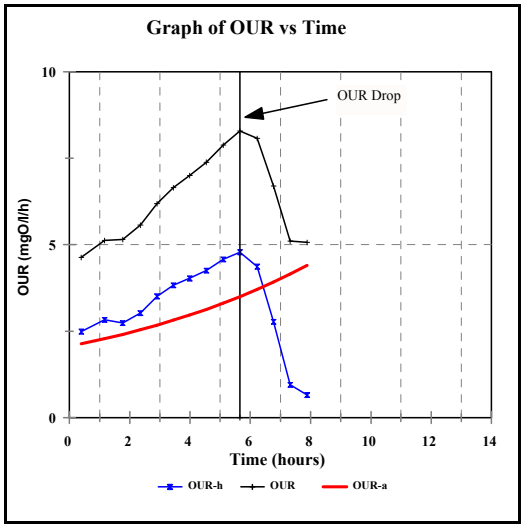

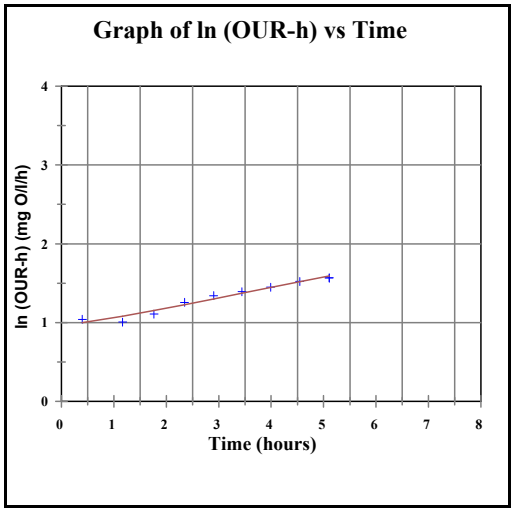

			Fitted Data			
Time	**NO_2**	**NO_3**	**NO_2**	**NO_3**	**Ln(NO_2)**	**Ln(NO_3)**
	conc.	**conc.**	**conc.**	**conc.**		
	[mg/l]	**[mg/l]**	**[mg/l]**	**[mg/l]**		
0.00	0.22	2.35	0.30	2.40	-1.51413	0.85442
1.00	0.55	2.87	0.50	2.72	-0.59784	1.05431
2.00	0.77	3.11	0.70	3.09	-0.26136	1.13462
3.00	0.90	3.36	0.91	3.50	-0.10536	1.21194
4.00	1.02	3.56	1.11	3.97	0.01980	1.26976
5.00	1.41	4.90	1.31	4.51	0.34359	1.58924
6.00	1.58	5.69	1.51	5.11	0.45742	1.73871
7.00	1.57	5.56	1.71	5.79	0.45108	1.71560
8.00	1.93	6.35	1.91	6.57	0.65752	1.84845

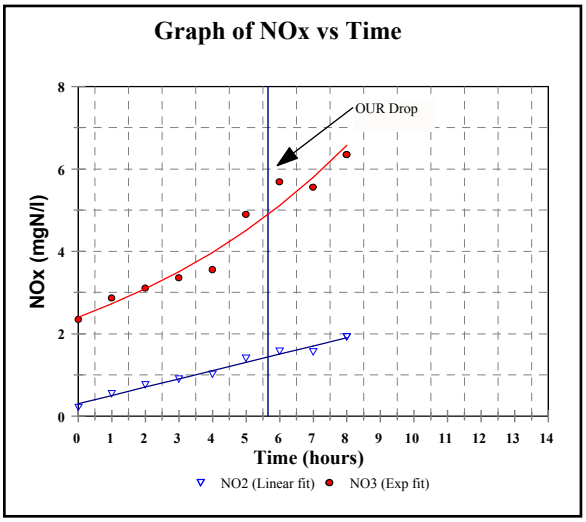

Sew. Batch No.	Batch test No.	Batch test date	Volume (L)		COD Recov. (%)	Regression			$Z_{BH(0)}$ (mgCOD/l)			
			WW	ML		Y-int	Slope	R^2	Measured		Theoretical	
									Batch Test	ML	Batch Test	ML
SB21/04	11	26-Oct	4.6	0.4	90.5	0.8483	0.131	0.973	28.9	360.8	77.8	972.0

BATCH TEST 12 DATA										
% COD Recovery		**End Time=**	8.00					**CODfilt.**	82	
COD t=o	**CODt=T**	**MOt**	**MOno2**	**MOno3**	**MOn**	**MOc**	**% Recovery**	So(mgCOD/l)	Xo(mgMLVSS/l)	**So/Xo**
198.00	172.00	47.70	3.96	11.46	15.42	32.28	103.17	75.44	176.32	0.428
								So(mgCOD/l)	Xo(mgMLAVSS/l)	**So/Xo**
Parent System		**fcv=**	**1.430**	**Batch Result**				75.44	54.377088	1.387
fav	**Xv**	**V_{ML}**	**ZBH(Theo)**	**$Z_{BH(0)}$**	**OUR_{SBCOD}**	**K_{MP}**	**U_H**	**t=s**		
0.3084	**2204**	400	77.8	66.77	4.022813333	1.59	1.28	6.347		

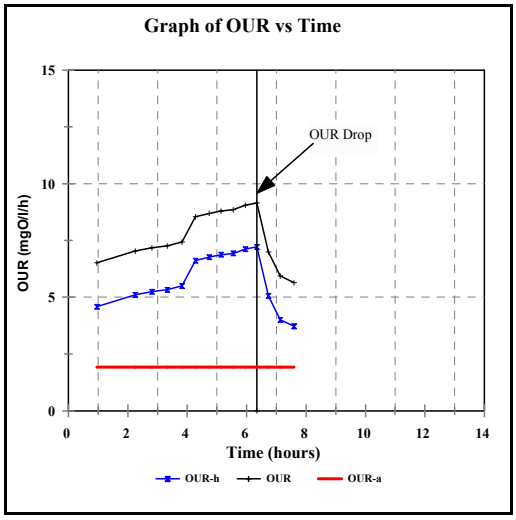

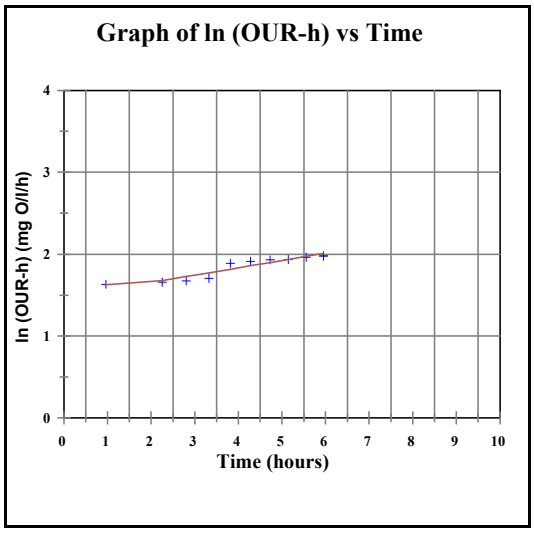

			Fitted Data			
Time	**NO2**	**NO3**	**NO2**	**NO3**	**Ln(NO2)**	**Ln(NO3)**
	conc.	**conc.**	**conc.**	**conc.**		
	[mg/l]	**[mg/l]**	**[mg/l]**	**[mg/l]**		
0.00	0.47	2.67	0.23	1.25	-0.75502	0.98208
1.00	0.29	1.06	0.38	1.56	-1.23787	0.05827
2.00	0.40	1.23	0.52	1.87	-0.91629	0.20701
3.00	0.62	1.65	0.66	2.19	-0.47804	0.50078
4.00	0.77	2.14	0.81	2.50	-0.26136	0.76081
5.00	0.88	2.62	0.95	2.81	-0.12783	0.96317
6.00	1.16	3.36	1.10	3.13	0.14842	1.21194
7.00	1.10	3.68	1.24	3.44	0.09531	1.30291
8.00	1.58	4.10	1.38	3.76	0.45742	1.41099

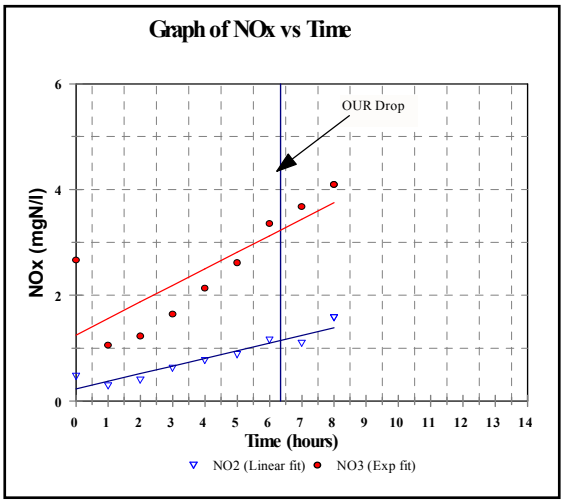

Sew. Batch No.	Batch test No.	Batch test date	Volume (L)		COD Recov. (%)	Regression			ZBH(0) (mgCOD/l)			
			WW	ML		Y-int	Slope	R_2	Measured		Theoretical	
									Batch Test	ML	Batch Test	ML
SB21/04	12	26 -Oct 04	4.6	0.4	103.2	1.4150	0.094	0.930	66.8	834.6	77.8	972.0

BATCH TEST 13 DATA										
% COD Recovery		**End Time=**	8.00					**CODfilt.**	82	
COD t=o	**CODt=T**	**MOt**	**MOno2**	**MOno3**	**MOn**	**MOc**	**% Recovery**	So(mgCOD/l)	Xo(mgMLVSS/l)	**So/Xo**
300.00	260.00	41.90	1.74	15.70	17.43	24.47	94.82	72.16	281.4	0.256
								So(mgCOD/l)	Xo(mgMLAVSS/l)	**So/Xo**
Parent System		**fcv=**	**1.470**	**Batch Result**				72.16	90.21684	0.800
fav	**Xv**	**V_{ML}**	**ZBH(Theo)**	**ZBH(O)**	**OUR_{SBCOD}**	**K_{MP}**	**U_H**	**t=s**		
0.3206	**2345**	600	132.6187548	21.87	2.9	2.31	2.60	5.66		

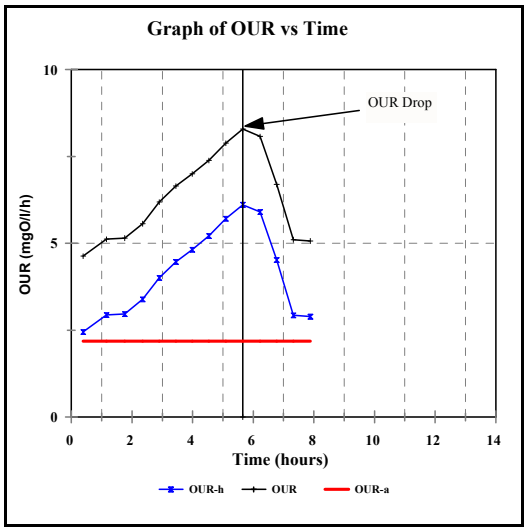

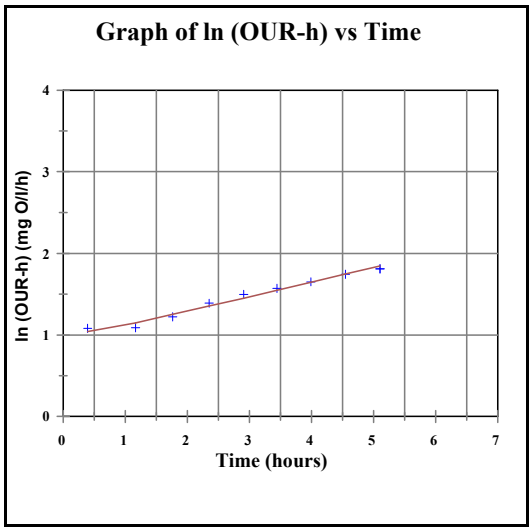

			Fitted Data			
Time	**NO2**	**NO3**	**NO2**	**NO3**	**Ln(NO2)**	**Ln(NO3)**
	conc.	**conc.**	**conc.**	**conc.**		
	[mg/l]	**[mg/l]**	**[mg/l]**	**[mg/l]**		
0.00	0.14	2.01	0.21	2.22	-1.96611	0.69813
1.00	0.29	2.75	0.27	2.65	-1.23787	1.01160
2.00	0.33	3.36	0.33	3.08	-1.10866	1.21194
3.00	0.44	3.60	0.40	3.51	-0.82098	1.28093
4.00	0.49	3.83	0.46	3.94	-0.71335	1.34286
5.00	0.54	4.23	0.52	4.37	-0.61619	1.44220
6.00	0.60	4.56	0.59	4.80	-0.51083	1.51732
7.00	0.65	5.46	0.65	5.23	-0.43078	1.69745
8.00	0.66	5.66	0.71	5.66	-0.41552	1.73342

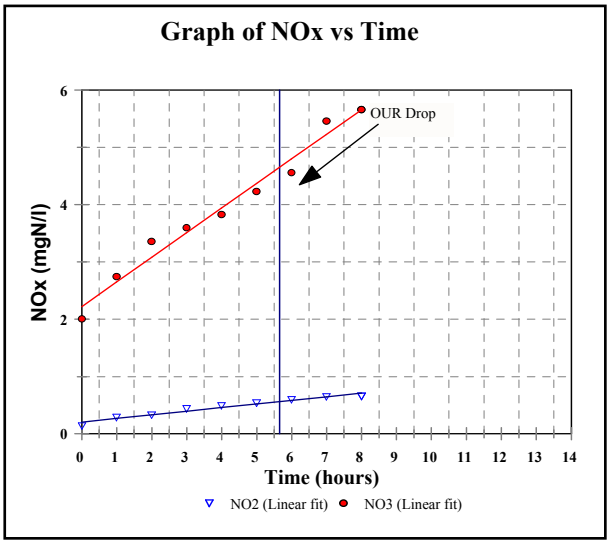

Sew. Batch No.	Batch test No.	Batch test date	Volume (l)		COD Recov. (%)	Regression			ZBH(0) (mgCOD/l)			
			WW	ML		Y-int	Slope	R2	Measured		Theoretical	
									Batch Test	ML	Batch Test	ML
SB21/04	13	28-Oct	4.4	0.6	94.8	0.8347	0.179	0.987	21.9	182.3	132.6	1105.2

BATCH TEST 14 DATA										
% COD Recovery		**End Time=**	8.00					**CODfilt.**	76	
COD t=o	**CODt=T**	**MOt**	**MOno2**	**MOno3**	**MOn**	**MOc**	**% Recovery**	So(mgCOD/l)	Xo(mgMLVSS/l)	**So/Xo**
320.00	312.00	39.50	4.49	9.31	13.80	25.70	105.53	68.4	234.5	0.292
								So(mgCOD/l)	Xo(mgMLAVSS/l)	**So/Xo**
Parent System		**fcv=**	**1.470**	**Batch Result**				68.4	75.1807	0.910
fav	**Xv**	**VML**	**ZBH(Theo)**	**$Z_{BH(0)}$**	**OUR_{SBCOD}**	**K_{MP}**	**U_H**	**t=s**		
0.3206	2345	500	110.515629	58.23	2.76	1.65	1.06	3.61		

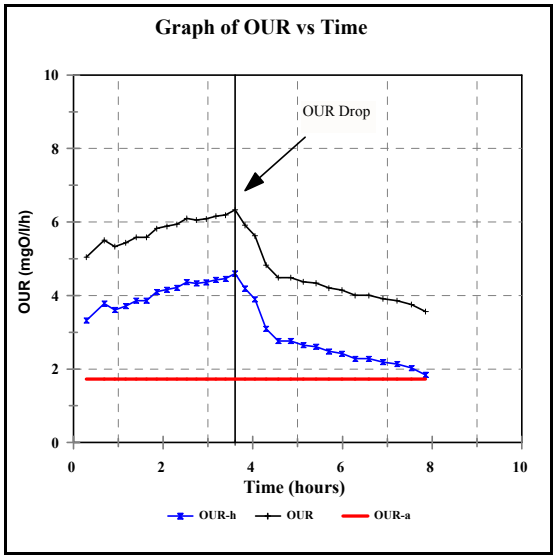

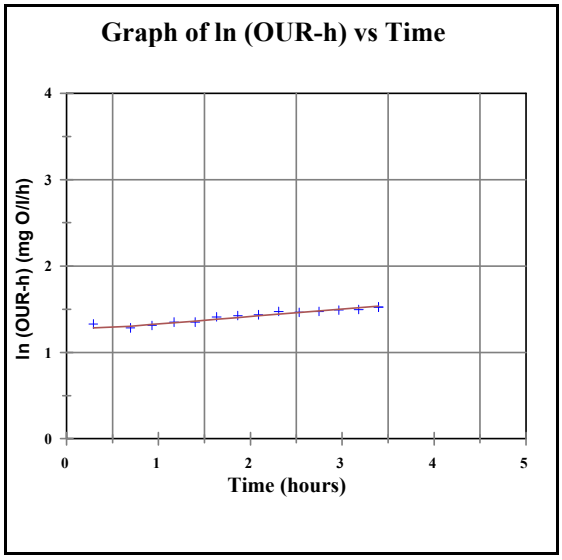

			Fitted Data			
Time	**NO_2**	**NO_3**	**NO_2**	**NO_3**	**Ln(NO_2)**	**Ln(NO_3)**
	conc.	**conc.**	**conc.**	**conc.**		
	[mg/l]	**[mg/l]**	**[mg/l]**	**[mg/l]**		
0.00	0.15	1.82	0.36	2.11	-1.89712	0.59884
1.00	0.59	2.24	0.52	2.36	-0.52763	0.80648
2.00	0.75	2.56	0.69	2.62	-0.28768	0.94001
3.00	0.89	3.16	0.85	2.87	-0.11653	1.15057
4.00	1.08	3.44	1.01	3.13	0.07696	1.23547
5.00	1.22	3.58	1.18	3.38	0.19885	1.27536
6.00	1.45	3.91	1.34	3.63	0.37156	1.36354
7.00	1.54	3.52	1.51	3.89	0.43178	1.25846
8.00	1.46	3.9	1.67	4.14	0.37844	1.36098

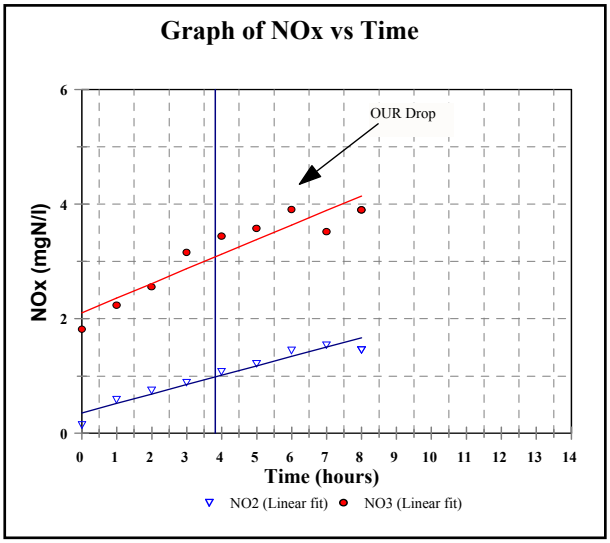

Sew. Batch No.	Batch test No.	Batch test date	Volume (L)		COD Recov. (%)	Regression			$Z_{BH(0)}$ (mgCOD/l)			
			WW	ML		Y-int	Slope	R^2	Measured		Theoretical	
									Batch Test	ML	Batch Test	ML
SB21/04	14	28-Oct	4.5	0.5	105.5	1.2230	0.087	0.930	58.2	582.3	110.5	1105.2

BATCH TEST 15 DATA										
% COD Recovery		**End Time=**	8.00					**CODfilt.**	82	
COD t=o	**CODt=T**	**MOt**	**MOno2**	**MOno3**	**MOn**	**MOc**	**% Recovery**	So(mgCOD/l)	Xo(mgMLVSS/l)	**So/Xo**
320.00	260.00	47.70	7.24	14.00	21.24	26.46	89.52	72.16	242.88	0.297
								So(mgCOD/l)	Xo(mgMLAVSS/l)	**So/Xo**
Parent System		**fcv=**	**1.490**	**Batch Result**				72.16	99.143616	0.728
fav	**Xv**	**VML**	**ZBH(Theo)**	**$Z_{BH(0)}$**	**OUR_{SBCOD}**	**K_{MP}**	**U_H**	**t=s**		
0.4082	**2024**	600	147.72	19.65	2.51	2.41	3.76	4.035		

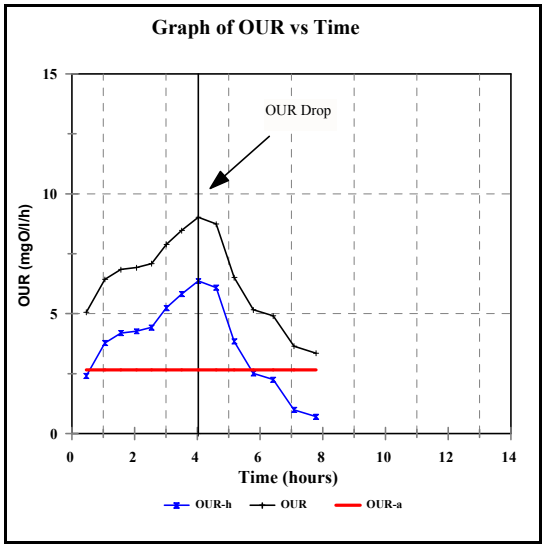

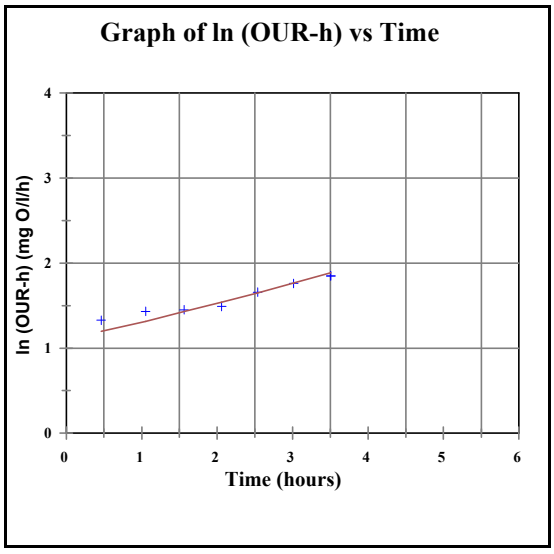

			Fitted Data			
Time	**NO2**	**NO3**	**NO2**	**NO3**	**Ln(NO2)**	**Ln(NO3)**
	conc.	**conc.**	**conc.**	**conc.**		
	[mg/l]	**[mg/l]**	**[mg/l]**	**[mg/l]**		
0.00	0.73	1.15	0.37	1.44	-0.31471	0.13976
1.00	0.54	1.97	0.63	1.82	-0.61619	0.67803
2.00	0.71	2.06	0.90	2.21	-0.34249	0.72271
3.00	1.13	2.6	1.16	2.59	0.12222	0.95551
4.00	1.21	3.29	1.43	2.97	0.19062	1.19089
5.00	1.69	3.71	1.69	3.36	0.52473	1.31103
6.00	1.86	3.74	1.95	3.74	0.62058	1.31909
7.00	2.33	3.94	2.22	4.12	0.84587	1.37118
8.00	2.63	4.3	2.48	4.51	0.96698	1.45862

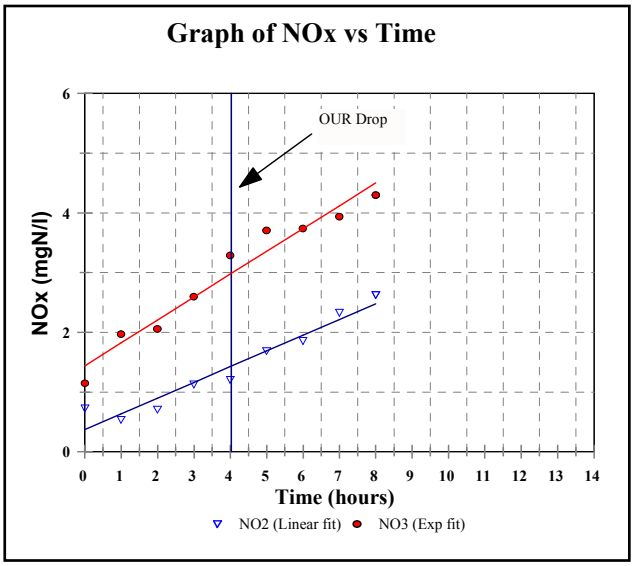

Sew. Batch No.	Batch test No.	Batch test date	Volume (L)		COD Recov. (%)	Regression			$Z_{BH(0)}$ (mgCOD/l)			
			WW	ML		Y-int	Slope	R^2	Measured		Theoretical	
									Batch Test	ML	Batch Test	ML
SB22/04	15	29-Oct	4.4	0.6	89.5	0.9556	0.231	0.891	19.7	163.8	147.7	1231.0

BATCH TEST 16 DATA										
% COD Recovery		**End Time=**	8.00					**CODfilt.**	80	
COD t=o	**CODt=T**	**MOt**	**MOno2**	**MOno3**	**MOn**	**MOc**	**% Recovery**	So(mgCOD/l)	Xo(mgMLVSS/l)	**So/Xo**
352.00	300.00	46.00	5.21	18.30	23.52	22.48	91.61	70.4	242.88	0.290
								So(mgCOD/l)	Xo(mgMLAVSS/l)	**So/Xo**
Parent System		**fcv=**	**1.490**	**Batch Result**				70.4	99.143616	0.710
fav	**Xv**	**VML**	**ZBH(Theo)**	**ZBH(O)**	**OUR_{SBCOD}**	**KMP**	**UH**	**t=s**		
0.4082	**2024**	600	147.72	34.57	1.605	1.13	3.15	4.445		

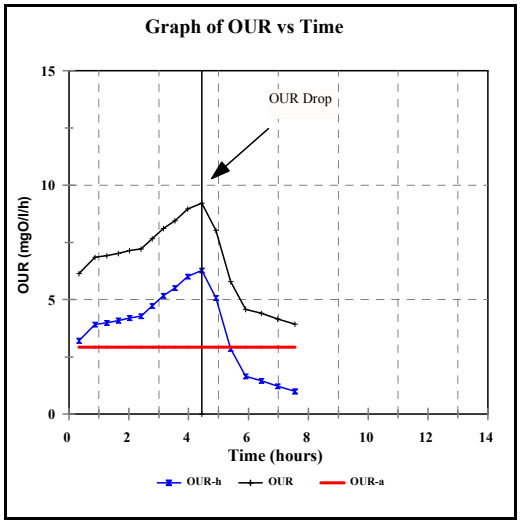

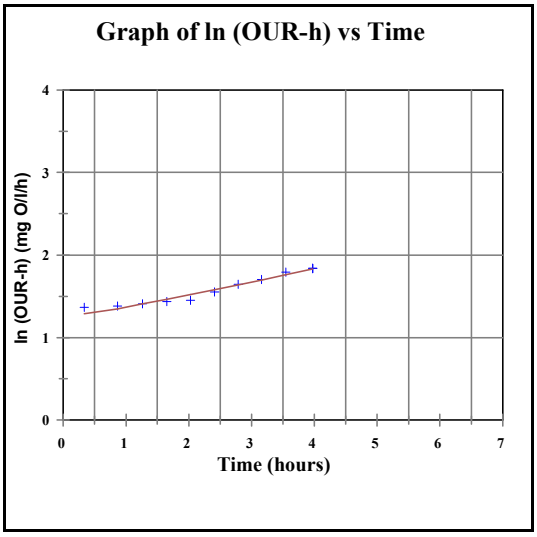

			Fitted Data			
Time	**NO_2**	**NO_3**	**NO_2**	**NO_3**	**Ln(NO_2)**	**Ln(NO_3)**
	conc.	**conc.**	**conc.**	**conc.**		
	[mg/l]	**[mg/l]**	**[mg/l]**	**[mg/l]**		
0.00	0.15	1.9	0.08	1.27	-1.89712	0.64185
1.00	0.29	1.48	0.27	1.77	-1.23787	0.39204
2.00	0.49	2.2	0.46	2.27	-0.71335	0.78846
3.00	0.56	2.6	0.65	2.77	-0.57982	0.95551
4.00	0.76	2.97	0.84	3.27	-0.27444	1.08856
5.00	0.98	3.41	1.03	3.77	-0.02020	1.22671
6.00	1.23	4.39	1.22	4.27	0.20701	1.47933
7.00	1.43	5.03	1.41	4.77	0.35767	1.61542
8.00	1.67	5.45	1.60	5.27	0.51282	1.69562

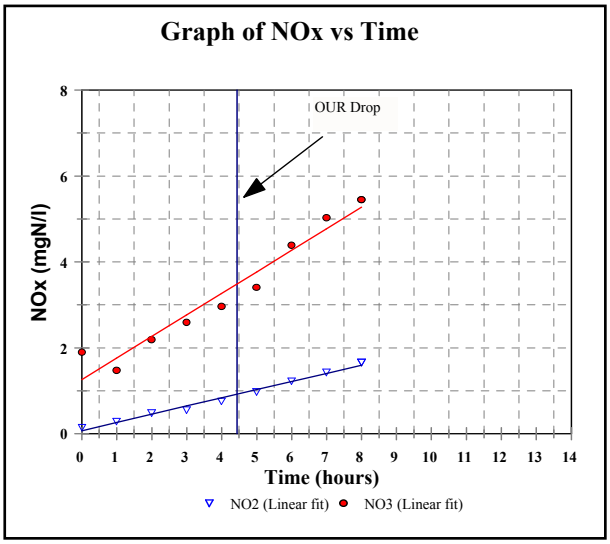

Sew. Batch No.	Batch test No.	Batch test date	Volume (l)		COD Recov. (%)	Regression			$Z_{BH(0)}$ (mgCOD/l)			
			WW	ML		Y-int	Slope	R^2	Measured		Theoretical	
									Batch Test	ML	Batch Test	ML
SB22/04	16	29oct	4.4	0.6	91.6	1.1559	0.153	0.961	34.6	288.1	147.7	1231.0

APPENDIX 11

Comprehensive FISH data for modified batch test

Table 11.1: All experimental FISH data for each modified batch tests; Cell counts (DAPI, EUB, NSO, NIT, NSR) means and standard deviations; percentages of DAPI and EUB are also listed. OHO cell count is determined from subtracting total nitrifiers from EUB cell count

Table 11.1: Comprehensive FISH data for modified batch tests

batch no	tcc(DAPI)	eub cc	nso cc	nit cc	nsr cc	total nitrif	OHO cc	OHO
	(cells/ml)	(cells/ml)	(cells/ml)	(cells/ml)	(cells/ml)	(cells/ml)	(cells/ml)	(mgCOD/l)
B1	3.25E+09	2.20E+09	2.78E+08	1.55E+07	2.89E+07	3.22E+08	1.88E+09	554.74
	3.04E+09	1.99E+09	2.99E+08	1.45E+07	3.05E+07	3.44E+08	1.65E+09	486.31
	2.80E+09	1.90E+09	2.87E+08	1.55E+07	3.15E+07	3.34E+08	1.57E+09	462.91
mean	**3.03E+09**	**2.03E+09**	**2.88E+08**	**1.52E+07**	**3.03E+07**	**3.33E+08**	**1.70E+09**	**501.32**
Stdev	**2.25E+08**	**1.54E+08**	**1.06E+07**	**5.63E+05**	**1.31E+06**	**1.08E+07**	**1.62E+08**	**47.72**
% EUB			14.18	0.75	1.49	16.42	83.58	
%DAPI		67.00	9.50	0.50	1.00	11.00	56.00	
Stdev		7.58						
	3.18E+09	2.64E+09	2.75E+08	3.05E+07	1.55E+08	4.61E+08	2.18E+09	639.50
B2	3.20E+09	2.55E+09	2.55E+08	3.25E+07	1.45E+08	4.33E+08	2.12E+09	621.30
	3.07E+09	2.65E+09	3.21E+08	3.15E+07	1.73E+08	5.25E+08	2.13E+09	624.68
mean	**3.15E+09**	**2.61E+09**	**2.84E+08**	**3.15E+07**	**1.58E+08**	**4.73E+08**	**2.14E+09**	**628.49**
stdev	**7.00E+07**	**5.63E+07**	**3.36E+07**	**1.00E+06**	**1.39E+07**	**4.72E+07**	**3.30E+07**	**9.68**
%EUB			10.84	1.20	6.02	18.07	81.93	
%DAPI		83.00	9.00	1.00	5.00	15.00	68.00	
stdev		2.15						
B3	2.55E+09	2.04E+09	2.44E+08	2.45E+07	1.50E+08	4.19E+08	1.62E+09	495.60
	2.45E+09	1.80E+09	2.20E+08	2.35E+07	1.44E+08	3.88E+08	1.41E+09	431.72
	2.20E+09	1.99E+09	2.56E+08	2.40E+07	1.38E+08	4.18E+08	1.57E+09	481.08
mean	**2.40E+09**	**1.94E+09**	**2.40E+08**	**2.40E+07**	**1.44E+08**	**4.08E+08**	**1.54E+09**	**469.46**
stdev	**1.80E+08**	**1.27E+08**	**1.83E+07**	**5.00E+05**	**6.00E+06**	**1.78E+07**	**1.10E+08**	**33.49**
%EUB			12.35	1.23	7.41	20.99	79.01	
%DAPI		81.00	10.00	1.00	6.00	17.00	64.00	
stdev		6.53						
B4	2.03E+09	1.77E+09	3.55E+08	4.34E+07	1.82E+08	5.80E+08	1.19E+09	351.47
	2.10E+09	1.84E+09	3.45E+08	4.12E+07	1.77E+08	5.63E+08	1.28E+09	377.23
	2.26E+09	2.20E+09	3.86E+08	4.32E+07	2.16E+08	6.46E+08	1.56E+09	460.70
mean	**2.13E+09**	**1.94E+09**	**3.62E+08**	**4.26E+07**	**1.92E+08**	**5.96E+08**	**1.34E+09**	**396.47**
stdev	**1.18E+08**	**2.34E+08**	**2.15E+07**	**1.22E+06**	**2.13E+07**	**4.35E+07**	**1.93E+08**	**57.10**
%EUB			18.68	2.20	9.89	30.77	69.23	
%DAPI		91.00	17.00	2.00	9.00	28.00	63.00	
stdev		12.05						
B5	1.94E+09	1.70E+09	2.62E+08	5.55E+07	1.33E+08	4.51E+08	1.25E+09	**366.62**
	1.20E+09	1.75E+09	2.22E+08	5.32E+07	1.26E+08	4.01E+08	1.35E+09	**395.76**
	2.38E+09	1.63E+09	2.89E+08	5.69E+07	1.27E+08	4.73E+08	1.16E+09	**338.98**
mean	**1.84E+09**	**1.69E+09**	**2.58E+08**	**5.52E+07**	**1.29E+08**	**4.42E+08**	**1.25E+09**	**367.12**
stdev	**5.96E+08**	**6.11E+07**	**3.36E+07**	**1.87E+06**	**3.70E+06**	**3.68E+07**	**9.68E+07**	**28.39**
%EUB			15.22	3.26	7.61	26.09	73.91	
%DAPI		92.00	14.00	3.00	7.00	24.00	68.00	

stdev		3.61						
B6	1.99E+09	1.82E+09	2.04E+08	3.74E+07	7.52E+07	3.17E+08	1.50E+09	459.50
	2.05E+09	1.97E+09	2.33E+08	3.94E+07	7.82E+07	3.51E+08	1.62E+09	494.95
	1.75E+09	1.54E+09	2.58E+08	3.90E+07	7.82E+07	3.75E+08	1.16E+09	355.09
mean	**1.93E+09**	**1.78E+09**	**2.32E+08**	**3.86E+07**	**7.72E+07**	**3.47E+08**	**1.43E+09**	**436.52**
stdev	**1.59E+08**	**2.20E+08**	**2.69E+07**	**1.06E+06**	**1.73E+06**	**2.93E+07**	**2.38E+08**	**72.71**
%EUB			13.04	2.17	4.35	19.57	80.43	
%DAPI		92.00	12.00	2.00	4.00	18.00	74.00	
stdev		12.39						
B7	2.22E+09	1.55E+09	3.04E+08	4.42E+07	1.85E+08	5.33E+08	1.02E+09	**306.63**
	2.10E+09	1.45E+09	3.29E+08	4.23E+07	2.09E+08	5.80E+08	8.70E+08	**262.27**
	2.16E+09	1.67E+09	3.39E+08	4.31E+07	1.89E+08	5.71E+08	1.09E+09	**330.00**
mean	**2.16E+09**	**1.56E+09**	**3.24E+08**	**4.32E+07**	**1.94E+08**	**5.62E+08**	**9.94E+08**	**299.63**
stdev	**6.00E+07**	**1.08E+08**	**1.80E+07**	**9.54E+05**	**1.28E+07**	**2.50E+07**	**1.14E+08**	**34.40**
%EUB			20.83	2.78	12.50	36.11	63.89	
%DAPI		72.00	15.00	2.00	9.00	26.00	46.00	
stdev		6.94						
B8	2.20E+09	1.56E+09	3.32E+08	2.40E+07	1.85E+08	5.41E+08	1.02E+09	317.68
	2.35E+09	1.44E+09	3.03E+08	2.35E+07	1.74E+08	5.01E+08	9.40E+08	292.89
	2.29E+09	1.79E+09	3.91E+08	2.09E+07	1.88E+08	6.00E+08	1.19E+09	370.33
mean	**2.28E+09**	**1.60E+09**	**3.42E+08**	**2.28E+07**	**1.82E+08**	**5.47E+08**	**1.05E+09**	**326.97**
stdev	**7.55E+07**	**1.77E+08**	**4.48E+07**	**1.66E+06**	**7.45E+06**	**5.01E+07**	**1.27E+08**	**39.55**
%EUB			21.43	1.43	11.43	34.29	65.71	
%DAPI		70.00	15.00	1.00	8.00	24.00	46.00	
stdev		11.08						
B9	3.12E+09	2.32E+09	3.33E+08	9.03E+07	2.22E+08	6.45E+08	1.67E+09	505.03
	2.87E+09	2.22E+09	3.18E+08	8.84E+07	2.45E+08	6.51E+08	1.57E+09	473.03
	2.98E+09	2.64E+09	3.36E+08	9.04E+07	2.51E+08	6.77E+08	1.96E+09	590.86
mean	**2.99E+09**	**2.39E+09**	**3.29E+08**	**8.97E+07**	**2.39E+08**	**6.58E+08**	**1.73E+09**	**522.97**
stdev	**1.25E+08**	**2.17E+08**	**9.54E+06**	**1.13E+06**	**1.52E+07**	**1.66E+07**	**2.02E+08**	**60.93**
%EUB			13.75	3.75	10.00	27.50	72.50	
%DAPI		80.00	11.00	3.00	8.00	22.00	58.00	
stdev		9.08						
B10	2.72E+09	2.32E+09	4.04E+08	2.88E+07	1.52E+08	5.85E+08	1.74E+09	509.13
	2.88E+09	2.02E+09	4.42E+08	2.76E+07	1.32E+08	6.02E+08	1.42E+09	416.18
	2.86E+09	2.51E+09	4.23E+08	2.82E+07	1.39E+08	5.90E+08	1.92E+09	564.06
mean	**2.82E+09**	**2.28E+09**	**4.23E+08**	**2.82E+07**	**1.41E+08**	**5.92E+08**	**1.69E+09**	**496.46**
stdev	**8.72E+07**	**2.48E+08**	**1.90E+07**	**6.00E+05**	**1.01E+07**	**8.58E+06**	**2.55E+08**	**74.75**
%EUB			18.52	1.23	6.17	25.93	74.07	
%DAPI		81.00	15.00	1.00	5.00	21.00	60.00	
stdev		10.87						
B11	1.91E+09	1.51E+09	3.33E+08	5.23E+07	2.05E+08	5.90E+08	9.20E+08	**269.85**

	1.75E+09	1.62E+09	3.15E+08	5.33E+07	1.84E+08	5.52E+08	1.07E+09	**313.28**
	1.77E+09	1.11E+09	3.29E+08	5.73E+07	2.08E+08	5.95E+08	5.10E+08	**149.76**
mean	**1.81E+09**	**1.41E+09**	**3.26E+08**	**5.43E+07**	**1.99E+08**	**5.79E+08**	**8.33E+08**	**244.30**
stdev	**8.72E+07**	**2.71E+08**	**9.52E+06**	**2.65E+06**	**1.32E+07**	**2.34E+07**	**2.89E+08**	**84.70**
%EUB			23.08	3.85	14.10	41.03	58.97	
%DAPI		78.00	18.00	3.00	11.00	32.00	46.00	
stdev		19.19						
B12	1.98E+09	1.85E+09	3.25E+08	6.23E+07	2.15E+08	6.02E+08	1.25E+09	363.55
	2.15E+09	1.98E+09	3.12E+08	5.89E+07	1.84E+08	5.55E+08	1.43E+09	415.24
	1.90E+09	1.84E+09	3.28E+08	5.97E+07	2.04E+08	5.92E+08	1.25E+09	363.26
mean	**2.01E+09**	**1.89E+09**	**3.22E+08**	**6.03E+07**	**2.01E+08**	**5.83E+08**	**1.31E+09**	**380.68**
stdev	**1.28E+08**	**7.87E+07**	**8.43E+06**	**1.78E+06**	**1.57E+07**	**2.48E+07**	**1.03E+08**	**2.99E+01**
%EUB			17.02	3.19	10.64	30.85	69.15	
%DAPI		94.00	16.00	3.00	10.00	29.00	65.00	
stdev		4.16						
B13	1.98E+09	1.30E+09	3.45E+08	2.01E+07	2.14E+08	5.79E+08	7.21E+08	**215.93**
	1.85E+09	1.45E+09	3.59E+08	1.92E+07	1.95E+08	5.73E+08	8.77E+08	**262.63**
	1.81E+09	1.42E+09	3.68E+08	1.71E+07	2.11E+08	5.96E+08	8.28E+08	**247.86**
mean	**1.88E+09**	**1.39E+09**	**3.57E+08**	**1.88E+07**	**2.07E+08**	**5.83E+08**	**8.08E+08**	**242.14**
stdev	**8.89E+07**	**8.01E+07**	**1.14E+07**	**1.54E+06**	**1.03E+07**	**1.19E+07**	**7.97E+07**	**23.87**
%EUB			25.68	1.35	14.86	41.89	58.11	
%DAPI		74.00	19.00	1.00	11.00	31.00	43.00	
stdev		5.76						
B14	2.05E+09	1.69E+09	2.64E+08	1.15E+08	2.24E+08	6.03E+08	1.09E+09	**325.59**
	1.95E+09	1.57E+09	2.48E+08	1.20E+08	2.05E+08	5.73E+08	9.97E+08	**298.63**
	1.97E+09	1.75E+09	2.64E+08	1.23E+08	2.28E+08	6.15E+08	1.14E+09	**341.40**
mean	**1.99E+09**	**1.67E+09**	**2.59E+08**	**1.19E+08**	**2.19E+08**	**5.97E+08**	**1.07E+09**	**321.87**
Stdev	**5.29E+07**	**9.38E+07**	**9.27E+06**	**4.13E+06**	**1.22E+07**	**2.16E+07**	**7.22E+07**	**21.63**
%EUB			15.48	7.14	13.10	35.71	64.29	
%DAPI		84.00	13.00	6.00	11.00	30.00	54.00	
stdev		5.61						
B15	2.15E+09	1.45E+09	2.23E+08	4.15E+07	1.01E+08	3.66E+08	1.08E+09	**329.26**
	2.12E+09	1.54E+09	2.35E+08	4.23E+07	1.12E+08	3.89E+08	1.15E+09	**349.36**
	2.03E+09	1.42E+09	2.35E+08	4.22E+07	1.02E+08	3.79E+08	1.04E+09	**315.99**
mean	**2.10E+09**	**1.47E+09**	**2.31E+08**	**4.20E+07**	**1.05E+08**	**3.78E+08**	**1.09E+09**	**331.53**
Stdev	**6.24E+07**	**6.24E+07**	**6.93E+06**	**4.36E+05**	**6.08E+06**	**1.19E+07**	**5.53E+07**	**16.80**
%EUB			15.71	2.86	7.14	25.71	74.29	
%DAPI		70.00	11.00	2.00	5.00	18.00	52.00	
stdev		4.25						
B16	2.50E+09	2.32E+09	2.33E+08	2.44E+07	1.20E+08	3.77E+08	1.94E+09	589.78
	2.44E+09	2.20E+09	2.42E+08	2.50E+07	1.33E+08	4.00E+08	1.80E+09	546.48
	2.53E+09	2.20E+09	2.35E+08	2.53E+07	1.21E+08	3.80E+08	1.82E+09	553.33
mean	**2.49E+09**	**2.24E+09**	**2.37E+08**	**2.49E+07**	**1.25E+08**	**3.86E+08**	**1.86E+09**	**563.20**

Stdev	**4.58E+07**	**6.84E+07**	**4.79E+06**	**4.58E+05**	**7.37E+06**	**1.23E+07**	**7.67E+07**	**23.27**
%EUB			10.56	1.11	5.56	17.22	82.78	
%DAPI		90.00	9.50	1.00	5.00	15.50	74.50	
Stdev		3.05						

APPENDIX 12

NO_3 vs. time plots for Autotrophic batch tests

- NO_3 vs. time and Ln (dNO_3/dt) vs. time profiles for autotrophic batch tests no. AB1 – AB10
- The nitrate/nitrite concentration vs. time profiles recorded during each batch test are also given

Autotrophic batch test 1 Data

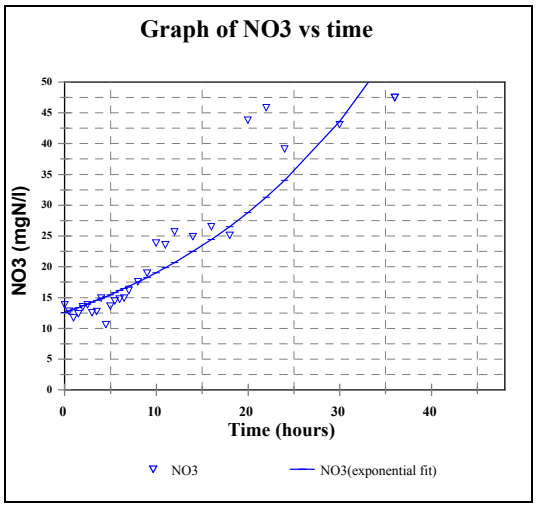

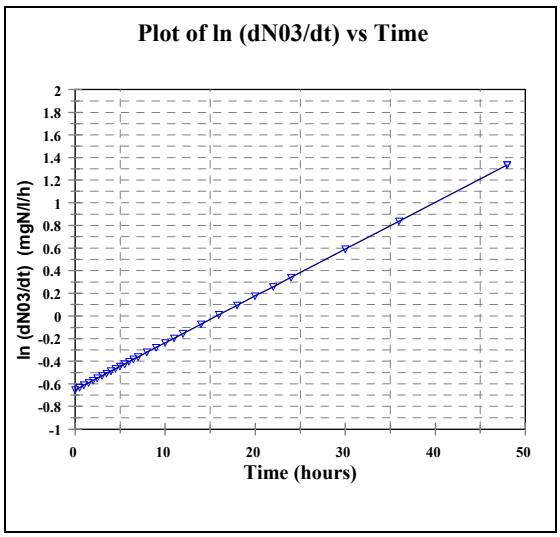

Time	NO_2	NO_3	fitted NO_3	$Ln(NO_3)$
	conc.	conc.	conc.	
	[mg/l]	[mg/l]	[mg/l]	
0.0	1.21	13.84	12.60	2.63
0.5	1.16	12.85	12.86	2.55
1.0	1.16	11.74	13.13	2.46
1.5	1.06	12.40	13.41	2.52
2.0	1.06	13.50	13.69	2.60
2.5	1.13	13.82	13.97	2.63
3.0	1.13	12.56	14.27	2.53
3.5	1.16	12.76	14.56	2.55
4.0	1.18	14.90	14.87	2.70
4.5	1.16	10.64	15.18	2.36
5.0	1.23	13.65	15.50	2.61
5.5	1.31	14.46	15.82	2.67
6.0	1.34	14.76	16.15	2.69
6.5	1.34	14.92	16.49	2.70
7.0	1.25	16.15	16.83	2.78
8.0	1.41	17.57	17.55	2.87
9.0	1.71	19.00	18.29	2.94
10.0	1.76	23.87	19.06	3.17
11.0	2.01	23.58	19.87	3.16
12.0	2.37	25.69	20.70	3.25
14.0	2.62	24.90	22.49	3.21
16.0	3.18	26.54	24.43	3.28
18.0	4.03	25.12	26.54	3.22
20.0	4.43	43.84	28.83	3.78
22.0	5.55	45.84	31.32	3.83
24.0	9.09	39.12	34.02	3.67
30.0	12.33	43.11	43.61	3.76
36.0	9.60	47.47	55.91	3.86
48.0	10.60	63.96	91.87	4.15

dNO_3/dt (mgN/l/h)	$\ln (dtNO_3/dt)$	best fit $\ln(dtNO_3/dt$
0.52	-0.65	-0.65
0.53	-0.63	-0.63
0.54	-0.61	-0.61
0.55	-0.59	-0.59
0.57	-0.57	-0.57
0.58	-0.55	-0.55
0.59	-0.53	-0.53
0.60	-0.51	-0.51
0.62	-0.49	-0.49
0.63	-0.46	-0.46
0.64	-0.44	-0.44
0.65	-0.42	-0.42
0.67	-0.40	-0.40
0.68	-0.38	-0.38
0.70	-0.36	-0.36
0.73	-0.32	-0.32
0.76	-0.28	-0.28
0.79	-0.24	-0.24
0.82	-0.20	-0.20
0.86	-0.15	-0.15
0.93	-0.07	-0.07
1.01	0.01	0.01
1.10	0.09	0.09
1.19	0.18	0.18
1.30	0.26	0.26
1.41	0.34	0.34
1.81	0.59	0.59
2.31	0.84	0.84
3.80	1.34	1.34

Autotrophic batch test 2 Data

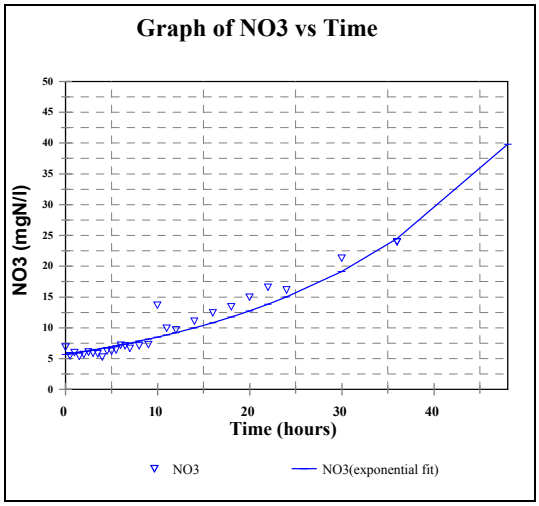

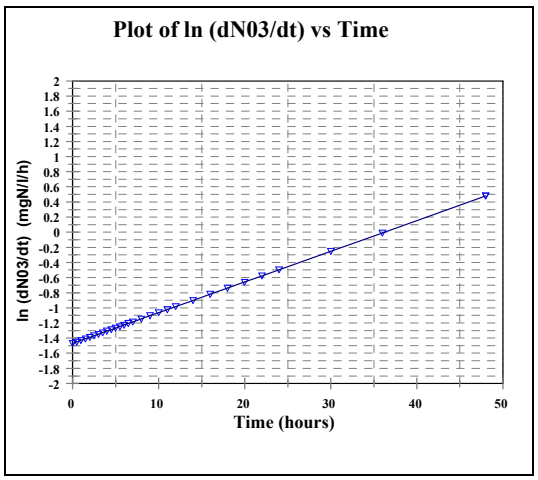

Time	NO_2	NO_3	fitted NO_3	$Ln(NO_3)$
	conc.	conc.	conc.	
	[mg/l]	[mg/l]	[mg/l]	
0.0	1.1	6.9	5.67	1.93
0.5	0.2	5.5	5.78	1.70
1.0	0.2	6	5.90	1.79
1.5	0.3	5.4	6.02	1.69
2.0	0.4	5.7	6.15	1.74
2.5	0.4	6.1	6.27	1.81
3.0	0.5	5.9	6.40	1.77
3.5	0.6	5.8	6.53	1.76
4.0	0.6	5.3	6.67	1.67
4.5	0.7	6.3	6.80	1.84
5.0	0.8	6.2	6.94	1.82
5.5	0.8	6.4	7.09	1.86
6.0	0.9	7.2	7.23	1.97
6.5	0.9	7.1	7.38	1.96
7.0	0.9	6.7	7.53	1.90
8.0	1	7.1	7.84	1.96
9.0	1.1	7.3	8.17	1.99
10.0	1.97	13.73	8.51	2.62
11.0	1.65	9.95	8.86	2.30
12.0	1.71	9.69	9.23	2.27
14.0	1.5	11.1	10.01	2.41
16.0	2.07	12.43	10.86	2.52
18.0	2.38	13.42	11.77	2.60
20.0	2.92	14.98	12.77	2.71
22.0	3.38	16.62	13.85	2.81
24.0	3.45	16.15	15.02	2.78
30.0	6.14	21.36	19.17	3.06
36.0	6.56	24	24.46	3.18
48.0	6.79	27.51	39.82	3.31

dNO_3/dt	$ln (dtNO_3/dt)$	best fit
(mgN/l/h)		$ln(dtNO_3/dt$
0.23	-1.47	-1.47
0.23	-1.45	-1.45
0.24	-1.43	-1.43
0.24	-1.41	-1.41
0.25	-1.39	-1.39
0.25	-1.37	-1.37
0.26	-1.35	-1.35
0.27	-1.33	-1.33
0.27	-1.31	-1.31
0.28	-1.29	-1.29
0.28	-1.27	-1.27
0.29	-1.25	-1.25
0.29	-1.23	-1.23
0.30	-1.20	-1.20
0.31	-1.18	-1.18
0.32	-1.14	-1.14
0.33	-1.10	-1.10
0.35	-1.06	-1.06
0.36	-1.02	-1.02
0.37	-0.98	-0.98
0.41	-0.90	-0.90
0.44	-0.82	-0.82
0.48	-0.74	-0.74
0.52	-0.66	-0.66
0.56	-0.58	-0.58
0.61	-0.49	-0.49
0.78	-0.25	-0.25
0.99	-0.01	-0.01
1.62	0.48	0.48

Autotrophic batch test 3 Data

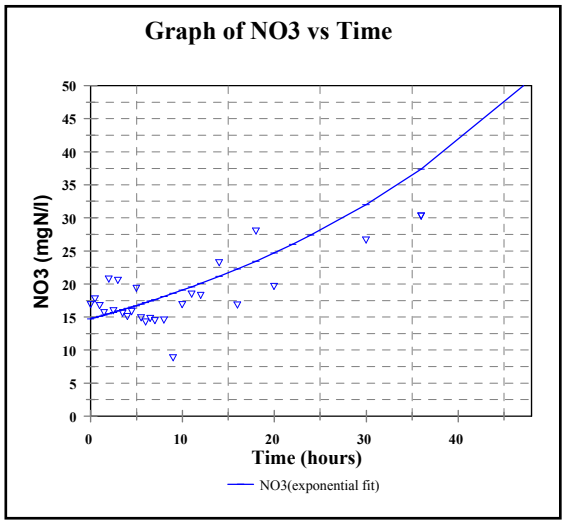

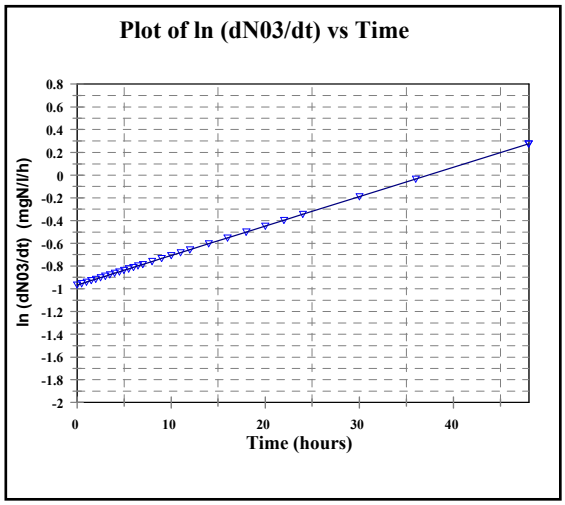

Time	NO_2 conc. [mg/l]	NO_3 conc. [mg/l]	fitted NO_3 conc. [mg/l]	$Ln(NO_3)$
0.0	1.5	16.88	14.72	2.83
0.5	1.45	17.76	14.91	2.88
1.0	1.41	16.74	15.11	2.82
1.5	1.45	15.71	15.30	2.75
2.0	1.77	20.78	15.50	3.03
2.5	1.51	15.98	15.71	2.77
3.0	1.51	20.56	15.91	3.02
3.5	1.59	15.58	16.12	2.75
4.0	1.96	15.1	16.33	2.71
4.5	1.77	15.85	16.54	2.76
5.0	1.82	19.37	16.75	2.96
5.5	1.78	14.87	16.97	2.70
6.0	1.88	14.27	17.19	2.66
6.5	1.92	14.8	17.42	2.69
7.0	2.28	14.48	17.64	2.67
8.0	2.1	14.59	18.11	2.68
9.0	2.34	8.84	18.58	2.18
10.0	2.37	16.88	19.07	2.83
11.0	2.43	18.46	19.57	2.92
12.0	2.5	18.26	20.08	2.90
14.0	2.97	23.23	21.15	3.15
16.0	3.14	16.84	22.27	2.82
18.0	4.1	28.02	23.45	3.33
20.0	4.73	19.67	24.70	2.98
22.0	5.65	62.52	26.01	4.14
24.0	5.63	62.43	27.39	4.13
30.0	7.17	26.69	31.99	3.28
36.0	9.87	30.3	37.37	3.41
48.0	18.97	43.52	50.97	3.77

$dtNO_3/dt$	ln ($dtNO_3$/dt)	best fit ln($dtNO_3$/dt)
0.38	-0.97	-0.97
0.39	-0.95	-0.95
0.39	-0.94	-0.94
0.40	-0.93	-0.93
0.40	-0.91	-0.91
0.41	-0.90	-0.90
0.41	-0.89	-0.89
0.42	-0.87	-0.87
0.42	-0.86	-0.86
0.43	-0.85	-0.85
0.43	-0.84	-0.84
0.44	-0.82	-0.82
0.44	-0.81	-0.81
0.45	-0.80	-0.80
0.46	-0.78	-0.78
0.47	-0.76	-0.76
0.48	-0.73	-0.73
0.49	-0.71	-0.71
0.51	-0.68	-0.68
0.52	-0.65	-0.65
0.55	-0.60	-0.60
0.58	-0.55	-0.55
0.61	-0.50	-0.50
0.64	-0.45	-0.45
0.67	-0.40	-0.40
0.71	-0.34	-0.34
0.83	-0.19	-0.19
0.97	-0.03	-0.03
1.32	0.28	0.28

Autotrophic batch test 4 Data

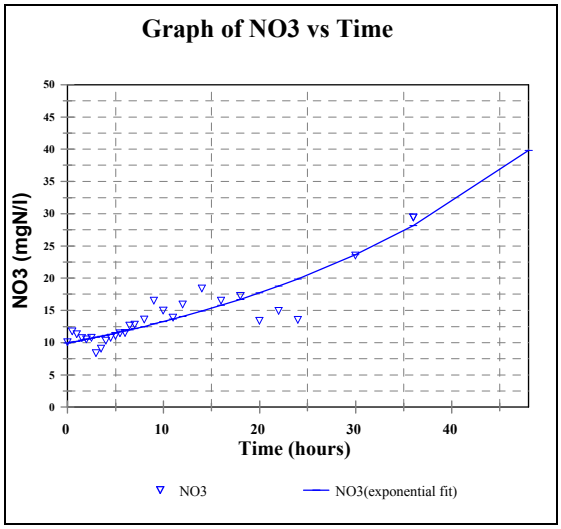

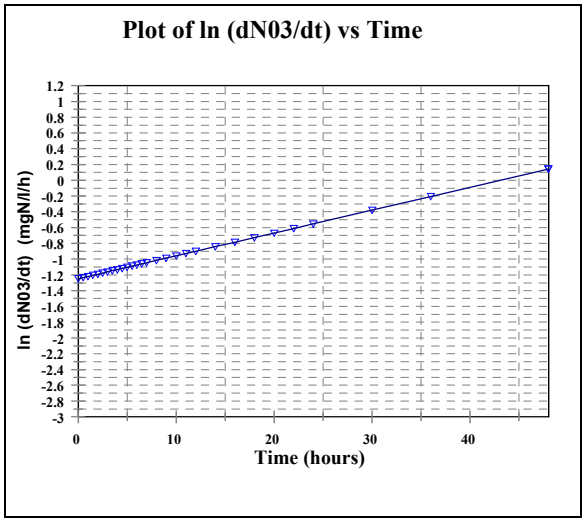

			fitted	
Time	NO_2	NO_3	NO_3	$Ln(NO_3)$
	conc.	conc.	conc.	
	[mg/l]	[mg/l]	[mg/l]	
0.0	1.3	10.11	9.94	2.31
0.5	1.44	11.75	10.09	2.46
1.0	1.4	11.3	10.23	2.42
1.5	1.42	10.73	10.38	2.37
2.0	1.47	10.54	10.53	2.36
2.5	1.53	10.79	10.69	2.38
3.0	1.26	8.37	10.84	2.12
3.5	1.58	9.09	11.00	2.21
4.0	1.71	10.33	11.16	2.34
4.5	1.76	10.78	11.32	2.38
5.0	1.83	11.08	11.49	2.41
5.5	1.88	11.45	11.65	2.44
6.0	1.9	11.52	11.82	2.44
6.5	2.01	12.67	12.00	2.54
7.0	1.97	12.85	12.17	2.55
8.0	2.17	13.6	12.53	2.61
9.0	2.14	16.52	12.90	2.80
10.0	2.6	15.02	13.27	2.71
11.0	1.58	13.91	13.66	2.63
12.0	1.89	15.92	14.06	2.77
14.0	2.24	18.41	14.90	2.91
16.0	3.12	16.52	15.79	2.80
18.0	3.16	17.29	16.73	2.85
20.0	3.79	13.4	17.73	2.60
22.0	4.74	14.94	18.78	2.70
24.0	3.92	13.56	19.90	2.61
30.0	6.45	23.53	23.67	3.16
36.0	8.45	29.45	28.16	3.38
48.0	18.55	48.82	39.84	3.89

dNO_3/dt	ln ($dtNO_3/dt$)	best fit
(mgN/l/h)		ln($dtNO_3/dt$
0.29	-1.25	-1.25
0.29	-1.23	-1.23
0.30	-1.22	-1.22
0.30	-1.20	-1.20
0.30	-1.19	-1.19
0.31	-1.17	-1.17
0.31	-1.16	-1.16
0.32	-1.15	-1.15
0.32	-1.13	-1.13
0.33	-1.12	-1.12
0.33	-1.10	-1.10
0.34	-1.09	-1.09
0.34	-1.07	-1.07
0.35	-1.06	-1.06
0.35	-1.04	-1.04
0.36	-1.02	-1.02
0.37	-0.99	-0.99
0.38	-0.96	-0.96
0.40	-0.93	-0.93
0.41	-0.90	-0.90
0.43	-0.84	-0.84
0.46	-0.78	-0.78
0.48	-0.73	-0.73
0.51	-0.67	-0.67
0.54	-0.61	-0.61
0.58	-0.55	-0.55
0.68	-0.38	-0.38
0.81	-0.21	-0.21
1.15	0.14	0.14

Autotrophic batch test 5 Data

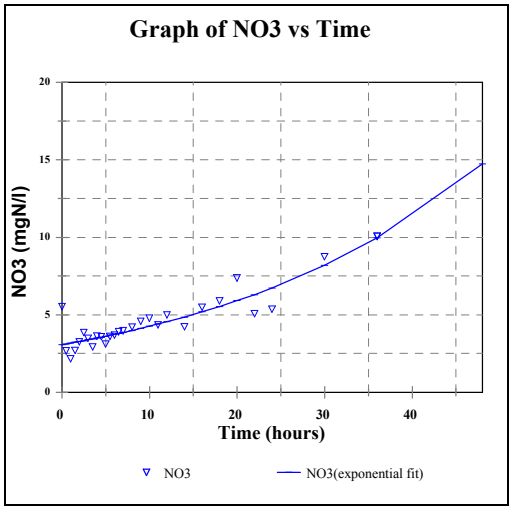

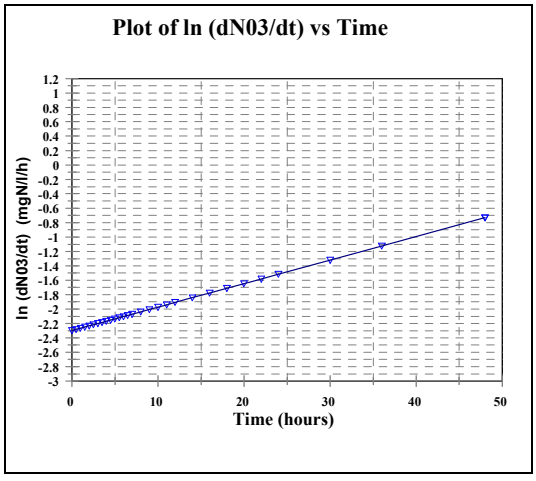

			fitted	
Time	NO_2	NO_3	NO_3	$Ln(NO_3)$
	conc.	conc.	conc.	
	[mg/l]	[mg/l]	[mg/l]	
0.0	1.08	5.54	3.08	1.71
0.5	0	2.67	3.13	0.98
1.0	0	2.17	3.18	0.77
1.5	0.03	2.7	3.23	0.99
2.0	0.04	3.27	3.29	1.18
2.5	0.04	3.87	3.34	1.35
3.0	0.05	3.5	3.40	1.25
3.5	0.04	2.93	3.45	1.08
4.0	0.05	3.62	3.51	1.29
4.5	0.11	3.59	3.57	1.28
5.0	0.09	3.12	3.62	1.14
5.5	0.08	3.61	3.68	1.28
6.0	0.03	3.71	3.74	1.31
6.5	0.12	3.91	3.81	1.36
7.0	0.11	3.97	3.87	1.38
8.0	0.18	4.21	4.00	1.44
9.0	0.18	4.59	4.13	1.52
10.0	0.12	4.78	4.27	1.56
11.0	0.17	4.36	4.41	1.47
12.0	0.12	5.01	4.55	1.61
14.0	0.39	4.24	4.86	1.44
16.0	0.87	5.48	5.19	1.70
18.0	0.51	5.91	5.54	1.78
20.0	1.14	7.38	5.91	2.00
22.0	1.7	5.09	6.31	1.63
24.0	1.8	5.37	6.74	1.68
30.0	2.13	8.75	8.20	2.17
36.0	5.13	10.07	9.97	2.31
48.0	9.05	15.07	14.75	2.71

dNO_3/dt	$ln (dtNO_3/dt)$	best fit
(mgN/l/h)		$ln(dtNO_3/dt$
0.10	-2.30	-2.30
0.10	-2.28	-2.28
0.10	-2.27	-2.27
0.11	-2.25	-2.25
0.11	-2.23	-2.23
0.11	-2.22	-2.22
0.11	-2.20	-2.20
0.11	-2.18	-2.18
0.11	-2.17	-2.17
0.12	-2.15	-2.15
0.12	-2.13	-2.13
0.12	-2.12	-2.12
0.12	-2.10	-2.10
0.12	-2.09	-2.09
0.13	-2.07	-2.07
0.13	-2.04	-2.04
0.13	-2.00	-2.00
0.14	-1.97	-1.97
0.14	-1.94	-1.94
0.15	-1.91	-1.91
0.16	-1.84	-1.84
0.17	-1.78	-1.78
0.18	-1.71	-1.71
0.19	-1.65	-1.65
0.21	-1.58	-1.58
0.22	-1.51	-1.51
0.27	-1.32	-1.32
0.33	-1.12	-1.12
0.48	-0.73	-0.73

Autotrophic batch test 6 Data

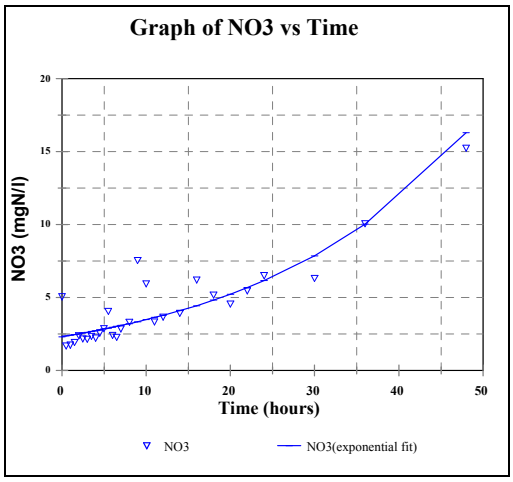

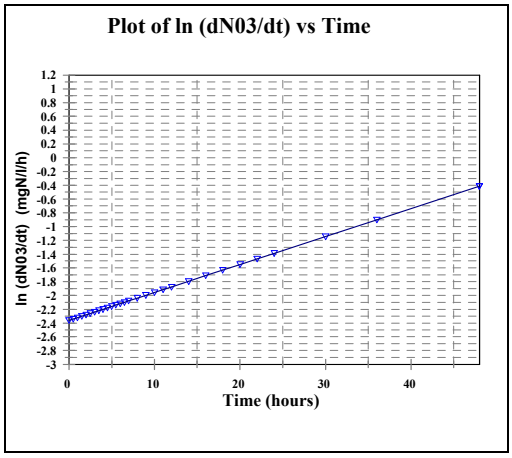

			fitted	
Time	NO_2	NO_3	NO_3	$Ln(NO_3)$
	conc.	conc.	conc.	
	[mg/l]	[mg/l]	[mg/l]	
0.0	1.09	5.05	2.32	1.62
0.5	0.02	1.7	2.37	0.53
1.0	0.03	1.75	2.42	0.56
1.5	0.06	1.93	2.47	0.66
2.0	0.05	2.38	2.52	0.87
2.5	0.06	2.17	2.57	0.77
3.0	0.24	2.15	2.62	0.77
3.5	0.12	2.35	2.68	0.85
4.0	0.08	2.23	2.73	0.80
4.5	0.14	2.56	2.79	0.94
5.0	0.14	2.87	2.85	1.05
5.5	0.18	4.05	2.90	1.40
6.0	0.15	2.41	2.96	0.88
6.5	0.12	2.27	3.02	0.82
7.0	0.14	2.85	3.09	1.05
8.0	0.18	3.32	3.21	1.20
9.0	0.25	7.54	3.35	2.02
10.0	0.1	5.93	3.49	1.78
11.0	0.16	3.33	3.63	1.20
12.0	0.23	3.66	3.78	1.30
14.0	0.24	3.92	4.10	1.37
16.0	0.74	6.2	4.45	1.82
18.0	0.59	5.17	4.82	1.64
20.0	1.69	4.56	5.23	1.52
22.0	2.28	5.45	5.67	1.70
24.0	2.93	6.49	6.15	1.87
30.0	2	6.3	7.85	1.84
36.0	2.07	10.07	10.01	2.31
48.0	9.27	15.23	16.30	2.72

dNO_3/dt	$ln (dtNO_3/dt)$	best fit
(mgN/l/h)		$ln(dtNO_3/dt$
0.09	-2.36	-2.36
0.10	-2.34	-2.34
0.10	-2.32	-2.32
0.10	-2.30	-2.30
0.10	-2.28	-2.28
0.10	-2.26	-2.26
0.11	-2.24	-2.24
0.11	-2.22	-2.22
0.11	-2.20	-2.20
0.11	-2.18	-2.18
0.12	-2.16	-2.16
0.12	-2.14	-2.14
0.12	-2.12	-2.12
0.12	-2.10	-2.10
0.13	-2.08	-2.08
0.13	-2.04	-2.04
0.14	-2.00	-2.00
0.14	-1.96	-1.96
0.15	-1.91	-1.91
0.15	-1.87	-1.87
0.17	-1.79	-1.79
0.18	-1.71	-1.71
0.20	-1.63	-1.63
0.21	-1.55	-1.55
0.23	-1.47	-1.47
0.25	-1.39	-1.39
0.32	-1.14	-1.14
0.41	-0.90	-0.90
0.66	-0.41	-0.41

Autotrophic batch test 7 Data

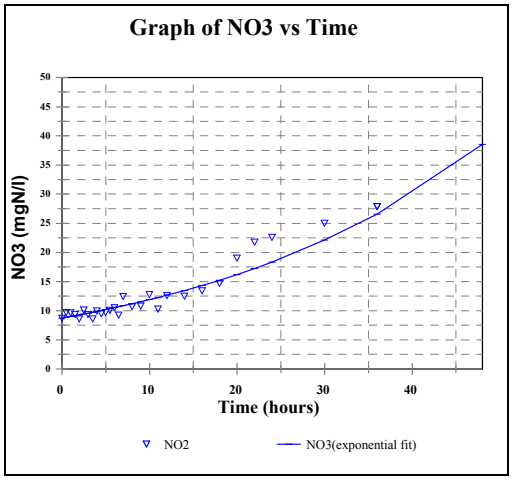

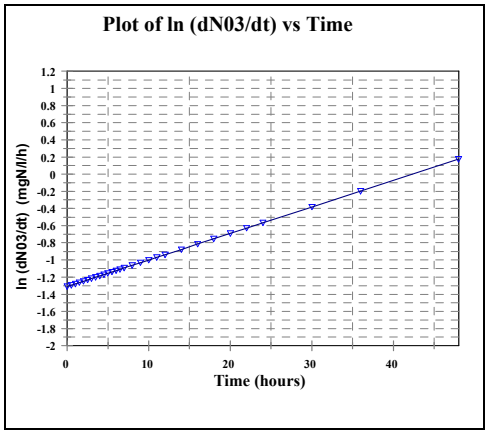

			fitted	
Time	NO_2	NO_3	NO_3	$Ln(NO_3)$
	conc.	conc.	conc.	
	[mg/l]	[mg/l]	[mg/l]	
0.0	0.33	8.73	8.74	2.17
0.5	0.12	9.71	8.88	2.27
1.0	0.11	9.67	9.02	2.27
1.5	0.1	9.38	9.16	2.24
2.0	0.11	8.6	9.30	2.15
2.5	0.11	10.14	9.44	2.32
3.0	0.16	9.39	9.59	2.24
3.5	0.19	8.63	9.74	2.16
4.0	0.19	10	9.89	2.30
4.5	0.23	9.48	10.05	2.25
5.0	0.28	9.71	10.20	2.27
5.5	0.31	10.08	10.36	2.31
6.0	0.38	10.51	10.52	2.35
6.5	0.39	9.24	10.69	2.22
7.0	0.4	12.41	10.85	2.52
8.0	0.47	10.66	11.19	2.37
9.0	0.54	10.82	11.55	2.38
10.0	0.54	12.77	11.91	2.55
11.0	0.55	10.3	12.28	2.33
12.0	0.65	12.61	12.67	2.53
14.0	0.83	12.51	13.48	2.53
16.0	0.97	13.42	14.33	2.60
18.0	1.25	14.67	15.25	2.69
20.0	1.13	19.05	16.22	2.95
22.0	1.58	21.79	17.26	3.08
24.0	4.35	22.61	18.36	3.12
30.0	5.48	25.06	22.09	3.22
36.0	4.38	27.89	26.60	3.33
48.0	10.53	29.5	38.54	3.38

dNO_3/dt	$ln (dtNO_3/dt)$	best fit
(mgN/l/h)		$ln(dtNO_3/dt$
0.27	-1.31	-1.31
0.27	-1.29	-1.29
0.28	-1.28	-1.28
0.28	-1.26	-1.26
0.29	-1.25	-1.25
0.29	-1.23	-1.23
0.30	-1.22	-1.22
0.30	-1.20	-1.20
0.31	-1.19	-1.19
0.31	-1.17	-1.17
0.32	-1.15	-1.15
0.32	-1.14	-1.14
0.33	-1.12	-1.12
0.33	-1.11	-1.11
0.34	-1.09	-1.09
0.35	-1.06	-1.06
0.36	-1.03	-1.03
0.37	-1.00	-1.00
0.38	-0.97	-0.97
0.39	-0.94	-0.94
0.42	-0.88	-0.88
0.44	-0.81	-0.81
0.47	-0.75	-0.75
0.50	-0.69	-0.69
0.53	-0.63	-0.63
0.57	-0.57	-0.57
0.68	-0.38	-0.38
0.82	-0.20	-0.20
1.19	0.17	0.17

Autotrophic batch test 8 Data

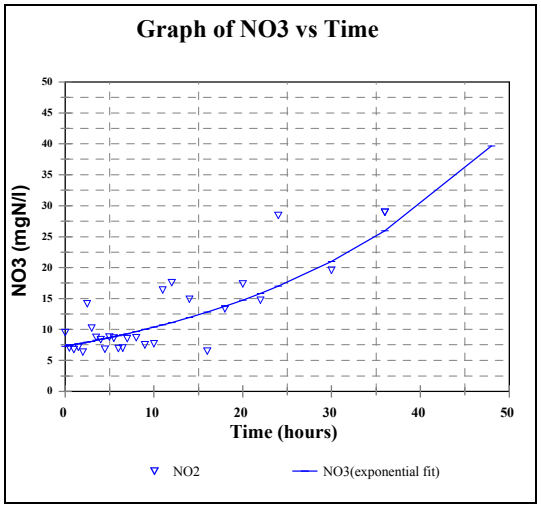

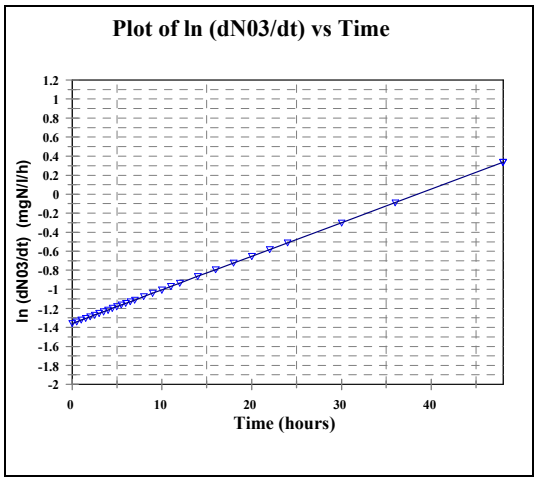

			fitted	
Time	NO_2	NO_3	NO_3	$Ln(NO_3)$
	conc.	conc.	conc.	
	[mg/l]	[mg/l]	[mg/l]	
0.0	0.36	9.48	7.30	2.25
0.5	0.12	7.05	7.43	1.95
1.0	0.1	6.77	7.56	1.91
1.5	0.09	7.14	7.69	1.97
2.0	0.1	6.36	7.83	1.85
2.5	0.09	14.17	7.97	2.65
3.0	0.12	10.27	8.11	2.33
3.5	0.15	8.74	8.26	2.17
4.0	0.17	8.39	8.40	2.13
4.5	0.19	6.84	8.55	1.92
5.0	0.22	8.82	8.71	2.18
5.5	0.26	8.6	8.86	2.15
6.0	0.29	6.93	9.02	1.94
6.5	0.3	7.02	9.18	1.95
7.0	0.34	8.55	9.34	2.15
8.0	0.39	8.69	9.68	2.16
9.0	0.43	7.55	10.02	2.02
10.0	0.46	7.71	10.38	2.04
11.0	0.54	16.4	10.76	2.80
12.0	0.55	17.58	11.14	2.87
14.0	0.74	14.88	11.96	2.70
16.0	0.89	6.52	12.83	1.87
18.0	1.14	13.34	13.77	2.59
20.0	0.96	17.35	14.78	2.85
22.0	0.97	14.74	15.86	2.69
24.0	2.79	28.44	17.01	3.35
30.0	4.95	19.59	21.02	2.98
36.0	9.21	28.98	25.98	3.37
48.0	12.23	33.75	39.67	3.52

dNO_3/dt	$ln (dtNO_3/dt)$	best fit
(mgN/l/h)		$ln(dtNO_3/dt$
0.26	-1.36	-1.36
0.26	-1.34	-1.34
0.27	-1.32	-1.32
0.27	-1.30	-1.30
0.28	-1.29	-1.29
0.28	-1.27	-1.27
0.29	-1.25	-1.25
0.29	-1.23	-1.23
0.30	-1.22	-1.22
0.30	-1.20	-1.20
0.31	-1.18	-1.18
0.31	-1.16	-1.16
0.32	-1.15	-1.15
0.32	-1.13	-1.13
0.33	-1.11	-1.11
0.34	-1.07	-1.07
0.35	-1.04	-1.04
0.37	-1.00	-1.00
0.38	-0.97	-0.97
0.39	-0.93	-0.93
0.42	-0.86	-0.86
0.45	-0.79	-0.79
0.49	-0.72	-0.72
0.52	-0.65	-0.65
0.56	-0.58	-0.58
0.60	-0.51	-0.51
0.74	-0.30	-0.30
0.92	-0.09	-0.09
1.40	0.34	0.34

Autotrophic batch test 9 Data

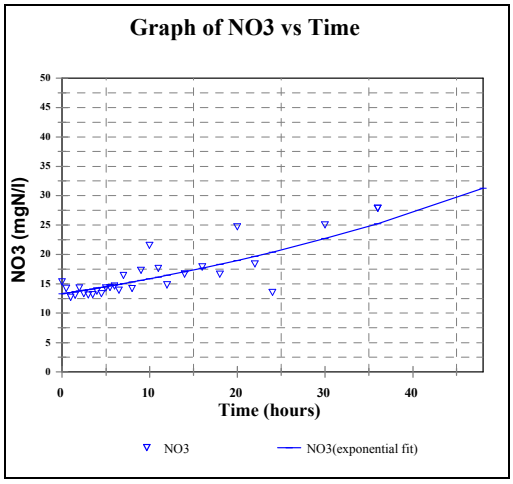

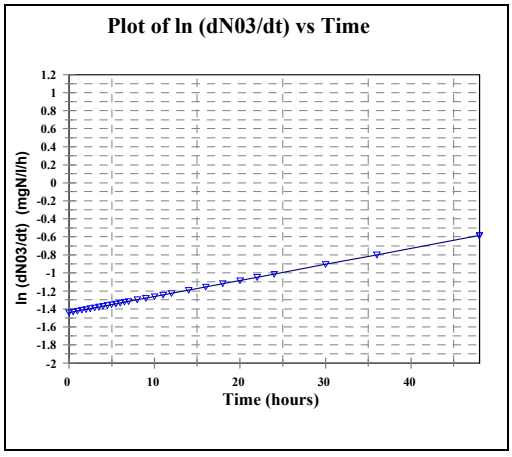

Time	NO_2	NO_3	fitted NO_3	$Ln(NO_3)$
	conc.	conc.	conc.	
	[mg/l]	[mg/l]	[mg/l]	
0.0	1.24	15.36	13.30	2.73
0.5	0.13	14.22	13.42	2.65
1.0	0.15	12.71	13.54	2.54
1.5	0.11	13.09	13.66	2.57
2.0	0.08	14.32	13.78	2.66
2.5	0.21	13.35	13.90	2.59
3.0	0.1	13.13	14.03	2.57
3.5	0.15	13.21	14.15	2.58
4.0	0.12	13.75	14.28	2.62
4.5	0.11	13.35	14.41	2.59
5.0	0.11	14.33	14.54	2.66
5.5	0.16	14.36	14.67	2.66
6.0	0.16	14.65	14.80	2.68
6.5	0.19	13.94	14.93	2.63
7.0	0.17	16.45	15.07	2.80
8.0	0.25	14.2	15.34	2.65
9.0	0.26	17.31	15.61	2.85
10.0	0.47	21.57	15.89	3.07
11.0	0.53	17.66	16.18	2.87
12.0	0.47	14.84	16.47	2.70
14.0	0.92	16.69	17.07	2.81
16.0	1.51	17.9	17.69	2.88
18.0	3.1	16.64	18.33	2.81
20.0	2.17	24.71	18.99	3.21
22.0	1.94	18.43	19.68	2.91
24.0	3.59	13.54	20.40	2.61
30.0	3.31	25.06	22.70	3.22
36.0	4.56	27.89	25.26	3.33
48.0	8.67	31.36	31.28	3.45

dNO_3/dt (mgN/l/h)	$\ln(dtNO_3/dt)$	best fit $\ln(dtNO_3/dt$
0.24	-1.44	-1.44
0.24	-1.43	-1.43
0.24	-1.42	-1.42
0.24	-1.41	-1.41
0.25	-1.40	-1.40
0.25	-1.40	-1.40
0.25	-1.39	-1.39
0.25	-1.38	-1.38
0.25	-1.37	-1.37
0.26	-1.36	-1.36
0.26	-1.35	-1.35
0.26	-1.34	-1.34
0.26	-1.33	-1.33
0.27	-1.32	-1.32
0.27	-1.32	-1.32
0.27	-1.30	-1.30
0.28	-1.28	-1.28
0.28	-1.26	-1.26
0.29	-1.24	-1.24
0.29	-1.23	-1.23
0.30	-1.19	-1.19
0.32	-1.15	-1.15
0.33	-1.12	-1.12
0.34	-1.08	-1.08
0.35	-1.05	-1.05
0.36	-1.01	-1.01
0.40	-0.91	-0.91
0.45	-0.80	-0.80
0.56	-0.58	-0.58

Autotrophic batch test 10 Data

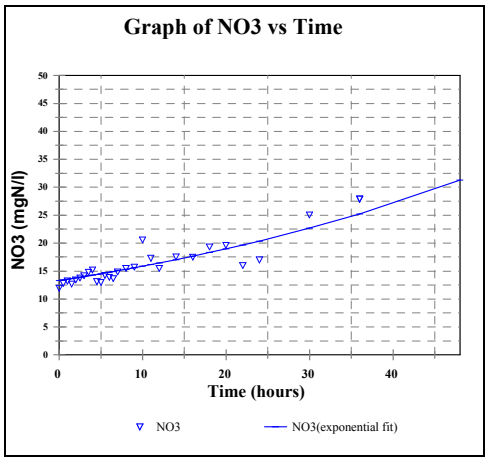

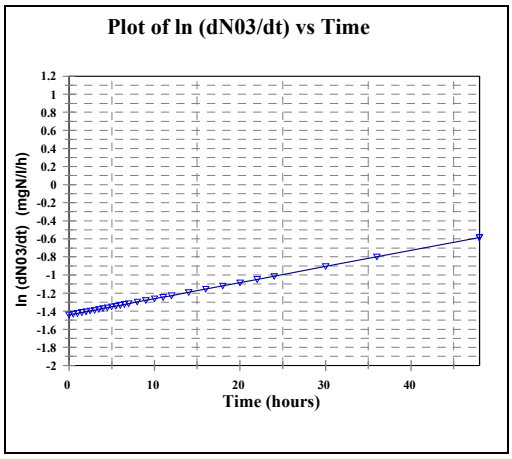

			fitted	
Time	NO_2	NO_3	NO_3	$Ln(NO_3)$
	conc.	conc.	conc.	
	[mg/l]	[mg/l]	[mg/l]	
0.0	1.38	11.94	13.30	2.48
0.5	0.15	12.83	13.42	2.55
1.0	0.15	13.24	13.54	2.58
1.5	0.14	12.68	13.66	2.54
2.0	0.13	13.45	13.78	2.60
2.5	0.11	13.77	13.90	2.62
3.0	0.13	14.17	14.03	2.65
3.5	0.14	14.8	14.15	2.69
4.0	0.15	15.2	14.28	2.72
4.5	0.16	13.13	14.41	2.57
5.0	0.15	12.94	14.54	2.56
5.5	0.16	14.22	14.67	2.65
6.0	0.19	13.86	14.80	2.63
6.5	0.19	13.68	14.93	2.62
7.0	0.23	14.88	15.07	2.70
8.0	0.27	15.49	15.34	2.74
9.0	0.32	15.72	15.61	2.75
10.0	0.35	20.59	15.89	3.02
11.0	0.5	17.3	16.18	2.85
12.0	0.35	15.49	16.47	2.74
14.0	0.36	17.56	17.07	2.87
16.0	0.77	17.48	17.69	2.86
18.0	0.91	19.33	18.33	2.96
20.0	1.68	19.6	18.99	2.98
22.0	3.91	16.01	19.68	2.77
24.0	2.8	17.01	20.40	2.83
30.0	2.13	25.06	22.70	3.22
36.0	5.21	27.89	25.26	3.33
48.0	9.15	30.88	31.28	3.43

dNO_3/dt	$ln (dtNO_3/dt)$	best fit
(mgN/l/h)		$ln(dtNO_3/dt$
0.24	-1.44	-1.44
0.24	-1.43	-1.43
0.24	-1.42	-1.42
0.24	-1.41	-1.41
0.25	-1.40	-1.40
0.25	-1.40	-1.40
0.25	-1.39	-1.39
0.25	-1.38	-1.38
0.25	-1.37	-1.37
0.26	-1.36	-1.36
0.26	-1.35	-1.35
0.26	-1.34	-1.34
0.26	-1.33	-1.33
0.27	-1.32	-1.32
0.27	-1.32	-1.32
0.27	-1.30	-1.30
0.28	-1.28	-1.28
0.28	-1.26	-1.26
0.29	-1.24	-1.24
0.29	-1.23	-1.23
0.30	-1.19	-1.19
0.32	-1.15	-1.15
0.33	-1.12	-1.12
0.34	-1.08	-1.08
0.35	-1.05	-1.05
0.36	-1.01	-1.01
0.40	-0.91	-0.91
0.45	-0.80	-0.80
0.56	-0.58	-0.58

APPENDIX 13

Comprehensive FISH data for autotrophic batch test

Table 13.1: All experimental FISH data for each batch tests; Cell counts (DAPI, EUB, NSO, NIT, NSR) means and standard deviations; percentages of DAPI, EUB and total nitrifiers are also listed.

Table 13.1: Comprehensive FISH data for all autotrophic batch test

batch no	tcc	eub cc	nso cc	nit cc	nsr cc	total nitrif	AUB
	(cells/ml)	(cells/ml)	(cells/ml)	(cells/ml)	(cells/ml)	(cells/ml)	mgCOD/l
b1	9.96E+08	8.12E+08	1.14E+08	4.57E+06	4.75E+07	1.66E+08	49.74
	9.56E+08	7.98E+08	1.09E+08	4.87E+06	4.58E+07	1.60E+08	47.83
	8.80E+08	7.97E+08	8.85E+07	4.72E+06	4.83E+07	1.42E+08	42.40
mean	**9.44E+08**	**8.02E+08**	**1.04E+08**	**4.72E+06**	**4.72E+07**	**1.56E+08**	**46.65**
std	5.89E+07	8.32E+06	1.35E+07	1.50E+05	1.28E+06	1.27E+07	**3.81**
%eub			12.94	0.59	5.88	19.41	
%Dapi		85.00	11.00	0.50	5.00	16.50	
%nitrifiers			66.67	3.03	30.30		
b2	**9.92E+08**	8.65E+08	1.44E+08	3.77E+06	6.98E+07	2.18E+08	**69.60**
	9.74E+08	8.55E+08	1.35E+08	3.85E+06	6.64E+07	2.05E+08	**65.66**
	9.98E+08	9.18E+08	1.66E+08	4.24E+06	7.13E+07	2.41E+08	**77.13**
mean	**9.88E+08**	8.79E+08	1.48E+08	3.95E+06	6.92E+07	2.21E+08	**70.80**
std	**1.25E+07**	**3.38E+07**	**1.57E+07**	**2.49E+05**	**2.50E+06**	**1.82E+07**	**5.83**
%eub			16.85	0.45	7.87	25.17	
%Dapi		89.00	15.00	0.40	7.00	22.40	
%nitrifiers			66.96	1.79	31.25		
b3	**8.73E+08**	7.32E+08	1.54E+08	1.79E+07	3.45E+07	2.06E+08	**64.35**
	8.63E+08	7.42E+08	1.77E+08	1.54E+07	3.62E+07	2.29E+08	**71.27**
	9.13E+08	7.78E+08	1.72E+08	1.97E+07	3.53E+07	2.27E+08	**70.85**
mean	8.83E+08	7.51E+08	1.68E+08	1.77E+07	3.53E+07	2.21E+08	**68.82**
std	2.65E+07	2.40E+07	1.22E+07	2.15E+06	8.52E+05	1.24E+07	3.88
%eub			22.35	2.35	4.71	29.41	
%dapi		85.00	19.00	2.00	4.00	25.00	
%nitrifiers			76.00	8.00	16.00		
b4	7.45E+08	5.62E+08	8.23E+07	7.22E+06	3.77E+07	1.27E+08	**39.66**
	7.33E+08	5.32E+08	8.11E+07	7.40E+06	3.55E+07	1.24E+08	**38.66**
	7.39E+08	7.68E+08	8.05E+07	7.55E+06	3.77E+07	1.26E+08	**39.18**
mean	**7.39E+08**	**6.21E+08**	**8.13E+07**	**7.39E+06**	**3.70E+07**	**1.26E+08**	**39.17**
std	6.00E+06	1.29E+08	9.30E+05	1.65E+05	1.26E+06	1.61E+06	
%eub			13.10	1.19	5.95	20.24	
%dapi		84.00	11.00	1.00	5.00	17.00	
%nitrifiers			64.71	5.88	29.41		
b5	7.14E+08	6.24E+08	1.24E+08	1.32E+07	3.33E+07	1.71E+08	**52.46**
	7.22E+08	6.42E+08	1.12E+08	1.44E+07	3.48E+07	1.61E+08	**49.60**
	6.67E+08	6.27E+08	1.43E+08	1.45E+07	3.71E+07	1.94E+08	**59.70**
mean	7.01E+08	6.31E+08	1.26E+08	1.40E+07	3.51E+07	1.75E+08	**53.92**
std	2.97E+07	9.71E+06	1.54E+07	7.11E+05	1.89E+06	1.69E+07	5.21
%eub			20.00	2.22	5.56	27.78	

%dapi		90.00	18.00	2.00	5.00	25.00	
%nitrifiers			72.00	8.00	20.00		
b6	9.56E+08	7.85E+08	1.01E+08	5.88E+07	7.85E+07	2.38E+08	**73.32**
	9.70E+08	7.77E+08	1.21E+08	5.92E+07	7.54E+07	2.56E+08	**78.64**
	9.75E+08	8.17E+08	1.26E+08	5.61E+07	7.82E+07	2.60E+08	**80.11**
mean	9.67E+08	7.93E+08	1.16E+08	5.80E+07	7.74E+07	2.51E+08	**77.36**
std	9.85E+06	2.11E+07	1.33E+07	1.71E+06	1.70E+06	1.16E+07	3.57
%eub			14.63	7.32	9.76	31.71	
%dapi		82.00	12.00	6.00	8.00	26.00	
%nitrifiers			46.15	23.08	30.77		
b7	1.66E+09	1.48E+09	4.24E+08	3.03E+07	8.50E+07	5.39E+08	**163.73**
	1.78E+09	1.30E+09	4.44E+08	3.45E+07	8.68E+07	5.65E+08	**171.63**
	1.60E+09	1.50E+09	3.92E+08	3.60E+07	8.02E+07	5.08E+08	**154.29**
mean	1.68E+09	1.43E+09	4.20E+08	3.36E+07	8.40E+07	5.38E+08	**163.22**
std	9.17E+07	1.11E+08	2.62E+07	2.95E+06	3.41E+06	2.86E+07	8.68
%eub			29.41	2.35	5.88	37.65	
%dapi		85.00	25.00	2.00	5.00	32.00	
%nitrifiers			78.13	6.25	15.63		
b8	1.80E+09	1.35E+09	2.67E+08	1.71E+07	5.21E+07	3.36E+08	**102.07**
	1.69E+09	1.21E+09	2.71E+08	1.79E+07	5.11E+07	3.40E+08	**103.22**
	1.70E+09	1.38E+09	2.92E+08	1.69E+07	5.25E+07	3.62E+08	**109.84**
mean	1.73E+09	1.31E+09	2.77E+08	1.73E+07	5.19E+07	3.46E+08	**105.05**
std	6.08E+07	9.24E+07	1.37E+07	5.29E+05	7.21E+05	1.38E+07	4.19
%eub			21.05	1.32	3.95	26.32	
%dapi		76.00	16.00	1.00	3.00	20.00	
%nitrifiers			80.00	5.00	15.00		
b9	1.32E+09	1.05E+09	8.45E+07	1.15E+07	4.78E+07	1.44E+08	**41.61**
	1.20E+09	1.12E+09	8.40E+07	1.32E+07	4.80E+07	1.45E+08	**42.01**
	1.14E+09	9.04E+08	8.77E+07	1.19E+07	5.06E+07	1.50E+08	**43.46**
mean	1.22E+09	1.02E+09	8.54E+07	1.22E+07	4.88E+07	1.46E+08	**42.36**
std	9.17E+07	1.10E+08	2.01E+06	8.89E+05	1.56E+06	3.36E+06	0.97
%eub			8.33	1.19	4.76	14.29	
%dapi		84.00	7.00	1.00	4.00	12.00	
%nitrifiers			58.33	8.33	33.33		
b10	1.13E+09	8.57E+08	1.11E+08	1.12E+07	4.21E+07	1.64E+08	**47.54**
	1.18E+09	8.60E+08	1.21E+08	1.15E+07	4.32E+07	1.76E+08	**50.84**
	9.00E+08	8.83E+08	1.21E+08	9.40E+06	4.31E+07	1.74E+08	**50.23**
mean	1.07E+09	8.67E+08	1.18E+08	1.07E+07	4.28E+07	1.71E+08	**49.53**
std	1.49E+08	1.43E+07	5.80E+06	1.14E+06	6.08E+05	6.07E+06	1.76
%eub			13.58	1.23	4.94	19.75	
%dapi		81.00	11.00	1.00	4.00	16.00	
%nitrifiers			68.75	6.25	25.00		

APPENDIX 14

DNA extraction and quantification

DNA extraction

Procedure: (Mayer and Palmer, 1996 and Kuhn *et al*., 2002)

- 1 ml of raw sample was added to 1.5 ml microtubes and centrifuged at 1400 rpm for 5 minutes at 4°C. Samples were done in duplicate.
- The supernatant is discarded and the pellet is resuspended in 500 µl 1 x PBS and centrifuged at 5000 rpm for 3 minutes.
- The pellet is resuspended in 75 µl of Tris-EDTA buffer with 25 µl of 10% SDS. Invert tubes 2 to 3 times to mix.
- Samples are incubated for 2 h at 65°C in a water-bath.
- 500 µl lysis buffer is added to the sample after incubation. Vortex gently.
- The cells are then lysed by the freeze thaw method consisting of dry ice and ethanol slurry for 2 minutes followed by 65°C for 5 minutes. This cycle is repeated 5 times.
- 500 µl of Tris-EDTA saturated Phenol was added to the sample and the sample was mixed by inversion.
- The sample is then centrifuged at 5700 rpm for 5 minutes.
- The top layer was removed and added to a clean microtube.
- An equal volume of phenol-chloroform (25:24) was added to the top layer which was removed. Sample was mixed by inversion and centrifuged at 5700 rpm for 5 minutes.
- The top layer was removed and added to a clean microtube and an equal volume of chloroform was added. Sample was mixed by inversion and centrifuged at 5700 rpm for 5 minutes.
- The top layer was removed and added to a clean microtube and an equal volume of 100% isopropyl alcohol was added and the sample was incubated at - 4ºC for 1 hour.
- The DNA was pelleted by centrifugation at 10500 rpm for 30 minutes.
- The pellet is then washed with 70% ethanol centrifuged at 4000 rpm for 5 minutes and then re-suspended in 30 µl of sterile distilled water.

Concentration of DNA: (Maniatis *et al*., 1982)

- To quantify the amount of DNA- readings are taken at 260 nm and 280 nm.
- Reading at 260 nm calculates the concentration of nucleic acids in the sample.
- An optical density of 1 corresponds to 50 µg/ml or double stranded DNA, 40 µg/ml for single stranded DNA and 20 ug/ml for oligonucleotides.
- The ratio between the readings 260nm and 280nm (OD_{260}/OD_{280}) provides an estimate for the purity of the DNA present.
- Pure preparations of DNA have (OD_{260}/OD_{280}) of 1.8 and 2.0 respectively.
- Contamination with protein or phenol causes the OD values to decrease significantly.

List of reagents:

1. Tris-EDTA Buffer:

- 10 mM Tris-HCl is added with to 1 mM EDTA, pH 8.

2. 10% SDS:

- 10 g SDS is dissolved in 100 ml sterile distilled water.

3. Lysis Buffer:

- 10% SDS is added to 0.1 M NaCl and 0.5 M Tris-HCl.

4. Equilibrium of Phenol (Tris-EDTA saturated buffer):

- Liquified phenol is stored at -20ºC therefore the phenol is melted at 68ºC in a water-bath.
- 50 ml phenol is added to a conical flask and 0.1 g of 8-Hydroxyquinoline is added.
- 50 ml of Tris-EDTA buffer is added and this solution is stirred on a magnetic stirrer for 15 minutes then turn off the stirrer and allow the two phases present to separate. When the two phases have separated, the top layer is aspirated.
- The last step is repeated until the pH reaches the pH of the Tris-EDTA buffer.
- After equilibration of the phenol the final aqueous layer is removed and 100 µl Tris-EDTA buffer containing 20 µl beta-mercaptoethanol is added.

5. 1 x PBS.

6. Liquidified Phenol.

7. Chloroform

APPENDIX 15

Polymerase chain reaction

Procedure: (Giovannoni, 1991)

- 0.2 ml sterile eppendorf tubes are used. The reaction mixture is added in specific quantities to the eppendorf tubes.
- PCR takes place in a Hybaid Thermal Cycler.
- The cycle format used to amplify the template DNA:

Table 15.1: Hybaid PCR Sprint Thermal Cycler Program (Hybaid Limited, UK)

STAGES		TEMPEATURE	TIME	CYCLES
STAGE 1	STEP 1	94ºC	4 minutes	x 1
STAGE 1	STEP 1	94ºC	1 minute	x 35
	STEP 2	53ºC	1 minute	
	STEP 3	72ºC	2 minutes	
STAGE 1	STEP 1	72ºC	4 minutes	x 1
HOLD		4ºC		

List of reagents:

1. 10 µl of 10 x PCR Buffer without $MgCl_2$: 50 mM KCl, 10 mM Tris-HCl, pH 8.4.
2. 6 µl of 2.5 mM $MgCl_2$.
3. 10 µl of 10 mM dNTP:dATP, dCTP, dGTP, dTTP each at a concentration of 10 mM.
4. 10 µl of 10 ng/µl Genomic DNA Template.
5. 2 µl of 50 pM Stock Solution of Primers.
6. 1 µl of 5units/µl *Taq* Polymerase

APPENDIX 16

Denaturing gradient gel electrophoresis

Procedure: (Bio-Rad Laboratories, 1994)

- Buffer Tempreature: Preheat running buffer in chamber or tank to 60ºC.
- Assembling the Glass Plates: The acrylamide gel was made between two clean glass plates of different heights. The smaller plate is placed on top of the longer rectangular plate. Spacers are placed between the glass plates and the plates are clamped together. The sandwich clamps are then loosened and an alignment card is inserted. Once a good alignment and seal was achieved, the clamp was tightened.
- The high and low density gel solutions (150 µl 10% Ammonium Pesulphate, 15 ml Denaturing Solution and 100 µl D-GENE dye to only the high density solution) are injected in between the two plates by using the delivery system (Model 475 Gradient Delivery System). A comb to produce wells was added and the gel was allowed to polymerise for 30-45 minutes.
- The samples were loaded into the washed wells (washed with 1 x TAE buffer). 8 µl samples were mixed with 2 µl D Gene dye solution and loaded into the wells using micropipettes.
- The DGGE apparatus (the sandwiched plates with the loaded gel) was placed in the pre-warmed tank. The voltage was set at 200V for 2 hours.
- After 2 hours the gel was carefully removed from the sandwiched plates and place in a container filled with 250 ml of 1 x TAE buffer and 15 µl of 10 mg/ml ethidium bromide. Staining took 5 minutes and the gel was transferred to another container which contained only the 250 ml 1 x TAE allowing for de-staining (unbound ethidium bromide was washed away from the gel).
- The gel was viewed on a UV transilluminator and photographed with a Polaroid camera (Hoefer Pharmacia Biotech, USA).

List of reagents:

1. 50 x TAE Buffer:

- 242 g of Tris-Base together with 57.1 ml glacial acetic acid and 100 ml 0.5 M EDTA. pH 8. Make to 1000 ml. Autoclave.

2. 1 x TAE Buffer:

- 20 ml 50 x TAE buffer is added to 980 ml sterile distilled water. Autoclave.

3. Running Buffer:

- 140 ml of 50 x TAE buffer is added to 6860 ml distilled water.

4. 40% Acrylamide/Bis-acrylamide:

- 38 g acrylamide and 2 g bis-acrylamide are made up to 100 ml. Filter through a Whatman No 1.

5. 30% Denaturing Solution:

- This is made up with 18.8 ml 40% Acrylamide/Bis-acrylamide, 2 ml 50 x TAE, **12 ml** Formamide and **12.6 g** Urea. Make up to 100 ml, and degas for 10 to 15 minutes.

6. 50% Denaturing Solution:

- This is made up with 18.8 ml 40% Acrylamide/Bis-acrylamide, 2 ml 50 x TAE, **20 ml** Formamide and **21 g** Urea. Make up to 100 ml, and degas for 10 to 15 minutes.

7. 10% Ammonium Persulphate:

- 0.1 g Ammonium Persulphate is added to 1 ml distilled water.

8. D GENE Dye Solution:

- 0.05 g Bromophenol Blue is added to 0.05 g Xylene Cyanol and 10 ml 1 x TAE buffer.